frontiers | Research Topics

Factors determining long term anti-tumor responses to immune checkpoint blockade therapy

Edited by
Alison Taylor, Graham Cook and Roberta Zappasodi

Published in
Frontiers in Immunology
Frontiers in Oncology

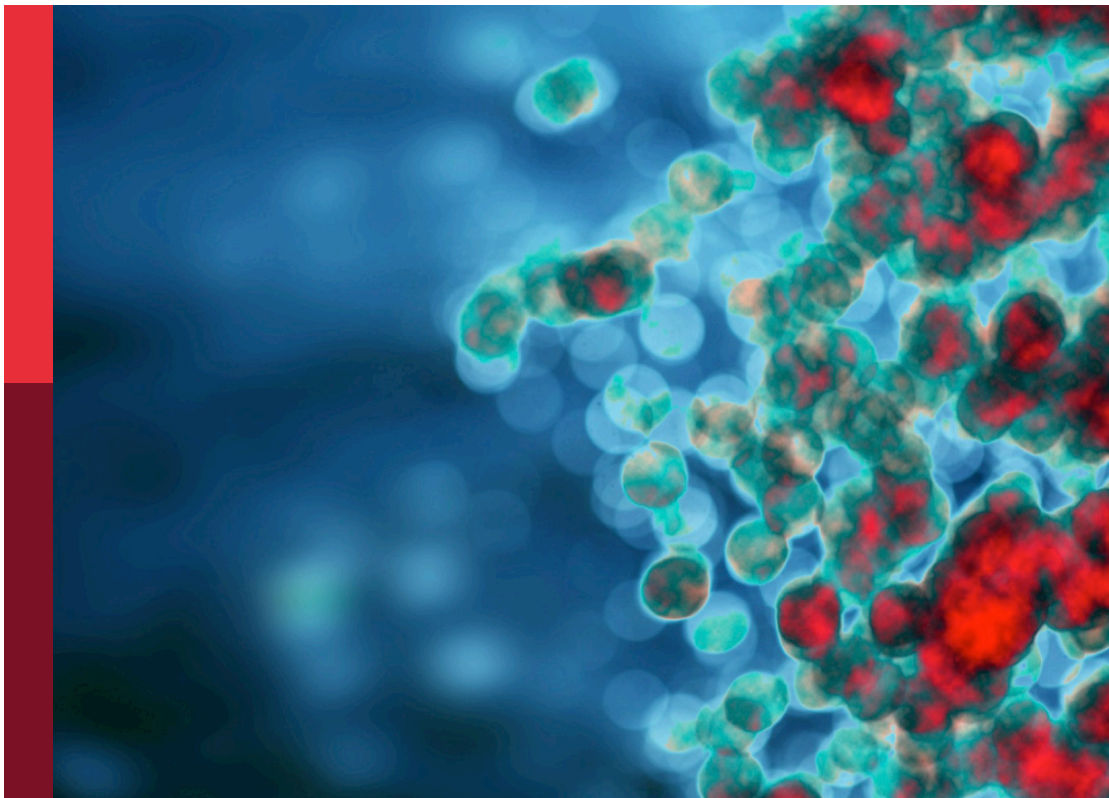

ISSN 1664-8714
ISBN 978-2-83251-277-7
DOI 10.3389/978-2-83251-277-7

About Frontiers

Frontiers is more than just an open access publisher of scholarly articles: it is a pioneering approach to the world of academia, radically improving the way scholarly research is managed. The grand vision of Frontiers is a world where all people have an equal opportunity to seek, share and generate knowledge. Frontiers provides immediate and permanent online open access to all its publications, but this alone is not enough to realize our grand goals.

Frontiers journal series

The Frontiers journal series is a multi-tier and interdisciplinary set of open-access, online journals, promising a paradigm shift from the current review, selection and dissemination processes in academic publishing. All Frontiers journals are driven by researchers for researchers; therefore, they constitute a service to the scholarly community. At the same time, the *Frontiers journal series* operates on a revolutionary invention, the tiered publishing system, initially addressing specific communities of scholars, and gradually climbing up to broader public understanding, thus serving the interests of the lay society, too.

Dedication to quality

Each Frontiers article is a landmark of the highest quality, thanks to genuinely collaborative interactions between authors and review editors, who include some of the world's best academicians. Research must be certified by peers before entering a stream of knowledge that may eventually reach the public - and shape society; therefore, Frontiers only applies the most rigorous and unbiased reviews. Frontiers revolutionizes research publishing by freely delivering the most outstanding research, evaluated with no bias from both the academic and social point of view. By applying the most advanced information technologies, Frontiers is catapulting scholarly publishing into a new generation.

What are Frontiers Research Topics?

Frontiers Research Topics are very popular trademarks of the *Frontiers journals series*: they are collections of at least ten articles, all centered on a particular subject. With their unique mix of varied contributions from Original Research to Review Articles, Frontiers Research Topics unify the most influential researchers, the latest key findings and historical advances in a hot research area.

Find out more on how to host your own Frontiers Research Topic or contribute to one as an author by contacting the Frontiers editorial office:
frontiersin.org/about/contact

Factors determining long term anti-tumor responses to immune checkpoint blockade therapy

Topic editors

Alison Taylor — University of Leeds, United Kingdom
Graham Cook — University of Leeds, United Kingdom
Roberta Zappasodi — Cornell University, United States

Citation

Taylor, A., Cook, G., Zappasodi, R., eds. (2023). *Factors determining long term anti-tumor responses to immune checkpoint blockade therapy*. Lausanne: Frontiers Media SA. doi: 10.3389/978-2-83251-277-7

Table of contents

frontiers | Frontiers in Immunology

TYPE Editorial
PUBLISHED 21 December 2022
DOI 10.3389/fimmu.2022.1120207

OPEN ACCESS

EDITED AND REVIEWED BY
Katy Rezvani, University of Texas MD Anderson Cancer Center, United States

*CORRESPONDENCE
Alison Taylor
A.Taylor1@leeds.ac.uk

SPECIALTY SECTION
This article was submitted to Cancer Immunity and Immunotherapy, a section of the journal Frontiers in Immunology

RECEIVED 09 December 2022
ACCEPTED 13 December 2022
PUBLISHED 21 December 2022

CITATION
Zappasodi R, Cook GP and Taylor A (2022) Editorial: Factors determining long term anti-tumor responses to immune checkpoint blockade therapy. *Front. Immunol.* 13:1120207. doi: 10.3389/fimmu.2022.1120207

Editorial: Factors determining long term anti-tumor responses to immune checkpoint blockade therapy

Roberta Zappasodi[1], Graham P. Cook[2] and Alison Taylor[2]*

[1]Weill Cornell Medicine, Cornell University and Memorial Sloan Kettering Cancer Center, New York City, NY, United States, [2]Leeds Institute of Medical Research, University of Leeds School of Medicine, Leeds, United Kingdom

KEYWORDS

immunotherapy, tumour immunology, immune checkpoint blockade, checkpoint inhibitors, cancer

Editorial on the Research Topic

Factors determining long term anti-tumor responses to immune checkpoint blockade therapy

Landmark studies performed in animal models more than twenty years ago revealed that the anti-tumour activity of T cells could be enhanced by blocking inhibitory signals arising from cell surface receptors now collectively termed immune checkpoints (1–3). This led to the development of therapeutic antibodies targeting these molecules, their clinical trials and to the approval of agents targeting CTLA-4, PD-1 and its ligand, PD-L1 (3–5). These agents have revolutionised treatment of several cancers and are under investigation for their value in the treatment of many others. Two pioneers of this field, immunologists James Allison and Tasuku Honjo, were awarded the 2018 Nobel Prize in Medicine or Physiology (4, 5).

Using antibodies to treat cancer is not new. Antibodies targeting CD20 expression on B cell malignancies (Rituximab and its derivatives) and HER2 in breast cancer (Trastuzumab) have been approved for clinical use since the late 1990s. However, the antibody-mediated targeting of immune checkpoints represents a paradigm shift in cancer treatment. Along with agents targeting vascular endothelial growth factor (VEGF), these treatments target components of the tumour microenvironment rather than direct targeting of the tumour cells. This strategy reflects our changing view of cancer and the way in which it is studied and treated (6, 7). Attention is no longer confined to just the malignant cells, but now extends to all components of the tumour microenvironment and beyond (for example, the effects of co-morbidities and the microbiome). Numerous cell types are under investigation for their contribution to tumour progression and, hence, for their potential as drug targets; immune checkpoint blockade is a success story resulting from such endeavours.

Unfortunately, this success is not universal. In the case of melanoma, roughly half of the patients treated will not benefit. Furthermore, side effects can be severe. These therapies target naturally occurring feedback inhibitory mechanisms that have evolved to limit the duration of the immune response and minimise damage to healthy tissue. This is exemplified by early studies of PD-1 and CTLA-4 in which knockout mice were shown to develop autoimmune phenotypes. Side effects, variable responses (and of course cost) mean there is a pressing need to better understand the nature of response (and non-response) and to identify those patients more likely to benefit from these treatments. This has been intensive area of research for several years and the collection of papers presented here reflect clinical needs and current mechanistic understanding. The papers include those addressing immune checkpoint blockade in a single malignancy, as well as more diverse studies. Indeed, the impact of immune checkpoint therapy on cancer treatment is demonstrated by the number of cancer types investigated in these papers, these include melanoma, bladder, lung, renal, pancreatic and colorectal cancers. Furthermore, case reports in pancreatic cancer and rhabdomyosarcoma demonstrate how these therapies can dramatically improve outcomes for individual patients.

Several of these studies focus on defining markers of response to immune checkpoint therapy. A diverse range of material and technological approaches are used. For example, studies utilise tumour genome and transcriptome data, inflammatory markers (serum proteins and neutrophil to lymphocyte ratio), markers of circulating tumour cells and the contribution of the gut microbiome and tumour metabolism. In addition, factors that determine outcome are discussed, these include drug-drug interactions, as well as underlying immunological mechanisms and how the tumour microenvironment regulates and responds to treatment. Of note, these papers highlight the interdisciplinarity of these studies; biomedical researchers, oncologists and other clinical professionals now regularly work alongside bioinformaticians, statisticians, clinical trials experts and computer scientists. Most importantly, this field (which is no longer exclusive to immunologists) makes a difference.

Author contributions

All authors listed have made a substantial, direct, and intellectual contribution to the work and approved it for publication.

Conflict of interest

The authors declare that the research was conducted in the absence of any commercial or financial relationships that could be construed as a potential conflict of interest.

Publisher's note

References

1. Leach DR, Krummel MF, Allison JP. Enhancement of antitumor immunity by CTLA-4 blockade. *Science* (1996) 271:1734–6. doi: 10.1126/science.271.5256.1734

2. Iwai Y, Ishida M, Tanaka Y, Okazaki T, Honjo T, Minato N, et al. Involvement of PD-L1 on tumor cells in the escape from host immune system and tumor immunotherapy by PD-L1 blockade. *Proc Natl Acad Sci U S A.* (2002) 99:12293–7. doi: 10.1073/pnas.192461099

3. Pardoll DM. The blockade of immune checkpoints in cancer immunotherapy. *Nat Rev Cancer.* (2012) 12:252–64. doi: 10.1038/nrc3239

4. *Nobel Prize in physiology or medicine 2018* . Available at: https://www.nobelprize.org/prizes/medicine/2018/press-release/.

5. Fritz JM, Lenardo MJ. Development of immune checkpoint therapy for cancer. *J Exp Med* (2019) 216:1244–54. doi: 10.1084/jem.20182395

6. Hanahan D, Weinberg RA. The hallmarks of cancer. *Cell* (2000) 100:57–70. doi: 10.1016/S0092-8674(00)81683-9

7. Hanahan D, Weinberg RA. Hallmarks of cancer: The next generation. *Cell* (2011) 144:646–74. doi: 10.1016/j.cell.2011.02.013

frontiers in Oncology

ORIGINAL RESEARCH
published: 01 April 2021
doi: 10.3389/fonc.2021.646883

Serum Levels of Soluble Urokinase Plasminogen Activator Receptor Predict Tumor Response and Outcome to Immune Checkpoint Inhibitor Therapy

Sven H. Loosen[1,2†], Joao Gorgulho[3,4†], Markus S. Jördens[1], Maximilian Schulze-Hagen[5], Fabian Beier[6], Mihael Vucur[1], Anne T. Schneider[3], Christiane Koppe[3], Alexander Mertens[1], Jakob N. Kather[2], Frank Tacke[7], Verena Keitel[1], Tim H. Brümmendorf[6‡], Christoph Roderburg[1,7‡] and Tom Luedde[1*‡]*

[1] Clinic for Gastroenterology, Hepatology and Infectious Diseases, University Hospital Düsseldorf, Medical Faculty of Heinrich Heine University Düsseldorf, Düsseldorf, Germany, [2] Department of Medicine III, University Hospital RWTH Aachen, Aachen, Germany, [3] Division of Gastroenterology, Hepatology and Hepatobiliary Oncology, University Hospital RWTH Aachen, Aachen, Germany, [4] Department of Oncology, Hematology and Bone Marrow Transplantation with Section of Pneumology, University Medical Centre Hamburg-Eppendorf, Hamburg, Germany, [5] Department of Diagnostic and Interventional Radiology, University Hospital RWTH Aachen, Aachen, Germany, [6] Department of Medicine IV, University Hospital RWTH Aachen, Aachen, Germany, [7] Department of Hepatology and Gastroenterology, Charité University Medicine Berlin, Berlin, Germany

Background: Immune checkpoint inhibitors (ICIs) have led to a paradigm shift in cancer therapy, improving outcomes in the treatment of various malignancies. However, not all patients benefit to the same extend from ICI. Reliable tools to predict treatment response and outcome are missing. Soluble urokinase plasminogen activator receptor (suPAR) is a marker of immune activation, whose levels are prognostic in various cancers. We evaluated circulating suPAR levels as a novel predictive and prognostic biomarker in patients receiving ICI therapy for solid tumors.

Methods: A total of n = 87 patients receiving ICI therapy for different solid malignancies as well as 32 healthy controls were included into this study. Serum levels of suPAR were measured by ELISA prior to and sequentially at two time points during ICI therapy.

Results: Baseline suPAR serum levels were significantly higher in solid tumor patients compared to healthy controls. Importantly, patients with low suPAR levels both before or during ICI treatment were more likely to have a favorable response to treatment at three and six months, respectively. This finding was confirmed by multivariate binary logistic regression analysis including several clinicopathological parameters. Moreover, circulating suPAR levels before and during therapy were an independent prognostic factor for overall survival (OS). As such, patients with initial suPAR levels above our ideal prognostic cut-off value (4.86 ng/ml) had a median OS of only 160 days compared to 705 days for patients

OPEN ACCESS

Edited by:
Alison Taylor,
University of Leeds, United Kingdom

Reviewed by:
Line Rasmussen,
Duke University, United States
Robert J. Canter,
University of California, Davis,
United States

***Correspondence:**
Tom Luedde
luedde@hhu.de
Sven H. Loosen
sven.loosen@med.uni-duesseldorf.de

†These authors share first authorship

‡These authors share senior authorship

Specialty section:
This article was submitted to Cancer Immunity and Immunotherapy, a section of the journal Frontiers in Oncology

Received: 28 December 2020
Accepted: 09 March 2021
Published: 01 April 2021

Citation:
Loosen SH, Gorgulho J, Joerdens MS, Schulze-Hagen M, Beier F, Vucur M, Schneider AT, Koppe C, Mertens A, Kather JN, Tacke F, Keitel V, Brümmendorf TH, Roderburg C and Luedde T (2021) Serum Levels of Soluble Urokinase Plasminogen Activator Receptor Predict Tumor Response and Outcome to Immune Checkpoint Inhibitor Therapy. Front. Oncol. 11:646883. doi: 10.3389/fonc.2021.646883

with suPAR levels below this cut-off value. Finally, low baseline suPAR levels identified a subgroup of patients who experienced ICI-related side effects which in turn were associated with favorable treatment response and outcome.

Conclusion: Our data suggest that measurements of suPAR serum levels are a previously unknown, easily accessible tool to predict individual treatment response and outcome to ICI therapy. Circulating suPAR might therefore be implemented into stratification algorithms to identify the ideal candidates for ICI treatment.

Keywords: immunotherapy, checkpoint inhibitors, prognosis, biomarker, nivolumab, pembrolizumab, IRAE

BACKGROUND

Cancer is the second leading cause of death in highly developed areas of the world such as Europe and the US (1). In 2013, cancer immunotherapy, or more precisely immune checkpoint inhibitors (ICIs), was deemed the "breakthrough of the year" by Science magazine (2). Several ICIs, mostly targeting the programmed cell death (PD)-L1/PD-1 (e.g. nivolumab, pembrolizumab) or the B7/cytotoxic T-lymphocyte-associated protein (CTLA)-4 (e.g. ipilimumab) pathway, have been approved either alone or in combination with e.g. chemotherapy for treatment of various cancer entities such as non-small cell lung cancer (NSCLC), malignant melanoma or urothelial carcinoma (3–5). However, tumor response rates and outcome to ICIs are very heterogeneous. While ICIs can achieve higher response and survival rates compared to conventional chemotherapy in several tumor entities, a subset of patients does not respond to immunotherapy. Although several, mostly tissue based, markers such as the expression of PD-L1, the tumor mutational burden (TMB) or the microsatellite instability (MSI) status have been suggested to predict ICI treatment response in selected tumor entities (3, 6–8), the identification of the ideal ICI patients who particularly benefit from ICI has remained challenging.

The soluble urokinase plasminogen activator receptor (suPAR) represents the cleavage product from the membrane-bound form of urokinase plasminogen activator receptor (uPAR/CD87) that is e.g. expressed on epithelial and immune cells (9). Circulating suPAR has recently been associated with inflammatory diseases and several cancer entities (10–15). During systemic inflammation, an increased shedding of uPAR on circulating neutrophils has been reported as a source of elevated suPAR levels (16). However, currently no data on a potential role of uPAR/suPAR in the context of ICIs exist. In the present study, we therefore aimed at evaluating a potential predictive and/or prognostic role of circulating suPAR as a novel biomarker in patients receiving ICIs for different solid tumor entities at the interdisciplinary tumor outpatient clinic of the University Hospital RWTH Aachen between 2018 and 2020.

METHODS

Study Design and Patient Characteristics

This observational cohort study was designed to evaluate a potential predictive and prognostic role of circulating suPAR in a cohort of patients receiving immune checkpoint inhibitors (ICI) for different tumor entities. A total of n = 87 patients who received ICI at the interdisciplinary cancer outpatient clinic at University Hospital RWTH Aachen for advanced stage disease were prospectively recruited 2018 and 2020 and enrolled into this study (see **Table 1**). Patient characteristics such as the Eastern Cooperative Oncology Group (ECOG) performance status were assessed by a trained physician during study enrollment based on established classification systems (17). Blood samples were drawn prior to ICI therapy as well as during the course of treatment (early time point: after one or two cycles of ICI, late time point: after three, four, or five cycles of ICI). Samples were then centrifuged for 10 min at 2,000*g*, and serum samples were stored in the RWTH centralized Biomaterial Bank at −80°C until use. As a control population we analyzed a total of n = 32 healthy, cancer-free blood donors with normal values for blood counts, C-reactive protein, kidney and liver function. The study protocol was approved by the ethics committee of the University Hospital RWTH Aachen, Germany (EK 206/09) and conducted in accordance with the ethical standards laid down in the Declaration of Helsinki. Written informed consent was obtained from the patients.

Assessment of Tumor Response, Overall Survival and Immune Related Adverse Events (IRAE)

Tumor response to ICI therapy was assessed on cross-sectional imaging modalities (CT or MRI scan) at three, six and twelve months based using the RECIST v1.1 criteria where applicable (18). Tumor response was classified using the standard nomenclature for RECIST: Complete response (CR), partial response (PR), stable disease (SD) and progressive disease (PD). CR, PR and SD were defined as "disease control" (DC) whereas patient with PD were classified into non-DC. Patients who died during the respective follow-up period were defined as non-DC. Patients were followed-up by a doctor with a specialization in oncology before every administration of ICI depending on the therapy regimen as well as in between therapy cycles. Overall survival (OS) was defined as time from the first administration of ICI to death. The median follow-up time of the study cohort (first ICI therapy to death/"last follow-up") was 261 days (IQR: 418). Immune related adverse events (IRAE) were assessed during follow up by a doctor with a specialization in oncology according to the Common Terminology Criteria for

TABLE 1 | Patient characteristics.

Parameter	Study cohort	Baseline suPAR levels [ng/ml, median and IQR]
Cancer patients	n = 87	5.36 (2.81)
Gender [%]:	67.8 (n = 59)	5.36 (3.24)
male	32.2 (n = 28)	5.40 (3.05)
female		
Age [years, median and range]	67.0 [38.0–87.0]	
BMI [kg/m^2, median and range]	24.1 [15.9–42.3]	
Tumor localization [%]:	36.8 (n = 32)	5.32 (3.40)
NSCLC	14.9 (n = 13)	3.91 (2.34)
Malignant melanoma	13.8 (n = 12)	5.69 (2.30)
Urothelial cancer	14.9 (n = 13)	6.25 (2.63)
GI cancer	10.3 (n = 9)	6.70 (2.27)
Head and neck cancer	9.2 (n = 8)	4.83 (2.51)
Others		
Staging [%]:	6.0 (n = 5)	
UICC III	94.0 (n = 79)	
UICC IV		
ICI regimen [%]:	57.5 (n = 50)	5.53 (2.97)
Nivolumab	25.3 (n = 22)	6.01 (3.21)
Pembrolizumab	9.2 (n = 8)	4.86 (3.02)
Nivolumab + Ipilimumab	8.0 (n = 7)	4.00 (2.06)
Others (e.g. Avelumab, Durvalumab)		
Previous systemic therapy before ICI? [%]:	70.1 (n = 61)	5.62 (2.70)
Yes	29.9 (n = 26)	4.80 (2.47)
No		
ECOG PS [%]:	7.1 (n = 6)	5.14 (3.01)
ECOG 0	52.9 (n = 45)	4.98 (3.47)
ECOG 1	40.0 (n = 34)	5.64 (2.29)
ECOG 2		
Smoking status [%]:	8.0 (n = 7)	4.95 (3.23)
Never	42.2 (n = 35)	5.70 (3.24)
Previous	19.5 (n = 17)	5.57 (2.25)
Present	32.2 (n = 28)	4.92 (2.98)
unknown		
Disease control at 3 months? [%]:	47.1 (n = 41)	4.68 (3.04)
Yes	52.9 (n = 46)	5.78 (2.19)
No		
Disease control at 6 months? [%]:	39.1 (n = 34)	4.66 (3.37)
Yes	60.9 (n = 53)	5.65 (2.29)
No		
Disease control at 12 months? [%]:	29.6 (n = 24)	4.74 (2.99)
Yes	70.4 (n = 57)	5.65 (2.39)
No		
Deceased during follow-up? [%]:	62.1 (n = 54)	5.68 (2.21)
Yes	37.9 (n = 33)	4.63 (3.02)
No		
Side effects to ICI? [%]:	42.5 (n = 37)	4.75 (2.44)
Yes	57.5 (n = 50)	5.99 (2.86)
No		
Healthy controls	n = 32	1.55 (0.635)

BMI, body mass index; NSCLC, non-small cell lung cancer; GI, gastrointestinal; UICC, Union for International Cancer Control; ICI, immune checkpoint inhibitor; ECOG PS, Eastern Cooperative Oncology Group performance status.

Adverse Events (CTCAE) classification. The following IRAE were documented during follow up (number of patients): hypothyroidism (four), hyperthyroidism (two), hepatitis (four), gastritis (two), pruritus/rash (nine), pneumonitis (six), colitis (four), rheumatic (two), myositis (two), vitiligo (one), pancreatitis (one).

Measurements of suPAR Serum Levels and Routine Laboratory Parameters

Serum levels of suPAR were measured using a commercial enzyme-linked immunosorbent assay (ELISA) according to the manufacturer's instructions (Nr. A001, suPARnostic, ViroGates, Birkerød, Denmark). Routine laboratory markers were analyzed in the central laboratory at University Hospital RWTH Aachen using a Sysmex XN9000 (Sysmex GmbH, Norderstedt, Germany) and Cobas 8000 c701 (Hoffmann-La Roche AG, Basel, Switzerland) platform according to manufacturer's instructions.

Statistical Analysis

Shapiro–Wilk-Test was used to test for normal distribution. Non-parametric data were compared using Mann–Whitney-U-Test and Kruskal–Wallis-Test. Related samples were compared using Wilcoxon signed-rank test. Box plot graphics display the median, quartiles and ranges. We generated receiver operating characteristics (ROC) curves by plotting the sensitivity against 1-specificity. Optimal cut-off values for ROC curves were calculated with the Youden-Index (YI) method (YI = sensitivity + specificity − 1). The predictive value of variables on treatment response was evaluated by uni- and multivariate binary logistic regression analyses. Parameters with a p-value of <0.250 in univariate testing were included into multivariate testing. The Odds ratio (OR) and 95% confidence interval are shown. Kaplan–Meier curves display the impact of a specific parameter on the overall survival (OS). The Log-rank test was used to test for statistical differences between subgroups. The ideal cut-off value for the identification of patients with an impaired OS was calculated by fitting Cox proportional hazard models to the dichotomized survival status as well as the survival time and defining the optimal cut-off as the point with the most significant split in the log-rank test. The prognostic value of variables was further tested by uni- and multivariate Cox regression analyses. Parameters with a p-value of <0.250 in univariate testing were included into multivariate testing. The hazard ratio (HR) and 95% confidence interval are displayed. In survival analyses of longitudinal suPAR alterations between baseline and the "early/late time-point", patients who died before this time-point were excluded from analysis. All statistical analyses were performed with SPSS 23 (SPSS, Chicago, IL, USA) and RStudio 1.2.5033 (RStudio Inc., Boston, MA, USA) (11). A p-value of <0.05 was considered statistically significant (*p <0.05; **p <0.01; ***p <0.001).

RESULTS

Patient Characteristics and Baseline suPAR Serum Levels

A total of n = 87 patients with advanced tumor stage scheduled to receive immune checkpoint inhibitor (ICI) therapy were included into this study prior to the first ICI administration. The median patients' age was 67 years (range: 38–87 years). 32.2% of patients were female and 67.8% were male. NSCLC represented the most common disease etiology (36.8%), followed

by malignant melanoma (14.9%), urothelial carcinoma (13.8%), GI cancer (14.9%), head and neck cancer (10.3%) and others (9.2%). Most patients (94.0%) presented with metastasized tumor stage (Union for International Cancer Control (UICC) IV), while 6.0% had UICC III tumor stage. 47.1% (n = 41/87), 39.1% (n = 34/87) and 29.6% (n = 24/81) of patients showed disease control at three, six and 12 months, respectively. **Table 1** provides a detailed overview of the study population.

To gain first insight into the regulation of circulating suPAR in patients with advanced stage cancer, we first compared serum suPAR levels in solid tumor patients and healthy controls without signs of malignant disease. Here, we observed 3.5-fold higher suPAR serum levels in cancer patients (median: 5.36 ng/ml) compared to healthy controls (median: 1.55, **Figure 1A**). While baseline suPAR levels were comparable between patients with different tumor stage (UICC stage III vs. IV, **Figure 1B**), we observed significantly lower levels in patients with malignant melanoma (MM) compared to most other tumor entities (**Figure 1C**). There was no significant difference in baseline suPAR levels regarding the scheduled ICI regimen (**Figure 1D**) as well as between patients who did or did not receive systemic cancer therapy previously (**Figure 1E**). We did also not observe a significant regulation of circulating suPAR with respect to different patient characteristics such the ECOG performance status, sex or the smoking status (**Figures 1F–H**). However, we observed a significant positive correlation between circulating suPAR levels and the neutrophil-to-lymphocyte ratio (NRL, r_S: 0.306, p = 0.005), which was shown to be a predictor of treatment response to ICI therapy (19).

Baseline suPAR Serum Levels Predict Treatment Response to Immune Checkpoint Inhibitors

Given its important role in the context of immune activation, we next hypothesized that suPAR serum levels before the first administration of ICI could have a predictive role regarding tumor response to immunotherapy. We therefore compared baseline suPAR levels between patients who showed "disease

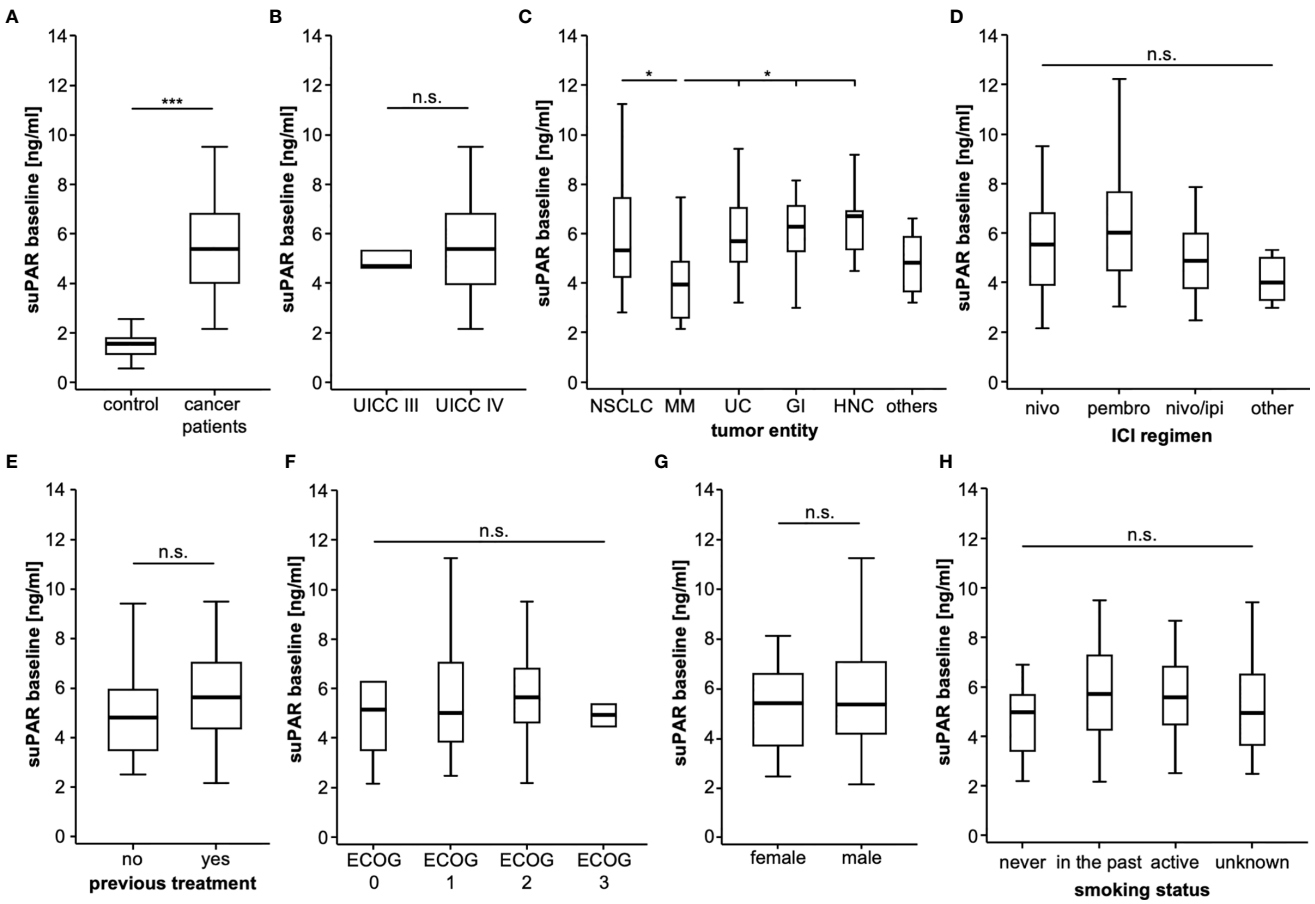

FIGURE 1 | SuPAR serum levels are significantly increased in cancer patients. **(A)** SuPAR serum levels are significantly elevated in cancer patients compared to healthy controls. While baseline suPAR levels are comparable between patients with different tumor stage **(B)**, patients with malignant melanoma have significantly lower suPAR levels compared to most other tumor entities **(C)**. There is no significant difference in baseline suPAR levels regarding the scheduled ICI regimen **(D)** as well as between patients who did or did not receive previous systemic cancer therapy **(E)**. There is no regulation of circulating suPAR with respect to the ECOG performance status **(F)**, gender **(G)** or the smoking status **(H)** n.s. non significant, *p < 0.05, ***p < 0.001.

control" (DC, n = 41, see *Methods* for detail) and patient with progressive disease (non-DC, n = 46) in the first staging scan at approximately three months after ICI therapy initialization. Strikingly, non-DC patients (median suPAR: 5.78 ng/ml) had significantly higher baseline suPAR concentrations compared to DC patients (median: 4.68 ng/ml, **Figure 2A**). ROC curve analysis revealed an AUC value of 0.645 for suPAR regarding the discrimination between DC and non-DC patients (**Figure 2B**). At the ideal predictive cut-off value of 4.804 ng/ml, suPAR showed a sensitivity and specificity of 78.3 and 56.1%. The discriminatory value of circulating suPAR was further confirmed by uni- and multivariate binary logistic regression analysis including several clinicopathological parameters (age, sex, UICC tumor stage and ECOG performance status) as well as standard laboratory markers of organ dysfunction (e.g., leucocyte count, bilirubin, creatinine, electrolytes, **Table 2**). Importantly, multivariate analysis revealed a pre-ICI suPAR concentration above 4.804 ng/ml as an independent predictor of non-DC at three months (OR: 0.215 [95% CI: 0.081–0.573], p = 0.002, **Table 2**). **Supplementary Table 1** provides a descriptive overview of baseline suPAR levels between DC/non-DC patients stratified by tumor entity and ICI regimen.

In a next step, we evaluated if initial suPAR levels might also be predictive for a prolonged response to ICI and compared suPAR levels in patients with DC at six or 12 months and patients who had progressed or died during this period of time (non-DC). Again, we observed significantly lower initial suPAR levels in patients with DC at six months and a non-significant trend (p = 0.069) towards lower suPAR levels in patients with DC at 12 months compared to non-DC patients at the respective time points (**Figures 2C, D**), indicating that baseline suPAR levels also predict a more durable ICI treatment response.

Baseline suPAR Levels Predict Overall Survival in Patients Receiving Immune Checkpoint Inhibitor Therapy

We next hypothesized that baseline suPAR levels might also be indicative for the patients' overall outcome. We therefore

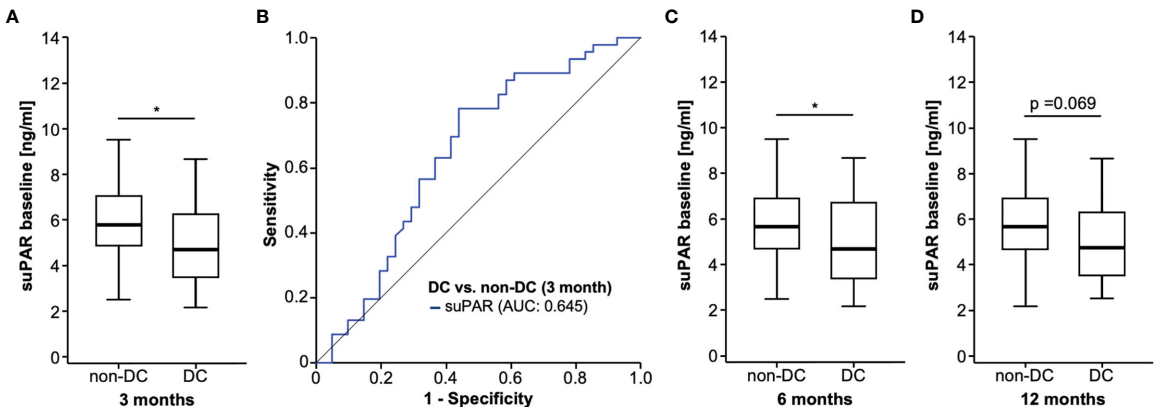

FIGURE 2 | Initial suPAR serum levels predict treatment response to ICI. **(A)** Patient who show disease control (DC) to ICI at 3 months have significantly lower baseline suPAR concentrations compared to non-DC patients. **(B)** ROC curve analysis reveals an AUC value of 0.645 for suPAR regarding the discrimination between DC and non-DC patients. Initial suPAR levels are significantly lower in patients with DC at 6 months **(C)** and show a strong trend (p = 0.069), **(D)** towards lower suPAR levels at 12 months compared to non-DC patients at the respective time points. *p<0.05.

TABLE 2 | Uni- and multivariate binary logistic regression analysis for the prediction of tumor response to checkpoint inhibitors.

Parameter	univariate binary logistic regression		multivariate binary logistic regression	
	p-value	Odds-Ratio (95% CI)	p-value	Odds-Ratio (95% CI)
suPAR pre-ICI >4.804 ng/ml	0.001	0.217 (0.085–0.553)	0.002	0.215 (0.081–0.573)
Age	0.515	0.987 (0.948–1.027)		
Sex	0.822	1.104 (0.466–2.617)		
UICC tumor stage	0.200	0.330 (0.061–1.800)	0.602	0.573 (0.070–4.663)
ECOG PS	0.490	0.793 (0.411–1.531)		
Leukocyte count	0.591	0.994 (0.971–1.017)		
Sodium	0.285	1.065 (0.949–1.196)		
Potassium	0.056	2.242 (0.979–5.133)	0.040	2.528 (1.043–6.125)
AST	0.321	0.992 (0.976–1.008)		
Bilirubin	0.251	0.483 (0.139–1.676)		
Creatinine	0.357	1.388 (0.691–2.788)		
LDH	0.285	1.002 (0.998–1.006)		

suPAR, soluble urokinase plasminogen activator receptor; AST, aspartate transaminase; ECOG PS, "Eastern Cooperative Oncology Group" performance status.

compared the overall survival (OS) of patients who presented with high or low circulating suPAR levels before initiation of ICI treatment. When using the median suPAR concentration (5.36 ng/ml) as a cut-off, patients with initial suPAR levels above this cut-off showed a significantly reduced OS compared to patients with low baseline suPAR levels (**Figure 3A**). The median OS was 202 days (standard error (SE): 107.4) and 658 days (293.5), respectively. We subsequently established an optimal prognostic cut-off value (see *Methods* for details). Using this optimal cut-off value of 4.86 ng/ml, initial suPAR serum levels were highly predictive for the patients' OS. As such, patients with a baseline suPAR concentration >4.86 ng/ml had a median OS of just 160 days (SE: 36.8) compared to 705 days (SE: 88.4) for patients with initial suPAR concentrations below the ideal cut-off (**Figure 3B**). Patient characteristics of the suPAR high/low group are displayed in **Table 3**. We next performed uni- and multivariate Cox-regression analyses to identify potential confounders on patients' outcome. In univariate analysis, baseline suPAR concentrations above the ideal cut-off value were highly predictive for OS (HR: 2.735 [95%CI: 1.501–4.985], p = 0.001, **Table 4**). Testing a broad variety of clinicopathological parameters and laboratory markers of organ dysfunction, we identified the ECOG PS, BMI, leucocyte count as well as sodium and AST levels as parameters of potential prognostic relevance for our cohort (p <0.250 in univariate analysis, **Table 4**). Importantly, in multivariate Cox-regression analysis including

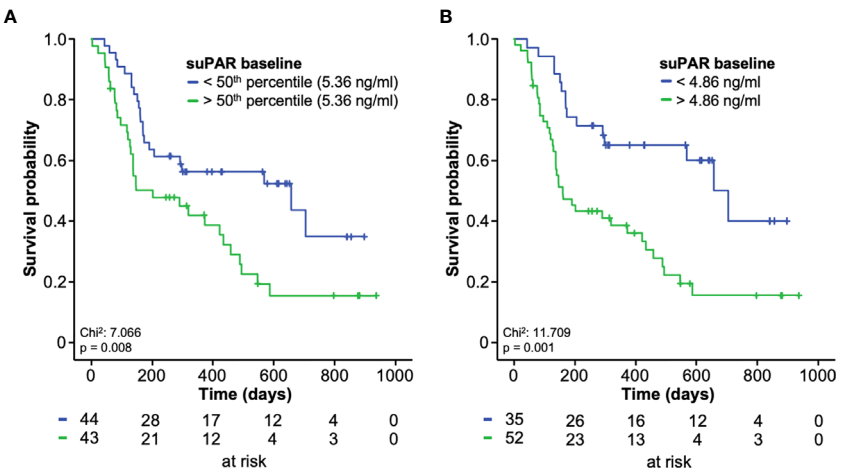

FIGURE 3 | Baseline suPAR levels predict overall survival in patients receiving ICI. **(A)** Using the median suPAR concentration (5.36 ng/ml) as a cut-off, patients with initial suPAR levels above this cut-off show a significantly reduced OS compared to patients with low baseline suPAR levels. **(B)** When applying the optimal cut-off value (4.86 ng/ml), patients with a baseline suPAR concentration >4.86 ng/ml have a median OS of just 160 days compared to 705 days for patients with initial suPAR concentrations below the ideal cut-off.

TABLE 3 | Comparison of clinical and pathological factors among patients with baseline suPAR levels below/above the ideal prognostic cut-off value.

	baseline suPAR level <4.86 ng/ml	baseline suPAR level >4.86 ng/ml
Total number of patients [n]:	35	52
Gender [n, (%)]:		
female/male	13/22 (37.1/62.9)	15/37 (28.8/71.2)
Age [years, median and range]	67 (45–87)	67 (38–87)
BMI [kg/m^2, median and range]	25.7 (17–41.4)	22.4 (15.9–42.3)
Staging [n, (%)]:		
UICC III/UICC IV	3/32 (8.6/91.4)	2/47 (4.1/95.9)
Previous systemic therapy before ICI? [n, (%)]:		
Yes/No	15/20 (42.9/57.1)	11/41 (21.2/78.8)
ECOG PS [n, (%)]:		
ECOG 0	3 (8.8)	3 (6)
ECOG 1	19 (55.9)	26 (52)
ECOG 2	12 (35.3)	21 (42)
Smoking status [n, (%)]:		
Never	3 (8.6)	4 (7.7)
Previous	13 (37.1)	22 (42.3)
Present	6 (17.1)	11 (21.2)
unknown	13 (37.2)	15 (28.8)

BMI, body mass index; ECOG PS, "Eastern Cooperative Oncology Group" performance status; ICI, immune checkpoint inhibitor; suPAR, soluble urokinase plasminogen activator receptor; UICC, Union for International Cancer Control.

these parameters, baseline suPAR levels above the ideal cut-off value turned out as an independent prognostic factor for OS (HR: 2.402 [95%CI: 1.250–4.616], p = 0.009, **Table 4**).

Prognostic Relevance of Circulating suPAR During ICI Treatment

We subsequently investigated a potential role of longitudinally assessed serum concentrations during ICI treatment at an early (after one or two cycles of immunotherapy) and a late (after three, four, or five cycles of immunotherapy) time point. Serum suPAR levels were available for a total of n = 76 and n = 57 patients at the early and late time point, respectively, and were not significantly altered compared to initial concentrations (p_{early}: 0.100 and p_{late}: 0.069, **Figure 4A**). In addition, suPAR serum levels at both time points did not significantly differ between patients with different tumor stage, tumor entity, ECOG PS, ICI regimen as well as male and female patients and patient with different smoking status (**Supplementary Figures 1**, **2**).

When comparing suPAR serum levels at the early and late time point during ICI treatment between patients with disease control (DC) and non-DC patients at three, six and 12 months, we observed significantly higher suPAR levels in non-DC patients at three and six months as well as a trend towards higher suPAR levels in non-DC patients at 12 months (**Supplementary Figures 3A–F**).

To analyze whether circulating suPAR levels also maintain their prognostic potential during the course of ICI therapy, we again established ideal prognostic cut-off values for the early and late time point. Similar to our previous results, patients with suPAR serum levels above the respective optimal cut-off value (early time point: 4.32 ng/ml, late time point: 7.58 ng/ml) showed a significantly impaired OS compared to patients with lower suPAR levels during the course of ICI treatment (**Figures 4B, C**). In line, univariate Cox-regression analyses confirmed the prognostic relevance of circulating suPAR above the ideal cut-off values for both the early and the late time point (HR_{early}: 3.059 [95%CI: 1.486-6.297], p=0.002; HR_{late}: 3.288 [95%CI: 1.578-6.852, p=0.001). Finally, we evaluated whether the longitudinal kinetic of circulating suPAR levels during ICI treatment might be indicative for the patients' outcome. We therefore compared the OS of patients who showed increasing suPAR levels between

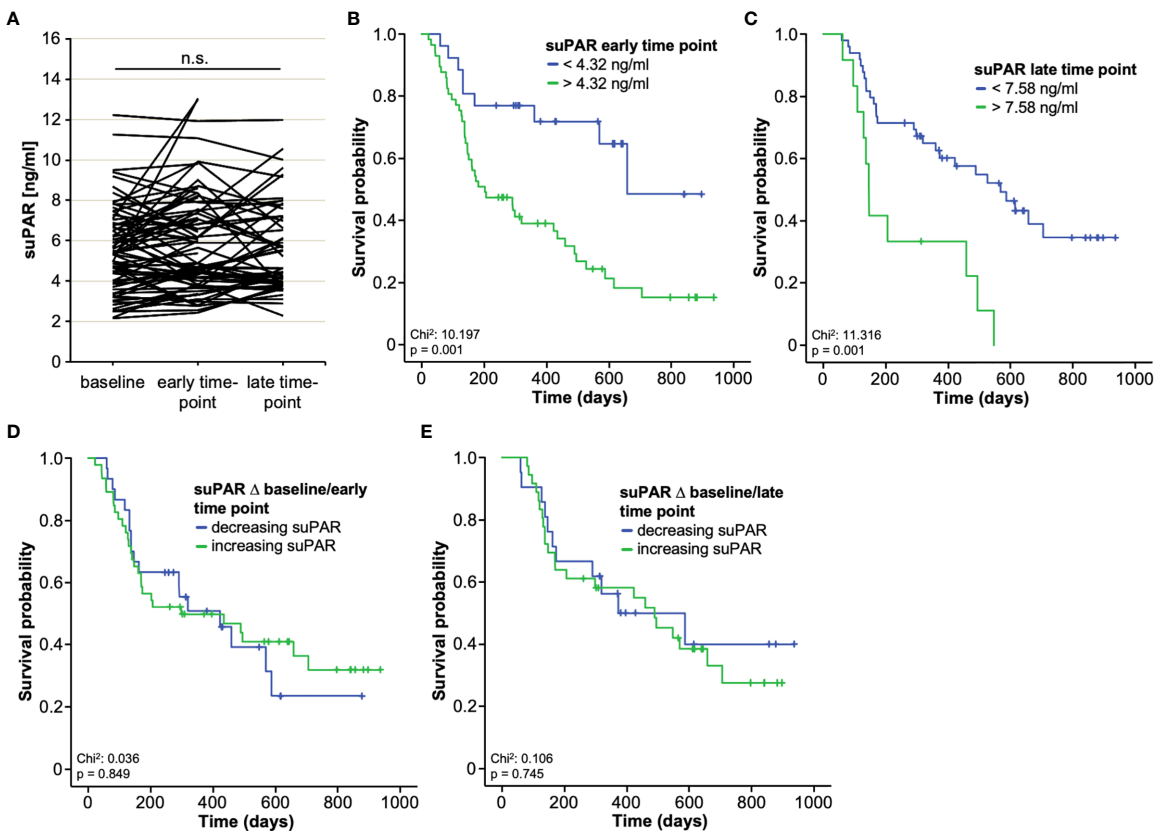

FIGURE 4 | Prognostic relevance of circulating suPAR during ICI treatment. **(A)** Serum suPAR levels at the early and late time point during ICI treatment are unaltered compared to initial concentrations. **(B, C)** Patients with suPAR serum levels above the respective optimal cut-off value (early time point: 4.32 ng/ml, late time point: 7.58 ng/ml) show a significantly impaired OS compared to patients with lower suPAR levels during the course of ICI treatment. **(D, E)** There is no survival benefit in patients who show increasing or decreasing suPAR concentrations at the early or late time point compared to baseline levels. n.s., non significant.

baseline and the early time point (n=30) to those patients with decreasing suPAR concentrations (n=46). However, we did not observe a significant difference of OS between the two groups (**Figure 4D**). There was also no survival benefit in patients who showed increasing (n=21) or decreasing (n=36) suPAR concentrations at the late time point compared to baseline levels (**Figure 4E**). In line, univariate Cox-regression analysis revealed no prognostic relevance of the individual suPAR kinetic at the early or late time point ($HR_{baseline/early}$: 0.943, 95%CI: 0.518-1.718, p= 0.849; $HR_{baseline/late}$: 1.127, 95%CI: 0.547-2.32, p= 0.745). A comparative analysis of overall survival between patients with increasing or decreasing suPAR levels stratified by their baseline suPAR value (above/below the ideal prognostic cut-off value) confirmed this finding and revealed that baseline suPAR levels rather than the individual kinetic during the course of treatment were of prognostic relevance (**Supplementary Figures 4A**, **B**). However, patients with low baseline suPAR levels and further decreasing suPAR levels between baseline and the late time point showed a slightly superior outcome compared to patients with low baseline suPAR levels but increasing levels (**Supplementary Figure 4B**).

Baseline suPAR Levels Correlate With Side Effects of ICI Therapy

Finally, we aimed at evaluating a potential association between baseline suPAR serum levels and potential side effects to ICI during the treatment course. Here, we observed significantly lower suPAR serum levels in patients who experienced immune related adverse events (IRAE) during the course of therapy compared to patients who did not (**Figure 5A**). Interestingly, patients with IRAE showed a significantly higher rate of disease control (DC) at three months (78.4% vs. 24.0%, p <0.001), six months (64.9% vs. 20.0%, p <0.001) and 12 months (52.9 vs. 12.8%, p <0.001), respectively. Moreover, OS was significantly higher in the subgroup of patients with IRAE to ICI (**Figure 5B**).

TABLE 4 | Uni- and multivariate Cox-regression analysis for the prediction of overall survival.

Parameter	univariate Cox-regression		multivariate Cox-regression	
	p-value	Hazard-Ratio (95% CI)	p-value	Hazard-Ratio (95% CI)
suPAR pre-ICI >4.86 ng/ml	0.001	2.735 (1.501–4.985)	0.009	2.402 (1.250-4.616)
Age	0.927	1.001 (0.975–1.028)		
Sex	0.486	0.820 (0.468–1.435)		
BMI	0.011	0.932 (0.882–0.984)	0.102	0.953 (0.899–1.010)
UICC tumor stage	0.267	3.078 (0.423–22.386)		
ECOG PS	0.020	1.644 (1.083–2.495)	0.055	1.542 (0.991–2.401)
Leukocyte count	0.009	1.004 (1.001–1.008)	0.193	1.003 (0.998–1.008)
Sodium	0.133	0.952 (0.893–1.015)	0.872	1.006 (0.933–1.085)
Potassium	0.782	0.932 (0.564–1.539)		
AST	0.245	1.005 (0.996–1.015)	0.929	0.999 (0.988–1.012)
Bilirubin	0.864	1.074 (0.477–2.416)		
Creatinine	0.492	0.864 (0.569–1.311)		
LDH	0.644	0.999 (0.997–1.002)		

suPAR, soluble urokinase plasminogen activator receptor; AST, aspartate transaminase; BMI, body mass index; ECOG PS, "Eastern Cooperative Oncology Group" performance status; LDH, lactase dehydrogenase.

DISCUSSION

Immune checkpoint inhibitors (ICI) have changed treatment paradigms for several tumor entities including NSCLC and malignant melanoma, often resulting in durable tumor responses with manageable site effects (4, 5). However, there is a subgroup of patients who do not or at least to a lesser extend benefit from ICI (20). The identification of these patients has remained challenging and up to now only very few reliable predictive markers could be established. To the best of our knowledge, we show for the first time that elevated levels of circulating suPAR predict both a poor tumor response and an

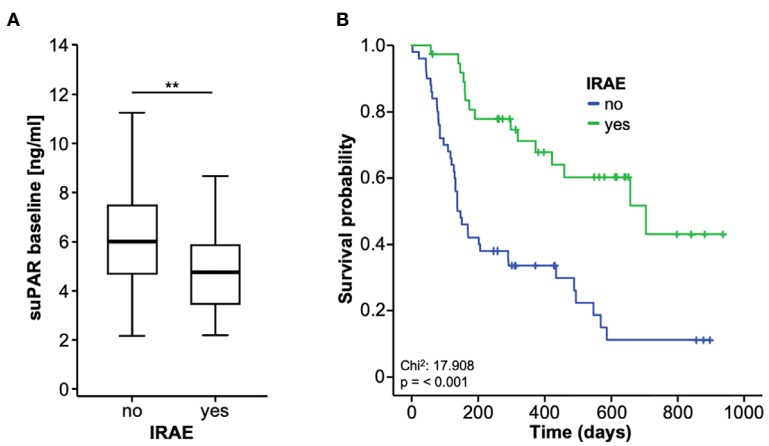

FIGURE 5 | Baseline suPAR levels correlate with side effects of ICI therapy. **(A)** Patients who experience immune-related adverse events (IRAE) to ICI therapy have significantly lower baseline suPAR serum levels compared to patients without IRAE. **(B)** Overall survival is significantly higher in the subgroup of patients experiencing IRAE. **p < 0.01.

impaired outcome in patients receiving ICI therapy for advanced stage solid malignancies. As such, patients with suPAR serum levels below the ideal predictive cut-off value (4.80 ng/ml) had a significantly higher probability of disease control under ICI therapy at three and six months, respectively. Moreover, baseline serum levels above the ideal prognostic cut-off value (4.86 ng/ml) were an independent prognostic factor for an impaired overall survival (OS). Patients with baseline suPAR levels above this cut-off value showed a median OS of only 160 days compared to 705 days for patients with initial suPAR concentrations below this cut-off. Finally, low baseline suPAR levels identified a subgroup of patients that experienced immune-related adverse event (IRAE) during the course of treatment, which in term was associated with a better treatment response an OS.

Although ICI are approved for an increasing number of malignancies including malignant melanoma, NSCLC and urothelial cancer (4, 5], the identification of individual patients who do not benefit from ICI therapy has remained a major challenge. Importantly, most of the existing stratification tools are tissue-based and therefore require an invasive tumor biopsy. As an example, microsatellite instability-high (MSI-H), or mismatch repair deficient (dMMR) solid tumors show a higher objective response rate to ICI, which lead to the FDA approval of pembrolizumab (anti-PD-1) as the first cancer treatment for any solid tumor with a specific genetic feature (21). Moreover, tissue expression levels of PD-L1 both in tumor and immune cells have been suggested as a predictive and/or prognostic marker in patients receiving ICI (22). In NSCLC, some ICI treatment regimens are only approved in patients with a PD-L1 tumor expression level above 50% (5). On the contrary, the potential role of PD-L1 tumor expression as a predictive marker is more controversial in other malignancies such as malignant melanoma (23). Most importantly, cut-off values for positivity (e.g. >1%, >10%, >50%), the precise cellular origin of PD-L1 expression (tumor cells, immune cells or the combination of both (combined positivity score, CPS)) and technical issues strongly vary between studies, limiting a wide-ranging clinical implementation of potential (24). In terms of circulating biomarkers, which are particularly interesting due their easy accessibility, only very few parameters have been suggested to date. In NSCLC and malignant melanoma patients receiving ICI, serum lactate dehydrogenase (LDH) levels were associated with worse survival (25, 26). A high neutrophil/lymphocyte ratio (NLR) correlated with an impaired outcome in NSCLC treated with ICI (26). In addition, serum CRP levels, a routine marker of inflammation, have been suggested to reflect treatment benefit during anti PD-(L)1 treatment in advanced NSCLC (27).

Our study provided evidence that elevated suPAR levels both before treatment initiation and during the course of treatment predict poor response and outcome to ICI. Although suPAR has been described as a prognostic marker for different treatment modalities (e.g., tumor resection, chemotherapy) of various cancer entities (10, 14, 28), this is the first study to evaluate its relevance in the context of ICI therapy. Nevertheless, the underlying molecular mechanism linking elevated suPAR levels with a poor response and outcome to ICI remains unknown. Circulating suPAR originates from shedding of the membrane bound plasminogen activator receptor (uPAR) that is expressed on immune and epithelial cells (29). During systemic inflammation, an increased shedding of uPAR on circulating immune cells, and neutrophils in particular, has been reported as a source of elevated suPAR levels (16). In proteinuric kidney disease, bone marrow-derived immature myeloid cells were identified as a main source of circulating suPAR (30). However, no data on a functional role of uPAR/suPAR in the context of ICI therapy exist to date. As a possible explanation, elevation of suPAR in the subgroup of patients with a poor response and outcome to ICI might reflect a chronically activated immune system, which in turn negatively influences the anti-tumoral effects of ICI. This hypothesis is corroborated by recent data suggesting markers of systemic inflammation such as the neutrophil-to-lymphocyte ratio (NLR) as negative predictive and/or prognostic markers for ICI therapy (31, 32). In line, it was shown that neutrophils dominate the NSCLC immune landscape being responsible for treatment failure under ICI therapy and a pro-inflammatory status was suggested to induce an "emergency granulopoiesis" leading to immature or poorly differentiated cells, which have been associated with tumor progression (26, 33). Importantly, we could show that circulating suPAR levels positively correlated with the NLR in our cohort of patients. Moreover, as it was recently shown that uPAR and suPAR can down-regulate the tumor suppressor phosphatase and tension homologue (PTEN) (34), novel data suggesting that a loss of PTEN promotes resistance to T-cell-mediated immunotherapy are of particular relevance (35, 36). However, further molecular studies are warranted to fully dissect a potential functional role of suPAR in the context of ICI therapy.

Interestingly, we observed significantly lower baseline suPAR serum levels in patients who experienced IRAE during the course of treatment compared to patients who did not. These patients had a significantly higher disease control rate and at three, six, and 12 months as well as an improved OS. There is a growing body of evidence showing that IRAE, which are believed to represent a bystander effect from activated T-cells, predict treatment response to ICI (37, 38). In this line of thinking, baseline suPAR levels could not only be useful to predict treatment response to ICI but also to identify a subgroup of patients that are more likely to experience IRAE, which in turn could trigger specific diagnostic and/or therapeutic measures to provide these patients with an optimal medical care during ICI treatment. With respect to a potential clinical implementation of circulating suPAR for the identification of the ideal candidates for ICI therapy, we suggest that suPAR should be implemented into existing or future stratification algorithms rather than being used as single biomarker. Particularly, as various more aggressive combinations of ICI as well as their combination with conventional therapies such as chemotherapy or loco-regional therapies are currently under clinical investigation (NCT04062708, NCT03572582), measurements of baseline suPAR levels might help to identify cancer patients who might

not sufficiently benefit from ICI therapy alone but could be suitable candidates for a combination of therapies.

Our results are limited by some aspects. First, the study was conducted in a basket design, meaning that we included patients with different solid tumor entities and different ICI regimens. While this approach argues for a potentially both entity- and ICI-regimen-independent role of circulating suPAR, further confirmatory studies including larger patient cohorts of a certain tumor entity (e.g., NSCLC or MM) are warranted to further dissect the role of suPAR in the context of ICI among different tumor entities. Secondly, we only included patients receiving ICI but did not evaluated suPAR levels and the clinical course of patients receiving an alternative treatment such as conventional chemotherapy. Moreover, tumor samples were not available in our cohort and we were thus unable to investigate a potential association between suPAR serum levels and established tissue-based markers of ICI treatment response such as tumoral PD-L1 expression or the TMB (8, 19). In this line of thinking, a combination of suPAR with other predictive biomarkers including patient characteristics such obesity, which was associated with a better survival of cancer patients receiving ICI therapy, should be considered (39–41). Finally, we are unable to provide information on the specific molecular mechanism being responsible for a poor treatment response and outcome to ICI in the subgroup of patients with high suPAR levels. Thus, further clinical trials including larger patient cohorts as well as molecular studies in e.g. uPAR knock-out mice (42) are warranted to corroborate our findings and to further evaluate the specific function of uPAR/suPAR in the context of ICI, which we hope to have encourage with our exploratory study.

In summary, our data suggest a previously unrecognized predictive and prognostic role of circulating suPAR in the context of ICI therapy. If these findings were confirmed in larger clinical trials, suPAR might represent a valuable stratification tool and complement existing algorithms to identify the ideal candidates for ICI in future.

DATA AVAILABILITY STATEMENT

The raw data supporting the conclusions of this article will be made available by the authors, without undue reservation.

ETHICS STATEMENT

The studies involving human participants were reviewed and approved by Ethics committee of the University Hospital RWTH Aachen, Germany (EK 206/09). The patients/participants provided their written informed consent to participate in this study.

AUTHOR CONTRIBUTIONS

TL and SL designed the study. JG and SL recruited patients. SL and JG performed experiments. SL, JK, and JG performed statistical analysis and generated figures and tables. MJ, MS-H, FB, MV, AS, CK, AM, VK, TB, and CR provided intellectual input. SL, JG, and TL drafted the manuscript. All authors contributed to the article and approved the submitted version.

FUNDING

Work in the lab of TL was funded from the European Research Council (ERC) under the European Union's Horizon 2020 research and innovation program through the ERC Consolidator Grant PhaseControl (Grant Agreement n° 771083). The lab of TL was further supported by the German Cancer Aid (Deutsche Krebshilfe 110043 and a Mildred-Scheel-Professorship), the German-Research-Foundation (SFB-TRR57/P06, LU 1360/3-1, CRC1380/A01, and CA 830/3-1), the Ernst-Jung-Foundation Hamburg, the IZKF (interdisciplinary centre of clinical research) Aachen, and a grant from the medical faculty of the RWTH Aachen. The suPAR ELISA kits were provided by Virogates (Denmark).

SUPPLEMENTARY MATERIAL

The Supplementary Material for this article can be found online at: https://www.frontiersin.org/articles/10.3389/fonc.2021.646883/full#supplementary-material

Supplementary Figure 1 | SuPAR serum levels at the early time point do not significantly differ between patients with different tumor stage **(A)** tumor entity **(B)** ECOG PS **(C)** ICI regimen **(D)** as well as male and female patients **(E)** and patient with different smoking status **(F)**.

Supplementary Figure 2 | SuPAR serum levels at the late time point do not significantly differ between patients with different tumor stage **(A)**, tumor entity **(B)**, ECOG PS **(C)**, ICI regimen **(D)** as well as male and female patients **(E)** and patient with different smoking status **(F)**.

Supplementary Figure 3 | (A, B) Patients with disease control (DC) at three months have significantly lower suPAR serum levels at the early and late time point during ICI treatment compared to non-DC patients. **(C, D)** Patients with disease control (DC) at six months have significantly lower suPAR serum levels at the early and late time point during ICI treatment compared to non-DC patients. **(E, F)** Patients with disease control (DC) at 12 months show a trend towards lower suPAR serum levels at the early and late time point during ICI treatment compared to non-DC patients.

Supplementary Figure 4 | (A) Kaplan-Meier curve analysis evaluating the overall survival of patients with high/low baseline suPAR levels (ideal prognostic cut-off value) and increasing or decreasing suPAR values between treatment initialization and the early time point. **(B)** Kaplan-Meier curve analysis evaluating the overall survival of patients with high/low baseline suPAR levels (ideal prognostic cut-off value) and increasing or decreasing suPAR values between treatment initialization and the late time point.

REFERENCES

1. Bray F, Ferlay J, Soerjomataram I, Siegel RL, Torre LA, Jemal A. Global cancer statistics 2018: GLOBOCAN estimates of incidence and mortality worldwide for 36 cancers in 185 countries. *CA Cancer J Clin* (2018) 68:394–424. doi: 10.3322/caac.21492
2. Couzin-Frankel J. Cancer immunotherapy. *Sci (80-)* (2013) 342:1432–3. doi: 10.1126/science.342.6165.1432

3. Herbst RS, Baas P, Kim D-W, Felip E, Pérez-Gracia JL, Han J-Y, et al. Pembrolizumab versus docetaxel for previously treated, PD-L1-positive, advanced non-small-cell lung cancer (KEYNOTE-010): a randomised controlled trial. *Lancet* (2016) 387:1540–50. doi: 10.1016/S0140-6736(15)01281-7
4. Larkin J, Chiarion-Sileni V, Gonzalez R, Grob JJ, Cowey CL, Lao CD, et al. Combined Nivolumab and Ipilimumab or Monotherapy in Untreated Melanoma. *N Engl J Med* (2015) 373:23–34. doi: 10.1056/NEJMc1509660
5. Bellmunt J, de Wit R, Vaughn DJ, Fradet Y, Lee J-L, Fong L, et al. Pembrolizumab as Second-Line Therapy for Advanced Urothelial Carcinoma. *N Engl J Med* (2017) 376:1015–26. doi: 10.1056/NEJMoa1613683
6. Le DT, Uram JN, Wang H, Bartlett BR, Kemberling H, Eyring AD, et al. PD-1 Blockade in Tumors with Mismatch-Repair Deficiency. *N Engl J Med* (2015) 372:2509–20. doi: 10.1056/NEJMoa1500596
7. Shi Y, Lei Y, Liu L, Zhang S, Wang W, Zhao J, et al. Integration of comprehensive genomic profiling, tumor mutational burden, and PD-L1 expression to identify novel biomarkers of immunotherapy in non-small cell lung cancer. *Cancer Med cam4* (2021) 10(7):2216–31. doi: 10.1002/cam4.3649
8. Patel SP, Kurzrock R. PD-L1 Expression as a Predictive Biomarker in Cancer Immunotherapy. *Mol Cancer Ther* (2015) 14:847–56. doi: 10.1158/1535-7163.MCT-14-0983
9. Thunø M, Macho B, Eugen-Olsen J. suPAR: the molecular crystal ball. *Dis Markers* (2009) 27:157–72. doi: 10.1155/2009/504294
10. Loosen SH, Breuer A, Tacke F, Kather JN, Gorgulho J, Alizai PH, et al. Circulating levels of soluble urokinase plasminogen activator receptor predict outcome after resection of biliary tract cancer. *JHEP Rep* (2020) 2:100080. doi: 10.1016/j.jhepr.2020.100080
11. Koch A, Voigt S, Kruschinski C, Sanson E, Dückers H, Horn A, et al. Circulating soluble urokinase plasminogen activator receptor is stably elevated during the first week of treatment in the intensive care unit and predicts mortality in critically ill patients. *Crit Care* (2011) 15:R63. doi: 10.1186/cc10037
12. Cobos E, Jumper C, Lox C. Pretreatment determination of the serum urokinase plasminogen activator and its soluble receptor in advanced small-cell lung cancer or non-small-cell lung cancer. *Clin Appl Thromb* (2003) 9:241–6. doi: 10.1177/107602960300900309
13. Fidan E, Mentese A, Ozdemir F, Deger O, Kavgaci H, Caner Karahan S, et al. Diagnostic and prognostic significance of CA IX and suPAR in gastric cancer. *Med Oncol* (2013) 30:540. doi: 10.1007/s12032-013-0540-9
14. Loosen SH, Tacke F, Püthe N, Binneboesel M, Wiltberger G, Alizai PH, et al. High baseline soluble urokinase plasminogen activator receptor (suPAR) serum levels indicate adverse outcome after resection of pancreatic adenocarcinoma. *Carcinogenesis.* (2019) 40(8):947–55. doi: 10.1093/carcin/bgz033
15. Chounta A, Ellinas C, Tzanetakou V, Pliarhopoulou F, Mplani V, Oikonomou A, et al. Serum soluble urokinase plasminogen activator receptor as a screening test for the early diagnosis of hepatocellular carcinoma. *Liver Int* (2015) 35:601–7. doi: 10.1111/liv.12705
16. Gussen H, Hohlstein P, Bartneck M, Warzecha KT, Buendgens L, Luedde T, et al. Neutrophils are a main source of circulating suPAR predicting outcome in critical illness. *J Intensive Care* (2019) 7:26. doi: 10.1186/s40560-019-0397-x
17. Oken MM, Creech RH, Tormey DC, Horton J, Davis TE, McFadden ET, et al. Toxicity and response criteria of the Eastern Cooperative Oncology Group. *Am J Clin Oncol* (1982) 5:649–55. doi: 10.1097/00000421-198212000-00014
18. Eisenhauer EA, Therasse P, Bogaerts J, Schwartz LH, Sargent D, Ford R, et al. New response evaluation criteria in solid tumours: Revised RECIST guideline (version 1.1). *Eur J Cancer* (2009) 45:228–47. doi: 10.1016/j.ejca.2008.10.026
19. Valero C, Lee M, Hoen D, Weiss K, Kelly DW, Adusumilli PS, et al. Pretreatment neutrophil-to-lymphocyte ratio and mutational burden as biomarkers of tumor response to immune checkpoint inhibitors. *Nat Commun* (2021) 12(1):729. doi: 10.1038/s41467-021-20935-9
20. Emens LA, Ascierto PA, Darcy PK, Demaria S, Eggermont AMM, Redmond WL, et al. Cancer immunotherapy: Opportunities and challenges in the rapidly evolving clinical landscape. *Eur J Cancer* (2017) 81:116–29. doi: 10.1016/j.ejca.2017.01.035
21. Marcus L, Lemery SJ, Keegan P, Pazdur R. FDA Approval Summary: Pembrolizumab for the Treatment of Microsatellite Instability-High Solid Tumors. *Clin Cancer Res* (2019) 25:3753–8. doi: 10.1158/1078-0432.CCR-18-4070
22. Meyers DE, Banerji S. Biomarkers of immune checkpoint inhibitor efficacy in cancer. *Curr Oncol* (2020) 27:S106–14. doi: 10.3747/co.27.5549
23. Wolchok JD, Chiarion-Sileni V, Gonzalez R, Rutkowski P, Grob J-J, Cowey CL, et al. Overall Survival with Combined Nivolumab and Ipilimumab in Advanced Melanoma. *N Engl J Med* (2017) 377:1345–56. doi: 10.1056/NEJMoa1709684
24. Duan Z, Gao J, Zhang L, Liang H, Huang X, Xu Q, et al. Phenotype and function of CXCR5+CD45RA−CD4+ T cells were altered in HBV-related hepatocellular carcinoma and elevated serum CXCL13 predicted better prognosis. *Oncotarget* (2015) 6:44239–53. doi: 10.18632/oncotarget.6235
25. Buder-Bakhaya K, Hassel JC. Biomarkers for clinical benefit of immune checkpoint inhibitor treatment-A review from the melanoma perspective and beyond. *Front Immunol* (2018) 9:1474. doi: 10.3389/fimmu.2018.01474
26. Mezquita L, Auclin E, Ferrara R, Charrier M, Remon J, Planchard D, et al. Association of the lung immune prognostic index with immune checkpoint inhibitor outcomes in patients with advanced non-small cell lung cancer. *JAMA Oncol* (2018) 4:351–7. doi: 10.1001/jamaoncol.2017.4771
27. Riedl JM, Barth DA, Brueckl WM, Zeitler G, Foris V, Mollnar S, et al. C-reactive protein (Crp) levels in immune checkpoint inhibitor response and progression in advanced non-small cell lung cancer: A bi-center study. *Cancers (Basel)* (2020) 12:1–21. doi: 10.3390/cancers12082319
28. Loosen SH, Tacke F, Binnebosel M, Leyh C, Vucur M, Heitkamp F, et al. Serum levels of soluble urokinase plasminogen activator receptor (suPAR) predict outcome after resection of colorectal liver metastases. *Oncotarget* (2018) 9:27027–38. doi: 10.18632/oncotarget.25471
29. Koch A, Zimmermann HW, Gassler N, Jochum C, Weiskirchen R, Bruensing J, et al. Clinical relevance and cellular source of elevated soluble urokinase plasminogen activator receptor (suPAR) in acute liver failure. *Liver Int* (2014) 34:1330–9. doi: 10.1111/liv.12512
30. Hahm E, Wei C, Fernandez I, Li J, Tardi NJ, Tracy M, et al. Bone marrow-derived immature myeloid cells are a main source of circulating suPAR contributing to proteinuric kidney disease. *Nat Med* (2017) 23:100–6. doi: 10.1038/nm.4242
31. Bagley SJ, Kothari S, Aggarwal C, Bauml JM, Alley EW, Evans TL, et al. Pretreatment neutrophil-to-lymphocyte ratio as a marker of outcomes in nivolumab-treated patients with advanced non-small-cell lung cancer. *Lung Cancer* (2017) 106:1–7. doi: 10.1016/j.lungcan.2017.01.013
32. Diem S, Kasenda B, Spain L, Martin-Liberal J, Marconcini R, Gore M, et al. Serum lactate dehydrogenase as an early marker for outcome in patients treated with anti-PD-1 therapy in metastatic melanoma. *Br J Cancer* (2016) 114:256–61. doi: 10.1038/bjc.2015.467
33. Kargl J, Busch SE, Yang GHY, Kim K-H, Hanke ML, Metz HE, et al. Neutrophils dominate the immune cell composition in non-small cell lung cancer. *Nat Commun* (2017) 8:14381. doi: 10.1038/ncomms14381
34. Unseld M, Chilla A, Pausz C, Mawas R, Breuss J, Zielinski C, et al. PTEN expression in endothelial cells is down-regulated by uPAR to promote angiogenesis. *Thromb Haemost* (2015) 114:379–89. doi: 10.1160/TH15-01-0016
35. Trujillo JA, Luke JJ, Zha Y, Segal JP, Ritterhouse LL, Spranger S, et al. Secondary resistance to immunotherapy associated with β-catenin pathway activation or PTEN loss in metastatic melanoma. *J Immunother Cancer* (2019) 7:295. doi: 10.1186/s40425-019-0780-0
36. Peng W, Chen JQ, Liu C, Malu S, Creasy C, Tetzlaff MT, et al. Loss of PTEN Promotes Resistance to T Cell-Mediated Immunotherapy. *Cancer Discovery* (2016) 6:202–16. doi: 10.1158/2159-8290.CD-15-0283
37. Das S, Johnson DB. Immune-related adverse events and anti-tumor efficacy of immune checkpoint inhibitors. *J Immunother Cancer* (2019) 7:306. doi: 10.1186/s40425-019-0805-8
38. Xing P, Zhang F, Wang G, Xu Y, Li C, Wang S, et al. Incidence rates of immune-related adverse events and their correlation with response in advanced solid tumours treated with NIVO or NIVO+IPI: a systematic review and meta-analysis. *J Immunother Cancer* (2019) 7:341. doi: 10.1186/s40425-019-0779-6
39. Wang F, Zhou L, Chen N, Li X. The effect of pretreatment BMI on the prognosis and serum immune cells in advanced LSCC patients who received ICI therapy. *Med (Baltimore)* (2021) 100:e24664. doi: 10.1097/MD.0000000000024664

40. Esposito A, Marra A, Bagnardi V, Frassoni S, Morganti S, Viale G, et al. Body mass index, adiposity and tumour infiltrating lymphocytes as prognostic biomarkers in patients treated with immunotherapy: A multi-parametric analysis. *Eur J Cancer* (2021) 145:197–209. doi: 10.1016/j.ejca.2020.12.028
41. Donnelly D, Bajaj S, Yu J, Hsu M, Balar A, Pavlick A, et al. The complex relationship between body mass index and response to immune checkpoint inhibition in metastatic melanoma patients. *J Immunother Cancer* (2019) 116 (9):1593–603. doi: 10.1186/s40425-019-0699-5
42. Connolly BM, Choi EY, Gardsvoll H, Bey AL, Currie BM, Chavakis T, et al. Selective abrogation of the uPA-uPAR interaction in vivo reveals a novel role in suppression of fibrin-associated inflammation. *Blood* (2010) 116:1593–603. doi: 10.1182/blood-2010-03-276642

Conflict of Interest: The authors declare that the research was conducted in the absence of any commercial or financial relationships that could be construed as a potential conflict of interest.

frontiers in Oncology

ORIGINAL RESEARCH
published: 14 June 2021
doi: 10.3389/fonc.2021.684110

Inflammatory Markers and Procalcitonin Predict the Outcome of Metastatic Non-Small-Cell-Lung-Cancer Patients Receiving PD-1/PD-L1 Immune-Checkpoint Blockade

Valerio Nardone[1], Rocco Giannicola[2], Giovanna Bianco[2], Diana Giannarelli[3], Paolo Tini[4], Pierpaolo Pastina[4], Antonia Consuelo Falzea[2], Sebastiano Macheda[5], Michele Caraglia[6,7], Amalia Luce[6], Silvia Zappavigna[6], Luciano Mutti[8], Luigi Pirtoli[8], Antonio Giordano[8,9] and Pierpaolo Correale[2,8]*

[1] Unit of Radiation Oncology, Ospedale del Mare, Naples, Italy, [2] Medical Oncology Unit, Grand Metropolitan Hospital "Bianchi-Melacrino-Morelli", Reggio Calabria, Italy, [3] Biostatistical Unit, National Cancer Institute "Regina Elena", IRCCS, Rome, Italy, [4] Section of Radiation Oncology, Medical School, University of Siena, Siena, Italy, [5] Unit of Intensive Care Medicine and Anesthesia, Grande Ospedale Metropolitano Bianchi Melacrino Morelli, Reggio Calabria, Italy, [6] Department of Precision Medicine, University of Campania "L. Vanvitelli", Naples, Italy, [7] Laboratory of Precision and Molecular Oncology, Institute of Genetic Research, Biogem Scarl, Ariano Irpino, Italy, [8] Sbarro Institute for Cancer Research and Molecular Medicine and Center of Biotechnology, College of Science and Technology, Temple University, Philadelphia, PA, United States, [9] Department of Medical Biotechnology, University of Siena, Siena, Italy

OPEN ACCESS

Edited by:
Roberta Zappasodi,
Memorial Sloan Kettering Cancer Center, United States

Reviewed by:
Yina Hsing Huang,
Dartmouth College, United States
Chengzhi Zhou,
First Affiliated Hospital of Guangzhou Medical University, China

***Correspondence:**
Michele Caraglia
michele.caraglia@unicampania.it

Specialty section:
This article was submitted to Cancer Immunity and Immunotherapy, a section of the journal Frontiers in Oncology

Received: 22 March 2021
Accepted: 24 May 2021
Published: 14 June 2021

Citation:
Nardone V, Giannicola R, Bianco G, Giannarelli D, Tini P, Pastina P, Falzea AC, Macheda S, Caraglia M, Luce A, Zappavigna S, Mutti L, Pirtoli L, Giordano A and Correale P (2021) Inflammatory Markers and Procalcitonin Predict the Outcome of Metastatic Non-Small-Cell-Lung-Cancer Patients Receiving PD-1/PD-L1 Immune-Checkpoint Blockade. Front. Oncol. 11:684110. doi: 10.3389/fonc.2021.684110

Peripheral-immune-checkpoint blockade (P-ICB) with mAbs to PD-1 (nivolumab and pembrolizumab) or PD-L1 (atezolizumab, durvalumab, avelumab) alone or combination with chemotherapy represents a novel active treatment for mNSCLC patients. However, this therapy can be associated to immune-related adverse events (irAEs) and high cost. Therefore, finding reliable biomarkers of response and irAEs is strongly encouraged to accurately select patients who may potentially benefit from the immuno-oncological treatment. This is a retrospective multi-institutional analysis performed on ninety-five mNSCLC patients who received real-world salvage therapy with nivolumab or atezolizumab between December 2015 and April 2020. The outcome of these patients in term of PFS and OS was evaluated in comparison with different serum levels of C-reactive protein (CRP), Erythrocyte Sedimention Rate (ESR) and Procalcitonin (PCT) by performing Kaplan–Meier and Log-rank test and multivariate analysis. We found that high baseline levels of CRP, ESR, and PCT were strongly predictive of poor outcome ($P < 0.05$) with the worse prognosis detected in those patients with a baseline levels of both ESR and PCT over the pre-established cut off (median OS recorded in patients with no marker over the cut off *vs*. those with just one marker over the cut off *vs*. those with both markers over the cut off: 40 ± 59 *vs*. 15.5 ± 5.5 *vs*. 5.5 ± 1.6 months, respectively; $P < 0.0001$). Our results suggest the predictive value of systemic inflammation and suggest a potential role of PCT in predicting a poor outcome in mNSCLC receiving PD-1/PD-L1 blocking mAbs. This finding also suggests a potential role of subclinical bacterial infections in defining the

response to PD-1/PD-L1 blocking mAbs that deserves further and more specific investigations.

Keywords: bacterial infections, immune-check point blockade, programmed cell death ligand-1, real-world salvage therapy, cell death receptor, prognostic factors of response, procalcitonin, inflammatory markers

INTRODUCTION

Peripheral immune-check point blockade (P-ICB) with mAbs to the programmed cell death receptor-1 (PD-1) (nivolumab and pembrolizumab) and PD-Ligand (PD-L1) (atezolizumab, avelumab and durvalumab) alone or in combination with chemotherapy is a promising treatment option for metastatic non-small cell lung cancer (mNSCLC) (1, 2).

These innovative immune-oncological strategies are often very effective in the management of mNSCLC patients; however, they may be hampered by frequent more or less severe immuno-related adverse events (irAEs) and rising costs. Additionally, their fast-track evaluation in controlled trials has allowed their introduction in the clinical practice leaving a large amount of questions to be addressed (3, 4).

This treatment has substantial differences by other anticancer strategies like chemotherapy, radiotherapy and molecular target therapy that exert a direct cytotoxic/cytostatic effect on the tumor. On the other hand, PD-1-ICB does not act on the tumor cells but they rather rescue the antitumor activity of tumor infiltrating cytotoxic T cells (CTLs) mostly attenuated as consequence of PD-1 binding to PD-L1/2 in the tumor (1, 5, 6).

In this context, micro-environmental conditions related to chronic inflammation and/or relapsing infections might greatly affect the efficacy of these immune-effectors at several levels. These conditions may induce CTL exhaustion or promote the synthesis of pro-inflammatory cytokines like Interleukin (IL-6) and chemokines that, in turn, can have the following effects: i) to hamper the CTL-mediated response; ii) to enhance the production of immunosuppressive cell lineages (Treg, MSDC, M2 macrophages etc.) and iii) to promote the activation of multiple peripheral and central immune-checkpoints including those related to the hypoxic induced factor (HIF) and the adenosine receptor pathway (7–10).

This events might be of critical interest in mNSCLC patients who often present coexisting subclinical inflammatory and/or infectious conditions eventually related to the smoking habit, to chronic pulmonary obstructive disease symptoms and to the presence of relapsing infections within the low airways (11–13).

On these bases, we believe that the study of both inflammatory and infection markers in mNSCLC patients addressed to receive immune-checkpoint blocking mAbs could have a key role in understanding their effective interference in CTL activation and consequently on the outcome of these patients. At the present, the majority of the studies in the literature rely on the prognostic role of unspecific inflammatory markers such as white cell counts, NLR, CRP, ESR, LDH or more sophisticated techniques including tumor immune-profiling or microbiology studies (14–17).

Therefore, we have hypothesized that the presence of inflammatory markers mostly associated to bacterial infections of the low airways such as procalcitonin (PCT), might be easily correlated to the clinical outcome of mNSCLC patients subjected to immuno-oncological treatments. PCT, is a 116 amino acid peptide physiologically synthesized by thyroid parafollicular C cells that contribute to maintain the calcium homeostasis once converted to the calcitonin hormone and released in the blood stream (18–20). In the presence of a bacterial infection provoking a systemic inflammatory response, PCT synthesis may be induced in nearly all the involved tissues leading to a massive release of the peptide in the blood stream. On these bases, it is recommended as a reliable marker of typical bacterial infections, a feature not shared by other common inflammatory markers (18, 20). Systemic PCT production is triggered by bacterial toxins (endotoxin) and by pro-inflammatory cytokines such as tumor necrosis factor (TNF)-α, interleukin-1-β (IL-1β), and interleukin-6 (IL-6) as an immunological danger signal able to alert the host of a possible bacterial infection (18–24). Serum PCT is undetectable in healthy persons while it is greatly risen in patients bearing clinical or subclinical bacterial infections (20). On the other hand, PCT synthesis is not induced in most viral infections due to their ability to trigger the release of cytokines such as interferon (IFN)-γ that, in turn, inhibits the production of PTC inducers such as TNF-α (25–30).

At the same time, preliminary reports show that PCT in NSCLC could be correlated to survival, with a worse survival in patients with a PCT >0.1 ng/ml (31–33).

On the light of all these considerations, we carried out a retrospective study aimed to investigate whether the blood levels of PCT compared with conventional inflammatory markers such as CRP and ESR may predict the outcome of mNSCLC patients receiving PD-1/PD-L1 immune-checkpoint inhibitor mAbs.

MATERIALS AND METHODS

Study Design and Patients

This work is part of a retrospective real-world evidence (RWE) multi-institutional database study including 95 chemo-refractory mNSCLC patients consecutively enrolled to receive salvage therapy with anti-PD-1 (nivolumab) or anti-PD-L1 (atezolizumab) mAb at the OU-RC, and ROU-SI between September 2015 and April 2020 with a median follow-up time of 28 months (34–36).

All the patients gave an informed consent for the anonymous use of their clinical data for the research aim. All procedures were undertaken in compliance with the ethical statements of the Helsinki Declaration (1964, amended most recently in 2008) of the World Medical Association and respect of their privacy. All patients received PD-1/PD-L1 blockade in *real world setting* as recommended by the international guidelines and regulatory

agencies following the standard procedures of administration for each drug. All patients according to their specific disease received: nivolumab (intravenous infusion of 3 mg/kg every two weeks) (84 patients) or atezolizumab (intravenous infusion of 1,200 mg every three weeks) (33 patients) until disease progression or occurrence of severe adverse events. All patients were fit for treatment with no heart, kidney, and liver failure, no alterations in the blood cell counts and no clear sign of infection. All of the patients aimed to receive the treatment presented a good performance status ≤1 according to the Eastern Cooperative Oncology Group (ECOG). A complete physical examination report, histological sampling, hematologic, biochemical, immune-biological, radiological, and instrumental monitoring were available at baseline. Clinical history, physical examination, and record of adverse events were reported prior to each treatment cycle. A CT scan was performed at baseline and repeated every 3 months or in any case of suspected progressive disease (PD). CT scans were evaluated according to the immune Response Evaluation Criteria in Solid Tumors (iRECIST 1.1) (37).

All patients were monitored for blood cell counts, biochemistry, CRP, ESR, and PCT before each treatment course and were also monitored for their adrenal hormone profile, ACTH, TSH, thyroid hormones, anti-thyroid auto-antibodies (AAbs), extractable nuclear antigen antibodies (ENA), anti-nucleus antibodies (ANA), anti-smooth cells antibodies (ASMA), and c/p- anti-neutrophil cytoplasmic antibodies (ANCA) each month from the beginning of treatment as reported in previous study (38–40). Only pre-therapy (before the start of immunotherapy) parameters PCR, CRP and ESR were considered for the present analysis.

Statistical Analysis

In order to perform a statistical correlation among continuous parameters and outcomes, we determined different cut-off for survival analysis (Kaplan–Meier analysis), on the overall population.

The PCT threshold chosen (0.1 ng/ml) was determined on the recent analysis from Kajikawa et al. (33), as it included only NSCLC patients and the same threshold was confirmed on multivariate analysis. For the other biomarkers (CRP, ESR), since a consensus in literature is lacking, we chose the median value as a cut-off (respectively CRP 1.6 mg/dl and ESR 40 mm/h).

Time to events was analyzed with the Kaplan–Meier method and statistics was performed by the log-rank test. Median survival and 95% confidence intervals were reported. Median follow-up was estimated with the reverse method. Hazard ratios (HRs) and their 95% confidence intervals were estimated through the Cox regression proportional model.

In the multivariate approach, a forward stepwise procedure was used and the enter and remove limit set to 0.05 and 0.10, respectively. Significant parameters at multivariate analysis were used to build a final model of survival, identifying different subgroups of patients. Chi-Square analysis was used to test the differences among the subgroup identified in terms of clinical variables.

Statistics were performed by the SPSS software 23.0 (International Business Machines Corp., New York, NY, USA).

RESULTS

Patients' Feature and Clinical Outcome

Our retrospective analysis was performed on a cohort of 95 patients with mNSCLC in our database who presented a parallel monitoring of serum CRP, ESR, and PCT values. In our series there were 77 males and 18 females who had been consecutively enrolled to receive salvage therapy with nivolumab (69 cases) or atezolizumab (26 cases) between November 2015 and April 2020 with a median follow of 28 months.

Patients' demographic and clinical characteristics are summarized in **Table 1**.

All of the patients were fit for the immunological treatment and presenting an ECOG performance status in a range of 0–1; no clinical or radiological sign of active infection at baseline and no major impairment of heart, liver and kidney functions were recorded.

Mean age was 66 years ± 9.9 years, median age 67 years, range 32–85 years.

On the overall, we recorded a median OS of 17.9 (95%CI; 11.0–24.6) months, with no statistical differences correlated with the treatment (nivolumab *vs*. atezolizumab, p: 0.378) (**Figure 1**). In this patients' series we recorded irAEs in 33.7% of the patients (32/95 patients, grades 1–3) and no other adverse events or major organ failures unrelated to the malignant disease progression.

Haematological parameters mean value and standard deviations were as follow: PCT 0.21 ± 0.50 ng/ml, ESR 44.2 ± 31.4 mm/H, CRP 3.3 ± 5 mg/dl. All the evaluated parameters are reported in **Supplementary Materials**.

Univariate Analysis of Survival

We carried out a statistical analysis aimed to compare the outcome of the patients presenting CRP, ESR and PCT

TABLE 1 | Clinical characteristics of the whole cohort of patients.

Characteristics	Percentage
Sex	
Males	77 (81.1%)
Females	18 (18.9%)
Immunotherapy	
Nivolumab	69 (72.6%)
Atezolizumab	26 (27.4%)
Histology	
Squamous	32 (33.7%)
Non-Squamous	63 (66.3%)
Immune-related Adverse Events	
Yes	32 (33.7%)
No	63 (66.3%)
Age	
<50 years	6 (4.2%)
50–65 years	38 (40%)
65–75 years	32 (33%)
>75 years	19 (20%)
Expression of PD-L1 tumor expression, categorized	
<1%	19 (20%)
1–50%	30 (31.5%)
>50%	15 (15.8%)
Missing	31 (32.7%)

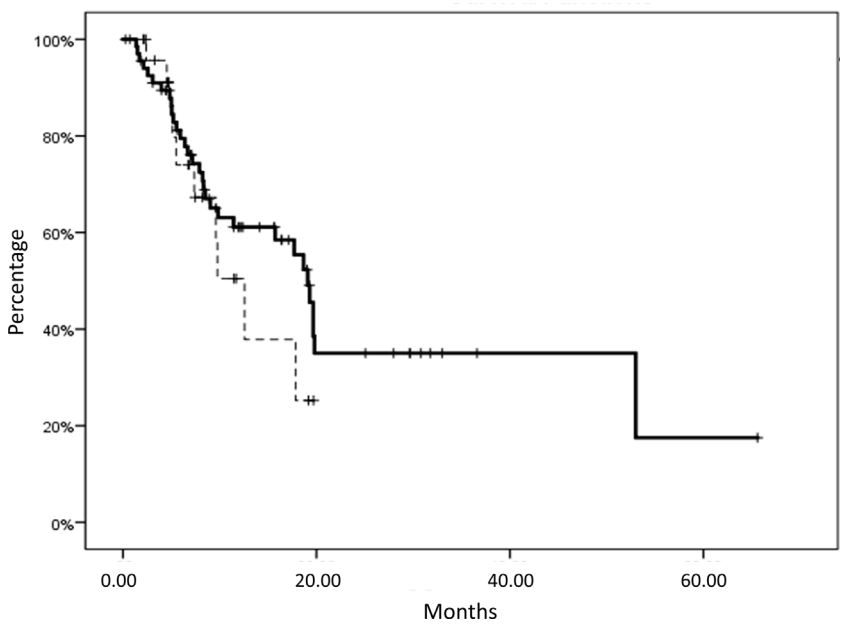

FIGURE 1 | Overall survival (OS) of patients with metastatic non-small cell lung cancer (mNSCLC) subjected to nivolumab (solid line) or atezolizumab treatment (dashed line). No statistical differences in survival were correlated with the treatment (nivolumab *vs*. atezolizumab, p:0.378). Nivolumab subgroup median OS: 19 ± 0.8 months, mean OS: 27.9 ± 3.9 months, *versus* Atezolizumab subgroup median OS: 12.5 ± 2.1 months, mean OS: 12.1 ± 1.6 months.

baseline values below or over the respective pre-established cut-off value. The overall survival was obtained for each specific marker (**Figures 2A–C**). In details, patients presenting baseline values of CRP≤ *vs*. >16 mg/L showed a median OS of 19.3 ± 0.6 (mean: 30.5 ± 4.7) *vs*. 9.7 ± 1.4 (mean: 15.9 ± 2.7) months, respectively, with a p-value of 0.033. Additionally, patients presenting baseline values of ESR≤ *vs*. >40 mm/h showed a median OS of 19.8 ± 1.5 (mean: 36.5 ± 5.4) *vs*. 9.8 ± 1.9 (mean: 17.7 ± 3.5) months, respectively, with a p-value of 0.01. Finally, patients presenting baseline values of PCT ≤ 0.1 *vs*. >0.1 mg/L showed a median OS of 19.6 ± 0.4 (mean: 31.0 ± 4.3) *vs*. 7.3 ± 0.6 (mean: 10.1 ± 1.4) months, respectively, with a p-value of 0.002.

Multivariate Analysis of Survival

Cox regression analysis of OS showed that only ESR (HR 2.11; 95% CI: 1.12–3.99; p = 0.02) and PCT (HR 2.64, 95% CI: 1.34–5.18; p = 0.005) were statistically significant. ESR and PCT were used to build a model of OS, dividing the cohort in three subgroups with the relative characteristics summarized in **Table 2**. Chi-Square analysis showed no significant difference among the three groups in terms of clinical variables (see **Table 2**). In the subgroup A were included patients (37 cases; 38.9%) with ESR and PCT baseline values equal to or below the respective cut-offs, who showed a prolonged OS (median OS not reached with a mean of 40 ± 5.9 months); in the subgroup B were included patients (43 cases; 45.3%) presenting just one of ESR or PCT baseline values over the respective cut off, who showed a median OS of 15.5 ± 5.5 (mean: 20.1 ± 4.0 months) months; finally, in the subgroup C were included patients (15 cases; 15.8%) with both ESR and PCT baseline values over the cut-off who showing the worst median OS of 5.5 ± 1.6 (mean: 8.3 ± 1.7) months. The differences among the three subgroups were statistically significant with a model p-value <0.001, HR 2.3, 95% CI 1.5–3.5 (**Figure 2D**).

DISCUSSION

Our retrospective multi-institutional analysis performed in real world setting and aimed to evaluate the effects of either inflammatory and/or infection markers in mNSCLC receiving PD-1/PD-L1 blocking mAbs, showed a direct correlation of CRP, ESR and PCT baseline values with a poor outcome in terms of survival. The PCT threshold chosen was determined on the recent analysis from Kajikawa et al. (33), as it included only NSCLC patients and the same threshold was confirmed on multivariate analysis. Conversely, other analyses included generally patients with lung cancer (both SCLC and NSCLC) and concluded that PCT is elevated in patients with lung cancer with neuroendocrine component or with metastases (31, 32). For the other biomarkers (CRP and ESR), since a consensus in literature is lacking, we chose the median value as a cut-off. The arbitrary choice of the cut-off must be recognized as a limitation of our retrospective study.

These results, however, are in line with our previous results and with what reported by several authors concerning the negative influence of inflammation on the outcome of patients subjected to palliative chemotherapy, radiotherapy and/or immunomodulating treatments for mNSCLC. On the basis of these data, it can be hypothesized that a coexisting chronic

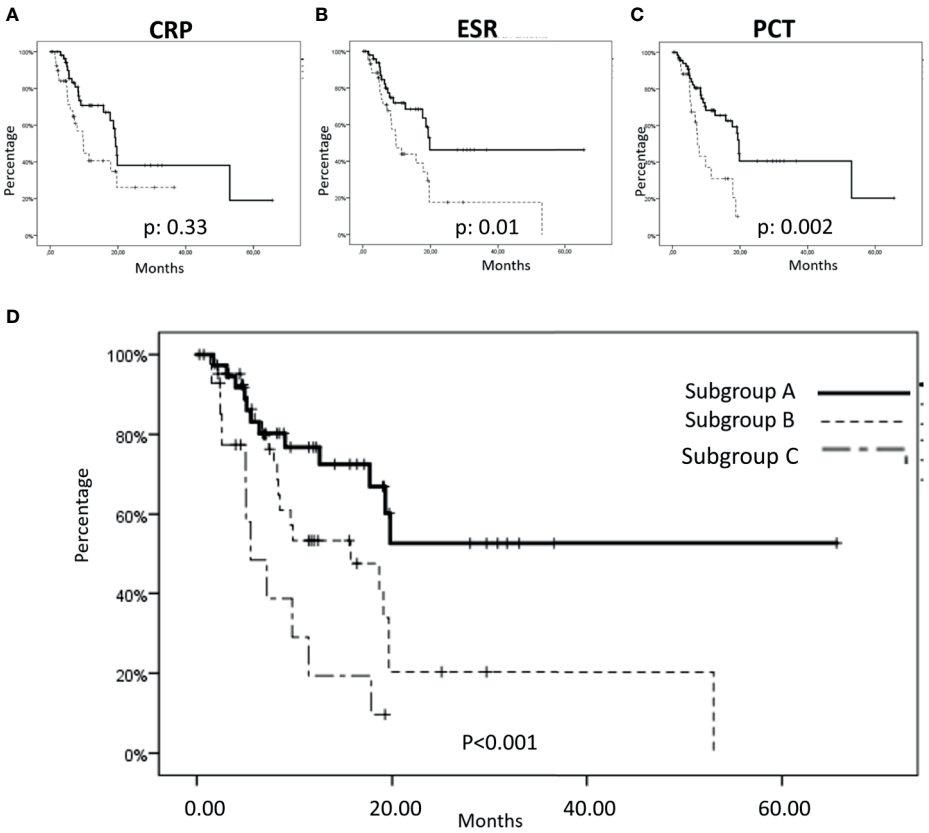

FIGURE 2 | Overall survival (OS) considering inflammation status markers in metastatic non-small cell lung cancer (mNSCLC) patients. **(A–C)** In our series, we found a significant cut-off of the baseline expression of CRP, ESR and PCT that was strongly correlated to a worse outcome in terms of OS; **(A)** Specifically, patients with a CRP ≤16 showed a median OS of 19.3 ± 0.6 months, mean: 30.5 ± 4.7 months, versus a median OS of 9.7 ± 1.4 months, mean: 15.9 ± 27 months in patients with a CRP >16, with a p-value of 0.033; **(B)** Patients with ESR ≤40 showed a median OS of 19.8 ± 1.5 months, mean: 36.5 ± 5.4 months, versus a median OS of 9.8 ± 1.9 months, mean: 17.7 ± 3.5 months in patients with an ESR >40, with a p-value of 0.01; **(C)** Finally, patients with a PCT ≤0.1 showed a median OS of 19.6 ± 0.4 months, mean: 31.0 ± 4.3 months, versus a median OS of 7.3 ± 0.6 months, mean: 10.1 ± 1.4 months, in patients with a PCT >0.10, with a p-value of 0.002. **(D)** OS in tree subgroups of patients: Subgroup A (Baseline ESR values ≤40 mm/h and baseline PCT values ≤0.10 mg/L, were detected in 37/95 patients) showed a median OS not reached, mean 40 ± 5.9 months; Subgroup B (baseline ESR values >40 mm/h or baseline PCT values >0.10 mg/L were detected in 43/95 patients) showed a mean OS of 15.5 ± 5.5 months, mean: 20.1 ± 4.0 months; Sugbroup C (baseline ESR values >40 mm/h and baseline PCT values >0.10 mg/L were detected in 15/95 patients) showed a median OS of 5.5 ± 1.6 months, mean OS: 8.3 ± 1.7 months.

inflammation in mNSCLC patients may affect the immune-balance between the immune-system and cancer growth affecting the anti-tumor activity of T cells and promoting the mechanisms of cancer immune-escape (39–41).

At the same time, additional analysis on the correlation between inflammation parameters and outcomes in the specific setting of immunotherapy is needed, in order to investigate whether these parameters are simply prognostic biomarkers (i.e.: they are correlated to the prognosis of lung cancer patients independently from the choice of the systemic therapies) or predictive biomarkers of response to immunotherapy.

It has already been shown that chronic inflammation is commonly associated to the production of cytokines/chemokines that can hamper the efficient CTL response; to the rise of immune-suppressive cell lineages (including T_{reg}s and MDSCs) and to the triggering of the activation of multiple immune-checkpoints and immune-suppressive adenosine receptors (42, 43).

The presence of inflammatory processes in mNSCLC patients may be related to the presence of malignancy itself, to concomitant smoke-associated bronchopulmonary chronic disease and to the presence of relapsing bacterial infections related to incomplete integrity the airways (44–49).

In this light, there are several evidences on the impairment of the existing balance between immune cell-mediated destruction and growth of cancer cells during a long-lasting inflammatory status in cancer patients. This can indeed result in an accelerated progression of the disease and a worse prognosis. In this context, our results highlighting the ability of PCT, an inflammatory marker associated to gram-positive bacterial infection, to predict the outcome of mNSCLC patients receiving immunotherapy, are in line with the results of other authors who recently showed that

TABLE 2 | Clinical characteristics of the three cohort of patients.

Characteristics	Subgroup A n. 37 patients	Subgroup B n. 43 patients	Subgroup C n. 15 patients
Sex			
p-value: 0.785			
Males	29 (78.4%)	35 (81.4%)	13 (86.7%)
Females	8 (21.6%)	8 (18.6%)	2 (13.3%)
Immunotherapy			
p-value: 0.818			
Nivolumab	28 (75.7%)	31 (72.1%)	10 (66.7%)
Atezolizumab	9 (24.3%)	12 (27.9%)	5 (33.3%)
Histology			
p-value: 0.973			
Squamous	12 (32.4%)	15 (34.9%)	5 (33.3%)
Non-squamous	25 (67.6%)	28 (65.15)	10 (66.7%)
IrAEs			
p-value: 0.465			
Yes	13 (35.1%)	16 (37.2%)	3 (20%)
No	24 (64.9%)	27 (62.8%)	12 (80%)
Age			
p-value: 0.156			
<50 years	1 (2.7%)	2 (4.7%)	2 (13.3%)
50–65 years	15 (40.5%)	17 (39.6%)	6 (40%)
65–75 years	13 (35.1%)	15 (34.8%)	6 (40%)
>75 years	8 (21.7%)	9 (20.9%)	1 (6.7%)
Expression of PD-L1 expression, categorized			
p-value: 0.818			
<1%	6 (16.2%)	9 (20.9%)	4 (26.6%)
1–50%	11 (29.8%)	15 (34.9%)	4 (26.7%)
>50%	8 (21.6%)	6 (13.9%)	1 (6.7%)
Missing	12 (32.4%)	13 (30.3%)	6 (40%)

Subgroup A included 37 patients with baseline ESR values ≤40 mm/h and baseline PCT values ≤0.10 ng/L. Subgroup B included 43 patients' baseline ESR values >40 mm/h or baseline PCT values >0.10 ng/L. Subgroup C included 15 patients with baseline ESR values >40 mm/h and baseline PCT values >0.10 ng/L. Chi-Square analysis showed no differences in clinical variables among the three groups.

high baseline levels of PCT are predictive of a poor prognosis in mNSCLC (31, 33, 50).

It is noteworthy to underline that in the setting of mNSCLC an increase of infection biomarkers, such as PCT, CRP and ESR, cannot be considered very specific for active infections, as these biomarkers may be related to the malignancy itself or to concomitant smoke-associated bronchopulmonary chronic disease (32), although PCT can be considered more specific and aid in the differential diagnosis between infectious fever and tumor fever (50, 51).

However, in our series we observed, in a multivariate analysis, that patients presenting at the same time ESR and PCT baseline values over the cut-off showed the worse outcome (mean OS = 8.3 ± 1.7 months) compared with the outcome recorded in patients with just one of the two marker values over the cut-off (mean OS = 20.1 ± 4.0 months) or in patients with both marker values below the cut-off (mean OS = 40 ± 5.9 months). This finding suggests that both inflammation and infection have an additive and independent detrimental effect on the outcome and on the treatment response to the immuno-oncological treatment with anti PD-1 and PD-L1 blocking mAbs.

PCT is considered a serum biomarker able to distinguish bacterial infection from other causes of infection or inflammation. This could be of particular interest in patients with infections of the lower respiratory tract where PCT may help in resolving diagnostic uncertainty and guiding to antibiotic therapy; in details, antibiotics' discontinuation in patients with pneumonia, is commonly recommended on defined PCT thresholds (below 0.25 or 0.5 ng/ml or decrease by ≥80% from peak if initial value is >5 ng/ml) in combination with clinical judgment (19, 52, 53). It is conceivable that this recommendation might be still valid in patients bearing a malignant disease and need to be investigated in appropriate trials.

It should be stated that not all bacterial infections cause similar PCT increase. The most common infections by typical bacteria such as *Streptococcus pneumonia* and *Haemophilus influentia*, are commonly associate to higher PCT levels (median blood values of 2.5 ng/ml) compared with atypical bacteria (like *Mycoplasma*, *Legionella*, *Chlamydia*, *Mycobacterium tubercolosis*, etc.), or other eukaryotic parasites (alike *Candida* and *Pneumocystis species*), (median blood values of 0.20 ng/ml) and viruses (median blood values of 0.09 ng/ml) (19, 52). On the other hand, systemic inflammation not associated with pathogens, including cancer (with the exception of neuroendocrine malignancies), shock, injuries and chronic kidney disease and more severe autoimmune diseases have a limited effect on PCT levels.

However, unspecific PCT rises have been sporadically reported upon treatment with immunomodulatory treatments such as T-cell antibodies, alemtuzumab, IL-2, and granulocyte transfusions even though in our setting we were unable to show

any significant increase in CRP, ESR and PCT related to the use of mAbs to PD-1 or PD-L1 (54–56).

Serum PCT blood levels commonly rise within few hours after the microbiological insult and roughly correlate with the severity of infection declining at a predictable fast rate with complete resolution. However, it should be taken in consideration that PCT production continues maintaining a plateau level when the infection/inflammatory stimulus is not completely solved (57–59). On these bases of the results derived from multiple observational studies, it has been hypothesized that PCT levels over the thresholds, reflect the existence of an active bacterial infection even though other clinical signs and symptoms are missing. Additionally, there is also evidence that the speed of rising in PCT serum levels correlates with the severity of the infection, a fact which allow the physicians to rely on this marker to monitor the systemic evolution of the ongoing infectious disease and the efficacy of the antibiotic therapy in elderly and cancer patients where the morbidity from bacterial infections is unpredictable and often lethal (60–64).

As an additional consideration, it is important to take in consideration the in mNSCLC patients receiving immuno-oncological treatments the role of the specific broncho-pulmonary microbiota that in analogy with what reported for the intestinal resident bacteria, may affect the immunological response of the host to the tumor and consequently the efficacy of immune-checkpoint inhibitors. In this context, it has been recently shown that the unspecific use of antibiotics prior to PD-1 blockade is correlated with a poor response to the treatment and it is commonly not advised, although some concerns of bias related to the selection of patients (65–71). In this regard, the use of infectious biomarkers such as PCT could help to properly select patients with active infections requiring antibiotics and to spare the unspecific use of these drugs avoiding their detrimental effects on specific microbiota.

Also, we did not find any correlation between the inflammation biomarkers and the development of irAEs. At this regard, we can speculate that basal parameters cannot predict the immune-related side effects, unfortunately, as immunotherapy has not started yet. We believe that the dynamic evaluation of these biomarkers during the course of immunotherapy (i.e.: in different time points, before each cycle of immunotherapy) could help in this prediction. A proper investigation of this phenomenon is needed in the next future with a dedicated prospective trial.

Our work recognizes the limitation of a monocentric retrospective study that deserves validation in external datasets and/or prospective validation. Presently, external validation was not possible, as PCT is not included in the routinary clinical management of mNSCLC.

In the present study we describe the detrimental effect of systemic inflammation and infection in mNSCLC receiving PD-1/PD-L1 blockade immunotherapy and suggest a perspective investigation of CRP, ESR and PCT as potential biomarker of response to the immuno-oncological treatment. The results of this study also open a new research scenario potentially played by bacterial influence and eventually on the preventive use of antibiotics in patients with high baseline levels of ESR and PCT, aimed to receive immune-checkpoint blockade.

DATA AVAILABILITY STATEMENT

The raw data supporting the conclusions of this article will be made available by the authors, without undue reservation.

ETHICS STATEMENT

Ethical review and approval was not required for the study on human participants in accordance with the local legislation and institutional requirements. The patients/participants provided their written informed consent to participate in this study.

AUTHOR CONTRIBUTIONS

VN, DG, MC, and PC conceived and designed the study and wrote the manuscript. RG, GB, PT, PP, AF, SM, and PC acquired the clinical data. DG performed statistical analysis. VN, LM, LP, AG and PC followed the patients, including planning clinical visits, blood sample collection and follow-up. AL, MC, PC and SZ revised the paper. All authors contributed to the article and approved the submitted version.

SUPPLEMENTARY MATERIAL

The Supplementary Material for this article can be found online at: https://www.frontiersin.org/articles/10.3389/fonc.2021.684110/full#supplementary-material

REFERENCES

1. Doroshow DB, Sanmamed MF, Hastings K, Politi K, Rimm DL, Chen L, et al. Immunotherapy in Non-Small Cell Lung Cancer: Facts and Hopes. *Clin Cancer Res* (2019) 25(15):4592–602. doi: 10.1158/1078-0432.CCR-18-1538
2. Dafni U, Tsourti Z, Vervita K, Peters S. Immune Checkpoint Inhibitors, Alone or in Combination With Chemotherapy, as First-Line Treatment for Advanced Non-Small Cell Lung Cancer. A Systematic Review and Network Meta-Analysis. *Lung Cancer* (2019) 134:127–40. doi: 10.1016/j.lungcan.2019.05.029
3. Huang Z, Su W, Lu T, Wang Y, Dong Y, Qin Y, et al. First-Line Immune-Checkpoint Inhibitors in Non-Small Cell Lung Cancer: Current Landscape and Future Progress. *Front Pharmacol* (2020) 11:578091. doi: 10.3389/fphar.2020.578091
4. Camidge DR, Doebele RC, Kerr KM. Comparing and Contrasting Predictive Biomarkers for Immunotherapy and Targeted Therapy of NSCLC. *Nat Rev Clin Oncol* (2019) 16(6):341–55. doi: 10.1038/s41571-019-0173-9
5. Philips GK, Atkins M. Therapeutic Uses of Anti-PD-1 and Anti-PD-L1 Antibodies. *Int Immunol* (2015) 27(1):39–46. doi: 10.1093/intimm/dxu095
6. Urwyler P, Earnshaw I, Bermudez M, Perucha E, Wu W, Ryan S, et al. Mechanisms of Checkpoint Inhibition-Induced Adverse Events. *Clin Exp Immunol* (2020) 200(2):141–54. doi: 10.1111/cei.13421

7. Hashimoto M, Kamphorst AO, Im SJ, Kissick HT, Pillai RN, Ramalingam SS, et al. CD8 T Cell Exhaustion in Chronic Infection and Cancer: Opportunities for Interventions. *Annu Rev Med* (2018) 69:301–18. doi: 10.1146/annurev-med-012017-043208
8. Saigi M, Alburquerque-Bejar JJ, Sanchez-Cespedes M. Determinants of Immunological Evasion and Immunocheckpoint Inhibition Response in Non-Small Cell Lung Cancer: The Genetic Front. *Oncogene* (2019) 38 (31):5921–32. doi: 10.1038/s41388-019-0855-x
9. Nowicki TS, Hu-Lieskovan S, Ribas A. Mechanisms of Resistance to PD-1 and PD-L1 Blockade. *Cancer J* (2018) 24(1):47–53. doi: 10.1097/PPO.0000000000000303
10. Najafi M, Hashemi Goradel N, Farhood B, Salehi E, Nashtaei MS, Khanlarkhani N, et al. Macrophage Polarity in Cancer: A Review. *J Cell Biochem* (2019) 120(3):2756–65. doi: 10.1002/jcb.27646
11. Seda G, Stafford CC, Parrish JS, Praske SP, Daheshia M. Chronic Obstructive Pulmonary Disease and Vascular Disease Delay Timeliness of Early Stage Lung Cancer Resectional Surgery. *COPD* (2013) 10(2):133–7. doi: 10.3109/15412555.2012.728260
12. McMullen S, Hess LM, Kim ES, Levy B, Mohamed M, Waterhouse D, et al. Treatment Decisions for Advanced Non-Squamous Non-Small Cell Lung Cancer: Patient and Physician Perspectives on Maintenance Therapy. *Patient* (2019) 12(2):223–33. doi: 10.1007/s40271-018-0327-3
13. Brown T, Pilkington G, Bagust A, Boland A, Oyee J, Tudur-Smith C, et al. Clinical Effectiveness and Cost-Effectiveness of First-Line Chemotherapy for Adult Patients With Locally Advanced or Metastatic Non-Small Cell Lung Cancer: A Systematic Review and Economic Evaluation. *Health Technol Assess* (2013) 17(31):1–278. doi: 10.3310/hta17310
14. Wojas-Krawczyk K, Kalinka E, Grenda A, Krawczyk P, Milanowski J. Beyond PD-L1 Markers for Lung Cancer Immunotherapy. *Int J Mol Sci* (2019) 20 (8):1915. doi: 10.3390/ijms20081915
15. Ni X-F, Wu J, Ji M, Shao Y-J, Xu B, Jiang J-T, et al. Effect of C-reactive Protein/Albumin Ratio on Prognosis in Advanced Non-Small-Cell Lung Cancer. *Asia Pac J Clin Oncol* (2018) 14(6):402–9. doi: 10.1111/ajco.13055
16. Thompson JC, Hwang W-T, Davis C, Deshpande C, Jeffries S, Rajpurohit Y, et al. Gene Signatures of Tumor Inflammation and Epithelial-to-Mesenchymal Transition (EMT) Predict Responses to Immune Checkpoint Blockade in Lung Cancer With High Accuracy. *Lung Cancer* (2020) 139:1–8. doi: 10.1016/j.lungcan.2019.10.012
17. Akamine T, Takada K, Toyokawa G, Kinoshita F, Matsubara T, Kozuma Y, et al. Association of Preoperative Serum CRP With PD-L1 Expression in 508 Patients With Non-Small Cell Lung Cancer: A Comprehensive Analysis of Systemic Inflammatory Markers. *Surg Oncol* (2018) 27(1):88–94. doi: 10.1016/j.suronc.2018.01.002
18. Becker KL, Nylén ES, White JC, Müller B, Snider RHJ. Clinical Review 167: Procalcitonin and the Calcitonin Gene Family of Peptides in Inflammation, Infection, and Sepsis: A Journey From Calcitonin Back to Its Precursors. *J Clin Endocrinol Metab* (2004) 89(4):1512–25. doi: 10.1210/jc.2002-021444
19. Christ-Crain M, Jaccard-Stolz D, Bingisser R, Gencay MM, Huber PR, Tamm M, et al. Effect of Procalcitonin-Guided Treatment on Antibiotic Use and Outcome in Lower Respiratory Tract Infections: Cluster-Randomised, Single-Blinded Intervention Trial. *Lancet (Lond Engl)* (2004) 363(9409):600–7. doi: 10.1016/S0140-6736(04)15591-8
20. Maruna P, Nedelníková K, Gürlich R. Physiology and Genetics of Procalcitonin. *Physiol Res* (2000) 49(Suppl 1):S57–61.
21. BalcI C, Sungurtekin H, Gürses E, Sungurtekin U, Kaptanoglu B. Usefulness of Procalcitonin for Diagnosis of Sepsis in the Intensive Care Unit. *Crit Care* (2003) 7(1):85–90. doi: 10.1186/cc1843
22. Dandona P, Nix D, Wilson MF, Aljada A, Love J, Assicot M, et al. Procalcitonin Increase After Endotoxin Injection in Normal Subjects. *J Clin Endocrinol Metab* (1994) 79(6):1605–8. doi: 10.1210/jcem.79.6.7989463
23. Reinhart K, Karzai W, Meisner M. Procalcitonin as a Marker of the Systemic Inflammatory Response to Infection. *Intensive Care Med* (2000) 26(9):1193–200. doi: 10.1007/s001340000624
24. Gendrel D, Raymond J, Coste J, Moulin F, Lorrot M, Guérin S, et al. Comparison of Procalcitonin With C-Reactive Protein, Interleukin 6 and Interferon-Alpha for Differentiation of Bacterial *vs.* Viral Infections. *Pediatr Infect Dis J* (1999) 18(10):875–81. doi: 10.1097/00006454-199910000-00008
25. Assicot M, Gendrel D, Carsin H, Raymond J, Guilbaud J, Bohuon C. High Serum Procalcitonin Concentrations in Patients With Sepsis and Infection. *Lancet (Lond Engl)* (1993) 341(8844):515–8. doi: 10.1016/0140-6736(93)90277-N
26. Harbarth S, Holeckova K, Froidevaux C, Pittet D, Ricou B, Grau GE, et al. Diagnostic Value of Procalcitonin, Interleukin-6, and Interleukin-8 in Critically Ill Patients Admitted With Suspected Sepsis. *Am J Respir Crit Care Med* (2001) 164(3):396–402. doi: 10.1164/ajrccm.164.3.2009052
27. Hamade B, Huang DT. Procalcitonin: Where Are We Now? *Crit Care Clin* (2020) 36(1):23–40. doi: 10.1016/j.ccc.2019.08.003
28. Choi JJ, McCarthy MW. Novel Applications for Serum Procalcitonin Testing in Clinical Practice. *Expert Rev Mol Diagn* (2018) 18(1):27–34. doi: 10.1080/14737159.2018.1407244
29. Schuetz P, Bolliger R, Merker M, Christ-Crain M, Stolz D, Tamm M, et al. Procalcitonin-Guided Antibiotic Therapy Algorithms for Different Types of Acute Respiratory Infections Based on Previous Trials. *Expert Rev Anti Infect Ther* (2018) 16(7):555–64. doi: 10.1080/14787210.2018.1496331
30. Wirz Y, Meier MA, Bouadma L, Luyt CE, Wolff M, Chastre J, et al. Effect of Procalcitonin-Guided Antibiotic Treatment on Clinical Outcomes in Intensive Care Unit Patients With Infection and Sepsis Patients: A Patient-Level Meta-Analysis of Randomized Trials. *Crit Care* (2018) 22(1):191. doi: 10.1186/s13054-018-2125-7
31. Avrillon V, Locatelli-Sanchez M, Folliet L, Carbonnaux M, Perino E, Fossard G, et al. Lung Cancer may Increase Serum Procalcitonin Level. *Infect Disord Drug Targets* (2015) 15(1):57–63. doi: 10.2174/1871526515666150320162950
32. Patout M, Salaün M, Brunel V, Bota S, Cauliez B, Thiberville L. Diagnostic and Prognostic Value of Serum Procalcitonin Concentrations in Primary Lung Cancers. *Clin Biochem* (2014) 47(18):263–7. doi: 10.1016/j.clinbiochem.2014.09.002
33. Kajikawa S, Ohashi W, Kato Y, Fukami M, Yonezawa T, Sato M, et al. Prognostic Impact of Serum Procalcitonin in Non-Small Cell Lung Cancer. *Tumori* (2020) 20:300891620966647. doi: 10.1177/0300891620966647
34. Giannicola R, D'arrigo G, Botta C, Agostino R, Del Medico P, Falzea AC, et al. Early Blood Rise in Auto-Antibodies to Nuclear and Smooth Muscle Antigens Is Predictive of Prolonged Survival and Autoimmunity in Metastatic-Non-Small Cell Lung Cancer Patients Treated With PD-1 Immune-Check Point Blockade by Nivolumab. *Mol Clin Oncol* (2019) 11(1):81–90. doi: 10.3892/mco.2019.1859
35. Correale P, Saladino RE, Giannarelli D, Giannicola R, Agostino R, Staropoli N, et al. Distinctive Germline Expression of Class I Human Leukocyte Antigen (HLA) Alleles and DRB1 Heterozygosis Predict the Outcome of Patients With Non-Small Cell Lung Cancer Receiving PD-1/PD-L1 Immune Checkpoint Blockade. *J Immunother Cancer* (2020) 8:e000733. doi: 10.1136/jitc-2020-000733
36. Correale P, Saladino RE, Giannarelli D, Sergi A, Mazzei MA, Bianco G, et al. HLA Expression Correlates to the Risk of Immune Checkpoint Inhibitor-Induced Pneumonitis. *Cells* (2020) 9(9):1964. doi: 10.3390/cells9091964
37. Seymour L, Bogaerts J, Perrone A, Ford R, Schwartz LH, Mandrekar S, et al. iRECIST: Guidelines for Response Criteria for Use in Trials Testing Immunotherapeutics. *Lancet Oncol* (2017) 18(3):e143–52. doi: 10.1016/S1470-2045(17)30074-8
38. Cusi MG, Botta C, Pastina P, Rossetti MG, Dreassi E, Guidelli GM, et al. Phase I Trial of Thymidylate Synthase Poly-Epitope Peptide (TSPP) Vaccine in Advanced Cancer Patients. *Cancer Immunol Immunother* (2015) 64(9):1159–73. doi: 10.1007/s00262-015-1711-7
39. Garner H, de Visser KE. Immune Crosstalk in Cancer Progression and Metastatic Spread: A Complex Conversation. *Nat Rev Immunol* (2020) 20 (8):483–97. doi: 10.1038/s41577-019-0271-z
40. Jiang X, Wang J, Deng X, Xiong F, Ge J, Xiang B, et al. Role of the Tumor Microenvironment in PD-L1/PD-1-Mediated Tumor Immune Escape. *Mol Cancer* (2019) 18(1):10. doi: 10.1186/s12943-018-0928-4
41. Nardone V, Pastina P, Giannicola R, Agostino R, Croci S, Tini P, et al. How to Increase the Efficacy of Immunotherapy in NSCLC and HNSCC: Role of Radiation Therapy, Chemotherapy, and Other Strategies. *Front Immunol* (2018) 9:2941. doi: 10.3389/fimmu.2018.02941
42. Berraondo P, Minute L, Ajona D, Corrales L, Melero I, Pio R. Innate Immune Mediators in Cancer: Between Defense and Resistance. *Immunol Rev* (2016) 274(1):290–306. doi: 10.1111/imr.12464
43. Chen DS, Mellman I. Elements of Cancer Immunity and the Cancer-Immune Set Point. *Nature* (2017) 541(7637):321–30. doi: 10.1038/nature21349
44. Nagy A, Müller V, Kolonics-Farkas AM, Eszes N, Vincze K, Horvath G. Worse Lung Cancer Outcome in Patients With Lower Respiratory Tract

Infection Confirmed at Time of Diagnosis. *Thorac Cancer* (2019) 10(9):1819–26. doi: 10.1111/1759-7714.13153
45. Jin J, Li Y, Zhang X, Chen T, Wang Y, Wang Z. Evaluation of Both Free Radical Scavenging Capacity and Antioxidative Damage Effect of Polydatin. *Adv Exp Med Biol* (2016) 923:57–62. doi: 10.1007/978-3-319-38810-6_8
46. Liu H, Liu B, Zheng F, Chen X, Ye L, He Y. Distribution of Pathogenic Bacteria in Lower Respiratory Tract Infection in Lung Cancer Patients After Chemotherapy and Analysis of Integron Resistance Genes in Respiratory Tract Isolates of Uninfected Patients. *J Thorac Dis* (2020) 12(8):4216–23. doi: 10.21037/jtd-20-928
47. Nakhaee M, Rezaee A, Basiri R, Soleimanpour S, Ghazvini K. Relation Between Lower Respiratory Tract Microbiota and Type of Immune Response Against Tuberculosis. *Microb Pathog* (2018) 120:161–5. doi: 10.1016/j.micpath.2018.04.054
48. Cho JY, Kim J, Lee JS, Kim YJ, Kim SH, Lee YJ, et al. Characteristics, Incidence, and Risk Factors of Immune Checkpoint Inhibitor-Related Pneumonitis in Patients With non-Small Cell Lung Cancer. *Lung Cancer* (2018) 125:150–6. doi: 10.1016/j.lungcan.2018.09.015
49. Tini P, Nardone V, Pastina P, Pirtoli L, Correale P, Giordano A. The Effects of Radiotherapy on the Survival of Patients With Unresectable Non-Small Cell Lung Cancer. *Expert Rev Anticancer Ther* (2018) 18(6). doi: 10.1080/14737140.2018.1458615
50. Zhao Z, Li X, Zhao Y, Wang D, Li Y, Liu L, et al. Role of C-Reactive Protein and Procalcitonin in Discriminating Between Infectious Fever and Tumor Fever in Non-Neutropenic Lung Cancer Patients. *Med (Baltimore)* (2018) 97 (33):e11930. doi: 10.1097/MD.0000000000011930
51. Tulek B, Koylu H, Kanat F, Arslan U, Ozer F. Serum C-Reactive Protein and Procalcitonin Levels in Non-Small Cell Lung Cancer Patients. *Contemp Oncol (Poznan Poland)* (2013) 17(1):68–72. doi: 10.5114/wo.2013.33777
52. Schuetz P, Christ-Crain M, Thomann R, Falconnier C, Wolbers M, Widmer I, et al. Effect of Procalcitonin-Based Guidelines *vs* Standard Guidelines on Antibiotic Use in Lower Respiratory Tract Infections: The ProHOSP Randomized Controlled Trial. *JAMA* (2009) 302(10):1059–66. doi: 10.1001/jama.2009.1297
53. de Jong E, van Oers JA, Beishuizen A, Vos P, Vermeijden WJ, Haas LE, et al. Efficacy and Safety of Procalcitonin Guidance in Reducing the Duration of Antibiotic Treatment in Critically Ill Patients: A Randomised, Controlled, Open-Label Trial. *Lancet Infect Dis* (2016) 16(7):819–27. doi: 10.1016/S1473-3099(16)00053-0
54. Dornbusch HJ, Strenger V, Sovinz P, Lackner H, Schwinger W, Kerbl R, et al. Non-Infectious Causes of Elevated Procalcitonin and C-Reactive Protein Serum Levels in Pediatric Patients With Hematologic and Oncologic Disorders. *Support Care Cancer* (2008) 16(9):1035–40. doi: 10.1007/s00520-007-0381-1
55. Sabat R, Höflich C, Döcke WD, Oppert M, Kern F, Windrich B, et al. Massive Elevation of Procalcitonin Plasma Levels in the Absence of Infection in Kidney Transplant Patients Treated With pan-T-Cell Antibodies. *Intensive Care Med* (2001) 27(6):987–91. doi: 10.1007/s001340100949
56. Dornbusch HJ, Strenger V, Kerbl R, Lackner H, Schwinger W, Sovinz P, et al. Procalcitonin and C-Reactive Protein Do Not Discriminate Between Febrile Reaction to Anti-T-Lymphocyte Antibodies and Gram-Negative Sepsis. *Bone Marrow Transplant* (2003) 32(9):941–5. doi: 10.1038/sj.bmt.1704265
57. Meisner M. Update on Procalcitonin Measurements. *Ann Lab Med* (2014) 34 (4):263–73. doi: 10.3343/alm.2014.34.4.263
58. Schuetz P, Maurer P, Punjabi V, Desai A, Amin DN, Gluck E. Procalcitonin Decrease Over 72 Hours in US Critical Care Units Predicts Fatal Outcome in Sepsis Patients. *Crit Care* (2013) 17(3):R115. doi: 10.1186/cc12787
59. Vijayan AL, Vanimaya, Ravindran S, Saikant R, Lakshmi S, Kartik R, et al. Procalcitonin: A Promising Diagnostic Marker for Sepsis and Antibiotic Therapy. *J Intensive Care* (2017) 5:51. doi: 10.1186/s40560-017-0246-8
60. Bele N, Darmon M, Coquet I, Feugeas J-P, Legriel S, Adaoui N, et al. Diagnostic Accuracy of Procalcitonin in Critically Ill Immunocompromised Patients. *BMC Infect Dis* (2011) 11:224. doi: 10.1186/1471-2334-11-224
61. Schüttrumpf S, Binder L, Hagemann T, Berkovic D, Trümper L, Binder C. Procalcitonin: A Useful Discriminator Between Febrile Conditions of Different Origin in Hemato-Oncological Patients? *Ann Hematol* (2003) 82 (2):98–103. doi: 10.1007/s00277-002-0584-y
62. Munsiff SS, Kambili C, Ahuja SD. Rifapentine for the Treatment of Pulmonary Tuberculosis. *Clin Infect Dis* (2006) 43(11):1468–75. doi: 10.1086/508278
63. Shomali W, Hachem R, Chaftari A-M, Jiang Y, Bahu R, Jabbour J, et al. Can Procalcitonin Distinguish Infectious Fever From Tumor-Related Fever in Non-Neutropenic Cancer Patients? *Cancer* (2012) 118(23):5823–9. doi: 10.1002/cncr.27602
64. El Haddad H, Chaftari A-M, Hachem R, Chaftari P, Raad II. Biomarkers of Sepsis and Bloodstream Infections: The Role of Procalcitonin and Proadrenomedullin With Emphasis in Patients With Cancer. *Clin Infect Dis* (2018) 67(6):971–7. doi: 10.1093/cid/ciy331
65. Banna GL, Passiglia F, Colonese F, Canova S, Menis J, Addeo A, et al. Immune-Checkpoint Inhibitors in Non-Small Cell Lung Cancer: A Tool to Improve Patients' Selection. *Crit Rev Oncol Hematol* (2018) 129:27–39. doi: 10.1016/j.critrevonc.2018.06.016
66. Derosa L, Hellmann MD, Spaziano M, Halpenny D, Fidelle M, Rizvi H, et al. Negative Association of Antibiotics on Clinical Activity of Immune Checkpoint Inhibitors in Patients With Advanced Renal Cell and Non-Small-Cell Lung Cancer. *Ann Oncol* (2018) 29(6):1437–44. doi: 10.1093/annonc/mdy103
67. Pinato DJ, Gramenitskaya D, Altmann DM, Boyton RJ, Mullish BH, Marchesi JR, et al. Antibiotic Therapy and Outcome From Immune-Checkpoint Inhibitors. *J Immunother Cancer* (2019) 7(1):287. doi: 10.1186/s40425-019-0775-x
68. Routy B, Le Chatelier E, Derosa L, Duong CPM, Alou MT, Daillère R, et al. Gut Microbiome Influences Efficacy of PD-1-Based Immunotherapy Against Epithelial Tumors. *Science* (2018) 359(6371):91–7. doi: 10.1126/science.aan3706
69. Nagasaka M, Sexton R, Alhasan R, Rahman S, Azmi AS, Sukari A. Gut Microbiome and Response to Checkpoint Inhibitors in Non-Small Cell Lung Cancer-A Review. *Crit Rev Oncol Hematol* (2020) 145:102841. doi: 10.1016/j.critrevonc.2019.102841
70. Pinato DJ, Howlett S, Ottaviani D, Urus H, Patel A, Mineo T, et al. Association of Prior Antibiotic Treatment With Survival and Response to Immune Checkpoint Inhibitor Therapy in Patients With Cancer. *JAMA Oncol* (2019) 5(12):1774–8. doi: 10.1001/jamaoncol.2019.2785
71. Remon J, Vilariño N, Reguart N. Immune Checkpoint Inhibitors in non-Small Cell Lung Cancer (NSCLC): Approaches on Special Subgroups and Unresolved Burning Questions. *Cancer Treat Rev* (2018) 64:21–9. doi: 10.1016/j.ctrv.2018.02.002

Conflict of Interest: The authors declare that the research was conducted in the absence of any commercial or financial relationships that could be construed as a potential conflict of interest.

frontiers in Immunology

ORIGINAL RESEARCH
published: 04 August 2021
doi: 10.3389/fimmu.2021.643282

Predictive Value of the *TP53/PIK3CA/ATM* Mutation Classifier for Patients With Bladder Cancer Responding to Immune Checkpoint Inhibitor Therapy

Yi-Hui Pan[1†], Jia-Xing Zhang[2†], Xu Chen[1†], Fei Liu[3†], Jia-Zheng Cao[4], Yu Chen[1], Wei Chen[1*] and Jun-Hang Luo[1*]*

[1] Department of Urology, First Affiliated Hospital, Sun Yat-sen University, Guangzhou, China, [2] Department of Oncology, First Affiliated Hospital, Sun Yat-sen University, Guangzhou, China, [3] Department of Urology, National Cancer Center/National Clinical Research Center for Cancer/Cancer Hospital, Chinese Academy of Medical Sciences and Peking Union Medical College, Beijing, China, [4] Department of Urology, Jiangmen Hospital, Sun Yat-sen University, Jiangmen, China

OPEN ACCESS

Edited by:
Roberta Zappasodi,
Memorial Sloan Kettering Cancer Center, United States

Reviewed by:
David Aggen,
Memorial Sloan Kettering Cancer Center, United States
Jeremie Nsengimana,
Newcastle University, United Kingdom

***Correspondence:**
Yu Chen
842691873@qq.com
Wei Chen
chenw3@mail.sysu.edu.cn
Jun-Hang Luo
luojunh@mail.sysu.edu.cn

[†]These authors have contributed equally to this work and share first authorship

Specialty section:
This article was submitted to Cancer Immunity and Immunotherapy, a section of the journal Frontiers in Immunology

Received: 17 December 2020
Accepted: 15 July 2021
Published: 04 August 2021

Citation:
Pan Y-H, Zhang J-X, Chen X, Liu F, Cao J-Z, Chen Y, Chen W and Luo J-H (2021) Predictive Value of the TP53/PIK3CA/ATM Mutation Classifier for Patients With Bladder Cancer Responding to Immune Checkpoint Inhibitor Therapy. Front. Immunol. 12:643282. doi: 10.3389/fimmu.2021.643282

Background: Only a proportion of patients with bladder cancer may benefit from durable response to immune checkpoint inhibitor (ICI) therapy. More precise indicators of response to immunotherapy are warranted. Our study aimed to construct a more precise classifier for predicting the benefit of immune checkpoint inhibitor therapy.

Methods: This multi-cohort study examined the top 20 frequently mutated genes in five cohorts of patients with bladder cancer and developed the *TP53/PIK3CA/ATM* mutation classifier based on the MSKCC ICI cohort. The classifier was then validated in a validation set consisting of IMvigor210 cohort and Broad/Dana-Farber cohort. The molecular profile and immune infiltration characteristics in each subgroup as defined by this classifier were explored.

Results: Among all 881 patients with bladder cancer, the mutation frequency of *TP53*, *PIK3CA*, and *ATM* ranked in the top 20 mutated genes. The *TP53/PIK3CA/ATM* mutation classifier was constructed based on the Memorial Sloan Kettering Cancer Center (MSKCC) ICI cohort and only showed predictive value for patients with bladder cancer who received ICI therapy (median overall survival: low-risk group, not reached; moderate-risk group, 13.0 months; high-risk group, 8.0 months; P<0.0001). Similar results were found in subgroups of MSKCC ICI cohort defined by tumor mutation burden. Multivariate Cox analysis revealed that the risk group defined by the classifier served as an independent prognostic factor for overall survival in patients with bladder cancer. Efficacy of the classifier was verified in a validation set consisting of IMvigor210 cohort and Broad/Dana-Farber cohort. Lower expression of PD-1/PD-L1 and less tumor immune infiltration were observed in the high-risk group than the other two groups of the TCGA cohort and the IMvigor210 cohort.

Conclusion: Our study constructed a *TP53/PIK3CA/ATM* mutation classifier to predict the benefit of immune checkpoint inhibitor therapy for patients with bladder cancer. This classifier can potentially complement the tumor mutation burden and guide clinical ICI treatment decisions according to distinct risk levels.

Keywords: bladder cancer, immune checkpoint inhibitor, mutation profile, immunotherapy, immune cell infiltration, signature

INTRODUCTION

Recently, an increasing number of researchers focused their attention on the relationship between tumor progression and the immune status. Immune checkpoint inhibitors (ICIs) have become the most promising therapeutic modality for patients with malignant neoplasms, including bladder cancer (BC). Antibodies targeting programmed cell death 1 (*PD-1*) (OMIM 600244)/programmed death-ligand 1 (*PD-L1*) (OMIM 6005402) and cytotoxic T-lymphocyte associated protein 4 (*CTLA-4*) (OMIM 123890) have shown high therapeutic efficacy. Over the past few years, five new ICIs have been approved for the second-line systemic therapy in the locally advanced or metastatic BC diseases (1). Unfortunately, only a proportion of unselected BC patients showed obvious improvement (2–5). In a phase 2 multicenter study, the objective response rate to atezolizumab (a PD-L1 inhibitor) was 15%, regardless of the expression of PD-L1 (3). Similar results were observed in the CheckMate 275. In this phase 2 trial of nivolumab (a PD-1 inhibitor), the objective response was confirmed as 19.6% (4). In an international phase 3 trial of pembrolizumab (a PD-1 inhibitor), the objective response rate was 21.1% (5). Therefore, researchers started to focus on finding new biomarkers for treatment stratification. Encouragingly, recent studies have identified some positive predictive biomarkers for ICI therapy, such as tumor mutation burden (TMB) and microsatellite instability (MSI) (6–8). High levels of TMB and MSI may be associated with accumulation of neoantigen and stimulate the immune response, resulting in favorable response to ICI therapy. Gene mutation signatures have also been gradually identified as a good complement (9, 10).

Nevertheless, few verified biomarkers of the response to ICI therapy in BCs have been reported. In the Checkmate 275 study, higher values of the 25-gene interferon-γ (IFN-γ) signature were associated with higher PD-L1 expression and improved response rate to nivolumab (4). Min et al. elucidated an association between the alterations in DNA damage response and repair (DDR) genes and response to ICI in advanced urothelial carcinomas (UC), whereas *ATM* was the most commonly altered genes among the DDR-related genes (11). Thiago et al. also found that, in muscle invasive bladder cancers, mutations of DDR genes were associated with the expression of tumor immune regulatory gene expression (12). Besides, Sangeeta et al. reported *ARID1A* mutation plus *CXCL13* expression as composite biomarkers to predict responses to ICI therapy in metastatic UC (13). Composite somatic mutations seem to be potential biomarkers in advanced or metastatic BCs. However, these observations still need to be validated in a larger cohort for future development.

Herein, we aimed to screen the most commonly mutated genes in BC patients and constructed a novel gene mutation classifier to predict the benefit of immune checkpoint inhibitor therapy more precisely. The mutation classifier was validated in an independent validation set. Comprehensive bioinformatics analyses were carried out to understand the underlying mechanisms and potential prognostic value of the classifier.

MATERIALS AND METHODS

Patients and Samples

Somatic mutation data and clinical data of patients with BC from the Memorial Sloan Kettering Cancer Center (MSKCC) ICI cohort (n=215) (6)[1], MSKCC non-ICI cohort (n=172) (14)[2], The Cancer Genome Atlas (TCGA) cohort (n=412) (15)[3, 4], Weill Cornell Medicine/University of Trento (Cornell/Trento) cohort (n=32) (16)[5], Dana-Farber Cancer Institute/MSKCC (DFCI/MSKCC) cohort (n=50) (17)[6], and Broad/Dana-Farber cohort(n=26) (18)[7] were downloaded from the cBioPortal and the TCGA data portal (19). Patients from the MSKCC center were distinguished by patient ID, history of drug use, and other clinical characteristics for fear of overlapping cases. Gene expression data in fragments per kilobase of transcripts per million mapped reads (FPKM) for 408 samples in the TCGA database were also obtained from the cBioPortal. Somatic mutation data, RNA-seq data, and matched clinical data of BC patients from IMvigor210 cohort (n=237) were obtained from IMvigor210CoreBiologies, a fully documented R package (20)[8]. 215 patients from the MSKCC ICI cohort were assigned to the training set. 263 patients from the IMvigor210 cohort and Broad/Dana-Farber cohort were assigned to the validation set. All the patients from the MSKCC ICI cohort, IMvigor210 cohort, and Broad/Dana-Farber cohort received at least one dose of ICI therapy. Patients from the training set and the validation set

[1] http://www.cbioportal.org/study/summary?id=tmb_mskcc_2018
[2] http://www.cbioportal.org/study/summary?id=msk_impact_2017
[3] https://portal.gdc.cancer.gov
[4] http://www.cbioportal.org/study/summary?id=blca_tcga_pub_2017
[5] http://www.cbioportal.org/study/summary?id=blca_cornell_2016
[6] http://www.cbioportal.org/study/summary?id=blca_dfarber_mskcc_2014
[7] http://www.cbioportal.org/study/summary?id=mixed_allen_2018
[8] http://research-pub.gene.com/IMvigor210CoreBiologies

with incomplete survival information, mutation data, and TMB data were excluded. The study was conducted according to the Strengthening the Reporting of Observational Studies in Epidemiology (STROBE) reporting guideline.

Construction of the Mutation Classifier

First, univariate Cox regression analysis was conducted in the top 20 most commonly mutated genes of 881 BC patients from five cohorts. Then, genes with a *P* value less than 0.05, which was determined by univariate Cox regression, were screened to perform a multivariate cox regression analysis. The risk score was calculated with the formula below:

Risk score = ($beta_1$× mutation status of $Gene_1$) + ($beta_2$× mutation status of $Gene_2$) + … + ($beta_n$× mutation status of $Gene_n$).

A mutated gene was coded as 1, and a wild type gene was coded as 0. Beta was the regression coefficient generated in the multivariate Cox regression analysis.

Division of Risk Scores With the X-Tile Software

X-tile software version 3.6.1 (Camp/Rimm, Yale University) described the substantial tumor subpopulations *via* dividing a population into three risk score levels (low-, moderate-, and high-level) (21). X-tile plot was shown in a right triangular grid, where each pixel represented a different cutoff point. Each division had a Chi-Sq (χ^2) value, which was shown with a color code on the grid. The X-tile software could automatically select the optimal division through χ^2 value. A *P* value calculated by standard Monte Carlo simulations was used to assess statistical significance.

Assessment of TMB

All non-synonymous mutations, including missense, frame-shift, nonsense, nonstop, splice site, and translation start site changes of *TP53*/*PIK3CA*/*ATM*, were considered. TMB was defined as the total number of somatic non-synonymous mutations normalized to the total number of megabases sequenced.

We collected TMB data of patients from the MSKCC ICI cohort, which generated from the Memorial Sloan Kettering-Integrated Mutation Profiling of Actionable Cancer Targets (MSK-IMPACT). A total of 215 patients with BC, whose tumors were profiled by next-generation sequencing. Genomic alterations of patients from the IMvigor210 cohort were assessed by FMOne panel (Foundation Medicine, Inc.). TMB data of patients from the Broad/Dana-Farber cohort were determined as the total number of mutations per sample, normalized by whole-exome sequencing (WES) coverage.

Oncoplot of the Mutated Genes

Mutation Annotation Format (MAF) files of BC patients were downloaded from the cBioPortal.

The oncoplot and summarized information were then graphed through the Maftools package in the R version 4.0.4 (22).

Construction of the Protein–Protein Interaction (PPI) Network

The PPI network functional enrichment analysis was conducted on the STRING website[9] and reconstructed using the Cytoscape software version 3.8.0 (23).

Gene Set Enrichment Analysis (GSEA)

The GSEA software version 4.1.0 (Broad Institute, Cambridge, MA, USA) was used to identify the notably altered gene sets between the pre-defined low-risk group and high-risk group in the TCGA cohort. Hallmark gene sets(hallmark gene sets as Gene Symbols), C2: curated gene sets (KEGG gene sets as Gene Symbols) and C7: immunologic signatures(ImmuneSigDB gene sets as Gene Symbols), which represented cell states and perturbations within the immune system, were applied to investigate the alteration in immune-related pathways. Gene expression profiles of the TCGA cohort with grouping information were prepared for GSEA. A *P* value < 0.05 and a false discovery rate (FDR) <0.25 were considered statistically significant.

Assessment of Immune Infiltration

The ESTIMATE algorithm was applied to calculate the stromal scores, immune score, estimate scores, and tumor purity, which depicted the fraction of stromal and immune cells in tumor samples using expression signatures (24).

The CIBERSORT algorithm was applied to characterize the immune cell composition of complex tissues via an LM22 gene signature matrix (25). The matrix contains 547 genes that distinguish 22 human hematopoietic cell phenotypes. The standardized processed gene expression profiles from TCGA database and IMvigor210CoreBiologies R package were uploaded to the CIBERSORT website[10] as mixture files. The LM22 signature matrix file was used to run CIBERSORTx, with 1000 permutations. Quantile normalization was disabled on RNA-seq data. The results of CIBERSORT included subsets of seven T cell types, naive and memory B cells, plasma cells, natural killer cells, and myeloid subsets. CIBERSORT conducted deconvolution with Monte Carlo sampling and derived an empirical *P* value. All 408 TCGA samples with gene expression data had *P* values < 0.05. In IMvigor210 cohort, 153 samples had *P* values < 0.05, and 84 samples had *P* values ≥ 0.05. Only samples with a *P* value less than 0.05 were included for the following analyses.

The TIMER algorithm was applied to estimate immune infiltrations (26, 27). The standardized processed gene expression profiles were uploaded to the TIMER2.0 website[11]. The results contained subsets of B cells, CD4+ T cells, CD8+ T cells, neutrophils, macrophages, and myeloid dendritic cells.

Statistical Analysis

Overall survival (OS) was measured from the date of ICI therapy initiation to the time of death or latest follow-up. For survival analysis, Kaplan–Meier survival curves were generated and

[9] https://string-db.org
[10] http://cibersort.stanford.edu
[11] http://timer.cistrome.org

compared using the log-rank test. Cox regression analysis was used to establish a multi-gene mutation classifier. Overall survival and overall patient survival status were used as the dependent variables in the univariate and multivariate cox regression analyses. X-tile plots were used to automatically select the optimal division of the classifier by selecting the highest χ^2 value. The cutoff point of TMB was defined by the quintile (top 20%). The two-tailed unpaired t-test and Kruskal–Wallis test were used to determine the differences between different groups with or without normal distribution, respectively. The Pearson χ^2 test was applied to estimate the correlations among various immune cell subsets. The SPSS software version 25.0 (IBM Corp., Armonk, NY, USA) and GraphPad Prism version 8.3.0 (GraphPad Software Inc., San Diego, CA, USA) were used to carry out the statistical analysis. All the statistical outcomes were two-sided, with P values < 0.05 denoting statistically significant differences. Data were collected and analyzed from March 14, 2020 to June 21, 2021.

RESULTS

Distribution and Clinical Significance of BC Gene Mutation Profile Landscape

Our study firstly collected somatic mutation data of 881 patients with BC, including 215 patients from the MSKCC ICI therapy cohort (mean [SD] age, 67.6 [9.9] years; 164 [76.3%] men), 172 patients from the MSKCC non-ICI therapy cohort (123 [71.5%] men), 412 patients from the TCGA cohort (mean [SD] age, 68.1 [10.6] years; 412 [73.5%] men), 32 patients from the Cornell/Trento cohort (mean [SD] age, 68.3 [9.4] years; 24 [75.0%] men), and 50 patients from the DFCI/MSKCC cohort (mean [SD] age, 62.5 [8.9] years; 37 [74%] men) (**Supplementary Figure 1**). The vast majority of variant classifications consisted of missense and nonsense mutations. Single nucleotide polymorphism is the most common variant type in BC (**Supplementary Figure 2**). The oncoplot showed the top 20 frequently mutated genes in these five BC patient cohorts (**Figure 1**). To better understand the interplay between frequently mutated genes, we constructed PPI networks of the top 20 mutated genes *via* the STRING database and subsequently conducted an analysis using Cytoscape (**Supplementary Figure 3**). Tumor protein p53 (*TP53*) (OMIM 191170), phosphatidylinositol-4,5-Bisphosphate 3-Kinase Catalytic Subunit Alpha (*PIK3CA*) (OMIM 171834), AT-Rich Interaction Domain 1A (*ARID1A*) (OMIM 603024), ataxia-telangiectasia mutated (ATM) (OMIM 607585), and Lysine Methyltransferase 2D (*KMT2D*) (OMIM 602113) were identified to possess higher stress and more edgecounts than other genes, which implied their central position and complex interactions in the PPI network of BC.

Predictive Value of the *TP53/PIK3CA/ATM* Mutation Classifier in Patients With BC Receiving ICI Therapy

To investigate the gene signatures of patients sensitive to ICI therapy, we selected the MSKCC ICI therapy cohort as the training set, where each patient underwent PD-1/PD-L1 inhibitor therapy or combination treatment with a CTLA-4 inhibitor. Somatic TMB, measured using the MSK-IMPACT, was provided in the clinical patient information. We firstly

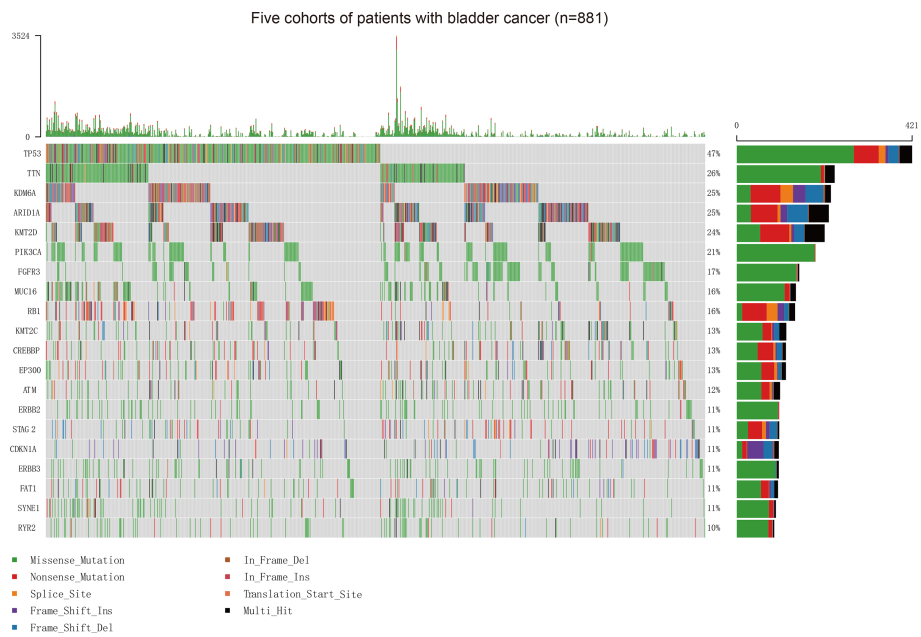

FIGURE 1 | Assessment of the Frequency of Mutated Genes and Mutation Patterns in Patients with BC from Five Cohorts. Oncoplot for the mutated genes of 881 patients with BC from five cohorts. The top 20 genes are listed by mutation frequencies. BC, bladder cancer.

utilized univariate cox regression analyses to examine the top 20 mutated genes. *TP53*, *PIK3CA*, *ATM*, and *CREBBP* showed statistical significance (**Supplementary Table 1**). After multivariate adjustment to 4 potential prognostic factors, only *TP53*, *PIK3CA*, and *ATM* showing independent predictive value ($P<0.05$) were selected as prognostic candidates (**Supplementary Table 2**). *CREBBP* had a P value > 0.05 and was excluded. Finally, *TP53*, *PIK3CA*, and *ATM* were included in the multivariate survival analysis, and we could generate a risk score for each patient with the cox regression coefficients in the model (**Supplementary Table 3**):

$$Risk\ Score = (-0.492 \star TP53) + (0.562 \star PIK3CA) - (1.454 \star ATM)$$

The risk scores of the 215 patients in the training set ranged from –1.946 to 0.562.

We evaluated the distribution of the risk score for the *TP53/PIK3CA/ATM* mutation classifier and survival status in patients who received ICI therapy. Patients with lower risk scores generally showed better response to ICI therapy than those with higher risk scores (**Figure 2A**). We next used the X-tile plots to determine the optimal cutoff point (**Supplementary Figure 4**). Patients with a score >0.07 or <0 were allocated to the high- and low-risk group, respectively. The remaining patients were allocated to the moderate-risk group (**Figure 2B**). Compared with patients in the moderate- and high-risk groups, those in the low-risk group exhibited better therapeutic response and OS (median OS, low-risk group: not reached; moderate-risk group: 13.0 months; high-risk group: 8.0 months; $P<0.0001$) (**Figure 2C**). According to the forest plot, we could confidently conclude that the risk group was a strong indicator of favorable OS among patients with BC (hazard ratio: 1.79; 95% CI: 1.37–2.34; $P<0.0001$) (**Figure 2D**). After multivariable adjustment, the risk group remained an independent predictive

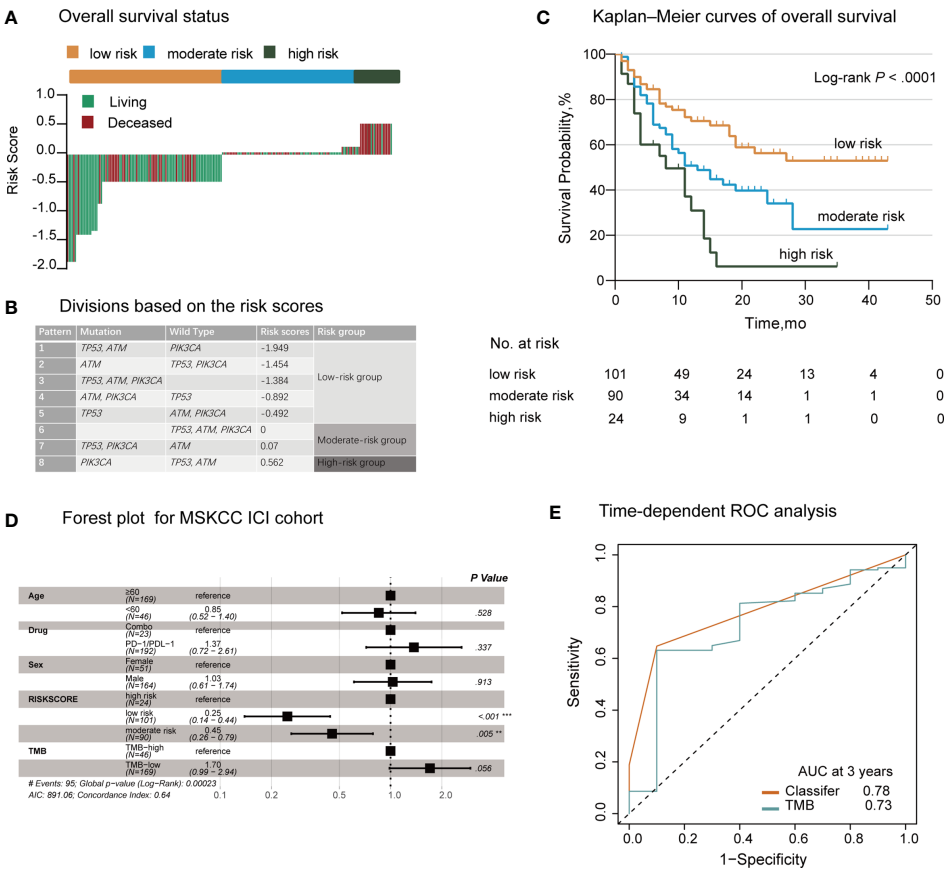

FIGURE 2 | Establishment of the *TP53/PIK3CA/ATM* Mutation Classifier in BC Patients Treated with Immune Checkpoint Inhibitors. **(A)** OS status in the MSKCC ICI cohort. "Living" and "Deceased" patients were marked green and red, respectively. **(B)** Schematic diagram of the divisions based on risk scores. **(C)** Kaplan–Meier curves of overall survival in the MSKCC ICI cohort based on the *TP53/PIK3CA/ATM* mutation classifier. The median overall survival was 8.0 months (95% CI: 13.1–20.9 months) in the high-risk group, 13.0 months (95% CI: 7.8–18.2 months) in the moderate-risk group, and not reached in the low-risk group. **(D)** Forest plot for 215 patients who received ICI therapy. The vertical line represents the hazard ratio (HR) of 1.0. **(E)** Time-dependent ROC curves and AUCs at 3 years were used to assess the predictive accuracy of the classifier compared with TMB. AUC, area under the curve; BC, bladder cancer; CI, confidence interval; ICI, immune checkpoint inhibitors; MSKCC, Memorial Sloan Kettering Cancer Center; OS, overall survival; ROC, receiver operating characteristic; TMB, tumor mutation burden.

factor (hazard ratio: 1.78; 95% CI: 1.35–2.36; $P<0.0001$) (**Supplementary Table 4**). When assessing the predictive accuracy of the classifier, the area under the curve (AUC) of the classifier and TMB at 3 years was 0.78 (95% CI: 0.69–0.88) and 0.73 (95% CI: 0.56–0.89), respectively (**Figure 2E**). Pearson correlation analysis showed a negative correlation between the risk score and TMB (r=−0.25; P=0.0002) (**Supplementary Figure 5**).

Subgroup Analysis of the *TP53/PIK3CA/ATM* Mutation Classifier in the MSKCC ICI Cohort by TMB

The median and range of TMB varied across tumor types (28). For this reason, we selected the higher TMB quintile (top 20%) as the cutoff point. According to the TMB cutoff (17.6), we divided patients into the high- and low-TMB groups. Patients in the low-TMB group showed notably poorer response and survival (median OS: low-TMB group, 15.0 months; high-TMB group, not reached; hazard ratio: 1.62; 95% CI: 1.00–2.60; P=0.047) (**Figure 3A**). When stratified by the TMB status, our *TP53/PIK3CA/ATM* mutation classifier became a more precise model for identifying patients sensitive to ICI therapy. In the high-TMB group, we observed that patients in the high-risk group showed the worst response to ICI therapy (median OS, low-risk group: not reached; moderate-risk group: not reached; high-risk group: 11.5 months; P=0.0025) (**Figure 3B**). Correspondingly, in the low-TMB group, patients in the low-risk group showed the best response to ICI therapy (median OS, low-risk group: 27.0 months; moderate-risk group: 11.0 months; high-risk group: 8.0 months; P=0.0027) (**Figure 3C**).

After adjusting for sex, age, and ICI treatment through multivariate Cox regression analysis, the classifier remained an independent prognostic factor in both subsets (**Supplementary Table 5**).

Validation of the *TP53/PIK3CA/ATM* Mutation Classifier

To estimate the efficacy of the *TP53/PIK3CA/ATM* mutation classifier, we tested the classifier in a 263-cases validation set. The validation set consisted of 237 BC patients from the IMvigor210 cohort (191 [80.6%] men) and 26 BC patients from the Broad/Dana-Farber cohort (18 [69.2%] men). All the patients in the validation set underwent ICI therapy. We once again evaluated the distribution of the risk score for the *TP53/PIK3CA/ATM* mutation classifier and survival status in the validation set. Patients with lower risk scores benefited more from the ICI therapy (**Figure 4A**), in accordance with the results of the training set. Patients in lower risk group showed better therapeutic response and OS (median OS, low-risk group: 16.5 months; moderate-risk group: 10.9 months; high-risk group: 8.1 months; P =0.039) (**Figure 4B**). A negative correlation between risk scores and TMB was also found in the validation set (**Figure 4C**). Univariate and multivariate cox regression analyses of BC patients in the validation set confirmed the results as well (**Supplementary Table 6**).

TP53/PIK3CA/ATM Mutation Classifier in Patients From the Non-ICI Therapy Cohort

When extended to patients with BC from the MSKCC non-ICI cohort, the *TP53/PIK3CA/ATM* mutation classifier did not show significant differences between the three groups (median OS, low-risk group: not reached; moderate-risk group: 30.5 months; high-risk group: not reached; P= 0.27) (**Supplementary Figure 6A**). Similar results were noted in patients with BC from the TCGA cohort (median OS, low-risk group: 26.9 months; moderate-risk group: 41.7 months; high-risk group: 22.1 months; P=0.55) (**Supplementary Figure 6B**). These findings demonstrated the specificity of the predictive value of the *TP53/PIK3CA/ATM* mutation classifier in patients with BC responding to ICI therapy.

Gene Signatures and Pathway Enrichment Analysis by the *TP53/PIK3CA/ATM* Mutation Classifier

To further investigate the gene signatures of the *TP53/PIK3CA/ATM* mutation classifier based on RNA-seq data, we utilized the TCGA cohort and IMvigor210 cohort. Lower expression of PD-1 (FPKM: 27.7 *vs.* 57.6, respectively; P<0.001) and PD-L1 (FPKM: 35.0 *vs.* 79.8, respectively; P=0.001) were observed in the high-risk group than the other two groups (**Figures 5A, B**) in the TCGA

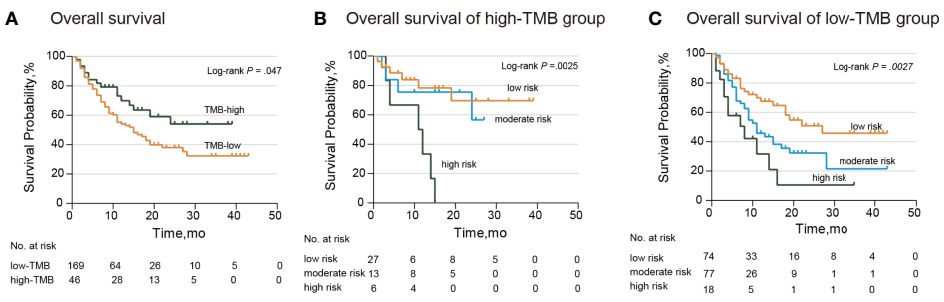

FIGURE 3 | Subgroup Analysis of Overall Survival in the MSKCC ICI cohort stratified by TMB. **(A)** Kaplan–Meier curves of overall survival in patients with BC by TMB. The median overall survival was 15.0 months (95% CI: 10.6–19.4 months) in the low-TMB group and not reached in the high-TMB group. **(B)** Kaplan–Meier curves of overall survival in patients from the high-TMB group. The median overall survival was 11.5 months (95% CI: 1.4–20.6 months) and not reached in the other two groups. **(C)** Kaplan–Meier curves of overall survival in patients from the low-TMB group. The median overall survival was 27.0 months (95% CI: not available) in the low-risk group, 11.0 months (95% CI: 7.5–14.5 months) in the moderate-risk group, and 7.0 months (95% CI: 10.6–19.4 months) in the high-risk group. BC, bladder cancer; CI, confidence interval; TMB, tumor mutation burden.

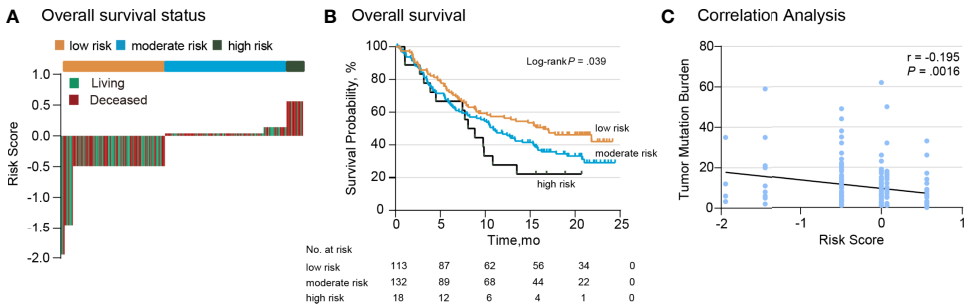

FIGURE 4 | Validation of the *TP53/PIK3CA/ATM* Mutation Classifier. **(A)** OS status in the validation set. "Living" and "Deceased" patients were marked green and red, respectively. **(B)** Kaplan–Meier curves of overall survival in the validation set based on the TP53/PIK3CA/ATM mutation classifier. The median overall survival was 8.1 months (95% CI: 5.8–10.4 months) in the high-risk group, 10.9 months (95% CI: 8.2–13.6 months) in the moderate-risk group, and 16.5 months (95% CI: 10.1–22.8 months) in the low-risk group. **(C)** Correlation between the risk score and TMB in the validation set.

cohort. Similar results were found in the IMvigor210 cohort (**Figures 5C–E**). The GSEA was performed between the low-risk group and high-risk group in the TCGA cohort to appraise the hallmark gene sets, C2: KEGG gene sets and C7: immunologic signature gene sets (**Supplementary Figure 7**). Intriguingly, we found that cell cycle-related pathways, such as the E2F targets (FDR=0.06) and G2M checkpoint (FDR=0.11), were enriched in hallmark gene sets. Altered pathways from the C2 subset in the low-risk group, including homologous recombination (FDR=0.03), pyrimidine metabolism (FDR=0.06), purine metabolism (FDR=0.08), and DNA replication (FDR=0.07), were related to the genomic stability status. Variation in these pathways may lead to higher TMB and MSI. In the C7 immunologic sets, 114 gene sets were significantly enriched in the low-risk group (FDR<0.25), indicating an intense immune activation status. Correspondingly, there was no set found in the high-risk group. In general, the GSEA uncovered enriched pathways in cell cycle, DNA repair, and immune infiltration.

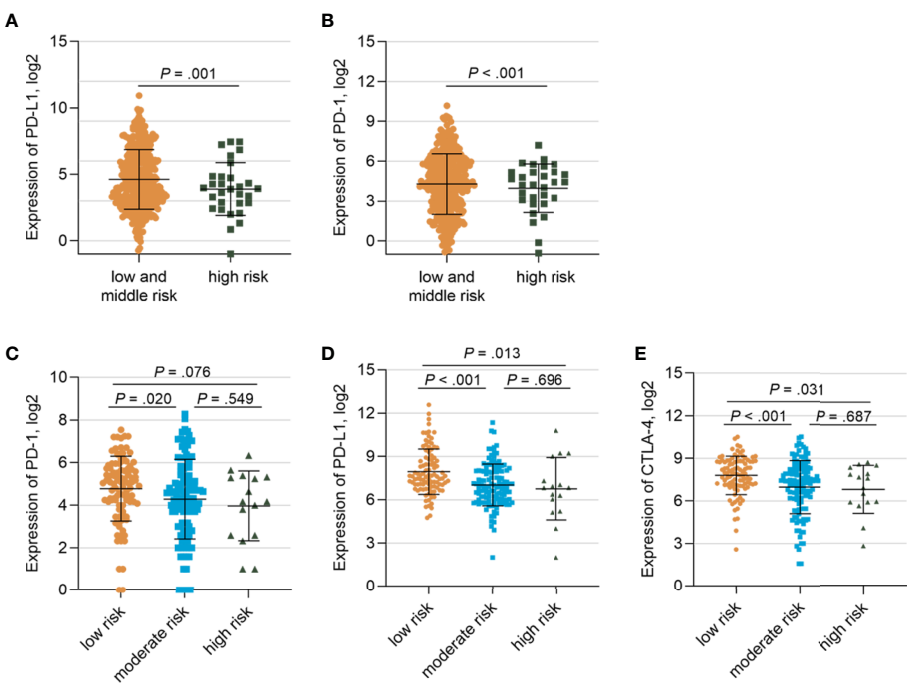

FIGURE 5 | Gene Expressions of Patients in the TCGA Cohort and IMvigor210 cohort stratified by the *TP53/PIK3CA/ATM* Mutation Classifier **(A)** Comparison of the expression of PD-1 between the low- and moderate-risk group and the high-risk group. **(B)** Comparison of the expression of PD-L1 between the low and moderate -risk group and the high-risk group. **(C)** Comparison of the expression of PD-1 among three risk groups in IMvigor210 cohort. **(D)** Comparison of the expression of PD-L1 among three risk groups in IMvigor210 cohort. **(E)** Comparison of the expression of CTLA-4 among three risk groups in IMvigor210 cohort.

Immune Infiltration Analysis by the *TP53/PIK3CA/ATM* Mutation Classifier

We ran the ESTIMATE algorithm to predict the tumor purity and infer the fractions of stromal cells and immune cells in the TCGA cohort and IMvigor210 cohort. There were conspicuous statistical differences in immune scores, estimate scores, and tumor purity among three risk groups in the TCGA cohort (**Figure 6A**). The low-risk group was infiltrated by more immune cells and consisted of fewer tumor cells than the high-risk group, in accordance with the better response to ICI therapy. Among the 22 immune cell subsets of the CIBERSORT algorithm in the TCGA cohort, M2 macrophages, M0 macrophages, helper T cells, resting memory CD4+ T cells, and CD8+ T cells were the five most abundant immune cell components, which accounted for >57.4% of immune cells (**Figure 6B**). The correlation between different fractions of immune cell subsets ranged from −0.38 to 0.38 (**Figure 6C**). The proportion of 22 immune cell subsets by the CIBERSORT algorithm and immune correlation heatmap in the IMvigor210 cohort were shown in **Supplementary Figures 8A, B**. The fractions of resting memory CD4+ T cells and monocytes were higher in the high-risk group of the TCGA cohort (**Figures 7A, B**). In contrast, the fraction of activated memory CD4+ T cells was higher in the low-risk group (**Figure 7C**). Higher expression of activated NK cells, M1 Macrophages, and gamma delta T cells were also observed in low-risk group of the IMvigor210 cohort (**Supplementary Figures 8C–E**). In addition, we utilized the TIMER algorithm and noticed a higher B cell fraction in the low-risk group of the TCGA cohort and a higher neutrophil fraction in the low-risk group of IMvigor210 cohort (**Figure 7D**; **Supplementary Figure 8F**). The heatmap of immune cells by the TIMER and CIBERSORT algorithms in the TCGA cohort also revealed more immune infiltration in the low-risk group (**Supplementary Figure 9**). Importantly, the low-risk group showed a more active immune response status compared with the high-risk group in both two cohorts.

DISCUSSION

Over the past few decades, platinum-based chemotherapy has become the standard option for the systemic management of muscle-invasive and advanced BC (29). However, with the rapid development in genomic sequencing technology in recent years, ICI therapy has shown great potential in advanced BC patients with high TMB. A subset of patients could benefit from durable response to ICI therapy. Then overcoming innate and adaptive resistance to therapy has been a top priority for investigators. Therefore, the discovery of novel biomarkers for predicting the therapeutic response to ICI therapy is urgently warranted. Gene expression signatures, MSI and TMB, have been proven to be effective (6, 8, 30, 31). Other indicators under evaluation include tumor-infiltrated

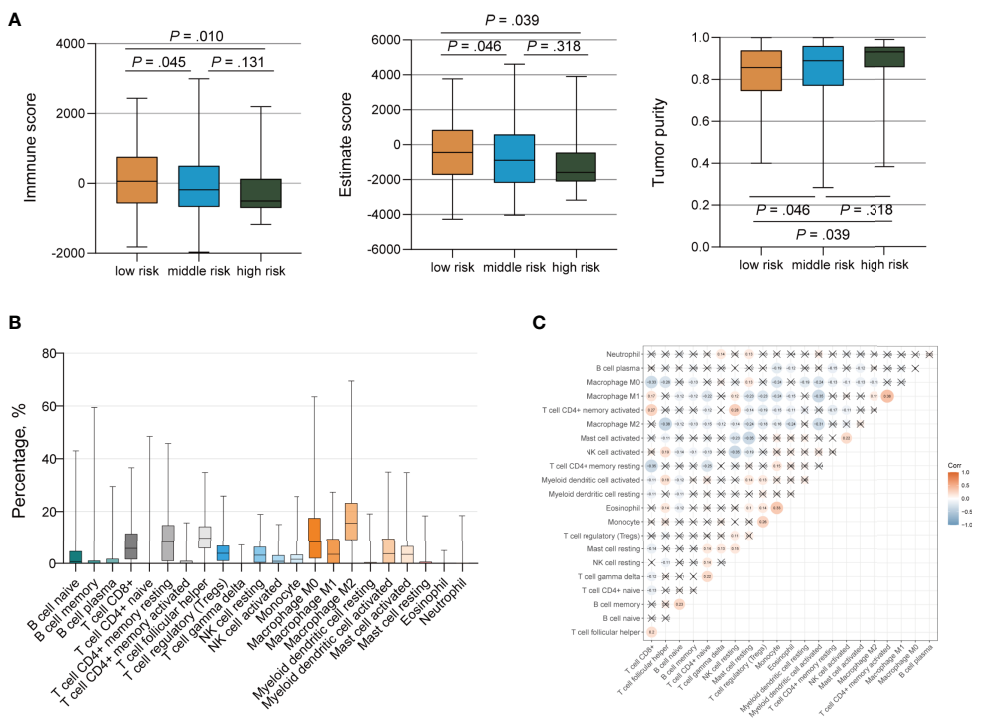

FIGURE 6 | Immune Infiltration of Tumor Cells by the *TP53/PIK3CA/ATM* Mutation Classifier. **(A)** Immune scores, estimate scores, and tumor purity distribution by the ESTIMATE algorithm. **(B)** Proportion of 22 immune cell subsets by the CIBERSORT algorithm. **(C)** Correlation heatmap of 22 immune cell subsets by the CIBERSORT algorithm. The blue color represents negative correlation, while the red color represents positive correlation. Correlations with a *P* value ≥ 0.05 were marked with a cross.

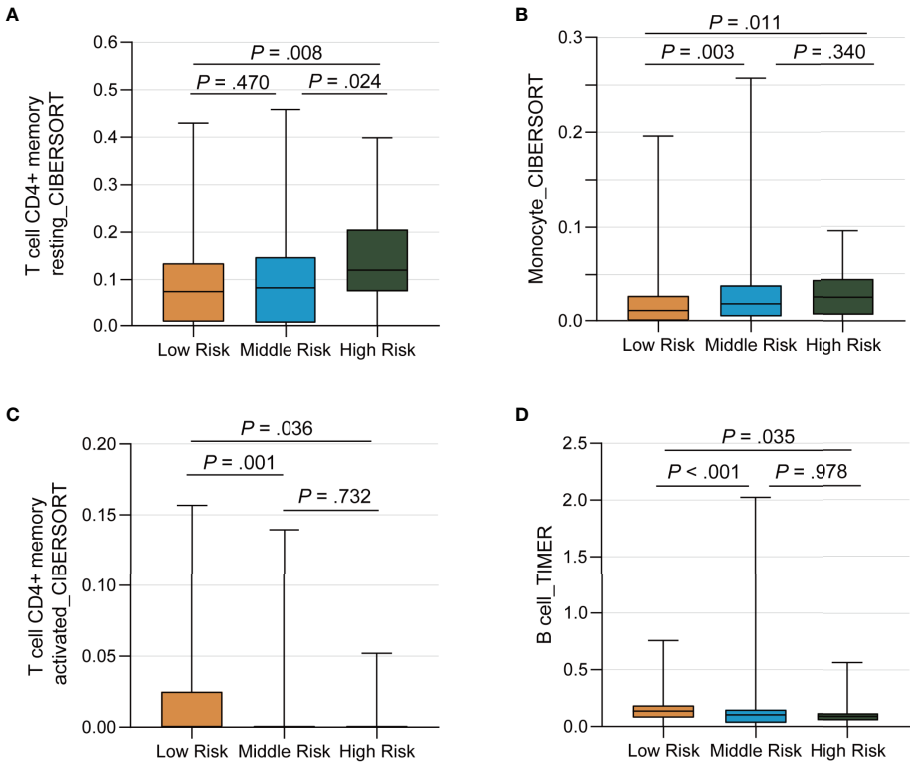

FIGURE 7 | Differential Distribution of Immune Infiltration Cells by the *TP53/PIK3CA/ATM* Mutation Classifier. **(A–C)** The fraction of resting memory CD4+ T cells, activated memory CD4+ T cells, and monocytes by the CIBERSORT algorithm, respectively. **(D)** The fraction of B cells by the TIMER algorithm.

lymphocytes, neoantigen burden, and gastrointestinal microbiome (32–35). In this study, we identified the top 20 frequently mutated genes in five BC cohorts, and established a *TP53*/*PIK3CA*/*ATM* mutation classifier according to the MSKCC ICI cohort. We subsequently confirmed the efficacy of the classifier in the validation set, and investigated its molecular profile and immune infiltration in the TCGA cohort and IMvigor 210 cohort. It could be concluded that BC patients with lower risk scores had a longer survival. Importantly, it seemed to only work on BC patients treated with ICIs. Moreover, BC patients with high-risk scores appeared to have a poorer immune infiltration than those with low- or moderate-risk scores.

Genome instability and mutation is a brand-new hallmark of cancers (36, 37). According to a study of the mutational landscape across 12 major types of cancer from TCGA program, *TP53* (41%) and *PIK3CA* (20%) are the top two most commonly mutated genes (38). The inclusion of these two genes improves the universality of the classifier. M. Choi et al. found that *PIK3CA* mutations were related to remarkably reduced peritumoral PD-1 and tumoral *PD-L1* in lung squamous cell carcinoma (LUSC) (39). Tao et al. also reported that *PIK3CA* mutations were connected with significantly lower infiltration of macrophage in LUSC (40). Generally speaking, *PIK3CA* mutations led to the activation of PI3K-AKT-mTOR signaling pathway. Activated PI3K-AKT-mTOR pathway increased production of free fatty acids, which were more effectively consumed by regulatory T cells and decreased effector T cell infiltration (41). Moreover, Borcoman et al. reported that PI3K inhibitors could increase the immune infiltration of BC with *PIK3CA* mutations, thus restoring the sensitivity to ICIs (42). These findings may partially interpret the attenuated response to ICI therapy in patients with *PIK3CA* mutations. *ATM* plays an important role in the regulation of the DNA damage response mechanism. Mutations in this gene are related to ataxia telangiectasia and tumor response to treatment, such as BC, prostate cancer, etc. (43). Its crucial role in response to double-strand breaks (DSB) has been noted, followed by the phosphorylation of extensive downstream signaling pathways (44). Phosphorylated p53 is subsequently stabilized and accumulated in the nucleus, acting as a central transcription factor for the regulation of DNA repair (45). The repair of DSB mainly involves homologous recombination and non-homologous end joining (46). Homologous recombination deficiency caused by mutation of *ATM*/*TP53* results in a preference to non-homologous end joining, which is a type of less accurate DSB repair and associated with higher TMB. Yu et al. discovered that comutation of *TP53* and *ATM* was associated with increased responses to ICIs in non–small cell lung cancer (9), while comutation of *TP53* and *ATM* was also divided into low-risk group in our classifier.

In our study, the low-risk group yielded a higher immune score than the other two groups, according to the ESTIMATE algorithm. Immune infiltration analysis revealed higher expression of B cells and activated memory CD4+ T cells, as well as lower expression of resting memory CD4+ T cells and monocytes in the low-risk group. Recent studies have shown that overexpression of monocytes enhanced the levels of glycolysis in the peritumoral area, leading to impaired cytotoxic T lymphocyte responses in tumors (47). Excessive production of interleukin-10 by monocytes leads to reversible dysfunction of CD4+ T cells (48). Accordingly, correlation analysis showed a positive correlation between monocytes and regulatory T cells. Importantly, the low-risk group exhibited a relatively more activated immune status than the high-risk group in two cohorts, indicating a greater benefit from ICI therapy.

The GSEA showed enriched pathways in cell cycle, DNA repair, and tumor metabolism in the low-risk group. Generally speaking, deficiencies in DNA damage response increase the tumor mutation load and the generation of neoantigen burden, which helps the immune system to recognize the tumor. The effect of *ATM*/*TP53* mutation may be amplified by the pathways, resulting in an accelerated accumulation of the mutation burden.

Compared with traditional chemotherapy and targeted therapy, ICI therapy requires a longer period of time to show its curative effects. In a retrospective study of 262 patients treated with anti-*PD-L1* monotherapy, 48 of 76 responder patients presented an objective response at 3 months (49). Our approach can distinguish patients who are sensitive to ICI therapy and accelerate the benefits of treatment. Meanwhile, we need to pay closer attention to the management of patients in the high-risk group. Since an undesirable curative response to ICI therapy is foreseeable, traditional chemotherapy or combined treatment with chemotherapy and targeted therapy need to be taken into consideration at the early stage of management.

Despite these promising findings, the present study had several limitations. Firstly, we conducted a retrospective study based on online published data. The findings should be verified in prospective studies with larger cohorts in the future. Secondly, we conducted substantial immune infiltration analyses through bioinformatics algorithms like the ESTIMATE algorithm, the CIBERSORT algorithm and the TIMER algorithm. The fidelity of reference profiles is the limitation of the signature gene-based algorithms. The results may deviate in tumor-induced dysregulation, phenotypic plasticity, and tumor heterogeneity. Besides, we could not ignore the different results among algorithms. Modified algorithms are needed to reconcile differences among the existing algorithms. Thirdly, the mechanisms underlying the *TP53*/*PIK3CA*/*ATM* mutations and response to ICI therapy remain unclear. Further investigation is warranted to understand the full impact of *TP53*/*PIK3CA*/*ATM* mutations.

In summary, our *TP53*/*PIK3CA*/*ATM* mutation classifier could predict the therapeutic response of patients with BC to ICI therapy. Only BC patients treated with ICIs and with lower risk scores had a longer survival. Stronger immune infiltration was observed in the low-risk group of the classifier. The present findings have important implications for clinical treatment strategy.

CONCLUSION

We established a *TP53/PIK3CA/ATM* mutation classifier to predict the therapeutic response of patients with BC to ICI therapy. This classifier has the potential to become a useful complement to TMB and guide the clinical treatment decision according to the levels of risk.

DATA AVAILABILITY STATEMENT

The original contributions presented in the study are included in the article/**Supplementary Material**. Further inquiries can be directed to the corresponding authors.

ETHICS STATEMENT

Ethical review and approval was not required for the study on human participants in accordance with the local legislation and institutional requirements. Written informed consent for participation was not required for this study in accordance with the national legislation and the institutional requirements.

AUTHOR CONTRIBUTIONS

J-HL and Y-HP made contributions to conception, design, statistical analysis and drafting of the manuscript. J-XZ, XC, and FL acquired the data. J-ZC, WC, and YC provide administrative, technical support. YC, WC, and J-HL supervised the study. All authors contributed to the article and approved the submitted version.

FUNDING

The article was supported by the National Natural Science Foundation of China (81725016, 81872094, 81772718, 81572522); Natural Science Foundation of Guangdong Province (2017B020227004). The funders had no role in the design and conduct of the study; collection, management, analysis, and interpretation of the data; preparation, review, or approval of the manuscript; and decision to submit the manuscript for publication.

ACKNOWLEDGMENTS

We thank the cBioPortal for Cancer Genomics and the TCGA for their efforts and providing data.

SUPPLEMENTARY MATERIAL

The Supplementary Material for this article can be found online at: https://www.frontiersin.org/articles/10.3389/fimmu.2021.643282/full#supplementary-material

REFERENCES

1. Aggen DH, Drake CG. Biomarkers for Immunotherapy in Bladder Cancer: A Moving Target. *J Immunother Cancer* (2017) 5(1):94. doi: 10.1186/s40425-017-0299-1
2. Balar AV, Galsky MD, Rosenberg JE, Powles T, Petrylak DP, Bellmunt J, et al. Atezolizumab as First-Line Treatment in Cisplatin-Ineligible Patients With Locally Advanced and Metastatic Urothelial Carcinoma: A Single-Arm, Multicentre, Phase 2 Trial. *Lancet* (2017) 389(10064):67–76. doi: 10.1016/S0140-6736(16)32455-2
3. Rosenberg JE, Hoffman-Censits J, Powles T, van der Heijden MS, Balar AV, Necchi A, et al. Atezolizumab in Patients With Locally Advanced and Metastatic Urothelial Carcinoma Who Have Progressed Following Treatment With Platinum-Based Chemotherapy: A Single-Arm, Multicentre, Phase 2 Trial. *Lancet* (2016) 387(10031):1909–20. doi: 10.1016/S0140-6736(16)00561-4
4. Sharma P, Retz M, Siefker-Radtke A, Baron A, Necchi A, Bedke J, et al. Nivolumab in Metastatic Urothelial Carcinoma After Platinum Therapy (CheckMate 275): A Multicentre, Single-Arm, Phase 2 Trial. *Lancet Oncol* (2017) 18(3):312–22. doi: 10.1016/S1470-2045(17)30065-7
5. Bellmunt J, de Wit R, Vaughn DJ, Fradet Y, Lee JL, Fong L, et al. Pembrolizumab as Second-Line Therapy for Advanced Urothelial Carcinoma. *N Engl J Med* (2017) 376(11):1015–26. doi: 10.1056/NEJMoa1613683
6. Samstein RM, Lee CH, Shoushtari AN, Hellmann MD, Shen R, Janjigian YY, et al. Tumor Mutational Load Predicts Survival After Immunotherapy Across Multiple Cancer Types. *Nat Genet* (2019) 51(2):202–6. doi: 10.1038/s41588-018-0312-8
7. Mandal R, Samstein RM, Lee KW, Havel JJ, Wang H, Krishna C, et al. Genetic Diversity of Tumors With Mismatch Repair Deficiency Influences Anti-PD-1 Immunotherapy Response. *Science* (2019) 364(6439):485–91. doi: 10.1126/science.aau0447
8. Petrelli F, Ghidini M, Ghidini A, Tomasello G. Outcomes Following Immune Checkpoint Inhibitor Treatment of Patients With Microsatellite Instability-High Cancers: A Systematic Review and Meta-Analysis. *JAMA Oncol* (2020) 6 (7):1068–71. doi: 10.1001/jamaoncol.2020.1046
9. Chen Y, Chen G, Li J, Huang YY, Li Y, Lin J, et al. Association of Tumor Protein P53 and Ataxia-Telangiectasia Mutated Comutation With Response to Immune Checkpoint Inhibitors and Mortality in Patients With Non-Small Cell Lung Cancer. *JAMA Netw Open* (2019) 2(9):e1911895. doi: 10.1001/jamanetworkopen.2019.11895
10. Wang F, Zhao Q, Wang YN, Jin Y, He MM, Liu ZX, et al. Evaluation of POLE and POLD1 Mutations as Biomarkers for Immunotherapy Outcomes Across Multiple Cancer Types. *JAMA Oncol* (2019) 50(10):1504–6. doi: 10.1001/jamaoncol.2019.2963
11. Teo MY, Seier K, Ostrovnaya I, Regazzi AM, Kania BE, Moran MM, et al. Alterations in DNA Damage Response and Repair Genes as Potential Marker of Clinical Benefit From PD-1/PD-L1 Blockade in Advanced Urothelial Cancers. *J Clin Oncol* (2018) 36(17):1685–94. doi: 10.1200/JCO.2017.75.7740
12. Vidotto T, Nersesian S, Graham C, Siemens DR, Koti M. DNA Damage Repair Gene Mutations and Their Association With Tumor Immune Regulatory Gene Expression in Muscle Invasive Bladder Cancer Subtypes. *J Immunother Cancer* (2019) 7(1):148. doi: 10.1186/s40425-019-0619-8
13. Goswami S, Chen Y, Anandhan S, Szabo PM, Basu S, Blando JM, et al. ARID1A Mutation Plus CXCL13 Expression Act as Combinatorial Biomarkers to Predict Responses to Immune Checkpoint Therapy in mUCC. *Sci Transl Med* (2020) 12(548):eabc4220. doi: 10.1126/scitranslmed.abc4220
14. Zehir A, Benayed R, Shah RH, Syed A, Middha S, Kim HR, et al. Mutational Landscape of Metastatic Cancer Revealed From Prospective Clinical Sequencing of 10,000 Patients. *Nat Med* (2017) 23(6):703–13. doi: 10.1038/nm.4333
15. Robertson AG, Kim J, Al-Ahmadie H, Bellmunt J, Guo G, Cherniack AD, et al. Comprehensive Molecular Characterization of Muscle-Invasive Bladder Cancer. *Cell* (2017) 171(3):540–56.e25. doi: 10.1016/j.cell.2017.09.007
16. Faltas BM, Prandi D, Tagawa ST, Molina AM, Nanus DM, Sternberg C, et al. Clonal Evolution of Chemotherapy-Resistant Urothelial Carcinoma. *Nat Genet* (2016) 48(12):1490–9. doi: 10.1038/ng.3692
17. Van Allen EM, Mouw KW, Kim P, Iyer G, Wagle N, Al-Ahmadie H, et al. Somatic ERCC2 Mutations Correlate With Cisplatin Sensitivity in Muscle-Invasive Urothelial Carcinoma. *Cancer Discovery* (2014) 4(10):1140–53. doi: 10.1158/2159-8290.CD-14-0623
18. Miao D, Margolis CA, Vokes NI, Liu D, Taylor-Weiner A, Wankowicz SM, et al. Genomic Correlates of Response to Immune Checkpoint Blockade in Microsatellite-Stable Solid Tumors. *Nat Genet* (2018) 50(9):1271–81. doi: 10.1038/s41588-018-0200-2
19. Cerami E, Gao J, Dogrusoz U, Gross BE, Sumer SO, Aksoy BA, et al. The Cbio Cancer Genomics Portal: An Open Platform for Exploring Multidimensional Cancer Genomics Data. *Cancer Discov* (2012) 2(5):401–4. doi: 10.1158/2159-8290.CD-12-0095
20. Mariathasan S, Turley SJ, Nickles D, Castiglioni A, Yuen K, Wang Y, et al. TGFbeta Attenuates Tumour Response to PD-L1 Blockade by Contributing to Exclusion of T Cells. *Nature* (2018) 554(7693):544–8. doi: 10.1038/nature25501
21. Camp RL, Dolled-Filhart M, Rimm DL. X-Tile: A New Bio-Informatics Tool for Biomarker Assessment and Outcome-Based Cut-Point Optimization. *Clin Cancer Res* (2004) 10(21):7252–9. doi: 10.1158/1078-0432.CCR-04-0713
22. Mayakonda A, Lin DC, Assenov Y, Plass C, Koeffler HP. Maftools: Efficient and Comprehensive Analysis of Somatic Variants in Cancer. *Genome Res* (2018) 28(11):1747–56. doi: 10.1101/gr.239244.118
23. Shannon P, Markiel A, Ozier O, Baliga NS, Wang JT, Ramage D, et al. Cytoscape: A Software Environment for Integrated Models of Biomolecular Interaction Networks. *Genome Res* (2003) 13(11):2498–504. doi: 10.1101/gr.1239303
24. Yoshihara K, Shahmoradgoli M, Martinez E, Vegesna R, Kim H, Torres-Garcia W, et al. Inferring Tumour Purity and Stromal and Immune Cell Admixture From Expression Data. *Nat Commun* (2013) 4:2612. doi: 10.1038/ncomms3612
25. Newman AM, Liu CL, Green MR, Gentles AJ, Feng W, Xu Y, et al. Robust Enumeration of Cell Subsets From Tissue Expression Profiles. *Nat Methods* (2015) 12(5):453–7. doi: 10.1038/nmeth.3337
26. Li B, Severson E, Pignon JC, Zhao H, Li T, Novak J, et al. Comprehensive Analyses of Tumor Immunity: Implications for Cancer Immunotherapy. *Genome Biol* (2016) 17(1):174. doi: 10.1186/s13059-016-1028-7
27. Li T, Fu J, Zeng Z, Cohen D, Li J, Chen Q, et al. TIMER2.0 for Analysis of Tumor-Infiltrating Immune Cells. *Nucleic Acids Res* (2020) 48(W1):W509–14. doi: 10.1093/nar/gkaa407
28. Alexandrov LB, Nik-Zainal S, Wedge DC, Aparicio SA, Behjati S, Biankin AV, et al. Signatures of Mutational Processes in Human Cancer. *Nature* (2013) 500 (7463):415–21. doi: 10.1038/nature12477
29. Patel VG, Oh WK, Galsky MD. Treatment of Muscle-Invasive and Advanced Bladder Cancer in 2020. *CA Cancer J Clin* (2020) 70(5):404–23. doi: 10.3322/caac.21631
30. Le DT, Uram JN, Wang H, Bartlett BR, Kemberling H, Eyring AD, et al. PD-1 Blockade in Tumors With Mismatch-Repair Deficiency. *N Engl J Med* (2015) 372(26):2509–20. doi: 10.1056/NEJMoa1500596
31. Schoenfeld AJ, Rizvi H, Bandlamudi C, Sauter JL, Travis WD, Rekhtman N, et al. Clinical and Molecular Correlates of PD-L1 Expression in Patients With Lung Adenocarcinomas. *Ann Oncol* (2020) 31(5):599–608. doi: 10.1016/j.annonc.2020.01.065
32. Mager LF, Burkhard R, Pett N, Cooke NCA, Brown K, Ramay H, et al. Microbiome-Derived Inosine Modulates Response to Checkpoint Inhibitor Immunotherapy. *Science* (2020) 369(6510):1481–9. doi: 10.1126/science.abc3421
33. McGranahan N, Furness AJ, Rosenthal R, Ramskov S, Lyngaa R, Saini SK, et al. Clonal Neoantigens Elicit T Cell Immunoreactivity and Sensitivity to Immune Checkpoint Blockade. *Science* (2016) 351(6280):1463–9. doi: 10.1126/science.aaf1490
34. Stanton SE, Adams S, Disis ML. Variation in the Incidence and Magnitude of Tumor-Infiltrating Lymphocytes in Breast Cancer Subtypes: A Systematic Review. *JAMA Oncol* (2016) 2(10):1354–60. doi: 10.1001/jamaoncol.2016.1061
35. Howitt BE, Shukla SA, Sholl LM, Ritterhouse LL, Watkins JC, Rodig S, et al. Association of Polymerase E-Mutated and Microsatellite-Instable Endometrial Cancers With Neoantigen Load, Number of Tumor-Infiltrating Lymphocytes, and Expression of PD-1 and PD-L1. *JAMA Oncol* (2015) 1 (9):1319–23. doi: 10.1001/jamaoncol.2015.2151
36. Hanahan D, Weinberg RA. Hallmarks of Cancer: The Next Generation. *Cell* (2011) 144(5):646–74. doi: 10.1016/j.cell.2011.02.013

37. Negrini S, Gorgoulis VG, Halazonetis TD. Genomic Instability–an Evolving Hallmark of Cancer. *Nat Rev Mol Cell Biol* (2010) 11(3):220–8. doi: 10.1038/nrm2858
38. Hoadley KA, Yau C, Wolf DM, Cherniack AD, Tamborero D, Ng S, et al. Multiplatform Analysis of 12 Cancer Types Reveals Molecular Classification Within and Across Tissues of Origin. *Cell* (2014) 158(4):929–44. doi: 10.1016/j.cell.2014.06.049
39. Choi M, Kadara H, Zhang J, Parra ER, Rodriguez-Canales J, Gaffney SG, et al. Mutation Profiles in Early-Stage Lung Squamous Cell Carcinoma With Clinical Follow-Up and Correlation With Markers of Immune Function. *Ann Oncol* (2017) 28(1):83–9. doi: 10.1093/annonc/mdw437
40. Jiang T, Shi J, Dong Z, Hou L, Zhao C, Li X, et al. Genomic Landscape and its Correlations With Tumor Mutational Burden, PD-L1 Expression, and Immune Cells Infiltration in Chinese Lung Squamous Cell Carcinoma. *J Hematol Oncol* (2019) 12(1):75. doi: 10.1186/s13045-019-0762-1
41. Kumagai S, Togashi Y, Sakai C, Kawazoe A, Kawazu M, Ueno T, et al. An Oncogenic Alteration Creates a Microenvironment That Promotes Tumor Progression by Conferring a Metabolic Advantage to Regulatory T Cells. *Immunity* (2020) 53(1):187–203.e8. doi: 10.1016/j.immuni.2020.06.016
42. Borcoman E, de la Rochere P, Richer W, Vacher S, Chemlali W, Krucker C, et al. Inhibition of PI3K Pathway Increases Immune Infiltrate in Muscle-Invasive Bladder Cancer. *Oncoimmunology* (2019) 8(5):e1581556. doi: 10.1080/2162402X.2019.1581556
43. Shiloh Y, Ziv Y. The ATM Protein Kinase: Regulating the Cellular Response to Genotoxic Stress, and More. *Nat Rev Mol Cell Biol* (2013) 14(4):197–210. doi: 10.1038/nrm3546
44. Alvarez-Quilon A, Serrano-Benitez A, Lieberman JA, Quintero C, Sanchez-Gutierrez D, Escudero LM, et al. ATM Specifically Mediates Repair of Double-Strand Breaks With Blocked DNA Ends. *Nat Commun* (2014) 5:3347. doi: 10.1038/ncomms4347
45. Jiang H, Reinhardt HC, Bartkova J, Tommiska J, Blomqvist C, Nevanlinna H, et al. The Combined Status of ATM and P53 Link Tumor Development With Therapeutic Response. *Genes Dev* (2009) 23(16):1895–909. doi: 10.1101/gad.1815309
46. Mao Z, Bozzella M, Seluanov A, Gorbunova V. Comparison of Nonhomologous End Joining and Homologous Recombination in Human Cells. *DNA Repair (Amst)* (2008) 7(10):1765–71. doi: 10.1016/j.dnarep.2008.06.018
47. Chen DP, Ning WR, Jiang ZZ, Peng ZP, Zhu LY, Zhuang SM, et al. Glycolytic Activation of Peritumoral Monocytes Fosters Immune Privilege *via* the PFKFB3-PD-L1 Axis in Human Hepatocellular Carcinoma. *J Hepatol* (2019) 71(2):333–43. doi: 10.1016/j.jhep.2019.04.007
48. Said EA, Dupuy FP, Trautmann L, Zhang Y, Shi Y, El-Far M, et al. Programmed Death-1-Induced Interleukin-10 Production by Monocytes Impairs CD4+ T Cell Activation During HIV Infection. *Nat Med* (2010) 16(4):452–9. doi: 10.1038/nm.2106
49. Gauci ML, Lanoy E, Champiat S, Caramella C, Ammari S, Aspeslagh S, et al. Long-Term Survival in Patients Responding to Anti-PD-1/PD-L1 Therapy and Disease Outcome Upon Treatment Discontinuation. *Clin Cancer Res* (2019) 25(3):946–56. doi: 10.1158/1078-0432.CCR-18-0793

Conflict of Interest: The authors declare that the research was conducted in the absence of any commercial or financial relationships that could be construed as a potential conflict of interest.

Publisher's Note: All claims expressed in this article are solely those of the authors and do not necessarily represent those of their affiliated organizations, or those of the publisher, the editors and the reviewers. Any product that may be evaluated in this article, or claim that may be made by its manufacturer, is not guaranteed or endorsed by the publisher.

frontiers in Oncology

REVIEW
published: 01 October 2021
doi: 10.3389/fonc.2021.706910

The Prognostic Value of ctDNA and bTMB on Immune Checkpoint Inhibitors in Human Cancer

Jiayan Wei†, Jia Feng†, Yiming Weng, Zexi Xu, Yao Jin, Peiwei Wang, Xue Cui, Peng Ruan, Ruijun Luo, Na Li and Min Peng**

Department of Oncology, Renmin Hospital of Wuhan University, Wuhan, China

OPEN ACCESS

Edited by:
Roberta Zappasodi, Memorial Sloan Kettering Cancer Center, United States

Reviewed by:
Yasin Senbabaoglu, Genentech, Inc., United States
David Stephen Guttery, University of Leicester, United Kingdom

***Correspondence:**
Na Li
nalirenmin@163.com
Min Peng
mpeng320@whu.edu.cn

†These authors share first authorship

Specialty section:
This article was submitted to Cancer Immunity and Immunotherapy, a section of the journal Frontiers in Oncology

Received: *08 May 2021*
Accepted: *13 September 2021*
Published: *01 October 2021*

Citation:
Wei J, Feng J, Weng Y, Xu Z, Jin Y, Wang P, Cui X, Ruan P, Luo R, Li N and Peng M (2021) The Prognostic Value of ctDNA and bTMB on Immune Checkpoint Inhibitors in Human Cancer. Front. Oncol. 11:706910. doi: 10.3389/fonc.2021.706910

Background: Circulating tumor DNA (ctDNA) levels and blood tumor mutation burden (bTMB) have a significant impact on the prognosis of tumor patients. However, their prognostic role in immune checkpoint inhibitors (ICIs) in cancer patients is still unclear.

Methods: We used the Review Manager software (version 5.3) to perform a meta-analysis based on the published literature to explore the prognostic value of ctDNA and bTMB in patients receiving immunotherapy. We extracted the hazard ratios (HRs) of progression-free survival (PFS) and overall survival (OS) for each included study and their respective 95% confidence intervals (CIs) and *p*-values for analysis.

Results: Thirteen studies were included in the meta-analysis. Higher ctDNA levels were significantly associated with shorter OS (HR = 3.35, 95%CI = 2.49–4.51, $p < 0.00001$) and PFS (HR = 3.28, 95%CI = 2.47–4.35, $p < 0.00001$). The results of ctDNA subgroup analysis showed that high posttreatment ctDNA levels significantly correlated with shorter OS in cancer patients receiving ICIs (HR = 5.09, 95%CI = 1.43–18.07, $p = 0.01$). Moreover, patients with ctDNA clearance had better OS (HR = 4.94, 95%CI = 2.96–8.26, $p < 0.00001$). Patients with high posttreatment ctDNA levels had shorter PFS (HR = 3.00, 95%CI = 2.02–4.46, $p < 0.00001$) and those with ctDNA clearance had longer PFS (HR = 4.61, 95%CI = 2.78–7.65, $p < 0.00001$). However, there was no statistically significant difference in the OS benefits between a high and a low bTMB after ICI therapy (HR = 0.68, 95%CI = 0.33–1.37, $p = 0.28$).

Conclusions: The host immune system and tumor burden together determine whether cancer patients can benefit from ICI therapy. Our systematic review and meta-analysis revealed for the first time that the levels of pretreatment and posttreatment ctDNA and the clearance of ctDNA can independently be used as prognostic factors for antitumor immunotherapy, while bTMB cannot. In conclusion, ctDNA levels have great potential as an assistant tool for radiological assessments to make clinical therapeutic decisions. The prognostic utility of bTMB still requires further exploration.

Keywords: ctDNA, bTMB, immune checkpoint inhibitor, prognosis, biomarker, meta-analysis

INTRODUCTION

Circulating tumor DNA (ctDNA), a component of cell-free DNA (cfDNA), is released from apoptotic or necrotic tumor cells (1). ctDNA can be measured by polymerase chain reaction (PCR) and next-generation sequencing (NGS) technology, and it is expected to be a new indicator for evaluating tumor burden and treatment response (2). Blood-based tumor mutation burden (bTMB) is the number of mutations per megabase (Mut/Mb) detected in the ctDNA sequencing region and is considered to be a neoantigen load marker that stimulates the immune response of T cells (3). In the past few decades, immune checkpoint inhibitors (ICIs) have been widely used and have shown remarkable effects in a variety of solid tumors, such as non-small cell lung cancer, melanoma, and renal cell carcinoma (4, 5). However, the objective response rate (ORR) was lower than 30% in unselected patients (6), highlighting the need for new biomarkers to identify patients who are more likely to benefit from ICI therapy. Tissue TMB (tTMB) has been used in multiple studies as a biomarker to predict the response to immunotherapy. However, owing to its invasiveness and organizational spatial heterogeneity, operable, easily accessible, and real-time ctDNA and bTMB have attracted more attention.

Several studies have focused on the prognostic impact of ctDNA and bTMB in patients receiving immunotherapy (7–9). However, most of them are characterized by small sample sizes and low universality. Therefore, we conducted a systematic review and meta-analysis on this topic.

MATERIALS AND METHODS

Search Strategy and Study Selection

Relevant published literature was searched for using MEDLINE (PubMed) and EMBASE. The following search terms were used: ctDNA OR circulating biomarker AND immune checkpoint AND cancer NOT review, ctDNA AND predictive AND cancer AND immunotherapy. The last search was updated on August 28, 2021.

The included studies met the following criteria: 1) cohort studies or clinical trials that use ICIs for treatment and ctDNA or bTMB to predict efficacy; 2) the prognostic value of ctDNA or bTMB in cancer patients who had received immunotherapy was investigated; 3) hazard ratios (HRs) of overall survival (OS) and progression-free survival (PFS), as well as their 95% CIs and *p*-values, or sufficient data to calculate them.

The exclusion criteria were as follows: 1) reviews, case reports, meeting abstracts, letters, expert opinions, and animal studies; and 2) no English translation of the study.

Data Extraction

Data were extracted from the included studies. The following pieces of information were extracted from each study: author name, year of publication, tumor type, study type, blood biomarker type, timing of biomarker, biomarker detection method, cutoff point of blood biomarker, type of ICI used, type of outcome, and results (HRs and 95% CIs).

Quality Assessment

The risk bias evaluation tool (Cochrane Handbook for Systematic Reviews of Interventions) was used to evaluate the quality of the included studies. Seven evaluation items were used to examine the quality of the research: random sequence generation, allocation concealment, blinding of participants and personnel, blinding of outcome assessment, incomplete outcome data, selective reporting, and other sources of bias.

Statistical Analysis

We used the Review Manager software (version 5.3) to analyze the prognostic effects of ctDNA and bTMB in tumor patients receiving ICI therapy. The HRs of PFS and OS and their 95% CIs were used to calculate the pooled estimates of the meta-analysis. Statistical significance was set at $p < 0.05$. The heterogeneity of each study was tested using the Higgins I^2 statistic. If I^2 was greater than 50%, it was considered that there was significant heterogeneity between the studies, so the random effects model was used; otherwise, when there was no significant heterogeneity ($I^2 < 50\%$), the fixed effects model was selected. There is no absolute definition of ctDNA or bTMB. The cutoff points for ctDNA and bTMB are not uniform because the studies we included used different techniques to detect biomarkers. To better analyze the data, we defined those biomarkers with values greater than the cutoff points and were detectable, positive, and unclear as high levels of ctDNA or bTMB and, conversely, as low levels of ctDNA or bTMB.

RESULTS

Study Characteristics

A total of 484 articles were retrieved through a database search. Using the exclusion criteria listed above, we removed 4 duplicate articles, 305 articles not related to ctDNA and bTMB, and 162 articles from non-clinical studies. Thirteen articles were finally included in our meta-analysis. The enrollment process of this study is shown in **Figure 1**. Among the 13 included studies, regarding tumor types, four studies were on non-small cell lung cancer (NSCLC), four were on melanoma, one was on colorectal cancer, one was on biliary tract cancer, and one was on urothelial carcinoma; the remaining two were studies on a mixture of different cancers. **Table 1** summarizes the characteristics of the 13 included studies.

Risk of Bias

Twelve of the 13 included studies were prospective cohort studies and only one was a retrospective cohort study, so the overall risk of bias was relatively low. **Figures 2A, B** summarize the risk bias of all the included studies. **Figures 3A, B** display the funnel plots showing no significant publication bias affecting the HRs of OS and PFS on ctDNA.

Outcomes of Included Studies

Relationship Between ctDNA Levels and Response to Immunotherapy

Overall, there were 10 studies on the prognostic value of ctDNA levels in the OS of patients receiving immunotherapy. Elevated

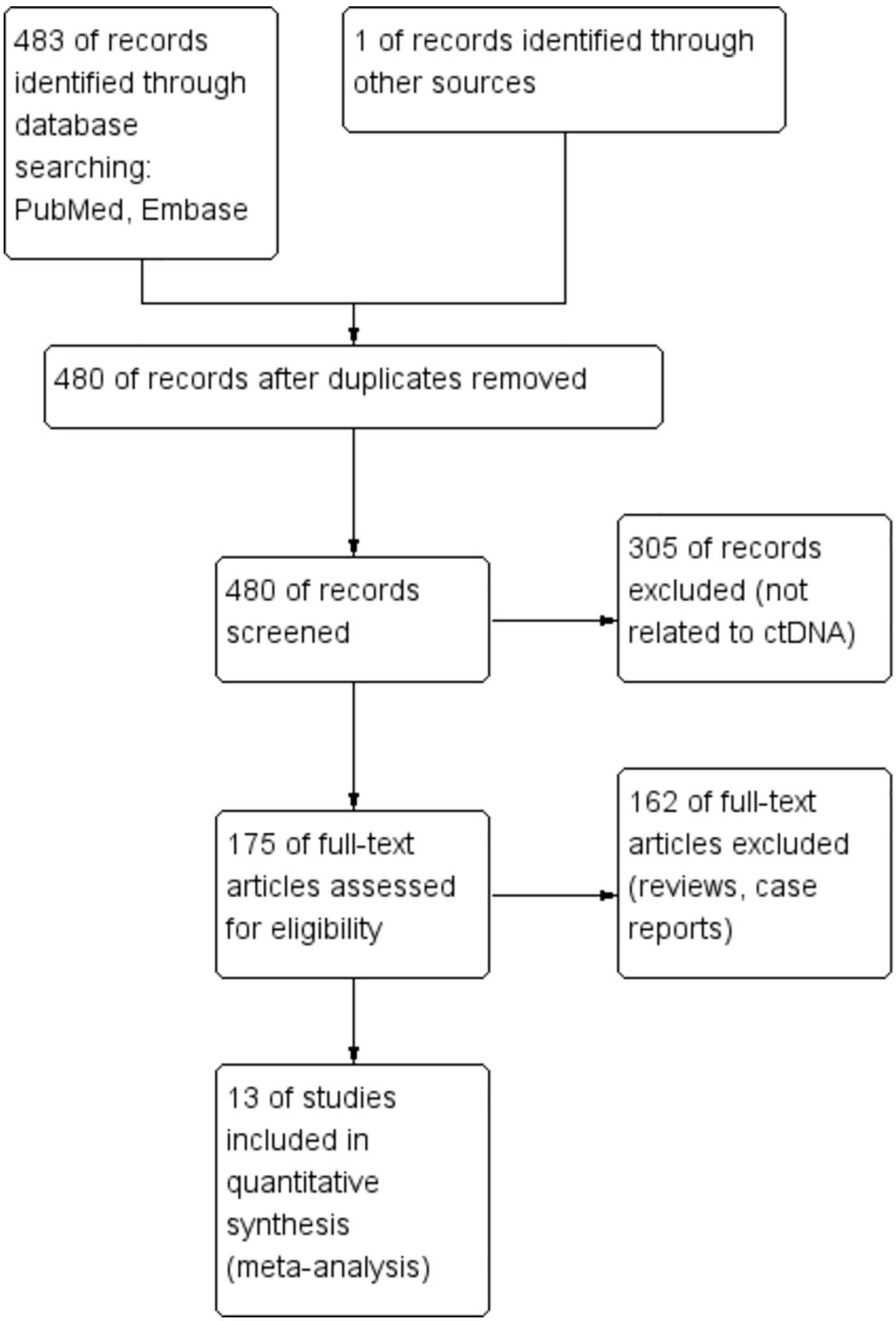

FIGURE 1 | Enrollment process of the included studies. The processes of identification, screening, eligibility, and inclusion are shown.

ctDNA levels were associated with shorter OS (HR = 3.35, 95% CI = 2.49–4.51, $p < 0.00001$) (**Figure 4A**). A total of nine studies were eligible for inclusion in the meta-analysis regarding the prognostic value of ctDNA levels in the PFS of patients receiving ICI therapy. A statistically significant poorer PFS was also observed in patients with higher ctDNA levels, with a pooled HR of 3.28 (95%CI = 2.47–4.35, $p < 0.00001$) (**Figure 4B**). In the subgroup analysis of the different timings of biomarkers, high

TABLE 1 | Characteristics of the included studies.

Authors	Year	Cancer type	Study type	Biomarker type	Timing of biomarker	Biomarker detection method	Cutoff point	ICI	Outcome of interest	Results
Chen et al.	2020	Colorectal cancer	Prospective	bTMB	Pretreatment	NGS	≥28 *vs*. <28 vts/Mb	Tremelimumab, durvalumab	OS	HR = 0.34, 90% CI = 0.18–0.63, p = 0.004
Lee et al.	2020	Melanoma	Prospective	ctDNA	Pretreatment	PCR	Undetectable *vs*. detectable	Pembrolizumab, nivolumab, ipilimumab	OS	HR = 0.51, 95% CI = 0.28–0.94, p = 0.03
Wang et al.	2020	NSCLC	Prospective	bTMB	Not mentioned	NGS	≥6 *vs*.<6 vts/Mb	Atezolizumab, nivolumab, pembrolizumab, tislelizumab, toripalimab	OS	HR = 0.92, 95% CI = 0.46–1.82, p = 0.80
Wang et al.	2020	NSCLC	Prospective	MSAF (ctDNA)	Not mentioned	NGS	Top 25% *vs*. bottom 75%	Atezolizumab, nivolumab, pembrolizumab, tislelizumab, toripalimab	OS	HR = 2.72, 95% CI = 1.33–5.59, p = 0.005
Chen et al.	2020	Biliary tract cancer	Prospective	ctDNA	Posttreatment	NGS	Positive *vs*. negative	Camrelizumab	OS and PFS	OS: HR = 1.77, 95%CI = 0.78–3.99, p = 0.16 PFS: HR = 2.83, 95%CI = 1.27–6.28, p = 0.007
Chen et al	2020	Biliary tract cancer	Prospective	bTMB	Not mentioned	NGS	Top 25% *vs*. bottom 75%	Camrelizumab	OS and PFS	OS: HR = 1.05, 95%CI = 0.43–2.54, p = 0.92 PFS: HR = 2.57, 95%CI = 1.08–6.12, p = 0.03
Pedersen et al.	2020	Melanoma	Prospective	ctDNA	Posttreatment	PCR	Detectable *vs*. undetectable	Pembrolizumab, nivolumab, ipilimumab	PFS	HR = 7.89, 95% CI = 1.40–44.6, p = 0.019
Marsavela et al.	2020	Melanoma	Prospective	ctDNA	Pretreatment	PCR	≤20 *vs*. >20 copies/ml	Nivolumab, pembrolizumab, ipilimumab	PFS	HR = 0.42, 95% CI = 0.22–0.83, p = 0.006
Anagnostou et al.	2020	NSCLC	Prospective	ctDNA	Clearance	NGS	No complete reduction *vs*. complete reduction	Unclear	OS and PFS	OS: HR = 6.91, 95%CI = 1.37–34.97, p = 0.02 PFS: HR = 5.36, 95%CI = 1.57–18.35, p = 0.007
Goldberg et al.	2018	NSCLC	Prospective	ctDNA	Clearance	NGS	>50% *vs*. ≤50% decrease in mutant allele fraction from baseline	Unclear	OS and PFS	OS: HR = 0.17, 95%CI = 0.05–0.62, p = 0.007 PFS: HR = 0.29, 95%CI = 0.09–0.89, p = 0.03
Cabel et al.	2017	NSCLC, etc.	Prospective	ctDNA	Posttreatment	NGS	Detectable *vs*. undetectable	Nivolumab, pembrolizumab	OS and PFS	OS: HR = 15, 95%CI = 2.5–94.9, p = 0.004 PFS: HR = 10.2, 95%CI = 2.5–41, p < 0.001
Herbreteau et al.	2021	Melanoma	Prospective	ctDNA	Clearance	PCR	Increase *vs*. decrease	Nivolumab/ nivolumab + ipilimumab	OS and PFS	OS: HR = 7.49, 95%CI = 2.59–24.10, p = 0.0002 PFS: HR = 12.74, 95%CI = 3.81–53.25, p < 0.0001

(Continued)

TABLE 1 | Continued

Authors	Year	Cancer type	Study type	Biomarker type	Timing of biomarker	Biomarker detection method	Cutoff point	ICI	Outcome of interest	Results
Ricciuti et al.	2021	NSCLC	Retrospective	ctDNA	Clearance	NGS	Decrease *vs.* increase	Pembrolizumab	OS and PFS	OS: HR = 0.34, 95%CI = 0.15–0.75, p = 0.008 PFS: HR = 0.29, 95%CI = 0.14–0.60, p = 0.0007
Zhang et al.	2020	Advanced cancers	Prospective	ctDNA	Posttreatment	Not mentioned	Below median *vs.* above median	Durvalumab ± tremelimumab	OS and PFS	HR = 0.13, 95% CI = 0.05–0.34 HR = 0.41, 95% CI = 0.25–0.68
Powles et al.	2021	Urothelial carcinoma	Prospective	ctDNA	Clearance	PCR	Clear *vs.* not clear	Atezolizumab	OS	HR = 0.14, 95% CI = 0.03–0.59

vts/Mb, variations per megabase; ctDNA, circulating tumor DNA; bTMB, blood tumor mutation burden; ICI, immune checkpoint inhibitor; HR, hazard ratio; NSCLC, non-small-cell lung cancer; MSAF, maximum somatic allele frequency; NGS, next-generation sequencing; PCR, polymerase chain reaction; OS, overall survival; PFS, progression-free survival.

posttreatment ctDNA levels significantly correlated with shorter OS in cancer patients receiving ICIs (HR = 5.09, 95%CI = 1.43–18.07, p = 0.01). In addition, patients without ctDNA clearance had worse OS (HR = 4.94, 95%CI = 2.96–8.26, p < 0.00001). There was only one study on the relationship between the pretreatment ctDNA levels and OS, and the results showed that high pretreatment ctDNA levels were correlated with worse overall survival (HR = 1.95, 95%CI = 1.06–3.57, p = 0.03) (**Figure 5**). As for PFS, patients with high posttreatment ctDNA levels had shorter PFS (HR = 3.00, 95%CI = 2.02–4.46, p < 0.00001). Similarly, patients with ctDNA clearance had longer PFS (HR = 4.61, 95%CI = 2.78–7.65, p < 0.00001). In addition, high levels of pretreatment ctDNA were significantly correlated with shorter PFS (HR = 2.34, 95%CI = 1.20–4.55, p = 0.01) (**Figure 6**).

Relationship Between bTMB and Response to Immunotherapy

There was only one study with PFS as an outcome indicator. Estimation of the prognostic value of bTMB in the PFS of patients receiving ICI therapy revealed that a high bTMB was significantly associated with shorter PFS (HR = 2.57, 95%CI = 1.08–6.12, p = 0.03). There were a total of three studies on the prognostic value of bTMB in the OS of cancer patients receiving immunotherapy. The pooled results showed that there was no statistically significant difference in the OS benefits between a higher and a lower bTMB (HR = 0.68, 95%CI = 0.33–1.37, p = 0.28) (**Figure 7**).

Heterogeneity

In the analysis of the prognostic effect of ctDNA in patients receiving immunotherapy, no significant heterogeneity was observed in the outcomes of PFS and OS (I^2 = 30%, p < 0.00001; I^2 = 45%, p < 0.00001); thus, both were analyzed with the fixed effects models. The heterogeneity between the studies on bTMB was greater than 50% (I^2 = 60%), so the random effects model was selected.

DISCUSSION

The efficacy of ICIs mainly depends on the tumor burden and the immune system of the host (10–12). At present, the main tools used to evaluate disease burden and the host immune status are radiologic assessments (CT and MRI) and tTMB (13–17), but they all have their own limitations. The clinical decision to continue or suspend ICI therapy is usually guided by continuous radiographic observations of changes in the tumor. However, CT and MRI are unable to identify patients who can achieve benefits early because tumors usually shrink slowly (18). In addition, radiographs often fail to identify whether transient tumor enlargements come from true disease progression or pseudoprogression, the latter referring to immune cell infiltration (18–20). Relevant evidence has shown that the existence of ctDNA occurs earlier than the recurrence of radiographic imaging, and it dynamically changes with the patient's response to treatment (21). As a prognostic factor of the host immune status, tTMB is also not completely satisfactory. Firstly, the measurement of tTMB requires tumor biopsy material, which may cause trauma and bleeding. Secondly, not all cancer patients meet the criteria for tissue biopsy (22). Thirdly, tTMB can only reflect the mutation burden of local tumor tissues and does not focus on the whole body (23). Finally, tTMB is unable to dynamically monitor tumor burden in real time. In order to more accurately identify patients who are most likely to benefit from immunotherapy, new biomarkers are needed to compensate for the lack of the evaluation tools mentioned above. ctDNA and bTMB are expected to become new biomarkers, but their exact prognostic roles in ICI therapy remain to be clarified. To the best of our knowledge, this is the first systematic review and meta-analysis on the prognostic impact of ctDNA and bTMB in patients undergoing immunotherapy.

Some studies claimed that a higher bTMB indicated better prognosis, which means longer PFS and OS in patients receiving immunotherapy (24, 25), while others hold the opposite opinion (26). The pooled results of our meta-analysis revealed that higher ctDNA levels resulted in shorter PFS (HR = 3.28, 95%CI = 2.47–

FIGURE 2 | Assessment of risk of bias at the study level. **(A)** Risk of bias graph: review authors' judgments of each risk of bias item presented as percentages across all included full report studies. **(B)** Risk of bias summary: review authors' judgments of each risk of bias item.

4.35, $p < 0.00001$) and OS (HR = 3.35, 95%CI = 2.49–4.51, $p < 0.00001$). In the subgroup analysis of biomarkers at different time points, patients with high levels of pretreatment or posttreatment ctDNA and patients without ctDNA clearance during treatment all had worse prognosis (PFS and OS) in immunotherapy. Regarding bTMB, no statistically significant difference was observed between a high and a low bTMB in OS prognosis (HR = 0.68, 95%CI = 0.33–1.37, $p = 0.28$).

ctDNA is a single- or double-stranded DNA released into the blood by tumor cells. The proportion of ctDNA in cfDNA ranges widely, and it is determined by the synthesis of tumor location, phenotype, and differentiation degree (27). Therefore, ctDNA can reflect the burden of tumors and carry the original tumor mutations (28). Theoretically, a higher ctDNA level reveals a greater tumor burden, resulting in a poorer prognosis. Zhao et al. (29) also observed that, in liver cancer, higher ctDNA levels were more associated with larger tumor volumes than was alpha-fetoprotein (AFP). This finding was consistent with the results of our meta-analysis.

Synonymous variation, non-synonymous variation, and variation of unknown significance (VUS) are the three methods used to calculate bTMB (3). New somatic mutations in tumor cells result in new antigen expression, and the production of tumor-specific antigens is an important

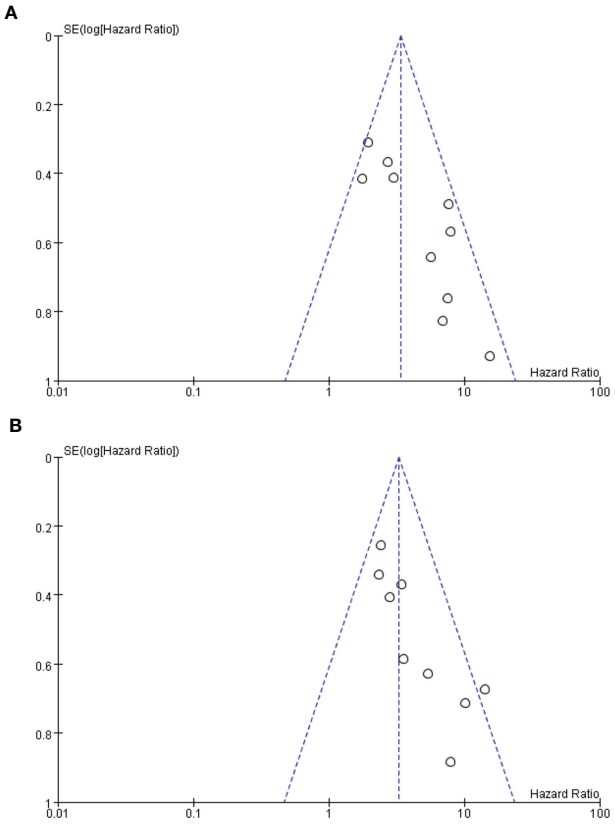

FIGURE 3 | **(A, B)** Funnel plots. Funnel plot analysis on potential publication bias for overall survival (OS) **(A)** and progression-free survival (PFS) **(B)**.

prerequisite for T cells to recognize tumors (30, 31). Moreover, neoantigens produced by mutations in tumor somatic cells have been confirmed to activate the immune response of T cells (32). Previous studies have demonstrated that a higher tTMB is associated with longer OS and PFS in patients receiving immunotherapy (33–35). The feasibility and accuracy of bTMB measured from blood samples based on ctDNA and the positive association between bTMB and TMB in tumor tissues have been confirmed (36, 37). Therefore, in theory, bTMB also has prognostic value in patients receiving ICIs, and a higher bTMB corresponds to better survival. However, the pooled results of our meta-analysis revealed no statistically significant relationship between a higher bTMB and better OS. Why bTMB cannot be a prognostic factor in patients receiving ICIs will be explained in the following. The detection method for bTMB inevitably leads to the following results: ctDNA levels have an important impact on the abundance of bTMB. In this way, a higher bTMB may be accompanied by higher ctDNA levels, and the latter is closely correlated with worse prognosis. As a consequence, a higher bTMB does not necessarily reveal longer OS and PFS; likewise, a lower bTMB is not necessarily related to shorter OS and PFS. In conclusion, some problems remain to be overcome before the clinical implementation of bTMB. To effectively determine the prognostic value of bTMB in cancer patients undergoing immunotherapy, the integration of bTMB and other blood biomarkers in the future may be required.

Our meta-analysis explored the prognostic value of high or low ctDNA and bTMB in patients receiving immunotherapy, but did not address the predictive effect of ctDNA or bTMB on the outcome of immunotherapy. The results of the trial, published in Nature by Powles et al., revealed that the ctDNA-positive patients in the atezolizumab group had better prognosis than those in the observation group, suggesting that ctDNA may be a predictor of the efficacy of ICIs. This conclusion is helpful in the clinical decision-making of clinicians. For patients with positive ctDNA after tumor surgery, the use of ICIs may be an option to improve survival. However, there are limited studies on the predictive indicators of the efficacy of immunotherapy, and this conclusion needs to be confirmed by more data in future studies.

Our study had certain limitations. Firstly, since the detection technology of ctDNA and bTMB in blood is still in the initial stages of development, there will be more or less inconsistencies between the measured values and the true values, which is also the main reason for the different cutoff points of ctDNA and bTMB in all the studies included in our meta-analysis. Therefore, the stability of our meta-analysis results was affected. Secondly, the number of studies included in the meta-analysis was relatively small, especially the number of studies on bTMB. Thirdly, in addition to the different cutoff points of the biomarkers that affect the results of the analysis, there are other factors that will cause heterogeneity in the meta-analysis results and affect the authenticity and reliability of the final results. Although we have performed a subgroup analysis on the prognostic value of ctDNA in patients receiving immunotherapy at different time points, the details of each study in each subgroup were diverse. For example, although they were all studies on the prognostic value of posttreatment ctDNA levels in patients receiving ICIs, some studies focused on ctDNA at 6–8 weeks after immunotherapy while others explored ctDNA at 8–10 weeks after immunotherapy. In addition, for studies on the prognostic impact of ctDNA clearance, the definition and the standard of ctDNA clearance were different. Finally, the detection methods for ctDNA and bTMB used by the studies included in our meta-analysis were not uniform (PCR and NGS, respectively), which would also impact the results of the analysis. This requires the continuous updating and improvement of the detection methods for these two biomarkers in the future.

CONCLUSION

In the past, ctDNA and bTMB have received increased attention in the field of targeted therapy and chemo/radiotherapy (38–41), but there has been no consensus regarding their prognostic role in patients receiving ICIs. Our meta-analysis results demonstrated that the levels and the clearance of ctDNA can be used as independent prognostic factors for immunotherapy, while the prognostic impact of bTMB in cancer patients undergoing immunotherapy is worth further discussion and exploration.

Monitoring the ctDNA levels for ICI therapy has the following advantages: it can be performed in real time, is noninvasive, and is

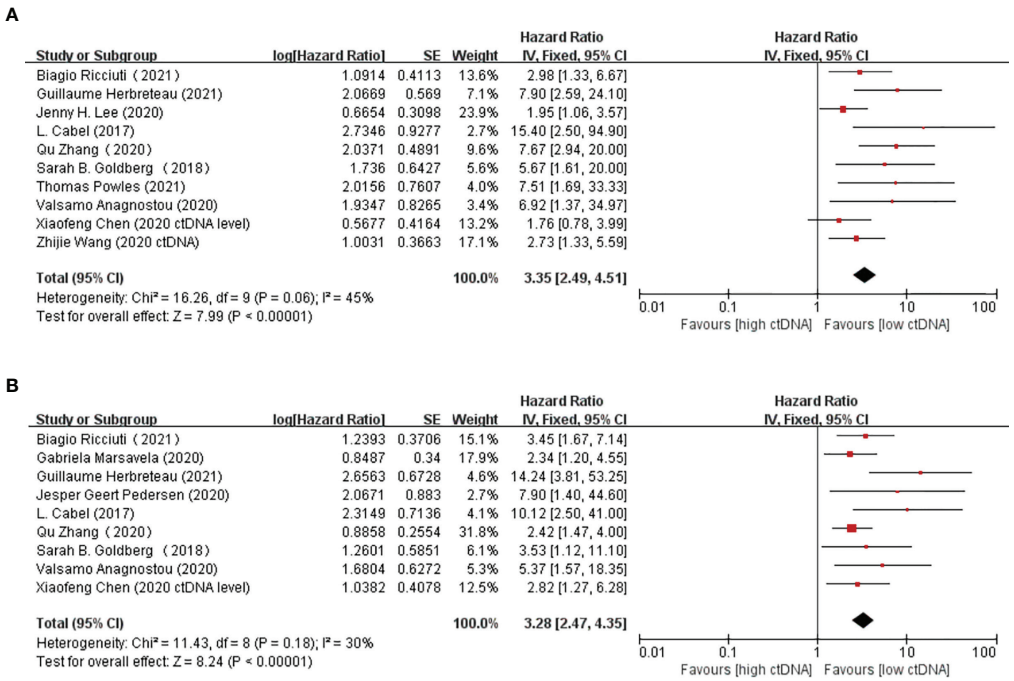

FIGURE 4 | **(A, B)** Forest plots of the fixed effects meta-analysis on the efficacy of circulating tumor DNA (ctDNA) for overall survival (OS) **(A)** and for progression-free survival (PFS) **(B)**.

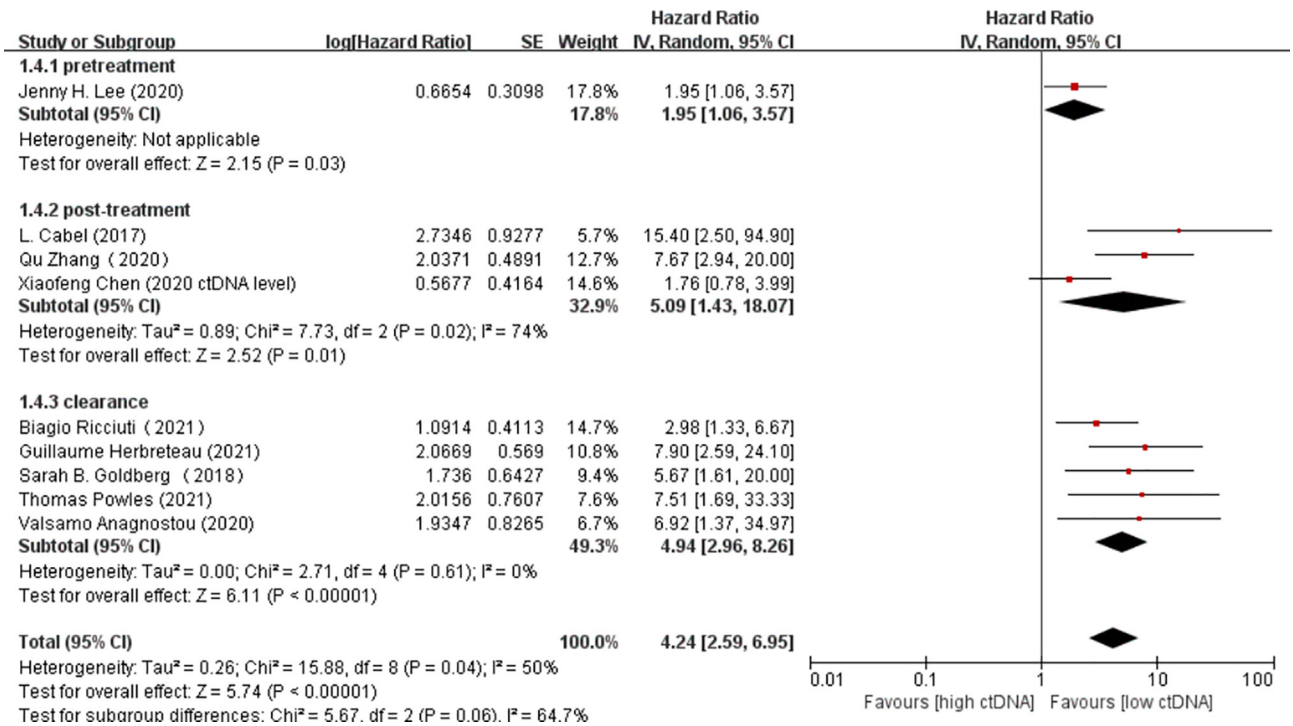

FIGURE 5 | Forest plot of the random effects meta-analysis on the efficacy of circulating DNA (ctDNA) for overall survival (OS) at different time points.

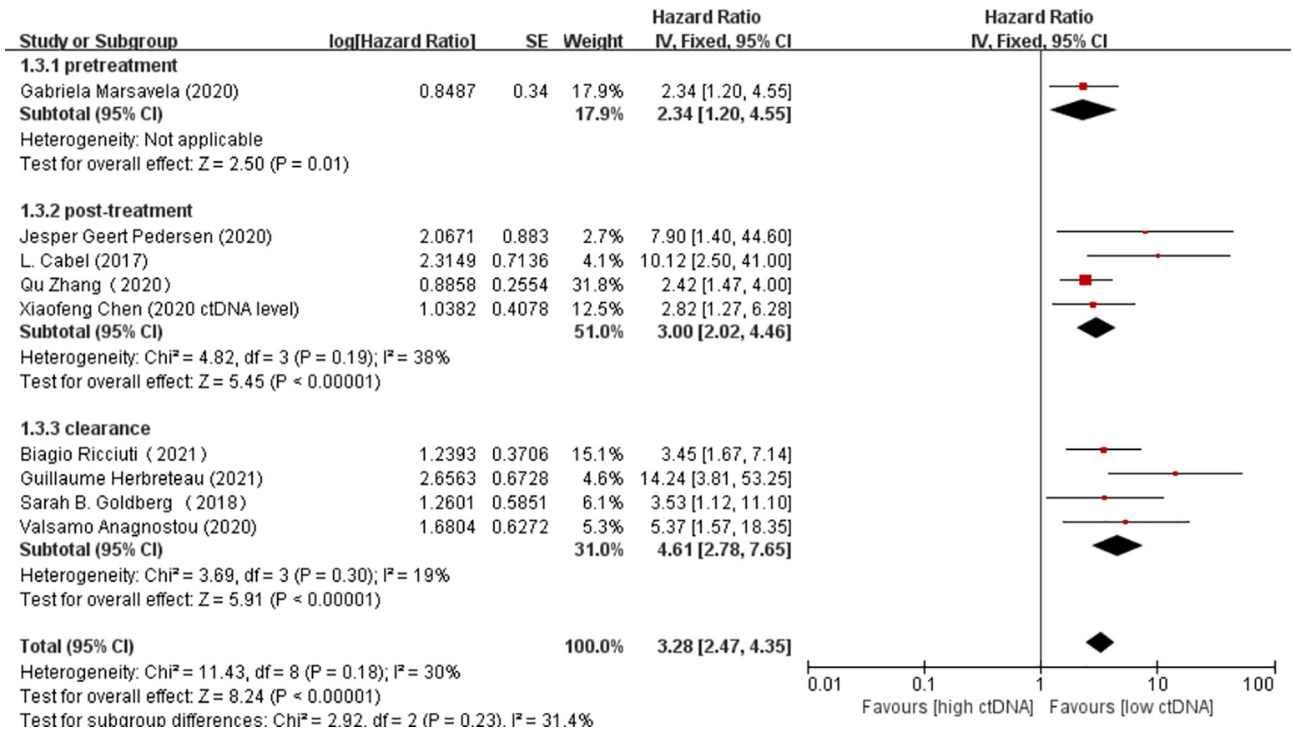

FIGURE 6 | Forest plot of the fixed effects meta-analysis on the efficacy of circulating DNA (ctDNA) for progression-free survival (PFS) at different time points.

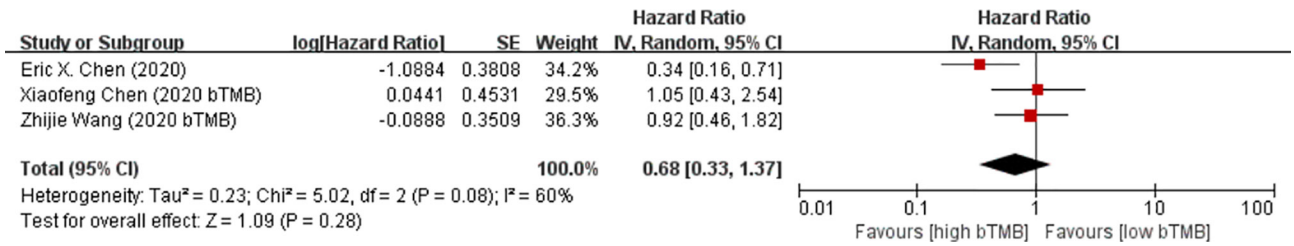

FIGURE 7 | Forest plot of the random effects meta-analysis on the efficacy of blood tumor mutation burden (bTMB) for overall survival (OS).

ultrasensitive. Therefore, it can be a good prognostic factor for immunotherapy in patients with cancer. Monitoring ctDNA can be used as an important supplement to conventional imaging and help in making timely therapeutic management decisions. Due to the limitations of the current detection technology and standards, bTMB cannot be directly used as a prognostic factor to effectively predict the survival of patients undergoing treatment with ICIs.

AUTHOR CONTRIBUTIONS

YW, NL, and MP conceptualized the study. PR, YJ, and ZX contributed to the methodology. JW helped with software. RL did the formal analysis. JW, JF, PW, and XC prepared the original draft. YW reviewed and edited the manuscript. All authors contributed to the article and approved the submitted version.

FUNDING

This work was supported by grants from the National Natural Science Foundation of China (81770169), National Natural Science Foundation of China (81802980) and National Natural Science Foundation of China (81102024).

REFERENCES

1. Cabel L, Proudhon C, Romano E, Girard N, Lantz O, Stern MH, et al. Clinical Potential of Circulating Tumour DNA in Patients Receiving Anticancer Immunotherapy. *Nat Rev Clin Oncol* (2018) 15(10):639–50. doi: 10.1038/s41571-018-0074-3
2. Boonstra PA, Wind TT, van Kruchten M, Schuuring E, Hospers G, van der Wekken AJ, et al. Clinical Utility of Circulating Tumor DNA as a Response and Follow-Up Marker in Cancer Therapy. *Cancer Metastasis Rev* (2020) 39 (3):999–1013. doi: 10.1007/s10555-020-09876-9
3. Chae YK, Davis AA, Agte S, Pan A, Simon NI, Iams WT, et al. Clinical Implications of Circulating Tumor DNA Tumor Mutational Burden (ctDNA TMB) in Non-Small Cell Lung Cancer. *Oncologist* (2019) 24(6):820–8. doi: 10.1634/theoncologist.2018-0433
4. McNamara MG, Jacobs T, Lamarca A, Hubner RA, Valle JW, Amir E. Impact of High Tumor Mutational Burden in Solid Tumors and Challenges for Biomarker Application. *Cancer Treat Rev* (2020) 89:102084. doi: 10.1016/j.ctrv.2020.102084
5. Motzer RJ, Escudier B, George S, Hammers HJ, Srinivas S, Tykodi SS, et al. Nivolumab Versus Everolimus in Patients With Advanced Renal Cell Carcinoma: Updated Results With Long-Term Follow-Up of the Randomized, Open-Label, Phase 3 CheckMate 025 Trial. *Cancer-Am Cancer Soc* (2020) 126(18):4156–67. doi: 10.1002/cncr.33033
6. Liu L, Bai X, Wang J, Tang XR, Wu DH, Du SS, et al. Combination of TMB and CNA Stratifies Prognostic and Predictive Responses to Immunotherapy Across Metastatic Cancer. *Clin Cancer Res* (2019) 25(24):7413–23. doi: 10.1158/1078-0432.CCR-19-0558
7. Anagnostou V, Forde PM, White JR, Niknafs N, Hruban C, Naidoo J, et al. Dynamics of Tumor and Immune Responses During Immune Checkpoint Blockade in Non-Small Cell Lung Cancer. *Cancer Res* (2019) 79(6):1214–25. doi: 10.1158/0008-5472.CAN-18-1127
8. Lee JH, Menzies AM, Carlino MS, McEvoy AC, Sandhu S, Weppler AM, et al. Longitudinal Monitoring of ctDNA in Patients With Melanoma and Brain Metastases Treated With Immune Checkpoint Inhibitors. *Clin Cancer Res* (2020) 26(15):4064–71. doi: 10.1158/1078-0432.CCR-19-3926
9. Marsavela G, Lee J, Calapre L, Wong SQ, Pereira MR, McEvoy AC, et al. Circulating Tumor DNA Predicts Outcome From First-, But Not Second-Line Treatment and Identifies Melanoma Patients Who May Benefit From Combination Immunotherapy. *Clin Cancer Res* (2020) 26(22):5926–33. doi: 10.1158/1078-0432.CCR-20-2251
10. Sakata Y, Kawamura K, Ichikado K, Shingu N, Yasuda Y, Eguchi Y, et al. The Association Between Tumor Burden and Severe Immune-Related Adverse Events in Non-Small Cell Lung Cancer Patients Responding to Immune-Checkpoint Inhibitor Treatment. *Lung Cancer* (2019) 130:159–61. doi: 10.1016/j.lungcan.2019.02.011
11. Seban RD, Mezquita L, Berenbaum A, Dercle L, Botticella A, Le Pechoux C, et al. Baseline Metabolic Tumor Burden on FDG PET/CT Scans Predicts Outcome in Advanced NSCLC Patients Treated With Immune Checkpoint Inhibitors. *Eur J Nucl Med Mol Imaging* (2020) 47(5):1147–57. doi: 10.1007/s00259-019-04615-x
12. Picard E, Verschoor CP, Ma GW, Pawelec G. Relationships Between Immune Landscapes, Genetic Subtypes and Responses to Immunotherapy in Colorectal Cancer. *Front Immunol* (2020) 11:369. doi: 10.3389/fimmu.2020.00369
13. Muhlberg A, Holch JW, Heinemann V, Huber T, Moltz J, Maurus S, et al. The Relevance of CT-Based Geometric and Radiomics Analysis of Whole Liver Tumor Burden to Predict Survival of Patients With Metastatic Colorectal Cancer. *Eur Radiol* (2021) 31(2):834–46. doi: 10.1007/s00330-020-07192-y
14. Sun G, Cheng C, Li X, Wang T, Yang J, Li D. Metabolic Tumor Burden on Postsurgical PET/CT Predicts Survival of Patients With Gastric Cancer. *Cancer Imaging* (2019) 19(1):18. doi: 10.1186/s40644-019-0205-9
15. Iv M, Liu X, Lavezo J, Gentles AJ, Ghanem R, Lummus S, et al. Perfusion MRI-Based Fractional Tumor Burden Differentiates Between Tumor and Treatment Effect in Recurrent Glioblastomas and Informs Clinical Decision-Making. *AJNR Am J Neuroradiol* (2019) 40(10):1649–57. doi: 10.3174/ajnr.A6211
16. Nan Z, Guoqing W, Xiaoxu Y, Yin M, Xin H, Xue L, et al. The Predictive Efficacy of Tumor Mutation Burden (TMB) on Nonsmall Cell Lung Cancer Treated by Immune Checkpoint Inhibitors: A Systematic Review and Meta-Analysis. *BioMed Res Int* (2021) 2021:1780860. doi: 10.1155/2021/1780860
17. Sholl LM, Hirsch FR, Hwang D, Botling J, Lopez-Rios F, Bubendorf L, et al. The Promises and Challenges of Tumor Mutation Burden as an Immunotherapy Biomarker: A Perspective From the International Association for the Study of Lung Cancer Pathology Committee. *J Thorac Oncol* (2020) 15(9):1409–24. doi: 10.1016/j.jtho.2020.05.019
18. Goldberg SB, Narayan A, Kole AJ, Decker RH, Teysir J, Carriero NJ, et al. Early Assessment of Lung Cancer Immunotherapy Response via Circulating Tumor DNA. *Clin Cancer Res* (2018) 24(8):1872–80. doi: 10.1158/1078-0432.CCR-17-1341
19. Markovic SN, Galli F, Suman VJ, Nevala WK, Paulsen AM, Hung JC, et al. Non-Invasive Visualization of Tumor Infiltrating Lymphocytes in Patients With Metastatic Melanoma Undergoing Immune Checkpoint Inhibitor Therapy: A Pilot Study. *Oncotarget* (2018) 9(54):30268–78. doi: 10.18632/oncotarget.25666
20. Cabel L, Riva F, Servois V, Livartowski A, Daniel C, Rampanou A, et al. Circulating Tumor DNA Changes for Early Monitoring of Anti-PD1 Immunotherapy: A Proof-of-Concept Study. *Ann Oncol* (2017) 28(8):1996–2001. doi: 10.1093/annonc/mdx212
21. Powles T, Assaf ZJ, Davarpanah N, Banchereau R, Szabados BE, Yuen KC, et al. ctDNA Guiding Adjuvant Immunotherapy in Urothelial Carcinoma. *Nature* (2021) 595(7867):432–7. doi: 10.1038/s41586-021-03642-9
22. Allgauer M, Budczies J, Christopoulos P, Endris V, Lier A, Rempel E, et al. Implementing Tumor Mutational Burden (TMB) Analysis in Routine Diagnostics-a Primer for Molecular Pathologists and Clinicians. *Transl Lung Cancer Res* (2018) 7(6):703–15. doi: 10.21037/tlcr.2018.08.14
23. Friedlaender A, Nouspikel T, Christinat Y, Ho L, McKee T, Addeo A. Tissue-Plasma TMB Comparison and Plasma TMB Monitoring in Patients With Metastatic Non-Small Cell Lung Cancer Receiving Immune Checkpoint Inhibitors. *Front Oncol* (2020) 10:142. doi: 10.3389/fonc.2020.00142
24. Chen EX, Jonker DJ, Loree JM, Kennecke HF, Berry SR, Couture F, et al. Effect of Combined Immune Checkpoint Inhibition vs Best Supportive Care Alone in Patients With Advanced Colorectal Cancer: The Canadian Cancer Trials Group CO.26 Study. *JAMA Oncol* (2020) 6(6):831–8. doi: 10.1001/jamaoncol.2020.0910
25. Killock D. bTMB is a Promising Predictive Biomarker. *Nat Rev Clin Oncol* (2019) 16(7):403. doi: 10.1038/s41571-019-0202-8
26. Wang Z, Duan J, Wang G, Zhao J, Xu J, Han J, et al. Allele Frequency-Adjusted Blood-Based Tumor Mutational Burden as a Predictor of Overall Survival for Patients With NSCLC Treated With PD-(L)1 Inhibitors. *J Thorac Oncol* (2020) 15(4):556–67. doi: 10.1016/j.jtho.2019.12.001
27. Pessoa LS, Heringer M, Ferrer VP. ctDNA as a Cancer Biomarker: A Broad Overview. *Crit Rev Oncol Hematol* (2020) 155:103109. doi: 10.1016/j.critrevonc.2020.103109
28. Cheng F, Su L, Qian C. Circulating Tumor DNA: A Promising Biomarker in the Liquid Biopsy of Cancer. *Oncotarget* (2016) 7(30):48832–41. doi: 10.18632/oncotarget.9453
29. Zhao W, Qiu L, Liu H, Xu Y, Zhan M, Zhang W, et al. Circulating Tumor DNA as a Potential Prognostic and Predictive Biomarker During Interventional Therapy of Unresectable Primary Liver Cancer. *J Gastrointest Oncol* (2020) 11(5):1065–77. doi: 10.21037/jgo-20-409
30. Lee M, Samstein RM, Valero C, Chan TA, Morris L. Tumor Mutational Burden as a Predictive Biomarker for Checkpoint Inhibitor Immunotherapy. *Hum Vaccin Immunother* (2020) 16(1):112–5. doi: 10.1080/21645515.2019.1631136
31. Subudhi SK, Vence L, Zhao H, Blando J, Yadav SS, Xiong Q, et al. Neoantigen Responses, Immune Correlates, and Favorable Outcomes After Ipilimumab Treatment of Patients With Prostate Cancer. *Sci Transl Med* (2020) 12(537). doi: 10.1126/scitranslmed.aaz3577
32. Jardim DL, Goodman A, de Melo GD, Kurzrock R. The Challenges of Tumor Mutational Burden as an Immunotherapy Biomarker. *Cancer Cell* (2021) 39 (2):154–73. doi: 10.1016/j.ccell.2020.10.001
33. Samstein RM, Lee CH, Shoushtari AN, Hellmann MD, Shen R, Janjigian YY, et al. Tumor Mutational Load Predicts Survival After Immunotherapy Across Multiple Cancer Types. *Nat Genet* (2019) 51(2):202–6. doi: 10.1038/s41588-018-0312-8
34. Alborelli I, Leonards K, Rothschild SI, Leuenberger LP, Savic PS, Mertz KD, et al. Tumor Mutational Burden Assessed by Targeted NGS Predicts Clinical Benefit From Immune Checkpoint Inhibitors in Non-Small Cell Lung Cancer. *J Pathol* (2020) 250(1):19–29. doi: 10.1002/path.5344

35. Greally M, Chou JF, Chatila WK, Margolis M, Capanu M, Hechtman JF, et al. Clinical and Molecular Predictors of Response to Immune Checkpoint Inhibitors in Patients With Advanced Esophagogastric Cancer. *Clin Cancer Res* (2019) 25(20):6160–9. doi: 10.1158/1078-0432.CCR-18-3603
36. Si H, Kuziora M, Quinn KJ, Helman E, Ye J, Liu F, et al. A Blood-Based Assay for Assessment of Tumor Mutational Burden in First-Line Metastatic NSCLC Treatment: Results From the MYSTIC Study. *Clin Cancer Res* (2021) 27 (6):1631–40. doi: 10.1158/1078-0432.CCR-20-3771
37. Zhang X, Zhao W, Wei W, You Z, Ou X, Sun M, et al. Parallel Analyses of Somatic Mutations in Plasma Circulating Tumor DNA (ctDNA) and Matched Tumor Tissues in Early-Stage Breast Cancer. *Clin Cancer Res* (2019) 25 (21):6546–53. doi: 10.1158/1078-0432.CCR-18-4055
38. Zhu C, Zhuang W, Chen L, Yang W, Ou WB. Frontiers of ctDNA, Targeted Therapies, and Immunotherapy in Non-Small-Cell Lung Cancer. *Transl Lung Cancer Res* (2020) 9(1):111–38. doi: 10.21037/tlcr.2020.01.09
39. Ji D, Zhang D, Zhan T, Jia J, Han W, Li Z, et al. Tumor Mutation Burden in Blood Predicts Benefit From Neoadjuvant Chemo/Radiotherapy in Locally Advanced Rectal Cancer. *Genomics* (2021) 113(1 Pt 2):957–66. doi: 10.1016/j.ygeno.2020.10.029
40. Nie W, Qian J, Xu MD, Gu K, Qian FF, Lu J, et al. Prognostic and Predictive Value of Blood Tumor Mutational Burden in Patients With Lung Cancer Treated With Docetaxel. *J Natl Compr Canc Netw* (2020) 18(5):582–9. doi: 10.6004/jnccn.2019.7383
41. Ma F, Guan Y, Yi Z, Chang L, Li Q, Chen S, et al. Assessing Tumor Heterogeneity Using ctDNA to Predict and Monitor Therapeutic Response in Metastatic Breast Cancer. *Int J Cancer* (2020) 146(5):1359–68. doi: 10.1002/ijc.32536

Conflict of Interest: The authors declare that the research was conducted in the absence of any commercial or financial relationships that could be construed as a potential conflict of interest.

Publisher's Note: All claims expressed in this article are solely those of the authors and do not necessarily represent those of their affiliated organizations, or those of the publisher, the editors and the reviewers. Any product that may be evaluated in this article, or claim that may be made by its manufacturer, is not guaranteed or endorsed by the publisher.

frontiers in Immunology

REVIEW
published: 18 October 2021
doi: 10.3389/fimmu.2021.754436

Kickstarting Immunity in Cold Tumours: Localised Tumour Therapy Combinations With Immune Checkpoint Blockade

*Elizabeth Appleton[1,2], Jehanne Hassan[2], Charleen Chan Wah Hak[1], Nanna Sivamanoharan[1], Anna Wilkins[1], Adel Samson[3], Masahiro Ono[2], Kevin J. Harrington[1], Alan Melcher[1] and Erik Wennerberg[1]**

[1] Department of Radiotherapy and Imaging, Institute of Cancer Research (ICR), London, United Kingdom, [2] Department of Life Sciences, Imperial College London, London, United Kingdom, [3] Leeds Institute of Medical Research at St. James, University of Leeds, Leeds, United Kingdom

OPEN ACCESS

Edited by:
Fernando Aranda,
Instituto de Investigación Sanitaria de Navarra (IdiSNA), Spain

Reviewed by:
Ariel Munitz,
Tel Aviv University, Israel
Bozena Kaminska,
Nencki Institute of Experimental Biology (PAS), Poland

***Correspondence:**
Erik Wennerberg
erik.ag.wennerberg@gmail.com

Specialty section:
This article was submitted to Cancer Immunity and Immunotherapy, a section of the journal Frontiers in Immunology

Received: 06 August 2021
Accepted: 29 September 2021
Published: 18 October 2021

Citation:
Appleton E, Hassan J, Chan Wah Hak C, Sivamanoharan N, Wilkins A, Samson A, Ono M, Harrington KJ, Melcher A and Wennerberg E (2021) Kickstarting Immunity in Cold Tumours: Localised Tumour Therapy Combinations With Immune Checkpoint Blockade. Front. Immunol. 12:754436. doi: 10.3389/fimmu.2021.754436

Cancer patients with low or absent pre-existing anti-tumour immunity ("cold" tumours) respond poorly to treatment with immune checkpoint inhibitors (ICPI). In order to render these patients susceptible to ICPI, initiation of *de novo* tumour-targeted immune responses is required. This involves triggering of inflammatory signalling, innate immune activation including recruitment and stimulation of dendritic cells (DCs), and ultimately priming of tumour-specific T cells. The ability of tumour localised therapies to trigger these pathways and act as *in situ* tumour vaccines is being increasingly explored, with the aspiration of developing combination strategies with ICPI that could generate long-lasting responses. In this effort, it is crucial to consider how therapy-induced changes in the tumour microenvironment (TME) act both as immune stimulants but also, in some cases, exacerbate immune resistance mechanisms. Increasingly refined immune monitoring in pre-clinical studies and analysis of on-treatment biopsies from clinical trials have provided insight into therapy-induced biomarkers of response, as well as actionable targets for optimal synergy between localised therapies and ICB. Here, we review studies on the immunomodulatory effects of novel and experimental localised therapies, as well as the re-evaluation of established therapies, such as radiotherapy, as immune adjuvants with a focus on ICPI combinations.

Keywords: oncolytic virus, radiotherapy, tumor microenvionment, immune checkpoint inhibitors, immunosuppression

HIGHLIGHTS

- Immune checkpoint inhibitors have revolutionised cancer therapy, however they remain largely ineffective in the treatment of poorly immunogenic "cold" tumours.
- Localised therapies can be used to enhance tumour immunogenicity and overcome resistance to checkpoint blockade, with minimal additive or overlapping side effects.
- Clinical studies to date have yielded mixed results, from negative studies to results that have already changed clinical practice.

- Future directions include novel combinations featuring alternative checkpoints, co-stimulatory agonists and agents that target pathways that may enhance antigenicity. Further considerations include the optimal scheduling of immune-modulatory agents.

INTRODUCTION

The last decade has seen a revolution in the field of immuno-oncology (IO), driven most notably by the approval and clinical implementation of immune checkpoint inhibitor (ICPI) therapy. In work later recognised in the 2018 Nobel Prize in Physiology or Medicine, James Allison and Tasuku Honjo separately identified two pivotal surface receptors that act as negative regulators of the effector T cell (Teff) response, Cytotoxic T Lymphocyte Associated Protein-4 (CTLA-4) (1) and Programmed Cell Death-1 (PD-1) (2), respectively. CTLA-4 is expressed on both effector and regulatory T cells and competes with the co-stimulatory receptor CD28 for shared ligands CD80 and CD86 (3), thereby inhibiting co-stimulatory signals essential for activation. PD-1 is expressed on activated immune cells and inhibits TCR signalling by binding with its ligands Programmed Cell Death-Ligand 1 (PD-L1) or PD-L2 (4). The checkpoints are immune gatekeepers, with receptor-ligand interactions acting to regulate the effector response to pathogens and maintain immune tolerance (3).

These pathways are frequently exploited by tumour cells as a mechanism of immune evasion. Upregulation of PD-L1 on tumour cells, or production of factors that upregulate checkpoint expression on immune cells, leads to exhausted and dysfunctional effector Teff and promotion of regulatory T cells (Treg) within the tumour microenvironment (TME). Monoclonal antibody (mAb) therapy targeting immune checkpoint pathways was shown to be a potent method of anti-cancer T cell re-invigoration, effectively releasing the brakes that are imposed on effector function by checkpoint-mediated immunosuppression. In 2011, the first anti-CTLA-4 mAb Ipilimumab was approved for clinical use, shortly followed by agents targeting the PD-1/PD-L1 axis (5).

Checkpoint inhibitors targeting CTLA-4, PD-1, and PD-L1 now form part of first or second-line standard-of-care in melanoma, non-small cell lung cancer (NSCLC), advanced head and neck squamous cell cancer (HNSCC), renal cancer and urothelial cancer, among others (targets summarised in **Table 1**). The result is a shift in outlook for a subset of patients with previously untreatable cancers (6), and for some a chance of long-term cure. In melanoma, for example, ICPI therapy has seen huge success. The Checkmate 067 trial of dual checkpoint blockade (CTLA-4/PD-1) in advanced melanoma showed a response rate of 58%, with a 52% 5-year survival in a historically poor-prognosis group (7), and patients with a complete response were shown to have a less than 10% chance of relapse on discontinuation of treatment in a study by Robert et al. with a 2-year median follow up (6).

These have undoubtedly been exciting times for the field of IO, and the potential for durable therapy with non-overlapping side-effects continues to bolster clinical and academic interest. Over 3000 clinical trials involving ICPI or other T cell modulators are currently ongoing worldwide. Furthermore, evidence for cancer therapy by inhibition of alternative checkpoints such as T cell and mucin-domain containing-3 (TIM-3), lymphocyte activation gene-3 (LAG-3) and T cell immunoreceptor with immunoglobulin and ITIM domain (TIGIT) is emerging (8).

Although ICPI have revolutionised the treatment landscape, low response rates and resistance still plague effective therapy for the majority. On average, only around 12% of patients gain benefit across all tumour types (9), with particularly low response rates in sites that are seen to be poorly immunogenic such as primary brain, pancreatic and ovarian cancer, and liver metastases (10, 11). Even in sites where ICPI therapy is well established, secondary resistance remains an issue, as seen in the aforementioned landmark Checkmate-067 trial which reported an 11.5-month median duration of response in advanced melanoma (7).

The enduring problem of primary and secondary resistance, combined with a lack of reliable predictive biomarkers of response, leaves a large proportion of patients at risk of ICPI-related toxicity without clinical benefit. A significant focus has therefore been placed on broadening mechanistic understanding of ICPI resistance, and developing strategies to augment response. One strategy is the use of locally-delivered, immune-modulatory therapies in combination with ICPI. These therapies, which include radiotherapy and treatments delivered by intratumoural injection such as oncolytic viruses (OV), can lead to remodelling of the TME to a more favourable phenotype for effective ICPI therapy.

Although accessibility of treatable lesions remains a limitation for some localised therapies, they have several advantages over

TABLE 1 | Current checkpoint inhibitors with regulatory approval.

Target	Checkpoint Inhibitor	Year of first FDA approval
PD-1	Pembrolizumab	2014
	Nivolumab	2014
	Cemiplimab	2018
	Dostarlimab	2021
PD-L1	Atezolizumab	2016
	Durvalumab	2017
	Avelumab	2017
CTLA-4	Ipilimumab	2011

systemic combinations. They enable targeted manipulation of the TME, minimising off-target effects and systemic or overlapping toxicity. In addition, local treatments have been shown to exert a systemic influence on TME composition and anti-cancer immunity, even in non-treated tumours. Examples of such effects include stimulation of immune cell influx, enhanced immune cell priming and increased expression of checkpoint targets (such as PD-1 or PD-L1). These characteristics form part of the metaphorical notion of the immunological "heat" of a tumour, and are commonly associated with response to ICPI. Accordingly, they are characteristically absent in "cold", ICPI-refractory tumours. Remodelling of the TME using localised therapies therefore provides potential for global synergy, and enhanced ICPI-responsiveness (12). This review will outline the rationale, pre-clinical and clinical evidence behind localised therapy-ICPI combinations and explore future directions.

Increasing the Immunological Heat

Immune checkpoints form only part of the complex picture of effective anti-cancer immunity. Huge diversity in mutational burden, antigen release and presentation, inflammatory signalling and TME composition all play a critical role in ICPI efficacy (13). This diversity and resultant dichotomy in ICPI response is apparent between patients of the same tumour type, and even within homogenous mouse tumour models (14).

The unifying concept of tumour Immunological "heat" is a global representation of this multifactorial diversity and represents the ability of a tumour to elicit effective anti-cancer immunity.

Immunostimulatory "hot" tumours are seen to be more responsive to immunotherapy. "Hot" characteristics include an immune-cell rich TME, high in $CD8^+$ Teff cells with a high CD8: Treg ratio, antigen-presenting cell (APC) and inflammatory M1-polarised macrophage infiltration, and immune-stimulatory cytokine production (such as Type I IFN). High tumour antigen (TAA) availability due to a high tumour mutational burden (TMB) or microsatellite instability (MSI) has also been associated with ICPI responsiveness, and checkpoint expression on activated, antigen-exposed immune cells, along with PD-L1 on tumour cells, provide targets for ICPI therapy (12).

Immunosuppressive "cold" tumours are seen to be less responsive to immunotherapy. They feature absent or excluded Teff, with a higher proportion of immunosuppressive Treg and M2 polarised macrophages. Poor antigen availability, for example in tumours with a low TMB and excluded APCs, means immune cell priming is suboptimal. This inhibits an effective anti-cancer immune response and renders ICPI therapy ineffective or even detrimental. For example, PD-1 blockade has been shown to drive T cell dysfunction and anti-PD-1 resistance in the absence of effective priming (15). A non-reactive gene signature and immunosuppressive cytokine production [such as IL10 and transforming growth factor β (TGF-β)] maintain a paucity of immune cells, and the immune-inhibitory effects of other TME constituents may predominate, for example cancer-associated fibroblasts (CAFs), hypoxia and abnormal vasculature (**Figure 1**) (16).

Although complex, and by no means universal, where a tumour sits on the axis of immunological heat is known to play a pivotal role in the response to ICPI therapy. Resistance mechanisms can remain dominant at the level of the TME even when circulating antigen-specific T cells are high (17), and local manipulation of the TME to increase the "heat" and improve ICPI responsiveness therefore presents a rational therapeutic strategy. Localised therapy/ICPI combinations involving radiotherapy or oncolytic virotherapy have gained the most clinical momentum to date. Further strategies in clinical development include agonists of immune-stimulatory pathways such as Stimulatory of Interferon Genes (STING) and Toll-Like Receptor (TLR) signalling, or physical modification or the TME using thermal treatments, such as high-intensity focused ultrasound (HIFU) or photothermaltherapy (18). This review will outline the effects of these treatments on TME composition and immunogenicity in "cold" tumours, and explore the evidence behind their combination with ICPI therapy.

Cellular and Molecular Mechanisms Underlying Immune Activation

Despite distinct differences in their mechanisms of action, the localised therapies featured in this review share some commonality in the basic immune-modulatory pathways through which they exert their immune effects and enhance ICPI therapy (summarised in **Table 2**). Advances in immunology research have validated radiotherapy-induced DNA damage as a viral mimic (34), triggering the same intrinsic anti-viral inflammatory pathways that are naturally stimulated by OV therapy (35). These protective pathways can also be targeted downstream by other agents such as TLR or STING agonists, and form the cellular machinery that enable recognition and presentation of pathogenic material or cellular defects - leading to an inflammatory signalling cascade and an innate and adaptive immune response.

Pattern-recognition receptors (PRRs) expressed on innate immune cells have evolved to detect microbial pathogenic molecules collectively known as pathogen-associated molecular patterns (PAMPs). The cytosolic nucleic acid sensors cyclic GMP-AMP synthase (cGAS) and retinoic acid inducible gene I (RIG-I) are not only important for detection of infected cells but also for immune recognition of cancer cells (36). Changes in the composition and abundance of cytosolic double-stranded DNA (dsDNA) and dsRNA induced during tumorigenesis, or by cellular stress following therapy, are detected by PRRs such as cGAS and RIG-I respectively, resulting in activation of STING and mitochondrial antiviral-signalling protein (MAVS). The resulting complex downstream signalling, including IRF3 and NFkB-dependent pathways, ultimately leads to expression of type I interferons (IFNs) and other pro-inflammatory cytokines (37, 38).

Two decades ago, Polly Matzinger postulated that immune activation can also occur in the absence of microbial products, instead being triggered by inflammatory signals released from stressed or dying cells (39), which are collectively named damage-associated molecular patterns (DAMPs). DAMPs such as ATP, HMGB1 and calreticulin are hallmarks of the highly inflammatory process of immunogenic cell death (ICD), which is defined as a regulated cell death mechanism capable of inducing

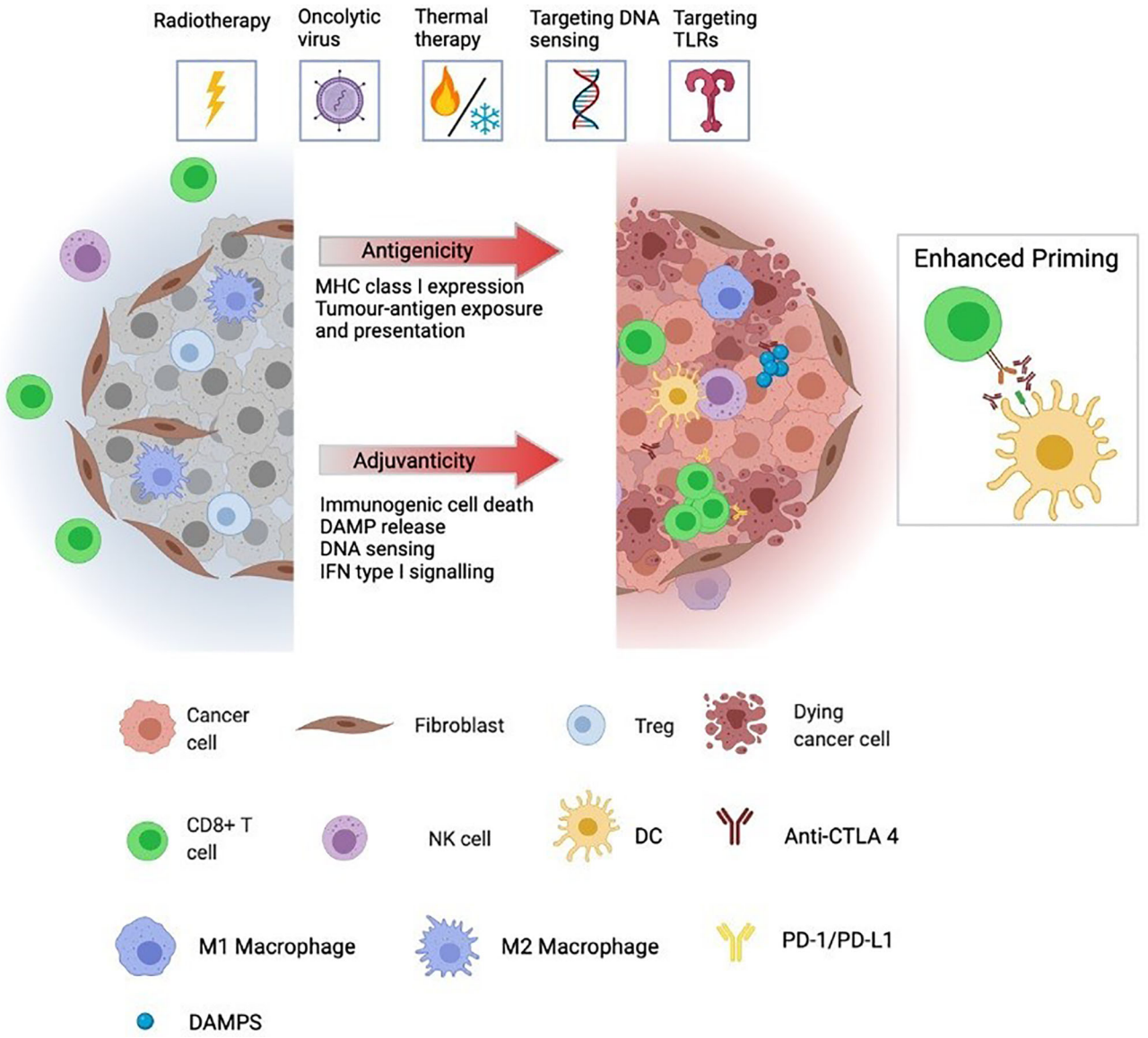

FIGURE 1 | Immunologically "cold" tumours are generally unresponsive to ICPI and characterised by low infiltration and/or exclusion of cytotoxic lymphocytes, including CD8 T cells and NK cells. Further, cold tumours often have high infiltration of immunosuppressive cells including Tregs, CAFs, and M2-polarized macrophages as well as low expression and presentation of tumour neoantigens preventing priming of de novo immune responses. Immunogenic localised therapies are designed to convert 'cold' tumours to a 'hot' by altering the adjuvanticity and antigenicity of the TME. Antigenicity is achieved by augmented expression, degradation and presentation of tumour neoantigens while adjuvanticity is associated with elevated levels of DAMPs, released from dying tumour cells, cytosolic DNA accumulation and sensing, and a transcriptional profile geared towards IFN type I signalling. Together, these factors promote recruitment, infiltration and activation of DCs allowing for increased antigen cross-presentation and priming of tumor-specific CD8 T cells. Triggering of these events by localised therapies creates a favourable environment for synergy with ICPI. The pool of activated cross-presenting DCs cooperates with anti-CTLA-4 treatment to generate a broadened repertoire of tumour neoantigen-specific T cells whose effector function can be augmented by anti-PD-1 treatment in their killing of tumour cells locally and systemically. TME, tumour microenvironment; DAMP, danger-associated molecular pattern; DC, dendritic cell; CAF, cancer-associated fibroblast; ICPI, immune checkpoint inhibitor; NK cell, natural killer cell.

an adaptive immune response in the host. Release of the metabolic mediator ATP into the extracellular space triggers recruitment and activation of DCs *via* P2Y2 and P2X7 receptors respectively (40, 41), while secretion of HMGB1 activates DCs *via* TLR-4 (42). Translocation of calreticulin to the cell surface provides an "eat-me" signal to antigen-presenting cells and results in phagocytosis of the target cell (43). In the context of cancer, ICD leads to release of tumour-associated antigens (TAA) and subsequent priming of a cancer-specific immune response.

TABLE 2 | Summary of key mechanisms of therapeutic synergy between localised therapy combinations and ICPI.

Therapy-induced mechanisms	Immunogenic effects promoting synergy with ICPI	References
Nucleic acid sensing	Induced IFN type I signalling	(19–23)
cGAS/STING activation	→ T cell recruitment	
RIG-I/MAVS activation	→ Augmented CD8 T cell cytotoxicity	
	→ Increased DC cross-priming	
DAMP release/exposure		
ATP	Recruitment and activation of DCs	(24–26)
HMGB1	Increased phagocytosis	
CALR	Production of pro-inflammatory cytokines	
Neo-antigen expression and processing	Increased peptide pool	(27–31)
	Increased diversity of TCR repertoire	
	Generation of tumour specific T cells	
MHC class I upregulation	Augmented CD8 T cell priming	(27)
	Enhanced tumour cell killing	
Death-receptor upregulation	Augmented NK cell and CD8 T cell cytotoxicity	(32, 33)

Together, therapy-induced inflammatory PAMP and DAMP signalling generate a favourable environment for activated DCs to process and cross-present tumour-derived antigens to naïve T cells, which can prime and sustain a systemic tumour-specific immune response in synergy with ICPI. Induction of ICD, and the resultant increase in adjuvanticity of the tumour, is therefore a key mechanism underlying the efficacy of immunogenic localised therapies such as OV and radiotherapy.

ONCOLYTIC VIROTHERAPY

Oncolytic viruses (OV) are naturally-occurring or genetically-modified (GM) viruses that selectively infect and destroy tumour cells through direct cell lysis and stimulation of an anti-cancer immune response (44). Many tumour cells are intrinsically sensitive to viral infection due to common deficiencies in key anti-viral machinery that enables unhindered viral replication while normal tissue is spared (45), a characteristic that can be optimized for safety and selectivity through variant selection or viral genetic modification.

The immune stimulatory effects of OV are multi-modal. Viral replication triggers cell lysis and ICD. This releases viral progeny to continue the lytic cascade in surrounding tumour cells, as well as TAA for cross-priming of APCs and DAMPs, subsequently leading to stimulation of a Type 1 IFN-mediated anti-tumour immune response (46). The cell intrinsic anti-viral apparatus also plays an integral role in OV-mediated immunity. Viral DNA and RNA are sensed by PRRs such as cGAS and RIG-I respectively, triggering an ATP-dependent inflammatory cascade mediated by STING, leading to JAK/STAT pathway upregulation and pro-inflammatory cytokine release (47).

The result is a switch to an immune-stimulatory TME, with influx of activated T cells and APCs, upregulation of MHC and co-stimulatory markers such as CD40, CD80 and CD86 (48), as well as enhanced antigen presentation. This leads to the upregulation of PD-1 and CTLA-4 by T cells, potentiating immune checkpoint inhibition. This OV-mediated immune-stmulation also presents a barrier to effective OV monotherapy, mediating adaptive resistance and leading to exhausted Teff and Treg influx. Synergy between ICPI and OV herefore has the potential to work both ways; OV may enhance response to ICPI, and conversely ICPI may enhance the efficacy of OV.

In 2015, the oncolytic Herpes Simplex Virus (oHSV), talimogene laherparepvec, became the first OV to gain regulatory approval for cancer therapy (49), leading to an acceleration in OV research. Since this milestone, evidence for the widespread clinical implementation of OV monotherapy has been limited. The 26% ORR and 23.3-month median OS seen with T-Vec in advanced melanoma was surpassed by dual checkpoint blockade, and to date no further OV have gained FDA approval.

What has become apparent is the potential of OV therapy as an immune adjuvant in combination with other immune-modulatory therapies, such as ICPI. In combination, OV present an appealing prospect. They exhibit anti-cancer activity and tumour selectivity, are generally well-tolerated with non-overlapping side-effects, and have the ability to increase the immunological heat of OV-injected and non-injected tumours – a phenomenon demonstrated in both pre-clinical animal models and patients (50).

A further advantage of OV therapy is the application of OV as viral vectors. The large backbone of some OV, such as oncolytic Herpes Simplex Virus (oHSV), Adenovirus (oADV) or Vaccinia Virus (oVV) can be manipulated by insertion of therapeutic transgenes, thus exploiting selective viral replication for concentrated delivery of immune-modulatory agents within the TME. This provides a unique opportunity, not only to manipulate the TME to enhance ICPI therapy, but to deliver the ICPI themselves. This is a particular advantage when considering the delivery of molecules where systemic administration may be limited by toxicity or pharmacokinetic considerations. Examples include the anti-CTLA-4 mAb, or potent immune-stimulators such as agonists of the 4-1BB co-stimulatory receptor or stimulatory cytokine IL-12.

Several clinical trials of OV/ICPI combinations are currently ongoing or have recently been completed, backed by pre-clinical evidence of synergistic effects. This section will focus on the rationale and evidence behind locally-delivered OV and ICPI

therapy combinations; strategies featuring systemic OV delivery are reviewed in detail elsewhere (51).

Localised OV and Checkpoint Blockade Combinations – Pre-Clinical Studies

Extensive pre-clinical research has evaluated the mechanisms behind OV remodelling of the TME in "cold" tumours, and the implications for subsequent checkpoint blockade. Among the most clinically advanced OV to date are variants of the oHSV and oADV viral platforms, double-stranded DNA viruses that are not only highly immune-stimulatory, but have large viral backbones that provide opportunity for transgene insertion.

Zhang et al. showed that oHSV therapy led to an increase in tumour-infiltrating CD4 and CD8 T cells and a decrease in Treg and suppressive TAM in a mouse model of pancreatic ductal adenocarcinoma (PDAC). PDAC is a notoriously immune-excluded, "cold" tumour, with a TME comprising immunosuppressive Treg, tumour associated macrophages (TAM), immunosuppressive cytokines and physical barriers to T cell infiltration such as CAFs and a desmoplastic stroma (52). Transcriptome profiling of immune cells following treatment showed enrichment of PD-1, LAG-3 and TIM-3 in the CD8 T cell population, and OX40 and CTLA-4 in the CD4 population (53). Accordingly, triple combination therapy (OV/PD-1/CTLA-4) was shown to significantly prolong survival in PDAC tumour-bearing mice.

HF-10 (Canepaturev, CRev) is a further oHSV1 which contains natural mutations that enhance selectivity. HF-10 treatment led to an influx of CD8 T cells in a poorly immunogenic HNSCC model, with infiltration of PD-L1-expressing macrophages and DCs in both OV-injected and non-injected tumours. Despite a PD-L1-enriched TME, a therapeutic effect was seen with single-agent HF-10 treatment; however, this was significantly enhanced by addition of anti-PD-L1 therapy. Interestingly, synergy was seen with high-dose, but not low-dose, anti-PD-L1 therapy highlighting a dose-dependent factor in the ability of ICPI to overcome either the intrinsic tumour-mediated immunosuppression or OV-induced checkpoint upregulation (54).

Saha et al. showed enhanced CD8 T cell infiltration in an 005-GSC-derived GBM mouse model following treatment with a third-generation triple-mutated oHSV encoding the immunostimulatory cytokine IL-12 (G47ΔV-mIL-12) (55). Glioblastoma multiforme (GBM) is a highly immunosuppressive tumour, with low response rates to single and dual checkpoint blockade and added immuno-therapeutic complexity provided by the blood-brain barrier and tissue hypoxia (55). In addition to Teff infiltration, changes were seen in other TME cell compartments, with a decrease in the proportion of Treg and an increase in the CD8 T cell/Treg ratio. A shift was seen towards pro-inflammatory M1-polarised macrophages with an increase in IFNy production, indicating a more-immunogenic tumour phenotype. Modest synergy was seen when G47ΔV-mIL-12 was combined with single agent ICPI (PD-1 or CTLA-4), however triple therapy (OV/PD-1/CTLA-4) led to long-term cures and protection from tumour re-challenge. This treatment effect was dependent on CD4 and CD8 T cells, as well as macrophages, highlighting the complex relationship between constituents of the TME, and the potential need for multi-targeted therapy to overcome tumour-mediated immunosuppression.

Adenovirus is a double-stranded DNA virus which has again been extensively investigated in the context of OV therapy, including for GBM. Stereotactic administration of low dose oADV was shown to upregulate PD-1 expression on tumour-infiltrating CD8 T cells, highlighting a mechanism of adaptive resistance. Synergy was seen with anti-PD-1 therapy, with significantly improved survival in GBM tumour-bearing mice (56).

Evidence of efficacy of an oADV encoding co-stimulatory ligand CD40-L was shown by Singh et al. in a mouse melanoma model. Melanoma has been well-established as an immunogenic "hot" tumour site. Despite this, 50% of patients do not respond to dual checkpoint blockade. The B16 mouse melanoma model is highly immunosuppressive, with an immune-excluded TME and production of immunosuppressive cytokines such as TGF-β. Remodelling of the TME was seen following treatment, with an influx of IFNy-producing CD8 T cells, an increase in the CD8:Treg ratio and upregulation of PD-L1 on tumour tissue. Combination treatment with anti-PD-L1 enhanced therapy and led to an increase in CTLA-4-expressing CD8 T cells. Subsequent triple therapy (OV/PD-L1/CTLA-4) significantly improved response, leading to regression of OV-injected and non-injected lesions (including brain metastases). A 45% cure rate was achieved, with protection from tumour re-challenge (57). Hu et al. also demonstrated synergy between a modified oADV, this time armed with immunostimulatory cytokine IL-24, and PD-1 blockade in B16-melanoma tumour-bearing mice. Treatment increased CD8 T cells, Tregs and CD11b+ myeloid cells, with MHC upregulation on APCs and production of inflammatory cytokines (58). Interestingly, although anti-tumour immunity was seen to be dependent on viral attachment and entry, the oADV did not successfuly infect and lyse cells and, therefore, lead to PAMP/DAMP release, and hence did not induce anti-tumour immunity through these mechanisms. Instead, oADV treatment appeared to label tumour cells as "non-self", leading to enhanced MHC-1 and co-stimulatory CD80 expression, and presentation of "non-self" viral epitopes on the tumour-cell surface, triggering an anti-cancer immune response. This highlights the complex mechanisms surrounding the immune-stimulatory effects of OV (59).

The vaccinia poxvirus, historically used as a vaccine for smallpox since the late 19th century, is also in clinical development as an OV. The modified oVV pexastimogene devacirepvec (JX-594) has yielded disappointing results in clinical trials to date, most notably with the failure of the phase 3 PHOCUS trial in liver cancer (60). However, it has shown pre-clinical promise in combination with ICPI therapy. Remodelling of the TME was demonstrated by Chon et al. following IT JX-594 therapy, with an influx of CD8 T cells and NK cells, upregulation of inflammatory genes and a switch to an immune-stimulatory TME in mouse breast and renal cancer models. As with other studies, combinaton with single-agent ICPI enhanced therapy, however triple therapy (OV/PD-1/CTLA-4) led to complete, durable tumour regression (61). Similar trends were seen in other studies of poorly immunogenic mouse colon and ovarian cancer models (62, 63).

An alternative therapeutic strategy is using OV as viral vectors to deliver ICPI therapy through insertion of transgenes encoding checkpoint blocking antibodies, an attractive prospect when considering complex immunomodulatory combinations and avoidance of systemic ICPI toxicity. Having said that, encoding ICPI or immune activating ligands within OV may present some limitations, not least of all the fact that the two components of therapy are obligatorily expressed within the same tissue compartment, which may not always be the optimum means of combination. Kleinpeter et al. showed that insertion of murine anti-PD-1 into an oVV backbone enhanced therapeutic effects in a poorly-immunogenic mouse fibrosarcoma model (64). Therapy led to a higher and more prolonged intra-tumoural anti-PD-1 concentration than IT injection of the antibody itself, highlighting the advantage of viral replication in dose amplification. Blood levels of anti-CTLA-4 mAb were also shown to be low following IT delivery of the GM oVV BT001 encoding anti-CTLA-4 and GM-CSF, while IT levels were sufficient to suppress CTLA-4 receptor function for days to weeks following injection (65).

Additional pre-clinical evidence was presented by Zuo et al. Up to 70% complete and durable tumour regression was seen in mouse tumour models following treatment with an oVV encoding novel checkpoint TIGIT, which is highly expressed on natural killer T cells (NKT) and Tregs. Treatment stimulated a CD8 T cell-mediated anti-tumour response with evidence of immune memory and protection from re-challenge. High levels of anti-TIGIT mAb were seen in tumour tissue, but not in blood from treated mice (66). A TK-gene deleted oVV expressing anti-PD-1 and an anti-4-1BB co-stimulatory receptor agonist was also shown to suppress tumour growth in mouse models of liver and pancreatic cancer (67).

The oHSV platform is also amenable to genetic modification. Coffin et al. developed the RP oHSV platform, featuring ICP34.5 and ICP47 deletions to attenuate neurovirulence and enhance antigen presentation and GALV-GP-R and hGM-CSF insertion to enhance OV-induced ICD. Further modification with insertion of ICPI or co-stimulatory ligands (CTLA-4, 4-1BB, CD40-L and OX40-L) was shown to increase therapeutic efficacy in tumour-bearing mice (68). Enhanced therapy, this time with an anti-PD-1 armed oADV was also demonstrated by Zhang et al. The un-modified oADV was shown to increase TME immune infiltration and promote PD-L1 upregulation but failed to prolong survival. Genetic modification with the addition of the extracellular domains of PD-1 and CD137L (4-1BBL) led to a 70% long-term cure rate in a sub-cutaneous hepatocellular carcinoma (HCC) model (69). A further modified oADV, LOAd703, also encodes 4-1BBL, along with TMZ-CD40-L, and has shown pre-clinical activity in PDAC mouse models (70).

Other OV in clinical development include polioviruses, Newcastle disease virus (NDV), reovirus and maraba virus. Clinical trials involving both reovirus and NDV in combination with ICPI therapy are ongoing, with pre-clinical evidence of synergy (3, 49, 71, 72); however, these are focused on systemic delivery, and as such are reviewed elsewhere. The non-neurovirulent rhinovirus:poliovirus chimera PVSRIPO was shown to synergise with anti-PD-1 and anti-PD-L1 therapy in mouse triple-negative breast cancer (TNBC) models (73) and is currently the subject of early-phase clinical trials. Maraba virus is a member of the Rhabdovirus family of RNA viruses, and was shown to increase Treg and PD-L1 expression when given prior to tumour resection in mouse breast cancer models. Post-operative addition of dual ICPI therapy (CTLA-4/PD-1) was shown significantly to prolong survival when compared to virus or ICPI alone (74).

CLINICAL TRANSLATION

Herpes Simplex Virus

Oncolytic viruses based on the Herpes Simplex Virus-1 (oHSV-1) have gained the most clinical traction to date following the approval of T-Vec in the treatment of melanoma. In T-Vec, the HSV backbone has been modified by deletion of ICP34.5 and ICP47 and insertion of GM-CSF to enhance selectivity and immune effects. T-vec was shown to induce antigen-specific local and systemic immunity in phase II studies, with an increase in CD8 T cell density in injected and non-injected lesions, increased checkpoint expression (50), and an increase in melanoma antigen-specific T cells (75).

T-Vec/ICPI combination therapy has to date yielded mixed results. A phase II trial of IT Tvec and Ipilimumab therapy in advanced melanoma showed a significant improvement in response (38% vs 18%) with regression of non-injected lesions and no additional safety concerns (76). However, a phase III study evaluating T-Vec in combination with Pembrolizumab was recently terminated due to futility at interim analysis (77), despite promising translational data in the phase 1b part of the the trial (78). The MASTERKEY-232 phase Ib study evaluated Tvec in combination with Pembrolizumab in recurrent or metastatic HNSCC. PFS and OS was comparable to documented results of Pembrolizumab monotherapy, and phase III was not pursued (79). As is a common IO theme, impressive and durable responses are seen for a minority. For example, Khaddour et al. reported a case of complete, durable tumour regression in a patient with melanoma with brain metastases following T -Vec, Atezolizumab and Temozolomide therapy (80). This highlights that there is much still to learn about the biology underpinning these and future complex combinatorial strategies. Several trials featuring T-Vec/ICPI combinations are ongoing (**Table 3**).

The spontaneous oHSV mutant HF-10 has also been evaluated in clinical trials in combination with ICPI therapy. A phase II study of HF-10 and Ipilimumab in advanced melanoma demonstrated an acceptable safety profile with a best overall response rate (BORR) of 41% and 19-month median PFS (81). Responding patients had influx of CD4 and CD8 T cells, along with increased CD4 ICOS expression and PD-L1 upregulation on monocytes. HF-10 was also evaluated in combination with Ipilimumab in patients with treatment-refractory acral and mucosal melanoma with an 11.1% BORR and 55.5% disease control rate (82).

The RP oHSV platform developed by Coffin et al. (RP1, RP2 and RP3) is undergoing clinical evaluation, with ongoing phase I and II trials in combination with anti-PD-1 or anti-PD-L1 agents

TABLE 3 | Summary of ongoing clinical trials evaluating oncolytic virotherapy in combination with immune checkpoint inhibition.

Oncolytic virus and NCT number	Combination	Status
Herpes Simplex Virus-1 (HSV-1)		
NCT04185311	T-Vec + Ipilimumab + Nivolumab	Active, not recruiting. Phase 1. Neo-adjuvant, breast cancer (TNBC, ER +HER2-)
NCT03842943	T-Vec + Pembrolizumab	Recruiting. Phase 2, neo-adjuvant, stage 3 resectable melanoma
NCT04068181	T-Vec + Pembrolizumab	Active, not recruiting. Phase 2, metastatic melanoma following progression on anti-PD1 therapy
NCT03069378	T-Vec + Pembrolizumab	Recruiting. Metastatic/locally advanced sarcoma
NCT02509507	T-Vec + Pembrolizumab	Recruiting, phase 1b/2. Liver tumours (HCC and liver metastases)
NCT04050436	RP1 + Cemiplimab	Recruiting Phase II Locally advanced or metastatic cutaneous SCC (CSCC)
NCT03767348	RP1 + Nivolumab	Recruiting Phase 1/2 Advanced and/or refractory solid tumours
NCT04336241	RP2 + Nivolumab	Recruiting Phase 1, advanced solid tumours
NCT04735978	RP3 + Nivolumab	Recruiting Phase 1, advanced solid tumours
NCT04348916	ONCR-177 + Pembrolizumab	Recruiting. Phase 1, advanced solid tumours and liver metastases
Adenovirus		
NCT04387461	Intravesical CG0070 + Pembrolizumab	Recruiting Phase 2, non-muscle invasive bladder cancer
NCT02636036	Enadenotucirev + Nivolumab	Active, not recruiting Phase 1, metastatic or advanced epithelial tumours
NCT02798406	DNX-2401 + Pembrolizumab	Active, not recruiting Phase 2, glioblastoma and gliosarcoma
NCT04123470	LOAd703 + Atezolizumab	Recruiting Phase 1/2, Metastatic melanoma
NCT02705196	LOAd703 + Atezolizumab + standard of care (Gemcitabine/nab-Paclitaxel)	Recruiting. Phase 1/2. Pancreatic cancer.
NCT03172819	OBP-301 + Pembrolizumab	Active, not recruiting Phase 1, advanced or metastatic solid tumours
NCT03921021	OBP-301 + Pembrolizumab	Recruiting Phase 2, esophagogastric adenocarcinoma
NCT03003676	ONCOS 102 + Pembrolizumab	Active, not recruiting. Phase 1, advanced melanoma after progression on anti-PD-1 therapy
NCT02963831	ONCOS 102 (intraperitoneal) + Durvalumab	Recruiting, phase II
Vaccinia virus		
NCT03294083	Pexa-Vec (JX-594) + Cemiplimab	Recruiting, phase 1b/2a, metastatic or unresectable RCC
NCT02977156	Pexa-Vec (JX-594) + Ipilimumab	Recruiting, phase 1, advanced solid tumours
Poliovirus		
NCT04577807	PVSRIPO + Nivolumab	Phase 2. Advanced, PD1 refractory melanoma
NCT03973879	PVSRIPO + Atezolizumab	Withdrawn (resubmission planned), phase 1/2 glioma
VSV		
NCT02923466	VSV-OFNb-NIS + Avelumab	Active, not recruiting. Phase 1, refractory solid tumours

in advanced solid tumours (**Table 3**). An oncolytic HSV-2 virus was also evaluated in a first-in-human phase 1b study in combination with anti-PD-1 therapy in metastatic oesophageal and rectal cancer patients. Remodelling of the TME was apparent, with CD8 T cell infiltration and increased PD-L1 expression, along with evidence of regression of both injected and non-injected lesions (52).

Adenovirus

Several oADV are in clinical development and have been tested in combination with ICPI therapy. ONCOS-102 is an oADV with a 24bp deletion in the E1A Rb binding site to attenuate replication in normal tissue, and addition of GM-CSF for immune augmentation. A two-part phase I study of ONCOS-102 in combination with concurrent or sequential anti-PD-1 therapy provided evidence of the ability of OV to overcome ICPI resistance. This trial recruited advanced melanoma patients that were refractory to prior anti-PD-1 therapy, and reported a 35% ORR in an early analysis (NCT03003676). A phase I study of ONCOS-102 in combination with Durvalumab in ovarian and colorectal cancer with peritoneal metastases showed an increase in CD8 T cell infiltration and PD-L1 expression following treatment. Some evidence of clinical activity was seen, but only 1 durable response. Phase II recruitment is ongoing (NCT02963831). DNX-2401 is a further oADV with E1A deletion. A phase II dose escalation study of IT DNX-2401 in

combination with Pembrolizumab in recurrent GBM noted an 11.9% ORR with 2 ongoing durable responses in the 49 patients recruited, median OS was 12.5 months (83). CG0070 is an oADV armed with GM-CSF. A phase II study evaluating intra-vesical CG0070 in combination with pembrolizumab in immunotherapy-refractory non-muscle-invasive bladder cancer (NMIBC) is ongoing (NCT04387461).

LOAd703 is a modified oADV armed with immune-stimulatory transgenes TMZ-CD40L and 4-1BBL. A phase 1/2 trial is currently recruiting and will evaluate LOAd703 in combination with standard of care chemotherapy (Gemcitabine/nab-Paclitaxel) and Atezolizumab in PDAC (NCT02705196). Pancreatic cancer is notoriously immune-excluded, however combination treatment was shown to increase antigen-specific T cells and reduce circulating MDSCs, with a partial response in 6/10 subjects in an interim report (84). Finally, the modified oADV TILT-123 encodes two immunostimulatory cytokines (IL2 and TNFa) with promising pre-clinical activity in combination with anti-PD-L1 therapy. A study combining TILT-123 with anti-PD-L1 agent Avelumab is planned for 2021.

Other Locally-Delivered OV in Clinical Development

Synergy has been demonstrated between oncolytic Coxsackie viral strain CVA21 (Cavatek) and ICPI therapy and, as with other OV, added toxicity in combination was minimal. Changes within the TME were seen following CVA21 treatment, with increased CD8 T cell infiltration and upregulation of PD-L1 and other immune checkpoint receptors. The phase Ib MITCI trial evaluated IT CVA21 therapy in combination with Ipilimumab in patients with advanced melanoma. An ORR of 38% was observed with no dose-limiting toxicity (85) (NCT02307149). Interim results of the phase I CAPRA study of IT CVA21 and Pembrolizumab therapy, also in advanced melanoma, showed an ORR of 73% with regression of injected and non-injected lesions (86), the study has completed although final results have not yet been published. The phase I CANON trial of intra-vesical CVA21 in NMIBC also showed transition of the TME to an inflamed phenotype along with upregulation of immune checkpoints such as PD-L1 and LAG-3 (87).

The modified vaccinia poxvirus JX-594 (Pexa-Vec) is also under investigation in combination with ICPI therapy. A recent phase Ib study in patients with renal cancer reported evidence of treatment response in combination with Cemiplimab therapy. The first phase of this trial involved IV oVV treatment, however the second phase will evaluate localised IT therapy (NCT03294083). A further study recruiting patients with advanced solid tumours for combined IT JX-594 with Ipilimumab is ongoing (NCT02977156).

Intratumoural injection of an oncolytic Vesicular Stomatitis Virus (oVSV) construct VSV-hIFNbetasodium iodide symporter is currently being tested in combination with avelumab in advanced solid tumours (NCT02923466). The oncolytic poliovirus, PVSRIPO, is also being tested in phase I trials in combination with nivolumab in PD-1-refractory melanoma (NCT0412759) and atezolizumab in glioma (NCT03973879). All trials are currently recruiting.

RADIOTHERAPY

Evidence of involvement of the immune system in the anti-tumour effect of radiotherapy has accumulated over many decades. Radiotherapy-induced regression of tumour lesions distant from the radiation field was first described almost 70 years ago and termed the "abscopal" effect (88). Over the years, this rare phenomenon has been reported in several malignancies (89, 90), while in mice, the role of T cells in controlling tumour growth following radiotherapy has been described more recently (91). These findings have spurred a growing field of research into elucidating the determinants of radiation-induced immune responses as well as the prospect of boosting the abscopal effect with immunostimulatory agents, although whether, or not, the abscopal designation truly applies when a systemic immunotherapy is part of treatment remains a moot point.

Radiotherapy has traditionally been used to treat cancer by utilizing the selective inability of cancer cells to repair DNA damage. When radiotherapy is used as an immune adjuvant, the aim is to transform the tumour into an individualized *in situ* vaccine. This process requires increasing the antigenicity as well as the adjuvanticity of the targeted tumour which is highly dependent on firstly the mode of cell death that the irradiated tumour cells undergo, secondly which molecular signalling pathways are induced and thirdly which DAMPs are released in the TME.

Radiation-Induced Tumour Antigenicity

Antigenicity is increased by inducing exposure and presentation of mutation-associated tumour neoantigens, which are the key targets for a T cell-mediated anti-tumour immune response, and which correlate with response to ICPI (92). Radiotherapy has been shown to promote an acute transcriptional programme including genes associated with DNA damage and repair, many of which are frequently mutated in tumours (93). Further, radiotherapy increases the peptide pool through augmented protein degradation and mTOR-regulated translation (27). When combined with increased MHC class I expression, this results in more antigenic peptides being presented for recognition by the host immune cells and enhanced TCR diversity (34). Indeed, Lhuillier and Lussier showed that irradiation upregulates genes harboring immunogenic mutations, resulting in selective elimination of irradiated tumour cells by neoantigen-specific CD8 T cells in the 4T1 mouse breast cancer model and KP mouse sarcoma model respectively (30, 94). *In vivo* focal irradiation of 4T1 tumours was shown to broaden the TCR repertoire with expansion of T cell clones driven by anti-CTLA-4 checkpoint inhibition (31). Importantly, in a patient with metastatic NSCLC who experienced a complete response to radiotherapy and ipilimumab, Formenti et al. detected clonal expansion of an immunogenic antigen derived from a gene upregulated by radiation (29).

Radiation-Induced Tumour Adjuvanticity

DNA damage induced by ionizing radiation causes accumulation of double-stranded DNA (dsDNA) in the cytosol, as well as

micronuclei formation. This dsDNA is recognized by cyclic GMP-AMP synthase (cGAS) (95) and subsequently activates stimulator of interferon genes (STING), thus triggering the transcription of Type I IFNs (96). A main role of IFNs in anti-tumour immunity is to recruit DCs (97) and facilitate their maturation and migration to tumour-draining lymph nodes allowing for cross-priming of naïve T cells (98). The resulting activation and bridging of innate and adaptive immune cell responses ultimately promote proliferation and activation of antigen-specific anti-tumour T cells.

ICD is defined by induction of certain DAMPs, all of which are induced by radiotherapy (99) resulting in DC activation in a dose and fractionation-dependent manner (100). The importance of HMGB1 release from irradiated tumour cells for effective radiation-induced tumour response was exemplified by Apetoh and colleagues in two studies reporting dependency of TLR-4 signalling for efficient antigen presentation by DCs and tumour susceptibility to radiotherapy in mice and humans (26, 101). Further, increased translocation of calreticulin in human breast, prostate and lung cancer cells following radiotherapy was shown to increase their sensitivity to CD8 T cell lysis (43). Conversely, radiotherapy was shown to downregulate CD47 in head and neck tumours, counteracting its suppressive effect on DC phagocytosis and resulting in pronounced radiation-induced anti-tumour effect (102).

Radiotherapy and ICPI Combinations – Pre-Clinical Studies

As evidence mounts of the ability of radiotherapy to alter the immune composition of the TME, there are increasing efforts to implement radiotherapy as an adjuvant to ICPI in patients that are unresponsive to immunotherapy alone.

Radiotherapy (RT) has been shown to promote PD-1/PD-L1-mediated immune resistance, setting the stage for potential synergistic effects. PD-L1 surface expression was shown to be elevated on tumour cells following radiotherapy, which has been attributed to IFNg release from tumour-infiltrating lymphocytes (TILs) (103). Tumour-infiltrating T cells have also exhibited increased expression of PD-1 and 4-1BB following *ex vivo* irradiation of colon- and gastric cancer tumour samples (104). Indeed, PD-1/PD-L1 blockade administered concomitantly with hypofractionated radiotherapy improved tumour control, compared to radiotherapy or ICPI alone, and generated sustained CD8 T cell responses and immunological memory (103) while simultaneously reducing immune suppression by myeloid-derived suppressor cells (MDSCs) (105).

Further, radiotherapy has been shown to potentiate the anti-tumour effect of CTLA-4 blockade in a CD8 T cell-dependent manner in the aggressive and poorly immunogenic breast cancer model 4T1 (31, 33, 106, 107). In this model, radiotherapy was shown to stabilize the immune synapse when CD8 T cells engaged natural killer cell group 2D (NKG2D) with its ligand retinoic acid inducible 1 (Rae-1) on target tumour cells (33). Radiotherapy was also shown to promote T cell recruitment and tumour infiltration by increasing production of the chemokine CXCL16 (107). An increase in the TCR repertoire was demonstrated following RT, with proliferation when RT was combined with anti-CTLA-4 therapy. This was in contrast to single-agent anti-CTLA-4 therapy, which led to fewer T cell clones (31). Similarly, in a melanoma mouse model, CTLA-4 blockade cooperated with radiotherapy to increase the CD8 effector T cell to Treg ratio and diversify the T cell receptor (TCR) repertoire resulting in therapeutic synergy. The anti-tumour effect was further improved by addition of PD-L1 blockade to boost clonal expansion and offset T cell exhaustion (28).

Recently, in the poorly immunogenic, ICPI-refractory KP mouse sarcoma model, which has low mutational status, Lussier et al. reported that low-dose irradiation of KP cells induced immunogenic mutations generating neo-antigens sufficient to convey T cell-mediated protection against the parental cell line *in vivo* when combined with anti-CLTA-4 and anti-PD-1 treatment (94).

Clinical Translation

Robust pre-clinical evidence has meant that combinations of radiotherapy and ICPI continues to be an area of ever-increasing research interest. There are currently over 500 studies involving clinical testing of these combinations, a number that has greatly increased in recent years (**Table 4**).

Several retrospective studies have evaluated the potential benefit of irradiation prior to checkpoint inhibition. Knispel et al. recently reported results of a multi-centre retrospective study of 835 patients with metastatic melanoma receiving anti-CTLA-4 or anti-PD-1 therapy with or without previous radiotherapy for unresectable metastases (108). No evidence of benefit was seen with preceding radiation therapy. In contrast, retrospective analysis of the KEYNOTE-001 phase I trial of

TABLE 4 | Summary of actively recruiting clinical trials evaluating radiotherapy in combination with immune checkpoint inhibition.

Target	Checkpoint inhibitor	Number of actively recruiting clinical trials
CTLA-4	Ipilimumab	51
PD-1	Nivolumab	138
	Pembrolizumab	161
	Cemiplimab	6
	Dostarlimab	3
PDL-1	Atezolizumab	59
	Durvalumab	115
	Avelumab	23

NSCLC patients treated with Pembrolizumab showed an improvement in PFS and OS in patients who had previously been treated with radiotherapy (109). Neither study reported an increased risk of adverse events with combination therapy.

A non-exhaustive selection of prospective clinical studies evaluating RT/ICPI combinations is summarised in **Table 5**. Formenti et al. investigated the mechanisms behind response to combination anti-CTLA-4 and radiotherapy in treatment-refractory NSCLC patients in a phase I/II study (NCT02221739). Evidence of response was seen in 33% of evaluable patients, with 2 complete responses. There was no association seen between CD8 T cell infiltration or PD-L1 expression and response, however RT-induced IFNb secretion and sustained TCR clonal expansion was associated with an abscopal response (29). Conversely, a recent phase I study evaluating RT in combination with anti-CTLA-4 in metastatic melanoma showed CD8 infiltration to be significantly correlated with PFS (NCT01557114) (110). McBride et al. also evaluated the mechanics of the abscopal effect in a phase II study of Nivolumab with or without SBRT in metastatic HNSCC. No statistically significant differences were seen between treatment groups, with no evidence of abscopal effects (NCT02684253) (111). The combination of Pembrolizumab and RT in the definitive setting in HNSCC is also being evaluated, a phase II study comparing ICPI therapy with conventional chemoradiotherapy is currently recruiting (NCT03383094).

Several key studies have evaluated combinations of RT and checkpoint blockade in breast cancer, a site where RT presents a cornerstone of treatment and where ICPI therapy has shown limited efficacy to date. Phase III trials have supported the approval of ICPI therapy in PD-L1-positive TNBC patients in combination with chemotherapy, and subsequent trials of combination ICPI/RT have yielded mixed results. Triple-negative breast cancer is classically seen to be poorly immunogenic, however has a high mutational burden with significantly higher PD-L1 expression than other sub-types (112). A phase II study of RT and Pembrolizumab in metastatic TNBC patients not selected for PD-L1 expression showed that treatment was well tolerated with some evidence of clinical activity in this poor-prognosis group (17.6% ORR). The study reported 3 complete responses and evidence of response outside the radiation field (NCT02730130) (113). In contrast, Barroso-Sousa et al. reported negative results of pembrolizumab and palliative radiotherapy in a small 8 patient study of heavily pre-treated hormone receptor positive metastatic breast cancer patients. No objective responses were seen, and the median overall survival was 2.9 months (NCT03051672) (114). Trials of additional combinations are planned, for example a phase 2 study combining Atezolizumab, radiotherapy and the TLR-7/8 agonist BDB001 is currently recruiting patients with PD-1/PD-L1-refractory TNBC (NCT03915678). Three trials combining RT/ICPI and Parp inhibitors are also planned in PD-L1-negative or ICPI refractory metastatic TNBC (NCT04690855, NCT04683679).

As previously discussed, pancreatic cancer is notoriously immune-excluded and ICPI-refractory. A phase I study recently evaluated the safety of stereotactic body radiation therapy (SBRT) and Durvalumab or Tremelimumab treatment. No dose-limiting toxicities were seen with combination therapy, and 2/39 patients had a partial response with an ORR of 5.1% and PFS between 0.9 and 9 months depending on treatment cohort (NCT02311361) (115).

The phase III PACIFIC trial showed that Durvalumab therapy significantly improved survival compared to standard of care concurrent chemo-radiotherapy in patients with locally advanced stage III unresectable NSCLC (NCT02125461). Antonia et al. reported a pronounced benefit in PFS with Durvalumab treatment compared with placebo (16.8 months vs 5.6 months respectively) (116), highlighting the potential for upfront combination therapy in the definitive management of

TABLE 5 | A non-exhaustive representative summary of key clinical trials evaluating radiotherapy in combination with immune checkpoint inhibition.

NCT number	Combination	Study design	Findings
NCT02125461	Sequential Durvalumab after concurrent chemoradiotherapy (PACIFIC trial)	Phase 3, stage III unresectable NSCLC	Median PFS 16.8 months (Durvalumab) vs 5.6 months (placebo)
NCT02444741	50 Gy in 5 fractions SBRT + concurrent Pembrolizumab	Phase 1/2, metastatic NSCLC	Improved ORR, did not reach statistical significance
NCT02492568	24 Gy in 3 fractions + sequential Pembrolizumab	Phase 2, metastatic NSCLC	Improved ORR, did not reach statistical significance
NCT02904954	24 Gy in 3 fractions SBRT+ concurrent Durvalumab prior to surgical resection	Phase 2, stage I, II, IIa NSCLC, neo-adjuvant	Significantly higher major pathological response rate with combination treatment (53.3%) *vs* single agent Durvalumab (6/7%)
NCT02221739	30 Gy in 5 fractions (later 28.5 Gy in 3 fractions) RT + concurrent Ipilimumab	Phase 1/2, metastatic NSCLC.	Evidence of response in 33% of evaluable patients.
NCT01557114	9, 15, 18 or 24 Gy in 3 fractions RT + concurrent Ipilimumab	Phase 1, advanced melanoma	31% ORR, increased CD8+ T cells associated with improved PFS
NCT02684253	27 Gy in 3 fractions + concurrent Nivolumab	Phase 2, HNSCC	No improvement in response and no evidence of abscopal effect
NCT02730130	30 Gy in 5 fractions + concurrent Pembrolizumab	Phase 2, TNBC	ORR 17.6%, 3/17 CR
NCT03051672	20 Gy in 5 fractions + Pembrolizumab 2-7 days prior then every 21 days	Phase 2, metastatic hormone receptor positive, HER-2 negative breast cancer	No objective responses, median OS 2.9 months
NCT02311361	8 Gy single fraction or 25 Gy in 5 fractions + Durvalumab/Tremelimumab/dual ICPI	Phase 1/2, PDAC	ORR 5.1%, PFS between 0.9 and 9 months depending on treatment cohort

locally-advanced disease despite the mixed results discussed above. These findings represent a pivotal milestone for the clinical implementation of RT/ICPI combination therapy, and the subsequent PACIFIC-4 trial has extended this combination to early-stage NSCLC in stage I/II node negative disease.

Conversely, in locally-advanced HNSCC, the phase 3 JAVELIN-100 trial evaluating avelumab in combination with standard-of-care chemoradiotherapy failed to meet its primary endpoint of prolonged PFS. Of relevance, subgroup analysis showed the only PFS benefit to be in patients with tumours expressing high levels of PD-L1 (>25%) at baseline, and further research is needed to evaluate the barriers to effective therapy in "cold" tumours (117).

In the metastatic setting, the PEMBRO-RT (phase 2, NCT02492568) (118) and MDACC (119) (phase 1/2, NCT02444741) trials both noted a treatment benefit with combination pembrolizumab/RT in NSCLC. This did not reach statistical significance overall due to a small sample size, however significance was noted in both studies in an exploratory analysis of the sub-group of patients with tumours expressing low levels of PD-L1 suggesting a potential benefit in "cold" tumours. A recent pooled analysis of these two studies showed a significant improvement in outcomes with the addition of RT when compared to single-agent Pembrolizumab, with an OS of 19.2 months vs 8.7 months respectively (120).

A further treatment setting under evaluation is neo-adjuvant treatment of patients with early-stage disease. A recent phase II study of Durvalumab and SBRT therapy in NSCLC (NCT02904954) showed a significant increase in major pathological response rates with combination therapy when compared to single agent Durvalumab (53.3% and 6.7% respectively), validating the strategy for a larger trial (121). This setting has also been evaluated in breast cancer. Pre-operative RT and Pembrolizumab prior to standard-of-care in patients with TNBC was shown to be well tolerated in published interim results, with a pCR or 67%. Of note, baseline TIL count of >10% was shown to corellate with complete response, but not change in TIL over treatment (122). Finally, encouraging results were seen in a recent phase Ib trial of neo-adjuvant SBRT and anti-PD-1 therapy in HNSCC (NCT03247712), where the combination was seen to be well tolerated with a high rate of major pathological response (86%) (123).

OTHER LOCALISED THERAPIES

Other strategies aimed at TME manipulation towards a more inflamed phenotype are also in clinical development. These include locally-delivered immune-adjuvants, non-viral oncolytics, and physical thermal therapies such as high intensity focused ultrasound (HIFU). A non-exhaustive selection of ongoing clinical studies are summarised in **Table 6**.

PV-10

Rose Bengal disodium is a small-molecule analogue of the commonly-used conjunctival dye fluorescein and is under clinical evaluation in its injectable form PV10 as a cancer immunotherapy. Intralesional PV-10 has been shown selectively to accumulate in lysosomes within tumour cells, leading to immunogenic cell death, PAMP, DAMP and TAA release, and an antigen-specific anti-cancer T cell response. Pre-clinical synergy has been shown with IT PV-10 and anti-PD-L1 therapy, with the initiation of a CD8 T cell-dependent anti-tumour immune response and depletion of Treg (124). A phase Ib trial combining PV-10 with pembrolizumab met its primary endpoint of safety in advanced melanoma and led to a complete response (CR) in 9% with partial response in 57% - translational correlative T cell data are awaited (125). Two expansion cohorts are currently recruiting patients with checkpoint-inhibitor-refractory melanoma (NCT02557321).

Toll-Like Receptor Agonists

Toll-like receptors (TLRs) are a family of PRRs that are most commonly found on DCs and macrophages, but also on T cells and tumour tissue. They play a key role in the innate and adaptive immune response, recognising potentially harmful

TABLE 6 | A non-exhaustive summary of ongoing clinical trials evaluating other localised therapies in combination with immune checkpoint inhibition.

Agent and NCT number	Combination	Study design	Status
Rose Bengal Disodium (PV-10)			
NCT02557321	PV-10 + Pembrolizumab	Phase 1, ICPI-refractory advanced melanoma	Recruiting
TLR agonists			
NCT03865082	Tilsotolimod (TLR-9 agonist) + Ipilimumab and Nivolumab	Phase 2, solid tumours	Recruiting
NCT04633278	CMP-001 (TLR-9 agonist) + Pembrolizumab	Phase 2, HNSCC	Recruiting
NCT03435640	NKTR-262 (TLR-7/8 agonist) + Nivolumab/pegylated-IL2	Phase 1/2, advanced solid tumours	Active, not recruiting
NCT03301896	LHC-165 (TLR-7 agonist) + PDR001 (anti-PD1)	Phase 1, advanced solid tumours	Active, not recruiting
NCT03317158	BCG + Durvalumab + RT	Phase 1/2, NMIBC	Recruiting
STING agonists			
NCT03010176	MK-1454 + Pembrolizumab	Phase 1, advanced solid tumours	Active, not recruiting
NCT04220866	MK-1454 + Pembrolizumab	Phase 2, HNSCC	Active, not recruiting
NCT03937141	ADU-S100 + Pembrolizumab	Phase 2, HNSCC	Active, not recruiting
Oncolytic Peptides			
NCT04796194	LTX-315 + Pembrolizumab or Ipilimumab	Phase 2, advanced solid tumours	Recruiting
Thermal treatments			
NCT03237572	HIFU + Pembrolizumab	Phase 1, metastatic breast cancer	Recruiting

PAMPs and DAMPs including microbial nucleic acids and TAA and triggering apoptosis and immune cell maturation and recruitment.

Bacillus Calmette Guerin (BCG) is a live attenuated strain of Mycobacterium Bovis, a potent agonist of TLR-2 and 4 that has been routinely used in the treatment of bladder cancer for decades. Schmidt et al. showed intra-tumoural injection of the TLR-9 agonist lefitolimod led to remodelling of the TME to a "hot" phenotype in mouse CRC models – with CD8 T cell influx, an increase in the CD8:Treg ratio and a greater proportion of M1-polarised macrophages (126). Enhanced therapeutic effect was seen in combination with anti-PD-1 therapy (127).

Several clinical trials are ongoing evaluating TLR agonist/ICPI combinations. The phase I/II ILLUMINATE-204 multi-centre study evaluated intra-tumoural TLR-9 agonist (tilsotolimod) therapy in combination with Ipilimumab in PD-1 refractory metastatic melanoma (NCT02644967). Responses were seen in local and distant lesions, with a 22.4% ORR (2 complete responses) and a 21-month median OS. Tumour biopsies showed evidence of an IFNa inflammatory gene signature and expansion of CD8 T cell clones (128). The subsequent ILLUMINATE-301 trial failed to achieve its primary end point, with no significant improvement in ORR over Ipilimumab alone (NCT03445533) (129). A further phase II study is ongoing recruiting patients with microsatellite stable (MSS) colorectal cancer (CRC) for intra-tumoural tilsotolimod in combination with ipilimumab (ILLUMINATE-206, NCT03865082). Early results showed the combination to be generally well tolerated with some evidence of response in injected and non-injected lesions.

Milhem et al. (130) reported early results of an ongoing phase 1b trial of a further TLR-9 agonist (CMP-001) and pembrolizumab in patients with PD-1-refractory melanoma. A best ORR of 23.5% was seen with a median duration of response of 19.9 months (NCT02680184). CMP-001 was also evaluated in a recently completed phase I study in combination with atezolizumab in PD-1-resistant NSCLC with or without radiation therapy (NCT03438318). CMP-001 was delivered SC (weeks 1 and 2) then IT (weeks 3-5) into visceral lesions. Treatment had a tolerable safety profile and stable disease was seen in a subset of patients. However, enrolment was stopped after Stage 1 due to no objective responses CMP-001 is also being evaluated in a Phase II trial in combination with Pembrolizumab in HNSCC (NCT04633278). Preliminary results of a Phase Ib study of TLR-7/8 agonist NKTR-262 in combination with Nivolumab and pegylated IL2 in advanced solid tumours (NCT03435640) showed enhanced immune infiltration and early evidence of clinical activity (131).

Other ongoing clinical trials include the IT TLR-7 agonist LHC165 in combination with anti-PD-1 in patients with advanced solid tumours (NCT03301896), the TLR-8 agonist motolimod in combination with anti-PD-1 agent nivolumab in HNSCC (Phase 1, NCT03906526) and BCG in combination with Durvalumab +/- RT in NMIBC (NCT03317158).

STING Agonists

The adaptor protein, STING, is a critical component of the previously discussed cGAS/STING pathway and acts as a bridge between innate and adaptive immunity. Cytosolic microbial or tumour-derived DNA is sensed by the PRR, cGAS, which undergoes conformational changes to catalyse ATP and GTP into the cyclic di-nucleodide (CDN) cGAMP. STING is activated on binding with cGAMP or other CDNs, leading to stimulation of a type 1 IFN response, immune cell recruitment, promotion of DC maturation and priming of antigen-specific immunity.

Most STING agonists in clinical development are human, bacterially-derived or synthetic CDNs mimicking cGAMP. As STING is located intracellularly on the ER, any agonist must penetrate the cell membrane, leading to low bioavailability of natural CDNs which are hydrophilic, electronegative and large in size. Localised delivery *via* intratumoural injection therefore provides a mechanism to enable therapeutic dosing within the TME, although emerging novel agents such as non-nucleotide small-molecule systemic STING agonists are in development for intravenous or oral administration (132).

Preclinical evidence provides rationale for the combination of STING agonism and ICPI therapy. In a poorly-immunogenic mouse sarcoma model, STING deficiency was shown to limit response to dual ICPI therapy highlighting an element of dependence on STING-mediated immunity (22). Ager et al. demonstrated that intratumoural injection of a STING agonist in a poorly-immunogenic bi-flank model of TRAMP-C2 mouse prostate cancer led to regression of injected but not non-injected tumours. Addition of checkpoint therapy led to synergistic effects in both injected and non-injected tumours, with an influx of CD8 effector cells, macrophage reprogramming and an increase in CD8:Treg ratio (133).

Combination treatment with STING agonism and anti-PD-1 therapy was shown to enhance therapeutic effects in the T cell-inflamed MOC1 mouse model of HNSCC. In contrast, the non-T cell-inflamed MOC2 model, used to represent "cold" tumours in work by Moore et al, did not respond to either single agent STING agonist or combination ICPI therapy. In these tumours, STING agonism induced a type I IFN response but did not result in CD8 TIL recruitment highlighting the inter-tumoural complexity in TME modification (134). Enhanced efficacy was seen with a combination of intraperitoneal STING agonist in combination with conventional carboplatin chemotherapy and anti-PD-1 checkpoint blockade in a model of high-grade serous ovarian cancer, a notoriously "cold" tumour site. STING agonism was shown significantly to enhance IFN production, the infiltration of activated PD-1-expressing CD8 T cells and MHCII expression in tumour-bearing mice (135).

A number of clinical trials evaluating STING agonism and ICPI combinations are currently ongoing. A first in human phase I study of the STING agonist MK-1454 in combination with Pembrolizumab in advanced solid tumours or lymphoma (NCT03010176) reported an encouraging safety profile and early evidence of efficacy (136). Phase II studies evaluating STING agonists MK-1454 (NCT04220866) and ADU-S100 (NCT03937141) in combination with Pembrolizumab in HNSCC are currently active.

Melphalan

Melphalan is a nitrogen mustard alkylating chemotherapeutic agent that has been widely used in cancer therapy. While

systemic therapy is known to cause lymphopaenia, localised therapy has been shown to enhance immune cell infiltration and antigen presentation through the initiation of apoptotic ICD, while minimising systemic side effects. Ariyan et al. showed synergy between local melphalan delivered *via* isolated limb perfusion and systemic anti-CTLA-4 therapy, with remodelling of the TME to an inflamed phenotype. This was translated into a phase II clinical trial, where combination therapy was shown to improve PFS with 62% complete responses and median PFS not reached. However, this did not reach significance over either treatment alone in the study of 26 patients (137).

Oncolytic Peptides

Designed to mimic natural antimicrobial peptides, oncolytic peptides (OPs) are short polypeptides with a net positive charge and a large proportion of hydrophobic amino acid residues (138). This allows them selectively to enter through negatively-charged phospholipid membranes, which are preferentially found in cancer cells due to higher phosphatidylserine exposure (139). Oncolytic peptides LTX-315/401 (140) and RT53 (141) have been shown to trigger ICD and DAMP release (ATP, HMGB1 and Calreticulin), as well as IFN I secretion, in melanoma and fibrosarcoma models; this was associated with local immune infiltration and tumour regression. In a mouse ovarian cancer model, local administration of the gonadotropin-releasing hormone receptor (GNRHR)-targeted peptide EP-100 was combined with anti-PD-L1-generating NK cell, DC and CD8 T cell tumour infiltration. In a process dependent on interleukin (IL)-33, T regs were simultaneously depleted. In mouse models of fibrosarcoma (MCA205) and lung carcinoma (TC-1), I.T. injections of LTX-315 (142)and LTX-401 (143) in combination with anti-PD-1 or anti-CTLA-4 promoted immune-dependent control of injected and abscopal (non-injected) tumour lesions.

LTX-315 is currently being explored in a phase I trial including patients with transdermally-accessible tumours in combination with pembrolizumab (NCT04796194).

Thermal and Ultrasound Based Treatments

High-intensity focused ultrasound (HIFU) is a non-invasive thermal modality, primarily used to treat solid tumours in cancer patients who are poor candidates for surgery and radiotherapy. HIFU was shown to induce ICD of human cancer cells promoting generation of DAMPs as well as cytokines that could polarize macrophages from a suppressive M2- to an anti-tumour M1-phenotype (144, 145). In immunocompetent mice, HIFU boosted DC infiltration in treated tumours and promoted CD8 T cell cytotoxicity (146). The documented effects of HIFU on DC recruitment, macrophage polarization and stromal dissociation indicate that HIFU treatment could skew the TME towards immune activation and possibly potentiate the effect of ICPI or immune agonists to generate systemic and tumour-specific immune responses. An ongoing phase 1 study is currently evaluating HIFU in combination with Pembrolizumab in metastatic breast cancer (NCT03237572).

Radiofrequency ablation (RFA) and microwave ablation (MWA) uses needle-like electrode probes to deliver radiofrequency and electromagnetic waves respectively, generating oscillation and subsequent heating of the tumour tissue. In two mouse models of breast (4T1) and colon (CT26) cancer, MWA of primary tumours followed by combined anti-PD-1 and anti-CTLA-4 treatment resulted in prolonged survival compared with MWA or ICPIs alone. MWA + ICPI treatment was also associated with increased frequencies of CD8 T cells in treated tumours and peripheral blood as well as increased plasma levels of IFNγ (147). Neo-adjuvant RFA of NSCLC tumours showed prominent CD8 and CD4 T cell infiltration in the peripheral regions of RFA-treated tumours as well as increased frequency of pro-inflammatory BDCA-3+ DCs in peripheral blood suggesting systemic immune activation (148). A retrospective study of colorectal cancer patients who had received preoperative RFA to liver metastases showed increased number of CD4 and CD8 TILs and increased PD-L1 expression in the resected primary tumours. An RFA-induced transient abscopal immune activation and PD-L1 induction was observed in a CT26 mouse tumour model with combined RFA and anti-PD-1 antibody treatment showing synergistic T-cell mediated systemic immunity (149).

Photothermal therapy (PTT) works by administering optically-absorbent nanoparticles which, when activated by near-infrared light, generates heat and localised thermal damage (18). PTT, in combination with a TLR-7 agonist and anti-CLTA-4 antibodies, induced abscopal effects in an orthotopic 4T1 breast cancer model (150). A recent case report describes a treatment-refractory HNSCC patient achieving a complete and sustained tumour response to photodynamic therapy (PDT) with anti-PD-1 antibody (151).

DISCUSSION AND FUTURE DIRECTIONS

Despite huge advances in recent years, ICPI therapy remains largely ineffective in the treatment of immunologically cold tumours. Although synergistic effects have been widely demonstrated between localised immune-modulatory therapies and ICPI, clinical response rates remain suboptimal. The mechanisms of response and resistance are highly complex, and it is likely that no single therapy will overcome tumour-mediated immunosuppression across multiple tumour histotypes. Multi-targeted combinations are likely to represent the future of immunotherapeutic strategies, and an overwhelming number of combinations are currently in clinical development.

Localised therapy combinations have been shown to have synergistic effects in some studies. RT has been shown to synergise with OV and ICPI, for example a CTLA-4 armed oNDV was shown to enhance sensitisation of melanoma cells to radiation (152). Oba et al. also demonstrated efficacy of *in situ* immune modulation using sequentially delivered local therapies – RT, DC recruitment agent Fms-like tyrosine kinase 3 ligand (Flt3L) and TLR-3/CD40 stimulation - in overcoming

checkpoint resistance in an immune-excluded mouse melanoma model (153). A further recent clinical study provided evidence that sequential oADV/HSV-TK, SBRT and anti-PD-1 was able to restore ICPI sensitivity in NSCLC patients, with a 64.2% clinical benefit rate (CBR) in patients that had received prior ICPI therapy (154). This highlights the potential benefit of a multi-targeted approach, even within localised therapies, and further triple combinations are emerging, such as STING or TLR agonists in combination with RT and ICPI.

Systemic targeted agents may also enhance treatment effects, and one novel strategy is the use of agents that target cellular DNA damage repair (DDR) pathways. An effective anti-cancer immune response is dependent on the formation of tumour neoantigens regardless of TME immunogenicity, a process that may be a key limiting factor in ICPI efficacy in cold tumours, due to a low mutational load. PARP inhibitors (PARPi) lead to un-repaired DNA damage which triggers a cascade of immunogenic events including enhanced PD-L1 expression on tumour cells, immune cell infiltration and TAA formation (155), providing rationale for combination treatment in cold tumours. PARPi was seen to enhance OV-mediated oncolysis in a model of anaplastic thyroid cancer (156). Treatment was also shown to enhance radiosensitivity, with PARPi/RT leading to chemokine secretion, immune infiltration and upregulation of PD-1/PD-L1 (157). Clinical trials evaluating triple combination with PARPi/RT/ICPI are ongoing (for example NCT04837209 and NCT04926324). The ataxia telangiectasia and Rad3-related (ATR) kinase is also integral to DDR pathways. Treatment with an ATR inhibitor was shown to synergise with radiotherapy and checkpoint inhibition in a pre-clinical model of liver cancer (158).

Combinations involving co-stimulatory agonists such as 4-1BB or CD40-L are also in clinical development. A recent study in an orthotopic mouse model of pancreatic ductal adenocarcinoma (PDA) revealed that an agonist targeting the co-stimulatory receptor CD40 synergized with radiotherapy to promote systemic tumour-targeted immune responses in combination with dual ICB (159). In mouse models of colorectal (MC38), melanoma (B16-OVA) and breast (4T1) cancer, radiotherapy administered concomitantly with a 4-1BB agonist resulted in local and abscopal anti-tumour immune responses and prolonged survival, which was dependent on CD8 T cells and conventional type I dendritic cells (cDC1a) (104). Such combinations have also been investigated in the context of oncolytic virotherapy, where the viral backbone presents an opportunity for delivery of these agents limiting toxicity. For example, Coffin et al. are currently testing an oHSV armed with anti-CTLA-4, a 4-1BB agonist and CD40-L in early phase clinical trials (68).

Novel checkpoints such as TIGIT, TIM-3, LAG3 (160) or other inhibitory targets such as the CEACAM proteins (161) are also under investigation, as are other triple combinations involving alternate immunotherapies such as CAR-T cells (162) or Bi-specific T cell engagers (BiTE) (163). As more is known about the effects of T cell modulatory therapies such as ICPI on the non T-cell constituents of the TME, the understanding and effective application of future ICPI combinations is likely to increase.

For example, the PD-1 pathway also regulates NK cells, B cells and macrophages, and evidence for the impact of the diverse cellular constituents of the TME on response to ICPI continues to accumulate. Indeed, a study of ICPI therapy in melanoma showed enrichment of B cell signatures in responding patients (164), and conditional knockout of novel checkpoint TIM-3 on DCs was shown to lead to inflammasome activation and anti-tumour immunity, an effect that was not seen with TIM-3 deletion on CD4 or CD8 Tcells (165).

Selective deletion of PD-1 in myeloid cells has also recently been shown to induce a more effective anti-cancer immune response than ablation on T cells (166), and other innate components such as Group 2 innate lymphoid cells (ILC2s) are also emerging as critical elements of checkpoint-mediated anti-cancer immunity (167). Understanding the complexities of these relationships will be essential in deciphering mechanisms of response, and identifying targets to overcome resistance.

As more complex combinations move into the spotlight, the question of optimal dose delivery and scheduling becomes of paramount importance both with regards to efficacy and toxicty. There is a rationale for checkpoint blockade as a priming agent before radiotherapy, and equally for OV administered prior to ICPI to prime for an effective anti-cancer immune response. Conversely, concurrent administration may enable maxiumum synergy, and sequential ICPI delivered after localised therapy may be the most effective way of sustaining immunity and overcoming T cell exhaustion. This is currently under investigation, and ongoing trials will begin to shed light on optimal scheduling. For example, a study evaluating priming vs concurrent atezolizumab in combination with conventional chemoradiotherapy in cervical cancer has recently finished recruiting (NCT03738228). A study combining an oADV with anti-PD-L1 agent Durvalumab is also currently recruiting and will evaluate concomitant *vs* sequential treatment (NCT03799744).

In the context of radiotherapy, the differential effects of dose-fractionation on immunogenicity are also largely unknown. Demaria et al. reported that RT doses above 12-18 Gy induced the Trex1 exonuclease and attenuated any immunogenic effects, while repeated lower doses led to IFN production, DC recruitment and immune-cell priming (23), and fractionated regimens have been preferred in some studies. For example, Dewan et al. reported that fractionated but not single dose (20 Gy) radiotherapy induced an abscopal effect in a murine model when combined with an anti-CTLA-4 antibody (168). In comparison, some studies report hypofractionated doses are more immunogenic, with a 15 Gy single fraction resulting in greater tumour control and increased activation and infiltration of antitumor T cells compared to 3 Gy x 5 in a B16/OVA murine model of melanoma (169). Further questions include treatment volume, especially when considering the immune effects of lymph node irradiation, which has been shown to attenuate adaptive anti-cancer immunity by altering CD8 T cell trafficking. Further evaluation may have an impact on radiotherapy target volumes of the future (170).

For OV treatment, a key limitation to optimal delivery is that many typically "cold" tumour sites such as brain, pancreatic and ovarian, do not have easily accessible lesions for repesated injection. Viral infectivity is highly heterogenous, and the barrier of anti-viral immunity, either from prior infection, vaccination or neutralizing antibodies (nAb) secondary to OV treatment, also hinders viral replication and therefore efficacy following systemic delivery. Novel methods of viral encapsulation to overcome the barrier of anti-viral immunity may provide a potential method of enhancing anti-tumour effects, for example, Francini et al. published evidence of ablation of nAb binding without viral inactivation using a new class of coating polymers (171).

There is much still to learn in order to overcome the lack of ICPI efficacy in cold tumours and to maximise the synergistic benefit of localised therapy combinations. However, continued research intended specifically to understand the biological changes occurring in tumours following administration of localised therapies is laying the groundwork for the design of more effective strategies. Checkpoint inhibitors have been proven to provide a widely-applicable method of immune rejuvenation, and are likely to form an integral part of future strategies. With the ability of localised therapies to manipulate the TME and enhance tumour immunogenicity without excessive additive side effects, they remain an attractive addition to the therapeutic armoury, with the potential of rendering more patients responsive to immune checkpoint blockade.

AUTHOR CONTRIBUTIONS

EA and EW devised and conceptualized the idea and drafted the manuscript. NS designed the figure. JH, CC, AW, AS, MO, AM, and KH have contributed to the writing of the manuscript. All authors contributed to the article and approved the submitted version.

FUNDING

Supported by Cancer Research UK (CRUK), the Institute of Cancer Research/Royal Marsden Hospital Centre for Translational Immunotherapy and RadNet Radiation Research Network.

REFERENCES

1. Leach DR, Krummel MF, Allison JP. Enhancement of Antitumor Immunity by CTLA-4 Blockade. *Science* (1996) 271(5256):1734–6.
2. Ishida Y, Agata Y, Shibahara K, Honjo T. Induced Expression of PD-1, a Novel Member of the Immunoglobulin Gene Superfamily, Upon Programmed Cell Death. *EMBO J* (1992) 11:3887–95. doi: 10.1002/j.1460-2075.1992.tb05481.x
3. Sharma P, Allison JP. The Future of Immune Checkpoint Therapy. *Science* (2015) 348:56–61. doi: 10.1126/science.aaa8172
4. Okazaki T, Chikuma S, Iwai Y, Fagarasan S, Honjo T. A Rheostat for Immune Responses: The Unique Properties of PD-1 and Their Advantages for Clinical Application. *Nat Immunol* (2013) 14:1212–8. doi: 10.1038/ni.2762
5. Robert C. A Decade of Immune-Checkpoint Inhibitors in Cancer Therapy. *Nat Commun* (2020) 11:3801 doi: 10.1038/s41467-020-17670-y
6. Robert C, Ribas A, Hamid O, Daud A, Wolchok JD, Joshua AM, et al. Durable Complete Response After Discontinuation of Pembrolizumab in Patients With Metastatic Melanoma. *J Clin Oncol* (2018) 36:1668–74. doi: 10.1200/JCO.2017.75.6270
7. Larkin J, Vanna Chiarion-Sileni MD, Rene Gonzalez MD, Jean-Jacques Grob MD, Piotr Rutkowski MD, Christopher D. Lao MD, et al. Five-Year Survival With Combined Nivolumab and Ipilimumab in Advanced Melanoma. *N Engl J Med* (2019) 381:1535–46. doi: 10.1056/NEJMoa1910836
8. Xin Yu J, Hubbard-Lucey VM, Tang J. Immuno-Oncology Drug Development Goes Global. *Nat Rev Drug Discovery* (2019) 18:899–900. doi: 10.1038/d41573-019-00167-9
9. Haslam A, Prasad V. Estimation of the Percentage of US Patients With Cancer Who Are Eligible for and Respond to Checkpoint Inhibitor Immunotherapy Drugs. *JAMA Netw Open* (2019) 2:192535. doi: 10.1001/jamanetworkopen.2019.2535
10. O'Leary K. Liver Metastases Cultivate an Immune Desert. *Nat Rev Cancer* (2021) 21:143–3. doi: 10.1038/s41568-021-00338-0
11. Yu J, Green MD, Yilun Sun SL, Journey SN, Choi JE, Rizvi SM, et al. Liver Metastasis Restrains Immunotherapy Efficacy *via* Macrophage-Mediated T Cell Elimination. *Nat Med* (2021) 27:152–64. doi: 10.1038/s41591-020-1131-x
12. Zemek RM, De Jong E, Chin WL, Schuster IS, Fear VS, Casey TH, et al. Sensitization to Immune Checkpoint Blockade Through Activation of a STAT1/NK Axis in the Tumor Microenvironment. *Sci Transl Med* (2019) 11:7816. doi: 10.1126/scitranslmed.aav7816
13. Tang T, Huang X, Zhang G, Hong Z, Bai X, Liang T. Advantages of Targeting the Tumor Immune Microenvironment Over Blocking Immune Checkpoint in Cancer Immunotherapy. *Signal Transduction Targeted Ther* (2021) 6:1–13. doi: 10.1038/s41392-020-00449-4
14. Joost Lesterhuis W, Bosco A, Millward MJ, Small M, Nowak AK, Lake RA. Dynamic Versus Static Biomarkers in Cancer Immune Checkpoint Blockade: Unravelling Complexity. *Nat Rev Drug Discovery* (2017) 16:264–72. doi: 10.1038/nrd.2016.233
15. Verma V, Shrimali RK, Ahmad S, Dai W, Wang H, Lu S, et al. PD-1 Blockade in Subprimed CD8 Cells Induces Dysfunctional PD-1 + CD38 Hi Cells and Anti-PD-1 Resistance. *Nat Immunol* (2019) 20:1231–43. doi: 10.1038/s41590-019-0441-y
16. Zemek RM, Chin WL, Nowak AK, Millward MJ, Lake RA, Lesterhuis WJ. Sensitizing the Tumor Microenvironment to Immune Checkpoint Therapy. *Front Immunol* (2020) 11:223. doi: 10.3389/fimmu.2020.00223
17. Gajewski TF. Next Hurdle in Cancer Immunorapy: Overcoming Non-T-Cell-Inflamed Tumor Microenvironment. *Semin Oncol* (2015) 42:663–71. doi: 10.1053/j.seminoncol.2015.05.011
18. Balakrishnan PB, Sweeney EE, Ramanujam AS, Fernandes R. Photothermal Therapies to Improve Immune Checkpoint Blockade for Cancer. *Int J Hyperthermia* (2020) 37:34–49. doi: 10.1080/02656736.2020.1797190
19. Reinert LS, Lopušná K, Winther H, Sun C, Thomsen MK, Nandakumar R, et al. Sensing of HSV-1 by the cGAS-STING Pathway in Microglia Orchestrates Antiviral Defence in the CNS. *Nat Commun* (2016) 7:13348. doi: 10.1038/ncomms13348
20. Diner BA, Lum KK, Toettcher JE, Cristea IM. Viral DNA Sensors IFI16 and Cyclic GMP-AMP Synthase Possess Distinct Functions in Regulating Viral Gene Expression, Immune Defenses, and Apoptotic Responses During Herpesvirus Infection. *MBio* (2016) 7(6):e01553–16. doi: 10.1128/mBio.01553-16
21. Harding SM, Benci JL, Irianto J, Discher DE, Minn AJ, Greenberg RA. Mitotic Progression Following DNA Damage Enables Pattern Recognition Within Micronuclei. *Nature* (2017) 548:466–70. doi: 10.1038/nature23470
22. STING-Dependent Cytosolic DNA Sensing Mediates Innate Immune Recognition of Immunogenic Tumors | Elsevier Enhanced Reader. Available at: https://reader.elsevier.com/reader/sd/pii/S1074761314003938?token=30C8669DE69F7B3D74D2F3A4DAECB74569C9D6B

369E7392C8F6370DA4E6D6FBA2A5CE54FFC035888A7C40C90A2A732AB&originRegion=eu-west-1&originCreation=20210615155149 (Accessed Accessed: 15th June 2021).
23. Vanpouille-Box C, Alard A, Aryankalayil MJ, Sarfraz Y, Diamond JM, Schneider RJ, et al. DNA Exonuclease Trex1 Regulates Radiotherapy-Induced Tumour Immunogenicity. *Nat Commun* (2017) 8:15618. doi: 10.1038/ncomms15618
24. Ghiringhelli F, Apetoh L, Tesniere A, Aymeric L, Ma Y, Ortiz C, et al. Activation of the NLRP3 Inflammasome in Dendritic Cells Induces IL-1beta-Dependent Adaptive Immunity Against Tumors. *Nat Med* (2009) 15 (10):1170–8. doi: 10.1038/nm.2028
25. Obeid M, Tesniere A, Ghiringhelli F, Fimia GM, Apetoh L, Perfettini JL, et al. Calreticulin Exposure Dictates the Immunogenicity of Cancer Cell Death. *Nat Med* (2007) 13(1):54–61. doi: 10.1038/nm1523
26. Apetoh L, Ghiringhelli F, Tesniere A, Obeid M, Ortiz C, Criollo A, et al. Toll-Like Receptor 4-Dependent Contribution of the Immune System to Anticancer Chemotherapy and Radiotherapy. *Nat Med* (2007) 13(5):1050–9. doi: 10.1038/nm1622
27. Reits EA, Hodge JW, Herberts CA, Groothuis TA, Chakraborty M, Wansley EK, et al. Radiation Modulates the Peptide Repertoire, Enhances MHC Class I Expression, and Induces Successful Antitumor Immunotherapy. *J Exp Med* (2006) 203(5):1259–71. doi: 10.1084/jem.20052494
28. Twyman-Saint Victor C, Rech AJ, Maity A, Rengan R, Pauken KE, Stelekati E, et al. Radiation and Dual Checkpoint Blockade Activate Non-Redundant Immune Mechanisms in Cancer. *Nature* (2015) 520:373–7. doi: 10.1038/nature14292
29. Formenti SC, Rudqvist NP, Golden E, Cooper B, Wennerberg E, Lhuillier C, et al. Radiotherapy Induces Responses of Lung Cancer to CTLA-4 Blockade. 24(12):1845–51. doi: 10.1038/s41591-018-0232-2
30. Lhuillier C, Rudqvist NP, Yamazaki T, Zhang T, Charpentier M, Galluzzi L, et al. Radiotherapy-Exposed CD8+ and CD4+ Neoantigens Enhance Tumor Control. *J Clin Invest* (2021) 131(5). doi: 10.1172/JCI138740
31. Rudqvist NP, et al. Radiotherapy and CTLA-4 Blockade Shape the Tcr Repertoire of Tumor-Infiltrating T Cells. *Cancer Immunol Res* (2018) 6:139–50. doi: 10.1158/2326-6066.CIR-17-0134
32. Gasser S, Orsulliuc S, Brown EJ, Raulet DH. The DNA Damage Pathway Regulates Innate Immune System Ligands of the NKG2D Receptor. *Nature* (2005) 436:1186–90. doi: 10.1038/nature03884
33. Ruocco MG, Pilones KA, Kawashima N, Cammer M, Huang J, Babb JS, et al. Suppressing T Cell Motility Induced by Anti-CTLA-4 Monotherapy Improves Antitumor Effects. *J Clin Invest* (2012) 122:3718–30. doi: 10.1172/JCI61931
34. Lhuillier C, Rudqvist NP, Elemento O, Formenti SC, Demaria S. Radiation Therapy and Anti-Tumor Immunity: Exposing Immunogenic Mutations to the Immune System. *Genome Med* (2019) 11:1–10. doi: 10.1186/s13073-019-0653-7
35. Wilkins A, Fontana E, Nyamundanda G, Ragulan C, Patil Y, Mansfield D, et al. Differential and Longitudinal Immune Gene Patterns Associated With Reprogrammed Microenvironment and Viral Mimicry in Response to Neoadjuvant Radiotherapy in Rectal Cancer. *J Immunother Cancer* (2021) 9(5). doi: 10.1136/jitc-2020-001717
36. Garg AD, Galluzzi L, Apetoh L, Baert T, Birge RB, Bravo-San Pedro JM, et al. Molecular and Translational Classifications of DAMPs in Immunogenic Cell Death. *Front Immunol* (2015) 6:588. doi: 10.3389/fimmu.2015.00588.
37. Rehwinkel J, Gack MU. RIG-I-Like Receptors: Their Regulation and Roles in RNA Sensing. *Nat Rev Immunol* (2020) 20:537–51. doi: 10.1038/s41577-020-0288-3
38. Goubau D, Deddouche S, Reis e Sousa C. Cytosolic Sensing of Viruses. *Immunity* (2013) 38:855–69. doi: 10.1016/j.immuni.2013.05.007
39. Matzinger P. Tolerance, Danger, and the Extended Family. *Annu Rev Immunol* (1994) 12:991–1045. doi: 10.1146/annurev.iy.12.040194.005015
40. Ma Y, Adjemian S, Mattarollo SR, Yamazaki T, Aymeric L, Yang H, et al. Anticancer Chemotherapy-Induced Intratumoral Recruitment and Differentiation of Antigen-Presenting Cells. *Immunity* (2013) 38(4):729–41. doi: 10.1016/j.immuni.2013.03.003
41. Ma Y, Adjemian S, Yang H, Catani JPP, Hannani D, Martins I, et al. ATP-Dependent Recruitment, Survival and Differentiation of Dendritic Cell Precursors in the Tumor Bed After Anticancer Chemotherapy. *Oncoimmunology* (2013) 2. doi: 10.4161/onci.24568
42. Kono K, Mimura K. Immunogenic Tumor Cell Death Induced by Chemoradiotherapy in a Clinical Setting. *Oncoimmunology* (2013) 2(1): e22197. doi: 10.4161/onci.22197
43. Gameiro SR, Jammeh ML, Wattenberg MM, Tsang KY, Ferrone S, Hodge JW. Radiation-Induced Immunogenic Modulation of Tumor Enhances Antigen Processing and Calreticulin Exposure, Resulting in Enhanced T-Cell Killign. *Oncotarget* (2014) 5(2):403–16. doi: 10.18632/oncotarget.1719
44. Ilett E, Kottke T, Thompson J, Rajani K, Zaidi S, Evgin L, et al. Prime-Boost Using Separate Oncolytic Viruses in Combination With Checkpoint Blockade Improves Anti-Tumour Therapy. *Gene Ther* (2017) 24(1):21–30. doi: 10.1038/gt.2016.70
45. Hwang JK, Hong J, Yun C-O. Molecular Sciences Oncolytic Viruses and Immune Checkpoint Inhibitors: Preclinical Developments to Clinical Trials. *Int J Mol Sci* (2020) 21(22):8627 doi: 10.3390/ijms21228627
46. Kaufman HL, Kohlhapp FJ, Zloza A. Oncolytic Viruses: A New Class of Immunotherapy Drugs. *Nat Rev Drug Discovery* (2015) 14:642–62. doi: 10.1038/nrd4663
47. Lee J, Ghonime MG, Wang R, Cassady KA. The Antiviral Apparatus: STING and Oncolytic Virus Restriction. *Mol Ther Oncolytics* (2019) 13:7–13. doi: 10.1016/j.omto.2019.02.002
48. Benencia F, Courrèges MC, Fraser NW, Coukos G. Herpes Virus Oncolytic Therapy Reverses Tumor Immune Dysfunction and Facilitates Tumor Antigen Presentation. *Cancer Biol Ther* (2008) 7:1194–205. doi: 10.4161/cbt.7.8.6216
49. Andtbacka RHI, Collichio F, Harrington KJ, Middleton MR, Downey G, Öhrling K, et al. Final Analyses of OPTiM: A Randomized Phase III Trial of Talimogene Laherparepvec Versus Granulocyte-Macrophage Colony-Stimulating Factor in Unresectable Stage III-IV Melanoma. *J Immunother Cancer* (2019) 7(1):145. doi: 10.1186/s40425-019-0623-z
50. Malvehy J, Samoylenko I, Schadendorf D, Gutzmer R, Grob JJ, Sacco JJ, et al. Talimogene Laherparepvec Upregulates Immune-Cell Populations in non-Injected Lesions: Findings From a Phase II, Multicenter, Open-Label Study in Patients With Stage IIIB-IVM1c Melanoma. *J Immunother Cancer* (2021) 9(3). doi: 10.1136/jitc-2020-001621
51. Chiu M, Armstrong EJL, Jennings V, Foo S, Crespo-Rodriguez E, Bozhanova G, et al. Combination Therapy With Oncolytic Viruses and Immune Checkpoint Inhibitors. *Expert Opin Biol Ther* (2020) 20(6):635–52. doi: 10.1080/14712598.2020.1729351
52. Zhang B, Huang J, Tang J, Hu S, Luo S, Luo Z, et al. Intratumoral OH2, an Oncolytic Herpes Simplex Virus 2, in Patients With Advanced Solid Tumors: A Multicenter, Phase I/II Clinical Trial. *J Immunother Cancer* (2021) 9(4):e002224. doi: 10.1136/jitc-2020-002224
53. Zhang L, Wang W, Wang R, Zhang N, Shang H, Bi Y, et al. Reshaping the Immune Microenvironment by Oncolytic Herpes Simplex Virus in Murine Pancreatic Ductal Adenocarcinoma. *Mol Ther* (2021) 29(2):744–61. doi: 10.1016/j.ymthe.2020.10.027
54. Ragab Eissa I, Mukoyama N, Abdelmoneim M, Naoe Y, Matsumura S, Bustos-Villalobos I, et al. Oncolytic Herpes Simplex Virus HF10 (Canerpaturev) Promotes Accumulation of CD8 + PD-1 – Tumor-Infiltrating T Cells in PD-L1-Enriched Tumor Microenvironment. (2021) 149(1):214–27. doi: 10.1002/ijc.33550
55. Saha D, Martuza RL, Rabkin SD. Oncolytic Herpes Simplex Virus Immunovirotherapy in Combination With Immune Checkpoint Blockade to Treat Glioblastoma. *Immunotherapy* (2018) 10:779–86. doi: 10.2217/imt-2018-0009
56. Belcaid Z, Berrevoets C, Choi J, van Beelen E, Stavrakaki E, Pierson T, et al. Low-Dose Oncolytic Adenovirus Therapy Overcomes Tumor-Induced Immune Suppression and Sensitizes Intracranial Gliomas to Anti-PD-1 Therapy. *Neuro-Oncol Adv* (2020) 2(1):vdaa011. doi: 10.1093/noajnl/vdaa011
57. Singh M, Vianden C, Cantwell MJ, Dai Z, Xiao Z, Sharma M, et al. Intratumoral CD40 Activation and Checkpoint Blockade Induces T Cell-Mediated Eradication of Melanoma in the Brain. *Nat Commun* (2017) 8 (1):1447. doi: 10.1038/s41467-017-01572-7
58. Hu HJ, Liang X, Li HL, Wang HY, Gu JF, Sun LY, et al. Enhanced Anti-Melanoma Efficacy Through a Combination of the Armed Oncolytic

Adenovirus ZD55-IL-24 and Immune Checkpoint Blockade in B16-Bearing Immunocompetent Mouse Model. *Cancer Immunol Immunother* (2021). doi: 10.1007/s00262-021-02946-z
59. Hu HJ, Liang X, Li HL, Du CM, Hao JL, Wang HY, et al. The Armed Oncolytic Adenovirus ZD55-IL-24 Eradicates Melanoma by Turning the Tumor Cells From the Self-State Into the Nonself-State Besides Direct Killing. *Cell Death Dis* (2020) 11(1):1022. doi: 10.1038/s41419-020-03223-0
60. *Pexa-Vec/Nexavar Combination Fails Phase III Trial in Liver Cancer* . Available at: https://www.genengnews.com/news/pexa-vec-nexavar-combination-fails-phase-iii-trial-in-liver-cancer/ (Accessed Accessed: 19th July 2021).
61. Chon HJ, Lee WS, Yang H, Kong SJ, Lee NK, Moon ES, et al. Tumor Microenvironment Remodeling by Intratumoral Oncolytic Vaccinia Virus Enhances the Efficacy of Immune-Checkpoint Blockade. *Clin Cancer Res* (2019) 25:1612–23. doi: 10.1158/1078-0432.CCR-18-1932
62. Liu Z, Ravindranathan R, Kalinski P, Guo ZS, Bartlett DL. Rational Combination of Oncolytic Vaccinia Virus and PD-L1 Blockade Works Synergistically to Enhance Therapeutic Efficacy. *Nat Commun* (2017) 8:14754. doi: 10.1038/ncomms14754
63. Lee YS, Lee WS, Kim CW, Lee SJ, Yang H, Kong SJ, et al. Oncolytic Vaccinia Virus Reinvigorates Peritoneal Immunity and Cooperates With Immune Checkpoint Inhibitor to Suppress Peritoneal Carcinomatosis in Colon Cancer. *J Immunother Cancer* (2020) 8(2):e000857. doi: 10.1136/jitc-2020-000857
64. Kleinpeter P, Fend L, Thioudellet C, Geist M, Sfrontato N, Koerper V, et al. Vectorization in an Oncolytic Vaccinia Virus of an Antibody, a Fab and a scFv Against Programmed Cell Death -1 (PD-1) Allows Their Intratumoral Delivery and an Improved Tumor-Growth Inhibition. *Oncoimmunology* (2016) 5(10). doi: 10.1080/2162402X.2016.1220467
65. Marchand J-B, Semmrich M, Fend L, Rehn M, Silvestre N, Teige I, et al. Abstract 5602: BT-001, an Oncolytic Vaccinia Virus Armed With a Treg-Depletion-Optimized Recombinant Human Anti-CTLA4 Antibody and GM-CSF to Target the Tumor Microenvironment. (2020) 5602. doi: 10.1158/1538-7445.am2020-5602
66. Zuo S, Wei M, He B, Chen A, Wang S, Kong L, et al. Enhanced Antitumor Efficacy of a Novel Oncolytic Vaccinia Virus Encoding a Fully Monoclonal Antibody Against T-Cell Immunoglobulin and ITIM Domain (TIGIT). *EBioMedicine* (2021) 64. doi: 10.1016/j.ebiom.2021.103240
67. Shi Z, Liu B, Huang C, Xie W, Cen Y, Chen L, et al. An Oncolytic Vaccinia Virus Armed With Anti-Human-PD-1 Antibody and Anti-Human-4-1BB Antibody Double Genes for Cancer-Targeted Therapy. *Biochem Biophys Res Commun* (2021) 559:176–82. doi: 10.1016/j.bbrc.2021.04.078
68. Thomas S, Kuncheria L, Roulstone V, Kyula JN, Mansfield D, Bommareddy PK, et al. Development of a New Fusion-Enhanced Oncolytic Immunotherapy Platform Based on Herpes Simplex Virus Type 1. *J Immunother Cancer* (2019) 7(1):214. doi: 10.1186/s40425-019-0682-1
69. Zhang Y, Zhang H, Wei M, Mou T, Shi T, Ma Y, et al. Recombinant Adenovirus Expressing a Soluble Fusion Protein PD-1/CD137L Subverts the Suppression of CD8+ T Cells in HCC. *Mol Ther* (2019) 27(11):1906–18. doi: 10.1016/j.ymthe.2019.07.019
70. Wenthe J, Eriksson E, Milenova I, Moreno R, Alemany R, Loskog A, et al. 516. A Novel Oncolytic Adenovirus Expressing Tumor Microenvironment Stimulators to Evoke and Facilitate Anti-Tumor Immune Responses. *Mol Ther* (2016) 24:S206. doi: 10.1016/S1525-0016(16)33325-1
71. Mostafa AA, Meyers DE, Thirukkumaran CM, Liu PJ, Gratton K, Spurrell J, et al. Oncolytic Reovirus and Immune Checkpoint Inhibition as a Novel Immunotherapeutic Strategy for Breast Cancer. *Cancers (Basel)* (2018) 10 (6). doi: 10.3390/cancers10060205
72. Annels NE, Simpson GR, Denyer M, Arif M, Coffey M, Melcher A, et al. Oncolytic Reovirus-Mediated Recruitment of Early Innate Immune Responses Reverses Immunotherapy Resistance in Prostate Tumors. *Mol Ther Oncolytics* (2021) 20:434–46. doi: 10.1016/j.omto.2020.09.010
73. Force J, Holl E, Brown M, Marcom PK, Grimm L, Boczkowski D, et al. Recombinant Oncolytic Poliovirus Combined With Checkpoint Blockade for Breast Cancer Therapy. *J Clin Oncol* (2018) 36(15_Supp):e12641–1. doi: 10.1200/JCO.2018.36.15_suppl.e12641
74. Bourgeois-Daigneault MC, Roy DG, Aitken AS, El Sayes N, Martin NT, Varette O, et al. Neoadjuvant Oncolytic Virotherapy Before Surgery Sensitizes Triple-Negative Breast Cancer to Immune Checkpoint Therapy. *Sci Transl Med* (2018) 10(422). doi: 10.1126/scitranslmed.aao1641
75. Kaufman HL, Kim DW, DeRaffele G, Mitcham J, Coffin RS, Kim-Schulze S. Local and Distant Immunity Induced by Intralesional Vaccination With an Oncolytic Herpes Virus Encoding GM-CSF in Patients With Stage IIIc and IV Melanoma. *Ann Surg Oncol* (2010) 17(3):718–30. doi: 10.1245/s10434-009-0809-6
76. Chesney J, Puzanov I, Collichio F, Singh P, Milhem MM, Glaspy J, et al. Randomized, Open-Label Phase II Study Evaluating the Efficacy and Safety of Talimogene Laherparepvec in Combination With Ipilimumab Versus Ipilimumab Alone in Patients With Advanced, Unresectable Melanoma. *J Clin Oncol* (2017) 36:1658–67. doi: 10.1200/JCO.2017.73.7379
77. Amgen Reports Fourth Quarter And Full Year 2020 Financial Results | Amgen Inc. Available at: https://investors.amgen.com/news-releases/news-release-details/amgen-reports-fourth-quarter-and-full-year-2020-financial/ (Accessed Accessed: 26th July 2021).
78. Ribas A, Dummer R, Puzanov I, VanderWalde A, Andtbacka RHI, Michielin O, et al. Oncolytic Virotherapy Promotes Intratumoral T Cell Infiltration and Improves Anti-PD-1 Immunotherapy. *Cell* (2017) 170(6):1109–1119.e10. doi: 10.1016/j.cell.2017.08.027
79. Harrington KJ, Kong A, Mach N, Chesney JA, Fernandez BC, Rischin D, et al. Talimogene Laherparepvec and Pembrolizumab in Recurrent or Metastatic Squamous Cell Carcinoma of the Head and Neck (MASTERKEY-232): A Multicenter, Phase 1b Study. *Clin Cancer Res* (2020) 26(19):5153–61. doi: 10.1158/1078-0432.CCR-20-1170
80. Khaddour K, Dowling J, Huang J, Council M, Chen D, Cornelius L, et al. Successful Administration of Sequential TVEC and Pembrolizumab Followed by Temozolomide in Immunotherapy Refractory Intracranial Metastatic Melanoma With Acquired B2M Mutation. *Oncotarget* (2021) 11:4836–44. doi: 10.18632/oncotarget.27848
81. Andtbacka RHI, Ross MI, Agarwala SS, Taylor MH, Vetto JT, Neves RI, Grossmann KF, et al. Final Results of a Phase II Multicenter Trial of HF10, a Replication-Competent HSV-1 Oncolytic Virus, and Ipilimumab Combination Treatment in Patients With Stage IIIB-IV Unresectable or Metastatic Melanoma. *J Clin Oncol* (2017) 35(15_Suppl):9510–0. doi: 10.1200/JCO.2017.35.15_suppl.9510
82. Yokota K, Isei T, Uhara H, Fujisawa Y, Takenouchi T, Kiyohara Y, et al. Final Results From Phase II of Combination With Canerpaturev (Formerly HF10), an Oncolytic Viral Immunotherapy, and Ipilimumab in Unresectable or Metastatic Melanoma in Second-or Later Line Treatment. *Ann Oncol* (2019) 30:v557. doi: 10.1093/annonc/mdz255.053
83. Zadeh G, Daras M, Cloughesy TF, Colman H, Kumthekar PU, Chen CC, et al. LTBK-04. Phase 2 Multicenter Study of the Oncolytic Adenovirus DNX-2401 (TASADENOTUREV) in Combination With Pembrolizumab for Recurrent Glioblastoma; Captive Study (Keynote-192). *Neuro Oncol* (2020) 22(Suppl_2):ii237–7. doi: 10.1093/neuonc/noaa215.989
84. Musher BL, Smaglo BG, Abidi W, Othman M, Patel K, Jing J, et al. A Phase I/II Study Combining a TMZ-CD40L/4-1BBL-Armed Oncolytic Adenovirus and Nab-Paclitaxel/Gemcitabine Chemotherapy in Advanced Pancreatic Cancer: An Interim Report. (2020) 38(4_Supp):716–6. doi: 10.1200/JCO.2020.38.4_suppl.716
85. Curti BD, Richards JM, Hallmeyer S, Faries MB, Andtbacka RHI, Daniels GA, et al. Activity of a Novel Immunotherapy Combination of Intralesional Coxsackievirus A21 and Systemic Ipilimumab in Advanced Melanoma Patients Previously Treated With Anti-PD1 Blockade Therapy. *J Clin Oncol* (2017) 35(15_Supp):3014–4. doi: 10.1200/JCO.2017.35.15_suppl.3014
86. Silk AW, Kaufman H, Gabrail N, Mehnert J, Bryan J, Norrell J, et al. Abstract CT026: Phase 1b Study of Intratumoral Coxsackievirus A21 (C V A 21) and Systemic P Emb R Olizumab in a Dvanced Melanoma Patients: Interim Results of the CAPRA Clinical Trial. *Cancer Res* (2017) 77(13_Suppl): CT026. American Association for Cancer Research (AACR). doi: 10.1158/1538-7445.AM2017-CT026
87. Annels NE, Mansfield D, Arif M, Ballesteros-Merino C, Simpson GR, Denyer M, et al. Phase I Trial of an ICAM-1-Targeted Immunotherapeutic-Coxsackievirus A21 (CVA21) as an Oncolytic Agent Against non Muscle-Invasive Bladder Cancer. *Clin Cancer Res* (2019) 25(19):5818–31. doi: 10.1158/1078-0432.CCR-18-4022

88. RH M. Whole Body Irradiation; Radiobiology or Medicine? *Br J Radiol* (1953) 26:234–41. doi: 10.1259/0007-1285-26-305-234
89. Abuodeh Y, Venkat P, Kim S. Systematic Review of Case Reports on the Abscopal Effect. *Curr Probl Cancer* (2016) 40:25–37. doi: 10.1016/j.currproblcancer.2015.10.001
90. Postow MA, Callahan MK, Barker CA, Yamada Y, Yuan J, Kitano S, et al. Immunologic Correlates of the Abscopal Effect in a Patient With Melanoma. *N Engl J Med* (2012) 366(10):925–31. doi: 10.1056/NEJMoa1112824
91. Demaria S, Ng B, Devitt ML, Babb JS, Kawashima N, Liebes L, et al. Ionizing Radiation Inhibition of Distant Untreated Tumors (Abscopal Effect) Is Immune Mediated. *Int J Radiat Oncol Biol Phys* (2004) 58(3):862–70. doi: 10.1016/j.ijrobp.2003.09.012
92. Rizvi NA, Hellmann MD, Snyder A, Kvistborg P, Makarov V, Havel JJ, et al. Mutational Landscape Determines Sensitivity to PD-1 Blockade in non-Small Cell Lung Cancer. *Science* (2015) 348(6230):124–8. doi: 10.1126/science.aaa1348
93. Tsai MH, Cook JA, Chandramouli GVR, DeGraff W, Yan H, Zhao S, et al. Gene Expression Profiling of Breast, Prostate, and Glioma Cells Following Single Versus Fractionated Doses of Radiation. *Cancer Res* (2007) 67 (8):3845–52. doi: 10.1158/0008-5472.CAN-06-4250
94. Lussier DM, Alspach E, Ward JP, Miceli AP, Runci D, White JM, et al. Radiation-Induced Neoantigens Broaden the Immunotherapeutic Window of Cancers With Low Mutational Loads. *Proc Natl Acad Sci U S A* (2021) 118.
95. MacKenzie KJ, Carroll P, Martin CA, Murina O, Fluteau A, Simpson DJ, et al. CGAS Surveillance of Micronuclei Links Genome Instability to Innate Immunity. *Nature* (2017) 548(7668):461–5. doi: 10.1038/nature23449
96. Brzostek-Racine S, Gordon C, Van Scoy S, Reich NC. The DNA Damage Response Induces IFN. *J Immunol* (2011) 187:5336–45. doi: 10.4049/jimmunol.1100040
97. Diamond MS, Kinder M, Matsushita H, Mashayekhi M, Dunn GP, Archambault JM, et al. Type I Interferon is Selectively Required by Dendritic Cells for Immune Rejection of Tumors. *J Exp Med* (2011) 208 (10):1989–2003. doi: 10.1084/jem.20101158
98. Fuertes MB, Kacha AK, Kline J, Woo SR, Kranz DM, Murphy KM, et al. Host Type I IFN Signals are Required for Antitumor CD8+ T Cell Responses Through CD8α+ Dendritic Cells. *J Exp Med* (2011) 208(10):2005–16. doi: 10.1084/jem.20101159
99. Golden EB, Frances D, Pellicciotta I, Demaria S, Barcellos-Hoff MH, Formenti SC. Radiation Fosters Dose-Dependent and Chemotherapy-Induced Immunogenic Cell Death. *Oncoimmunology* (2014) 3(4). doi: 10.4161/onci.28518
100. Kulzer L, Rubner Y, Deloch L, Allgäuer A, Frey B, Fietkau R, et al. Norm- and Hypo-Fractionated Radiotherapy is Capable of Activating Human Dendritic Cells. *J Immunotoxicol* (2014) 11(4):328–36. doi: 10.3109/1547691X.2014.880533
101. Apetoh L, Ghiringhelli F, Tesniere A, Criollo A, Ortiz C, Lidereau R, et al. The Interaction Between HMGB1 and TLR4 Dictates the Outcome of Anticancer Chemotherapy and Radiotherapy. *Immunol Rev* (2007) 220:47–59. doi: 10.1111/j.1600-065X.2007.00573.x
102. Vermeer DW, Spanos WC, Vermeer PD, Bruns AM, Lee KM, Lee JH. Radiation-Induced Loss of Cell Surface CD47 Enhances Immune-Mediated Clearance of Human Papillomavirus-Positive Cancer. *Int J Cancer* (2013) 133(1):120–9. doi: 10.1002/ijc.28015
103. Dovedi SJ, Adlard AL, Lipowska-Bhalla G, McKenna C, Jones S, Cheadle EJ, et al. Acquired Resistance to Fractionated Radiotherapy can be Overcome by Concurrent PD-L1 Blockade. *Cancer Res* (2014) 74(19):5458–68. doi: 10.1158/0008-5472.CAN-14-1258
104. Rodriguez-Ruiz ME, Rodriguez I, Garasa S, Barbes B, Solorzano JL, Perez-Gracia JL, et al. Abscopal Effects of Radiotherapy Are Enhanced by Combined Immunostimulatory Mabs and Are Dependent on CD8 T Cells and Crosspriming. *Cancer Res* (2016) 76(20):5994–6005. doi: 10.1158/0008-5472.CAN-16-0549
105. Deng L, Liang H, Burnette B, Beckett M, Darga T, Weichselbaum RR, et al. Irradiation and Anti-PD-L1 Treatment Synergistically Promote Antitumor Immunity in Mice. *J Clin Invest* (2014) 124:687–95. doi: 10.1172/JCI67313
106. Demaria S, Kawashima N, Yang AM, Devitt ML, Babb JS, Allison JP, et al. Immune-Mediated Inhibition of Metastases After Treatment With Local Radiation and CTLA-4 Blockade in a Mouse Model of Breast Cancer. *Clin Cancer Res* (2005) 11(2 Pt 1):728–34.
107. Matsumura S, Wang B, Kawashima N, Braunstein S, Badura M, Cameron TO, et al. Radiation-Induced CXCL16 Release by Breast Cancer Cells Attracts Effector T Cells. *J Immunol* (2008) 181:3099–107. doi: 10.4049/jimmunol.181.5.3099
108. Knispel S, Stang A, Zimmer L, Lax H, Gutzmer R, Heinzerling L, et al. Impact of a Preceding Radiotherapy on the Outcome of Immune Checkpoint Inhibition in Metastatic Melanoma: A Multicenter Retrospective Cohort Study of the DeCOG. *J Immunother Cancer* (2020) 8(1). doi: 10.1136/jitc-2019-000395
109. Shaverdian N, Lisberg AE, Bornazyan K, Veruttipong D, Goldman JW, Formenti SC, et al. Previous Radiotherapy and the Clinical Activity and Toxicity of Pembrolizumab in the Treatment of Non-Small-Cell Lung Cancer: A Secondary Analysis of the KEYNOTE-001 Phase 1 Trial. *Lancet Oncol* (2017) 18(7):895–903. doi: 10.1016/S1470-2045(17)30380-7
110. Boutros C, Chaput-Gras N, Lanoy E, Larive A, Mateus C, Routier E, et al. Dose Escalation Phase 1 Study of Radiotherapy in Combination With Anti-Cytotoxic-T-Lymphocyte-Associated Antigen 4 Monoclonal Antibody Ipilimumab in Patients With Metastatic Melanoma. *J Immunother Cancer* (2020) 8(2):627. doi: 10.1136/jitc-2020-000627
111. McBride S, Sherman E, Jillian Tsai C, Baxi S, Aghalar J, Eng J, et al. Randomized Phase II Trial of Nivolumab With Stereotactic Body Radiotherapy Versus Nivolumab Alone in Metastatic Head and Neck Squamous Cell Carcinoma. *J Clin Oncol* (2021) 39(1):30–7. doi: 10.1200/JCO.20.00290
112. Mittendorf EA, Philips AV, Meric-Bernstam F, Qiao N, Wu Y, Harrington S, et al. PD-L1 Expression in Triple-Negative Breast Cancer. *Cancer Immunol Res* (2014) 2(4):361–70. doi: 10.1158/2326-6066.CIR-13-0127
113. Ho AY, Barker CA, Arnold BB, Powell SN, Hu ZI, Gucalp A, et al. A Phase 2 Clinical Trial Assessing the Efficacy and Safety of Pembrolizumab and Radiotherapy in Patients With Metastatic Triple-Negative Breast Cancer. *Cancer* (2020) 126(4):850–60. doi: 10.1002/cncr.32599
114. Barroso-Sousa R, Krop IE, Trippa L, Tan-Wasielewski Z, Li T, Osmani W, et al. A Phase II Study of Pembrolizumab in Combination With Palliative Radiotherapy for Hormone Receptor-Positive Metastatic Breast Cancer. *Clin Breast Cancer* (2020) 20(3):238–45. doi: 10.1016/j.clbc.2020.01.012
115. Xie C, Duffy AG, Brar G, Fioravanti S, Mabry-Hrones D, Walker M, et al. Immune Checkpoint Blockade in Combination With Stereotactic Body Radiotherapy in Patients With Metastatic Pancreatic Ductal Adenocarcinoma. *Clin Cancer Res* (2020) 26(10):2318–26. doi: 10.1158/1078-0432.CCR-19-3624
116. Antonia SJ, Villegas A, Daniel D, Vicente D, Murakami S, Hui R, et al. Durvalumab After Chemoradiotherapy in Stage III Non–Small-Cell Lung Cancer. *N Engl J Med* (2019) 377(20):1919–29. doi: 10.1056/NEJMoa1709937
117. Lee NY, Ferris RL, Psyrri A, Haddad RI, Tahara M, Bourhis J, et al. Avelumab Plus Standard-of-Care Chemoradiotherapy Versus Chemoradiotherapy Alone in Patients With Locally Advanced Squamous Cell Carcinoma of the Head and Neck: A Randomised, Double-Blind, Placebo-Controlled, Multicentre, Phase 3 Trial. *Lancet Oncol* (2021) 22 (4):450–62. doi: 10.1016/S1470-2045(20)30737-3
118. Theelen WSME, Peulen HMU, Lalezari F, van der Noort V, de Vries JF, Aerts JGJV, et al. Effect of Pembrolizumab After Stereotactic Body Radiotherapy vs Pembrolizumab Alone on Tumor Response in Patients With Advanced Non–Small Cell Lung Cancer: Results of the PEMBRO-RT Phase 2 Randomized Clinical Trial. *JAMA Oncol* (2019) 5(9):1276–82. doi: 10.1001/jamaoncol.2019.1478
119. Welsh J, Menon H, Chen D, Verma V, Tang C, Altan M, et al. Pembrolizumab With or Without Radiation Therapy for Metastatic Non-Small Cell Lung Cancer: A Randomized Phase I/II Trial. *J Immunother Cancer* (2020) 8:e001001. doi: 10.1136/JITC-2020-001001
120. Theelen WSME, Chen D, Verma V, Hobbs BP, Peulen HMU, Aerts JGJV, et al. Pembrolizumab With or Without Radiotherapy for Metastatic Non-Small-Cell Lung Cancer: A Pooled Analysis of Two Randomised Trials. *Lancet Respir Med* (2021) 9(5):467–75. doi: 10.1016/S2213-2600(20)30391-X
121. Altorki NK, Altorki NK, McGraw TE, Borczuk AC, Saxena A, Port JL, Stiles BM, et al. Neoadjuvant Durvalumab With or Without Stereotactic Body

Radiotherapy in Patients With Early-Stage non-Small-Cell Lung Cancer: A Single-Centre, Randomised Phase 2 Trial. *Lancet Oncol* (2021) 22(6):824–35. doi: 10.1016/S1470-2045(21)00149-2

122. McArthur H, McArthur H, Shiao S, Karlan S, Basho R, Amersi F, Arnold B, et al. Abstract PS12-09: Pre-Operative Pembrolizumab (Pembro) With Radiation Therapy (RT) in Patients With Operable Triple-Negative Breast Cancer (TNBC). *Cancer Res* (2021) 81(4_Suppl):PS12–09. doi: 10.1158/1538-7445.SABCS20-PS12-09
123. R L, Leidner R, Crittenden M, Young K, Xiao H, Wu Y, Couey MA, et al. Neoadjuvant Immunoradiotherapy Results in High Rate of Complete Pathological Response and Clinical to Pathological Downstaging in Locally Advanced Head and Neck Squamous Cell Carcinoma. *J Immunother Cancer* (2021) 9:e002485. doi: 10.1136/jitc-2021-002485
124. Liu H, Weber A, Morse J, Kodumudi K, Scott E, Mullinax J, et al. T Cell Mediated Immunity After Combination Therapy With Intralesional PV-10 and Blockade of the PD-1/PD-L1 Pathway in a Murine Melanoma Model. *PloS One* (2018) 13(4). doi: 10.1371/journal.pone.0196033
125. Agarwala SS, Ross MI, Zager JS, Shirai K, Essner R, Smithers BM, et al. Phase 1b Study of PV-10 and Anti-PD-1 in Advanced Cutaneous Melanoma. *J Clin Oncol* (2019) 37(15_Supp):9559–9. doi: 10.1200/JCO.2019.37.15_suppl.9559
126. Schmidt M, Oswald D, Volz B, Wittig B, Kapp K. Modulation of T Cell and Macrophage Tumor Infiltration by the TLR9 Agonist Lefitolimod in a Murine Model of Colorectal Cancer. *J Clin Oncol* (2018) 36:687–7. doi: 10.1200/JCO.2018.36.4_suppl.687
127. Schmidt M, Kapp K, Volz B, Oswald D, Wittig B. TLR9 Agonist Lefitolimod to Improve Antitumor Effect of Checkpoint Inhibitors *In Vivo*. *J Clin Oncol* (2017) 35:e14625–5. doi: 10.1200/JCO.2017.35.15_suppl.e14625
128. Haymaker C, Andtbacka RHI, Johnson DB, Shaheen MF, Rahimian S, Chunduru S, et al. 1083mo Final Results From ILLUMINATE-204, a Phase I/II Trial of Intratumoral Tilsotolimod in Combination With Ipilimumab in PD-1 Inhibitor Refractory Advanced Melanoma. *Ann Oncol* (2020) 31:S736. doi: 10.1016/j.annonc.2020.08.1207
129. Idera Pharmaceuticals Announces Results From ILLUMINATE-301. Available at: https://www.globenewswire.com/fr/news-release/2021/03/18/2195815/33448/en/Idera-Pharmaceuticals-Announces-Results-From-ILLUMINATE-301-Trial-of-Tilsotolimod-Ipilimumab-in-anti-PD-1-Refractory-Advanced-Melanoma.html (Accessed Accessed: 9th June 2021).
130. Milhem M, Zakharia Y, d D, Buchbinder E, Medina T, Daud A, et al. 304 Intratumoral Injection of CMP-001, A Toll-Like Receptor 9 (TLR9) Agonist, in Combination With Pembrolizumab Reversed Programmed Death Receptor 1 (PD-1) Blockade Resistance in Advanced Melanoma. *J ImmunoTher Cancer* (2020) 8. doi: 10.1136/jitc-2020-SITC2020.0304
131. Diab A, Marcondes M, Kotzin B, Tagliaferri MA, Hoch U, Li Y, et al. Phase Ib: Preliminary Clinical Activity and Immune Activation for NKTR-262 [TLR 7/8 Agonist] Plus NKTR-214 [CD122-Biased Agonist] in Patients (Pts) With Locally Advanced or Metastatic Solid Tumors (REVEAL Phase Ib/II Trial). *J Clin Oncol* (2019) 37(8_Supp):26–6. doi: 10.1200/JCO.2019.37.8_suppl.26
132. Crunkhorn S. Strengthening the Sting of Immunotherapy. *Nat Rev Drug Discovery* (2020) 19:669. doi: 10.1038/d41573-020-00148-3
133. Ager CR, Reilley MJ, Nicholas C, Bartkowiak T, Jaiswal AR, Curran MA. Intratumoral STING Activation With T-Cell Checkpoint Modulation Generates Systemic Antitumor Immunity. (2017) 5(8):676–84. doi: 10.1158/2326-6066.CIR-17-0049
134. Moore E, Clavijo PE, Davis R, Cash H, Van Waes C, Kim Y, et al. Established T Cell-Inflamed Tumors Rejected After Adaptive Resistance Was Reversed by Combination STING Activation and PD-1 Pathway Blockade. *Cancer Immunol Res* (2016) 4(2). doi: 10.1158/2326-6066.CIR-16-0104
135. Ghaffari A, Peterson N, Khalaj K, Vitkin N, Robinson A, Francis JA, et al. Sting Agonist Therapy in Combination With Pd-1 Immune Checkpoint Blockade Enhances Response to Carboplatin Chemotherapy in High-Grade Serous Ovarian Cancer. *Br J Cancer* (2018) 119(4):440–9. doi: 10.1038/s41416-018-0188-5
136. Harrington KJ, Brody J, Ingham M, Strauss J, Cemerski S, Wang M, et al. Preliminary Results of the First-in-Human (FIH) Study of MK-1454, an Agonist of Stimulator of Interferon Genes (STING), as Monotherapy or in Combination With Pembrolizumab (Pembro) in Patients With Advanced Solid Tumors or Lymphomas. *Ann Oncol* (2018) 29:viii712. doi: 10.1093/annonc/mdy424.015
137. Ariyan CE, Brady MS, Siegelbaum RH, Hu J, Bello DM, Rand J, et al. Robust Antitumor Responses Result From Local Chemotherapy and CTLA-4 Blockade. *Cancer Immunol Res* (2018) 6(2):189–200. doi: 10.1158/2326-6066.CIR-17-0356
138. Tornesello AL, Borrelli A, Buonaguro L, Buonaguro FM, Tornesello ML. Antimicrobial Peptides as Anticancer Agents: Functional Properties and Biological Activities. *Molecules* (2020) 25(12):2850. doi: 10.3390/molecules25122850
139. Sharma B, Kanwar SS. Phosphatidylserine: A Cancer Cell Targeting Biomarker. *Semin Cancer Biol* (2018) 52:17–25. doi: 10.1016/j.semcancer.2017.08.012
140. Camilio KA, Berge G, Ravuri CS, Rekdal Ø, Sveinbjørnsson B. Complete Regression and Systemic Protective Immune Responses Obtained in B16 Melanomas After Treatment With LTX-315. *Cancer Immunol Immunother* (2014) 63:601–13. doi: 10.1007/s00262-014-1540-0
141. Pasquereau-Kotula E, Habault J, Kroemer G, Poyet JL. The Anticancer Peptide RT53 Induces Immunogenic Cell Death. *PloS One* (2018) 13(8):e0201220. doi: 10.1371/journal.pone.0201220
142. Yamazaki T, et al. The Oncolytic Peptide LTX-315 Overcomes Resistance of Cancers to Immunotherapy With CTLA4 Checkpoint Blockade. *Cell Death Differ* (2016) 23:1004–15. doi: 10.1038/cdd.2016.35
143. Xie W, Mondragón L, Mauseth B, Wang Y, Pol J, Lévesque S, et al. Tumor Lysis With LTX-401 Creates Anticancer Immunity. *Oncoimmunology* (2019) 8(7). doi: 10.1080/2162402X.2019.1594555
144. Pahk KJ, Shin CH, Bae IY, Yang Y, Kim SH, Pahk K, et al. Boiling Histotripsy-Induced Partial Mechanical Ablation Modulates Tumour Microenvironment by Promoting Immunogenic Cell Death of Cancers. *Sci Rep* (2019) 9(1). doi: 10.1038/s41598-019-45542-z
145. Hu Z, et al, Xiao YY, Liu Y, Morse MA, Lyerly HK, Clay TM. Release of Endogenous Danger Signals From HIFU-Treated Tumor Cells and Their Stimulatory Effects on APCs. *Biochem Biophys Res Commun* (2005) 335 (1):124–31. doi: 10.1016/j.bbrc.2005.07.071
146. Hu Z, Yang XY, Liu Y, Sankin GN, Pua EC, Morse MA, et al. Investigation of HIFU-Induced Anti-Tumor Immunity in a Murine Tumor Model. *J Transl Med* (2007) 5:34. doi: 10.1186/1479-5876-5-34
147. Zhu J, Yu M, Chen L, Kong P, Li L, Ma G, et al. Enhanced Antitumor Efficacy Through Microwave Ablation in Combination With Immune Checkpoints Blockade in Breast Cancer: A Pre-Clinical Study in a Murine Model. *Diagn Interv Imaging* (2018) 99(3):135–42. doi: 10.1016/j.diii.2017.12.011
148. Schneider T, Hoffmann H, Dienemann H, Herpel E, Heussel CP, Enk AH, et al. Immune Response After Radiofrequency Ablation and Surgical Resection in Nonsmall Cell Lung Cancer. *Semin Thorac Cardiovasc Surg* (2016) 28(2):585–92. doi: 10.1053/j.semtcvs.2016.02.008
149. Shi L, Chen L, Wu C, Zhu Y, Xu B, Zheng X, et al. PD-1 Blockade Boosts Radiofrequency Ablation-Elicited Adaptive Immune Responses Against Tumor. *Clin Cancer Res* (2016) 22(5):1173–84. doi: 10.1158/1078-0432.CCR-15-1352
150. Chen Q, Xu L, Liang C, Wang C, Peng R, Liu Z. Photothermal Therapy With Immune-Adjuvant Nanoparticles Together With Checkpoint Blockade for Effective Cancer Immunotherapy. *Nat Commun* (2016) 7. doi: 10.1038/ncomms13193
151. Santos LL, Oliveira J, Monteiro E, Santos J, Sarmento C. Treatment of Head and Neck Cancer With Photodynamic Therapy With Redaporfin: A Clinical Case Report. *Case Rep Oncol* (2018) 11(1):769–76. doi: 10.1159/000493423
152. Vijayakumar G, Palese P, Goff PH. Oncolytic Newcastle Disease Virus Expressing a Checkpoint Inhibitor as a Radioenhancing Agent for Murine Melanoma. *EBioMedicine* (2019) 49:96–105. doi: 10.1016/j.ebiom.2019.10.032
153. Oba T, Long MD, Keler T, Marsh HC, Minderman H, Abrams SI, et al. Overcoming Primary and Acquired Resistance to Anti-PD-L1 Therapy by Induction and Activation of Tumor-Residing Cdc1s. *Nat Commun* (2020) 11:1–20. doi: 10.1038/s41467-020-19192-z
154. Guerrero C, Ensor JE, Sun K, Farach AM, Nair S, Zhang J, et al. Stereotactic Body Radiation Therapy and *in Situ* Oncolytic Virus Therapy Followed by

Immunotherapy in Metastatic non-Small Cell Lung Cancer. *J Clin Oncol* (2021) 39(15_Supp):9115–5. doi: 10.1200/JCO.2021.39.15_suppl.9115
155. Peyraud F, Italiano A. Combined Parp Inhibition and Immune Checkpoint Therapy in Solid Tumors. *Cancers* (2020) 12:1–28. doi: 10.3390/cancers12061502
156. Passaro C, Volpe M, Botta G, Scamardella E, Perruolo G, Gillespie D, et al. PARP Inhibitor Olaparib Increases the Oncolytic Activity of Dl922-947 in Invitro and Invivo Model of Anaplastic Thyroid Carcinoma. *Mol Oncol* (2015) 9:78–92. doi: 10.1016/j.molonc.2014.07.022
157. Césaire M, Thariat J, Candéias SM, Stefan D, Saintigny Y, Chevalier F. Combining PARP Inhibition, Radiation, and Immunotherapy: A Possible Strategy to Improve the Treatment of Cancer? *Int J Mol Sci* (2018) 19. doi: 10.3390/ijms19123793
158. Sheng H, Huang Y, Xiao Y, Zhu Z, Shen M, Zhou P, et al. ATR Inhibitor AZD6738 Enhances the Antitumor Activity of Radiotherapy and Immune Checkpoint Inhibitors by Potentiating the Tumor Immune Microenvironment in Hepatocellular Carcinoma. *J Immunother Cancer* (2020) 8(1):340. doi: 10.1136/jitc-2019-000340
159. Rech AJ, Dada H, Kotzin JJ, Henao-Mejia J, Minn AJ, Twyman-Saint Victor C, et al. Radiotherapy and CD40 Activation Separately Augment Immunity to Checkpoint Blockade in Cancer. *Cancer Res* (2018) 78(15):4282–91. doi: 10.1158/0008-5472.CAN-17-3821
160. Qin S, Xu L, Yi M, Yu S, Wu K, Luo S. Novel Immune Checkpoint Targets: Moving Beyond PD-1 and CTLA-4. *Mol Cancer* (2019) 18:1–14. doi: 10.1186/s12943-019-1091-2
161. Han ZW, Lyv ZW, Cui B, Wang YY, Cheng JT, Zhang Y, et al. The Old CEACAMs Find Their New Role in Tumor Immunotherapy. *Investigational New Drugs* (2020) 38:1888–98. doi: 10.1007/s10637-020-00955-w
162. Rosewell Shaw A, Porter CE, Watanabe N, Tanoue K, Sikora A, Gottschalk S, et al. Adenovirotherapy Delivering Cytokine and Checkpoint Inhibitor Augments CAR T Cells Against Metastatic Head and Neck Cancer. *Mol Ther* (2017) 25(11):2440–51. doi: 10.1016/j.ymthe.2017.09.010
163. Porter CE, Rosewell Shaw A, Jung Y, Yip T, Castro PD, Sandulache VC, et al. Oncolytic Adenovirus Armed With BiTE, Cytokine, and Checkpoint Inhibitor Enables CAR T Cells to Control the Growth of Heterogeneous Tumors. *Mol Ther* (2020) 28(5):1251–62. doi: 10.1016/j.ymthe.2020.02.016
164. Helmink BA, Reddy SM, Gao J, Zhang S, Basar R, Thakur R, et al. B Cells and Tertiary Lymphoid Structures Promote Immunotherapy Response. *Nature* (2020) 577(7791):549–55. doi: 10.1038/s41586-019-1922-8
165. Dixon KO, Tabaka M, Schramm MA, Xiao S, Tang R, Dionne D, et al. TIM-3 Restrains Anti-Tumour Immunity by Regulating Inflammasome Activation. *Nature* (2021) 595(7865):101–6. doi: 10.1038/s41586-021-03626-9
166. Strauss L, Mahmoud MAA, Weaver JD, Tijaro-Ovalle NM, Christofides A, Wang Q, et al. Targeted Deletion of PD-1 in Myeloid Cells Induces Antitumor Immunity. *Sci Immunol* (2020) 5(43):eaay1863. doi: 10.1126/sciimmunol.aay1863
167. Jacquelot N, Seillet C, Wang M, Pizzolla A, Liao Y, Hediyeh-Zadeh S, et al. Blockade of the Co-Inhibitory Molecule PD-1 Unleashes ILC2-Dependent Antitumor Immunity in Melanoma. *Nat Immunol* (2021) 22(7):851–64. doi: 10.1038/s41590-021-00943-z
168. Dewan MZ, Galloway AE, Kawashima N, Dewyngaert JK, Babb JS, Formenti SC, et al. Fractionated But Not Single-Dose Radiotherapy Induces an Immune-Mediated Abscopal Effect When Combined With Anti-CTLA-4 Antibody. *Clin Cancer Res* (2009) 15(17):5379–88. doi: 10.1158/1078-0432.CCR-09-0265
169. Lugade AA, Moran JP, Gerber SA, Rose RC, Frelinger JG, Lord EM. Local Radiation Therapy of B16 Melanoma Tumors Increases the Generation of Tumor Antigen-Specific Effector Cells That Traffic to the Tumor. *J Immunol* (2005) 174(12):7516–23. doi: 10.4049/jimmunol.174.12.7516
170. Marciscano AE, Ghasemzadeh A, Nirschl TR, Theodros D, Kochel CM, Francica BJ, et al. Elective Nodal Irradiation Attenuates the Combinatorial Efficacy of Stereotactic Radiation Therapy and Immunotherapy. *Clin Cancer Res* (2018) 24(20):5058–71. doi: 10.1158/1078-0432.CCR-17-3427
171. Francini N, Cochrane D, Illingworth S, Purdie L, Mantovani G, Fisher K, et al. Polyvalent Diazonium Polymers Provide Efficient Protection of Oncolytic Adenovirus Enadenotucirev From Neutralizing Antibodies While Maintaining Biological Activity in Vitro and in Vivo. *Bioconjug Chem* (2019) 30(4):1244–57. doi: 10.1021/acs.bioconjchem.9b00189

Conflict of Interest: The authors declare that the research was conducted in the absence of any commercial or financial relationships that could be construed as a potential conflict of interest.

frontiers in Oncology

SYSTEMATIC REVIEW
published: 11 November 2021
doi: 10.3389/fonc.2021.746976

Neutrophil-to-Lymphocyte Ratio as a Prognostic Biomarker for Patients With Metastatic Renal Cell Carcinoma Treated With Immune Checkpoint Inhibitors: A Systematic Review and Meta-Analysis

Xiuqiong Chen[1,2,3,4], *Fanqiao Meng*[5] *and Richeng Jiang*[1,2,3,4*]

[1] Tianjin Medical University Cancer Institute and Hospital, National Clinical Research Center for Cancer, Tianjin, China, [2] Key Laboratory of Cancer Prevention and Therapy, Tianjin, China, [3] Tianjin's Clinical Research Center for Cancer, Tianjin, China, [4] Department of Thoracic Oncology, Tianjin Lung Cancer Center, Tianjin Cancer Institute and Hospital, Tianjin Medical University, Tianjin, China, [5] Department of Hematology, Tianjin Medical University General Hospital, Tianjin, China

OPEN ACCESS

Edited by:
Roberta Zappasodi, Memorial Sloan Kettering Cancer Center, United States

Reviewed by:
Khaled Murshed, Hamad Medical Corporation, Qatar
Marco Maruzzo, Veneto Institute of Oncology (IRCCS), Italy

***Correspondence:**
Richeng Jiang
jiangricheng@tjmuch.com

Specialty section:
This article was submitted to Cancer Immunity and Immunotherapy, a section of the journal Frontiers in Oncology

Received: *25 July 2021*
Accepted: *25 October 2021*
Published: *11 November 2021*

Citation:
Chen X, Meng F and Jiang R (2021) Neutrophil-to-Lymphocyte Ratio as a Prognostic Biomarker for Patients With Metastatic Renal Cell Carcinoma Treated With Immune Checkpoint Inhibitors: A Systematic Review and Meta-Analysis. Front. Oncol. 11:746976. doi: 10.3389/fonc.2021.746976

There is increasing evidence to suggest that the neutrophil-to-lymphocyte ratio (NLR) is related to the prognosis of patients with renal cell carcinoma (RCC) treated with immune checkpoint inhibitors (ICIs). However, these findings are inconsistent. The present study was performed with the aim of exploring the utility of NLR in patients with RCC treated with ICIs. For this purpose, a comprehensive search of PubMed, Web of Science, and Embase was performed to find studies evaluating the prognostic value of NLR. The overall survival (OS) and progression-free survival (PFS) were the assessed clinical outcomes. All statistical analysis was performed using Stata version 12.0 software. The combined hazard ratios (HRs) and 95% confidence intervals (CIs) of NLR for OS and PFS were calculated using the random-effect models. Heterogeneity was evaluated based on the I^2 value and Cochran's Q test. Egger's and Begg's tests were applied to precisely assess the publication bias. The "trim and fill" method was adopted to perform the sensitivity analysis to determine whether the results were stable. In total, 12 studies encompassing 1,275 patients were included in the final analysis. The results revealed that a high NLR at baseline or pre-therapy was associated with a poor OS (HR, 2.23; 95% CI, 1.84–2.70; $p < 0.001$) and PFS (HR, 1.78; 95% CI, 1.72–2.09; $p < 0.001$). During the course of treatment, a decrease in the NLR was associated with a significantly longer OS (HR, 0.34; 95% CI, 0.20–0.56; $p < 0.001$) and PFS (HR, 0.44; 95% CI, 0.30–0.63; $p < 0.001$) compared to an increase in NLR. As a preliminary screening of other risk factors, age, sex, race, and IMDC risk may have a certain prognostic value for RCC treated with ICIs. People over 70 years old had better OS compared to people younger than 70 (HR, 0.65; 95% CI, 0.48–0.89). Non-Caucasians treated with immunotherapy had a worse OS (HR, 8.67; 95% CI, 2.87–26.2) and PFS (HR, 2.65; 95% CI, 1.28–5.48) than Caucasians. Males had a worse OS than females (HR, 1.48; 95% CI, 1.14–1.93). Compared with the IMDC favorable risk

group, the OS of the IMDC poor risk group was worse (HR, 2.59; 95% CI, 1.56–4.32). There was no significant publication bias or heterogeneity observed in the present study. On the whole, the present study demonstrated that an elevated NLR is associated with an adverse OS and PFS in patients with RCC treated with ICIs. The NLR may thus be used as a readily available prognostic biomarker for these patients. Age, sex, race, and IMDC risk may have potential predictive value for the prognosis of RCC treated with ICIs. However, further investigations are warranted to validate these results.

Keywords: neutrophil-to-lymphocyte ratio, renal cell cancer, immune checkpoint inhibitor, prognosis, biomarker

INTRODUCTION

According to the 2018 GLOBLE data, 403,000 individuals are diagnosed with kidney cancer each year, accounting for 2.2% of all cancers worldwide (1). The most common subtype of renal cell carcinoma (RCC) is clear cell carcinoma, which accounts for ~75% of all cases (2). RCC accounts for 5% and 3% of all malignancies among adult males and females, respectively. It is the sixth most common type of cancer among males and the ninth among females (3). Approximately one-third of patients with RCC have experienced metastasis by the time of diagnosis (4).

For patients with advanced RCC, the selection of effective treatment options is critical. Recently, several immune checkpoint inhibitors (ICIs) have been shown to be effective against metastatic RCC (mRCC). RCC tissues are infiltrated by a large number of inflammatory cells, such as T cells, natural killer cells, dendritic cells, and macrophages, rendering immunotherapy a possible effective treatment. The Checkmate-025 study revealed that when Nivolumab monotherapy was used in the second- or third-line therapy of mRCC, both programmed death-ligand (PD-L)1(+) and PD-L1(−) patients benefited from immunotherapy (5). However, for first-line therapy, whether PD-L1 expression is positive or negative, patients with mRCC can benefit from treatment with PD-1 monoclonal antibody, such as Pembrolizumab or PD-L1 monoclonal antibody, such as Atezolizumab and Avelumab combined with vascular targeted therapy (6–8). However, in the CheckMate 214 study, 776 subjects were tested for PD-L1 expression. According to PD-L1 expression, stratified analysis found that for patients with PD-L1 ≥1%, the objective response rate (ORR) was significantly higher in the combined treatment group than in the Sunitinib control group (58% vs. 22%; $p < 0.001$), and median progression-free survival (PFS) was extended by 16.9 months [22.8 vs. 5.9 months; hazard ratio (HR), 0.46; 95% confidence interval (CI), 0.31–0.67]. Of note, in terms of patients with PD-L1 <1%, the ORR was still significantly higher in the immune combination group than in the Sunitinib control group (37% vs. 28%; $p = 0.03$), and the difference in PFS was not statistically significant (11.0 vs. 10.4 months; HR, 1.00, 95% CI, 0.80–1.26) (9). Therefore, PD-L1 is not a perfect predictor of clinical outcomes in immunotherapy for RCC. Thus, the identification of factors associated with the efficacy of immunotherapy for mRCC is essential for guiding precise therapy and surveillance of disease.

In recent years, it has become clear that tumor-related inflammatory responses, such as local and systemic inflammation, and decreased or increased myelopoiesis, substantially contribute to the development and progression of malignancies (10). The alteration of peripheral blood biomarkers, such as the neutrophil-to-lymphocyte ratio (NLR) can represent the systemic inflammatory response in patients. Several studies have demonstrated that the NLR is a potent prognostic biomarker related to a worse overall survival (OS) in several tumor types, including mRCC in the pre-immunotherapy era (11–15). Currently, a growing number of peripheral blood biomarkers, particularly NLR, have been found to be associated with ICI treatment outcomes for various types of cancer (16). Inflammatory indicators related to therapeutic efficacy may guide clinical decision-making.

Currently, although several studies have explored the prognostic value of NLR in patients receiving immunotherapy for RCC (17–28), it is still difficult to verify the prognostic role of NLR in patients with RCC treated with ICIs. Certain studies have suggested that the NLR is not associated with the prognosis of patients with RCC treated with immunotherapy (21, 26). Additionally, some of the published studies had a small sample size (17, 18, 28). Hence, the present comprehensive meta-analysis was conducted in order to precisely evaluate the prognostic significance of the NLR in patients with RCC receiving immunotherapy.

DATA AND METHODS

Literature Search

A comprehensive search strategy was applied to identify all relevant literature in the PubMed, Web of Science, and Embase databases up to July 2021. The search terms were as follows: "Neutrophil to lymphocyte" OR "inflammatory biomarkers" OR "Immunoinflammatory measures" OR "Inflammatory indices" OR "NLR" OR "Neutrophil-to-Lymphocyte Ratio" AND "PD-L1" OR "PD-1" OR "nivolumab" OR "immune checkpoint blockade" OR "Immune Checkpoint Inhibitors" OR "immunotherapy" AND "renal cancer" OR "kidney carcinoma" OR "kidney cancer" OR "RCC" OR "renal cell carcinoma". The reference lists of the identified studies were also examined.

Inclusion Criteria

Studies that fulfilled the following criteria were included: (i) All patients were diagnosed with mRCC according to the current clinical guidelines and treated with ICIs; (ii) the NLR of patients

was calculated, and the association between NLR and prognosis was also investigated; (iii) HR values and 95% CIs could be extracted from the studies or described in the studies; (iv) survival information included the OS and PFS; (v) articles were written in the English language.

Quality Evaluation

The quality assessment methods from Hayden et al. (29) were used in the present study. It was recommended that the quality appraisal of prognostic studies consider six potential biases: Study attrition, study participation, outcome measurement, prognostic factor measurement, analysis and confounding measurement, and account. The evaluation of risk for bias should be completed by at least two independent reviewers. The score for each item in the quality assessment is 0–2, the maximum score for each study is 12 points, and a score of ≥8 is considered high quality.

Data Extraction

The information obtained from the studies included the year of publication, first author, country, the number of patients, age, sex, histological type, race, Eastern Cooperative Oncology Group (ECOG) status, prior nephrectomy, the number of prior anti-VEGF therapies, International Metastatic RCC Database Consortium (IMDC) risk group, number of metastatic sites, study type, testing time, cutoff value for NLR, and survival outcomes. Survival data included the HR and 95% CI values for OS and PFS. If the HR and 95% CI values could not be directly extracted from the original study, the reported methods from Tierney et al. (30) and Parmar et al. (31) were used to calculate these statistical variables.

Statistical Analysis

Authoritative statistical software (Stata 12.0: Stata Corporation) was used to perform the meta-analysis. The HR and 95% CI values were applied to estimate the prognostic value of NLR for patients treated with ICIs. Individual HR and 95% CI values were combined to an overall HR and 95% CI. An HR >1 indicated a worse survival for the experimental group, a 95% CI containing the no. 1 and $p < 0.05$ indicated a significant difference statistically between the two groups. The I^2 statistic and Cochran Q test were applied to detect the heterogeneity between studies; $p \leq 0.1$ and $I^2 > 50\%$ indicated a substantial heterogeneity between studies and random effects models were adopted. When significant heterogeneity existed, subgroup analysis could be employed to identify the source of heterogeneity. Begg's test, Egger's test, and visual inspection of a funnel plot were carried out to evaluate the possibility of publication bias. Egger's test result was the primary indicator, and a symmetry funnel plot with a p-value ≥0.05 was considered as an insignificant publication bias.

RESULTS

Literature Characteristics

A total of 495 references were collected from PubMed, Web of Science, and Embase. In total, 369 records were left after deleting the duplicates. After examining titles and abstracts, 19 studies were identified. A total of seven studies had insufficient data following a full-text review, leaving 12 records included according to the eligibility criteria (**Figure 1**) (17–28). The literature search was performed by two investigators, and any disagreements between them were settled by consensus. The basic features of the included trials are summarized in **Tables 1**, **2**. The total number of patients from the included studies was 1,275, ranging from 37 to 404 cases per trial. In total, 9 studies were from Western countries, including the USA (17–21, 28), Italy (24, 27), and France (25). Another three were from Japan (22, 23, 26). Only one study was prospective (24) and the remaining studies were retrospective studies. The majority of studies measured the number of neutrophils and lymphocytes at baseline or pre-treatment, and then calculated the NLR; four trials also tested the number under therapy (19, 22, 25, 28). The cutoff values of the majority of studies were 3 (18, 23–28); those in three studies were 3.9 (19), 4.2 (20), and 5.5 (17), and the values in other studies were 5 (21, 22). Both the OS and PFS were evaluated in all nine studies (17–19, 22, 23, 25–28), In total, two studies (21, 24) only had OS and one study (20) only had PFS data available. The scores of quality evaluation for the included trials ranged from 7 to 11; 10 scored >8 (17–20, 22–27), and 2 scored <8 (21, 28).

NLR and OS for RCC

A total of 10 studies containing 1,148 patients reported the association between NLR at baseline or pre-therapy and OS in patients with RCC treated with ICIs. The random-effects model was used to estimate the combined HR and corresponding 95% CI values. The results revealed that the high NLR group at baseline or pre-therapy had a shorter OS than the low group (combined HR, 2.23; 95% CI, 1.84–2.70; $p < 0.001$; **Figure 2**), which suggested that a high NLR at baseline or pre-therapy was an important predictor of a poor prognosis. The I^2 (27.4%) and Q test ($p = 0.192$) results for OS indicated that there was no obvious heterogeneity among the studies. A total of four studies including 330 patients reported the effect of NLR during treatment on OS. The present study revealed that a decrease in NLR during treatment was a predictor of a longer OS (HR, 0.34; 95% CI, 0.20–0.56; $p < 0.001$; **Figure 3**). Correspondingly, the heterogeneity test revealed no statistically significant heterogeneity between the studies ($I^2 = 0\%$, Q test $p = 0.932$).

NLR and PFS in RCC

As performed for the OS analysis, the association between the NLR at baseline or pre-therapy and PFS was estimated. A total of nine studies including a total of 1,173 subjects were used to investigate the clinical outcome, and a final combined HR of 1.78 (95% CI, 1.72–2.09; $p < 0.001$; **Figure 4**) indicated that a higher NLR was associated with a worse PFS in patients with RCC treated with ICIs. A low heterogeneity in the present analysis in terms of PFS ($I^2 = 37.8\%$, Q test $p = 0.116$) was found. The association between changes in NLR during treatment and PFS was also explored. As observed in the OS analyses and in the PFS comparison, an increase in NLR during treatment resulted in a worse PFS (HR, 0.44; 95% CI, 0.30–0.63; $p < 0.001$; **Figure 5**) and no significant heterogeneity existed ($I^2 = 0\%$, Q test $p = 0.584$).

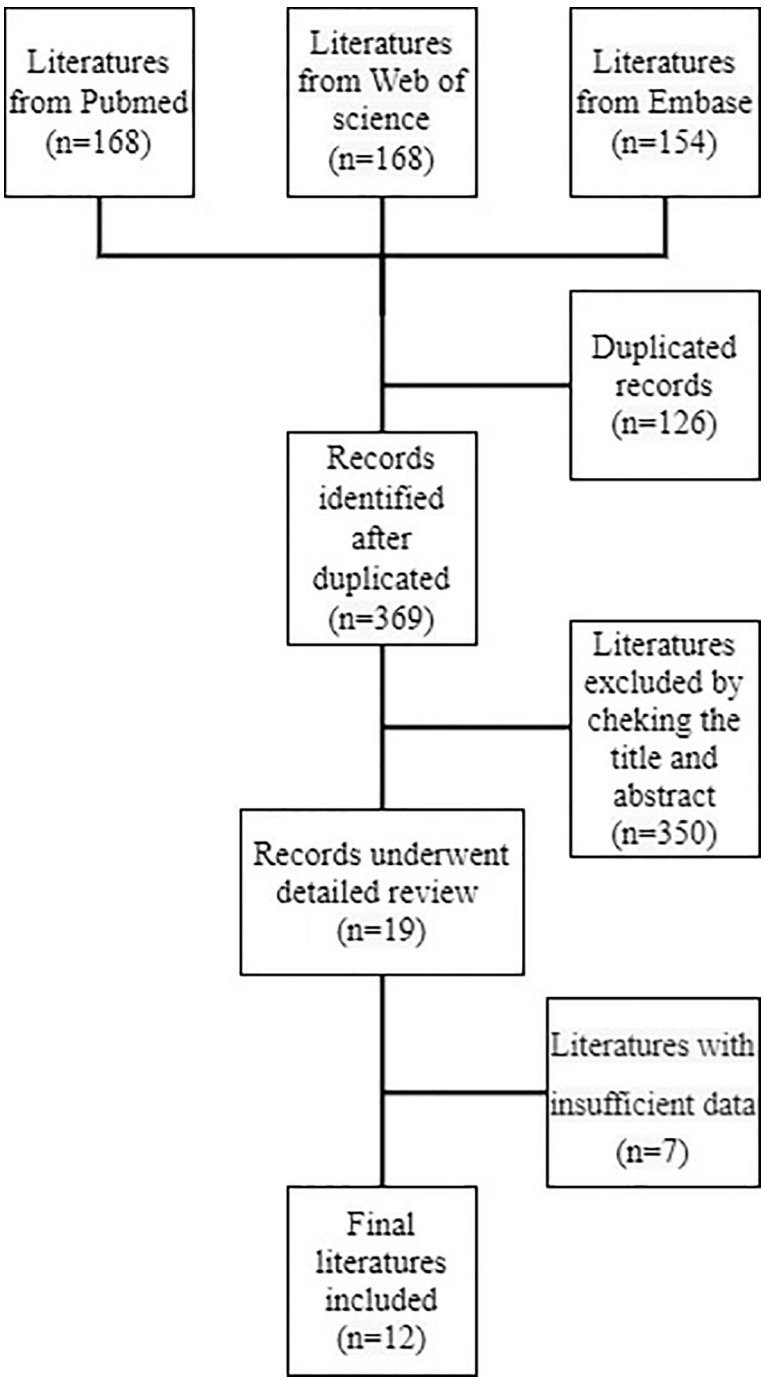

FIGURE 1 | Flow diagram of record selection.

Other Risk Factors, and PFS and OS in RCC

The association between the efficacy of immunotherapy for mRCC and other possible risk factors including age, sex, race, histological type, ECOG status, prior nephrectomy, number of prior anti-VEGF therapies, IMDC risk group, and the number of metastatic sites was also explored. The results are presented in **Table 2**. Among all the risk factors, age, sex, race, and IMDC risk grouping may be prognostic factors for mRCC treated with immunotherapy. Males had a worse OS than females (HR, 1.48; 95% CI, 1.14–1.93); there was no significant difference in PFS between the two groups (HR, 1.10; 95% CI, 0.85–1.44). People over 70 years old had better OS compared to people younger than 70 (HR, 0.65; 95% CI, 0.48–0.89);

TABLE 1 | Study features of the 12 eligible records.

Author (Year)	Country	Study type	Patients	Testing time	Group	Clinical outcome	Quality score
Asim M (2017)	USA	Retrospective	38	Pretherapy	≥5.5 *vs.* <5.5	PFS, OS	10
Jeyakumar G (2017)	USA	Retrospective	42	Pretherapy	≥3 *vs.* <3	PFS, OS	11
Lalani A (2018)	USA	Retrospective	142	Under therapy	deNLR *vs.* inNLR	PFS, OS	10
				Baseline	≥3.9 *vs.* <3.9	PFS, OS	
Zahoor H (2018)	USA	Retrospective	90	Baseline	≥4.2 *vs.* <4.2	PFS	8
Rohit K (2018)	USA	Retrospective	65	Pretherapy	≥5 vs<5	OS	7
Suzuki K (2019)	Japan	Retrospective	65	Under therapy	deNLR *vs.* inNLR	PFS, OS	9
				Pretherapy	≥5 vs<5	PFS, OS	
Ishihara H (2019)	Japan	Retrospective	58	Pretherapy	≥3 *vs.* <3	PFS, OS	8
Giorgi U (2019)	Italy	Prospective	196	Baseline	≥3 *vs.* <3	OS	9
Simonaggio A (2020)	France	Retrospective	86	Under therapy	deNLR *vs.* inNLR	PFS, OS	10
				Baseline	≥3 *vs.* <3	PFS, OS	
Nishiyama N (2020)	Japan	Retrospective	52	Baseline	≥3 *vs.* <3	PFS, OS	8
Rebuzzi S (2020)	Italy	Retrospective	404	Baseline	≥3 *vs.* <3	PFS, OS	8
Arnab B (2020)	USA	Retrospective	37	Under therapy	deNLR *vs.* inNLR	PFS, OS	7

deNLR, decrease of NLR; inNLR, increase of NLR; OS, overall survival; PFS, progression-free survival.

however, there was no significant difference in PFS between the two groups (HR, 0.73; 95% CI, 0.51–1.06). Non-Caucasians treated with immunotherapy had a worse OS (HR, 8.67; 95% CI, 2.87–26.2) and PFS (HR, 2.65; 95% CI, 1.28–5.48) than Caucasians. Compared with the IMDC favorable risk group, the OS of the IMDC poor risk group was worse (HR, 2.59; 95% CI, 1.56–4.32); there was no statistically significant difference in PFS between the two groups (HR, 1.20; 95% CI, 0.74–1.94). Other risk factors including histologic type, ECOG, prior nephrectomy, number of prior anti-VEGF therapies, and number of metastatic sites did not affect the prognosis of patients treated with ICIs. However, the number of studies involving the prognostic value of these risk factors was too small. The results of the present study can be used as a preliminary screening of prognostic factors, and a more specific meta-analysis can be performed for further exploration in the future.

Publication Bias

The publication bias for OS and PFS was then assessed. In terms of the impact of NLR on the OS and PFS, Egger's test revealed no obvious publication bias ($p > 0.05$); however, Begg's test raised a high risk of publication bias ($p = 0.05$) in terms of the impact of NLR at baseline or pre-therapy on the OS and PFS (**Table 3**); funnel plots revealed a slight basic asymmetry by visual assessment (**Figure 6A**). To resolve this issue, a sensitivity analysis was implemented using the "trim and fill" method in STATA software, which removed or supplemented certain trials to examine the changes in the pooled effect size. If the conclusions were consistent, the publication bias was not obvious and the results were relatively stable. As far as OS was concerned, before the "trim and fill method", the combined effect size Log (HR) and the corresponding 95% CIs were 0.80 (0.61–0.99). After three studies were supplemented, the pooled HR and 95% CIs were 2.13 (1.76–2.57). In terms of PFS, the effect size [Log (HR) and HR] and 95% CIs before and after "trim and fill" were 0.58 (0.42–0.74) and 1.78 (1.52–2.09), respectively. The above data showed that the conclusions were consistent, indicating that the result was stable. The imputed studies produced a symmetrical funnel plot (**Figure 6B**), which showed no publication bias; thus, the results were reliable in the current meta-analysis.

DISCUSSION

As one of the inflammatory factor indicators, NLR can predict the efficacy of various therapeutic options, such as surgical resection

TABLE 2 | The association between other risk factors and overall survival and progression-free survival of patients with renal cell carcinoma treated with immunotherapy.

Factor	Studies number (OS/PFS)	OS		PFS	
		HR	95% CI	HR	95% CI
Gender (male vs female)	5/4	1.48	1.14-1.93	1.10	0.85-1.44
Histologic type (clear cell vs non-clear cell)	4/3	0.84	0.52-1.35	0.82	0.52-1.28
Age (≥70 vs <70)	4/3	0.65	0.48-0.89	0.73	0.51-1.06
Race (non-caucasian vs caucasian)	1/2	8.67	2.87-26.2	2.65	1.28-5.48
ECOG (0-1 vs 2-4)	1/1	0.42	0.10–1.74	0.46	0.16–1.31
Prior Nephrectomy (yes vs no)	3/3	0.65	0.33-1.29	1.24	0.72-2.12
Number of Prior anti-VEGF Therapies (>1 vs ≤1)	3/3	1.70	0.98-2.96	1.09	0.75-1.59
IMDC Risk Group (poor vs favorable)	3/4	2.59	1.56-4.32	1.20	0.74-1.94
Number of metastatic sites (≥ 2 vs <2)	3/5	1.11	0.67-1.85	0.98	0.52-1.83

ECOG, Eastern Cooperative Oncology Group; VEGF, vascular endothelial growth factor; IMDC, International Metastatic Renal Cell Carcinoma Database Consortium.

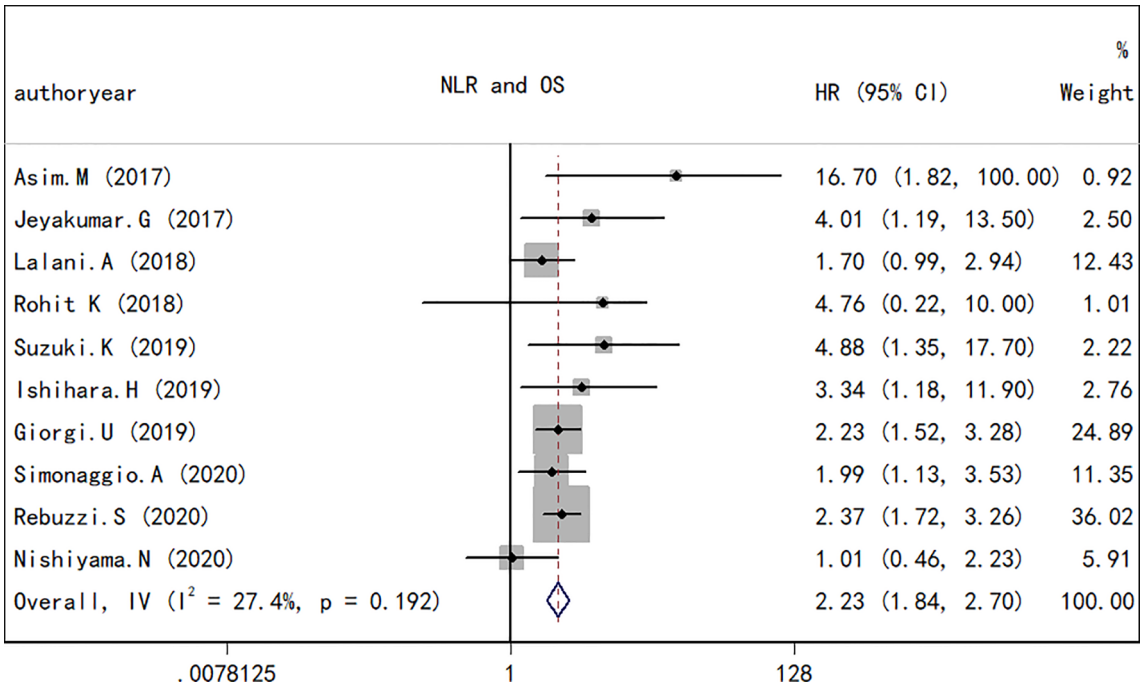

FIGURE 2 | Forest plot of hazard ratios for the association between the neutrophil-to-lymphocyte ratio at baseline or pre-therapy and overall survival in renal cell carcinoma.

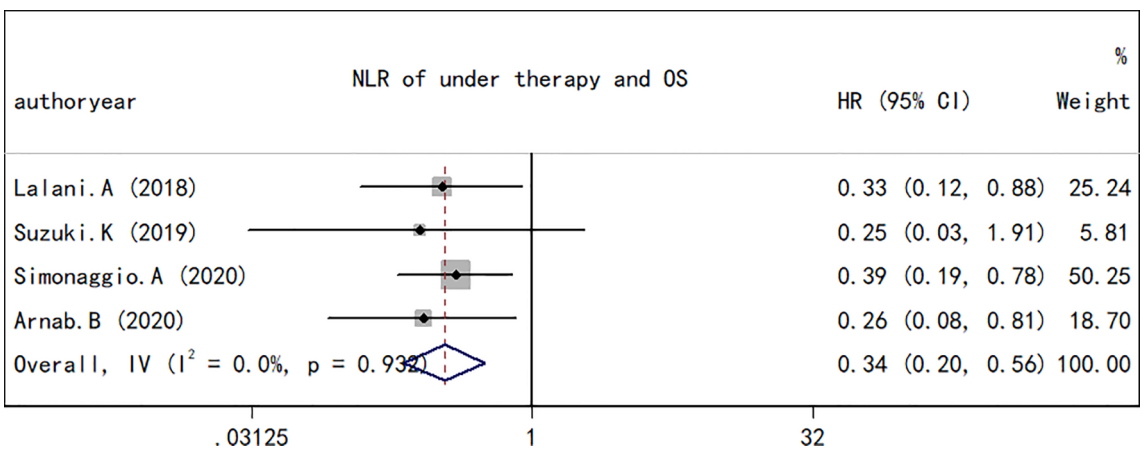

FIGURE 3 | Forest plot of hazard ratios for the association between the neutrophil-to-lymphocyte ratio at baseline or pre-therapy and progression-free survival in renal cell carcinoma.

and VEGR inhibitors in RCC (32, 33). The prognostic value of NLR in a variety of solid tumors undergoing immunotherapy has also been extensively explored (34, 35), and these findings suggest that a high NLR is a predictor of a poor survival in patients undergoing immunotherapy, which was consistent with the findings of the present study. Although the association between NLR and the prognosis of patients receiving immunotherapy has also been widely investigated in RCC, it remains a difficult task to determine the prognostic value of NLR in patients due to the small sample sizes of individual studies and the conflicting results of various studies. The present study provides strong evidence that NLR may be applied as a prognostic marker for patients with RCC receiving immunotherapy.

As the first meta-analysis (to the best of our knowledge) fully investigating the association between NLR and the prognosis of patients with RCC receiving immunotherapy, the present study summarized the available credible evidence from 12 studies encompassing 1,275 cases. The integrated HR confirmed that

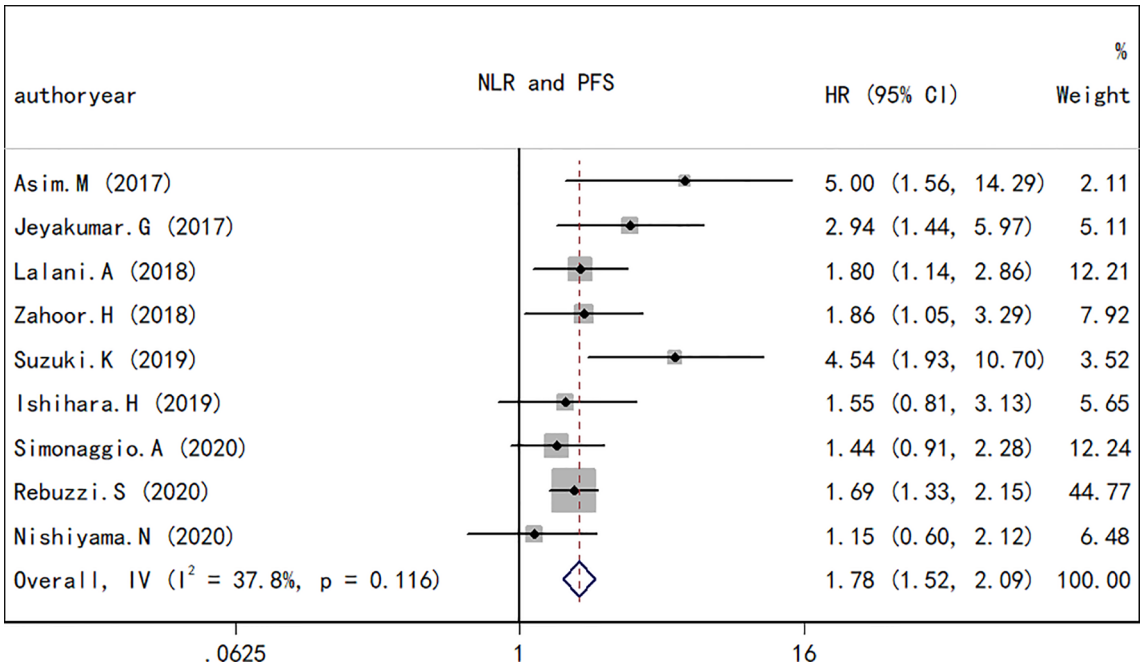

FIGURE 4 | Forest plot of hazard ratios for the association between the neutrophil-to-lymphocyte ratio under therapy and overall survival in renal cell carcinoma.

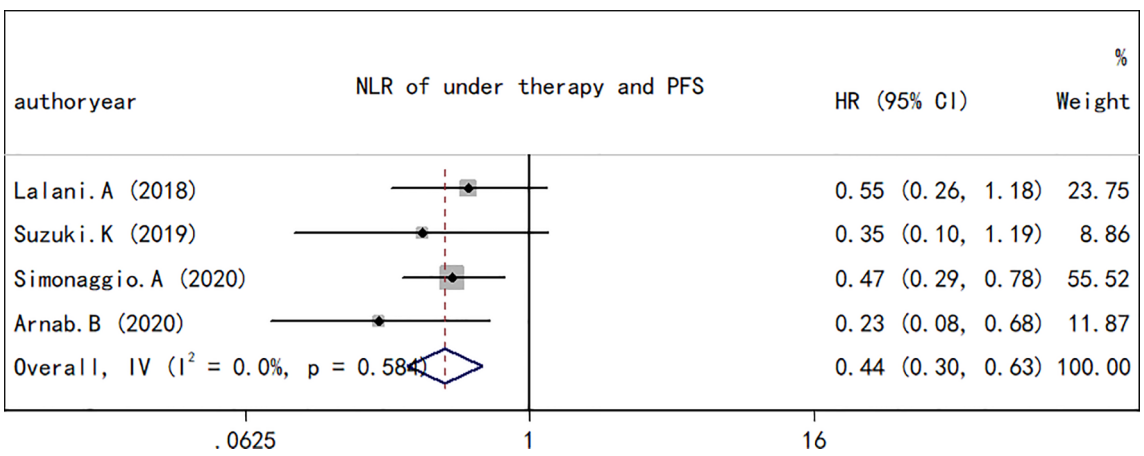

FIGURE 5 | Forest plot of hazard ratios for the association between the neutrophil-to-lymphocyte ratio under therapy and progression-free survival in renal cell carcinoma.

an elevated NLR at pre-therapy or at baseline was associated with a poor OS (HR, 2.23; 95% CI, 1.84–2.70; $p < 0.001$) and PFS (HR, 1.78; 95% CI, 1.72–2.09; $p < 0.001$). A significant association was also found between a decrease in NLR under therapy and an improved OS (HR, 0.34; 95% CI, 0.20–0.56; $p < 0.001$) and PFS (HR, 0.44; 95% CI, 0.30–0.63; $p < 0.001$). These results confirm that the NLR may be used as a prognostic indicator in patients with CC receiving immunotherapy.

Numerous studies have suggested that systemic inflammatory responses and the tumor microenvironment play a critical role in cancer progression and affect a patient's response to treatment. At different stages of tumorigenesis, invasion, and metastasis, tumor cells and related inflammatory cells release a large amount of cytokines, chemokines, and other inflammatory factors to promote tumor initiation (10, 36). Thus, the systemic inflammatory response is significantly associated with the outcome of patients and related inflammatory indicators, such as the NLR, and this may be used as a biomarker for the prognosis of patients with cancer, and may effectively estimate the prognosis of these patients (37, 38). Neutrophils can promote

TABLE 3 | Results of Egger's and Begg's tests for publication bias.

Outcome	Study number	Egger's test (*p*)	Begg's test (*p*)
OS	10	0.18	0.05
PFS	9	0.15	0.05
OS for under therapy group	4	0.15	0.31
PFS for under therapy group	4	0.35	0.73

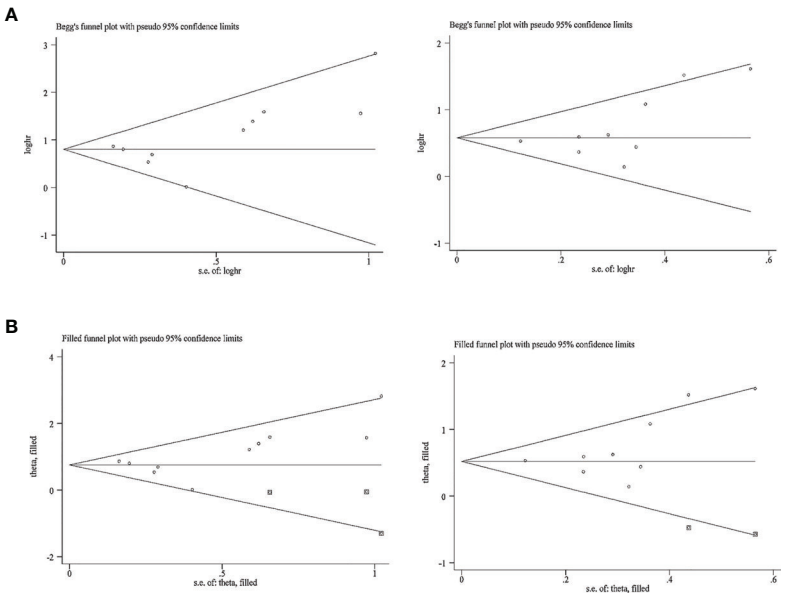

FIGURE 6 | Funnel plot for the evaluation of publication bias considering the association between the neutrophil-to-lymphocyte ratio at baseline or pre-therapy and clinical outcomes in this analysis. **(A)** Funnel plot for 10 studies regarding overall survival and 9 studies considering progression-free survival before the "trim and fill" method. **(B)** Funnel plot for 10 studies considering overall survival and 9 studies considering progression-free survival after the "trim and fill" method.

cancer progression by directly acting on tumor cells or indirectly altering the tumor microenvironment (39). In the tumor microenvironment, neutrophils are separated into high-density neutrophils (HDNs) and low-density neutrophils (LDN) due to functional differences. LDNs suppress T cells through arginase expression and promote tumor angiogenesis by upregulating tumor vascular endothelial cytokines (VEGF), thus promoting tumor progression. Instead, HDNs function as antitumor agents either by acting directly on cancer cells or by provoking T-cell-mediated immune responses. In the context of inflammation, neutrophils primarily display an HDN phenotype in the early stages of inflammation, whereas the LDN phenotype is inclined to accumulate when the inflammation subsides (39, 40). As immune response cells, lymphocytes play a dominant role in the antitumor effect. Lymphocyte infiltration in tumor tissue is associated with a better therapeutic response and outcome, while the decrease in lymphocytes in the tumor microenvironment leads to a decrease in antitumor ability, which causes the emergence of immune tolerance and the escape of tumor cells (41). In addition, the reduction in peripheral blood lymphocytes can provide an appropriate tumor microenvironment for the proliferation and metastasis of tumor cells by impairing the antitumor response mediated by lymphocytes (42). Theoretically, neutrophilia represents the response to systematic inflammation, whereas lymphocytes reflect an impaired cell-mediated immunity. Therefore, a decreased NLR is associated with a better response to immunotherapy.

The predictive value of the NLR in the efficacy of immunotherapy for esophageal cancer, lung cancer, melanoma, and other solid tumors has been fully explored. As regards esophageal cancer, the PFS in patients with a high NLR at 6 weeks post-treatment was shown to be lower than that of patients with a low NLR (HR, 2.097; 95% CI, 0.996–4.417; $p = 0.027$) (16). An elevated NLR at pre-treatment has been shown to be associated with a shorter OS and lower response rates in patients with metastatic NSCLC treated with Nivolumab independently of other prognostic factors (34). In another study, a similar association was observed between the NLR and the efficacy of Ipilimumab in the treatment of melanoma (35). All the aforementioned independent studies confirmed the prognostic value of NLR in immunotherapy; however, these individual studies were retrospective studies and the sample sizes were small.

Another two high-quality meta-analyses also explored the association between NLR and the survival of patients with solid

tumors treated with immunotherapy. A previous meta-analysis included 27 studies incorporating 4,647 patients with advanced cancers consisting of non-small cell lung cancer (NSCLC), RCC, and hepatocellular carcinoma, among other types. The pooled analyses indicated that a high blood NLR at pre-therapy was associated with a significant shorter OS (HR, 1.98; 95% CI, 1.66–2.36; $p < 0.001$) and PFS (HR, 1.78; 95% CI, 1.48–2.15; $p < 0.001$). In that study, immunotherapy was defined as a form of treatment that acted on the immune microenvironment, including CTLA-4, PD-1, PD-L1, VEGF, and VEGFR, among other targets, and the involved patients with RCC were all treated with Sunitinib and Sorafenib (43). However, in the present study, the patients with RCC were treated with ICIs, including CTLA-4, PD-L1, and PD-1. In another meta-analysis, seven studies were included, containing three trials on melanoma, three studies on NSCLC, and only one study on RCC. The pooled results revealed that a high NLR contributed to a worse OS (HR, 1.92; 95% CI, 1.29–2.87; $p < 0.001$) and PFS (HR, 1.66; 95% CI, 1.38–2.01; $p < 0.001$) (44). Although both studies assessed the prognostic value of NLR in patients with malignant tumor receiving immunotherapy, the predictive significance of NLR in patients with malignant tumors receiving immunotherapy remains unknown due to differences in the definition of immunotherapy and fewer studies involving RCC. In the present study, the prognostic value of NLR in patients with RCC receiving ICIs was comprehensively identified. The pooled results showed that a high NLR was significantly associated with a poor OS and PFS, indicating that blood NLR was a significative predictive biomarker in patients with RCC receiving immunotherapy.

However, the present study has several limitations. Firstly, Egger's test indicated that a slight publication bias was present; although a "trim and fill" analysis was conducted, the combined results should be treated with caution. Secondly, the current meta-analysis is a literature-based analysis rather than individual patient data-based analysis, which renders the results less reliable. Thirdly, studies that could not provide sufficient information to calculate the HR were excluded, which would cause the combined effect size to differ from true values to a certain extent. Considering these factors, further more robust analyses are required to verify or update these results in the future.

In conclusion, in view of the current meta-analysis, the results revealed that a high blood NLR was associated with a poor OS and PFS across studies of patients with RCC treated with ICIs. Therefore, the NLR may be used as a prognostic indicator for patients with RCC accepting ICIs based on available trials, which may help to direct clinical decision-making. Nevertheless, future prospective randomized controlled trials are required to confirm and better understand this biomarker and its role in the employment of ICIs in RCC.

DATA AVAILABILITY STATEMENT

The original contributions presented in the study are included in the article/supplementary material. Further inquiries can be directed to the corresponding author.

AUTHOR CONTRIBUTIONS

XC and RJ designed and performed the study, and wrote the manuscript. FM extracted the data, and assisted in data collection and analysis. XC and FM critically revised the manuscript, and ensured correct data analysis. RJ and XC confirmed the authenticity of all the raw data. All authors contributed to the article and approved the submitted version.

FUNDING

The present study was funded by the Nature Science Foundation of Tianjin City (grant no. 18JCZDJC98800).

REFERENCES

1. Padala SA, Barsouk A, Thandra KC, Saginala K, Mohammed A, Vakiti A, et al. Epidemiology of Renal Cell Carcinoma. *World J Oncol* (2020) 11(3):79–87. doi: 10.14740/wjon1279
2. Jemal A, Siegel R, Ward E, Murray T, Xu J, Thun MJ. Cancer Statistics, 2007. *CA: Cancer J Clin* (2007) 57(1):43–66. doi: 10.3322/canjclin.57.1.43
3. Siegel RL, Miller KD, Fuchs HE, Jemal A. Cancer Statistics, 2021. *CA: Cancer J Clin* (2021) 71(1):7–33. doi: 10.3322/caac.21654
4. Bianchi M, Sun M, Jeldres C, Shariat SF, Trinh QD, Briganti A, et al. Distribution of Metastatic Sites in Renal Cell Carcinoma: A Population-Based Analysis. *Ann Oncol Off J Eur Soc Med Oncol* (2012) 23(4):973–80. doi: 10.1093/annonc/mdr362
5. Motzer RJ, Escudier B, George S, Hammers HJ, Srinivas S, Tykodi SS, et al. Nivolumab Versus Everolimus in Patients With Advanced Renal Cell Carcinoma: Updated Results With Long-Term Follow-Up of the Randomized, Open-Label, Phase 3 CheckMate 025 Trial. *Cancer* (2020) 126 (18):4156–67. doi: 10.1002/cncr.33033
6. Rini BI, Plimack ER, Stus V, Gafanov R, Hawkins R, Nosov D, et al. Pembrolizumab Plus Axitinib Versus Sunitinib for Advanced Renal-Cell Carcinoma. *New Engl J Med* (2019) 380(12):1116–27. doi: 10.1056/NEJMoa1816714
7. Motzer RJ, Penkov K, Haanen J, Rini B, Albiges L, Campbell MT, et al. Avelumab Plus Axitinib Versus Sunitinib for Advanced Renal-Cell Carcinoma. *New Engl J Med* (2019) 380(12):1103–15. doi: 10.1056/NEJMoa1816047
8. Rini BI, Powles T, Atkins MB, Escudier B, McDermott DF, Suarez C, et al. Atezolizumab Plus Bevacizumab Versus Sunitinib in Patients With Previously Untreated Metastatic Renal Cell Carcinoma (IMmotion151): A Multicentre, Open-Label, Phase 3, Randomised Controlled Trial. *Lancet (London England)* (2019) 393(10189):2404–15. doi: 10.1016/s0140-6736(19)30723-8
9. Motzer RJ, Rini BI, McDermott DF, Arén Frontera O, Hammers HJ, Carducci MA, et al. Nivolumab Plus Ipilimumab Versus Sunitinib in First-Line Treatment for Advanced Renal Cell Carcinoma: Extended Follow-Up of Efficacy and Safety Results From a Randomised, Controlled, Phase 3 Trial. *Lancet Oncol* (2019) 20(10):1370–85. doi: 10.1016/s1470-2045(19)30413-9
10. Diakos CI, Charles KA, McMillan DC, Clarke SJ. Cancer-Related Inflammation and Treatment Effectiveness. *Lancet Oncol* (2014) 15(11): e493–503. doi: 10.1016/s1470-2045(14)70263-3
11. Leitch EF, Chakrabarti M, Crozier JE, McKee RF, Anderson JH, Horgan PG, et al. Comparison of the Prognostic Value of Selected Markers of the Systemic

Inflammatory Response in Patients With Colorectal Cancer. *Br J Cancer* (2007) 97(9):1266–70. doi: 10.1038/sj.bjc.6604027
12. Guthrie GJ, Charles KA, Roxburgh CS, Horgan PG, McMillan DC, Clarke SJ. The Systemic Inflammation-Based Neutrophil-Lymphocyte Ratio: Experience in Patients With Cancer. *Crit Rev Oncol/Hematol* (2013) 88(1):218–30. doi: 10.1016/j.critrevonc.2013.03.010
13. Nunno VD, Mollica V, Gatto L, Santoni M, Cosmai L, Porta C, et al. Prognostic Impact of Neutrophil-to-Lymphocyte Ratio in Renal Cell Carcinoma: A Systematic Review and Meta-Analysis. *Immunotherapy* (2019) 11(7):631–43. doi: 10.2217/imt-2018-0175
14. Su S, Liu L, Li C, Zhang J, Li S. Prognostic Role of Pretreatment Derived Neutrophil to Lymphocyte Ratio in Urological Cancers: A Systematic Review and Meta-Analysis. *Int J Surg (London England)* (2019) 72:146–53. doi: 10.1016/j.ijsu.2019.10.043
15. Boissier R, Campagna J, Branger N, Karsenty G, Lechevallier E. The Prognostic Value of the Neutrophil-Lymphocyte Ratio in Renal Oncology: A Review. *Urologic Oncol* (2017) 35(4):135–41. doi: 10.1016/j.urolonc.2017.01.016
16. Wu X, Han R, Zhong Y, Weng N, Zhang A. Post Treatment NLR Is a Predictor of Response to Immune Checkpoint Inhibitor Therapy in Patients With Esophageal Squamous Cell Carcinoma. *Cancer Cell Int* (2021) 21(1):356. doi: 10.1186/s12935-021-02072-x
17. Bilen MA, Dutcher GMA, Liu Y, Ravindranathan D, Kissick HT, Carthon BC, et al. Association Between Pretreatment Neutrophil-To-Lymphocyte Ratio and Outcome of Patients With Metastatic Renal-Cell Carcinoma Treated With Nivolumab. *Clin Genitourinary Cancer* (2018) 16(3):e563–e75. doi: 10.1016/j.clgc.2017.12.015
18. Jeyakumar G, Kim S, Bumma N, Landry C, Silski C, Suisham S, et al. Neutrophil Lymphocyte Ratio and Duration of Prior Anti-Angiogenic Therapy as Biomarkers in Metastatic RCC Receiving Immune Checkpoint Inhibitor Therapy. *J Immunother Cancer* (2017) 5(1):82. doi: 10.1186/s40425-017-0287-5
19. Lalani AKA, Xie W, Martini DJ, Norton CK, Steinharter JA, Bosse D, et al. Change in Neutrophil-to-Lymphocyte Ratio (NLR) in Response to Immunotherapy for Metastatic Renal Cell Carcinoma (mRCC). *Ann Oncol* (2017) 6(1):5. doi: 10.1186/s40425-018-0315-0
20. Zahoor H, Barata PC, Jia X, Martin A, Allman KD, Wood LS, et al. Patterns, Predictors and Subsequent Outcomes of Disease Progression in Metastatic Renal Cell Carcinoma Patients Treated With Nivolumab. *J Immunother Cancer* (2018) 6(1):107. doi: 10.1186/s40425-018-0425-8
21. Jain RK, Gosain R, George S. High Neutrophil to Lymphocyte Ratio Is Associated With Poor Outcome During Immunotherapy Treatment in Metastatic Renal Cell Carcinoma. *J Clin Oncol* (2018) 36(15):15_suppl.e15140. doi: 10.1200/JCO.2018.36.15_suppl.e15140
22. Suzuki K, Terakawa T, Furukawa J, Harada K, Hinata N, Nakano Y, et al. C-Reactive Protein and the Neutrophil-to-Lymphocyte Ratio Are Prognostic Biomarkers in Metastatic Renal Cell Carcinoma Patients Treated With Nivolumab. *Int J Clin Oncol* (2020) 25(1):135–44. doi: 10.1007/s10147-019-01528-5
23. Ishihara H, Tachibana H, Takagi T, Kondo T, Fukuda H, Yoshida K, et al. Predictive Impact of Peripheral Blood Markers and C-Reactive Protein in Nivolumab Therapy for Metastatic Renal Cell Carcinoma. *Targeted Oncol* (2019) 14(4):453–63. doi: 10.1007/s11523-019-00660-6
24. De Giorgi U, Procopio G, Giannarelli D, Sabbatini R, Bearz A, Buti S, et al. Association of Systemic Inflammation Index and Body Mass Index With Survival in Patients With Renal Cell Cancer Treated With Nivolumab. *Clin Cancer Res an Off J Am Assoc Cancer Res* (2019) 25(13):3839–46. doi: 10.1158/1078-0432.Ccr-18-3661
25. Simonaggio A, Elaidi R, Fournier L, Fabre E, Ferrari V, Borchiellini D, et al. Neutrophil to Lymphocyte Ratio (NLR) Kinetics as Predictors of Outcomes in Metastatic Renal Cell Carcinoma (mRCC) and Non-Small Cell Lung Cancer (NSCLC) Patients Treated With Nivolumab (N). *Ann Oncol* (2019) 69 (12):2513–22. doi: 10.1093/annonc/mdz253.080
26. Nishiyama N, Hirobe M, Kikushima T, Matsuki M, Takahashi A, Yanase M, et al. The Neutrophil-Lymphocyte Ratio has a Role in Predicting the Effectiveness of Nivolumab in Japanese Patients With Metastatic Renal Cell Carcinoma: A Multi-Institutional Retrospective Study. *BMC Urol* (2020) 20 (1):110. doi: 10.1186/s12894-020-00679-2
27. Rebuzzi SE, Buti S, Galli L, Procopio G, De Giorgi U, Baldessari C, et al. Baseline and Early Change of Neutrophil to Lymphocyte Ratio (bNLR and.NLR) as Prognostic Factors in Metastatic Renal Cell Carcinoma (mRCC) Patients Treated With Nivolumab: Preliminary Results of the Meet-URO 15 (I-BIO-REC) Study. *J Clin Oncol* (2020) 38(6):15_suppl.e17081. doi: 10.1200/JCO.2020.38.6_suppl.752
28. Basu A, Suri Y, Nandagopal L, Deshazo M, Norian L, Yang E. Nlr (Neutrophil Lymphocyte Ratio) And Plr (Platelet Lymphocyte Ratio) Changes As A Predictor Of Eventual Treatment Failure And Death On Nivolumab Therapy In Renal Cell Carcinoma. *J Immunother Cancer* (2020) 8:A16–A7. doi: 10.1136/jitc-2020-SITC2020.0030
29. Hayden JA, Côté P, Bombardier C. Evaluation of the Quality of Prognosis Studies in Systematic Reviews. *Ann Intern Med* (2006) 144(6):427–37. doi: 10.7326/0003-4819-144-6-200603210-00010
30. Tierney JF, Stewart LA, Ghersi D, Burdett S, Sydes MR. Practical Methods for Incorporating Summary Time-to-Event Data Into Meta-Analysis. *Trials* (2007) 8:16. doi: 10.1186/1745-6215-8-16
31. Parmar MK, Torri V, Stewart L. Extracting Summary Statistics to Perform Meta-Analyses of the Published Literature for Survival Endpoints. *Stat Med* (1998) 17(24):2815–34. doi: 10.1002/(sici)1097-0258(19981230)17:24<2815::aid-sim110>3.0.co;2-8
32. Patel A, Ravaud A, Motzer RJ, Pantuck AJ, Staehler M, Escudier B, et al. Neutrophil-To-Lymphocyte Ratio as a Prognostic Factor of Disease-Free Survival in Postnephrectomy High-Risk Locoregional Renal Cell Carcinoma: Analysis of the S-TRAC Trial. *Clin Cancer Res an Off J Am Assoc Cancer Res* (2020) 26(18):4863–8. doi: 10.1158/1078-0432.Ccr-20-0704
33. Park YH, Ku JH, Kwak C, Kim HH. Post-Treatment Neutrophil-to-Lymphocyte Ratio in Predicting Prognosis in Patients With Metastatic Clear Cell Renal Cell Carcinoma Receiving Sunitinib as First Line Therapy. *SpringerPlus* (2014) 3:243. doi: 10.1186/2193-1801-3-243
34. Diem S, Schmid S, Krapf M, Flatz L, Born D, Jochum W, et al. Neutrophil-To-Lymphocyte Ratio (NLR) and Platelet-To-Lymphocyte Ratio (PLR) as Prognostic Markers in Patients With Non-Small Cell Lung Cancer (NSCLC) Treated With Nivolumab. *Lung Cancer (Amsterdam Netherlands)* (2017) 111:176–81. doi: 10.1016/j.lungcan.2017.07.024
35. Cassidy MR, Wolchok RE, Zheng J, Panageas KS, Wolchok JD, Coit D, et al. Neutrophil to Lymphocyte Ratio Is Associated With Outcome During Ipilimumab Treatment. *EBioMedicine* (2017) 18:56–61. doi: 10.1016/j.ebiom.2017.03.029
36. Oguma K, Oshima H, Aoki M, Uchio R, Naka K, Nakamura S, et al. Activated Macrophages Promote Wnt Signalling Through Tumour Necrosis Factor-Alpha in Gastric Tumour Cells. *EMBO J* (2008) 27(12):1671–81. doi: 10.1038/emboj.2008.105
37. Kim TW, Lee JH, Shim KH, Choo SH, Choi JB, Ahn HS, et al. Prognostic Significance of Preoperative and Follow-Up Neutrophil-to-Lymphocyte Ratio and Platelet-to-Lymphocyte Ratio in Patients With Non-Metastatic Clear Cell Renal Cell Carcinoma. *Invest Clin Urol* (2019) 60(1):14–20. doi: 10.4111/icu.2019.60.1.14
38. Zhou W, Zhang GL. C-Reactive Protein to Albumin Ratio Predicts the Outcome in Renal Cell Carcinoma: A Meta-Analysis. *PloS One* (2019) 14 (10):e0224266. doi: 10.1371/journal.pone.0224266
39. Shaul ME, Fridlender ZG. Tumour-Associated Neutrophils in Patients With Cancer. *Nat Rev Clin Oncol* (2019) 16(10):601–20. doi: 10.1038/s41571-019-0222-4
40. Moses K, Brandau S. Human Neutrophils: Their Role in Cancer and Relation to Myeloid-Derived Suppressor Cells. *Semin Immunol* (2016) 28(2):187–96. doi: 10.1016/j.smim.2016.03.018
41. Gooden MJ, de Bock GH, Leffers N, Daemen T, Nijman HW. The Prognostic Influence of Tumour-Infiltrating Lymphocytes in Cancer: A Systematic Review With Meta-Analysis. *Br J Cancer* (2011) 105(1):93–103. doi: 10.1038/bjc.2011.189
42. Wang B, Gu W, Wan F, Shi G, Ye D. Prognostic Significance of the Dynamic Changes of Systemic Inflammatory Response in Metastatic Renal Cell Carcinoma. *Int Braz J urol Off J Braz Soc Urol* (2019) 45(1):89–99. doi: 10.1590/s1677-5538.Ibju.2017.0500
43. Jiang T, Qiao M, Zhao C, Li X, Gao G, Su C, et al. Pretreatment Neutrophil-to-Lymphocyte Ratio Is Associated With Outcome of Advanced-Stage Cancer Patients Treated With Immunotherapy: A Meta-Analysis. *Cancer Immunol Immunother CII* (2018) 67(5):713–27. doi: 10.1007/s00262-018-2126-z

44. Sacdalan DB, Lucero JA, Sacdalan DL. Prognostic Utility of Baseline Neutrophil-to-Lymphocyte Ratio in Patients Receiving Immune Checkpoint Inhibitors: A Review and Meta-Analysis. *Onco J Targets Ther* (2018) 11:955–65. doi: 10.2147/ott.S153290

Conflict of Interest: The authors declare that the research was conducted in the absence of any commercial or financial relationships that could be construed as a potential conflict of interest.

Publisher's Note: All claims expressed in this article are solely those of the authors and do not necessarily represent those of their affiliated organizations, or those of the publisher, the editors and the reviewers. Any product that may be evaluated in this article, or claim that may be made by its manufacturer, is not guaranteed or endorsed by the publisher.

frontiers in Immunology

REVIEW
published: 16 November 2021
doi: 10.3389/fimmu.2021.755304

The Emerging Interplay Between Recirculating and Tissue-Resident Memory T Cells in Cancer Immunity: Lessons Learned From PD-1/PD-L1 Blockade Therapy and Remaining Gaps

Silvia Gitto[1,2], *Ambra Natalini*[1], *Fabrizio Antonangeli*[1] *and Francesca Di Rosa*[1]*

[1] Institute of Molecular Biology and Pathology, National Research Council of Italy (CNR), Rome, Italy, [2] Department of Molecular Medicine, University of Rome "Sapienza", Rome, Italy

OPEN ACCESS

Edited by:
Roberta Zappasodi,
Cornell University, United States

Reviewed by:
Niroshana Anandasabapathy,
Weil Cornell Medicine, United States
Chien-Huan Weng,
Memorial Sloan Kettering Cancer Center, United States

***Correspondence:**
Francesca Di Rosa
francesca.dirosa@cnr.it

Specialty section:
This article was submitted to Cancer Immunity and Immunotherapy, a section of the journal Frontiers in Immunology

Received: 08 August 2021
Accepted: 01 November 2021
Published: 16 November 2021

Citation:
Gitto S, Natalini A, Antonangeli F and Di Rosa F (2021) The Emerging Interplay Between Recirculating and Tissue-Resident Memory T Cells in Cancer Immunity: Lessons Learned From PD-1/PD-L1 Blockade Therapy and Remaining Gaps. Front. Immunol. 12:755304. doi: 10.3389/fimmu.2021.755304

Remarkable progress has been made in the field of anti-tumor immunity, nevertheless many questions are still open. Thus, even though memory T cells have been implicated in long-term anti-tumor protection, particularly in prevention of cancer recurrence, the bases of their variable effectiveness in tumor patients are poorly understood. Two types of memory T cells have been described according to their traffic pathways: recirculating and tissue-resident memory T cells. Recirculating tumor-specific memory T cells are found in the cell infiltrate of solid tumors, in the lymph and in the peripheral blood, and they constantly migrate in and out of lymph nodes, spleen, and bone marrow. Tissue-resident tumor-specific memory T cells (TRM) permanently reside in the tumor, providing local protection.

Anti-PD-1/PD-L1, a type of immune checkpoint blockade (ICB) therapy, can considerably re-invigorate T cell response and lead to successful tumor control, even in patients at advanced stages. Indeed, ICB has led to unprecedented successes against many types of cancers, starting a ground-breaking revolution in tumor therapy. Unfortunately, not all patients are responsive to such treatment, thus further improvements are urgently needed. The mechanisms underlying resistance to ICB are still largely unknown. A better knowledge of the dynamics of the immune response driven by the two types of memory T cells before and after anti-PD-1/PD-L1 would provide important insights on the variability of the outcomes. This would be instrumental to design new treatments to overcome resistance.

Here we provide an overview of T cell contribution to immunity against solid tumors, focusing on memory T cells. We summarize recent evidence on the involvement of recirculating memory T cells and TRM in anti-PD-1/PD-L1-elicited antitumor immunity, outline the open questions in the field, and propose that a synergic action of the two types

of memory T cells is required to achieve a full response. We argue that a T-centric vision focused on the specific roles and the possible interplay between TRM and recirculating memory T cells will lead to a better understanding of anti-PD-1/PD-L1 mechanism of action, and provide new tools for improving ICB therapeutic strategy.

Keywords: immune checkpoint blockade, memory T cells, TRM, bone marrow, anti-tumor immunity

INTRODUCTION

T cells are major players of anti-tumoral immunity. During the induction phase of an adaptive immune response against cancer cells, dendritic cells (DCs) uptake tumor antigens released by damaged/dying tumor cells and migrate to secondary lymphoid organs, such as tumor-draining lymph nodes (LNs). In these organs DCs present tumor antigen-derived peptides in the context of Major Histocompatibility Complex (MHC) molecules of class I (MHC-I) and class II (MHC-II) to naïve CD8 and CD4 T cells, respectively. MHC-peptide complexes and costimulatory molecules expressed by DCs jointly lead to T cell priming (**Figure 1**). In most cases, effective naïve CD8 T cell priming requires CD4 T cell help. This is mediated *via* $CD40L^+$ CD4 T cell interaction with $CD40^+$ DCs. The DCs are thus "licensed" and can provide all the costimulatory signals needed for naïve CD8 T cell priming (1–4) (**Figure 1**). Primed CD4 and CD8 T cells proliferate and generate a progeny of short-lived effector and long-lived memory cells that migrate out of LNs. Effector T cells enter the tumor bed, recognize tumor-antigens in this site and display their protective function. Specifically, cytotoxic CD8 T cells kill tumor cells *via* degranulation of secretory granules or activation of the Fas/FasL molecular pathway, whereas CD4 T cells provide help for CD8 T cell stimulation, and produce pro-inflammatory cytokines (e.g. TNF-α, IFN-γ, etc.) and chemokines that attract further effector T cells into the tumor (**Figures 1** and **2A**). After the acute phase of an immune response, antigen is cleared, effector T cells die, and a few memory T cells remain over long time in the blood and in tissue reservoirs, including the bone marrow (BM) (7, 8) (**Figure 1**). Memory T cells are more abundant than their naïve precursors, and are poised to proliferate, differentiate and display prompt effector function upon secondary stimulation, resulting in a more rapid and efficient antigen elimination than in the primary response. Unfortunately, T cell response against cancer cells does not always lead to antigen clearance. Tumor-bearing patients typically present with a chronic immune response, characterized by persisting antigen, and deficient and/or dysfunctional anti-tumor T cells (**Figures 1** and **2**).

The mechanisms underlying qualitatively and quantitatively effective T cell memory are largely unclear. The most accepted view is that antigen-specific memory T cells are maintained for years by a fine equilibrium between quiescence and self-renewal. It has been proposed that a duality of BM niches supports memory T cells persistence over time, without consuming their proliferative potential (8). Two major types of memory T cells have been recently distinguished according to their migratory behavior, i.e. recirculating memory T cells and tissue-resident memory T cells (TRM) (**Figure 1**). Recirculating memory T cells include central memory T cells (TCM) and effector memory T cells (TEM), that are discriminated based on the expression of CCR7, a lymph node (LN) homing receptor (10). Recirculating memory T cells migrate through the blood and the lymph, and patrol the whole body. In contrast, TRM are found in peripheral sites, in disconnection from circulation, thus these cells provide local and/or tissue-wide protection (5, 6). Despite increasing knowledge on T cell memory, many gaps still remain to be filled, especially in respect to TRM, given the relatively recent discovery of these cells. For example, while recirculating memory T cells with phenotype and transcriptional signature similar to hematopoietic stem cells (T stem cell memory cells, TSCM) have been implicated in long-term memory (11–13), a similar TRM subset has been only partially characterized (14, 15). It is also unknown whether TRM residing in different tissues have a diverse longevity (6). Furthermore, many questions about the role of TRM in anti-tumoral immunity, and their interplay with recirculating memory T cells, remain open.

Anti-tumor T cell response takes place in the context of a complex relationship between a growing tumor and the immune system. According to the concept of "Cancer Immunoediting", this relationship is a multi-step process including three phases, i.e. elimination, equilibrium and escape (the so-called three "Es" of cancer immunoediting) (9) (**Figure 2**). The elimination phase is characterized by the physical deletion of $MHC\text{-}I^+$ tumor cells by infiltrating effector CD8 T cells, which are triggered by recognition of tumor antigen-derived peptides in the context of MHC-I. Similarly, tumor-specific effector CD4 T cells can be triggered to release pro-inflammatory cytokines and chemokines by antigen-MHC-II complexes presented by DCs in the tumor microenvironment (TME). Intratumoral DCs further emphasize anti-tumor immunity by restimulating effector T cells locally (**Figure 2A**). In the equilibrium phase there is a dynamic interplay between genetically heterogeneous tumor cells, and the immune cell infiltrate. Tumor-infiltrating lymphocytes (TILs) exert a containing function, without eradicating the tumor. In fact, some tumor cell variants acquire mutations that give them a survival advantage and/or enable them to resist to the antitumoral immune response. Selective killing of tumor cells by functional effector T cells contributes to tumor editing, a sort of "Darwinian selection" that gives advantages to tumor cells able to avoid immune cell recognition or killing (16) (**Figure 2B**). The escape phase is characterized by the expansion of tumor cell variants, which have often lost their sensitivity to the immune attack through several genetic and epigenetic alterations. At this stage, the TME is typically immunosuppressive, e.g. enriched with regulatory T cells (Tregs), myeloid-derived suppressor cells

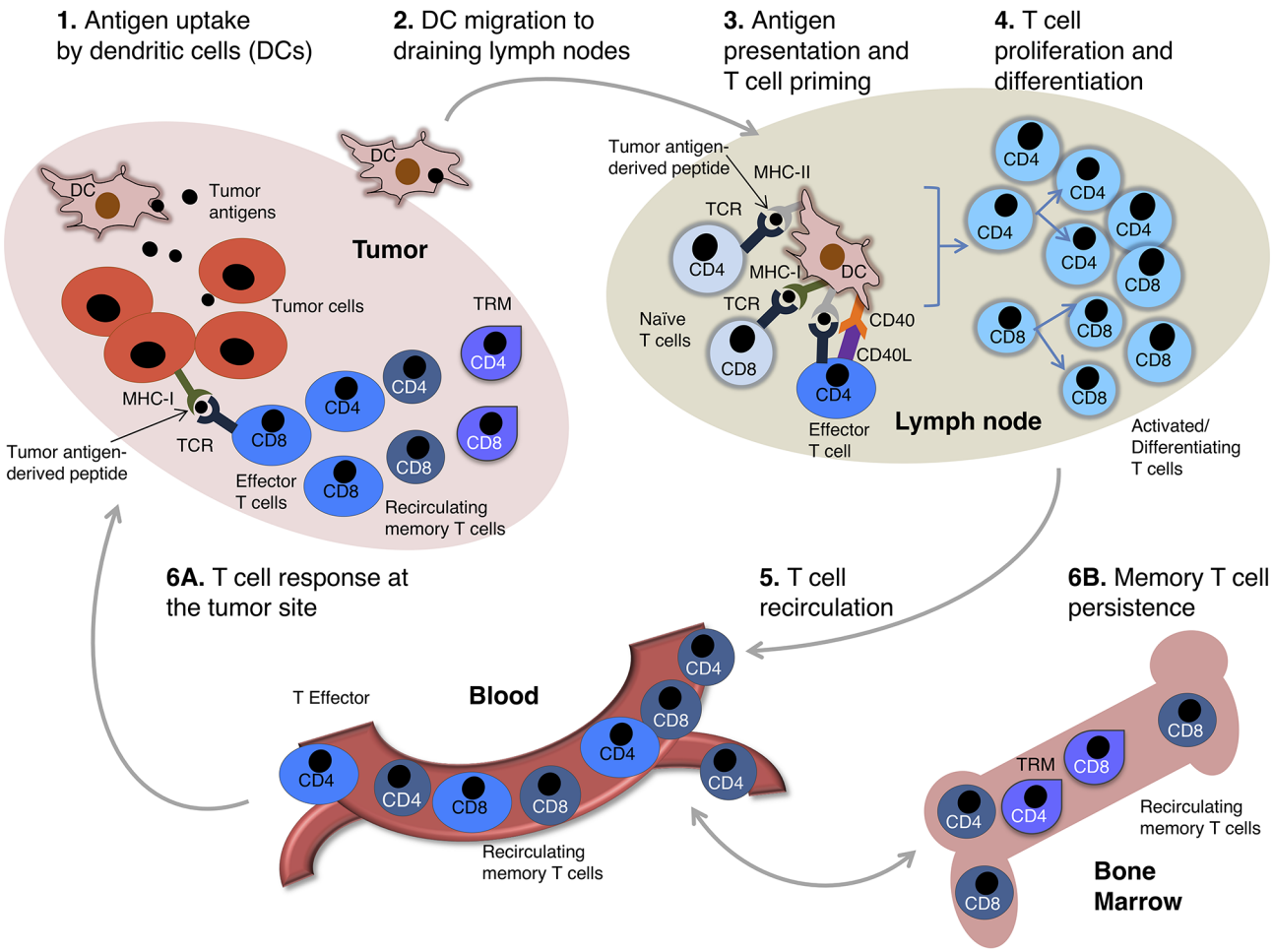

FIGURE 1 | The circuit of anti-tumor T cell immunity. A scheme of anti-tumor T cell response is depicted. Intratumoral DCs uptake antigens released by damaged/dying tumor cells (**1**). DCs get activated and migrate to tumor draining lymph nodes (LNs) (**2**) wherein they present tumor antigen-derived peptides in the context of MHC molecules, plus costimulatory signals, to naïve tumor-specific T cells. Tumor antigen-derived peptides presented in MHC-II and MHC-I molecules are recognized by CD4 and CD8 T cells, respectively. Activated CD4 T cells differentiating into effector cells up-regulate CD40L and provide help for naïve CD8 T cells by modulating DC costimulatory capability (so-called DC "licensing", mediated by CD40L-CD40 interaction) (1–4). Licensed DCs are enabled to provide full costimulation for naïve CD8 T cell priming (**3**) (note that DC-provided costimulatory signals for T cell priming are not depicted for simplicity). Activated tumor-specific CD4 and CD8 T cells proliferate and differentiate (**4**), and migrate out of LNs into the blood stream (**5**). The differentiated progeny includes effector and memory T cells, which extravasate from the blood and enter the tumor sites (**6A**). Tissue-resident memory T cells (TRM) are non-migratory cells that persist in the tumor (5), whereas recirculating memory T cells go back to circulation and migrate all over the body (6). They preferentially accumulate in the bone marrow (BM), a key organ for long-term memory T cell maintenance (7, 8) (**6B**).

(MDSCs), etc., and the infiltrating tumor-specific CD4 and CD8 T cells are often dysfunctional (**Figure 2C**). In addition to Tregs and MDSCs, several players of cancer-initiated negative circuits have been identified in advanced cancer-bearing individuals, for example γδ T cells, macrophages and neutrophils can cooperate in suppressing CD8 T cells (17). Dysfunctional anti-tumor T cells in tumor-bearing patients are often considered the equivalent of "exhausted" anti-viral T cells in mice chronically infected with lymphocytic choriomeningitis virus (LCMV) (18–20). Typically, exhausted T cells are exposed to high dose/persisting antigen and have impaired effector function, nevertheless the concept of T cell-exhaustion has been differently defined in diverse contexts, generating potential misunderstanding (21). We will use it here to indicate the complex phenotype of dysfunctional tumor-specific T cells in patients with clinically evident tumors (**Figure 2C**).

When a patient presents with a clinically evident tumor, the above-described tumor-host interaction is mostly in the escape phase (9). Anti-cancer T cells are inhibited by so-called immune checkpoints, i.e. negative feedback pathways that normally prevent excessive activation in chronic immune responses. A series of inhibitory receptor/ligand pairs controlling T cell response have been described, e.g., PD-1/PD-L1, CTLA4/B7, LAG-3/MHCII, TIM-3/Galectin-9 (**Figure 2C**). Unleashing T

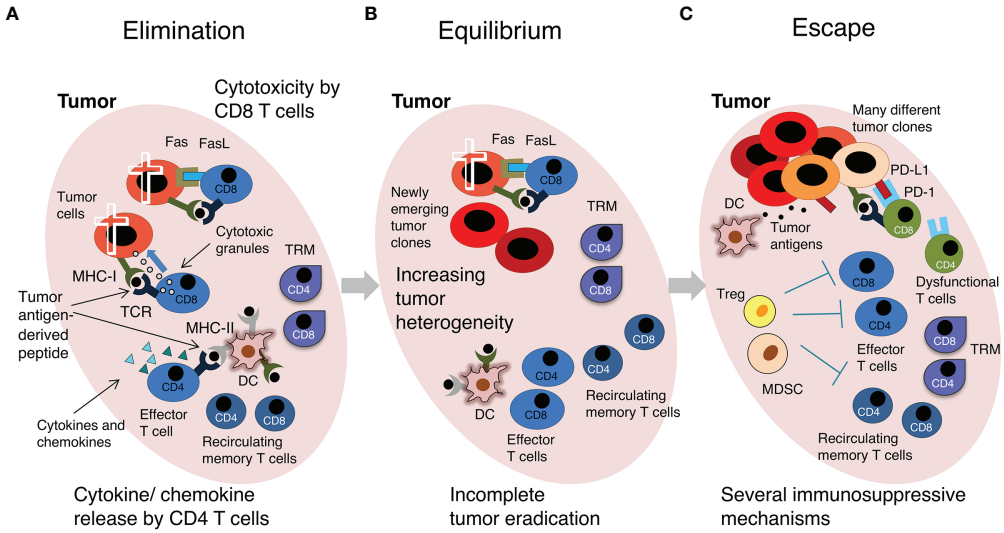

FIGURE 2 | The "Cancer Immunoediting" concept: effector versus exhausted T cells. A scheme of the 3 phases of "Cancer Immunoediting" is represented, with emphasis on T cells. **(A)** Elimination. The tumor has low heterogeneity. Effector CD8 T triggered by recognition of tumor-derived peptides in the context of MHC-I molecules on the surface of tumor cells kill these cells by release of secretory granules (containing perforin, granzymes, etc.) and FasL/Fas interaction. Effector CD4 T cells triggered by recognition of tumor-derived peptides in the context of MHC-II molecules on the surface of DCs and other tumor-infiltrating immune cells release cytokines and chemokines. **(B)** Equilibrium. There is moderate intratumoral heterogeneity, and tumor mass contains some genetically different tumor clones. TILs control tumor growth without inducing tumor regression. **(C)** Escape. Tumor is genetically unstable and highly heterogeneous. The immune cell infiltrate contains a few effector T cells and high levels of regulatory T cells (Tregs) and Myeloid Derived Suppressor Cells (MDSCs), which contribute to create an immunosuppressive environment. DCs do not effectively present tumor-derived antigens and T cell-inhibitory circuits are dominant, for example that induced by the interaction between PD-L1$^+$ tumor cells and PD-1$^+$ T cells. Most intratumoral T cells are dysfunctional. The tumor grows. For simplicity, only some cells are depicted. See text and original reference (9) for more details.

cell-activity by immune checkpoint blockade (ICB) therapy has been a real breakthrough in the treatment of human cancers. ICB is able to determine partial or even complete regression of primary solid tumors and metastatic lesions, for example in melanoma and lung cancer patients (22, 23). Unfortunately, only a small fraction of ICB-treated patients responds to therapy, with some variability in the percentage of responsive patients across different tumor types. Reinvigoration of tumor-antigen specific T cells and high tumor-derived neo-antigen burden have been associated to clinical response (24). The effectiveness of ICB, even though only in some of the patients, supports the concept that functional exhaustion of T cells is not an irreversible state, and/or that resetting of anti-tumor immunity can result in an effective T cell response even at advanced cancer stages. Nevertheless, a better knowledge is required to understand why the majority of patients do not respond, or experience tumor progression after an initial partial response. It is also important to understand why a few of the non-responder patients develop the so called hyper-progressive disease (HPD), which is characterized by accelerated tumor growth associated with drastic worsening of clinical conditions (25).

Anti-PD-1 and anti-PD-L1 monoclonal antibodies (mAbs) are among the most effective ICB, currently used in several tumor types (**Table 1**). PD-1 is a lymphocyte inhibitory receptor expressed by antigen-activated T cells, that binds to PD-L1 and PD-L2 expressed on the surface of other cells. PD-L1 and PDL-2 have different expression patterns; PD-L1 is expressed by several cell types, including Antigen Presenting Cells (APCs) such as macrophages and DCs, MDSCs, and tumor cells (32), whereas PD-L2 is mostly expressed by APCs and lymphocytes (33). PD-1-mediated feedback loop contributes to maintain tissue homeostasis and prevent cell damage, especially in conditions of chronic immune stimulation, e.g. chronic infections and autoimmune diseases (32). Nevertheless, PD-1 induced T-cell inhibition could be detrimental in case of anti-tumor T cell response. One mechanism of action of anti-PD-1/PD-L1 mAbs in anti-cancer treatment is to block the molecular interaction between the corresponding receptor-ligand pair, thus relieving PD-1$^+$ T cells from PD-L1-mediated inhibition exerted by PD-L1$^+$ tumor cells and/or myeloid cells in the tumor infiltrate (34). Additional mechanisms have been described, unraveling the complexity of the biological response to anti-PD-1/PD-L1 mAb. It has been proposed that cancer patient treatment with the PD-L1 mAb Avelumab might result in elimination of PD-L1$^+$ cells by Antibody Dependent Cellular Cytotoxicity (ADCC), as suggested by *in vitro* data (30, 31); in contrast, the PD-L1 mAbs Atezolizumab and Durvalumab have an engineered Fc region to reduce ADCC (28, 29). Notably, ADCC has not been reported for the PD-1 mAbs Pembrolizumab and Nivolumab (26, 27) (**Table 1**). A detailed overview of anti-PD-1/PD-L1 mAb effects

TABLE 1 | Anti-PD-1/PD-L1 monoclonal antibodies (mAbs) in anti-cancer immunotherapy.

Drug name	Target	Isotype	Degreeof humanization	Time to market	Antibody-dependent cellular cytotoxicity (ADCC) *in vitro* activity	Cancer types
Pembrolizumab	PD-1	IgG4, κ	Fully humanized	2014	NO (26)	Non small cell lung cancer (NSCLC), melanoma, renal cell carcinoma (RCC), urothelial carcinoma, Merkel cell carcinoma, hepatocellular carcinoma, colorectal cancer (CRC), cervical cancer
Nivolumab	PD-1	IgG4, κ	Fully human	2014	NO (27)	NSCLC, small cell lung cancer (SCLC), melanoma, RCC, urothelial carcinoma, CRC, Merkel cell carcinoma, hepatocellular carcinoma
Atezolizumab	PD-L1	IgG1, κ	Humanized	2016	NO (28)	Urothelial carcinoma, SCLC, NSCLC, triple-negative breast cancer
Durvalumab	PD-L1	IgG1, κ	Human	2017	NO (29)	NSCLC, SCLC, urothelial
Avelumab	PD-L1	IgG1, λ	Human	2017	YES (30, 31)	Urothelial carcinoma, Merkel call carcinoma

The table summarizes the main features of the most common anti-PD-1/PD-L1 mAbs currently employed in anti-cancer immunotherapy.

on immune response goes beyond the scope of this paper; the reader is referred to excellent recent articles on this topic (35–37).

In this article we will provide a T memory-centric vision of anti-tumor immunity. We will start with a brief outline of tumor-immune system interaction, with a focus on Tumor Infiltrating Lymphocytes (TILs). We will then give an overview of the distinct roles played by TRM and re-circulating memory T cells in antitumor immune response, and discuss emerging evidence on the effects of anti-PD-1/PD-L1 on the two types of T cells. We will propose that a better knowledge of the interplay between TRM and re-circulating memory T cells in anti-tumor immunity will provide an insightful framework to better understand the mechanisms underlying anti-PD-1/PD-L1 immunotherapy, offering new perspectives on how to improve it.

TUMOR INFILTRATING LYMPHOCYTES (TIL)

Tumor Infiltrating Lymphocytes (TILs) are a heterogeneous mixture containing tumor antigen-specific T cells, T cells of unknown specificities, Tregs, etc. (38). TILs comprise both TRM, and T cells belonging to the recirculating pool. Despite some pre-existing evidence of long-term retention of memory T cells in peripheral extra-lymphoid sites (39, 40), it was only about a decade ago that TRM were recognized as a clearly defined T cell memory subset, characterized by its own functional and molecular signature (41). Thus, in many studies TILs were examined without a separate analysis of the TRM component in them. We will briefly summarize here some of these TIL studies that lack TRM analysis, and then focus on TRM and memory recirculating T cells in the next paragraphs.

TILs have been an extraordinary tool to gain knowledge on T cell response against tumors, clone tumor antigens, and develop anti-tumor immunotherapies (42). One of the classical approaches in immunotherapy has been to re-invigorate TILs *in vitro* by treatment with IL-2, and then infuse them back into the patient (43). It was later recognized that IL-2 expanded mostly NK cells, which mediated tumor cytotoxicity upon infusion (44). Despite some success, this treatment had severe side effects, and was replaced in subsequent years by more effective tumor-tailored adoptive T cell therapies, often based on tumor-specific T cells isolated from TILs (45–47).

TILs contain cytotoxic CD8 T cells and helper CD4 T cells, as well as Tregs. When a tumor reaches a clinically evident stage, TILs have predominantly a terminally differentiated phenotype, but they somehow failed to clear the tumor. Indeed, they are inhibited by a variety of immunosuppressive mechanisms in the TME, including inhibition by high levels of TGF-β and/or other cytokines, negative regulation by innate cells such as Tumor Associated Macrophages (TAM) and MDSCs, metabolic competition with tumor cells (48), and an imbalance among T cell subsets, with a Treg dominance (49). It has been proposed that TIL exhausted phenotype is under the control of the transcription factor TOX (50, 51), nevertheless TOX has been also implicated in terminal differentiation of effector T cells, thus questioning its exhaustion-specific expression (52, 53). It should be noted that "exhaustion" is a comprehensive term which includes different T cell-phenotypes described in diverse experimental models, as mentioned above (21). A likely scenario is that a set of transcription factors (e.g. Eomes, T-bet, TCF-1, TOX, etc.) jointly regulates effective and dysfunctional T cell differentiation, as suggested by experimental findings in mouse models (54–56). Advanced technologies, including multidimensional flow cytometry, TCR sequencing and single cell -omics, have greatly contributed to our growing understanding of TIL heterogeneity (57–59). Patient-derived organoids from tumor biopsies are a new highly promising tool to investigate TILs embedded in their original TME, and gain information on the functional and/or exhausted profile of TIL subsets (60).

Anti-PD-1/PD-L1 treatment is aimed at unleashing T cell response against the tumor, thus it is expected that in responder patients TILs change following treatment, for example their number might increase due to recruitment of T cells from circulation and/or local proliferation. In fact, TIL quantification and characterization are considered among the "dynamic" biomarkers of response to ICB, which can be

examined in tumor biopsies (49). Experimental studies performed with single cell approaches have been recently used to track changes occurring in TILs in response to ICB (61). One of these studies has questioned that all TILs are exhausted in advanced tumors, and has proposed instead that even without treatment a few are functional (e.g. those expressing TCF-1), and they are simply expanded by ICB (62), in agreement with the proposed role of TCF-1 in mouse models of chronic infections (63). Once again, reaching a consensus on the definition of exhaustion might help to solve some current discrepancies (21).

Changes in the Treg fraction of TILs have been associated with clinical response to ICB. About 10% of gastric cancer patients treated with anti-PD-1 experience HPD. In these patients, Tregs with effector phenotype ($FoxP3^{high}CD45RA^{-}$ CD4 T cells) expressing the cell cycle marker Ki-67 increased among TILs after treatment, whereas in non-HPD patients these cells diminished, suggesting that Treg expansion in TME supports increased local immunosuppression and disease worsening (64).

TISSUE-RESIDENT MEMORY T CELLS (TRM)

TRM characterization is essential for a full evaluation of T cell response in TME. This subset of non-migratory memory T cells was identified about 10 years ago, in the course of seminal studies on peripheral immune defense against viral infections, which focused on CD8 TRM (5, 65). It was shown that CD8 T cells recruited to the skin upon Herpes Virus infection generated a population of skin-resident memory CD8 T cells that did not go back to circulation and controlled viral growth locally (65). CD4 TRM have been subsequently identified, and are currently under intense investigation in diverse settings (66). TRM can be found in many epithelial barriers (i.e. skin, lung, gastroenteric and reproductive tracts) and also in internal organs (e.g. kidney, brain) to ensure long-term immunity against infections, tumors and other types of tissue damage (5, 67–69). TRM have a remarkable capacity for exerting protective functions, e.g. cytokine production, etc. (5).

A distinct set of surface molecules is typically expressed by TRM, including the adhesion molecule CD103 (the αE integrin subunit) and the activation marker CD69 (70), nevertheless there are also $CD103^{-}$ TRM (5, 6). Notably, TRM differ from other T-memory subsets, such as TCM or TEM, in terms of transcription profile, metabolism, kinetics of response, and migration capability into extracellular matrix (71, 72). The signals required for priming and differentiation of TRM have been only partially disclosed. For example, it is unclear whether αE/β7 integrin interaction with E-cadherin, which is highly expressed in epithelial tissues, provides survival and/or other signals to $CD103^{+}$ TRM, and what are the differences between $CD103^{+}$ and $CD103^{-}$ TRM (5). Moreover, it has been shown that DCs expressing DNGR-1 (the C-type lectin receptor for F-actin) are required for optimal priming of TRM but not of recirculating T cells in a mouse model of viral infection (73). The degree of plasticity of antigen-experienced effector and memory T cell subsets to generate TRM remains to be determined (74). It should be noted that perturbation of normal T cell traffic is required to definitely identify TRM, that by definition are non-recirculating cells; this question is normally addressed in mouse models.

Recent evidence indicated that human $CD8^{+}$ TILs from epithelial cancers contain TRM-like cells (i.e. cells expressing TRM markers) and that their abundance is associated with strong anti-tumor activity (75). For example, Guo and colleagues performed single-cell sequencing analysis of TILs within Non-Small-Cell-Lung Cancer (NSCLC) specimens, and identified several intratumoral CD4 and CD8 T cell clusters, including TRM-like cells expressing high levels of mRNA coding for CD69, for the chemokine receptor CXCR6, and for the integrins CD49a (ITGA1 gene), and CD103 (ITGAE gene) (76). Studies in lung cancer showed that patients with greater intratumoral density of TRM-like cells had a better prognosis (77). Similarly, high intratumoral frequency of $CD103^{+}$ $CD39^{+}$ $CD8^{+}$ T cells was associated with better overall survival in patients with head-and-neck squamous cell carcinoma, another type of epithelial cancer (78). Recent findings in mouse models suggest that TILs with $CD69^{+}$ $CD103^{+}$ TRM-like phenotype are found also in non-epithelial cancers, such as rhabdomyosarcoma (79).

Since TRM may express different inhibitory receptors, this subset represents a potential target for ICB (80, 81). A preferential expression of PD-1 and TIM-3 by intratumoral TRM-like cells has been observed in lung, cervical, ovarian, endometrial cancer and melanoma, both in mice and humans (82). Remarkable changes in TRM-like cells have been documented in patients responding to ICB (83–85). In one of these studies, a positive response of NSCLC patients to anti-PD-1/PD-L1 therapy was correlated to an increased intratumoral density of $CD8^{+}$ $CD103^{+}$ TILs, which displayed typical transcriptomic and phenotypic profiles of TRM (83). Similarly, in anti-PD-1-treated lung cancer patients, it was observed that $CD8^{+}$ $CD103^{+}$ TILs accumulated in patients with better progression-free survival; these TILs were enriched with TRM-like cells having a unique Tc1/Tc17 effector signature, further emphasizing the distinguished differentiation program of TRM and their critical role in response to ICB (84). TCR sequencing studies in melanoma showed that TRM-like clones were diverse in different metastatic lesions from the same patient, with implications for heterogeneity of ICB-induced unleashing of anti-tumoral activity at each site (80)

RECIRCULATING MEMORY T CELLS

Recirculating memory T cells are found in the lymph and in the peripheral blood, and migrate in and out of lymph nodes, spleen, BM, and extra-lymphoid tissues, thus patrolling the whole body to provide systemic protection. Upon tumor antigen-recognition, recirculating memory T cells can develop highly efficient secondary responses, resulting in tumor cell killing, cytokine release, etc. In a study on mouse melanoma, it has been shown that CD8 mAb treatment inducing 82%–99% reduction of circulating CD8 T cells resulted in rapid

metastasis outgrowth in visceral organs, suggesting that CD8 T cells were cytostatic and kept in check disseminated dormant tumor cells in this model (86). Conversely, there are some rare cases of T cells favoring the metastatic process. For example, T cell pro-osteoclastogenic activity can favor bone erosion and remodeling, supporting breast cancer cell metastatization to the bones (87). Recirculating T cells migrating to tissues distant from primary tumor are likely to be involved in this case, nevertheless TRM contribution was not investigated and cannot be excluded.

Peripheral blood samples from cancer patients have been extensively screened for the presence of tumor antigen-specific T cells, that have been identified and characterized in a number of patients (88–90). In some cancer patients at advanced stages, TCR repertoire skewing and impairment of peripheral blood T cell function have been observed (91). For example, in breast, lung and cervical cancers a decreased TCR diversity correlated with reduced capacity of IFN-γ and IL-2 production by peripheral CD4 and CD8 T cells (92, 93). Furthermore, T cell signaling defects have been reported in individuals with advanced cancers (94).

Notably, tumor antigen-specific T cells recirculate in the bone marrow (BM), and it has been shown that they are enriched in this organ as compared to peripheral blood in many patients with solid tumors, for example in subjects with melanoma and pancreatic cancer (88, 89). This is perhaps not surprising, considering that the BM has a central role in long-lived memory T cell maintenance in a variety of settings (7, 95). In solid cancer patients it cannot be excluded that BM T cells are actively engaged in micrometastasis control in this organ, even in the absence of evident metastases. BM tumor-specific T cells are functional, for example they produce IFN-γ and TNF-α (89, 96), and in most cases they are not inhibited by Tregs in the organ (97, 98). Considering that the BM represents a reservoir of functional memory T cells in tumor-bearing individuals, innovative anti-tumor T cell transfer approaches exploiting the BM as a source of T cells have been proposed (99–101). A related strategy is based on the adoptive transfer of CXCR4-engineered T cells with increased homing to the BM (102).

The re-invigoration of recirculating T cells induced by ICB has been investigated in mouse models of chronic infections and tumors, focusing on exhausted T cells. In LCMV chronic infection, the prototypical model of T cell exhaustion, it has been observed that ICB-induced functional CD8 T cells derived from rare $CXCR5^+$ CD8 T cell precursors in lymphoid organs that shared molecular signature with follicular helper CD4 T cells and hematopoietic stem cell progenitors (103). Studies in other mouse models implicated T cell-intrinsic CD28 expression in the proliferative CD8 T cell response to PD-1 blockade, suggesting that engagement of the CD28/B7 co-stimulatory pathways, possibly occurring in lymphoid organs, has a central role in response to treatment (104).

Remarkably, in many human studies, distinct changes of peripheral blood T cells following PD-1/PD-L1 blockade have been associated with response to treatment. For example, it has been shown that $Ki\text{-}67^+$ CD8 T cells appeared in peripheral blood of lung cancer patients treated with anti-PD-1, suggesting that these cells switched from a quiescent to an activated/proliferative state and were mobilized in the circulation (104, 105). Functional memory CD4 T cells in peripheral blood at baseline and increased proportions of $Ki\text{-}67^+$ CD4 T cells after anti-PD-1/PD-L1 have been associated with better responses to treatment in NSCLC patients (106). These changes in peripheral blood T cells can potentially be exploited as biomarkers of response.

The intra-tumoral recruitment of recirculating T cells upon anti-PD-1/PD-L1 treatment has been investigated in depth by a few reports. In a big transcriptomic study, in which >300 million T-cell derived mRNA transcripts were sequenced, the same expanded clonotypes of T cells were found in the tumor, in normal adjacent tissue, and in peripheral blood, thus suggesting that non-exhausted recirculating T cells from non-tumoral sites are recruited into the tumor in response to anti-PD-L1 (107). Replacement of intratumoral T cell clones with newly recruited T cells upon PD-1 blockade therapy has been shown in basal and squamous cell carcinoma (108). It is tempting to speculate that the newly recruited T cells may include memory T cells switching to an effector phenotype in the tumor bed upon local restimulation with antigen.

THE EMERGING DIVISION OF LABOR BETWEEN TRM AND RECIRCULATING MEMORY T CELLS IN ANTI-TUMORAL IMMUNITY

That local and systemic anti-tumor immunity might be discordant has long been known. One example is the phenomenon of concomitant immunity, that was described some decades ago in transplantable tumor models, when it was shown that an individual bearing a primary growing tumor rejected a secondary syngeneic tumor at a distant site (109). Rejection was T-cell mediated and occurred only at early times after primary tumor inoculation, before the growing tumor evoked a population of suppressor T cells that inhibited anti-tumor response in the whole body (110). These old experiments were then revisited more recently, as there was a resurgent interest for Tregs (111, 112). It would be interesting to reconsider concomitant immunity in the light of the dichotomy between TRM and recirculating memory T cells. For example, one can envision that in the old experiments with transplantable tumors, the sensitizing primary tumor induced antigen-specific recirculating T cells, but was not seeded by local TRMs, resulting in incomplete anti-tumor protection. This experimental model might resemble human cancers that are resistant to T-cell infiltration.

As concerns T-cell infiltrated tumors, it is conceivable that tumor antigen-specific TRM, that permanently reside in the tumor bed and are chronically antigen-exposed, display more evident signs of exhaustion than recirculating memory T cells, which are intermittently exposed to tumor-derived antigens, e.g. in tumor-draining LNs, as suggested by studies on TRM-like cells in human urinary bladder cancer (113). Furthermore, many other factors in TME can promote T-cell exhaustion locally, including infiltrating Tregs, MDSCs, inhibitory cytokines, etc., as

discussed above. In this context, migration of recirculating tumor-specific T cells to the BM might sustain their persistence and functionality, in agreement with the supporting role of the BM in long-term memory (7). From this organ, tumor-specific recirculating memory T cells can be mobilized into the blood and recruited into the tumor to exert their protective activity (7, 100).

Conversely, TRM may have an advantage over recirculating memory T cells because of their interaction with distinct types of intratumoral DCs. Indeed, it has been shown that CXCR6$^+$ T cell contact with CCR7$^+$ DC expressing the CXCR6 ligand CXCL16 and transpresenting IL-15 supported T cell survival in intratumoral perivascular niches (114). In this context, CXCR6 up-regulation could represent a transitory rescue signal for terminally differentiated or exhausted T cells (114). Furthermore, considering that most secondary CD8 T cell responses rely on CD4 T cell help (115), which is mediated by the antigen-presenting DC (1–4), it is conceivable to envision that CD4 TRM can license intratumoral DCs for productive restimulation of TRM and/or recirculating memory CD8 T cells infiltrating the tumor (**Figure 3A**). This possibility is consistent with recent findings showing that CD4 TRM provide help for memory CD8 T cells in antiviral immune responses in the lungs (116).

TRM AND RECIRCULATING MEMORY T CELLS IN PD-1/PD-L1 BLOCKADE AND COMBINATION THERAPIES

Beyond the well-established specialization of TRM and recirculating memory T cells in providing local and systemic protection, respectively, an insightful mouse study proposed that PD-1/PD-L1 blockade can strengthen their interplay. Indeed, anti-PD-1 treatment promoted intratumoral infiltration of intravenously transferred tumor antigen-specific TCM, without increasing the numbers or frequency of these cells in tumor-draining LNs (117). In this study, adoptively transferred tumor antigen-specific TCM showed potential to give rise to TRM-like cells upon tumor inoculation (117). These findings point to the developmental plasticity of memory T cells, a topic deserving further investigation for a better understanding of T cell response to ICB. Furthermore, building on these results (117), it can be envisioned that recirculating memory T cells recruited into the tumor after anti-PD-1/PD-L1 are enriched in recently mobilized BM T cells (**Figure 3B**).

Since PD-1/PD-L1 blockade is a systemic treatment, it can have a broad effect on T cell responses, beyond those on tumor-specific T cells. Peripheral blood T cells are probably more

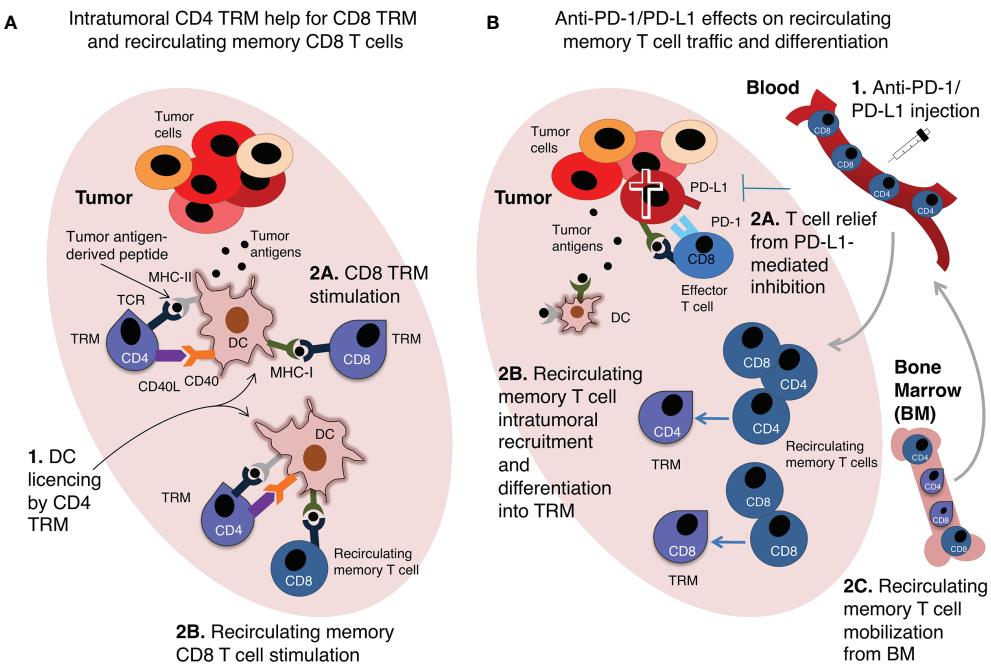

FIGURE 3 | Tissue-resident memory T cells (TRM) and recirculating memory T cell collaboration in anti-tumor immunity. Two examples of possible interplay between TRM and recirculating memory T cell are shown. **(A)** Intratumoral CD4 TRM provide help to recirculating memory CD8 T cells and CD8 TRM. A hypothetical scenario of intratumoral DCs presenting tumor antigen-derived peptides to memory CD4 and CD8 T cells is shown. In this scenario, memory CD4 T cells are intratumoral TRM, and license DCs *via* CD40L-CD40 interaction (1). This enables DCs to fully stimulate either CD8 TRM (2A) or recirculating memory CD8 T cells (2B). **(B)** Recirculating memory T cells unleashed by anti-PD-1/PD-L1 therapy promote intratumoral TRM response. Upon anti-PD-1/PD-L1 intravenous injection (1), tumor-specific effector CD8 T cells expressing PD-1 are relieved from PD-L1-mediated inhibition and kill tumor cells **(2A)**. Recirculating memory CD4 and CD8 T cells migrate *via* blood into the tumor, and differentiate into TRM **(2B)**, augmenting TIL number and anti-tumoral activity. Recirculating memory CD4 and CD8 T cells are mobilized from BM into the blood, and are then recruited into the tumor, thus contributing to re-invigorate anti-tumor T cell immunity **(2C)**. These hypothetical examples echo data obtained in mouse models of immune response against viruses **(A)** (116) and transplanted tumors **(B)** (117).

informative than TRM about the potential re-invigoration of T cells specific for non-tumoral antigens, and/or cross-reactive T cells, occurring in cancer patients after ICB (118). Early identification of this phenomenon might be important to reduce the potential risks of immune-related Adverse Events (irAEs) due to activation of auto-reactive T cells (49, 119). Conversely, cross-reactivity of T cell clones might be exploited against tumor cells. For example, it has been shown that some memory T cells in peripheral blood specific for melanoma antigens were able to recognize also antigens of common pathogens such as Herpes Simplex Virus-1, and *Mycoplasma penetrans* (120, 121).

Ideally, anti-PD-1/PD-L1 should reset both local and systemic T cell reactions against tumor cells, resulting in effective tumor elimination, and long-term prevention of recurrence and/or metastases. Unfortunately, only some patients benefit of this therapy. To explain the mechanisms underlying anti PD-1/PD-L1 resistance, it has been proposed that tumors are "cold" in non-responder patients, with reduced T cell infiltration, lack of tumor antigens, defect in antigen presentation, or presence of mechanisms blocking T cell migration into the tumor site (122). Of note, intratumoral flu vaccination is able to transform immunologically "cold" tumors into "hot" tumors, and in combination with ICB is highly effective against mouse melanoma (123). It is also possible that anti-cancer T cell response is either quantitatively or qualitatively inadequate to effectively eliminate the tumor, in at least some of the patients who do not respond to anti-PD-1/PD-L1. Thus, these patients would better benefit of anti-cancer vaccination, and/or other strategies aimed at boosting proinflammatory (Th1) CD4 T cells and cytotoxic CD8 T cells (34). To increase the proportion of responder patients, combinations of anti-PD-1/PD-L1 and conventional chemotherapy have been tried. A significant improvement of therapeutic response has been reported in advanced human NSCLC and renal cell carcinoma treated with anti-PD-1/PD-L1 mAbs combined with standard chemotherapics (124–126). Chemotherapics may trigger immunogenic tumor cell death, resulting in stronger antigen presentation and co-stimulation, tumor-specific T-cell activation/traffic and tumor cell destruction (127, 128). A comprehensive discussion of the many combination ICB therapies, already in use or at different stages of development, and of their proposed underlying mechanisms, goes beyond the scope of this review. We would only propose here that combining ICB with drugs strengthening a productive collaboration between TRM and non-migratory memory T cells might open new avenues for cancer immunotherapy.

CONCLUDING REMARKS

The concerted anti-tumoral action of TRM and recirculating memory T cells may be required for efficient and durable protection, and for response to anti-PD-1/PD-L1(**Box 1**). However, the role of T cell migration and residency in anti-tumor response has not been fully investigated and many questions remain still open in the field (**Box 2**). Multi-organ analysis could provide critical information on the contribution of the two types of T cells to either protective or pro-tumorigenic mechanisms in tumor-bearing hosts (129). We would like to stress that, among other mechanisms, failure of T cell response in the majority of anti-PD-1/PD-L1-treated cancer patients might derive from insufficient re-invigoration of either TRM or recirculating memory T cells, and from a non-productive interplay between the two types of T cells (**Figure 3**). It is tempting to suggest that revising the "Cancer immunoediting" concept to take into consideration the migratory behavior of anti-tumoral T cells might contribute to achieve a more

BOX 1 Key Points.

- It is still poorly understood how local and systemic T-cell immunity collaborate in anti-tumor response, before and after the administration of anti-PD-1/PD-L1 mAbs.
- Tumor-infiltrating T cells (TILs) comprise both tissue-resident memory T cells (TRM), which are non-migratory T cells that permanently reside in the tumor, and recirculating memory T cells, that can be recruited into the tumor.
- TRM are constantly exposed to local signals, mostly immunosuppressive, in the Tumor Microenvironment (TME).
- Recirculating memory T cells can be recruited to the tumor site after anti-PD-1/PD-L1 mAbs treatment.
- Migration of recirculating tumor-specific T cells to the bone marrow (BM) might support their persistence and functionality; from this organ they can be mobilized into the blood and recruited into the tumor.
- Multi-organ analysis could be highly informative about the contribution of different T cell subsets to either protective or pro-tumorigenic mechanisms.
- We propose to revise the "Cancer immunoediting" concept to take into consideration the migratory behavior of anti-tumoral T cells, to achieve a comprehensive view of TRM and recirculating memory T cell response to solid cancers before and after anti-PD-1/PD-L1 mAb treatment.

BOX 2 Open Questions in the Field.

- Which is the role of tissue-resident memory T cells (TRM) and recirculating memory T cells in anti-tumor response before and after anti-PD-1/PD-L1 therapy?
- Are recirculating memory T cells exposed to less immunosuppressive environments compared to intratumoral TRM (e.g. in the bone marrow)?
- Can TRM and recirculating memory T cells influence the immune cell composition of the tumor infiltrate?
- Which is the role of environmental factors, infectious agents or microbiota in anticancer TRM response before and after anti-PD-1/PD-L1 therapy?
- Which is the role of environmental factors, infectious agents or microbiota in anticancer recirculating memory T cell response before and after anti-PD-1/PD-L1 therapy?

comprehensive view of anti-PD-1/PD-L1 mechanism of action, and consequently to improve anti-cancer therapy, for example by combining ICB with drugs able to modulate T-cell homing pathways.

AUTHOR CONTRIBUTIONS

SG wrote the initial draft of the manuscript. AN and FA edited the manuscript. FD revised the final version of the manuscript. All authors contributed to the article and approved the submitted version.

FUNDING

Grant sponsor: Italian Minister of Research and University (MIUR), grant number: 2017K55HLC.

ACKNOWLEDGMENTS

We thank Gabriele Favaretto, Lorenzo Lucantonio and Alexandru Turcan for helpful discussion, and precious inputs on the figures. We are in debt with Maria Teresa Fiorillo and Sonia Simonetti for generous help in revising the text.

REFERENCES

1. Ridge JP, Di Rosa F, Matzinger P. A Conditioned Dendritic Cell can be a Temporal Bridge Between a CD4+ T-Helper and a T-Killer Cell. *Nature* (1998) 393:474–8. doi: 10.1038/30989
2. Bennett SR, Carbone FR, Karamalis F, Flavell RA, Miller JF, Heath WR. Help for Cytotoxic-T-Cell Responses Is Mediated by CD40 Signalling. *Nature* (1998) 393:478–80. doi: 10.1038/30996
3. Schoenberger SP, Toes RE, van der Voort EI, Offringa R, Melief CJ. T-Cell Help for Cytotoxic T Lymphocytes Is Mediated by CD40-CD40L Interactions. *Nature* (1998) 393:480–3. doi: 10.1038/31002
4. Lanzavecchia A. Immunology. Licence to Kill. *Nature* (1998) 393:413–4. doi: 10.1038/30845
5. Masopust D, Soerens AG. Tissue-Resident T Cells and Other Resident Leukocytes. *Annu Rev Immunol* (2019) 37:521–46. doi: 10.1146/annurev-immunol-042617-053214
6. Di Rosa F, Gebhardt T. Bone Marrow T Cells and the Integrated Functions of Recirculating and Tissue-Resident Memory T Cells. *Front Immunol* (2016) 7:51. doi: 10.3389/fimmu.2016.00051
7. Di Rosa F, Pabst R. The Bone Marrow: A Nest for Migratory Memory T Cells. *Trends Immunol* (2005) 26:360–6. doi: 10.1016/j.it.2005.04.011
8. Di Rosa F. Two Niches in the Bone Marrow: A Hypothesis on Life-Long T Cell Memory. *Trends Immunol* (2016) 37:503–12. doi: 10.1016/j.it.2016.05.004
9. Dunn GP, Bruce AT, Ikeda H, Old LJ, Schreiber RD. Cancer Immunoediting: From Immunosurveillance to Tumor Escape. *Nat Immunol* (2002) 3:991–8. doi: 10.1038/ni1102-991
10. Sallusto F, Lenig D, Forster R, Lipp M, Lanzavecchia A. Two Subsets of Memory T Lymphocytes With Distinct Homing Potentials and Effector Functions. *Nature* (1999) 401:708–12. doi: 10.1038/44385
11. Luckey CJ, Bhattacharya D, Goldrath AW, Weissman IL, Benoist C, Mathis D. Memory T and Memory B Cells Share a Transcriptional Program of Self-Renewal With Long-Term Hematopoietic Stem Cells. *Proc Natl Acad Sci U S A* (2006) 103:3304–9. doi: 10.1073/pnas.0511137103
12. Gattinoni L, Speiser DE, Lichterfeld M, Bonini C. T Memory Stem Cells in Health and Disease. *Nat Med* (2017) 23:18–27. doi: 10.1038/nm.4241
13. Graef P, Buchholz VR, Stemberger C, Flossdorf M, Henkel L, Schiemann M, et al. Serial Transfer of Single-Cell-Derived Immunocompetence Reveals Stemness of CD8(+) Central Memory T Cells. *Immunity* (2014) 41:116–26. doi: 10.1016/j.immuni.2014.05.018
14. Boddupalli CS, Nair S, Gray SM, Nowyhed HN, Verma R, Gibson JA, et al. ABC Transporters and NR4A1 Identify a Quiescent Subset of Tissue-Resident Memory T Cells. *J Clin Invest* (2016) 126:3905–16. doi: 10.1172/JCI85329
15. Eberhardt CS, Kissick HT, Patel MR, Cardenas MA, Prokhnevska N, Obeng RC, et al. Functional HPV-Specific PD-1^{+} Stem-Like CD8 T Cells in Head and Neck Cancer. *Nature* (2021) 597:279–84. doi: 10.1038/s41586-021-03862-z
16. Dunn GP, Old LJ, Schreiber RD. The Immunobiology of Cancer Immunosurveillance and Immunoediting. *Immunity* (2004) 21:137–48. doi: 10.1016/j.immuni.2004.07.017
17. Coffelt SB, Kersten K, Doornebal CW, Weiden J, Vrijland K, Hau CS, et al. IL-17-Producing γδ T Cells and Neutrophils Conspire to Promote Breast Cancer Metastasis. *Nature* (2015) 522:345–8. doi: 10.1038/nature14282
18. Moskophidis D, Lechner F, Pircher H, Zinkernagel RM. Virus Persistence in Acutely Infected Immunocompetent Mice by Exhaustion of Antiviral Cytotoxic Effector T Cells. *Nature* (1993) 362:758–61. doi: 10.1038/362758a0
19. Gallimore A, Glithero A, Godkin A, Tissot AC, Plückthun A, Elliott T, et al. Induction and Exhaustion of Lymphocytic Choriomeningitis Virus-Specific Cytotoxic T Lymphocytes Visualized Using Soluble Tetrameric Major Histocompatibility Complex Class I-Peptide Complexes. *J Exp Med* (1998) 187:1383–93. doi: 10.1084/jem.187.9.1383
20. Zajac AJ, Blattman JN, Murali-Krishna K, Sourdive DJD, Suresh M, Altman JD, et al. Viral Immune Evasion Due to Persistence of Activated T Cells Without Effector Function. *J Exp Med* (1998) 188:2205–13. doi: 10.1084/jem.188.12.2205
21. Kaminski H, Lemoine M, Pradeu T. Immunological Exhaustion: How to Make a Disparate Concept Operational. *PloS Pathog* (2021) 17:e1009892. doi: 10.1371/journal.ppat.1009892
22. Reckamp KL. Advances in Immunotherapy for Non-Small Cell Lung Cancer. *Clin Adv Hematol Oncol* (2015) 13:847–53.
23. Márquez-Rodas I, Cerezuela P, Soria A, Berrocal A, Riso A, González-Cao M, et al. Immune Checkpoint Inhibitors: Therapeutic Advances in Melanoma. *Ann Transl Med* (2015) 3:267. doi: 10.3978/j.issn.2305-5839.2015.10.27
24. Rizvi NA, Hellmann MD, Snyder A, Kvistborg P, Makarov V, Havel JJ, et al. Cancer Immunology. Mutational Landscape Determines Sensitivity to PD-1 Blockade in Non-Small Cell Lung Cancer. *Science* (2015) 348:124–8. doi: 10.1126/science.aaa1348
25. Arasanz, Zuazo, Bocanegra, Gato, Martínez-Aguillo, Morilla, et al. Early Detection of Hyperprogressive Disease in Non-Small Cell Lung Cancer by Monitoring of Systemic T Cell Dynamics. *Cancers* (2020) 12:344. doi: 10.3390/cancers12020344
26. Hutchins B, Starling GC, McCoy MA, Herzyk D, Poulet FM, Dulos J, et al. Biophysical and Immunological Characterization and *In Vivo* Pharmacokinetics and Toxicology in Non-Human Primates of the Anti-PD-1 Antibody Pembrolizumab. *Mol Cancer Ther* (2020) 19:1298–307. doi: 10.1158/1535-7163.mct-19-0774. molcanther.0774.2019.
27. Wang C, Thudium KB, Han M, Wang XT, Huang H, Feingersh D, et al. *In Vitro* Characterization of the Anti-PD-1 Antibody Nivolumab, BMS-936558, and *In Vivo* Toxicology in Non-Human Primates. *Cancer Immunol Res* (2014) 2:846–56. doi: 10.1158/2326-6066.CIR-14-0040
28. Park J-E, Kim S-E, Keam B, Park H-R, Kim S, Kim M, et al. Anti-Tumor Effects of NK Cells and Anti-PD-L1 Antibody With Antibody-Dependent Cellular Cytotoxicity in PD-L1-Positive Cancer Cell Lines. *J ImmunoTherapy Cancer* (2020) 8:e000873. doi: 10.1136/jitc-2020-000873
29. Stewart R, Morrow M, Hammond SA, Mulgrew K, Marcus D, Poon E, et al. Identification and Characterization of MEDI4736, an Antagonistic Anti–PD-L1 Monoclonal Antibody. *Cancer Immunol Res* (2015) 3:1052–62. doi: 10.1158/2326-6066.cir-14-0191
30. Boyerinas B, Jochems C, Fantini M, Heery CR, Gulley JL, Tsang KY, et al. Antibody-Dependent Cellular Cytotoxicity Activity of a Novel Anti-PD-L1

Antibody Avelumab (MSB0010718C) on Human Tumor Cells. *Cancer Immunol Res* (2015) 3:1148–57. doi: 10.1158/2326-6066.CIR-15-0059
31. Juliá EP, Amante A, Pampena MB, Mordoh J, Levy EM. Avelumab, an IgG1 Anti-PD-L1 Immune Checkpoint Inhibitor, Triggers NK Cell-Mediated Cytotoxicity and Cytokine Production Against Triple Negative Breast Cancer Cells. *Front Immunol* (2018) 9:2140. doi: 10.3389/fimmu.2018.02140
32. Antonangeli F, Natalini A, Garassino MC, Sica A, Santoni A, Di Rosa F. Regulation of PD-L1 Expression by NF-κb in Cancer. *Front Immunol* (2020) 11:584626. doi: 10.3389/fimmu.2020.584626
33. Messal N, Serriari NE, Pastor S, Nunès JA, Olive D. PD-L2 is Expressed on Activated Human T Cells and Regulates Their Function. *Mol Immunol* (2011) 48:2214–9. doi: 10.1016/j.molimm.2011.06.436
34. Pardoll DM. The Blockade of Immune Checkpoints in Cancer Immunotherapy. *Nat Rev Cancer* (2012) 12:252–64. doi: 10.1038/nrc3239
35. Patsoukis N, Wang Q, Strauss L, Boussiotis VA. Revisiting the PD-1 Pathway. *Sci Adv* (2020) 6(eabd2712):1–13. doi: 10.1126/sciadv.abd2712
36. Buckle I, Guillerey C. Inhibitory Receptors and Immune Checkpoints Regulating Natural Killer Cell Responses to Cancer. *Cancers* (2021) 13:4263. doi: 10.3390/cancers13174263
37. Liu X, Hogg GD, DeNardo DG. Rethinking Immune Checkpoint Blockade: 'Beyond the T Cell'. *J Immunother Cancer* (2021) 9(e001460):1–10. doi: 10.1136/jitc-2020-001460
38. Scheper W, Kelderman S, Fanchi LF, Linnemann C, Bendle G, de Rooij MAJ, et al. Low and Variable Tumor Reactivity of the Intratumoral TCR Repertoire in Human Cancers. *Nat Med* (2019) 25:89–94. doi: 10.1038/s41591-018-0266-5
39. Masopust D, Vezys V, Marzo AL, Lefrancois L. Preferential Localization of Effector Memory Cells in Nonlymphoid Tissue. *Science* (2001) 291:2413–7. doi: 10.1126/science.1058867
40. Reinhardt RL, Khoruts A, Merica R, Zell T, Jenkins MK. Visualizing the Generation of Memory CD4 T Cells in the Whole Body. *Nature* (2001) 410:101–5. doi: 10.1038/35065111
41. Schenkel JM, Masopust D. Tissue-Resident Memory T Cells. *Immunity* (2014) 41:886–97. doi: 10.1016/j.immuni.2014.12.007
42. Rosenberg SA. Development of Cancer Immunotherapies Based on Identification of the Genes Encoding Cancer Regression Antigens. *J Natl Cancer Inst* (1996) 88:1635–44. doi: 10.1093/jnci/88.22.1635
43. Rosenberg SA. The Immunotherapy of Solid Cancers Based on Cloning the Genes Encoding Tumor-Rejection Antigens. *Annu Rev Med* (1996) 47:481–91. doi: 10.1146/annurev.med.47.1.481
44. Pross HF, Lotzová E. Role of Natural Killer Cells in Cancer. *Nat Immun* (1993) 12:279–92.
45. Dudley ME, Wunderlich JR, Robbins PF, Yang JC, Hwu P, Schwartzentruber DJ, et al. Cancer Regression and Autoimmunity in Patients After Clonal Repopulation With Antitumor Lymphocytes. *Science* (2002) 298:850–4. doi: 10.1126/science.1076514
46. June CH. Principles of Adoptive T Cell Cancer Therapy. *J Clin Invest* (2007) 117:1204–12. doi: 10.1172/JCI31446
47. Freitag F, Maucher M, Riester Z, Hudecek M. New Targets and Technologies for CAR-T Cells. *Curr Opin Oncol* (2020) 32:510–7. doi: 10.1097/CCO.0000000000000653
48. Chang CH, Qiu J, O'Sullivan D, Buck MD, Noguchi T, Curtis JD, et al. Metabolic Competition in the Tumor Microenvironment Is a Driver of Cancer Progression. *Cell* (2015) 162:1229–41. doi: 10.1016/j.cell.2015.08.016
49. Zappasodi R, Wolchok JD, Merghoub T. Strategies for Predicting Response to Checkpoint Inhibitors. *Curr Hematol Malig Rep* (2018) 13:383–95. doi: 10.1007/s11899-018-0471-9
50. Scott AC, Dündar F, Zumbo P, Chandran SS, Klebanoff CA, Shakiba M, et al. TOX is a Critical Regulator of Tumour-Specific T Cell Differentiation. *Nature* (2019) 571:270–4. doi: 10.1038/s41586-019-1324-y
51. Khan O, Giles JR, McDonald S, Manne S, Ngiow SF, Patel KP, et al. TOX Transcriptionally and Epigenetically Programs $CD8^+$ T Cell Exhaustion. *Nature* (2019) 571:211–8. doi: 10.1038/s41586-019-1325-x
52. Sekine T, Perez-Potti A, Nguyen S, Gorin J-B, Wu VH, Gostick E, et al. TOX is Expressed by Exhausted and Polyfunctional Human Effector Memory CD8+ T Cells. *Sci Immunol* (2020) 5:eaba7918. doi: 10.1126/sciimmunol.aba7918
53. Utzschneider DT, Kallies A. Human Effector T Cells Express TOX-Not So "TOX"Ic After All. *Sci Immunol* (2020) 5(eabc8272):1–2. doi: 10.1126/sciimmunol.abc8272
54. Pais Ferreira D, Silva JG, Wyss T, Fuertes Marraco SA, Scarpellino L, Charmoy M, et al. Central Memory CD8(+) T Cells Derive From Stem-Like Tcf7(hi) Effector Cells in the Absence of Cytotoxic Differentiation. *Immunity* (2020) 53:985–1000.e11. doi: 10.1016/j.immuni.2020.09.005
55. McLane LM, Ngiow SF, Chen Z, Attanasio J, Manne S, Ruthel G, et al. Role of Nuclear Localization in the Regulation and Function of T-Bet and Eomes in Exhausted CD8 T Cells. *Cell Rep* (2021) 35:109120. doi: 10.1016/j.celrep.2021.109120
56. Philip M, Schietinger A. $CD8^+$ T Cell Differentiation and Dysfunction in Cancer. *Nat Rev Immunol* (2021). doi: 10.1038/s41577-021-00574-3
57. Reuben A, Zhang J, Chiou SH, Gittelman RM, Li J, Lee WC, et al. Comprehensive T Cell Repertoire Characterization of Non-Small Cell Lung Cancer. *Nat Commun* (2020) 11:603. doi: 10.1038/s41467-019-14273-0
58. Loo K, Tsai KK, Mahuron K, Liu J, Pauli ML, Sandoval PM, et al. Partially Exhausted Tumor-Infiltrating Lymphocytes Predict Response to Combination Immunotherapy. *JCI Insight* (2017) 2(e93433):1–8. doi: 10.1172/jci.insight.93433
59. Paijens ST, Vledder A, de Bruyn M, Nijman HW. Tumor-Infiltrating Lymphocytes in the Immunotherapy Era. *Cell Mol Immunol* (2021) 18:842–59. doi: 10.1038/s41423-020-00565-9
60. Neal JT, Li X, Zhu J, Giangarra V, Grzeskowiak CL, Ju J, et al. Organoid Modeling of the Tumor Immune Microenvironment. *Cell* (2018) 175:1972–88.e16. doi: 10.1016/j.cell.2018.11.021
61. Gibellini L, De Biasi S, Porta C, Lo Tartaro D, Depenni R, Pellacani G, et al. Single-Cell Approaches to Profile the Response to Immune Checkpoint Inhibitors. *Front Immunol* (2020) 11:490. doi: 10.3389/fimmu.2020.00490
62. Kurtulus S, Madi A, Escobar G, Klapholz M, Nyman J, Christian E, et al. Checkpoint Blockade Immunotherapy Induces Dynamic Changes in $PD\text{-}1^-$ $CD8^+$ Tumor-Infiltrating T Cells. *Immunity* (2019) 50:181–94.e6. doi: 10.1016/j.immuni.2018.11.014
63. Utzschneider DT, Charmoy M, Chennupati V, Pousse L, Ferreira DP, Calderon-Copete S, et al. T Cell Factor 1-Expressing Memory-Like CD8 (+) T Cells Sustain the Immune Response to Chronic Viral Infections. *Immunity* (2016) 45:415–27. doi: 10.1016/j.immuni.2016.07.021
64. Kamada T, Togashi Y, Tay C, Ha D, Sasaki A, Nakamura Y, et al. $PD\text{-}1^+$ Regulatory T Cells Amplified by PD-1 Blockade Promote Hyperprogression of Cancer. *Proc Natl Acad Sci U S A* (2019) 116:9999–10008. doi: 10.1073/pnas.1822001116
65. Gebhardt T, Wakim LM, Eidsmo L, Reading PC, Heath WR, Carbone FR. Memory T Cells in Nonlymphoid Tissue That Provide Enhanced Local Immunity During Infection With Herpes Simplex Virus. *Nat Immunol* (2009) 10:524–30. doi: 10.1038/ni.1718
66. Beura LK, Fares-Frederickson NJ, Steinert EM, Scott MC, Thompson EA, Fraser KA, et al. $CD4^+$ Resident Memory T Cells Dominate Immunosurveillance and Orchestrate Local Recall Responses. *J Exp Med* (2019) 216:1214–29. doi: 10.1084/jem.20181365
67. Clark RA, Chong B, Mirchandani N, Brinster NK, Yamanaka ,K-i, Dowgiert RK, et al. The Vast Majority of CLA+ T Cells Are Resident in Normal Skin. *J Immunol* (2006) 176:4431–9. doi: 10.4049/jimmunol.176.7.4431
68. Wakim LM, Woodward-Davis A, Liu R, Hu Y, Villadangos J, Smyth G, et al. The Molecular Signature of Tissue Resident Memory CD8 T Cells Isolated From the Brain. *J Immunol* (2012) 189:3462–71. doi: 10.4049/jimmunol.1201305
69. Milner JJ, Toma C, He Z, Kurd NS, Nguyen QP, McDonald B, et al. Heterogenous Populations of Tissue-Resident $CD8^+$ T Cells Are Generated in Response to Infection and Malignancy. *Immunity* (2020) 52:808–824.e7. doi: 10.1016/j.immuni.2020.04.007
70. Mackay LK, Rahimpour A, Ma JZ, Collins N, Stock AT, Hafon ML, et al. The Developmental Pathway for CD103(+)CD8+ Tissue-Resident Memory T Cells of Skin. *Nat Immunol* (2013) 14:1294–301. doi: 10.1038/ni.2744
71. Kumar BV, Ma W, Miron M, Granot T, Guyer RS, Carpenter DJ, et al. Human Tissue-Resident Memory T Cells Are Defined by Core Transcriptional and Functional Signatures in Lymphoid and Mucosal Sites. *Cell Rep* (2017) 20:2921–34. doi: 10.1016/j.celrep.2017.08.078
72. Pan Y, Tian T, Park CO, Lofftus SY, Mei S, Liu X, et al. Survival of Tissue-Resident Memory T Cells Requires Exogenous Lipid Uptake and Metabolism. *Nature* (2017) 543:252–6. doi: 10.1038/nature21379

73. Iborra S, Martínez-López M, Khouili S, Enamorado M, Cueto F, Conde-Garrosa R, et al. COptimal Generation of Tissue-Resident But Not Circulating Memory T Cells During Viral Infection Requires Crosspriming by DNGR-1 + Dendritic Cells. *Immunity* (2016) 45:847–60. doi: 10.1016/j.immuni.2016.08.019
74. Enamorado M, Khouili SC, Iborra S, Sancho D. Genealogy, Dendritic Cell Priming, and Differentiation of Tissue-Resident Memory CD8+ T Cells. *Front Immunol* (2018) 9:1751. doi: 10.3389/fimmu.2018.01751
75. Williams JB, Kupper TS. Resident Memory T Cells in the Tumor Microenvironment. *Adv Exp Med Biol* (2020) 1273:39–68. doi: 10.1007/978-3-030-49270-0_3
76. Guo X, Zhang Y, Zheng L, Zheng C, Song J, Zhang Q, et al. Global Characterization of T Cells in Non-Small-Cell Lung Cancer by Single-Cell Sequencing. *Nat Med* (2018) 24:978–85. doi: 10.1038/s41591-018-0045-3
77. Ganesan AP, Clarke J, Wood O, Garrido-Martin EM, Chee SJ, Mellows T, et al. Tissue-Resident Memory Features are Linked to the Magnitude of Cytotoxic T Cell Responses in Human Lung Cancer. *Nat Immunol* (2017) 18:940–50. doi: 10.1038/ni.3775
78. Duhen T, Duhen R, Montler R, Moses J, Moudgil T, de Miranda NF, et al. Co-Expression of CD39 and CD103 Identifies Tumor-Reactive CD8 T Cells in Human Solid Tumors. *Nat Commun* (2018) 9(2724):1–13. doi: 10.1038/s41467-018-05072-0
79. Liikanen I, Lauhan C, Quon S, Omilusik K, Phan AT, Bartrolí LB, et al. Hypoxia-Inducible Factor Activity Promotes Antitumor Effector Function and Tissue Residency by CD8+ T Cells. *J Clin Invest* (2021) 131(e143729):1–17. doi: 10.1172/JCI143729
80. Boddupalli CS, Bar N, Kadaveru K, Krauthammer M, Pornputtapong N, Mai Z, et al. Interlesional Diversity of T Cell Receptors in Melanoma With Immune Checkpoints Enriched in Tissue-Resident Memory T Cells. *JCI Insight* (2016) 1(e88955):1–13. doi: 10.1172/jci.insight.88955
81. van der Gracht ETI, Behr FM, Arens R. Functional Heterogeneity and Therapeutic Targeting of Tissue-Resident Memory T Cells. *Cells* (2021) 10 (164):1–17. doi: 10.3390/cells10010164
82. Mami-Chouaib F, Blanc C, Corgnac S, Hans S, Malenica I, Granier C, et al. Resident Memory T Cells, Critical Components in Tumor Immunology. *J Immunother Cancer* (2018) 6:87. doi: 10.1186/s40425-018-0399-6
83. Djenidi F, Adam J, Goubar A, Durgeau A, Meurice G, de Montpréville V, et al. CD8+CD103+ Tumor–Infiltrating Lymphocytes Are Tumor-Specific Tissue-Resident Memory T Cells and a Prognostic Factor for Survival in Lung Cancer Patients. *J Immunol* (2015) 194:3475–86. doi: 10.4049/jimmunol.1402711
84. Corgnac S, Malenica I, Mezquita L, Auclin E, Voilin E, Kacher J, et al. $CD103^{+}CD8^{+}$ T_{RM} Cells Accumulate in Tumors of Anti-PD-1-Responder Lung Cancer Patients and Are Tumor-Reactive Lymphocytes Enriched With Tc17. *Cell Rep Med* (2020) 1:100127. doi: 10.1016/j.xcrm.2020.100127
85. Banchereau R, Chitre AS, Scherl A, Wu TD, Patil NS, de Almeida P, et al. Intratumoral CD103+ CD8+ T Cells Predict Response to PD-L1 Blockade. *J Immunother Cancer* (2021) 9(e002231):1–14. doi: 10.1136/jitc-2020-002231
86. Eyles J, Puaux AL, Wang X, Toh B, Prakash C, Hong M, et al. Tumor Cells Disseminate Early, But Immunosurveillance Limits Metastatic Outgrowth, in a Mouse Model of Melanoma. *J Clin Invest* (2010) 120:2030–9. doi: 10.1172/JCI42002
87. Monteiro AC, Leal AC, Goncalves-Silva T, Mercadante AC, Kestelman F, Chaves SB, et al. T Cells Induce Pre-Metastatic Osteolytic Disease and Help Bone Metastases Establishment in a Mouse Model of Metastatic Breast Cancer. *PloS One* (2013) 8:e68171. doi: 10.1371/journal.pone.0068171
88. Letsch A, Keilholz U, Assfalg G, Mailander V, Thiel E, Scheibenbogen C. Bone Marrow Contains Melanoma-Reactive CD8+ Effector T Cells and, Compared With Peripheral Blood, Enriched Numbers of Melanoma-Reactive CD8+ Memory T Cells. *Cancer Res* (2003) 63:5582–6.
89. Schmitz-Winnenthal FH, Volk C, Z'graggen K, Galindo L, Nummer D, Ziouta Y, et al. High Frequencies of Functional Tumor-Reactive T Cells in Bone Marrow and Blood of Pancreatic Cancer Patients. *Cancer Res* (2005) 65:10079–87. doi: 10.1158/0008-5472.CAN-05-1098
90. Gros A, Parkhurst MR, Tran E, Pasetto A, Robbins PF, Ilyas S, et al. Prospective Identification of Neoantigen-Specific Lymphocytes in the Peripheral Blood of Melanoma Patients. *Nat Med* (2016) 22:433–8. doi: 10.1038/nm.4051
91. Noguchi A, Kaneko T, Naitoh K, Saito M, Iwai K, Maekawa R, et al. Impaired and Imbalanced Cellular Immunological Status Assessed in Advanced Cancer Patients and Restoration of the T Cell Immune Status by Adoptive T-Cell Immunotherapy. *Int Immunopharmacol* (2014) 18:90–7. doi: 10.1016/j.intimp.2013.11.009
92. Verronèse E, Delgado A, Valladeau-Guilemond J, Garin G, Guillemaut S, Tredan O, et al. Immune Cell Dysfunctions in Breast Cancer Patients Detected Through Whole Blood Multi-Parametric Flow Cytometry Assay. *OncoImmunology* (2016) 5:e1100791. doi: 10.1080/2162402x.2015.1100791
93. Hiam-Galvez KJ, Allen BM, Spitzer MH. Systemic Immunity in Cancer. *Nat Rev Cancer* (2021) 21:345–59. doi: 10.1038/s41568-021-00347-z
94. Frey AB, Monu N. Signaling Defects in Anti-Tumor T Cells. *Immunol Rev* (2008) 222:192–205. doi: 10.1111/j.1600-065x.2008.00606.x
95. Di Rosa F. Maintenance of Memory T Cells in the Bone Marrow: Survival or Homeostatic Proliferation? *Nat Rev Immunol* (2016) 16:271. doi: 10.1038/nri.2016.31
96. Safi S, Yamauchi Y, Stamova S, Rathinasamy A, op den Winkel J, Jünger S, et al. Bone Marrow Expands the Repertoire of Functional T Cells Targeting Tumor-Associated Antigens in Patients With Resectable Non-Small-Cell Lung Cancer. *OncoImmunology* (2019) 8:e1671762. doi: 10.1080/2162402x.2019.1671762
97. Guichelaar T, Emmelot ME, Rozemuller H, Martini B, Groen RW, Storm G, et al. Human Regulatory T Cells do Not Suppress the Antitumor Immunity in the Bone Marrow: A Role for Bone Marrow Stromal Cells in Neutralizing Regulatory T Cells. *Clin Cancer Res* (2013) 19:1467–75. doi: 10.1158/1078-0432.CCR-12-2177
98. Rathinasamy A, Domschke C, Ge Y, Böhm HH, Dettling S, Jansen D, et al. Tumor Specific Regulatory T Cells in the Bone Marrow of Breast Cancer Patients Selectively Upregulate the Emigration Receptor S1P1. *Cancer Immunol Immunother* (2017) 66:593–603. doi: 10.1007/s00262-017-1964-4
99. Feuerer M, Beckhove P, Bai L, Solomayer EF, Bastert G, Diel IJ, et al. Therapy of Human Tumors in NOD/SCID Mice With Patient-Derived Reactivated Memory T Cells From Bone Marrow. *Nat Med* (2001) 7:452–8. doi: 10.1038/86523
100. Di Rosa F, Santoni A. Bone Marrow CD8 T Cells are in a Different Activation State Than Those in Lymphoid Periphery. *Eur J Immunol* (2002) 32:1873–80. doi: 10.1002/1521-4141(200207)32:7<1873::AID-IMMU1873>3.0.CO;2-P
101. Schuetz F, Ehlert K, Ge Y, Schneeweiss A, Rom J, Inzkirweli N, et al. Treatment of Advanced Metastasized Breast Cancer With Bone Marrow-Derived Tumour-Reactive Memory T Cells: A Pilot Clinical Study. *Cancer Immunol Immunother* (2009) 58:887–900. doi: 10.1007/s00262-008-0605-3
102. Khan AB, Carpenter B, Santos E Sousa P, Pospori C, Khorshed R, Griffin J, et al. Redirection to the Bone Marrow Improves T Cell Persistence and Antitumor Functions. *J Clin Invest* (2018) 128:2010–24. doi: 10.1172/JCI97454
103. Im SJ, Hashimoto M, Gerner MY, Lee J, Kissick HT, Burger MC, et al. Defining CD8+ T Cells That Provide the Proliferative Burst After PD-1 Therapy. *Nature* (2016) 537:417–21. doi: 10.1038/nature19330
104. Kamphorst AO, Wieland A, Nasti T, Yang S, Zhang R, Barber DL, et al. Rescue of Exhausted CD8 T Cells by PD-1-Targeted Therapies is CD28-Dependent. *Science* (2017) 355:1423–7. doi: 10.1126/science.aaf0683
105. Kamphorst AO, Pillai RN, Yang S, Nasti TH, Akondy RS, Wieland A, et al. Proliferation of PD-1+ CD8 T Cells in Peripheral Blood After PD-1-Targeted Therapy in Lung Cancer Patients. *Proc Natl Acad Sci U S A* (2017) 114:4993–8. doi: 10.1073/pnas.1705327114
106. Zuazo M, Arasanz H, Fernández-Hinojal G, Garcia-Granda MJ, Gato M, Bocanegra A, et al. Functional Systemic CD4 Immunity is Required for Clinical Responses to PD-L1/PD-1 Blockade Therapy. *EMBO Mol Med* (2019) 11:e10293. doi: 10.15252/emmm.201910293
107. Wu TD, Madireddi S, de Almeida PE, Banchereau R, Chen YJ, Chitre AS, et al. Peripheral T Cell Expansion Predicts Tumour Infiltration and Clinical Response. *Nature* (2020) 579:274–8. doi: 10.1038/s41586-020-2056-81
108. Yost KE, Satpathy AT, Wells DK, Qi Y, Wang C, Kageyama R, et al. Clonal Replacement of Tumor-Specific T Cells Following PD-1 Blockade. *Nat Med* (2019) 25:1251–9. doi: 10.1038/s41591-019-0522-3

109. North RJ, Kirstein DP. T-Cell-Mediated Concomitant Immunity to Syngeneic Tumors. I. Activated Macrophages as the Expressors of Nonspecific Immunity to Unrelated Tumors and Bacterial Parasites. *J Exp Med* (1977) 145:275–92. doi: 10.1084/jem.145.2.275
110. DiGiacomo A, North RJ. T Cell Suppressors of Antitumor Immunity. The Production of Ly-1-,2+ Suppressors of Delayed Sensitivity Precedes the Production of Suppressors of Protective Immunity. *J Exp Med* (1986) 164:1179–92. doi: 10.1084/jem.164.4.1179
111. Turk MJ, Guevara-Patiño JA, Rizzuto GA, Engelhorn ME, Sakaguchi S, Houghton AN. Concomitant Tumor Immunity to a Poorly Immunogenic Melanoma is Prevented by Regulatory T Cells. *J Exp Med* (2004) 200:771–82. doi: 10.1084/jem.20041130
112. De Rosa V, Di Rella F, Di Giacomo A, Matarese G. Regulatory T Cells as Suppressors of Anti-Tumor Immunity: Role of Metabolism. *Cytokine Growth Factor Rev* (2017) 35:15–25. doi: 10.1016/j.cytogfr.2017.04.001
113. Hartana CA, Ahlén Bergman E, Broomé A, Berglund S, Johansson M, Alamdari F, et al. Tissue-Resident Memory T Cells are Epigenetically Cytotoxic With Signs of Exhaustion in Human Urinary Bladder Cancer. *Clin Exp Immunol* (2018) 194:39–53. doi: 10.1111/cei.13183
114. Di Pilato M, Kfuri-Rubens R, Pruessmann JN, Ozga AJ, Messemaker M, Cadilha BL, et al. CXCR6 Positions Cytotoxic T Cells to Receive Critical Survival Signals in the Tumor Microenvironment. *Cell* (2021) 184:4512–30.e22. doi: 10.1016/j.cell.2021.07.015
115. Di Rosa F, Matzinger P. Long-Lasting CD8 T Cell Memory in the Absence of CD4 T Cells or B Cells. *J Exp Med* (1996) 183:2153–63. doi: 10.1084/jem.183.5.2153
116. Son YM, Cheon IS, Wu Y, Li C, Wang Z, Gao X, et al. Tissue-Resident CD4(+) T Helper Cells Assist the Development of Protective Respiratory B and CD8(+) T Cell Memory Responses. *Sci Immunol* (2021) 6(eabb6852):1–15. doi: 10.1126/sciimmunol.abb6852
117. Enamorado M, Iborra S, Priego E, Cueto FJ, Quintana JA, Martínez-Cano S, et al. Enhanced Anti-Tumour Immunity Requires the Interplay Between Resident and Circulating Memory CD8+ T Cells. *Nat Commun* (2017) 8 (16073):1–11. doi: 10.1038/ncomms16073
118. Bakacs T, Moss RW, Kleef R, Szasz MA, Anderson CC. Exploiting Autoimmunity Unleashed by Low-Dose Immune Checkpoint Blockade to Treat Advanced Cancer. *Scand J Immunol* (2019) 90:e12821. doi: 10.1111/sji.12821
119. Oh DY, Cham J, Zhang L, Fong G, Kwek SS, Klinger M, et al. Immune Toxicities Elicted by CTLA-4 Blockade in Cancer Patients Are Associated With Early Diversification of the T-Cell Repertoire. *Cancer Res* (2017) 77:1322–30. doi: 10.1158/0008-5472.can-16-2324
120. Loftus DJ, Castelli C, Clay TM, Squarcina P, Marincola FM, Nishimura MI, et al. Identification of Epitope Mimics Recognized by CTL Reactive to the Melanoma/Melanocyte-Derived Peptide MART-1(27-35). *J Exp Med* (1996) 184:647–57. doi: 10.1084/jem.184.2.647
121. Vujanovic L, Shi J, Kirkwood JM, Storkus WJ, Butterfield ,LH. Molecular Mimicry of MAGE-A6 and Mycoplasma Penetrans HF-2 Epitopes in the Induction of Antitumor $CD8^+$ T-Cell Responses. *Oncoimmunology* (2014) 3: e954501. doi: 10.4161/21624011.2014.954501
122. Bonaventura P, Shekarian T, Alcazer V, Valladeau-Guilemond J, Valsesia-Wittmann S, Amigorena S, et al. Cold Tumors: A Therapeutic Challenge for Immunotherapy. *Front Immunol* (2019) 10:168. doi: 10.3389/fimmu.2019.00168
123. Newman JH, Chesson CB, Herzog NL, Bommareddy PK, Aspromonte SM, Pepe R, et al. Intratumoral Injection of the Seasonal Flu Shot Converts Immunologically Cold Tumors to Hot and Serves as an Immunotherapy for Cancer. *Proc Natl Acad Sci* (2020) 117:1119–28. doi: 10.1073/pnas.1904022116
124. Gandhi L, Rodríguez-Abreu D, Gadgeel S, Esteban E, Felip E, De Angelis F, et al. Pembrolizumab Plus Chemotherapy in Metastatic Non-Small-Cell Lung Cancer. *N Engl J Med* (2018) 378:2078–92. doi: 10.1056/NEJMoa1801005
125. Melosky B, Juergens R, Hirsh V, McLeod D, Leighl N, Tsao MS, et al. Amplifying Outcomes: Checkpoint Inhibitor Combinations in First-Line Non-Small Cell Lung Cancer. *Oncologist* (2020) 25:64–77. doi: 10.1634/theoncologist.2019-0027
126. Chamoto K, Hatae R, Honjo T. Current Issues and Perspectives in PD-1 Blockade Cancer Immunotherapy. *Int J Clin Oncol* (2020) 25:790–800. doi: 10.1007/s10147-019-01588-7
127. Lake RA, Robinson BW. Immunotherapy and Chemotherapy–a Practical Partnership. *Nat Rev Cancer* (2005) 5:397–405. doi: 10.1038/nrc1613
128. Kim JM, Chen DS. Immune Escape to PD-L1/PD-1 Blockade: Seven Steps to Success (or Failure). *Ann Oncol* (2016) 27:1492–504. doi: 10.1093/annonc/mdw217
129. Spitzer MH, Carmi Y, Reticker-Flynn NE, Kwek SS, Madhireddy D, Martins MM, et al. Systemic Immunity Is Required for Effective Cancer Immunotherapy. *Cell* (2017) 168:487–502.e15. doi: 10.1016/j.cell.2016.12.022

Conflict of Interest: The authors declare that the research was conducted in the absence of any commercial or financial relationships that could be construed as a potential conflict of interest.

Publisher's Note: All claims expressed in this article are solely those of the authors and do not necessarily represent those of their affiliated organizations, or those of the publisher, the editors and the reviewers. Any product that may be evaluated in this article, or claim that may be made by its manufacturer, is not guaranteed or endorsed by the publisher.

frontiers in Immunology

ORIGINAL RESEARCH
published: 19 November 2021
doi: 10.3389/fimmu.2021.782106

Avoiding Absolute Quantification Trap: A Novel Predictive Signature of Clinical Benefit to Anti-PD-1 Immunotherapy in Non-Small Cell Lung Cancer

Chengming Liu[1,2†], Sihui Wang[1,2†], Sufei Zheng[1,2], Fei Xu[3], Zheng Cao[4], Xiaoli Feng[4], Yan Wang[3], Qi Xue[1], Nan Sun[1,2] and Jie He[1,2*]*

[1] Department of Thoracic Surgery, National Cancer Center/National Clinical Research Center for Cancer/Cancer Hospital, Chinese Academy of Medical Sciences and Peking Union Medical College, Beijing, China, [2] State Key Laboratory of Molecular Oncology, National Cancer Center/National Clinical Research Center for Cancer/Cancer Hospital, Chinese Academy of Medical Sciences and Peking Union Medical College, Beijing, China, [3] Department of Medical Oncology, National Cancer Center/National Clinical Research Center for Cancer/Cancer Hospital, Chinese Academy of Medical Sciences and Peking Union Medical College, Beijing, China, [4] Department of Pathology, National Cancer Center/National Clinical Research Center for Cancer/Cancer Hospital, Chinese Academy of Medical Sciences and Peking Union Medical College, Beijing, China

Immunotherapy has been focused on by many oncologists and researchers. While, due to technical biases of absolute quantification, few traditional biomarkers for anti-PD-1 immunotherapy have been applied in regular clinical practice of non-small cell lung cancer (NSCLC). Therefore, there is an urgent and unmet need for a feasible tool—immune to data source bias—for identifying patients who might benefit from ICIs in clinical practice. Using the strategy based on the relative ranking of gene expression levels, we herein proposed the novel BRGP index (BRGPI): four BRGPs significantly related with progression-free survival of NSCLC patients treated with anti-PD-1 immunotherapy in the multicohort analysis. Moreover, stratification and multivariate Cox regression analyses demonstrated that BRGPI was an independent prognostic factor. Notably, compared to PD-L1, BRGPI exerted the best predictive ability. Further analysis showed that the patients in the BRGPI-low and PD-L1-high subgroup derived more clinical benefits from anti-PD-1 immunotherapy. In conclusion, the prospect of applying the BRGPI to real clinical practice is promising owing to its powerful and reliable predictive value.

Keywords: NSCLC, immune checkpoint inhibitors, clinical benefit, prognosis, BRGPI

OPEN ACCESS

Edited by:
Alison Taylor,
University of Leeds, United Kingdom

Reviewed by:
Chun-Yi Hao,
Peking University Cancer Hospital, China
Yuping Sun,
Shandong First Medical University and Shandong Academy of Medical Sciences, China

****Correspondence:***
Jie He
prof.jiehe@gmail.com
Nan Sun
sunnan@vip.126.com

[†]These authors have contributed equally to this work

Specialty section:
This article was submitted to Cancer Immunity and Immunotherapy, a section of the journal Frontiers in Immunology

Received: *23 September 2021*
Accepted: *03 November 2021*
Published: *19 November 2021*

Citation:
Liu C, Wang S, Zheng S, Xu F, Cao Z, Feng X, Wang Y, Xue Q, Sun N and He J (2021) Avoiding Absolute Quantification Trap: A Novel Predictive Signature of Clinical Benefit to Anti-PD-1 Immunotherapy in Non-Small Cell Lung Cancer. Front. Immunol. 12:782106. doi: 10.3389/fimmu.2021.782106

INTRODUCTION

Non-small cell lung cancer (NSCLC) is related with the highest cancer-related mortality worldwide. It features a high mortality rate and only 19% of those diagnosed with NSCLC will be alive 5 years later (1, 2). Over the years, the application of molecular targeted therapy and immunotherapy has allowed many patients to survive longer (3). Although some patients can benefit from targeted molecular therapy, rapid

resistance limits its effectiveness in lung cancer treatment (4). Immune-checkpoint inhibitors (ICIs)—such as pembrolizumab and nivolumab targeting PD-1—have revolutionarily improved the prognosis of patients with NSCLC. Clinical trials (5–9) and real-world data (10–12) have demonstrated that anti-PD-1/PD-L1 immunotherapy effectively improves long-term response and durable disease control. Unfortunately, only a small number of patients can derive benefit from ICIs; therefore, reliable biomarkers are needed to identify these candidate patients (13).

Biomarkers predicting immunotherapy benefits have recently emerged, including those correlated with the inflammatory tumor microenvironment, such as PD-L1 protein expression in cancer and antigen-presenting cells, and markers demonstrating the increase of tumor-specific neoantigens like tumor mutational burden (TMB) (14, 15). PD-L1 expression is the most widely recognized biomarker for ICIs targeting PD-1/PD-L1. Nevertheless, the sensitivity and specificity of this approach are modest (16). Most patients do not respond to ICIs but given high PD-L1 expression, a small group of PD-L1-low/negative patients do respond to ICIs (17). Also, due to the different antibodies and cut-off values, PD-L1 expression varies among different platforms for detection (18). Application of PD-L1 alone may be insufficient to predict the response to immunotherapy. Beyond PD-L1 expression, TMB has also been recommended as a critical marker related to the response of immunotherapy (19). Theoretically—as TMB is correlated with the number of neoantigens—the higher the TMB is, the better the immunotherapy effect will be. Yet TMB alone fails to represent the complexity of tumor immunogenicity. Anti-tumor cytotoxicity does not correlate with neoantigen load, and high TMB does not equivalent to immunogenicity and activation of anti-tumor immunity (20, 21). Like PD-L1, TMB also varies largely among different detecting platforms and there is no agreed-upon clinically validated TMB cut-off. Therefore, predictive markers—comprehensively reflecting anti-tumor immunity—are urgently needed to determine the patients who might derive benefit from anti-PD-1 immunotherapy in clinical practice, and without data platform limitations.

Opening gene expression sources in public databases enable the development of reliable gene-based biomarkers for cancer research. Some gene expression-based signatures have been proposed for diagnosis and treatment planning for patients with NSCLC. Unfortunately, few of them have been applied in regular clinical practice because of issues such as overfitting in small training datasets and insufficient validation (22, 23). Generally, adequate normalization was needed before the gene expression raw data were used, and this is difficult to accomplish owing to technical biases in different measuring platforms and sample heterogeneity among datasets. The ranking of gene relative expressions is a new approach to avoid data preprocessing, such as normalization and scaling. Methods based on this have been effective for cancer classification, immune status determination, and analyses of patients' outcomes (24–26).

The objective of this study was to construct a predictive signature based on benefit-related gene pairs (BRGPs)—represented by four BRGPs significantly related with progression-free survival (PFS)—in NSCLC patients who received the treatment of ICIs. Considering all these decisive immune genes that may influence the response to ICIs, we constructed a predictive pattern to remedy the deficiencies of existing biomarkers.

MATERIALS AND METHODS

Study Design and Data Collection

We enrolled 74 patients with advanced NSCLC who received the treatment of ICIs in three independent cohorts. We recruited 35 patients from GSE93157 as the signature-training dataset. We then collected 20 patients from the GSE136961 cohort and 19 patients from the CICAMS cohort for signature validation of the prognostic model. The analysis pipeline of the construction and validation of benefit-related gene-pair index (BRGPI) is shown in **Supplementary Figure S1**.

We downloaded normalized RNA-seq by expectation maximization (RSEM)-estimated count data of the GSE93157 cohort and transcripts per million (TPM) data of the GSE136961 cohort from the Gene Expression Omnibus (GEO, http://www.ncbi.nlm.nih.gov/geo), and corresponding clinical information were obtained. The CICAMS cohort included 19 LUAD patients who received the treatment of ICIs at the Cancer Hospital/Institute, Chinese Academy of Medical Sciences (CICAMS, Beijing, China) from April 2016 to July 2019. Moreover, formalin fixation paraffin embedding (FFPE) specimens of all enrolled patients prior to the initiation of ICIs were available. According to the Response Evaluation Criteria in Solid Tumors, version 1.1, the tumor response to ICIs was categorized as a complete response (CR), a partial response (PR), stable disease (SD), or progressive disease (PD). Noticeably, non-PD refers to the patients with CR, PR, or SD (27). Progression-free survival (PFS) was defined as the time from the initiation of ICIs administration to the time of PD. The Ethics Committee of CICAMS approved and oversaw this study (approval number 20/242-2438). The characteristics of individuals included in the various patient cohorts are shown in **Supplementary Table S1**.

Construction and Validation of a Predictive Signature Based on BRGPs

We constructed BRGPI based on immune-related genes. Those immune-related genes were downloaded from the Pan-Cancer Immune Profiling Panel, including cytokines and their receptors, and genes correlated with the adaptive immune response such as antigen processing and presentation, T-cell activation, and infiltration (28). We selected 222 immune-related genes that were shared with all the cohorts to construct 2526 gene pairs for pairwise comparison. Each gene pair was scored on the basis of normalized RSEM-estimated count data of GSE93157, TPM data of GSE136961, and proteomic data of CICAMS. Noticeably, we used the immunohistochemistry (IHC) method to obtain the protein expression values of the selected BRGPs. A BRGP score was assigned on the basis of the relative expression of two genes in the pairs (26). For example, BRG1 expression was more than BRG2 expression, the BRGP score was scored with 1, the BRGP score was

scored 0 otherwise. The established BRGPI score of tumor sample completely based on the relative expression of the gene-pair method avoids the batch effect or bias on measurement platforms and is no need for normalization. Then, 311 BRGPs significantly associated with PFS determined by univariate Cox regression analysis (P<0.05) in the signature-training set (GSE93157) were candidates to develop a personalized immune prognostic model in NSCLC. To make the predictive signature more optimized and practical, we selected four gene pairs with the best predictive performance using multivariate Cox regression. Next, we weighted the score of the selected BRGPs by their respective coefficients to obtain the BRGPI. We then determined the best cut-off value to distribute patients into BRGPI-high or BRGPI-low groups by a time-dependent receiver operating characteristic (ROC) curve at one year in the training cohort (29). The predictive performance of the novel BRGPI for immunotherapy response was evaluated in three independent cohorts using the ROC and Kaplan–Meier survival analyses.

IHC Analysis

We collected the FFPE samples of 19 patients who received anti-PD-1 immunotherapy to obtain the protein expression values of the chosen four gene pairs in the CICAMS cohort. Expression levels of eight genes were determined *via* the IHC method using an anti-human C-C motif chemokine ligand 2 (CCL2, MCP1) antibody (Cat# 25542-1-AP, Proteintech, USA), an anti-human vascular endothelial growth factor A (VEGFA) antibody (Cat# ab52917, Abcam, USA), an anti-human cyclin dependent kinase 1 (CDK1) antibody (Cat# ab133327, Abcam, USA), an anti-human C-X-C motif chemokine ligand 9 (CXCL9, MIG) antibody (Cat# 22355-1-AP, Proteintech, USA), an anti-human major histocompatibility complex, class II, DO beta (HLA-DOB) antibody (Cat# NBP1-87469, NOVUS, USA), an anti-human LCK proto-oncogene, Src family tyrosine kinase (LCK) antibody (Cat# ab32149, Abcam, USA), an anti-human interleukin 12A (IL-12A) antibody (Cat# ab131039, Abcam, USA), and an anti-human T-box 21 (TBX21) antibody (Cat# ab150440, Abcam, USA). Importantly, all IHC slides were assessed based on the evaluation method of the previously published study (30–33). Representative staining images of eight genes from the BRGPI model are shown in **Supplementary Figure S2**.

Statistical Analysis

Data analysis was performed using GraphPad Prism software (version 5.0) and R software (version 3.6.0).

Survival was assessed using the log-rank test and Kaplan-Meier analysis. Differences between the two groups were evaluated using Chi-square or Mann–Whitney U test. Notably, all statistical analyses were double-sided, and statistical significance was defined as P values less than 0.05.

RESULTS

Establishment and Definition of the BRGPI in the Training Cohort

To develop a signature to predict patients who might benefit from ICIs, we selected 222 immune-related genes shared by all cohorts and constructed 2526 immune-related gene pairs by pairwise comparison. Next, 311 prognostic BRGPs that were significantly related with PFS (P<0.05) were chosen *via* the univariate Cox proportional hazards regression modelling. We then used multivariate Cox regression to determine gene pairs with the best prognostic performance to obtain the optimized and practical value. According to the minimum criteria, a novel prognostic signature with four BRGPs was proposed (**Figure 1A**). The four selected BRGPs and their coefficients are listed in **Supplementary Table S2**. Next, *via* the multivariate Cox regression, the BRGPI for each patient was scored based on the following formula (33): BRGPI score= 1.521 × value of CCL2|VEGFA +1.257 × value of CDK1|CXCL9 −1.495 × value of HLA-DOB|LCK +1.812 × value of IL-12A|TBX21. According to the optimal cut-off value of 0.317, we classified patients into the BRGPI-low (n=18) and BRGPI-high groups (n=17).

Furthermore, we calculated the AUC value of the ROC and performed Kaplan–Meier survival analysis to validate the predictive performance of the novel BRGPI. The results showed that the AUC value at one-year PFS was 0.842 (**Figure 1B**). Patients with high BRGPI had significantly worse PFS than those with low BRGPI (P<0.001; **Figure 1C**). Next, univariate and multivariate Cox regression analyses were conducted in the training cohort and results showed that BRGPI was an independent prognostic factor (BRGPI: P<0.001, **Figures 1D, E**). We also analyzed the distributions of the BRGPI among the patient subgroups with a different response to immunotherapy. These results showed that patients had a better response in the BRGPI-low group. Furthermore—regardless of the evaluation criteria of the response group—the BRGPI was higher in patients with worse immunotherapy responses, which supports the prediction value of the index (CR/PR, SD, and PD, P=0.0033, **Figure 1F**; response and non-response, P=0.0436, **Figure 1G**; PD and non-PD, P=0.0009, **Figure 1H**). Overall, the predictive ability of the BRGPI for the clinical response of immunotherapy in patients with NSCLC is initially verified and expected to carry next research.

External Validation of the BRGPI in the Test Cohort

To confirm the prediction power of BRGPI for anti-PD-1 immunotherapy in NSCLC, we used the same formula for the data in the testing dataset from the GSE136961 cohort. The index of each patient in the GSE136961 cohort was performed and then 20 patients were assigned to the BRGPI-low group (n=11) and BRGPI-high group (n=9) according to the training cohort's cut-off value. By constructing a ROC curve, the AUC value at a progression-free survival was 0.869. This demonstrated BRGPI had an accurate predictive value for patient prognosis in the testing dataset (**Figure 2A**). *Via* the Kaplan–Meier survival analysis, the results showed that patients with the low-BRGPI score had prominently better PFS than those with the high-BRGPI score (P=0.004; **Figure 2B**). Consistent with the previous findings, univariate and multivariate Cox regression analyses indicated that BRGPI was an independent prognostic factor after

adjustment by sex and pathology (BRGPI: P=0.003, **Figure 2C**; BRGPI: P<0.001, **Figure 2D**).

Independent Validation of the BRGPI in the CICAMS Cohort

To further access the robustness and practicability of BRGPI, we used protein expression values to investigate its prognostic power in an independent cohort consisting of 19 patients with NSCLC. For each sample, pairwise comparisons for the protein expression values of 8 genes were performed to acquire a score (0 or 1) for each gene pair. We then calculated the BRGPI score of each patient using the mentioned above formula. Representative staining images of eight genes from the BRGPI model are shown in **Supplementary Figure S2**. Given that the AUC value for one year of PFS was 0.849, the BRGPI for patients with NSCLC who received ICIs was a reliable predictive signature at the protein level (**Figure 3A**). We then stratified the 19 patients into a BRGPI-low-group (n=9) and a BRGPI-high

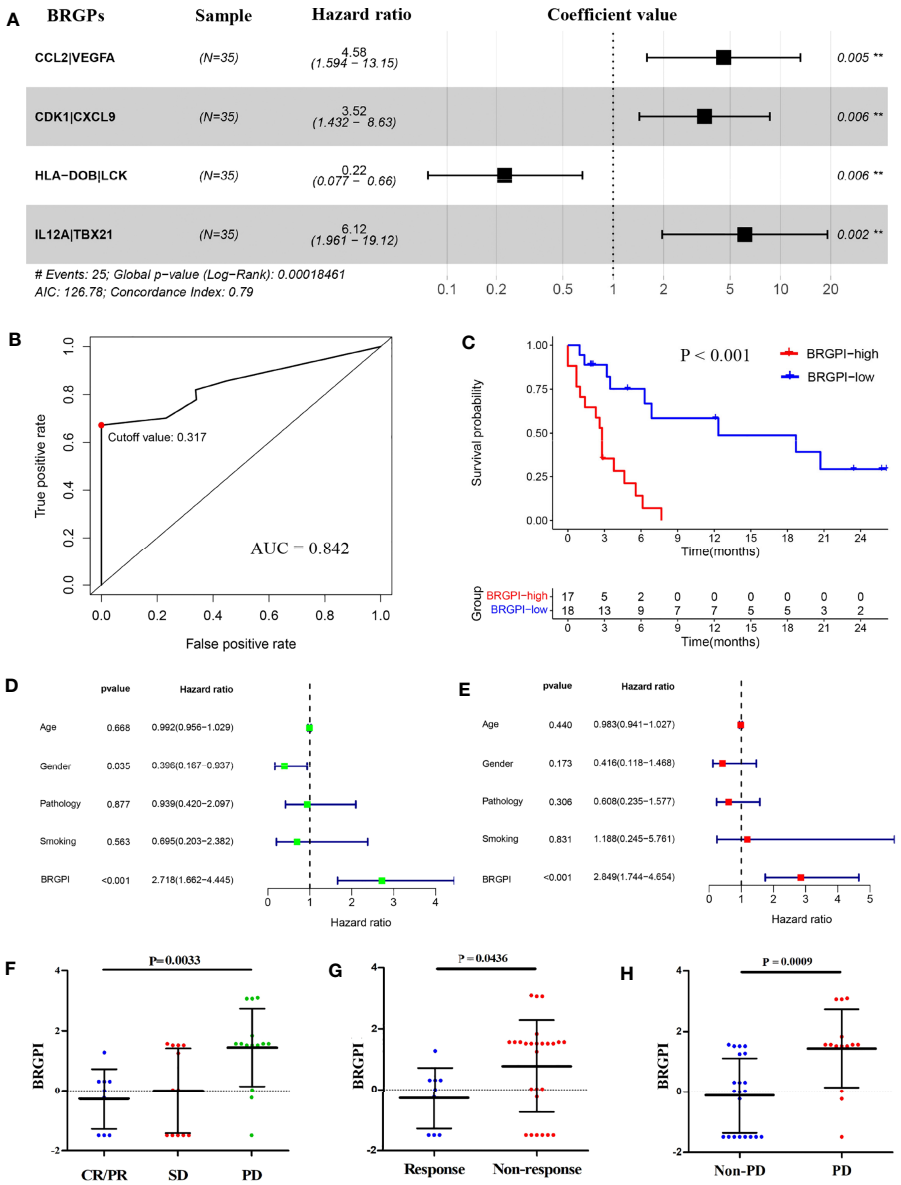

FIGURE 1 | Construction and definition of the BRGPI for patients with NSCLC treated with anti-PD-1 immunotherapy in the training cohort. **(A)** Prognostic values of four selected BRGPs. **(B)** ROC analysis of the BRGPI for progression-free survival. **(C)** Survival curve of progression-free survival for patients with NSCLC treated with anti-PD-1 immunotherapy according to the BRGPI. **(D, E)** Univariate **(D)** and multivariate **(E)** regression analyses of the associations between BRGPI and clinical variables for the predictive ability of progression-free survival. **(F)** The distributions of the BRGPI scores among the patients receiving CR/PR, SD, and PD. **(G)** The distributions of the BRGPI scores between the two groups (response and non-response). **(H)** The distributions of the BRGPI scores between the two groups (Non-PD and PD). **P < 0.01.

group (n=10) with the same cut-off value. The results revealed a notable difference in PFS between the two groups *via* the Kaplan–Meier survival analysis (P<0.001; **Figure 3B**). Consistent with the prior results, univariate and multivariate Cox regression analysis results show that BRGPI was an independent prognostic factor of anti-PD-1 immunotherapy (BRGPI: P=0.012, **Figure 3C**; BRGPI: P=0.011, **Figure 3D**). Further, BRGPI of the CICAMS cohort also can stratify clinically defined groups of patients with different responses (PR, SD, and PD, P=0.0212, **Figure 3E**; response and non-response, P=0.0274, **Figure 3F**; PD and non-PD, P=0.0351, **Figure 3G**), which support the clinical practice value of the prognostic signature.

Stratification Analysis of BRGPI for Its Predictive Value

To verify the reliability of the BRGPI considering pathology for NSCLC, we performed Kaplan–Meier survival analysis in patients grouped by pathological type for each of the three independent cohorts. Notably, the BRGPI remained highly prognostic for the immunotherapy outcome. In the multicohort analysis—in patients with both non-squamous and squamous-cell NSCLC who were treated with anti-PD-1 immunotherapy—those in the BRGPI-low groups had better PFS than those in the BRGPI-high groups (non-squamous tumors in GSE93157: P<0.001, **Supplementary Figure S3A**; squamous tumors in GSE93157: P=0.032, **Supplementary Figure S3B**; non-squamous tumors in GSE136961: P=0.016, **Supplementary Figure S3C**; squamous tumors in GSE136961: P=0.088, **Supplementary Figure S3D**; non-squamous tumors in CICAMS: P=0.013, **Supplementary Figure S3E**; squamous tumors in CICAMS: P=0.016, **Supplementary Figure S3F**). Noticeably, the statistical significance of Kaplan–Meier survival analysis in squamous tumors from GSE136961 was not significant, but the Kaplan–Meier survival curves of the two groups were slightly separated owning to the very small sample size.

Association of BRGPI and PD-L1

Given the widespread use of PD-L1 expression level on the cell surface as a validated prediction marker for the response of ICIs, we supposed that BRGPI could improve the prognostic value in combination with the corresponding PD-L1 expression level, although PD-L1 was not a prognostic risk factor in multivariate analyses of CICAMS cohort. Therefore, the prognostic performance of PD-L1 was first assessed *via* the ROC and Kaplan–Meier survival analyses. The AUC value of PD-L1 at PFS was 0.579 for the CICAMS cohort (**Supplementary Figure S4A**). Also, Kaplan–Meier survival analyses did not show a significant difference in PFS of patients with high-expression (n=7) and low-expression (n=12) PD-L1 (**Supplementary Figure S4B**). Nonetheless, the results of the Kaplan–Meier survival analyses the in subset grouped by expression of PD-L1 show that regardless of the expression level of PD-L1, patients in the BRGPI-low group demonstrated longer PFS (P<0.05; **Supplementary Figures S4C, D**), which highlighted the reliable predictive ability of the novel BRGPI. Next, we classified the patients into three subgroups according to the

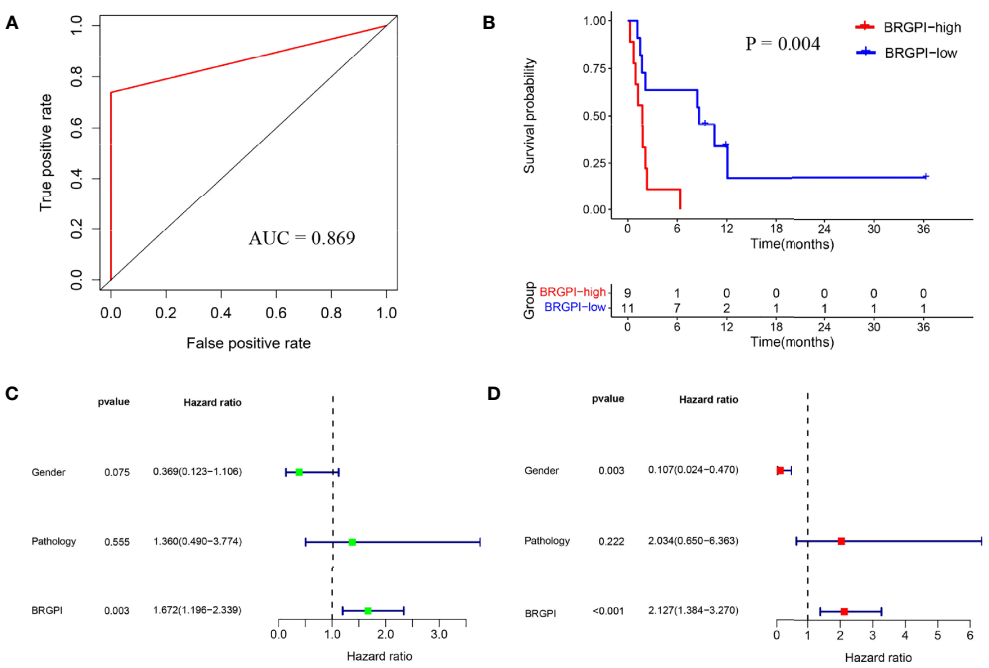

FIGURE 2 | External validation of the BRGPI for patients with NSCLC treated with anti-PD-1 immunotherapy in the test cohort. **(A)** ROC analysis of the BRGPI for progression-free survival. **(B)** Survival curve of progression-free survival for patients with NSCLC treated with anti-PD-1 immunotherapy according to the BRGPI. **(C, D)** Univariate **(C)** and multivariate **(D)** regression analyses of the associations between BRGPI and clinical variables for the predictive ability of progression-free survival.

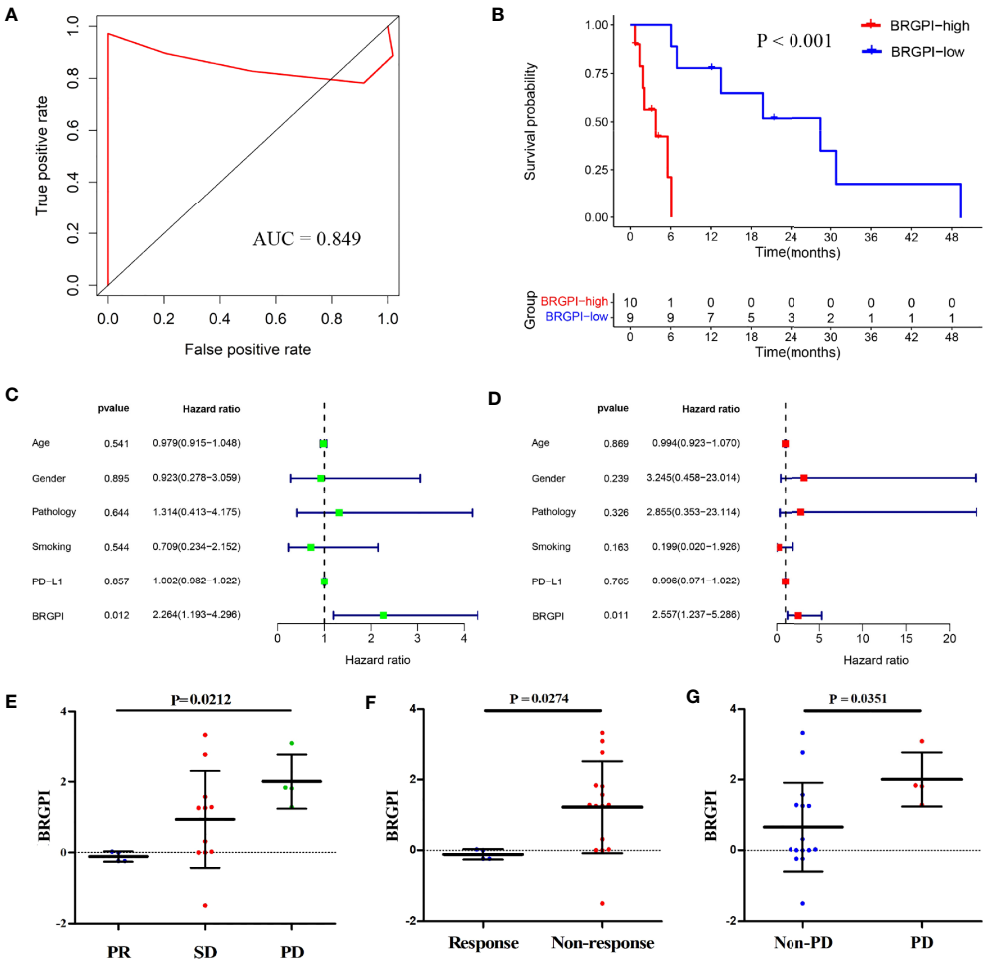

FIGURE 3 | Independent validation of the BRGPI for patients with NSCLC treated with anti-PD-1 immunotherapy in the CICAMS cohort. **(A)** ROC analysis of the BRGPI for progression-free survival. **(B)** Survival curve of progression-free survival for patients with NSCLC treated with anti-PD-1 immunotherapy according to the BRGPI. **(C, D)** Univariate **(C)** and multivariate **(D)** regression analyses of the associations between BRGPI and clinical variables for the predictive ability of progression-free survival. **(E)** The distributions of the BRGPI scores among the patients receiving PR, SD, and PD. **(F)** The distributions of the BRGPI scores between the two groups (response and non-response). **(G)** The distributions of the BRGPI scores between the two groups (Non-PD and PD).

BRGPI and expression level of PD-L1: the BRGPI-low and PD-L1-high group, the BRGPI-low or PD-L1-high group, and the BRGPI-high and PD-L1-low group. As expected, the patients in BRGPI-low and PD-L1-high subgroup derived more clinical benefit while the BRGPI-high and PD-L1-low subgroups derived less clinical benefit (P=0.047; **Supplementary Figure S4E**).

DISCUSSION

Immunotherapy is revolutionizing cancer treatment, including NSCLC treatment. There has been a rapid rise in the number of ICIs targeting the PD-1/PD-L1 axis clinical trials in NSCLC over the past 15 years. However, it is not effective for all patients. Only a subset will demonstrate durable responses and improved survival after receiving ICI treatment. Although biomarker-related responses to ICI therapy for patients with NSCLC holds promise, there are very few studies within medical literature. Numerous prognostic factors of NSCLC have been continually reported such as PD-L1 expression level and TMB. Currently, detection of PD-L1 expression level is still the standard means of identifying which patients are more likely to benefit from immunotherapy. While owing to different platforms and various cut-off points for the expression between different immunotherapy agents, PD-L1 remains a controversial biomarker for immunotherapy response. In addition, TMB also faces a similar situation as PD-L1. Data across platforms cause biases and the cut-off points may not be reproducible. Therefore, there is an urgent and unmet need for a feasible tool—immune to data source bias—for identifying patients who might derive benefit from anti-PD-1 immunotherapy in clinical practice.

Recent studies show that the immunologic gene expression is correlated with the response to immunotherapy (34).

Immunogenic genes related to tumor antigen presentation, chemokine expression, and cytotoxic activity. These features were sufficient for the immunologic landscape (35, 36). A better presentation of the tumor immunologic microenvironment could help identify reliable biomarkers for immunotherapy. The relative ranking of paired-gene expressions provides new ideas for avoiding data preprocessing, such as normalization and scaling. The established BRGPI of the tumor sample, completely based on the relative expression of the gene-pairs method, avoids the batch effect or bias on measurement platforms; there is no need for normalization. The immune-related gene-pair model appears promising for predicting immunotherapy response. Here, we constructed a prognostic BRGPI based on the relative ranking of gene expression values.

In this study, 222 shared immune-related genes from Pan-Cancer Immune Profiling Panel were selected to construct 2526 BRGPs. Then, 311 BRGPs significantly associated with PFS were determined by univariate Cox regression analysis in the signature-training set (GSE93157) and four BRGPs were selected using multivariate Cox regression to calculate the BRGPI. Remarkably, BRGPI can act as an independent prognostic factor and help identify patients in different response groups. By external validation, the GSE136961 cohort also supports the predictive value of BRGPI. Moreover, we further validated the discriminatory performance of BRGPI using protein expression values, acquired using the IHC technique, in an independent CICAMS cohort. The IHC method might be more suitable and convenient for clinical application because of its simplicity and low cost. Considering pathological type—whether non-squamous or squamous-cell NSCLC—patients in BRGPI-low groups had better PFS times than those in the BRGPI-high groups. This indicated that the BRGPI signature is promising preliminary value. We also investigated the association of BRGPI and PD-L1 expression. The predictive ability of PD-L1 was poor in the analyses of the CICAMS cohort. This might be because multiple immune-related genes may better represent the complex immune microenvironment. When patients were grouped by the PD-L1 expression, we found that—no matter PD-L1 expression level—the BRGPI-low subgroup showed longer PFS. Further analysis demonstrated that the patients in BRGPI-low and PD-L1-high subgroup derived more clinical benefit while the BRGPI-high and PD-L1-low subgroups derived less clinical benefit. The combination with PD-L1 underscores the reliability and predictive validity for predicting immunotherapy response, in addition to clinical utility.

BRGPI was constructed by pairwise comparison and the score of each patient was calculated based on his or her own corresponding gene expression. Thus, our prognostic model can avoid the batch effect or bias inherent to different measurement platforms. Additionally, there is no need for data normalization. According to these advantages—and considering the same formula and cut-off value in the training set—this method can be translated into clinical practice as a tool for predicting a patient with NSCLC's response to immunotherapy.

Nevertheless, the limitations of this study should be acknowledged. First, the size of the three datasets was relatively small, despite our attempts to enroll as many datasets as possible, and inclusion of the GEO and CICAMS cohorts increase the rigor of our biomarker validation process. Second, because this was a retrospective study, further validation of this signature should be conducted in prospective paradigms.

In conclusion, this study was the first to highlight a BRGPI based on benefit-related gene pairs. This method may emerge as a powerful prognostic tool for immunotherapy and help further optimize the ICI paradigm of personalized medicine for patients with advanced NSCLC.

DATA AVAILABILITY STATEMENT

The datasets presented in this study can be found in online repositories. The names of the repository/repositories and accession number(s) can be found in the article/**Supplementary Material**.

ETHICS STATEMENT

The Ethics Committee of CICAMS approved the human tissue study protocol, and the approval number was 20/242-2438. The patients/participants provided their written informed consent to participate in this study.

AUTHOR CONTRIBUTIONS

CL and SW designed the study, performed experiments, analyzed data, and wrote the manuscript. SZ, FX, ZC, XF, YW, and XQ performed experiments and analyzed data. JH and NS conceived and designed the study and wrote the manuscript. All authors contributed to the article and approved the submitted version.

FUNDING

This work was supported by the National Key Basic Research Development Plan (grant number 2018YFC1312105), the National Natural Science Foundation of China (grant numbers 81802299, 81502514), the Graduate Innovation Funds of Peking Union Medical College (grant number 2019-1002-06), the National Key R&D Program of China (grant numbers 2018YFC1312100, 2018YFC1312102), the CAMS Innovation Fund for Medical Sciences (grant numbers 2016-I2M-1-001, 2017-I2M-1-005), and the Fundamental Research Funds for the Central Universities (grant number 3332018070).

SUPPLEMENTARY MATERIAL

The Supplementary Material for this article can be found online at: https://www.frontiersin.org/articles/10.3389/fimmu.2021.782106/full#supplementary-material

Supplementary Table 1 | Demographic characteristics of NSCLC patients treated with anti-PD-1 immunotherapy in three cohorts.

Supplementary Table 2 | Model information about BRGPI.

Supplementary Figure 1 | The analysis pipeline of the construction and validation of BRGPI for NSCLC patients treated with anti-PD-1 immunotherapy.

Supplementary Figure 2 | Representative staining images of eight genes from the BRGPI model and PD-L1 at different levels.

Supplementary Figure 3 | Stratification analysis of BRGPI for its predictive value of progression-free survival in NSCLC patients treated with anti-PD-1 immunotherapy. **(A, B)** Kaplan-Meier survival curve of progression-free survival for non-squamous **(A)** and squamous-cell **(B)** NSCLC patients treated with anti-PD-1 immunotherapy based on the BRGPI in the GSE93157 cohort. **(C, D)** Kaplan-Meier survival curve of progression-free survival for non-squamous **(C)** and squamous-cell **(D)** NSCLC patients treated with anti-PD-1 immunotherapy based on the BRGPI in the GSE136961 cohort. **(E, F)** Kaplan-Meier survival curve of progression-free survival for non-squamous **(E)** and squamous-cell **(F)** NSCLC patients treated with anti-PD-1 immunotherapy based on the BRGPI in the CICAMS cohort.

Supplementary Figure 4 | Association of BRGPI and PD-L1 for NSCLC patients treated with anti-PD-1 immunotherapy in the CICAMS cohort. **(A)** ROC analysis of PD-L1 expression for progression-free survival. **(B)** Kaplan-Meier survival curve of progression-free survival for NSCLC patients treated with anti-PD-1 immunotherapy classified by PD-L1 status. **(C, D)** Kaplan-Meier survival curve of progression-free survival for NSCLC patients with **(C)** and without **(D)** positive PD-L1 expression based on the BRGPI after anti-PD-1 immunotherapy. **(E)** Kaplan-Meier survival curve of progression-free survival for NSCLC patients treated with anti-PD-1 immunotherapy among subgroups categorized by BRGPI and PD-L1.

REFERENCES

1. Bray F, Ferlay J, Soerjomataram I, Siegel RL, Torre LA, Jemal A. Global Cancer Statistics 2018: GLOBOCAN Estimates of Incidence and Mortality Worldwide for 36 Cancers in 185 Countries. *CA: Cancer J Clin* (2018) 68:394–424. doi: 10.3322/caac.21492
2. Miller KD, Nogueira L, Mariotto AB, Rowland JH, Yabroff KR, Alfano CM, et al. Cancer Treatment and Survivorship Statistics, 2019. *CA: Cancer J Clin* (2019) 69:363–85. doi: 10.3322/caac.21565
3. Ettinger DS, Aisner DL, Wood DE, Akerley W, Bauman J, Chang JY, et al. NCCN Guidelines Insights: Non-Small Cell Lung Cancer, Version 5.2018. *J Natl Compr Cancer Network JNCCN* (2018) 16:807–21. doi: 10.6004/jnccn.2018.0062
4. Gainor JF, Shaw AT. Emerging Paradigms in the Development of Resistance to Tyrosine Kinase Inhibitors in Lung Cancer. *J Clin Oncol* (2013) 31:3987–96. doi: 10.1200/JCO.2012.45.2029
5. Herbst RS, Baas P, Kim DW, Felip E, Perez-Gracia JL, Han JY, et al. Pembrolizumab Versus Docetaxel for Previously Treated, PD-L1-Positive, Advanced Non-Small-Cell Lung Cancer (KEYNOTE-010): A Randomised Controlled Trial. *Lancet (Lond Engl)* (2016) 387:1540–50. doi: 10.1016/S0140-6736(15)01281-7
6. Rittmeyer A, Barlesi F, Waterkamp D, Park K, Ciardiello F, von Pawel J, et al. Atezolizumab Versus Docetaxel in Patients With Previously Treated Non-Small-Cell Lung Cancer (OAK): A Phase 3, Open-Label, Multicentre Randomised Controlled Trial. *Lancet (Lond Engl)* (2017) 389:255–65. doi: 10.1016/S0140-6736(16)32517-X
7. Borghaei H, Paz-Ares L, Horn L, Spigel DR, Steins M, Ready NE, et al. Nivolumab Versus Docetaxel in Advanced Nonsquamous Non-Small-Cell Lung Cancer. *N Engl J Med* (2015) 373:1627–39. doi: 10.1056/NEJMoa1507643
8. Brahmer J, Reckamp KL, Baas P, Crino L, Eberhardt WE, Poddubskaya E, et al. Nivolumab Versus Docetaxel in Advanced Squamous-Cell Non-Small-Cell Lung Cancer. *N Engl J Med* (2015) 373:123–35. doi: 10.1056/NEJMoa1504627
9. Wu YL, Lu S, Cheng Y, Zhou C, Wang J, Mok T, et al. Nivolumab Versus Docetaxel in a Predominantly Chinese Patient Population With Previously Treated Advanced NSCLC: CheckMate 078 Randomized Phase III Clinical Trial. *J Thorac Oncol* (2019) 14(5):867–75. doi: 10.1016/j.jtho.2019.01.006
10. Brustugun OT, Sprauten M, Helland A. Real-World Data on Nivolumab Treatment of Non-Small Cell Lung Cancer. *Acta Oncol (Stockholm Sweden)* (2017) 56:438–40. doi: 10.1080/0284186X.2016.1253865
11. Dudnik E, Moskovitz M, Daher S, Shamai S, Hanovich E, Grubstein A, et al. Effectiveness and Safety of Nivolumab in Advanced Non-Small Cell Lung Cancer: The Real-Life Data. *Lung Cancer (Amsterdam Netherlands)* (2018) 126:217–23. doi: 10.1016/j.lungcan.2017.11.015
12. Ahn BC, Pyo KH, Xin CF, Jung D, Shim HS, Lee CY, et al. Comprehensive Analysis of the Characteristics and Treatment Outcomes of Patients With Non-Small Cell Lung Cancer Treated With Anti-PD-1 Therapy in Real-World Practice. *J Cancer Res Clin Oncol* (2019) 145(6):1613–23. doi: 10.1007/s00432-019-02899-y
13. Yoneda K, Imanishi N, Ichiki Y, Tanaka F. Immune Checkpoint Inhibitors (ICIs) in Non-Small Cell Lung Cancer (NSCLC). *J UOEH* (2018) 40:173–89. doi: 10.7888/juoeh.40.173
14. Bodor JN, Boumber Y, Borghaei H. Biomarkers for Immune Checkpoint Inhibition in Non-Small Cell Lung Cancer (NSCLC). *Cancer* (2020) 126:260–70. doi: 10.1002/cncr.32468
15. Choucair K, Morand S, Stanbery L, Edelman G, Dworkin L, Nemunaitis J. TMB: A Promising Immune-Response Biomarker, and Potential Spearhead in Advancing Targeted Therapy Trials. *Cancer Gene Ther* (2020) 27(12):841–53. doi: 10.1038/s41417-020-0174-y
16. Prelaj A, Tay R, Ferrara R, Chaput N, Besse B, Califano R. Predictive Biomarkers of Response for Immune Checkpoint Inhibitors in Non-Small-Cell Lung Cancer. *Eur J Cancer (Oxford Engl 1990)* (2019) 106:144–59. doi: 10.1016/j.ejca.2018.11.002
17. Schoenfeld AJ, Rizvi H, Bandlamudi C, Sauter JL, Travis WD, Rekhtman N, et al. Clinical and Molecular Correlates of PD-L1 Expression in Patients With Lung Adenocarcinomas. *Ann Oncol* (2020) 31:599–608. doi: 10.1016/j.annonc.2020.01.065
18. Mehnert JM, Monjazeb AM, Beerthuijzen JMT, Collyar D, Rubinstein L, Harris LN. The Challenge for Development of Valuable Immuno-Oncology Biomarkers. *Clin Cancer Res* (2017) 23:4970–9. doi: 10.1158/1078-0432.CCR-16-3063
19. Wang Z, Duan J, Cai S, Han M, Dong H, Zhao J, et al. Assessment of Blood Tumor Mutational Burden as a Potential Biomarker for Immunotherapy in Patients With Non-Small Cell Lung Cancer With Use of a Next-Generation Sequencing Cancer Gene Panel. *JAMA Oncol* (201) 5(5):696–702. doi: 10.1001/jamaoncol.2018.7098
20. Hellmann MD, Ciuleanu TE, Pluzanski A, Lee JS, Otterson GA, Audigier-Valette C, et al. Nivolumab Plus Ipilimumab in Lung Cancer With a High Tumor Mutational Burden. *N Engl J Med* (2018) 378:2093–104. doi: 10.1056/NEJMoa1801946
21. Hellmann MD, Nathanson T, Rizvi H, Creelan BC, Sanchez-Vega F, Ahuja A, et al. Genomic Features of Response to Combination Immunotherapy in Patients With Advanced Non-Small-Cell Lung Cancer. *Cancer Cell* (2018) 33:843–52.e844. doi: 10.1016/j.ccell.2018.03.018
22. Xiong Y, Liu L, Bai Q, Xia Y, Qu Y, Wang J, et al. Individualized Immune-Related Gene Signature Predicts Immune Status and Oncologic Outcomes in Clear Cell Renal Cell Carcinoma Patients. *Urol Oncol* (2020) 38:7 e1–8. doi: 10.1016/j.urolonc.2019.09.014
23. Sun XY, Yu SZ, Zhang HP, Li J, Guo WZ, Zhang SJ. A Signature of 33 Immune-Related Gene Pairs Predicts Clinical Outcome in Hepatocellular Carcinoma. *Cancer Med* (2020) 9:2868–78. doi: 10.1002/cam4.2921
24. Leek JT, Scharpf RB, Bravo HC, Simcha D, Langmead B, Johnson WE, et al. Tackling the Widespread and Critical Impact of Batch Effects in High-Throughput Data. *Nat Rev Genet* (2010) 11:733–9. doi: 10.1038/nrg2825
25. Popovici V, Budinska E, Tejpar S, Weinrich S, Estrella H, Hodgson G, et al. Identification of a Poor-Prognosis BRAF-Mutant–Like Population of Patients

With Colon Cancer. *J Clin Oncol* (2012) 30:1288–95. doi: 10.1200/JCO.2011.39.5814
26. Ciccarese C, Iacovelli R, Bria E, Modena A, Massari F, Brunelli M, et al. The Incidence and Relative Risk of Pulmonary Toxicity in Patients Treated With Anti-PD1/PD-L1 Therapy for Solid Tumors: A Meta-Analysis of Current Studies. *Immunotherapy* (2017) 9:579–87. doi: 10.2217/imt-2017-0018
27. Rizvi H, Sanchez-Vega F, La K, Chatila W, Jonsson P, Halpenny D, et al. Molecular Determinants of Response to Anti-Programmed Cell Death (PD)-1 and Anti-Programmed Death-Ligand 1 (PD-L1) Blockade in Patients With Non-Small-Cell Lung Cancer Profiled With Targeted Next-Generation Sequencing. *J Clin Oncol* (2018) 36:633–41. doi: 10.1200/JCO.2017.75.3384
28. Cesano A. Ncounter((R)) PanCancer Immune Profiling Panel (NanoString Technologies, Inc., Seattle, Wa). *J Immunother Cancer* (2015) 3:42. doi: 10.1186/s40425-015-0088-7
29. Li B, Cui Y, Diehn M, Li R. Development and Validation of an Individualized Immune Prognostic Signature in Early-Stage Nonsquamous Non-Small Cell Lung Cancer. *JAMA Oncol* (2017) 3:1529–37. doi: 10.1001/jamaoncol.2017.1609
30. Liu C, Zheng S, Jin R, Wang X, Wang F, Zang R, et al. The Superior Efficacy of Anti-PD-1/PD-L1 Immunotherapy in KRAS-Mutant Non-Small Cell Lung Cancer That Correlates With an Inflammatory Phenotype and Increased Immunogenicity. *Cancer Lett* (2020) 470:95–105. doi: 10.1016/j.canlet.2019.10.027
31. Long J, Wang A, Bai Y, Lin J, Yang X, Wang D, et al. Development and Validation of a TP53-Associated Immune Prognostic Model for Hepatocellular Carcinoma. *EBioMedicine* (2019) 42:363–74. doi: 10.1016/j.ebiom.2019.03.022
32. Alsaleem MA, Ball G, Toss MS, Raafat S, Aleskandarany M, Joseph C, et al. A Novel Prognostic Two-Gene Signature for Triple Negative Breast Cancer. *Modern Pathol* (2020) 33(11):2208–20. doi: 10.1038/s41379-020-0563-7
33. Liu C, Zheng S, Wang S, Wang X, Feng X, Sun N, et al. Development and External Validation of a Composite Immune-Clinical Prognostic Model Associated With EGFR Mutation in East-Asian Patients With Lung Adenocarcinoma. *Ther Adv Med Oncol* (2021) 13:17588359211006949. doi: 10.1177/17588359211006949
34. Prat A, Navarro A, Pare L, Reguart N, Galvan P, Pascual T, et al. Immune-Related Gene Expression Profiling After PD-1 Blockade in Non-Small Cell Lung Carcinoma, Head and Neck Squamous Cell Carcinoma, and Melanoma. *Cancer Res* (2017) 77:3540–50. doi: 10.1158/0008-5472.CAN-16-3556
35. Lee CK, Man J, Lord S, Cooper W, Links M, Gebski V, et al. Clinical and Molecular Characteristics Associated With Survival Among Patients Treated With Checkpoint Inhibitors for Advanced Non-Small Cell Lung Carcinoma: A Systematic Review and Meta-Analysis. *JAMA Oncol* (2018) 4:210–6. doi: 10.1001/jamaoncol.2017.4427
36. Ribas A, Wolchok JD. Cancer immunotherapy using checkpoint blockade. *Science* (2018) 359:1350–5. doi: 10.1126/science.aar4060

Conflict of Interest: The authors declare that the research was conducted in the absence of any commercial or financial relationships that could be construed as a potential conflict of interest.

Publisher's Note: All claims expressed in this article are solely those of the authors and do not necessarily represent those of their affiliated organizations, or those of the publisher, the editors and the reviewers. Any product that may be evaluated in this article, or claim that may be made by its manufacturer, is not guaranteed or endorsed by the publisher.

frontiers in Immunology

ORIGINAL RESEARCH
published: 23 November 2021
doi: 10.3389/fimmu.2021.758004

S100A2 Is a Prognostic Biomarker Involved in Immune Infiltration and Predict Immunotherapy Response in Pancreatic Cancer

Yuan Chen[†], *Chengcheng Wang*[†], *Jianlu Song*, *Ruiyuan Xu*, *Rexiati Ruze and Yupei Zhao*[*]

Department of General Surgery, State Key Laboratory of Complex Severe and Rare Diseases, Peking Union Medical College Hospital, Chinese Academy of Medical Sciences, Peking Union Medical College, Beijing, China

OPEN ACCESS

Edited by:
Alison Taylor,
University of Leeds, United Kingdom

Reviewed by:
Xiaokang Li,
Shandong University, China
Stefano Ugel,
University of Verona, Italy

***Correspondence:**
Yupei Zhao
zhao8028@263.net

[†]*These authors have contributed equally to this work*

Specialty section:
This article was submitted to Cancer Immunity and Immunotherapy, a section of the journal Frontiers in Immunology

Received: *13 August 2021*
Accepted: *02 November 2021*
Published: *23 November 2021*

Citation:
Chen Y, Wang C, Song J, Xu R, Ruze R and Zhao Y (2021) S100A2 Is a Prognostic Biomarker Involved in Immune Infiltration and Predict Immunotherapy Response in Pancreatic Cancer. Front. Immunol. 12:758004. doi: 10.3389/fimmu.2021.758004

Pancreatic cancer (PC) is a highly fatal and aggressive disease with its incidence and mortality quite discouraging. It is of great significance to construct an effective prognostic signature of PC and find the novel biomarker for the optimization of the clinical decision-making. Due to the crucial role of immunity in tumor development, a prognostic model based on nine immune-related genes was constructed, which was proved to be effective in The Cancer Genome Atlas (TCGA) training set, TCGA testing set, TCGA entire set, GSE78229 set, and GSE62452 set. Furthermore, S100A2 (S100 Calcium Binding Protein A2) was identified as the gene occupying the most paramount position in risk model. Gene set enrichment analysis (GSEA), ESTIMATE and CIBERSORT algorithm revealed that S100A2 was closely associated with the immune status in PC microenvironment, mainly related to lower proportion of CD8+T cells and activated NK cells and higher proportion of M0 macrophages. Meanwhile, patients with high S100A2 expression might get more benefit from immunotherapy according to immunophenoscore algorithm. Afterwards, our independent cohort was also used to demonstrate S100A2 was an unfavorable marker of PC, as well as its remarkably positive correlation with the expression of PD-L1. In conclusion, our results demonstrate S100A2 might be responsible for the preservation of immune-suppressive status in PC microenvironment, which was identified with significant potentiality in predicting prognosis and immunotherapy response in PC patients.

Keywords: S100A2, tumor microenvironment, immune cells, prognostic model, immunotherapy, PD-L1, pancreatic cancer

INTRODUCTION

Pancreatic cancer (PC) is one of the most aggressive malignancies, with a five-year survival rate of only 10% in the United States (1). According to the latest epidemiological data, there are 495,773 new cases and 466,003 deaths of PC worldwide in 2020, making ratio of incidence and mortality close to 1:1 (2). In addition to the lack of sensitive screening methods and the rapid progression of PC, the dismal prognosis of this disease is largely attributable to the lack of valid risk prediction models and biomarkers in PC development (3). Therefore, it is of great significance to construct an effective prognostic signature of PC and find the novel biomarker for the optimization of the clinical decision-making.

Tumor microenvironment (TME), a concept developed from Paget's "seed and soil" theory, is regarded as both a cause and consequence of tumorigenesis, which is demonstrated to provide a permissive environment for tumor initiation and progression (4, 5). In addition to fibroblasts endothelial cells, stromal cells, blood vessels and secreted factors, the TME comprises innate and adaptive immune cells, which have a profound impact on tumor development (6, 7). In recent years, the vital role of immune cells in the occurrence and progression of PC is gradually revealed (8–10). For example, Yamamoto et al. identified NBR1-mediated selective macroautophagy/autophagy of MHC-I hindered cancer cell recognition and clearance by CD8+ T cells in PC (11), and granulin secretion by metastasis-associated macrophages activates resident hepatic stellate cells into myofibroblasts, resulting in a fibrotic microenvironment that sustains metastatic PC growth (12). Meanwhile, although immunotherapy is almost ineffective for PC (13, 14), PC patients who exhibited high effector T-cell infiltration in tumor had longer overall survival (15, 16), implying that valuing immune heterogeneity and remodeling the immune microenvironment may hold promise for PC treatment. Therefore, we considered a prognostic model based on immune-related genes (IRGs) to better predict the prognosis of PC patients and optimize the clinical decision-making. Furthermore, the most paramount gene and its potential mechanisms were further explored, as well as its ability to predict patients' response to immunotherapy.

In the present study, we constructed a prognostic model based on nine IRGs and the corresponding nomogram, which were proved to be an independent risk factor and was validated in the training set, testing set, entire set, GSE78229 set and GSE62452 set. S100A2 (S100 Calcium Binding Protein A2), a highly conserved elongation factor (EF)-hand calcium-binding protein, was identified as the gene occupying the most paramount position in the risk signature. GSEA, ESTIMATE and CIBERSORT algorithm revealed that S100A2 was closely associated with the immune status in the PC microenvironment, mainly related to lower proportion of CD8+T cells and activated NK cells and higher proportion of M0 macrophages. Meanwhile, the results of immunophenoscore (IPS) algorithm proved that patients with high S100A2 expression might get more benefit from immunotherapy. Afterwards, our own independent cohort (PUMCH cohort) was also utilized to demonstrate S100A2 was an unfavorable marker of PC, as well as its remarkably positive correlation with the expression of PD-L1.

MATERIALS AND METHODS

Datasets Sources and Processing

Immune-related genes were extracted and integrated from the ImmPort database (https://immport.niaid.nih.gov; ≤March 1, 2021) (17). Gene expression profile, clinical information, and mutation profile of the patients were downloaded from The Cancer Genome Atlas (TCGA) dataset (https://portal.gdc.cancer.gov/; ≤March 1, 2021). Samples with inadequate clinical information and follow-up period less than 30 days were excluded. Finally, 166 cases with corresponding gene expression profiles and clinical information were included in the study (**Table 1**, detailed in **Table S1**). Gene IDs was converted to gene symbol using a GFF3 file, which was downloaded from GENCODE (https://www.gencodegenes.org/). The gene expression data was converted to TPM (Transcripts Per Kilobase Million), and log2(TPM + 0.01) was used throughout the analysis unless otherwise noted. The samples of tumor tissues in TCGA set were randomly divided into to a training set and a testing set by a ratio of 7:3 using "sample" function of R software.

Meanwhile, GSE15471, GSE28735, GSE62165, GSE62452, GSE78229, and GSE71729 dataset were downloaded from the Gene Expression Omnibus (GEO) (http://www.ncbi.nlm.nih.gov/geo/) (18–23), in which GSE62452 and GSE78229 with corresponding clinical information were used for external validation (**Table 2**, detailed in **Tables S2**, **S3**). Expression values were calculated using the robust multi-array average (RMA) algorithm except GSE71729. The normalized expression matrix of microarray data can be directly download from the GEO dataset. They were performed on GPL570, GPL6244, GPL13667, and GPL20769 platform. Probes were matched to the gene symbols using the annotation files provided by the manufacturer.

Furthermore, a single-cell dataset CRA001160 was analyzed through Tumor Immune Single-cell Hub (TISCH) database (http://tisch.comp-genomics.org/) and Seurat package, and also cell type clustering and gene expression location analysis (24, 25). The expression profile of 51 pancreatic cell lines was integrated from the CCLE database (https://portals.broadinstitute.org/ccle) (26).

Construction and Validation of a Risk Signature Associated With Survival of PC Patients

Limma package was applied to screen differentially expressed genes (DEGs) in GSE15471, GSE28735, and GSE62165 datasets respectively (27). |Fold Change| >1.5 and false discovery rate (FDR) <0.05 were set as the cutoffs for the DEGs. The intersection of DEGs were selected as candidate genes. Univariate Cox regression was used to identify genes that were significantly associated with overall survival (OS) of PC patients

TABLE 1 | Clinical and pathologic information of training set, testing set and entire set.

Character	TRAINING SET		TESTING SET		ENTIRE SET	
	Number	%	Number	%	Number	%
Age						
Median	65		64.5		65	
Range	35–85		39–88		35–88	
OS (M)						
Median	15.3		16.1		15.6	
Range	1.1–72.7		1.0–91.4		1.0–91.4	
STATUS						
ALIVE	52	44.83	24	48.00	76	45.78
DEAD	64	55.17	26	52.00	90	54.22
gender						
Male	66	56.90	24	48.00	90	54.22
Female	50	43.10	26	52.00	76	45.78
AJCC_stage						
I	14	12.07	4	8.00	18	10.84
II	97	83.62	44	88.00	141	84.94
III	2	1.72	1	2.00	3	1.81
IV	3	2.59	1	2.00	4	2.41
Grade						
G1	17	14.66	9	18.00	26	15.66
G2	65	56.03	26	52.00	91	54.82
G3	32	27.59	15	30.00	47	28.31
G4	2	1.72	0	0.00	2	1.21
T STAGE						
T1	3	2.59	3	6.00	6	3.61
T2	16	13.79	5	10.00	21	12.65
T3	95	81.90	41	82.00	136	81.93
T4	2	1.72	1	2.00	3	1.81
N STAGE						
N0	32	27.59	13	26.00	45	27.11
N1	81	69.82	37	74.00	118	71.08
NX	3	2.59	0	0.00	3	1.81
M STAGE						
M0	59	50.86	17	34.00	76	45.78
M1	3	2.59	1	2.00	4	2.41
MX	54	46.55	32	64.00	86	51.81

in the training set (P <0.01). Subsequently, Least absolute shrinkage and selection operator (LASSO) regression analysis was further used to screen out the optimal gene combination for constructing the risk signature. According to the regression coefficient-weighted pseudogene expression, the risk signature was established as follows: Risk score = $(expr_{gene1} \times Coef_{gene1}) + (expr_{gene2} \times Coef_{gene2}) + \ldots + (expr_{genen} \times Coef_{genen})$. The efficiency and independence of the risk signature were assessed by Kaplan–Meier (K–M) curve, time-dependent receiver operating characteristic (ROC) curve and survival point diagram in both the internal validation set (training set, testing set, and entire set) and the external validation set (GSE78229 set and GSE62452 set). Copy number variation information of the nine genes was extracted from the cBioportal database (http://www.cbioportal.org/) (28), and protein expression in normal and tumor tissues was obtained from the Human Protein Atlas (HPA) database (https://www.proteinatlas.org/).

Meanwhile, in order to make the prediction model more accurate, the clinicopathological information was also incorporated with the riskscore to establish a nomogram, which was based on the results of the univariate and multivariate analysis by using the 'rms' package in R language. The C-index, calibration curve and time-dependent ROC curve of 1-, 1.5-, and 2-year were applied to evaluate the predictive effectiveness of the nomogram.

Differential Gene Analysis, Co-Expression Network Construction and Functional Enrichments Analysis Between S100A2 High and Low Expression Group

The pan-cancer expression analysis of S100A2 was performed through the GEPIA2 database (29). edgeR package was used to perform DEGs analysis between S100A2 high and low expression group, in which |Log2FC| >2 and FDR <0.001 were considered statistically significant (30). The pheatmap package, tidyverse package, and ggrepel package were utilized to create the heatmap and the volcano plot in R language. Approximately 50 genes with the most significant differences were shown in the heatmap, and those genes with their P values $<1 \times 10^{-20}$ and |logFC| >4 were labeled in the volcano plot. Afterwards, the co-expression network was constructed and visualized with STRING database

TABLE 2 | Clinical and pathologic information of GSE62452 and GSE78229 dataset.

Character	GSE62452 (N = 66)		GSE78229 (N = 49)	
	Number	%	Number	%
OS (M)				
Median	14.6		14.2	
Range	0.9–70.8		0.9–70.8	
STATUS				
Alive	16	24.24	14	28.57
DEAD	50	75.76	35	71.43
AJCC_stage				
I	4	6.06	4	8.16
II	45	68.18	44	89.80
III	11	16.67	1	2.04
IV	6	9.09	0	0
Grade				
G1	2	3.03	2	4.08
G2	32	48.48	24	48.98
G3	30	45.45	21	42.86
G4	1	1.52	1	2.04
GX	1	1.52	1	2.04

and Cytoscape. The minimum required interaction score was set to be high confidence (0.700) and disconnected nodes were hidden in the network, therefore not all genes were represented. To further elucidate the mechanism of S100A2 in the development of PC, we performed GSEA analysis of the DEGs (31). The ALL ontology of the DEGs was analyzed by Gene Ontology (GO) (32), while pathway enrichment was analyzed by the Kyoto Encyclopedia of Genes and Genomes (KEGG) (33). The number of random sample permutations was set at 1,000, and NOM p-value <0.05 and FDR q-value <0.25 were set as the significance threshold.

Estimation of Tumor Infiltrating Immune Cells

CIBERSORT algorithm could calculate the ratios of infiltrating immune cells from tissue transcriptional profiles by a deconvolution algorithm (34). Based on the expression profiles of patients in the TCGA and GSE71729 datasets, we calculated the relative abundance of 22 types of tumor infiltrating immune cells in each patient. Meanwhile, stromal, immune, and estimate scores were outputted respectively by the R package 'estimate' (35).

Tumor Mutation Burden Analysis

The mutation profile was acquired from TCGA data portal (https://portal.gdc.cancer.gov/; ≤March 1, 2021). Somatic variants data of patients were analyzed and visualized by maftools package in R language (36). Then the tumor mutation burden (TMB) of each patient was calculated and analyzed by TCGA mutations package.

Prediction of the Patients' Response to Immunotherapy

Immunophenoscore (IPS) was a scoring scheme for the quantification of tumor immunogenicity, which was verified to positively correlated to the probability to respond to immunotherapy (37). The Cancer Immunome Atlas (https://tcia.at/) characterized the intratumoral immune landscapes and the cancer antigenomes from 20 solid cancers (37). The IPS data of PC patients was extracted for the following analysis, including the scores for anti-PD-1/PD-L1 treatment and anti-CTLA-4 treatment. Meanwhile, the correlation between S100A2 and immune checkpoints was also investigated in TCGA entire set, including PD-1, PD-L1, and CTLA-4.

Clinical Specimens

A total of 65 patients with primary PDAC who underwent surgical resection at the Peking Union Medical College Hospital (PUMCH) were included in this study (PUMCH cohort, April 2019–November 2020). TNM staging was evaluated according to the 8th edition of the American Joint Committee on Cancer (AJCC) staging system for PC (38). Sequential sections of each patient were used for following studies. Written informed consent were obtained from all the patients enrolled in this study. This project was approved by the Ethics Committee of Peking Union Medical College Hospital.

Cell Culture

All pancreatic cancer cell lines were purchased from the American Type Culture Collection (ATCC). All the cell lines were tested for mycoplasma every two months and identified by STR (Short Tandem Repeat) identification. HPNE, PANC-1, T3M4 and MIACaPa-2 cell lines were cultured in high glucose Dulbecco's modified Eagle's medium (DMEM; CORNING, Manassas, USA), BxPC-3, AsPC-1, SW1990, PATU 8988 cell lines were cultured in RPMI-1640 medium (CORNING, Manassas, USA), and Capan-1 and CFPAC-1 cell lines were cultured in Iscove's Modified Dulbecco Medium (IMDM; CORNING, Manassas, USA). All medium was supplemented with 10% fetal bovine serum (HyClone, Logan, UT, USA). All cell lines were routinely maintained at 37°C with 5% CO2 in a humidified incubator.

Immunohistochemistry

Manual staining was performed as the protocol previously described in this research (39). For primary antibody incubation of each patient, two sequential sections were incubated with rabbit monoclonal anti-S100A2 antibody (1:250) (Abcam, ab109494) for 1 h and rabbit monoclonal anti-PD-L1 antibody (1:200) (Abcam, ab205921) for 1 h respectively.

RNA Isolation and RT-PCR

Total RNA was extracted from PDAC cell lines by Trizol reagent (Ambion, Life Technologies, 15596026). The cDNA was synthesized using a cDNA Reverse Transcription kit (Thermo scientific, K1622). Quantitative PCR was performed using PowerUp™ SYBR™ Green Master Mix (Applied Biosystems, A25742) in StepOnePlus™ (Applied Biosystems) according to the manufacturer's protocols. The primer sequences were used as follows:

S100A2: Forward 5′-GCCAAGAGGGCGACAAGTT-3',
Reverse 5′-AGGAAAACAGCATACTCCTGGA-3';
GAPDH: Forward 5′-GTCTCCTCTGACTTCAACAGCG-3',
Reverse 5'-ACCACCCTGTTGCTGTAGCCAA-3'.

All the values were normalized to GAPDH, and the $2^{-\Delta Ct}$ method was used to quantify the fold change.

Statistical Analysis

All the statistical analyses and visualization were performed using Rstudio (version 4.1.0) and GraphPad Prism 8 (version 8.0.1), including DEGs analysis, univariate and multivariate Cox regression analysis, LASSO regression analysis, correlation analysis, clinicopathological factor analysis, ROC curve analysis, and K-M survival analysis. A two-sided P <0.05 was considered as statistically significant unless otherwise noted.

RESULTS

Nine Immune-Related Genes Were Screened Out For Constructing A Risk Signature

The flowchart of the whole analysis was illustrated in **Figure S1**. A total of 1,793 IRGs were integrated from the ImmPort database (**Table S4**) 17. First, DEGs of normal and tumor samples in GSE15471 (Normal = 36, Tumor = 36), GSE28735 (Normal = 45, Tumor = 45), and GSE62165 (Normal = 13, Tumor = 118) datasets were analyzed by limma package (|Fold Change| >1.5 and P <0.05 were considered statistically significant). Approximately 50 genes with the most significant differences were shown in the heatmap respectively (**Figures 1A**–**C**).

Then we intersected the three differential gene sets, and finally obtained 86 common DEGs (**Figure 1D**). Subsequently, univariate Cox regression analysis of 86 candidate genes was applied in TCGA training set (n = 116) to identify prognosis-related genes (P <0.01), resulting in 26 genes with Hazard Ratio (HR) >1 and one gene with HR <1 (**Table S5**). LASSO regression analysis was further performed on the prognosis-related genes in order to avoid overfitting problems and construct the risk signature, and nine genes (*AREG*, *CXCL10*, *MET*, *OAS1*, *PI3*, *PLAU*, *S100A14*, *S100A2*, and *SPP1*) were finally screened out according to the optimal lambda value (**Figures 1E, F**, log (lambda.min) = −2.554188). At the same time, the copy number variation and the protein expression status of these nine genes were also explored through the cBioportal database and the HPA database (**Figures S2**, **S3**).

CONSTRUCTION OF A RISK SIGNATURE FOR PREDICTING SURVIVAL RATE OF PC

Base on the expression level of nine IRGs and the regression coefficient derived from LASSO regression model, we designed a risk-score formula for PC patients' survival prediction in training set. The risk score for each patient was calculated as follows: Risk score = (0.0356 × expression level of AREG) + (0.0651 × expression level of CXCL10) + (0.1030 × expression level of MET) + (0.0269 × expression level of OAS1) + (0.0002 × expression level of PI3) + (0.0129 × expression level of PLAU) + (0.0455 × expression level of S100A14) + (0.0519 × expression level of S100A2) + (0.0404 × expression level of SPP1). Then the patients in the training set were divided into high-risk group (n = 58) and low-risk group (n = 58) according to the median cut-off value of the risk scores.

To evaluate the competitive performance of the nine immune-related genes signature, Kaplan–Meier (K–M) curve analysis and time-dependent receiver operating characteristic (ROC) curve analysis were applied (**Figure 2A**). As shown in the Kaplan–Meier curves, patients in the high-risk group suffered worse prognosis than the patients in the low-risk group (**Figure 2B**, P <0.001). At the same time, the area under curves (AUCs) of the risk signature were 0.797 for 1 year survival, 0.740 for 1.5 year survival, 0.766 for 2 year survival, 0.794 for 2.5 year survival and 0.834 for 3 year survival (**Figure 2B**), proving a high prognostic value for survival prediction in the training set. Compared with the low-risk group, the expressions of *S100A2*, *AREG*, *CXCL10*, *MET*, *OAS1*, *PI3*, *PLAU*, *S100A14*, and *SPP1* increased in the high-risk group. Consistent with this, the number of deaths increased with the risk scores rising (**Figure 2B**).

Effectiveness and Independence Validation of the Risk Signature for the Survival Prediction

We next performed internal validation of the risk signature in testing set (n = 50) and the entire set (n = 166), and external validation in GSE78229 dataset (n = 49) and GSE62452 dataset (n = 66). By calculating the risk scores for each patient based on the above-mentioned formula, the patients in these datasets were divided into high-risk group and low risk group using the same criteria. Consistent with the results in the training set, patients in the high-risk group had significantly lower overall survival (OS) than those in the low-risk group (**Figures 2C, D**, P <0.05). The AUCs of ROC curves for predicting 1-, 1.5-, 2-, 2.5-, and 3-year survival of PC patients in the testing set were 0.772, 0.633, 0.623,

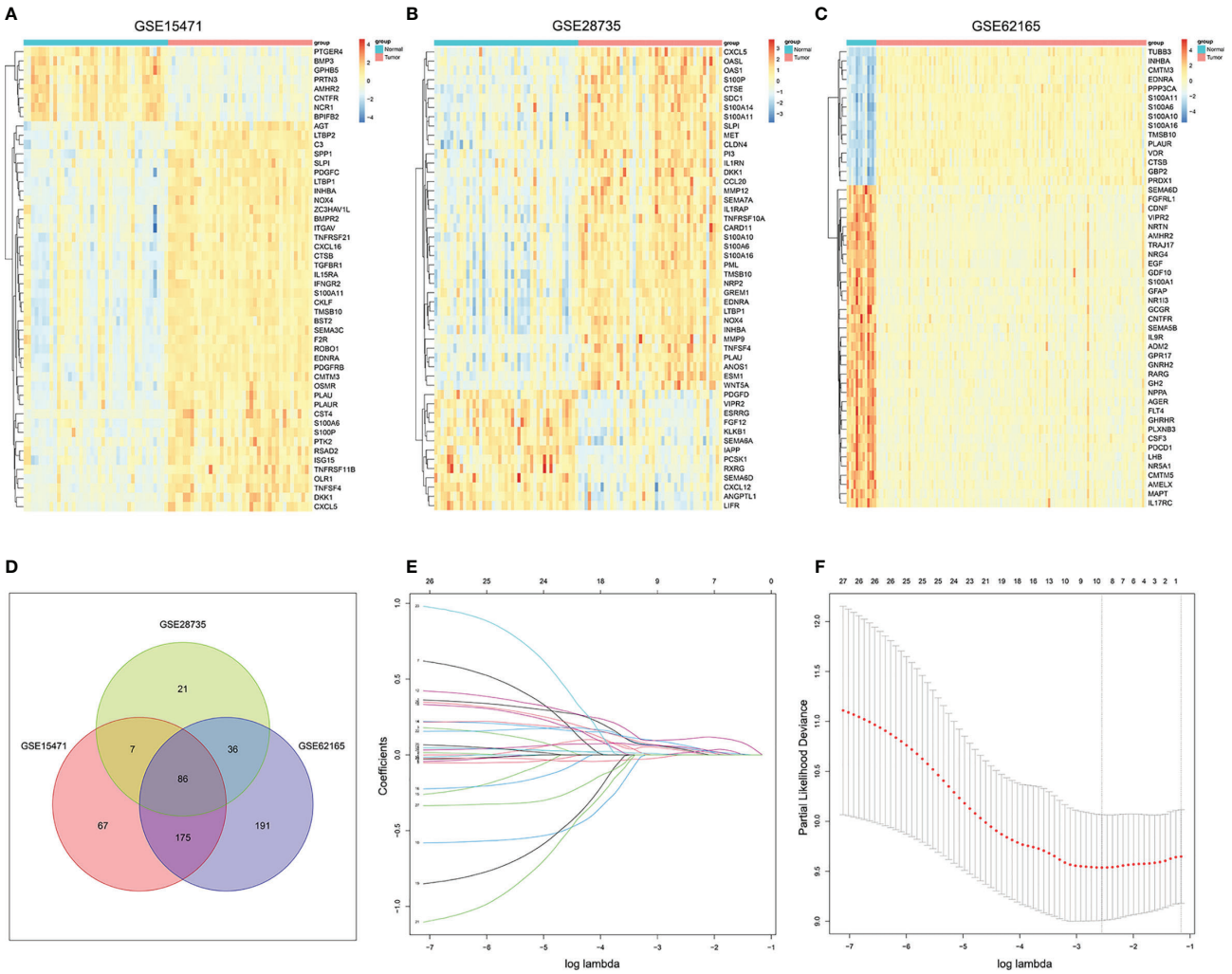

FIGURE 1 | Screening out immune-related genes for constructing a risk signature. **(A–C)**. Heatmap of immune-related DEGs between PC and normal tissue in GSE15471, GSE28735, and GSE62165. **(D)** Venn plot of the intersection of three DEGs dataset. **(E)** LASSO coefficient profiles of 27 prognostic IRGs. **(F)** Cross-validation for tuning parameter selection in the LASSO model.

0.634, and 0.671 respectively (**Figure 2C**), and those in the entire set were 0.790, 0.701, 0.725, 0.747, and 0.764 (**Figure 2D**). As for external validation, the AUCs of ROC curves were 0.541, 0.626, 0.761, 0.755, and 0.842 in GSE78229 dataset, and 0.512, 0.579, 0.739, 0.745, and 0.814 in GSE62452 dataset (**Figures 2E, F**). Meanwhile, the expressions of the nine hub IRGs increased significantly and the number of deaths was remarkably higher in the high-risk group, which was consistent with the results of the training set (**Figures 2E, F**).

Afterwards, we intended to investigate whether the survival prediction based on the risk signature was independent of other clinical factors (**Table 1**). Univariate Cox regression analysis and multivariate Cox regression analysis were conducted on these factors in the training set, testing set and entire set respectively. And the results showed that the risk signature was independent of other clinical factors, including age, gender, AJCC_stage, grade, T stage and N stage (**Figures S4A–F**, P <0.05 in all dataset for risk score). The prognostic value of the risk signature was also explored in different cohorts stratified by age, gender, tumor grade and T stage (**Figures S5A–L**, P <0.05 in all subgroups). Regardless of the subgroup, patients in the high-risk group suffered significantly poorer prognosis than those in the low-risk group, further confirming that this risk signature was an independent prognostic factor for PC.

Construction and Validation of a Nomogram Based on the Nine-Gene Signature of PC

In order to better optimize the risk signature, detailed clinical information of 166 PC patients in the TCGA dataset was collected, including age, gender, tumor grade, AJCC tumor

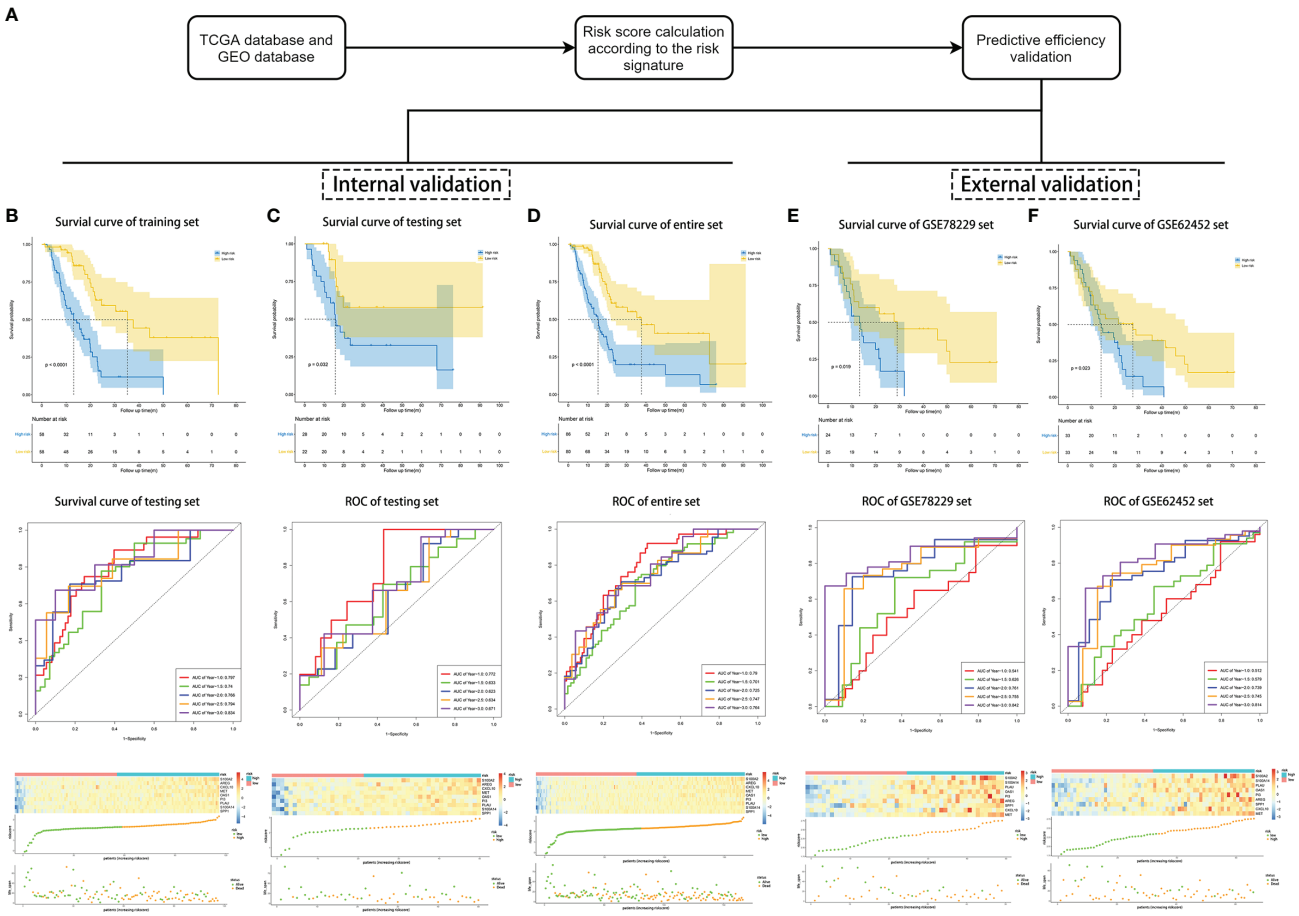

FIGURE 2 | Validation of the risk signature for survival prediction in training set, testing set, entire TCGA set, GSE78229 set, and GSE62452 set. **(A)** The process of the risk signature validation. **(B–F)** Kaplan–Meier analysis of OS of the risk signature, time-dependent ROC analysis of the risk signature, heatmap of the nine hub genes expression, the risk scores distribution and survival status of the patients in training set **(B)**, testing set **(C)**, entire TCGA set **(D)**, GSE78229 set **(E)**, and GSE62452 set **(F)**.

stage and TNM stage (**Table 1**). First, we performed univariate Cox regression analyses on all the factors in training set, and then factors with P <0.2 were included in the multivariate analysis (**Figures 3A, B**). Concomitantly, we reconfirmed that risk score was an independent prognostic factor in this process. Finally, risk score, age, T stage and N stages were incorporated into the construction of nomogram for predicting 1-, 1.5-, and 2-year survival rate of PC. In the nomogram, the patients' 1-, 1.5-, and 2-year survival rates were estimated by the total points obtained by adding up the point of each factor (**Figure 3C**). The C-index of the training set, the testing set and entire set were 0.718, 0.686, and 0.708 respectively, indicating the excellent performance of the nomogram. Subsequently, time-dependent ROC curve and calibration plot were applied to further evaluate the effectiveness of the nomogram. The AUCs of ROC curves for predicting 1-, 1.5-, and 2-year survival were 0.764, 0761, and 0.807 in the training set (**Figure 3D**), 0.785, 0.692, and 0.723 in the test set (**Figure 3E**), and 0.767, 0.732, and 0.777 in the entire set, respectively (**Figure 3F**). In addition, the calibration plot showed good agreement between the predicted and actual outcome of 1-year, 1.5-year, and 2-year OS of the nomogram in training set (**Figures S6A–C**), testing set (**Figures S6D–F**) and entire set (**Figures S6G–I**).

S100A2 Is Highly Expressed and Correlates With Unfavorable Prognosis in PC

In the DEGs analysis between the high and low risk groups, the increased expression of S100A2 occupied the most significant position (**Figure 4A**, FDR = 5.55×10^{-36}, $\log_2$FC = 4.36). Furthermore, due to its high proportion in the risk signature, we tended to consider that S100A2 occupied the core position in the risk signature. A pan-cancer analysis of S100A2 was performed, showing that PC experienced one of the most remarkably increase of S100A2 expression among all types of cancer (**Figure S7**). To be specific, a joint analysis of TCGA and GTEx databases confirmed that the expression of S100A2 in PC

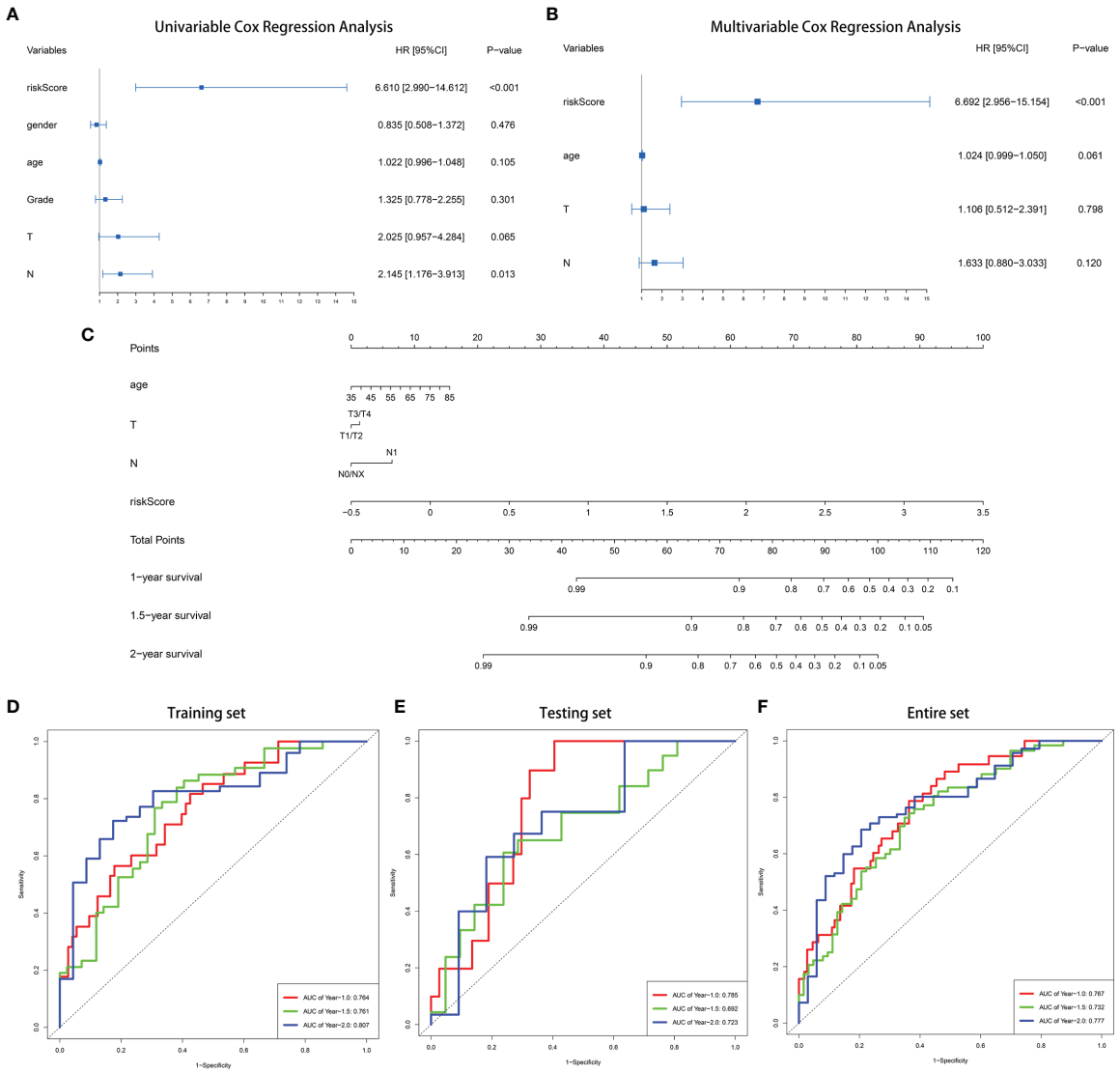

FIGURE 3 | Construction of a nomogram for predicting 1-, 1.5-, and 2-year survival rate of PC. **(A)** Forrest plot of univariate Cox regression analysis in training set. **(B)** Forrest plot of multivariate Cox regression analysis in in training set. **(C)** Nomogram integrating nine IRGs-based risk score, age, T stage and N stage. **(D–F)** Time-dependent ROC analysis of the nomogram in training set, testing set and entire TCGA set.

tissues was significantly higher than that in normal tissues (**Figure 4B**, P <0.001). Meanwhile, TCGA entire set was divided into S100A2 high and low expression groups based on S100A2 median expression. The Kaplan–Meier analysis elucidated that PC patients with S100A2 high expression suffered a poor prognosis than those with S100A2 low expression (**Figure 4C**, P <0.01). Concomitantly, the association between S100A2 expression and patients' clinicopathological information was further investigated. Notably, the expression of S100A2 was significantly increased along with the progression of tumor grade, AJCC_stage, age and T stage (**Figures 4D–I**).

In order to further verify the above findings, we conducted clustering on the single-cell dataset CRA001160 and explored the predominant expression cells of S100A2 (24, 25). It was found that S100A2 was mainly expressed by cancer cells in PC tissues (**Figure 5A**). Subsequently, the significantly high expression of S100A2 in tumor cells was confirmed by qRT-PCR in pancreatic normal cell line (HPNE) and pancreatic cancer cell lines (AsPC-1, BxPC-3, Capan-1, CFPAC-1, MIA PaCa-2, PATU 8988, PANC-1, SW1990, and T3M4) (**Figure 5B**). Meanwhile, PUMCH cohort (n = 65) was utilized to further validate that high expression of S100A2 was associated with poor prognosis in PC (**Table 3**). Comprehensive analysis of S100A2

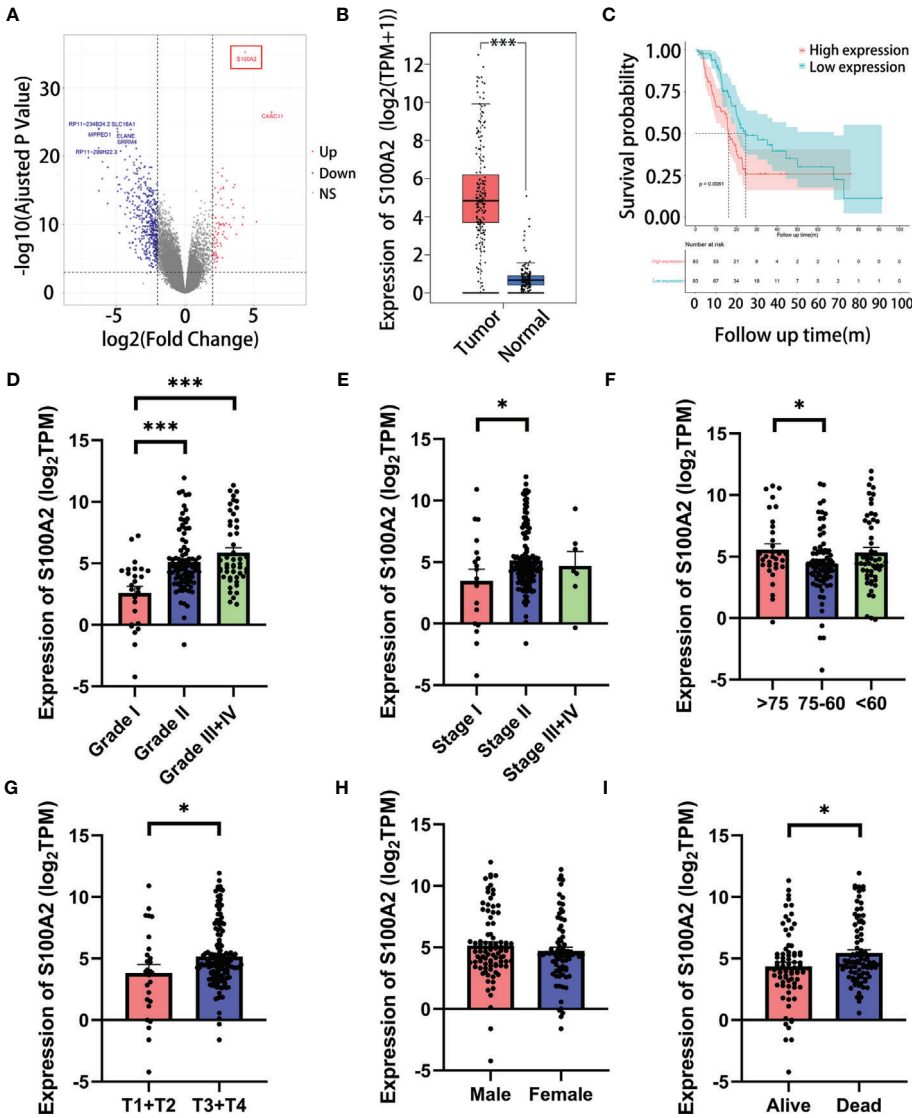

FIGURE 4 | The correlation of the expression of S100A2 and clinicopathological features of PC patients in TCGA entire set. **(A)** Screening out the most paramount gene in risk signature by DEGs analysis between high and low risk groups (the gene in red box). **(B)** Expression difference of S100A2 between PC tissue and normal tissue according to the cBioPortal database. **(C)** Kaplan-Meier analysis of OS between the high S100A2 expression group and low S100A2 expression group. **(D–I)** The correlation of S100A2 expression with clinicopathological features, including grade, AJCC_stage, age, T stage, N stage and status. *P < 0.05; ***P<0.001.

immunohistochemical scores and clinicopathologic information revealed that tumor with high S100A2 expression experienced higher T stage and poorer differentiation (**Figures 5C–E**). Collectively, these results indicated that high S100A2 expression in PC patients was correlated with unfavorable prognosis.

S100A2 Predicts the Infiltration of Immune Cells Into PC Microenvironment

Next, in order to investigate the in-depth mechanism of S100A2 leading to poor prognosis of PC, DEGs analysis was performed between the S100A2 high expression group (n = 83) and S100A2 low expression group (n = 83) in TCGA entire set (**Figure 6A**). As predicted, S100A2 was the gene with the most significant difference between the two groups, supporting the accuracy of the analysis. Then the co-expression network was constructed and visualized with STRING database and Cytoscape (**Figure 6B**).

To further elucidate the mechanism of S100A2, GSEA analysis was conducted on DEGs, in which P <0.05 and q <0.25 was considered statistically significant. Five representative pathways for the Kyoto Encyclopedia of Genes and Genomes (KEGG) and the Gene Ontology (GO) analyses were presented respectively (**Figures 6C, D**). Collectively, it was uncovered that part of the

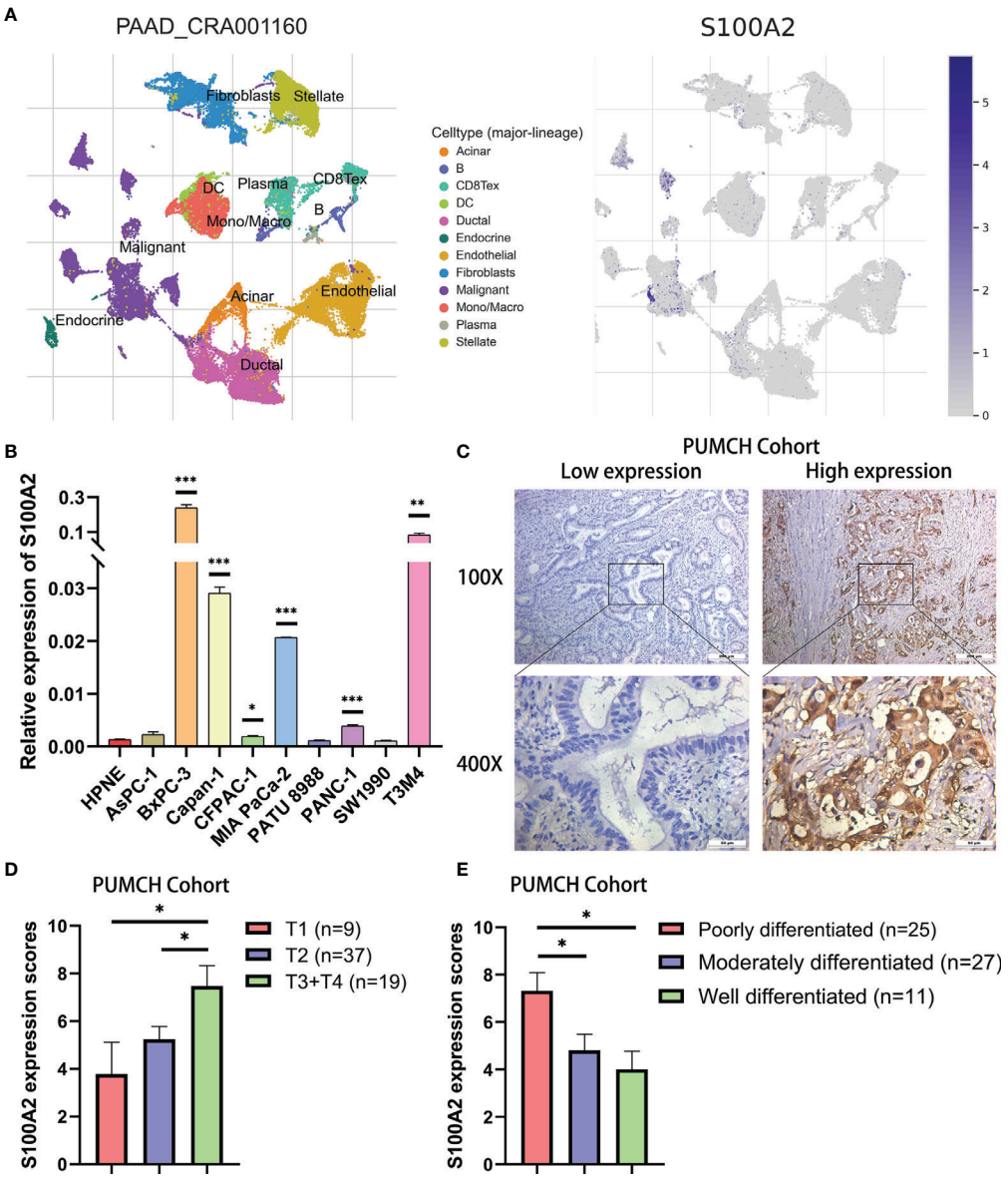

FIGURE 5 | Validation of high expression of S100A2 in PC cancer cells and its association with poor prognosis. **(A)** The results of clustering and S100A2 expression distribution in single cell dataset CRA001160. **(B)** The expression difference of S100A2 between normal and pancreatic cancer cell lines detected by qRT-PCR. The difference between each PC cell line and HPNE was analyzed. **(C)** Representative images of low and high expression of S100A2 in PUMCH cohort (n = 65). **(D–E)** Correlation between S100A expression and T stage and differentiation status in PUMCH cohort. *P < 0.05; **P < 0.01; ***P < 0.001.

pathways of DEGs enrichment were associated with immune response and associated signaling pathways.

Therefore, CIBERSORT algorithm was applied to detect the proportions of 22 kinds of immune cells in TCGA entire set (**Figure 6E**). The results showed that relatively higher proportion of M0 macrophages cells and a lower proportion of resting memory CD4+ T cells were found in the S100A2 high expression group compared with the low expression group (**Figure 6F**). To further verify this conclusion, the number of macrophages and CD4+ T cells in the single cell dataset CRA001160 was statistically analyzed, which were divided into S100A2 high-expression group, S100A2 moderate-expression group and S100A2 low-expression group. Consistent with the previous results, with the increase of S100A2 expression, the proportion of macrophages gradually increased while that of CD4+T cells declined (**Figures S8A–C**) and immunohistochemical images also support these findings, in which patients with high S100A2 expression exhibited higher CD68 expression and lower CD4 expression (**Figures S8D, E**).

Moreover, in order to prove the universality of the results, GSE71729 dataset (n = 125) was also included for following

TABLE 3 | Clinical and pathologic information of the PUMCH cohort.

Character	Total (n = 65)		S100A2 high expressioN (N = 34)		S100A2 low expression (n = 31)	
	Number	%	Number	%	Number	%
Age						
Median	65		64.5		65	
Range	38–81		40–81		38–80	
S100A2 score						
Median	6		9		3	
Range	0–12		6–12		0–4	
PD-L1 SCORE						
Median	8		8		4	
Range	1–12		2–12		1–12	
gender						
Male	28	43.08	17	50.00	11	35.48
Female	37	56.92	17	50.00	20	64.52
differentiation						
POORLY	25	38.46	18	52.94	7	22.58
MODERATELY	27	41.54	13	38.24	14	45.16
WELL	11	16.92	2	5.88	9	29.03
UNknown	2	3.08	1	2.94	1	3.23
T stage						
T1	9	13.85	2	5.88	7	22.58
T2	37	56.92	18	52.94	19	61.29
T3	17	26.15	13	38.24	4	12.90
T4	2	3.08	1	2.94	1	3.23
N stage						
N0	28	43.08	17	50.00	11	35.48
N1	30	46.15	15	44.12	15	48.39
N2	7	10.77	2	5.88	5	16.13
M stage						
M0	63	96.92	32	94.12	31	100.00
M1	2	3.08	2	5.88	0	0

analysis. It was discovered that the expression of S100A2 had a significant positive correlation with M0 macrophages and activated dendritic cells, while a remarkable negative correlation with CD8+ T cells and activated NK cells (**Figure 6G**). In addition, ESTIMATE package was also used to score the immune microenvironment, which revealed that the immune score of the group with high S100A2 expression was significantly lower than that of the group with low S100A2 expression (**Figure 6H**).

S100A2 Is Associated With Patients' TMB and Response to Immunotherapy

The mutation profiles of each PC patients were analyzed and visualized (**Figure S9**). For the TCGA dataset, the ten genes with the highest mutation rate were KRAS, TP53, SMAD4, CDKN2A, TTN, MUC16, RNF43, GNAS, ARID1A, and PCDH15 (**Figure 7A**). Meanwhile, we calculated the tumor mutation burden (TMB) of each sample and found that the TMB was higher in the group with high S100A2 expression (**Figure 7B**, P <0.05). Combined with the fact that patients with high TMB suffered a worse prognosis (**Figure 7C**, P <0.05), it was hypothesized that the effect of S100A2 on the progression of PC might result from a higher TMB.

IPS is a machine learning-based scoring system, which was able to predict patients' response to immunotherapy including anti-PD-1/PD-L1 and anti-CTLA-4 treatment (37). Combined analysis of the expression S100A2 and IPS score proved that patients with high S100A2 expression had a relative high probability to respond to anti-PD-1/PD-L1 treatment and anti-CTLA-4 treatment (**Figures 7D, E**, P <0.05). These results indicated that patients with high S100A2 expression are more suitable for immunotherapy such as anti-PD-1/PD-L1 treatment and anti-CTLA-4 treatment.

The Expression of S100A2 Was Positively Correlated With PD-L1 in PC Cells

In addition, it was discovered the expression of S100A2 in tumor tissues was remarkably positively correlated with the expression of PD-L1 (**Figure 8A**, P = 0.001, r = 0.25) and CTLA-4 (**Figure 8A**, P <0.01, r = 0.23), especially PD-L1. It might partly explain why samples with high expression of S100A2 experienced fewer CD8+ and CD4+ T cell infiltration, as well as better therapeutic effect on anti-PD1/PD-L1 therapy and anti-CTLA-4 therapy.

Since the relationship between S100A2 and PD-L1 was the most remarkable, PUMCH cohort (n = 65) was used to further demonstrate the positive correlation between S100A2 and PD-L1 (**Figure 8B** and **Table 3**). There was a significantly increased expression of PD-L1 in patients with high expression of S100A2 according to the immunohistochemical analysis of sequential sections staining S100A2 and PD-L1 (**Figure 8C**, P <0.001).

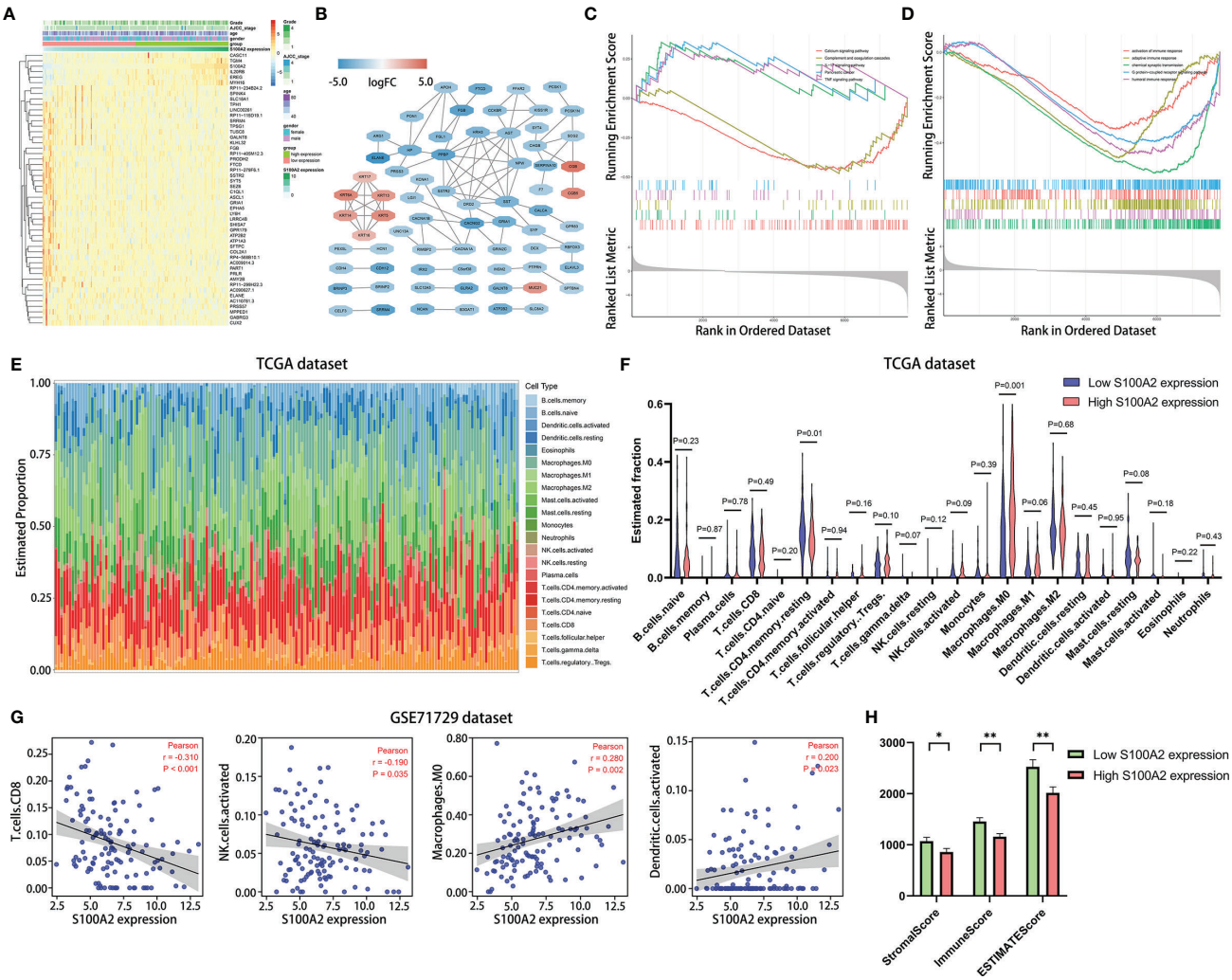

FIGURE 6 | Differential gene analysis, co-expression network construction and functional enrichments analysis between S100A2 high and low expression groups, as well as the correlation analysis of the expression of S100A2 and immune cell infiltration. **(A)** Heatmap of top 50 DEGs in PC between S100A2 high and low expression groups. **(B)** Co-expression network of DEGs constructed and visualized with STRING database and Cytoscape. **(C, D)** Gene Set Enrichment Analysis between S100A2 high and low expression groups. The representative 5 KEGG enrichments **(C)** and GO enrichments **(D)** were displayed respectively. **(E)** The abundance ratio of the 22 types of immune cells in TCGA entire set. **(F)** Differential immune cell type abundance between S100A2 high and low expression groups. **(G)** Correlation analysis between the expression of S100A2 and the proportion of immune cells in GSE71729 dataset. Immune cell types with $P < 0.05$ were shown. **(H)** Differences in immune scores between high and low S100A2 expression groups. *$P < 0.05$; **$P < 0.01$.

Meanwhile, the expression profiles of 51 pancreatic cancer cell lines in Cancer Cell Line Encyclopedia (CCLE) database also supported above results (**Figure 8D**, $P < 0.05$).

DISCUSSION

PC is one of the leading causes of cancer-related death worldwide, which is expected to become the second most common cause of cancer-related death by 2030 after lung cancer (40). There are a number of crucial reasons for this dismal status, and one of them is the lack of effective risk prediction models and biomarkers, which hinders individualized treatment of PC. Herein, due to the critical role of tumor microenvironment in the carcinogenesis and progression of PC (41, 42), we explored an IRGs-based predictive model to evaluate the prognosis of PC patients. Nine prognosis-specific IRGs were identified by a series of bioinformatics analysis: *S100A2*, *AREG*, *CXCL10*, *MET*, *OAS1*, *PI3*, *PLAU*, *S100A14*, and *SPP1*. Among them, AREG, CXCL10, MET, PLAU, S100A14, and SPP1 have been reported to be involved in the carcinogenesis and progression of PC (43–48), implying that our risk signature has considerable prognostic

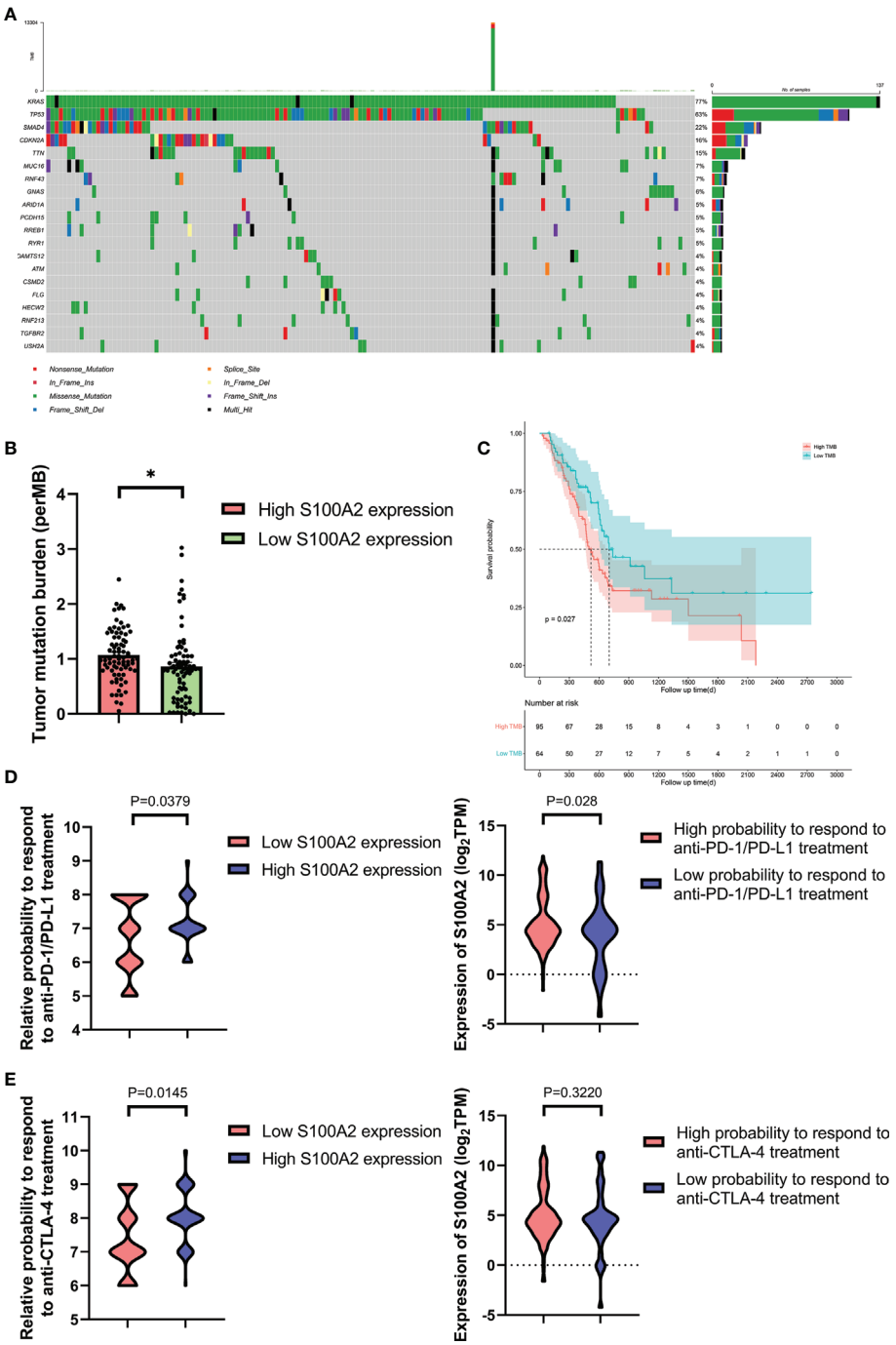

FIGURE 7 | Figure 7. The mutation profile, TMB and relative probabilities to respond to immunotherapy in S100A2 high and low expression groups. **(A)** Mutation profile of PC patients in TCGA dataset. **(B)** The difference of TMB between S100A2 high and low expression groups. **(C)** Kaplan-Meier analysis of OS between the high TMB group and low TMB group. **(D, E)** The association between S100A2 expression and the relative probabilities to respond to immunotherapy, including anti-PD-1/PD-L1 therapy and anti-CTLA-4 therapy. *P < 0.05.

value. The remaining three genes, including S100A2, OAS1, and PI3, have not been well documented for their participation in PC development. Since S100A2 occupied the most paramount position in the risk signature-based DEGs analysis, and S100A2 accounted for a relatively high proportion in the risk signature, we tended to consider that S100A2 occupied the core position in the risk signature. Therefore, we gave special attention to S100A2 in the following exploration.

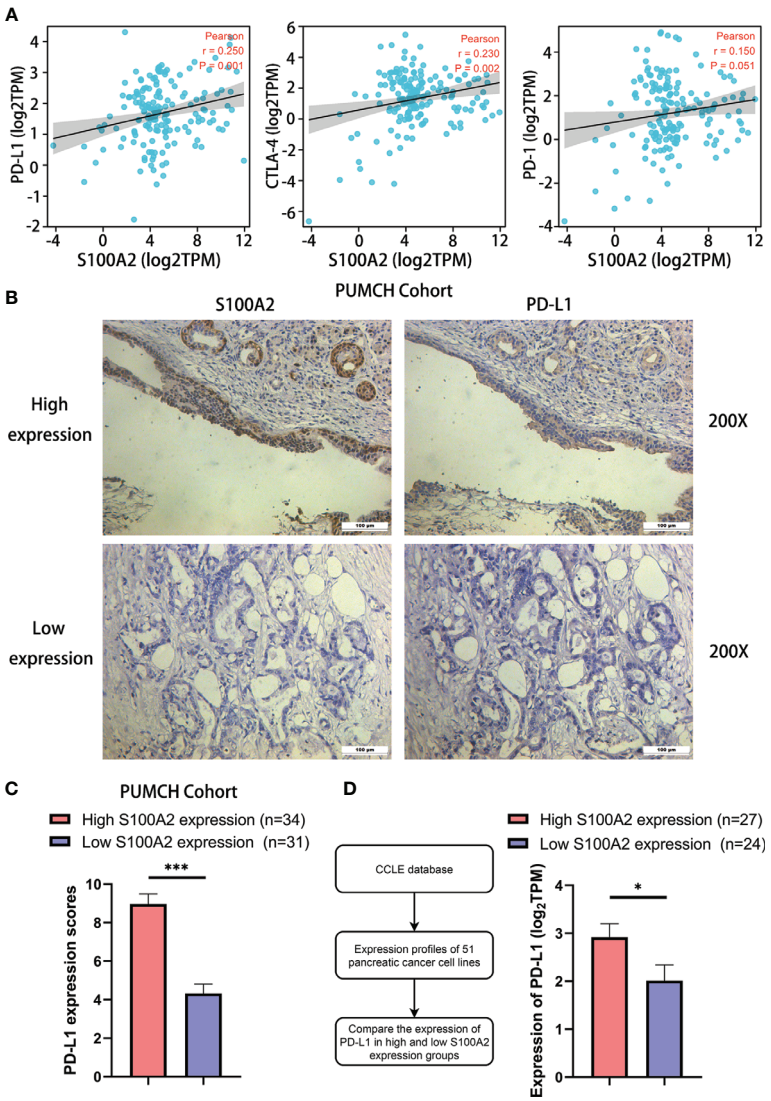

FIGURE 8 | Correlation between S100A2 expression and PD-L1 expression in PC. **(A)** Correlation analysis between the expression of S100A2 and immune checkpoint, including PD-L1, PD-1 and CTLA-4. **(B)** Representative images of positive correlation between S100A2 and PD-L1 expression in sequential sections of PUMCH cohort. **(C)** Expression difference of PD-L1 in high and low S100A2 expression groups in PUMCH cohort (n = 65). **(D)** Expression difference of PD-L1 in pancreatic cancer cell lines with high and low S100A2 expression. *P < 0.05; ***P < 0.001.

S100A2 is an important member of the S100 protein family, which is a group of highly conserved elongation factor (EF)-hand calcium-binding proteins (49, 50). Aberrant expression of S100A2 affects a range of cellular physiological functions, such as calcium homeostasis, enzyme activities and protein phosphorylation (51, 52). Notably, the role of S100A2 in tumors appears to be dual (53). Li et al. have reported that S100A2 activated the PI3K/AKT signaling pathway and upregulated GLUT1 expression in colorectal cancer, which induced glycolytic reprogramming and consequently increased tumor proliferation (54). Conversely, S100A2 was also identified to be one of the crucial tumor suppressor genes involved in the lung carcinogenesis (55). And our results supported its deteriorating effect in PC development. Previous clinical studies have proved S100A2 to be an independent poor prognostic factor and an indicator of less benefit to pancreatectomy for PC (56, 57). However, the underlying mechanism by which S100A2 promotes the progression of PC has not been fully revealed, which is also the main content of this study, especially the relationship between S100A2 and the tumor immune microenvironment. GSEA analysis revealed that the high expression of S100A2 was closely associated with the tumor immune microenvironment and corresponding pathways, enhanced interleukin-17 (IL-17), and tumor necrosis factor

(TNF) signaling pathways, and also weakened adaptive immune response, which have been widely reported to participate in tumor progression (58–62).

Therefore, CIBERSORT algorithm was applied to further elucidate the abundance ratios of 22 types of immune cells in each PC patients from TCGA entire set. It was found that compared with S100A2 low expression patients, S100A2 high expression patients experienced significantly higher proportions of M0 macrophages cells and activated dendritic cells, as well as remarkable lower proportions of CD8+ T cells, resting memory CD4+ T cells and activated NK cells. Among them, CT8+T cells, the immune cell with the most prominent tumor killing ability (63, 64), were significantly reduced in S100A2 high expression group, which partially explained the poor prognosis of patients with high S100A2 expression. Meanwhile, NK cells, another major tumor killer cells (65, 66), showed a similar trend in S100A2 high expression group. In addition, M0 macrophages have been demonstrated to be associated with worse prognosis of PC (67), but some other researches reached the opposite conclusion (68). In our analysis, the high expression of S100A2 was associated with the increase of M0 macrophages, but whether this is related to the mechanism of S100A2 leading to PC progression remained to be explored. It was also possible that the increase of M0 macrophages is a precursor to the increase of tumor-associated macrophages (TAMs), and the immune profiles reflected in the TCGA and GSE71729 datasets were both prior to the differentiation of M0 macrophages. In addition, it was worth noting that the expression of S100A2 was positively correlated with the activation of dendritic cells, which played a pivotal role in anti-tumor immunity (69). For this phenomenon, we suspected that it might be due to the negative feedback effect caused by the decrease and functional deficiency of T cells.

In recent years, immunotherapy has been proved to be one of the most promising therapies for cancer therapy and has made a profound progress in prolonging the survival time of patients with of various types of tumors (70, 71). However, the immunotherapy is almost ineffective for pancreatic cancer (72, 73). Promisingly, a small subset of patients who exhibited high effector T-cell infiltration in tumor had longer overall survival (15, 16), implying that immunotherapy still had certain application value for PC patients.

Since we have previously explored the role of S100A2 in predicting tumor immune microenvironment, we wondered whether S100A2 has any predictive effect in predicting the efficacy of immunotherapy for PC. In the past years, studies have revealed that tumor mutation burden is positively related to the efficacy of immunotherapy (74, 75). Specifically, the more TMB a tumor has, the more neoantigens it is also likely to form and T-cells released by immune checkpoint inhibitors are more likely to recognize the neoantigens and thus attack the tumor cell. Therefore, we explored the relationship between the expression level of S100A2 and TMB. The results showed that patients with high S100A2 expression had higher TMB, which indirectly indicated that patients with high S100A2 expression might have better therapeutic effect on immunotherapy. Apart from that, according to the IPS algorithm (37), it was estimated that patients with high expression of S100A2 displayed relatively significant anti-PD1/PD-L1 and anti-CTLA-4 therapeutic effects. Moreover, the expression of S100A2 was remarkably positively correlated with the expression of PD-L1 and CTLA-4, especially with the expression of PD-L1. It has been reported that PD-L1 was able to inhibit the activation of T cells by binding to PD-1 receptor on the surface of T cells (76). In our study, we found that the expression of PD-L1 was significantly increased in patients with high S100A2 expression, suggesting that patients with high S100A2 expression may have fewer T cells infiltration in tumor microenvironment. Meanwhile, the results obtained by CIBERSORT algorithm also showed that patients with high S100A2 expression had fewer CD8+ T cells, which was exactly consistent with the previous speculation. To further verify the correlation between the expression of S100A2 and PD-L1, immunohistochemistry was performed on sequential sections of PUMCH cohort (n = 65) for S100A2 and PD-L1 respectively. According to comprehensive analysis of immunohistochemical scores, it was confirmed that patients with high S100A2 expression had higher PD-L1 expression in tumor tissues. In addition, expression profile of S100A2 and PD-L1 in all pancreatic cell lines was integrated from the CCLE database, and similar results were obtained. Regarding the co-expression of S100A2 and PD-L1, studies have shown that overexpression of S100A2 in A549 lung cancer cells enhanced Akt phosphorylation (77). Meanwhile, numerous studies have revealed that Akt activation could increase the expression of PD-L1 (78, 79). On this basis, we hypothesized that the co-expression of S100A2 and PD-L1 in pancreatic cancer might be based on the activation of the S100A2-Akt-PD-L1 signaling pathway.

In spite of the positive results, several limitations in our study should also be acknowledged. Firstly, due to the extremely poor prognosis of PC, the survival time of patients rarely exceeds three years, which may bring some imprecise results when we want to predict long-term prognosis. Besides, IPS algorithm is applied to mimic patients' response to immunotherapy. Although the prediction of immunotherapy efficacy by IPS algorithm has been verified in several independent datasets, it still cannot completely replace the actual therapeutic effect.

In summary, a risk signature consisting of nine immune-related genes was constructed through a series of bioinformatics analysis, which was validated in TCGA training set, TCGA testing set, TCGA entire set, GSE78229 set and GSE62452 set. Subsequently, a nomogram was also developed to establish a more accurate prognostic prediction model for PC. Furthermore, S100A2 was identified as the gene occupying the core position in risk model, which was demonstrated to be significantly associated with the progression of tumor grade, AJCC_stage, age and T stage. Mechanically, GSEA, ESTIMATE and CIBERSORT algorithm analysis revealed that the deteriorating effect of S100A2 was associated with dysfunctional tumor immune microenvironment, mainly related to lower proportion of CD8+T cells and activated NK cells and higher proportion of M0 macrophages. Meanwhile, the results of IPS algorithm revealed that patients with high expression of S100A2 might get more benefit from immunotherapy. Finally, our

independent cohort was applied to demonstrate a remarkably positive correlation between the expression of S100A2 and PD-L1, as well as the positive relationship between S100A2 expression and unfavorable prognosis of PC patients. Our findings demonstrate S100A2 might be responsible for the preservation of immune-suppressive status in PC microenvironment, which contributes to accurate assessment of the prognosis of PC patients and optimization of the clinical decision-making.

DATA AVAILABILITY STATEMENT

The original contributions presented in the study are included in the article/**Supplementary Material**. Further inquiries can be directed to the corresponding author.

ETHICS STATEMENT

Written informed consent was obtained from all the patients enrolled in this study. This project was approved by the Ethics Committee of Peking Union Medical College Hospital.

AUTHOR CONTRIBUTIONS

Study concept and design: YC, CW, JS, RX, RR, and YZ. Experimental design and implementation: YC and CW. Drafting of the manuscript: YC. Critical revision of the manuscript for important intellectual content: YC, CW, JS, RX, RR, and YZ. Obtained funding: YZ. All authors contributed to the article and approved the submitted version.

FUNDING

This study was supported by the CAMS Innovation Fund For Medical Sciences (2021, 2021-1-I2M-002, to YZ), National Nature Science Foundation of China (2021, 82102810, to CW) and fellowship of China Postdoctoral Science Foundation (2021, 2021M700501, to CW).

SUPPLEMENTARY MATERIAL

The Supplementary Material for this article can be found online at: https://www.frontiersin.org/articles/10.3389/fimmu.2021.758004/full#supplementary-material

Supplementary Figure 1 | Flowchart of the whole study.

Supplementary Figure 2 | The copy number variation information of the nine hub IRGs in TCGA dataset.

Supplementary Figure 3 | Representative images of hub IRGs expression status except CXCL10 in normal pancreas and PC tissues. (The expression information of CXCL10 was unavailable in HPA database)

Supplementary Figure 4 | Independence of the risk signature and the other clinical variables, including gender, age, AJCC_stage and grade. **(A, C, E)** Univariate Cox regression analyses in the training set, testing set and entire set. **(B, D, F)** Multivariate Cox regression analyses in the training set testing set and entire set.

Supplementary Figure 5 | Stratification analyses of all patients using the risk signature. **(A–C)** The Kaplan-Meier analysis of the younger stratum (age ≤ 65, n=88), older stratum (age >65, n=78) and all patients with PC (n=166). **(D–F)** The Kaplan-Meier analysis of the male stratum (n=90), female stratum n=76) and all patients with PC (n=166). **(G–I)** The Kaplan-Meier analysis of the Grade I/II stratum (n=117), Grade III/IV stratum (n=49) and all patients with PC (n=166). **(J-L)** The Kaplan-Meier analysis of the T1+T2 stratum (n=27), T3+T4 stratum (n=139) and all patients with PC (n=166).

Supplementary Figure 6 | Validation of the nomogram in training set, testing set and entire set. **(A–I)** The calibration plot of the nomogram for agreement test between 1-, 1.5- and 2-year OS prediction and actual outcome in the training set, testing set and entire set.

Supplementary Figure 7 | A pan-cancer analysis of S100A2 on 33 types of tumors. Red represented a significant increase in tumor, green represented a significant decrease in tumor, and black meant no significant change.

Supplementary Figure 8 | The change of macrophages and CD4+ T cells with the increase of S100A2 expression. **(A)** The expression of S100A2 in cancer cells from 24 PDAC patients in single cell dataset CRA001160 (From high to low). **(B, C)** The proportion of macrophages and CD4+ T cells in high S100A2 expression group, moderate S100A2 expression group and low S100A2 expression group. **(D, E)** Representative images of S100A2 and CD68/CD4 expression by immunohistochemistry in HPA database.

Supplementary Figure 9 | The mutation profiles of patients in TCGA dataset.

Supplementary Table 1 | Detailed clinical and pathologic information of TCGA entire set.

Supplementary Table 2 | Detailed clinical and pathologic information of GSE62452 dataset.

Supplementary Table 3 | Detailed clinical and pathologic information of GSE78229 dataset.

Supplementary Table 4 | Immune-related genes obtained from the ImmPort database.

Supplementary Table 5 | Prognosis-related genes obtained by differential expressed gene analysis and univariate Cox regression analysis.

REFERENCES

1. Siegel RL, Miller KD, Fuchs HE, Jemal A. Cancer Statistics, 2021. *CA: Cancer J Clin* (2021) 71:7–33. doi: 10.3322/caac.21654
2. Sung H, Ferlay J, Siegel RL, Laversanne M, Soerjomataram I, Jemal A, et al. Global Cancer Statistics 2020: GLOBOCAN Estimates of Incidence and Mortality Worldwide for 36 Cancers in 185 Countries. *CA: Cancer J Clin* (2021) 71(3):209–49. doi: 10.3322/caac.21660
3. Mizrahi JD, Surana R, Valle JW, Shroff RT. Pancreatic Cancer. *Lancet (London England)* (2020) 395:2008–20. doi: 10.1016/s0140-6736(20)30974-0
4. Kaymak I, Williams KS, Cantor JR, Jones RG. Immunometabolic Interplay in the Tumor Microenvironment. *Cancer Cell* (2021) 39:28–37. doi: 10.1016/j.ccell.2020.09.004
5. Casey SC, Amedei A, Aquilano K, Azmi AS, Benencia F, Bhakta D, et al. Cancer Prevention and Therapy Through the Modulation of the Tumor Microenvironment. *Semin Cancer Biol* (2015) 35 Suppl:S199–223. doi: 10.1016/j.semcancer.2015.02.007
6. Hinshaw DC, Shevde LA. The Tumor Microenvironment Innately Modulates Cancer Progression. *Cancer Res* (2019) 79:4557–66. doi: 10.1158/0008-5472.Can-18-3962

7. Byrne A, Savas P, Sant S, Li R, Virassamy B, Luen SJ, et al. Tissue-Resident Memory T Cells in Breast Cancer Control and Immunotherapy Responses. *Nat Rev Clin Oncol* (2020) 17:341–8. doi: 10.1038/s41571-020-0333-y
8. Hegde S, Krisnawan VE, Herzog BH, Zuo C, Breden MA, Knolhoff BL, et al. Dendritic Cell Paucity Leads to Dysfunctional Immune Surveillance in Pancreatic Cancer. *Cancer Cell* (2020) 37:289–307.e289. doi: 10.1016/j.ccell.2020.02.008
9. Pushalkar S, Hundeyin M, Daley D, Zambirinis CP, Kurz E, Mishra A, et al. The Pancreatic Cancer Microbiome Promotes Oncogenesis by Induction of Innate and Adaptive Immune Suppression. *Cancer Discov* (2018) 8:403–16. doi: 10.1158/2159-8290.Cd-17-1134
10. Daley D, Zambirinis CP, Seifert L, Akkad N, Mohan N, Werba G, et al. γδ T Cells Support Pancreatic Oncogenesis by Restraining αβ T Cell Activation. *Cell* (2016) 166:1485–99.e1415. doi: 10.1016/j.cell.2016.07.046
11. Yamamoto K, Venida A, Perera RM, Kimmelman AC. Selective Autophagy of MHC-I Promotes Immune Evasion of Pancreatic Cancer. *Autophagy* (2020) 16:1524–5. doi: 10.1080/15548627.2020.1769973
12. Nielsen SR, Quaranta V, Linford A, Emeagi P, Rainer C, Santos A, et al. Macrophage-Secreted Granulin Supports Pancreatic Cancer Metastasis by Inducing Liver Fibrosis. *Nat Cell Biol* (2016) 18:549–60. doi: 10.1038/ncb3340
13. Bear AS, Vonderheide RH, O'Hara MH. Challenges and Opportunities for Pancreatic Cancer Immunotherapy. *Cancer Cell* (2020) 38:788–802. doi: 10.1016/j.ccell.2020.08.004
14. Balachandran VP, Beatty GL, Dougan SK. Broadening the Impact of Immunotherapy to Pancreatic Cancer: Challenges and Opportunities. *Gastroenterology* (2019) 156:2056–72. doi: 10.1053/j.gastro.2018.12.038
15. Morrison AH, Byrne KT, Vonderheide RH. Immunotherapy and Prevention of Pancreatic Cancer. *Trends Cancer* (2018) 4:418–28. doi: 10.1016/j.trecan.2018.04.001
16. Balachandran VP, Łuksza M, Zhao JN, Makarov V, Moral JA, Remark R, et al. Identification of Unique Neoantigen Qualities in Long-Term Survivors of Pancreatic Cancer. *Nature* (2017) 551:512–6. doi: 10.1038/nature24462
17. Bhattacharya S, Andorf S, Gomes L, Dunn P, Schaefer H, Pontius J, et al. ImmPort: Disseminating Data to the Public for the Future of Immunology. *Immunol Res* (2014) 58:234–9. doi: 10.1007/s12026-014-8516-1
18. Badea L, Herlea V, Dima SO, Dumitrascu T, Popescu I. Combined Gene Expression Analysis of Whole-Tissue and Microdissected Pancreatic Ductal Adenocarcinoma Identifies Genes Specifically Overexpressed in Tumor Epithelia. *Hepato-Gastroenterology* (2008) 55:2016–27.
19. Zhang G, He P, Tan H, Budhu A, Gaedcke J, Ghadimi BM, et al. Integration of Metabolomics and Transcriptomics Revealed a Fatty Acid Network Exerting Growth Inhibitory Effects in Human Pancreatic Cancer. *Clin Cancer Res an Off J Am Assoc Cancer Res* (2013) 19:4983–93. doi: 10.1158/1078-0432.Ccr-13-0209
20. Janky R, Binda MM, Allemeersch J, Van den Broeck A, Govaere O, Swinnen JV, et al. Prognostic Relevance of Molecular Subtypes and Master Regulators in Pancreatic Ductal Adenocarcinoma. *BMC Cancer* (2016) 16:632. doi: 10.1186/s12885-016-2540-6
21. Yang S, He P, Wang J, Schetter A, Tang W, Funamizu N, et al. A Novel MIF Signaling Pathway Drives the Malignant Character of Pancreatic Cancer by Targeting Nr3c2. *Cancer Res* (2016) 76:3838–50. doi: 10.1158/0008-5472.Can-15-2841
22. Wang J, Yang S, He P, Schetter AJ, Gaedcke J, Ghadimi BM, et al. Endothelial Nitric Oxide Synthase Traffic Inducer (NOSTRIN) is a Negative Regulator of Disease Aggressiveness in Pancreatic Cancer. *Clin Cancer Res an Off J Am Assoc Cancer Res* (2016) 22:5992–6001. doi: 10.1158/1078-0432.Ccr-16-0511
23. Moffitt RA, Marayati R, Flate EL, Volmar KE, Loeza SG, Hoadley KA, et al. Virtual Microdissection Identifies Distinct Tumor- and Stroma-Specific Subtypes of Pancreatic Ductal Adenocarcinoma. *Nat Genet* (2015) 47:1168–78. doi: 10.1038/ng.3398
24. Sun D, Wang J, Han Y, Dong X, Ge J, Zheng R, et al. TISCH: A Comprehensive Web Resource Enabling Interactive Single-Cell Transcriptome Visualization of Tumor Microenvironment. *Nucleic Acids Res* (2021) 49:D1420–30. doi: 10.1093/nar/gkaa1020
25. Peng J, Sun BF, Chen CY, Zhou JY, Chen YS, Chen H, et al. Single-Cell RNA-Seq Highlights Intra-Tumoral Heterogeneity and Malignant Progression in Pancreatic Ductal Adenocarcinoma. *Cell Res* (2019) 29:725–38. doi: 10.1038/s41422-019-0195-y
26. Barretina J, Caponigro G, Stransky N, Venkatesan K, Margolin AA, Kim S, et al. The Cancer Cell Line Encyclopedia Enables Predictive Modelling of Anticancer Drug Sensitivity. *Nature* (2012) 483:603–7. doi: 10.1038/nature11003
27. Ritchie ME, Phipson B, Wu D, Hu Y, Law CW, Shi W, et al. Limma Powers Differential Expression Analyses for RNA-Sequencing and Microarray Studies. *Nucleic Acids Res* (2015) 43:e47. doi: 10.1093/nar/gkv007
28. Cerami E, Gao J, Dogrusoz U, Gross BE, Sumer SO, Aksoy BA, et al. The Cbio Cancer Genomics Portal: An Open Platform for Exploring Multidimensional Cancer Genomics Data. *Cancer Discov* (2012) 2:401–4. doi: 10.1158/2159-8290.Cd-12-0095
29. Tang Z, Kang B, Li C, Chen T, Zhang Z. GEPIA2: An Enhanced Web Server for Large-Scale Expression Profiling and Interactive Analysis. *Nucleic Acids Res* (2019) 47:W556–60. doi: 10.1093/nar/gkz430
30. Robinson MD, McCarthy DJ, Smyth GK. Edger: A Bioconductor Package for Differential Expression Analysis of Digital Gene Expression Data. *Bioinf (Oxford England)* (2010) 26:139–40. doi: 10.1093/bioinformatics/btp616
31. Subramanian A, Tamayo P, Mootha VK, Mukherjee S, Ebert BL, Gillette MA, et al. Gene Set Enrichment Analysis: A Knowledge-Based Approach for Interpreting Genome-Wide Expression Profiles. *Proc Natl Acad Sci USA* (2005) 102:15545–50. doi: 10.1073/pnas.0506580102
32. Harris MA, Clark J, Ireland A, Lomax J, Ashburner M, Foulger R, et al. The Gene Ontology (GO) Database and Informatics Resource. *Nucleic Acids Res* (2004) 32:D258–61. doi: 10.1093/nar/gkh036
33. Kanehisa M, Goto S. KEGG: Kyoto Encyclopedia of Genes and Genomes. *Nucleic Acids Res* (2000) 28:27–30. doi: 10.1093/nar/28.1.27
34. Newman AM, Liu CL, Green MR, Gentles AJ, Feng W, Xu Y, et al. Robust Enumeration of Cell Subsets From Tissue Expression Profiles. *Nat Methods* (2015) 12:453–7. doi: 10.1038/nmeth.3337
35. Yoshihara K, Shahmoradgoli M, Martínez E, Vegesna R, Kim H, Torres-Garcia W, et al. Inferring Tumour Purity and Stromal and Immune Cell Admixture From Expression Data. *Nat Commun* (2013) 4:2612. doi: 10.1038/ncomms3612
36. Mayakonda A, Lin DC, Assenov Y, Plass C, Koeffler HP. Maftools: Efficient and Comprehensive Analysis of Somatic Variants in Cancer. *Genome Res* (2018) 28:1747–56. doi: 10.1101/gr.239244.118
37. Charoentong P, Finotello F, Angelova M, Mayer C, Efremova M, Rieder D, et al. Pan-Cancer Immunogenomic Analyses Reveal Genotype-Immunophenotype Relationships and Predictors of Response to Checkpoint Blockade. *Cell Rep* (2017) 18:248–62. doi: 10.1016/j.celrep.2016.12.019
38. van Roessel S, Kasumova GG, Verheij J, Najarian RM, Maggino L, de Pastena M, et al. International Validation of the Eighth Edition of the American Joint Committee on Cancer (AJCC) TNM Staging System in Patients With Resected Pancreatic Cancer. *JAMA Surg* (2018) 153:e183617. doi: 10.1001/jamasurg.2018.3617
39. Chen Y, Xu R, Ruze R, Yang J, Wang H, Song J, et al. Construction of a Prognostic Model With Histone Modification-Related Genes and Identification of Potential Drugs in Pancreatic Cancer. *Cancer Cell Int* (2021) 21:291. doi: 10.1186/s12935-021-01928-6
40. Rahib L, Smith BD, Aizenberg R, Rosenzweig AB, Fleshman JM, Matrisian LM. Projecting Cancer Incidence and Deaths to 2030: The Unexpected Burden of Thyroid, Liver, and Pancreas Cancers in the United States. *Cancer Res* (2014) 74:2913–21. doi: 10.1158/0008-5472.Can-14-0155
41. Ho WJ, Jaffee EM, Zheng L. The Tumour Microenvironment in Pancreatic Cancer - Clinical Challenges and Opportunities. *Nat Rev Clin Oncol* (2020) 17:527–40. doi: 10.1038/s41571-020-0363-5
42. Ren B, Cui M, Yang G, Wang H, Feng M, You L, et al. Tumor Microenvironment Participates in Metastasis of Pancreatic Cancer. *Mol Cancer* (2018) 17:108. doi: 10.1186/s12943-018-0858-1
43. Nagathihalli NS, Beesetty Y, Lee W, Washington MK, Chen X, Lockhart AC, et al. Novel Mechanistic Insights Into Ectodomain Shedding of EGFR Ligands Amphiregulin and TGF-α: Impact on Gastrointestinal Cancers Driven by Secondary Bile Acids. *Cancer Res* (2014) 74:2062–72. doi: 10.1158/0008-5472.Can-13-2329
44. Hirth M, Gandla J, Höper C, Gaida MM, Agarwal N, Simonetti M, et al. CXCL10 and CCL21 Promote Migration of Pancreatic Cancer Cells Toward Sensory Neurons and Neural Remodeling in Tumors in Mice, Associated

With Pain in Patients. *Gastroenterology* (2020) 159:665–81.e613. doi: 10.1053/j.gastro.2020.04.037
45. Li Z, Yanfang W, Li J, Jiang P, Peng T, Chen K, et al. Tumor-Released Exosomal Circular RNA PDE8A Promotes Invasive Growth *via* the miR-338/MACC1/MET Pathway in Pancreatic Cancer. *Cancer Lett* (2018) 432:237–50. doi: 10.1016/j.canlet.2018.04.035
46. Zhao X, Liu Z, Ren Z, Wang H, Wang Z, Zhai J, et al. Triptolide Inhibits Pancreatic Cancer Cell Proliferation and Migration *via* Down-Regulating PLAU Based on Network Pharmacology of Tripterygium Wilfordii Hook F. *Eur J Pharmacol* (2020) 880:173225. doi: 10.1016/j.ejphar.2020.173225
47. Zhu H, Gao W, Li X, Yu L, Luo D, Liu Y, et al. S100A14 Promotes Progression and Gemcitabine Resistance in Pancreatic Cancer. *Pancreatol Off J Int Assoc Pancreatol (IAP) [et al.]* (2021) 21:589–98. doi: 10.1016/j.pan.2021.01.011
48. Cao J, Li J, Sun L, Qin T, Xiao Y, Chen K, et al. Hypoxia-Driven Paracrine Osteopontin/Integrin αvβ3 Signaling Promotes Pancreatic Cancer Cell Epithelial-Mesenchymal Transition and Cancer Stem Cell-Like Properties by Modulating Forkhead Box Protein M1. *Mol Oncol* (2019) 13:228–45. doi: 10.1002/1878-0261.12399
49. Schäfer BW, Heizmann CW. The S100 Family of EF-Hand Calcium-Binding Proteins: Functions and Pathology. *Trends Biochem Sci* (1996) 21:134–40. doi: 10.1016/s0968-0004(96)80167-8
50. Bresnick AR, Weber DJ, Zimmer DB. S100 Proteins in Cancer. *Nat Rev Cancer* (2015) 15:96–109. doi: 10.1038/nrc3893
51. Heizmann CW, Fritz G, Schäfer BW. S100 Proteins: Structure, Functions and Pathology. *Front Biosc J Virtual Library* (2002) 7:d1356–68. doi: 10.2741/A846
52. Ji YF, Huang H, Jiang F, Ni RZ, Xiao MB. S100 Family Signaling Network and Related Proteins in Pancreatic Cancer (Review). *Int J Mol Med* (2014) 33:769–76. doi: 10.3892/ijmm.2014.1633
53. Wolf S, Haase-Kohn C, Pietzsch J. S100A2 in Cancerogenesis: A Friend or a Foe? *Amino Acids* (2011) 41:849–61. doi: 10.1007/s00726-010-0623-2
54. Li C, Chen Q, Zhou Y, Niu Y, Wang X, Li X, et al. S100A2 Promotes Glycolysis and Proliferation *via* GLUT1 Regulation in Colorectal Cancer. *FASEB J Off Publ Fed Am Societies Exp Biol* (2020) 34:13333–44. doi: 10.1096/fj.202000555R
55. Feng G, Xu X, Youssef EM, Lotan R. Diminished Expression of S100A2, a Putative Tumor Suppressor, at Early Stage of Human Lung Carcinogenesis. *Cancer Res* (2001) 61:7999–8004.
56. Dreyer SB, Pinese M, Jamieson NB, Scarlett CJ, Colvin EK, Pajic M, et al. Precision Oncology in Surgery: Patient Selection for Operable Pancreatic Cancer. *Ann Surg* (2020) 272:366–76. doi: 10.1097/sla.0000000000003143
57. Biankin AV, Kench JG, Colvin EK, Segara D, Scarlett CJ, Nguyen NQ, et al. Expression of S100A2 Calcium-Binding Protein Predicts Response to Pancreatectomy for Pancreatic Cancer. *Gastroenterology* (2009) 137:558–568, 568.e551-511. doi: 10.1053/j.gastro.2009.04.009
58. Coffelt SB, Kersten K, Doornebal CW, Weiden J, Vrijland K, Hau CS, et al. IL-17-Producing γδ T Cells and Neutrophils Conspire to Promote Breast Cancer Metastasis. *Nature* (2015) 522:345–8. doi: 10.1038/nature14282
59. Li X, Bechara R, Zhao J, McGeachy MJ, Gaffen SL. IL-17 Receptor-Based Signaling and Implications for Disease. *Nat Immunol* (2019) 20:1594–602. doi: 10.1038/s41590-019-0514-y
60. Vanamee É S, Faustman DL. TNFR2: A Novel Target for Cancer Immunotherapy. *Trends Mol Med* (2017) 23:1037–46. doi: 10.1016/j.molmed.2017.09.007
61. Balkwill F. Tumour Necrosis Factor and Cancer. *Nat Rev Cancer* (2009) 9:361–71. doi: 10.1038/nrc2628
62. Ward EM, Flowers CR, Gansler T, Omer SB, Bednarczyk RA. The Importance of Immunization in Cancer Prevention, Treatment, and Survivorship. *CA: Cancer J Clin* (2017) 67:398–410. doi: 10.3322/caac.21407
63. van der Leun AM, Thommen DS, Schumacher TN. CD8(+) T Cell States in Human Cancer: Insights From Single-Cell Analysis. *Nat Rev Cancer* (2020) 20:218–32. doi: 10.1038/s41568-019-0235-4
64. Jansen CS, Prokhnevska N, Master VA, Sanda MG, Carlisle JW, Bilen MA, et al. An Intra-Tumoral Niche Maintains and Differentiates Stem-Like CD8 T Cells. *Nature* (2019) 576:465–70. doi: 10.1038/s41586-019-1836-5
65. Myers JA, Miller JS. Exploring the NK Cell Platform for Cancer Immunotherapy. *Nat Rev Clin Oncol* (2021) 18:85–100. doi: 10.1038/s41571-020-0426-7
66. Souza-Fonseca-Guimaraes F, Cursons J, Huntington ND. The Emergence of Natural Killer Cells as a Major Target in Cancer Immunotherapy. *Trends Immunol* (2019) 40:142–58. doi: 10.1016/j.it.2018.12.003
67. Xu C, Sui S, Shang Y, Yu Z, Han J, Zhang G, et al. The Landscape of Immune Cell Infiltration and its Clinical Implications of Pancreatic Ductal Adenocarcinoma. *J Adv Res* (2020) 24:139–48. doi: 10.1016/j.jare.2020.03.009
68. Tekin C, Aberson HL, Bijlsma MF, Spek CA. Early Macrophage Infiltrates Impair Pancreatic Cancer Cell Growth by TNF-α Secretion. *BMC Cancer* (2020) 20:1183. doi: 10.1186/s12885-020-07697-1
69. Cubillos-Ruiz JR, Silberman PC, Rutkowski MR, Chopra S, Perales-Puchalt A, Song M, et al. ER Stress Sensor XBP1 Controls Anti-Tumor Immunity by Disrupting Dendritic Cell Homeostasis. *Cell* (2015) 161:1527–38. doi: 10.1016/j.cell.2015.05.025
70. Sanmamed MF, Chen L. A Paradigm Shift in Cancer Immunotherapy: From Enhancement to Normalization. *Cell* (2018) 175:313–26. doi: 10.1016/j.cell.2018.09.035
71. Hegde PS, Chen DS. Top 10 Challenges in Cancer Immunotherapy. *Immunity* (2020) 52:17–35. doi: 10.1016/j.immuni.2019.12.011
72. Henriksen A, Dyhl-Polk A, Chen I, Nielsen D. Checkpoint Inhibitors in Pancreatic Cancer. *Cancer Treat Rev* (2019) 78:17–30. doi: 10.1016/j.ctrv.2019.06.005
73. Leinwand J, Miller G. Regulation and Modulation of Antitumor Immunity in Pancreatic Cancer. *Nat Immunol* (2020) 21:1152–9. doi: 10.1038/s41590-020-0761-y
74. Chan TA, Yarchoan M, Jaffee E, Swanton C, Quezada SA, Stenzinger A, et al. Development of Tumor Mutation Burden as an Immunotherapy Biomarker: Utility for the Oncology Clinic. *Ann Oncol Off J Eur Soc Med Oncol* (2019) 30:44–56. doi: 10.1093/annonc/mdy495
75. Rizvi NA, Hellmann MD, Snyder A, Kvistborg P, Makarov V, Havel JJ, et al. Cancer Immunology. Mutational Landscape Determines Sensitivity to PD-1 Blockade in non-Small Cell Lung Cancer. *Sci (New York NY)* (2015) 348:124–8. doi: 10.1126/science.aaa1348
76. Cha JH, Chan LC, Li CW, Hsu JL, Hung MC. Mechanisms Controlling PD-L1 Expression in Cancer. *Mol Cell* (2019) 76:359–70. doi: 10.1016/j.molcel.2019.09.030
77. Naz S, Bashir M, Ranganathan P, Bodapati P, Santosh V, Kondaiah P. Protumorigenic Actions of S100A2 Involve Regulation of PI3/Akt Signaling and Functional Interaction With Smad3. *Carcinogenesis* (2014) 35:14–23. doi: 10.1093/carcin/bgt287
78. Lastwika KJ, Wilson W3rd, Li QK, Norris J, Xu H, Ghazarian SR, et al. Control of PD-L1 Expression by Oncogenic Activation of the AKT-mTOR Pathway in Non-Small Cell Lung Cancer. *Cancer Res* (2016) 76:227–38. doi: 10.1158/0008-5472.Can-14-3362
79. Gao Y, Yang J, Cai Y, Fu S, Zhang N, Fu X, et al. IFN-γ-Mediated Inhibition of Lung Cancer Correlates With PD-L1 Expression and Is Regulated by PI3K-AKT Signaling. *Int J Cancer* (2018) 143:931–43. doi: 10.1002/ijc.31357

Conflict of Interest: The authors declare that the research was conducted in the absence of any commercial or financial relationships that could be construed as a potential conflict of interest.

Publisher's Note: All claims expressed in this article are solely those of the authors and do not necessarily represent those of their affiliated organizations, or those of the publisher, the editors and the reviewers. Any product that may be evaluated in this article, or claim that may be made by its manufacturer, is not guaranteed or endorsed by the publisher.

frontiers in Immunology

REVIEW
published: 24 November 2021
doi: 10.3389/fimmu.2021.752042

Thymic Function and T-Cell Receptor Repertoire Diversity: Implications for Patient Response to Checkpoint Blockade Immunotherapy

Antonella Cardinale[1†], *Carmen Dolores De Luca*[2†], *Franco Locatelli*[1,2] *and Enrico Velardi*[1*]

[1] Department of Pediatric Hematology and Oncology, Bambino Gesù Children's Hospital, Istituto di Ricovero e Cura a Carattere Scientifico (IRCCS), Rome, Italy, [2] Department of Maternal and Child Health, Sapienza University of Rome, Rome, Italy

OPEN ACCESS

Edited by:
Roberta Zappasodi,
Cornell University, United States

Reviewed by:
Kellie Smith,
Johns Hopkins University,
United States
Ann Chidgey,
Monash University, Australia

***Correspondence:**
Enrico Velardi
enrico.velardi@opbg.net

[†]These authors have contributed equally to this work

Specialty section:
This article was submitted to Cancer Immunity and Immunotherapy, a section of the journal Frontiers in Immunology

Received: 02 August 2021
Accepted: 05 November 2021
Published: 24 November 2021

Citation:
Cardinale A, De Luca CD, Locatelli F and Velardi E (2021) Thymic Function and T-Cell Receptor Repertoire Diversity: Implications for Patient Response to Checkpoint Blockade Immunotherapy. Front. Immunol. 12:752042. doi: 10.3389/fimmu.2021.752042

The capacity of T cells to recognize and mount an immune response against tumor antigens depends on the large diversity of the T-cell receptor (TCR) repertoire generated in the thymus during the process of T-cell development. However, this process is dramatically impaired by immunological insults, such as that caused by cytoreductive cancer therapies and infections, and by the physiological decline of thymic function with age. Defective thymic function and a skewed TCR repertoire can have significant clinical consequences. The presence of an adequate pool of T cells capable of recognizing specific tumor antigens is a prerequisite for the success of cancer immunotherapy using checkpoint blockade therapy. However, while this approach has improved the chances of survival of patients with different types of cancer, a large proportion of them do not respond. The limited response rate to checkpoint blockade therapy may be linked to a suboptimal TCR repertoire in cancer patients prior to therapy. Here, we focus on the role of the thymus in shaping the T-cell pool in health and disease, discuss how the TCR repertoire influences patients' response to checkpoint blockade therapy and highlight approaches able to manipulate thymic function to enhance anti-tumor immunity.

Keywords: immune reconstitution, thymus, immunotherapy, TCR repertoire diversity, T cells

INTRODUCTION

Optimal immunological response to a large array of unknown antigens requires the presence of a diverse T-cell receptors (TCRs) repertoire, which represents the primary determinant for the likelihood of recognizing specific antigens (1). The thymus is the primary lymphoid organ with the exclusive role for generating and maintaining in the periphery a broadly diverse pool of T cells able to recognize tumor and pathogenic antigens. Once considered to take only a marginal part in maintaining a healthy immune system in adult life, the adult thymus plays a crucial role in sustaining the peripheral TCR repertoire diversity under physiological and clinical conditions. Thymic function and T-cell output are dynamic processes that can be severely compromised by

acute immunological insults (resulting from infections, stress or antineoplastic therapies) and by chronic dysfunctions (such as the ones correlated to age-associated involution and recurrent infections). Suboptimal thymic function and skewed TCR repertoire can have profound immunological and clinical consequences for patients' response to different forms of immunotherapy (**Figure 1**).

THYMIC FUNCTION AND THE GENERATION OF A DIVERSE TCR REPERTOIRE

During the process of T-cell development, thymocytes undergo a series of well-characterized and sequential developmental steps that ultimately lead to the formation of CD4 or CD8 single-positive T cells. These developmental steps are orchestrated by the crosstalk between bone marrow (BM)-derived T-cell progenitors and the supportive thymic stromal microenvironment, which primarily consists of thymic epithelial cells (TECs), endothelial cells (ECs), mesenchymal cells, dendritic cells and macrophages (2). A crucial step in T-cell development process is the generation of TCR molecules able to recognize antigenic peptides presented on heterologous cells. The recognition of a specific antigen is granted by three complementarity-determining regions (CDRs) of the TCR. The CDR3 regions are generated by somatic rearrangement between noncontiguous variable (V) and joining (J) gene segments for α and γ loci and between V, diversity (D), and J segments for the β and δ loci. The existence of multiple V, D and J gene segments in germline DNA allows the generation of a large variety of distinct CDR3 sequences that can be encoded (3). TCR rearrangement occurs in the thymic cortical and medullary regions where, respectively, the positive and negative selection of developing thymocytes occurs (4). Once the formation of a functional TCR is completed, T cells leave the thymus and enter the circulation where they impact the peripheral TCR diversity, specifically, of the *naïve* T-cell compartment.

The integrity of thymic function is essential for the generation of T cells with a diverse TCR. However, the thymus is particularly susceptible to negative insults that can come from infections, stress, acute and chronic Graft-*versus*-Host disease,

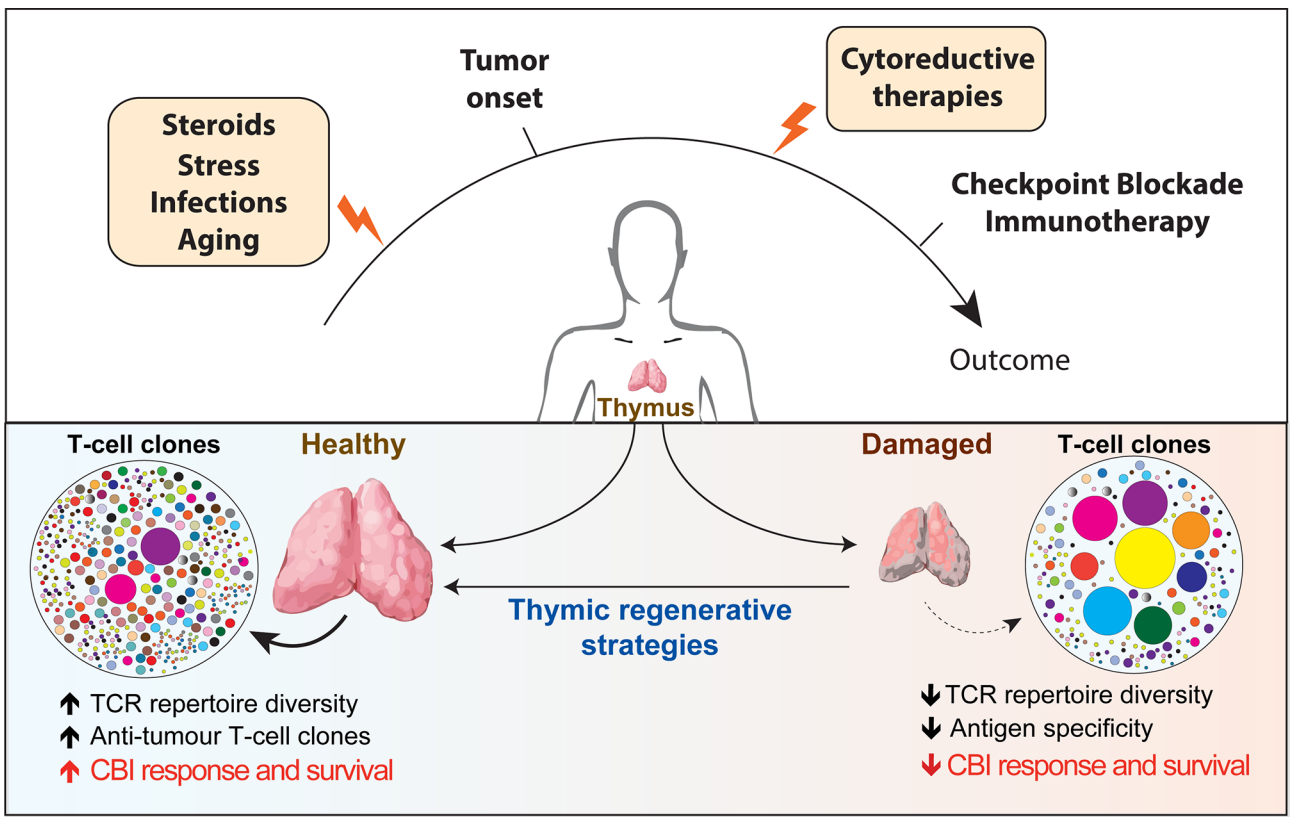

FIGURE 1 | Overview of the factors affecting thymic function and their potential role in regulating patients' response to checkpoint blockade immunotherapy. Thymus is particularly sensitive to negative insults that can come from infections, stress, cytoreductive therapies and the physiological process of aging (yellow boxes). The reduction in thymic functionality and in the TCR diversity impaired immune surveillance and may provide a supportive environment for tumors to elude T-cell-mediated response. Instead, a broader TCR repertoire in patients receiving CBI would increase the chance of tumor antigen recognition and favorable long-term clinical outcome. The use of regenerative factors aimed to boost thymic function could improve TCR repertoire diversity and have the potential to significantly extend the clinical efficacy of CBI. TCR, T cell repertoire; CBI, checkpoint blockade immunotherapy; SSA, sex steroids ablation.

cytoreductive therapies such as chemo and radiotherapy (5). These effects lead to a qualitative and quantitative decline in T-cell output with consequent restricted TCR repertoire diversity and impaired immune responses. At a specific time of an individual's life, the peripheral diversity of TCR repertoire reflects and is shaped by multiple intrinsic and extrinsic factors, including the residual thymic functionality, previous response to pathogens, previous diseases and therapies, and many others.

In addition, the physiological process of aging has important effects on thymic function and TCR diversity. While the adult thymus can still generate new T cells up to the seventh decade of life, this process is severely compromised (6–8). It is well recognized that the size of peripheral *naïve* T-cell pool and the functionality of the immune system progressively decline with age (9). Particularly, aging impairs the normal process of T-cell development at multiple levels, including reduced numbers of lymphoid progenitors generated in the BM, decreased clonal deletion during negative selection (which increases the risk of releasing autoreactive T cells in the periphery), altered thymic microenvironment, reduced output of new T cells (6, 10). As a result, it has been estimated that only ~30–40% of elderly people are capable of mounting sufficient immune responses to the influenza vaccine (11). In addition, studies in pre-clinical models linked the skewed TCR repertoire occurring during aging to infection susceptibility (12). Although in healthy individuals thymic involution is not associated with any clinical consequences, the age-associated decline of thymic function significantly impairs the endogenous process of thymic repair following cytoreductive therapies further delaying the immune reconstitution in cancer patients (6).

Overall, reduction in thymic functionality and in the peripheral T-cell diversity are important contributors of the decline in immune surveillance observed in the elderly and this may eventually provide a supportive environment for infections and tumors to elude T-cell-mediated response. Even though there is a temporal correlation, the connection between decreased thymic function and increased incidence of cancers during age is still largely debated (13, 14).

IMPACT OF THYMIC FUNCTION AND TCR DIVERSITY IN CLINICAL CONDITIONS

In several clinical conditions, damage to thymic function and changes in TCR repertoire diversity correlate with patients' response to therapy and clinical outcome. In this section, we will provide a brief overview of how thymic functionality correlates with TCR diversity in human diseases and how TCR repertoire has been used to monitor and predict patient response to therapies.

Infections lead to severe thymic dysfunction, including reduced thymic output, altered thymic architecture and skewed TCR repertoire (15). Given that the degree of TCR diversity correlates with the chance of recognizing pathogenic antigens, the skewed TCR repertoire would probably represent a major factor in the reduced immune response to infections observed in HIV seropositive patients (16).

In patients affected by symptomatic SARS-CoV2 infection, lymphopenia, particularly in the CD8+ T cell compartment, has been shown to predict poor prognosis and can represent an early indicator for admission to the intensive care unit (17, 18). While there are not yet data on potential detrimental effects of SARS-Cov2 infection on thymic function, a recent study showed that Thymosin-α1 administration, which boosts immunity through thymic dependent and independent effects, increased survival of Covid-19 patients (19). Few studies are investigating the dynamic of TCR repertoire modification during infection demonstrating trends towards reduced TCR diversity in patients with pneumonia compared to those with mild disease (20). A clinical trial is ongoing to better characterize B- and T-cell repertoire and immune response in patients with acute and resolved Covid-19 infection (NCT04362865).

In patients receiving hematopoietic cell transplantation (HCT), impaired thymic function and suboptimal reconstitution of T-cell compartment have deleterious consequences. Thymic function is highly sensitive to conditioning regimens associated with the transplant procedure and delayed or defective recovery of its function has been linked to adverse clinical outcomes (21–24). Although mature T cells transferred with the graft or T cell clones resistant to conditioning procedure can expand and contribute to the recovery of the absolute lymphocyte counts early after HCT, the resulting T-cell immunity has a limited efficacy due to the skewed TCR repertoire. Low levels of tumor antigen-specific clonally expanded T cells are associated with higher risk of disease relapse (25). Indeed, higher TCR diversity has been correlated with lower relapse rates, presumably due to a greater probability of having T cell clones endowed with Graft-*versus*-Leukemia capacity (26). Similarly, delayed T-cell recovery and restricted TCR diversity post HCT are associated with increased risks of infection and leukemia relapse (27).

T-cell immunity is critical to control cancer occurrence and relapse; a more diverse TCR repertoire increases the likelihood of tumor-antigen recognition and mounting an effective immune response. For instance, reduced TCR diversity, when compared to healthy individuals, has been demonstrated in lung cancer patients (28). In addition, the TCR repertoire was particularly restricted in those patients carrying a more severe disease, which would indicate a defective antitumor immunity (28). In patients affected by cervical cancers, TCR repertoire diversity was lower than in patients with cervical intraepithelial neoplasia and healthy women, with a gradual decrease in TCR repertoire diversity during carcinogenesis and progression of the disease (29). Likewise, a recent study found that TCR repertoire diversity in renal cell carcinoma patients could predict better prognosis and the diversity was significantly higher in early disease stages. Interestingly, cytoreductive nephrectomy could restore TCR diversity, reduce T-cell exhaustion and induce mobilization of *naïve* T cells (30).

Checkpoint Blockade Immunotherapy

Immunotherapy with monoclonal antibody-based immune checkpoint blockade (CBI) enhances the function of anti-

tumor T lymphocytes in cancer patients, by targeting co-inhibitory signaling pathways.

Cytotoxic T-Lymphocyte Antigen 4 (CTLA4) is an early negative regulator of T-cell activation. It binds to CD80/CD86 (which provides co-stimulatory signal through CD28) and inhibits the acquisition of T-cell effector function. CTLA4 inhibits the priming of naive CD4+ T cells and reduces the function of memory CD8+ T cells. CTLA4 is also expressed on CD4+ FOXP3+ regulatory T cells (Tregs), contributing to their immunosuppressive property (31). Anti-CTLA4 monoclonal antibodies constrain Tregs immune suppression in the tumor microenvironment and enhance CD4+ and CD8+ T cells primary and memory function (32). Anti-CTLA4 monoclonal antibodies are used in several clinical settings, including stage III/IV melanoma, renal cell carcinoma, non-small-cell lung carcinoma (NSCLC) and prostate cancer (33).

Programmed death-ligand 1 (PD-L1) and 2 (PD-L2), expressed by tumor cells and tumor-associated APCs (in tumor inflammatory microenvironment), are Programmed Death 1 (PD1) ligands and represent important immune checkpoint molecules. The interaction between the ligand and its receptor inhibits T-cell effector activity (34), primary T-cell response (35) and inducible Tregs suppression function (36). Given the critical role of PD1 in mediating T-cell exhaustion, anti-PD1 blocking antibodies have been developed to restore effector function of anti-tumor T cells. Monoclonal anti-PD1 antibodies, either alone or in combination with other agents, are used to manage advanced cancer stages such as melanoma, advanced squamous-cell lung carcinoma, NSCLC, advanced renal cell carcinoma, recurrent squamous cell carcinoma of the head and neck, advanced hepatocellular carcinoma and Hodgkin Lymphoma. Monoclonal antibodies against PD-L1 are used in NSCLC, advanced urothelial carcinoma, metastatic Merkel cell carcinoma (31).

TCR Repertoire Diversity and Patients' Response to CBI

The success of CBI depends on the presence of T cells able to recognize specific tumor antigens. The capacity of an individual to elicit an effective immune response is also directly correlated with tumor mutation load, which increases the likelihood of generating immunogenic neo-antigens and the chance to stimulate an anti-tumor immune response (37, 38). Thus, a broader TCR repertoire in patients receiving CBI would increase the chance of tumor antigen recognition and favorable long-term clinical outcome. Profiling TCR repertoire in patients before and after CBI has been used to assess dynamics of T-cell expansion and changes in T-cell clonotype diversity to predict and monitor patient response to therapy (39). Here we will highlight studies in which TCR diversity has been evaluated in the most commonly used CBI approaches: anti-CTLA4 e anti-PD1/PD-L1.

Anti-CTLA4 therapy shapes T-cell pool involved in anti-tumor recognition by indiscriminately broadening blood TCR repertoire (which also increase treatment side effects) (40, 41) and by increasing the number of tumor reactive T-cell clones (42, 43). Indeed, it has been shown that anti-CTLA4 therapy drove polyclonal expansion of TCR clones in tumor microenvironment (44) even those not specific for tumor antigens (45, 46). Analysis of pre-treatment TCR clonality in metastatic melanoma patients suggested that T-cell clonality within the tumor did not predict response to CTLA4 blockade (47). On the other hand, melanoma patients receiving anti-PD1 therapy showed increased TCR clonality (which was ten times greater in responders than in non-responders) and reduction in TCR diversity of intra-tumoral infiltrating lymphocytes (47).

Studies have found that higher peripheral blood TCR diversity is associated with improved clinical outcome in melanoma patients receiving anti-CTLA4 (48, 49) or anti-PD1 therapy (49). A similar study in melanoma patients observed that high pre-therapy clonality was associated with poor response to CTLA4, whereas it predicted good response to PD1 blockade (50). Higher baseline TCR diversity has been found to correlate with better disease control in patients with gastrointestinal cancers (51) and relapsed/refractory classical Hodgkin Lymphoma (52) receiving anti-PD1 therapy. Similarly, low T-cell clonality prior to anti-PD-L1 therapy and its increase in the periphery after immunotherapy has been associated with clinical benefits in patients with metastatic urothelial cancer (53). More recently, in a small group of patients affected by renal cell carcinoma receiving anti-PD1 therapy it was found which pre-treatment TCR diversity could not predict patients' outcome and that restriction of TCR diversity early post-treatment (with following increase in TCR clonality) correlated with good response to therapy (54).

Thus, higher blood TCR diversity at baseline and increased TCR clonality following CBI have been associated with better clinical outcomes and increased survival in several studies, although not in all. Several factors can explain this discrepancy including the type of disease, the intra-tumoral mutation burden rate, patient previous therapies and method used to evaluate TCR diversity. In particular, the sample used to estimate TCR diversity could play a major role in the results. In addition to analysis in peripheral blood (which is representative of non-tumor and tumor specific TCRs), specific blood T-cell subsets could better help to characterize the association between TCR diversity and response to CBI. For instance, peripheral PD1+ T cells, in the case of anti-PD1 blockade therapy, which should be representative of tumor-specific T cells (46, 55), may represent an ideal target to assess TCR diversity. Indeed, contrary to analysis performed on bulk CD8+ T cells, melanoma patients with higher pre-treatment TCR diversity and reduced diversity post anti-PD1 treatment in CD8+ PD1+ showed longer progression free survival (46). In addition, higher pre-treatment TCR diversity on sorted PD1+ CD8+ T cells was also reported in those NSCLC patients with longer progression-free survival and better overall survival before anti-PD1/PDL1 therapy (56).

Overall, a broader T-cell receptor before CBI immunotherapy has been largely associated with a better clinical outcome in cancer patients (**Figure 1**). This may suggest that approaches that improve TCR repertoire diversity could render more patients receptive to CBI treatment.

As already discussed above, the decline of thymic function and the reduction of T cell repertoire diversity with age lead to holes in the repertoire that could compromise the efficacy of CBI. An increasing number of studies have been evaluating the possible association between age and response to CBI therapy in clinical studies, as well as in pre-clinical mouse models. In triple-negative breast cancer mouse model, one study demonstrated that young (8-12 weeks of age) and aged (>12 months of age) animals equally respond to anti-PD1. However, response to anti-CTLA4 therapy was significantly impaired in aged animals when tumor growth and survival were compared to young animals (57). Mechanistically, a lower number of infiltrating lymphocytes and a reduction in the expression of genes associated with antigen presentation and inflammation was observed in the tumor microenvironment of aged animals. Another study found that advanced age was associated with decreased overall survival in aged mice (>22 months of age) treated with anti-PD1 (58). Interestingly, the same study also demonstrated that survival of glioblastoma patients were inversely correlated with CBI therapy as such that older patients have worse survival compared to younger patients.

However, a large amount of clinical evidence suggests that CBI therapy remains effective even in patients over the age of 75 and similar clinical response has been observed when patients are stratified by age (59, 60). For instance, response to CBI immunotherapy has been found to be independent of age in patients affected with IV stage melanoma and treated with anti-CTLA4 (61). Surprisingly, other studies found that the response of melanoma patients to anti-PD1 was even better in older than in younger patients (62). A large meta-analysis of 19 CBI trials in advanced cancers found no significant association between age and response to therapy.

While multiple studies have found that age does not affect patients' response to CBI, this possibility is still under debate. In particular, as several of the reported studies are limited due to the retrospective nature of the analysis, prospective clinical studies that would include larger cohorts of elderly patients would be required to answer this question.

MANIPULATING THYMIC FUNCTION TO ENHANCE EFFICACY OF CANCER IMMUNOTHERAPY

Although the thymus is extremely sensitive to injury, it maintains a remarkable capacity for repair (63, 64). Therapies aimed to enhance the regeneration of thymic function are an attractive strategy to restore a diverse T-cell pool and long-term immunity (65). Several studies explored the use of regenerative factors to enhance and broaden immune responses in individuals with thymic insufficiency and immunodeficiency resulting from infections, cancer therapies and immunosenescence (**Table 1** and **Figure 1**). Several therapies have been developed over time in preclinical models, some of which have been translated into clinical trials (5).

IL-7

One of the most widely studied molecules with immune regenerative capacity is the cytokine IL-7, a key lymphopoietic factor with the ability to enhance the proliferation of lymphocytes and lymphoid precursors (66). Several pre-clinical studies demonstrated that IL-7 cytokine controls the size of the peripheral T-cell pool and plays an important role in regulating overall T-cell homeostasis (69, 72). Moreover, in patients enrolled in a phase I dose-escalation trial, recombinant human IL-7 (rhIL-7) administration safely induced polyclonal T-cell expansion, resulting in increased T-cell counts. Specifically, 4 of the 6 enrolled subjects showed a statistically significant increase in TCR repertoire diversity 1 week after the end of rhIL-7 treatment compared to their baseline levels in $CD4^+$ and $CD8^+$ populations (73). RhIL-7 therapy also augmented immune responses to weak antigens and spare Tregs expansion (73). In a phase I clinical trial (NCT00684008) in which the immune-regenerative properties of rhIL-7 were assessed in patients receiving T-cell-depleted allogeneic HCT, the majority of participants displayed enhanced TCR repertoire diversity that persisted several weeks after the end of rhIL-7 therapy (70).

A recombinant form of the human interleukin-7 (NT-I7), in combination with PD-L1 inhibition, will be assessed in a Phase 2 study for the treatment of NSCLC patients.

KGF

Normal thymic T-cell development is strongly contingent on the regular maintenance of the stromal microenvironment. Thus, molecules that can promote recovery of stromal function, in particular of TECs, would support T-cell development and enhance T-cell reconstitution after damage. Keratinocyte Growth Factor (KGF) is a potent growth factor expressed by thymic stroma that binds to its receptor on TECs and induces thymic epithelial cells (TEC) proliferation (115). Given its peculiarity to protect thymic stromal compartment from damage, KGF administration has been exploited in thymic regeneration therapies (116). The impact of exogenous administration of KGF on TEC function and thymic regrowth has been extensively assessed in several mouse studies. It has been found that KGF administration significantly increased thymic cellularity in mouse models of aging and following acute damage caused by radiation or chemotherapy (88, 117). Moreover, several studies in mice and non-human primates demonstrated the efficacy of KGF for improving thymic-dependent T-cell recovery following HCT. In particular, KGF-treated animals showed increased numbers of T-cell receptor excision circles (TRECs), which measure thymic function in peripheral blood, up to 3 months following treatment (118).

RANKL

The role of RANKL in the regeneration of the thymic microenvironment has been well characterized (82). Following thymic damage, RANKL induces up-regulation of lymphotoxin-α (LTα) which can bind to LTβ receptor on thymic epithelial progenitor cells and TECs, and promote their regeneration (83). Exogenous administration of recombinant RANKL boosts

TABLE 1 | Approaches, discussed in the review, to promote thymic function, their targets and their evaluation in clinical trials.

Therapeutic Approach	Targets cells	Clinical Translation		References
		Trial	Setting	
Cytokines				
IL-7	HSPCs, thymocytes, mature T cells	NCT01190111	HIV	(66)
		NCT01241643	HIV	(67)
		NCT00839436	ICL	(68)
		NCT00684008	HCT	(69)
		NCT00477321	HIV	(70)
		NCT04332653	**Advanced solid tumors (anti-PD1)**	(70)
				(71)
				(72, 73)
IL-12	Thymocytes	Pre-clinical		(74)
				(75)
IL-21	HSPCs, thymocytes	Pre-clinical		(76)
				(77)
				(78)
IL-22	TECs	Pre-clinical		(79)
				(80)
RANKL	TECs	Pre-clinical		(81)
				(82)
				(83)
Growth Factors				
KGF	TECs	NCT00593554	HCT	(84)
		NCT02356159	HCT	(85)
		NCT03042585	HCT	(86)
		NCT01233921	HCT	(87)
		NCT01712945	MS	(88)
				(69)
				(89)
IGF-1	TECs	Pre-clinical		(90)
BMP4	TECs	Pre-clinical		(91)
Hormones				
Thymosin-α1	Thymocytes	NCT00580450	HCT	(92, 93)
		NCT00911443*	**Melanoma***	(94)
				(92)
				(95)
GH	TECs, thymocytes	NCT00287677	HIV	(96)
		NCT00071240	HIV	(97)
		NCT00050921	HIV	(98)
		NCT00119769	HIV	(99)
		NCT04375657	Immunosenescence	(100)
				(101)
Sex steroid ablation	TECs, HSPCs, thymocytes	NCT01746849	HCT	(102)
		NCT01338987	HCT	(63)
		NCT03650894	**Breast cancer (anti-PD1+ anti-CTLA4)**	(103)
				(104)
				(105)
				(106)
				(105)
				(107)
				(108, 109)
Artificial Tissue				
Artificial Thymus	TECs, thymocytes	Pre-clinical		(110)
				(111)
				(112, 113)
				(114)

In bold, clinical studies on CBI in combination with immune boosting strategy. (GH, growth hormone; HSPCs, hematopoietic stem and progenitor cells; KGF, keratinocyte growth factor; IL, interleukin; RANKL, receptor activator of nuclear factor-κB ligand; TECs, thymic epithelial cells; IGF1, insuline-like growth factor 1; HCT, hematopoietic cell transplantation; MS, multiple sclerosis; ICL, Idiopathic CD4+ lymphocytopenia; HIV, Human Immunodeficiency Virus).

**Clinical trial on the efficacy of thymosin-α1 in combination with dacarbazine in melanoma patients. Patients were subsequently treated with anti-CTLA4 in a separate study.*

regeneration of TECs and improves T-cell progenitor homing and *de novo* thymopoiesis. Overall, these effects lead to enhanced T-cell development (81).

Thymosin-α1

Thymic stroma, particularly TECs, also produces Thymosin-α1 (Tα1) that is able to increase thymocytes differentiation, boost T-cell function and promote immune recovery following hematologic insults (119). Several evidence in pre-clinical models have highlighted the immunomodulatory properties of Tα1; thus, this therapy has been studied in the clinic for the treatment of patients experiencing viral infections, immunodeficiency and hematological malignancies (92, 94). Treatment with Tα1 resulted in earlier appearance of pathogen-specific T-cell responses against pathogens such as cytomegalovirus and *Aspergillus* species after HCT (93). Interestingly, recent clinical studies also suggested that Tα1 may also have synergistic effects when used in combination with CBI. It has been shown that sequentially treatment with Tα1 and anti-CTLA4 significantly increased overall survival of melanoma patients (95).

Growth Hormone and Insulin-Like Growth Factor-1

Growth Hormone (GH) is a small peptide hormone implicated in the regulation of hematopoietic function. It has been demonstrated that *in vivo* administration of a recombinant form of GH or insulin-like growth factor-1 (IGF1) (which represents one of the principal mediators of GH effects) can reverse thymic involution, increases TCR diversity and enhances recovery of hematopoietic compartments in patients with adult GH deficiency (90, 101, 120). Moreover, the administration of human recombinant GH in HIV-infected patients promoted thymic function and peripheral immune function (96, 99). A recent study also suggested that GH treatment can regenerate thymic tissue in healthy adults between 51 and 65 years of age (100). This treatment resulted in significant increase of both $CD4^+$ and $CD8^+$ naive T cells, and in decrease of $PD1^+CD8^+$ T cells (100).

Ablation of Sex Steroids

Sexual dimorphism in the immune system is well recognized and it is broadly summarized with the concept that women tend to develop more autoimmune diseases than men, while men are more vulnerable to some infectious diseases. Sex hormones, and in particular androgens, heavily influence thymic function primarily through the regulation of TEC differentiation and function (121, 122). Studies in murine models demonstrated that age-related thymic dysfunction is faster in males than in females. Similarly, in humans, the rate of thymic involution is greater in males as demonstrated by evaluation of TRECs in patient peripheral blood (123, 124). As direct evidence of the close connection between sex hormones and thymic function, many pre-clinical studies have demonstrated that sex steroid ablation (SSA), by surgical or chemical approaches, transiently reverses thymic involution and promotes rejuvenation of lymphoid tissues. SSA induces thymic reconstitution and peripheral immune cells recovery after radiation, chemotherapy and HCT (63, 104–107). Recent studies have also shown that the effects of SSA are not restricted to the lymphoid lineage, as extensive regenerative signals are also directed towards the hematopoietic stem and progenitor cells and their niche (103, 108). While the underlying mechanisms are still not completely understood, experimental evidence demonstrated that some of the regenerative effects are mediated by the removal of the inhibitory effects of sex steroids, primarily of androgens, on endogenous B and T lymphopoiesis. The increase in androgens during life could also explain and contribute to the faster rate of thymic-involution observed after puberty. Most of our mechanistic understanding of the effects of hormones on thymic function is largely restricted to the effects of androgens in male subjects. However, recent studies have started characterizing genders differences in thymic function and in response to SSA (122, 125). It has been shown that, in female mice, age induces a higher degree of central tolerance imbalance characterized by the reduction of medullary TECs expressing the autoimmune regulator gene (AIRE), which could contribute to the increased risk of autoimmune disease observed in middle-aged women (126). In addition, middle-aged females are less affected by the regenerative effects triggered by SSA therapy compared to males but are more responsive when thymic regeneration was evaluated in response to acute thymic damage (125).

Interestingly, when transferred into the clinic, SSA has been shown to enhance neutrophil and lymphocyte recovery, thymic function and T-cell repertoire regeneration in patients receiving autologous and allogeneic HCT, independently from gender (109). Thus, while the precise mechanisms of action of SSA on lymphoid regeneration is still not completely understood, this approach represents an appealing therapy to enhance immune recovery in patients. Importantly, a clinical trial has been recently opened to evaluate if the regeneration of thymus and peripheral T-cell pool induced by SSA can enhance response to dual ICB with anti-PD1 and anti-CTLA4 therapy in metastatic breast cancer patients (127).

There is an incredible effort in the field to identify novel pathways and targets that can enhance thymic and immune recovery as the currently identified approaches are limited. In addition to IL-7, KGF, RANKL, SSA, GH and Thymosin α1, studies have found that other cytokines and growth factors have the potential to restore thymic function following immune insults. Administration of IL-12 induces thymocyte proliferation through increased IL-7 and IL-2 signaling (74). IL-21 delivery can also imprint regenerative signals to the thymus after immunological injuries such as glucocorticoid-induced thymic atrophy, aging and allogeneic HCT (76–78). IL-22 cytokine can mediate thymic regeneration by promoting TECs survival and proliferation through activation of STAT3 and STAT5 and expression of the antiapoptotic molecule *Mcl1* (80, 128). Furthermore, BMP4 produced by thymic endothelial cells can drive thymic regeneration by binding to its receptor expressed on TECs and stimulating the upregulation of *FoxN1* and its target genes (91). Critically, in patients with extensive thymic aplasia due to repetitive cycles of chemo or radiotherapy

and/or aging, the presence of residual thymic tissue that could receive the regenerative signals and start organ recovery can be insufficient. In those conditions, the implant of artificial thymic tissue could represent an attractive alternative to repopulate the *naive* T-cell pool (110–114).

While some of the above-mentioned strategies have made some steps into the clinic, at present, there is no standard of care approach to promote immune reconstitution. In addition, their beneficial use in elderly cancer patients, which would greatly benefit from immune rejuvenating approaches, still requires additional research. Recent work observed that the increased disorganization and fibrosis of lymph nodes with age can limit the efficacy of thymic rejuvenation strategies (129). Thus, further studies are needed to determine whether secondary lymphoid organs are also rejuvenated with immune regenerative treatments, or whether approaches that could target both the thymus and the lymph nodes would represent a more effective therapy for immune recovery.

Breaking Central Tolerance to Enhance CBI Efficacy

Central tolerance takes place in the thymus, where T cell clones that are reactive to self are deleted to protect against the development of autoimmunity. Although on the one hand, this process allows the elimination of T cells reactive against tissue-specific self-antigens (130), on the other hand, the majority of tumor cells, which express self-antigens, could be recognized by the same self-reactive T cells deleted by negative selection in the thymus (131). AIRE plays a crucial role in establishing central T cell tolerance controlling the expression of tissue-specific self-antigens in medullary TECs. AIRE deficiency leads to multiple autoimmune disorders in mice and patients. AIRE knock-out mice, which show expanded auto reactive T cell repertoire, have enhanced ability to mount anti-tumor response when challenged with syngeneic melanoma cells (132). Interestingly, a polymorphism in AIRE, which can decrease the stability of the mRNA, has been associated with protection from melanoma (133). Thus, while protecting against autoimmunity, AIRE also limits antitumor immunity. Thus, recent studies have been investigating alternative approaches to enhance T cell-mediated antitumor immunity and response to CBI, which are based on temporary disruption of central T cell tolerance through the inhibition of AIRE (131). Evidence of this approach has been provided in pre-clinical settings by the infusion of anti-RANKL antibody, which depleted AIRE-expressing TEC in the thymus and allowed self/melanoma-reactive T cells to escape negative selection and increase in the peripheral pool. Combination of anti-RANKL and anti-CTLA4 antibody therapy enhanced anti-tumor response and survival after melanoma challenge (134). Similarly, the use of anti-RANKL/PD-1 dual targeting antibody has been shown to promote anti-tumor response in pre-clinical tumor models (135).

While the depletion of AIRE+ TECs and the suppression of central tolerance after anti-RANKL therapy could play an important role in the enhanced anti-tumor activity when combined with CBI, further studies are needed to better characterize the contribution of RANKL antagonism on the tumor microenvironment.

CONCLUSIONS

T-cell immunity is critical to control cancer occurrence and relapse. A more diverse TCR repertoire increases the likelihood of tumor-antigen recognition and of mounting an effective immune response. As the thymus represents the primary site of T-cell development and its function directly shapes the peripheral TCR diversity, robust residual thymic function in adult life can be associated with greater chance of establishing effective tumor immunity. However, direct evidence of the connection between thymic function and cancer is still under investigation. While thymic boosting approaches can have an immediate impact to enhance immune reconstitution after cytoreductive therapies, which would significantly reduce morbidly and improve survival in HCT patients, their potential use to extend the benefit of CBI is just beginning to be investigated. Indeed, although CBI has tremendously improved the chances of survival of cancer patients, a large proportion of them do not respond. Would patients with greater residual thymic functionality have greater chance to respond to CBI? In addition, multiple studies have investigated the use of TCR-seq as a predictive and prognostic tool for patient's response to CBI. Broader TCR diversity has been linked to greater response to CBI in multiple studies. However, the methodology is associated with significant cost and methodological bias. Thus, can the assessment of thymic function, for example through the evaluation of TRECs or recent thymic emigrants, better and more precisely stratify patients that could benefit from CBI? Clinical trials in progress will be fundamental to answer to these questions and explore these intriguing possibilities.

AUTHOR CONTRIBUTIONS

AC and CD conducted the literature review, created the figures, and wrote the bulk of the manuscript. FL contributed to writing and editing. EV conceived the review and contributed to the planning, editing and writing. All authors contributed to the article and approved the submitted version.

FUNDING

EV was supported by grants from the Amy Strelzer Manasevit Research Program; the Italian Association for Cancer Research (AIRC); and the Italian Ministry of Health ("Ricerca Corrente"). FL was supported by grants from AIRC (Special Program Metastatic disease: the key unmet need in oncology 5 per mille 2018 Project Code 21147 and Accelerator Award 2017 INCAR); Ministero dell'Istruzione, dell'Università e della Ricerca, PRIN ID 2017 WC8499_004; Ministero della Salute, RF-20 16-02364388.

REFERENCES

1. Nikolich-Zugich J, Slifka MK, Messaoudi I. The Many Important Facets of T-Cell Repertoire Diversity. *Nat Rev Immunol* (2004) 4(2):123–32. doi: 10.1038/nri1292
2. Takahama Y. Journey Through the Thymus: Stromal Guides for T-Cell Development and Selection. *Nat Rev Immunol* (2006) 6(2):127–35. doi: 10.1038/nri1781
3. Hou X, Lu C, Chen S, Xie Q, Cui G, Chen J, et al. High Throughput Sequencing of T Cell Antigen Receptors Reveals a Conserved TCR Repertoire. *Med (Baltimore)* (2016) 95(10):e2839. doi: 10.1097/MD.0000000000002839
4. Takahama Y, Ohigashi I, Baik S, Anderson G. Generation of Diversity in Thymic Epithelial Cells. *Nat Rev Immunol* (2017) 17(5):295–305. doi: 10.1038/nri.2017.12
5. Velardi E, Tsai JJ, van den Brink MRM. T Cell Regeneration After Immunological Injury. *Nat Rev Immunol* (2021) 21(5):277–91. doi: 10.1038/s41577-020-00457-z
6. Lynch HE, Goldberg GL, Chidgey A, Van den Brink MR, Boyd R, Sempowski GD. Thymic Involution and Immune Reconstitution. *Trends Immunol* (2009) 30(7):366–73. doi: 10.1016/j.it.2009.04.003
7. Yoshida K, Nakashima E, Kubo Y, Yamaoka M, Kajimura J, Kyoizumi S, et al. Inverse Associations Between Obesity Indicators and Thymic T-Cell Production Levels in Aging Atomic-Bomb Survivors. *PLoS One* (2014) 9(3):e91985. doi: 10.1371/journal.pone.0091985
8. Mold JE, Réu P, Olin A, Bernard S, Michaëlsson J, Rane S, et al. Cell Generation Dynamics Underlying Naive T-Cell Homeostasis in Adult Humans. *PLoS Biol* (2019) 17(10):e3000383. doi: 10.1371/journal.pbio.3000383
9. Nikolich-Zugich J. The Twilight of Immunity: Emerging Concepts in Aging of the Immune System. *Nat Immunol* (2018) 19(1):10–9. doi: 10.1038/s41590-017-0006-x
10. Coder BD, Wang H, Ruan L, Su DM. Thymic Involution Perturbs Negative Selection Leading to Autoreactive T Cells That Induce Chronic Inflammation. *J Immunol* (2015) 194(12):5825–37. doi: 10.4049/jimmunol.1500082
11. Thompson WW, Shay DK, Weintraub E, Brammer L, Cox N, Anderson LJ, et al. Mortality Associated With Influenza and Respiratory Syncytial Virus in the United States. *JAMA J Am Med Assoc* (2003) 289(2):179–86. doi: 10.1001/jama.289.2.179
12. Cicin-Sain L, Smyk-Pearson S, Currier N, Byrd L, Koudelka C, Robinson T, et al. Loss of Naive T Cells and Repertoire Constriction Predict Poor Response to Vaccination in Old Primates. *J Immunol* (2010) 184(12):6739–45. doi: 10.4049/jimmunol.0904193
13. Palmer S, Albergante L, Blackburn CC, Newman TJ. Thymic Involution and Rising Disease Incidence With Age. *Proc Natl Acad Sci USA* (2018) 115(8):1883–8. doi: 10.1073/pnas.1714478115
14. Jimenez-Alonso JJ, Calderon-Montano JM, Lopez-Lazaro M. Are Most Cancer Cases a Consequence of an Immune Deficiency Caused by Thymic Involution? *Proc Natl Acad Sci USA* (2018) 115(19):E4314–5. doi: 10.1073/pnas.1803180115
15. Savino W. The Thymus Is a Common Target Organ in Infectious Diseases. *PLoS Pathog* (2006) 2(6):e62. doi: 10.1371/journal.ppat.0020062
16. Heather JM, Best K, Oakes T, Gray ER, Roe JK, Thomas N, et al. Dynamic Perturbations of the T-Cell Receptor Repertoire in Chronic HIV Infection and Following Antiretroviral Therapy. *Front Immunol* (2015) 6:644. doi: 10.3389/fimmu.2015.00644
17. Liu Z, Long W, Tu M, Chen S, Huang Y, Wang S, et al. Lymphocyte Subset (CD4+, CD8+) Counts Reflect the Severity of Infection and Predict the Clinical Outcomes in Patients With COVID-19. *J infection* (2020) 81(2):318–56. doi: 10.1016/j.jinf.2020.03.054
18. Urra JM, Cabrera CM, Porras L, Rodenas I. Selective CD8 Cell Reduction by SARS-CoV-2 Is Associated With a Worse Prognosis and Systemic Inflammation in COVID-19 Patients. *Clin Immunol* (2020) 217:108486. doi: 10.1016/j.clim.2020.108486
19. Liu Y, Pang Y, Hu Z, Wu M, Wang C, Feng Z, et al. Thymosin Alpha 1 (Talpha1) Reduces the Mortality of Severe COVID-19 by Restoration of Lymphocytopenia and Reversion of Exhausted T Cells. *Clin Infect Dis an Off Publ Infect Dis Soc Am* (2020) 71(16):2150–7. doi: 10.1093/cid/ciaa630
20. Chang CM, Feng PH, Wu TH, Alachkar H, Lee KY, Chang WC. Profiling of T Cell Repertoire in SARS-CoV-2-Infected COVID-19 Patients Between Mild Disease and Pneumonia. *J Clin Immunol* (2021) 41:1131–45. doi: 10.1007/s10875-021-01045-z
21. Atkinson K. Reconstruction of the Haemopoietic and Immune Systems After Marrow Transplantation. *Bone Marrow Transplant* (1990) 5(4):209–26.
22. Storek J, Witherspoon RP, Storb R. T Cell Reconstitution After Bone Marrow Transplantation Into Adult Patients Does Not Resemble T Cell Development in Early Life. *Bone Marrow Transplant* (1995) 16(3):413–25.
23. Weinberg K, Annett G, Kashyap A, Lenarsky C, Forman SJ, Parkman R. The Effect of Thymic Function on Immunocompetence Following Bone Marrow Transplantation. *Biol Blood Marrow Transplant* (1995) 1(1):18–23.
24. Velardi E, Clave E, Arruda LCM, Benini F, Locatelli F, Toubert A. The Role of the Thymus in Allogeneic Bone Marrow Transplantation and the Recovery of the Peripheral T-Cell Compartment. *Semin Immunopathol* (2021) 43(1):101–17. doi: 10.1007/s00281-020-00828-7
25. Kapp M, Stevanovic S, Fick K, Tan SM, Loeffler J, Opitz A, et al. CD8+ T-Cell Responses to Tumor-Associated Antigens Correlate With Superior Relapse-Free Survival After Allo-SCT. *Bone Marrow Transplant* (2009) 43(5):399–410. doi: 10.1038/bmt.2008.426
26. Yew PY, Alachkar H, Yamaguchi R, Kiyotani K, Fang H, Yap KL, et al. Quantitative Characterization of T-Cell Repertoire in Allogeneic Hematopoietic Stem Cell Transplant Recipients. *Bone Marrow Transplant* (2015) 50(9):1227–34. doi: 10.1038/bmt.2015.133
27. Van Heijst JWJ, Ceberio I, Lipuma LB, Samilo DW, Wasilewski GD, Gonzales AMR, et al. Quantitative Assessment of T Cell Repertoire Recovery After Hematopoietic Stem Cell Transplantation. *Nat Med* (2013) 19(3):372–7. doi: 10.1038/nm.3100
28. Liu YY, Yang QF, Yang JS, Cao RB, Liang JY, Liu YT, et al. Characteristics and Prognostic Significance of Profiling the Peripheral Blood T-Cell Receptor Repertoire in Patients With Advanced Lung Cancer. *Int J Cancer* (2019) 145(5):1423–31. doi: 10.1002/ijc.32145
29. Cui JH, Lin KR, Yuan SH, Jin YB, Chen XP, Su XK, et al. TCR Repertoire as a Novel Indicator for Immune Monitoring and Prognosis Assessment of Patients With Cervical Cancer. *Front Immunol* (2018) 9:2729. doi: 10.3389/fimmu.2018.02729
30. Guo L, Bi X, Li Y, Wen L, Zhang W, Jiang W, et al. Characteristics, Dynamic Changes, and Prognostic Significance of TCR Repertoire Profiling in Patients With Renal Cell Carcinoma. *J Pathol* (2020) 251(1):26–37. doi: 10.1002/path.5396
31. Hargadon KM, Johnson CE, Williams CJ. Immune Checkpoint Blockade Therapy for Cancer: An Overview of FDA-Approved Immune Checkpoint Inhibitors. *Int Immunopharmacol* (2018) 62:29–39. doi: 10.1016/j.intimp.2018.06.001
32. Wei SC, Levine JH, Cogdill AP, Zhao Y, Anang NAS, Andrews MC, et al. Distinct Cellular Mechanisms Underlie Anti-CTLA-4 and Anti-PD-1 Checkpoint Blockade. *Cell* (2017) 170(6):1120–33.e17. doi: 10.1016/j.cell.2017.07.024
33. Topalian SL, Drake CG, Pardoll DM. Immune Checkpoint Blockade: A Common Denominator Approach to Cancer Therapy. *Cancer Cell* (2015) 27(4):450–61. doi: 10.1016/j.ccell.2015.03.001
34. Gordon J, Freeman AJL, Iwai Y, Bourque K, Chernova T, Nishimura H, et al. Engagement of the PD-1 Immunoinhibitory Receptor by a Novel B7 Family Member. *J Exp Med* (2000) 192(7):1027–34. doi: 10.1084/jem.192.7.1027
35. Goldberg MV, Maris CH, Hipkiss EL, Flies AS, Zhen L, Tuder RM, et al. Role of PD-1 and Its Ligand, B7-H1, in Early Fate Decisions of CD8 T Cells. *Blood* (2007) 110(1):186–92. doi: 10.1182/blood-2006-12-062422
36. Francisco LM, Salinas VH, Brown KE, Vanguri VK, Freeman GJ, Kuchroo VK, et al. PD-L1 Regulates the Development, Maintenance, and Function of Induced Regulatory T Cells. *J Exp Med* (2009) 206(13):3015–29. doi: 10.1084/jem.20090847
37. Schumacher TN, Kesmir C, van Buuren MM. Biomarkers in Cancer Immunotherapy. *Cancer Cell* (2015) 27(1):12–4. doi: 10.1016/j.ccell.2014.12.004
38. McGranahan N, Furness AJ, Rosenthal R, Ramskov S, Lyngaa R, Saini SK, et al. Clonal Neoantigens Elicit T Cell Immunoreactivity and Sensitivity to Immune Checkpoint Blockade. *Science* (2016) 351(6280):1463–9. doi: 10.1126/science.aaf1490

39. Kidman J, Principe N, Watson M, Lassmann T, Holt RA, Nowak AK, et al. Characteristics of TCR Repertoire Associated With Successful Immune Checkpoint Therapy Responses. *Front Immunol* (2020) 11:587014. doi: 10.3389/fimmu.2020.587014
40. Cha E, Klinger M, Hou Y, Cummings C, Ribas A, Faham M, et al. Improved Survival With T Cell Clonotype Stability After Anti-CTLA-4 Treatment in Cancer Patients. *Sci Transl Med* (2014) 6(238):238ra70. doi: 10.1126/scitranslmed.3008211
41. Oh DY, Cham J, Zhang L, Fong G, Kwek SS, Klinger M, et al. Immune Toxicities Elicted by CTLA-4 Blockade in Cancer Patients Are Associated With Early Diversification of the T-Cell Repertoire. *Cancer Res* (2017) 77 (6):1322–30. doi: 10.1158/0008-5472.CAN-16-2324
42. Hopkins AC, Yarchoan M, Durham JN, Yusko EC, Rytlewski JA, Robins HS, et al. T Cell Receptor Repertoire Features Associated With Survival in Immunotherapy-Treated Pancreatic Ductal Adenocarcinoma. *JCI Insight* (2018) 3(13):e122092. doi: 10.1172/jci.insight.122092
43. Robert L, Tsoi J, Wang X, Emerson R, Homet B, Chodon T, et al. CTLA4 Blockade Broadens the Peripheral T-Cell Receptor Repertoire. *Clin Cancer Res* (2014) 20(9):2424–32. doi: 10.1158/1078-0432.CCR-13-2648
44. Page DB, Yuan J, Redmond D, Wen YH, Durack JC, Emerson R, et al. Deep Sequencing of T-Cell Receptor DNA as a Biomarker of Clonally Expanded TILs in Breast Cancer After Immunotherapy. *Cancer Immunol Res* (2016) 4 (10):835–44. doi: 10.1158/2326-6066.CIR-16-0013
45. Simoni Y, Becht E, Fehlings M, Loh CY, Koo SL, Teng KWW, et al. Bystander CD8(+) T Cells Are Abundant and Phenotypically Distinct in Human Tumour Infiltrates. *Nature* (2018) 557(7706):575–9. doi: 10.1038/s41586-018-0130-2
46. Gros A, Parkhurst MR, Tran E, Pasetto A, Robbins PF, Ilyas S, et al. Prospective Identification of Neoantigen-Specific Lymphocytes in the Peripheral Blood of Melanoma Patients. *Nat Med* (2016) 22(4):433–8. doi: 10.1038/nm.4051
47. Whijae Roh P-LC, Reuben A, Spencer CN, Prieto PA, Miller JP, Gopalakrishna V, et al. Integrated Molecular Analysis of Tumor Biopsies on Sequential CTLA-4 and PD-1 Blockade. *Cancer* (2017) 9(379):eaah3560. doi: 10.1126/scitranslmed.aah3560
48. Postow MA, Manuel M, Wong P, Yuan J, Dong Z, Liu C, et al. Peripheral T Cell Receptor Diversity Is Associated With Clinical Outcomes Following Ipilimumab Treatment in Metastatic Melanoma. *J Immunother Cancer* (2015) 3:23. doi: 10.1186/s40425-015-0070-4
49. Arakawa A, Vollmer S, Tietze J, Galinski A, Heppt MV, Burdek M, et al. Clonality of CD4(+) Blood T Cells Predicts Longer Survival With CTLA4 or PD-1 Checkpoint Inhibition in Advanced Melanoma. *Front Immunol* (2019) 10:1336. doi: 10.3389/fimmu.2019.01336
50. Hogan SA, Courtier A, Cheng PF, Jaberg-Bentele NF, Goldinger SM, Manuel M, et al. Peripheral Blood TCR Repertoire Profiling May Facilitate Patient Stratification for Immunotherapy Against Melanoma. *Cancer Immunol Res* (2019) 7(1):77–85. doi: 10.1158/2326-6066.CIR-18-0136
51. Ji S, Li J, Chang L, Zhao C, Jia R, Tan Z, et al. Peripheral Blood T-Cell Receptor Repertoire as a Predictor of Clinical Outcomes in Gastrointestinal Cancer Patients Treated With PD-1 Inhibitor. *Clin Transl Oncol* (2021) 23 (8):1646–56. doi: 10.1007/s12094-021-02562-4
52. Cader FZ, Hu X, Goh WL, Wienand K, Ouyang J, Mandato E, et al. A Peripheral Immune Signature of Responsiveness to PD-1 Blockade in Patients With Classical Hodgkin Lymphoma. *Nat Med* (2020) 26(9):1468–79. doi: 10.1038/s41591-020-1006-1
53. Snyder A, Nathanson T, Funt SA, Ahuja A, Buros Novik J, Hellmann MD, et al. Contribution of Systemic and Somatic Factors to Clinical Response and Resistance to PD-L1 Blockade in Urothelial Cancer: An Exploratory Multi-Omic Analysis. *PLoS Med* (2017) 14(5):e1002309. doi: 10.1371/journal.pmed.1002309
54. Kato T, Kiyotani K, Tomiyama E, Koh Y, Matsushita M, Hayashi Y, et al. Peripheral T Cell Receptor Repertoire Features Predict Durable Responses to Anti-PD-1 Inhibitor Monotherapy in Advanced Renal Cell Carcinoma. *Oncoimmunology* (2021) 10(1):1862948. doi: 10.1080/2162402X.2020.1862948
55. Huang AC, Postow MA, Orlowski RJ, Mick R, Bengsch B, Manne S, et al. T-Cell Invigoration to Tumour Burden Ratio Associated With Anti-PD-1 Response. *Nature* (2017) 545(7652):60–5. doi: 10.1038/nature22079
56. Han J, Duan J, Bai H, Wang Y, Wan R, Wang X, et al. TCR Repertoire Diversity of Peripheral PD-1(+)CD8(+) T Cells Predicts Clinical Outcomes After Immunotherapy in Patients With Non-Small Cell Lung Cancer. *Cancer Immunol Res* (2020) 8(1):146–54. doi: 10.1158/2326-6066.CIR-19-0398
57. Sceneay J, Goreczny GJ, Wilson K, Morrow S, DeCristo MJ, Ubellacker JM, et al. Interferon Signaling Is Diminished With Age and Is Associated With Immune Checkpoint Blockade Efficacy in Triple-Negative Breast Cancer. *Cancer Discov* (2019) 9(9):1208–27. doi: 10.1158/2159-8290.CD-18-1454
58. Ladomersky E, Zhai L, Lauing KL, Bell A, Xu J, Kocherginsky M, et al. Advanced Age Increases Immunosuppression in the Brain and Decreases Immunotherapeutic Efficacy in Subjects With Glioblastoma. *Clin Cancer Res* (2020) 26(19):5232–45. doi: 10.1158/1078-0432.CCR-19-3874
59. Kaiser M, Semeraro MD, Herrmann M, Absenger G, Gerger A, Renner W. Immune Aging and Immunotherapy in Cancer. *Int J Mol Sci* (2021) 22 (13):7016. doi: 10.3390/ijms22137016
60. Pawelec G. Does Patient Age Influence Anti-Cancer Immunity? *Semin Immunopathol* (2019) 41(1):125–31. doi: 10.1007/s00281-018-0697-6
61. Hodi FS, O'Day SJ, McDermott DF, Weber RW, Sosman JA, Haanen JB, et al. Improved Survival With Ipilimumab in Patients With Metastatic Melanoma. *N Engl J Med* (2010) 363(8):711–23. doi: 10.1056/NEJMoa1003466
62. Kugel CH3rd, Douglass SM, Webster MR, Kaur A, Liu Q, Yin X, et al. Age Correlates With Response to Anti-PD1, Reflecting Age-Related Differences in Intratumoral Effector and Regulatory T-Cell Populations. *Clin Cancer Res* (2018) 24(21):5347–56. doi: 10.1158/1078-0432.CCR-18-1116
63. Goldberg GL, Dudakov JA, Reiseger JJ, Seach N, Ueno T, Vlahos K, et al. Sex Steroid Ablation Enhances Immune Reconstitution Following Cytotoxic Antineoplastic Therapy in Young Mice. *J Immunol* (2010) 184(11):6014–24. doi: 10.4049/jimmunol.0802445
64. van den Broek T, Delemarre EM, Janssen WJ, Nievelstein RA, Broen JC, Tesselaar K, et al. Neonatal Thymectomy Reveals Differentiation and Plasticity Within Human Naive T Cells. *J Clin Invest* (2016) 126(3):1126–36. doi: 10.1172/JCI84997
65. Roux E, Dumont-Girard F, Starobinski M, Siegrist CA, Helg C, Chapuis B, et al. Recovery of Immune Reactivity After T-Cell-Depleted Bone Marrow Transplantation Depends on Thymic Activity. *Blood* (2000) 96(6):2299–303. doi: 10.1182/blood.V96.6.2299
66. Chu YW, Memon SA, Sharrow SO, Hakim FT, Eckhaus M, Lucas PJ, et al. Exogenous IL-7 Increases Recent Thymic Emigrants in Peripheral Lymphoid Tissue Without Enhanced Thymic Function. *Blood* (2004) 104 (4):1110–9. doi: 10.1182/blood-2003-10-3635
67. Mackall CL, Fry TJ, Bare C, Morgan P, Galbraith A, Gress RE. IL-7 Increases Both Thymic-Dependent and Thymic-Independent T-Cell Regeneration After Bone Marrow Transplantation. *Blood* (2001) 97(5):1491–7. doi: 10.1182/blood.v97.5.1491
68. Fry TJ, Moniuszko M, Creekmore S, Donohue SJ, Douek DC, Giardina S, et al. IL-7 Therapy Dramatically Alters Peripheral T-Cell Homeostasis in Normal and SIV-Infected Nonhuman Primates. *Blood* (2003) 101(6):2294–9. doi: 10.1182/blood-2002-07-2297
69. Alpdogan O, Muriglan SJ, Eng JM, Willis LM, Greenberg AS, Kappel BJ, et al. IL-7 Enhances Peripheral T Cell Reconstitution After Allogeneic Hematopoietic Stem Cell Transplantation. *J Clin Invest* (2003) 112 (7):1095–107. doi: 10.1172/JCI17865
70. Perales MA, Goldberg JD, Yuan J, Koehne G, Lechner L, Papadopoulos EB, et al. Recombinant Human Interleukin-7 (CYT107) Promotes T-Cell Recovery After Allogeneic Stem Cell Transplantation. *Blood* (2012) 120 (24):4882–91. doi: 10.1182/blood-2012-06-437236
71. Sheikh V, Porter BO, DerSimonian R, Kovacs SB, Thompson WL, Perez-Diez A, et al. Administration of Interleukin-7 Increases CD4 T Cells in Idiopathic CD4 Lymphocytopenia. *Blood* (2016) 127(8):977–88. doi: 10.1182/blood-2015-05-645077
72. Andrew D, Aspinall R. Il-7 and Not Stem Cell Factor Reverses Both the Increase in Apoptosis and the Decline in Thymopoiesis Seen in Aged Mice. *J Immunol* (2001) 166(3):1524–30. doi: 10.4049/jimmunol.166.3.1524
73. Sportes C, Hakim FT, Memon SA, Zhang H, Chua KS, Brown MR, et al. Administration of rhIL-7 in Humans Increases *In Vivo* TCR Repertoire Diversity by Preferential Expansion of Naive T Cell Subsets. *J Exp Med* (2008) 205(7):1701–14. doi: 10.1084/jem.20071681

74. Li L, Hsu HC, Stockard CR, Yang P, Zhou J, Wu Q, et al. IL-12 Inhibits Thymic Involution by Enhancing IL-7- and IL-2-Induced Thymocyte Proliferation. *J Immunol* (2004) 172(5):2909–16. doi: 10.4049/jimmunol.172.5.2909
75. Chen T, Burke KA, Zhan Y, Wang X, Shibata D, Zhao Y. IL-12 Facilitates Both the Recovery of Endogenous Hematopoiesis and the Engraftment of Stem Cells After Ionizing Radiation. *Exp Hematol* (2007) 35(2):203–13. doi: 10.1016/j.exphem.2006.10.002
76. Rafei M, Dumont-Lagace M, Rouette A, Perreault C. Interleukin-21 Accelerates Thymic Recovery From Glucocorticoid-Induced Atrophy. *PLoS One* (2013) 8(9):e72801. doi: 10.1371/journal.pone.0072801
77. Al-Chami E, Tormo A, Pasquin S, Kanjarawi R, Ziouani S, Rafei M. Interleukin-21 Administration to Aged Mice Rejuvenates Their Peripheral T-Cell Pool by Triggering *De Novo* Thymopoiesis. *Aging Cell* (2016) 15 (2):349–60. doi: 10.1111/acel.12440
78. Tormo A, Khodayarian F, Cui Y, Al-Chami E, Kanjarawi R, Noé B, et al. Interleukin-21 Promotes Thymopoiesis Recovery Following Hematopoietic Stem Cell Transplantation. *J Hematol Oncol* (2017) 10(1):120. doi: 10.1186/s13045-017-0490-3
79. Dudakov JA, Mertelsmann AM, O'Connor MH, Jenq RR, Velardi E, Young LF, et al. Loss of Thymic Innate Lymphoid Cells Leads to Impaired Thymopoiesis in Experimental Graft-Versus-Host Disease. *Blood* (2017) 130(7):933–42. doi: 10.1182/blood-2017-01-762658
80. Pan B, Zhang F, Lu Z, Li L, Shang L, Xia F, et al. Donor T-Cell-Derived Interleukin-22 Promotes Thymus Regeneration and Alleviates Chronic Graft-*Versus*-Host Disease in Murine Allogeneic Hematopoietic Cell Transplant. *Int Immunopharmacol* (2019) 67:194–201. doi: 10.1016/j.intimp.2018.12.023
81. Lopes N, Vachon H, Marie J, Irla M. Administration of RANKL Boosts Thymic Regeneration Upon Bone Marrow Transplantation. *EMBO Mol Med* (2017) 9(6):835–51. doi: 10.15252/emmm.201607176
82. Lee HW, Park HK, Na YJ, Kim CD, Lee JH, Kim BS, et al. RANKL Stimulates Proliferation, Adhesion and IL-7 Expression of Thymic Epithelial Cells. *Exp Mol Med* (2008) 40(1):59–70. doi: 10.3858/emm.2008.40.1.59
83. Borelli A, Irla M. Lymphotoxin: From the Physiology to the Regeneration of the Thymic Function. *Cell Death Differ* (2021) 28:2305–14. doi: 10.1038/s41418-021-00834-8
84. Seggewiss R, Lore K, Guenaga FJ, Pittaluga S, Mattapallil J, Chow CK, et al. Keratinocyte Growth Factor Augments Immune Reconstitution After Autologous Hematopoietic Progenitor Cell Transplantation in Rhesus Macaques. *Blood* (2007) 110(1):441–9. doi: 10.1182/blood-2006-12-065623
85. Rizwan R, Levine JE, Defor T, Ferarra JL, Weisdorf DJ, Blazar BR, et al. Peritransplant Palifermin Use and Lymphocyte Recovery After T-Cell Replete, Matched Related Allogeneic Hematopoietic Cell Transplantation. *Am J Hematol* (2011) 86(10):879–82. doi: 10.1002/ajh.22136
86. Jacobson JM, Wang H, Bordi R, Zheng L, Gross BH, Landay AL, et al. A Randomized Controlled Trial of Palifermin (Recombinant Human Keratinocyte Growth Factor) for the Treatment of Inadequate CD4+ T Lymphocyte Recovery in Patients With HIV-1 Infection on Antiretroviral Therapy. *J Acquir Immune Defic Syndr* (2014) 66(4):399–406. doi: 10.1097/QAI.0000000000000195
87. Coles AJ, Azzopardi L, Kousin-Ezewu O, Mullay HK, Thompson SA, Jarvis L, et al. Keratinocyte Growth Factor Impairs Human Thymic Recovery From Lymphopenia. *JCI Insight* (2019) 5. doi: 10.1172/jci.insight.125377
88. Rossi S, Blazar BR, Farrell CL, Danilenko DM, Lacey DL, Weinberg KI, et al. Keratinocyte Growth Factor Preserves Normal Thymopoiesis and Thymic Microenvironment During Experimental Graft-*Versus*-Host Disease. *Blood* (2002) 100(2):682–91. doi: 10.1182/blood.v100.2.682
89. Rossi SW, Jeker LT, Ueno T, Kuse S, Keller MP, Zuklys S, et al. Keratinocyte Growth Factor (KGF) Enhances Postnatal T-Cell Development *via* Enhancements in Proliferation and Function of Thymic Epithelial Cells. *Blood* (2007) 109(9):3803–11. doi: 10.1182/blood-2006-10-049767
90. Chu YW, Schmitz S, Choudhury B, Telford W, Kapoor V, Garfield S, et al. Exogenous Insulin-Like Growth Factor 1 Enhances Thymopoiesis Predominantly Through Thymic Epithelial Cell Expansion. *Blood* (2008) 112(7):2836–46. doi: 10.1182/blood-2008-04-149435
91. Wertheimer T, Velardi E, Tsai J, Cooper K, Xiao S, Kloss CC, et al. Production of BMP4 by Endothelial Cells Is Crucial for Endogenous Thymic Regeneration. *Sci Immunol* (2018) 3(19):eaal2736. doi: 10.1126/sciimmunol.aal2736
92. Ding J-H, Wang L-L, Chen Z, Wang J, Yu Z-P, Zhao G, et al. The Role of Tα1 on the Infective Patients After Hematopoietic Stem Cell Transplantation. *Int J Hematol* (2013) 97(2):280–3. doi: 10.1007/s12185-012-1208-5
93. Perruccio K, Bonifazi P, Topini F, Tosti A, Bozza S, Aloisi T, et al. Thymosin Alpha1 to Harness Immunity to Pathogens After Haploidentical Hematopoietic Transplantation. *Ann NY Acad Sci* (2010) 1194:153–61. doi: 10.1111/j.1749-6632.2010.05486.x
94. Wang F, Yu T, Zheng H, Lao X. Thymosin Alpha1-Fc Modulates the Immune System and Down-Regulates the Progression of Melanoma and Breast Cancer With a Prolonged Half-Life. *Sci Rep* (2018) 8(1):12351. doi: 10.1038/s41598-018-30956-y
95. Danielli R, Cisternino F, Giannarelli D, Calabro L, Camerini R, Savelli V, et al. Long-Term Follow Up of Metastatic Melanoma Patients Treated With Thymosin Alpha-1: Investigating Immune Checkpoints Synergy. *Expert Opin Biol Ther* (2018) 18(sup1):77–83. doi: 10.1080/14712598.2018.1494717
96. Napolitano LA, Lo JC, Gotway MB, Mulligan K, Barbour JD, Schmidt D, et al. Increased Thymic Mass and Circulating Naive CD4 T Cells in HIV-1-Infected Adults Treated With Growth Hormone. *AIDS* (2002) 16(8):1103–11. doi: 10.1097/00002030-200205240-00003
97. Chen BJ, Cui X, Sempowski GD, Chao NJ. Growth Hormone Accelerates Immune Recovery Following Allogeneic T-Cell-Depleted Bone Marrow Transplantation in Mice. *Exp Hematol* (2003) 31(10):953–8. doi: 10.1016/s0301-472x(03)00196-6
98. Dixit VD, Yang H, Sun Y, Weeraratna AT, Youm YH, Smith RG, et al. Ghrelin Promotes Thymopoiesis During Aging. *J Clin Invest* (2007) 117 (10):2778–90. doi: 10.1172/JCI30248
99. Napolitano LA, Schmidt D, Gotway MB, Ameli N, Filbert EL, Ng MM, et al. Growth Hormone Enhances Thymic Function in HIV-1-Infected Adults. *J Clin Invest* (2008) 118(3):1085–98. doi: 10.1172/JCI32830
100. Fahy GM, Brooke RT, Watson JP, Good Z, Vasanawala SS, Maecker H, et al. Reversal of Epigenetic Aging and Immunosenescent Trends in Humans. *Aging Cell* (2019) 18(6):e13028. doi: 10.1111/acel.13028
101. Morrhaye G, Kermani H, Legros JJ, Baron F, Beguin Y, Moutschen M, et al. Impact of Growth Hormone (GH) Deficiency and GH Replacement Upon Thymus Function in Adult Patients. *PLoS One* (2009) 4(5):e5668. doi: 10.1371/journal.pone.0005668
102. Goldberg GL, King CG, Nejat RA, Suh DY, Smith OM, Bretz JC, et al. Luteinizing Hormone-Releasing Hormone Enhances T Cell Recovery Following Allogeneic Bone Marrow Transplantation. *J Immunol* (2009) 182(9):5846–54. doi: 10.4049/jimmunol.0801458
103. Velardi E, Tsai JJ, Radtke S, Cooper K, Argyropoulos KV, Jae-Hung S, et al. Suppression of Luteinizing Hormone Enhances HSC Recovery After Hematopoietic Injury. *Nat Med* (2018) 24(2):239. doi: 10.1038/nm.4470
104. Lai KP, Lai JJ, Chang P, Altuwaijri S, Hsu JW, Chuang KH, et al. Targeting Thymic Epithelia AR Enhances T-Cell Reconstitution and Bone Marrow Transplant Grafting Efficacy. *Mol Endocrinol* (2013) 27(1):25–37. doi: 10.1210/me.2012-1244
105. Heng TS, Reiseger JJ, Fletcher AL, Leggatt GR, White OJ, Vlahos K, et al. Impact of Sex Steroid Ablation on Viral, Tumour and Vaccine Responses in Aged Mice. *PLoS One* (2012) 7(8):e42677. doi: 10.1371/journal.pone.0042677
106. Velardi E, Tsai JJ, Holland AM, Wertheimer T, Yu VWC, Zakrzewski JL, et al. Sex Steroid Blockade Enhances Thymopoiesis by Modulating Notch Signaling. *J Exp Med* (2014) 211(12):2341–9. doi: 10.1084/Jem.20131289
107. Dudakov JA, Goldberg GL, Reiseger JJ, Vlahos K, Chidgey AP, Boyd RL. Sex Steroid Ablation Enhances Hematopoietic Recovery Following Cytotoxic Antineoplastic Therapy in Aged Mice. *J Immunol* (2009) 183(11):7084–94. doi: 10.4049/jimmunol.0900196
108. Khong DM, Dudakov JA, Hammett MV, Jurblum MI, Khong SM, Goldberg GL, et al. Enhanced Hematopoietic Stem Cell Function Mediates Immune Regeneration Following Sex Steroid Blockade. *Stem Cell Rep* (2015) 4 (3):445–58. doi: 10.1016/j.stemcr.2015.01.018
109. Sutherland JS, Spyroglou L, Muirhead JL, Heng TS, Prieto-Hinojosa A, Prince HM, et al. Enhanced Immune System Regeneration in Humans Following Allogeneic or Autologous Hemopoietic Stem Cell

Transplantation by Temporary Sex Steroid Blockade. *Clin Cancer Res* (2008) 14(4):1138–49. doi: 10.1158/1078-0432.CCR-07-1784
110. Fan Y, Tajima A, Goh SK, Geng X, Gualtierotti G, Grupillo M, et al. Bioengineering Thymus Organoids to Restore Thymic Function and Induce Donor-Specific Immune Tolerance to Allografts. *Mol Ther J Am Soc Gene Ther* (2015) 23(7):1262–77. doi: 10.1038/mt.2015.77
111. Shah NJ, Mao AS, Shih T-Y, Kerr MD, Sharda A, Raimondo TM, et al. An Injectable Bone Marrow–Like Scaffold Enhances T Cell Immunity After Hematopoietic Stem Cell Transplantation. *Nat Biotechnol* (2019) 37:293–302. doi: 10.1038/s41587-019-0017-2
112. Otsuka R, Wada H, Tsuji H, Sasaki A, Murata T, Itoh M, et al. Efficient Generation of Thymic Epithelium From Induced Pluripotent Stem Cells That Prolongs Allograft Survival. *Sci Rep* (2020) 10(1):224. doi: 10.1038/s41598-019-57088-1
113. Bredenkamp N, Ulyanchenko S, O'Neill KE, Manley NR, Vaidya HJ, Blackburn CC. An Organized and Functional Thymus Generated From FOXN1-Reprogrammed Fibroblasts. *Nat Cell Biol* (2014) 16(9):902–8. doi: 10.1038/ncb3023
114. Bortolomai I, Sandri M, Draghici E, Fontana E, Campodoni E, Marcovecchio GE, et al. Gene Modification and Three-Dimensional Scaffolds as Novel Tools to Allow the Use of Postnatal Thymic Epithelial Cells for Thymus Regeneration Approaches. *Stem Cells Transl Med* (2019) 8(10):1107–22. doi: 10.1002/sctm.18-0218
115. Finch PW, Rubin JS. Keratinocyte Growth Factor/Fibroblast Growth Factor 7, a Homeostatic Factor With Therapeutic Potential for Epithelial Protection and Repair. *Adv Cancer Res* (2004) 91:69–136. doi: 10.1016/S0065-230X(04)91003-2
116. Alpdogan O, Hubbard VM, Smith OM, Patel N, Lu S, Goldberg GL, et al. Keratinocyte Growth Factor (KGF) Is Required for Postnatal Thymic Regeneration. *Blood* (2006) 107(6):2453–60. doi: 10.1182/blood-2005-07-2831
117. Min D, Panoskaltsis-Mortari A, Kuro OM, Hollander GA, Blazar BR, Weinberg KI. Sustained Thymopoiesis and Improvement in Functional Immunity Induced by Exogenous KGF Administration in Murine Models of Aging. *Blood* (2007) 109(6):2529–37. doi: 10.1182/blood-2006-08-043794
118. Wils EJ, Aerts-Kaya FS, Rombouts EJ, van Mourik I, Rijken-Schelen A, Visser TP, et al. Keratinocyte Growth Factor and Stem Cell Factor to Improve Thymopoiesis After Autologous CD34+ Cell Transplantation in Rhesus Macaques. *Biol Blood Marrow Transplant* (2012) 18(1):55–65. doi: 10.1016/j.bbmt.2011.09.010
119. Hirokawa K, McClure JE, Goldstein AL. Age-Related Changes in Localization of Thymosin in the Human Thymus. *Thymus* (1982) 4(1):19–29.
120. Taub DD, Murphy WJ, Longo DL. Rejuvenation of the Aging Thymus: Growth Hormone-Mediated and Ghrelin-Mediated Signaling Pathways. *Curr Opin Pharmacol* (2010) 10(4):408–24. doi: 10.1016/j.coph.2010.04.015
121. Olsen NJ, Olson G, Viselli SM, Gu X, Kovacs WJ. Androgen Receptors in Thymic Epithelium Modulate Thymus Size and Thymocyte Development. *Endocrinology* (2001) 142(3):1278–83. doi: 10.1210/endo.142.3.8032
122. Wilhelmson AS, Lantero Rodriguez M, Johansson I, Svedlund Eriksson E, Stubelius A, Lindgren S, et al. Androgen Receptors in Epithelial Cells Regulate Thymopoiesis and Recent Thymic Emigrants in Male Mice. *Front Immunol* (2020) 11:1342. doi: 10.3389/fimmu.2020.01342
123. Just HL, Deleuran M, Vestergaard C, Deleuran B, Thestrup-Pedersen K. T-Cell Receptor Excision Circles (TREC) in CD4+ and CD8+ T-Cell Subpopulations in Atopic Dermatitis and Psoriasis Show Major Differences in the Emission of Recent Thymic Emigrants. *Acta Dermato-Venereologica* (2008) 88(6):566–72. doi: 10.2340/00015555-0550
124. Pido-Lopez J, Imami N, Aspinall R. Both Age and Gender Affect Thymic Output: More Recent Thymic Migrants in Females Than Males as They Age. *Clin Exp Immunol* (2001) 125(3):409–13. doi: 10.1046/j.1365-2249.2001.01640.x
125. Hun ML, Wong K, Gunawan JR, Alsharif A, Quinn K, Chidgey AP. Gender Disparity Impacts on Thymus Aging and LHRH Receptor Antagonist-Induced Thymic Reconstitution Following Chemotherapeutic Damage. *Front Immunol* (2020) 11:302. doi: 10.3389/fimmu.2020.00302
126. Fairweather D, Frisancho-Kiss S, Rose NR. Sex Differences in Autoimmune Disease From a Pathological Perspective. *Am J Pathol* (2008) 173(3):600–9. doi: 10.2353/ajpath.2008.071008
127. Page DB, Kim IK, Chun B, Redmond WL, Martel M, Mori M, et al. A Phase II Study of Dual Immune Checkpoint Blockade (ICB) Plus Androgen Receptor (AR) Blockade to Enhance Thymic T-Cell Production and Immunotherapy Response in Metastatic Breast Cancer (MBC). *J Clin Oncol* (2019) 37(15_suppl): TPS1106–TPS. doi: 10.1200/JCO.2019.37.15_suppl.TPS1106
128. Dudakov JA, Hanash AM, Jenq RR, Young LF, Ghosh A, Singer NV, et al. Interleukin-22 Drives Endogenous Thymic Regeneration in Mice. *Science* (2012) 336(6077):91–5. doi: 10.1126/science.1218004
129. Thompson HL, Smithey MJ, Uhrlaub JL, Jeftic I, Jergovic M, White SE, et al. Lymph Nodes as Barriers to T-Cell Rejuvenation in Aging Mice and Nonhuman Primates. *Aging Cell* (2019) 18(1):e12865. doi: 10.1111/acel.12865
130. Cheng M, Anderson MS. Thymic Tolerance as a Key Brake on Autoimmunity. *Nat Immunol* (2018) 19(7):659–64. doi: 10.1038/s41590-018-0128-9
131. Wang W, Thomas R, Sizova O, Su DM. Thymic Function Associated With Cancer Development, Relapse, and Antitumor Immunity - A Mini-Review. *Front Immunol* (2020) 11:773. doi: 10.3389/fimmu.2020.00773
132. Trager U, Sierro S, Djordjevic G, Bouzo B, Khandwala S, Meloni A, et al. The Immune Response to Melanoma Is Limited by Thymic Selection of Self-Antigens. *PLoS One* (2012) 7(4):e35005. doi: 10.1371/journal.pone.0035005
133. Conteduca G, Ferrera F, Pastorino L, Fenoglio D, Negrini S, Sormani MP, et al. The Role of AIRE Polymorphisms in Melanoma. *Clin Immunol* (2010) 136(1):96–104. doi: 10.1016/j.clim.2010.03.002
134. Bakhru P, Zhu ML, Wang HH, Hong LK, Khan I, Mouchess M, et al. Combination Central Tolerance and Peripheral Checkpoint Blockade Unleashes Antimelanoma Immunity. *JCI Insight* (2017) 2(18):e93265. doi: 10.1172/jci.insight.93265
135. Dougall WC, Roman Aguilera A, Smyth MJ. Dual Targeting of RANKL and PD-1 With a Bispecific Antibody Improves Anti-Tumor Immunity. *Clin Transl Immunol* (2019) 8(10):e01081. doi: 10.1002/cti2.1081

Conflict of Interest: The authors declare that the research was conducted in the absence of any commercial or financial relationships that could be construed as a potential conflict of interest.

Publisher's Note: All claims expressed in this article are solely those of the authors and do not necessarily represent those of their affiliated organizations, or those of the publisher, the editors and the reviewers. Any product that may be evaluated in this article, or claim that may be made by its manufacturer, is not guaranteed or endorsed by the publisher.

frontiers in Oncology

ORIGINAL RESEARCH
published: 02 December 2021
doi: 10.3389/fonc.2021.733533

OPEN ACCESS

Edited by:
Alison Taylor,
University of Leeds, United Kingdom

Reviewed by:
Chengzhi Zhou,
Clinical Management Department of National Respiratory Medical Center, China
Weilai Dong,
Yale University, United States

***Correspondence:**
Yun Li
liyun28@mail.sysu.edu.cn
Yuhong Liang
rainbowliang1230@163.com
Bihui Huang
bihui_huang@126.com

†ORCID:
Yun Li
orcid.org/0000-0003-0949-6519
Yuhong Liang
orcid.org/0000-0003-1157-984X
Bihui Huang
orcid.org/0000-0003-3084-7096

‡These authors have contributed equally to this work and share the first authorship

§These authors have contributed equally to this work and share the last authorship

Specialty section:
This article was submitted to Cancer Immunity and Immunotherapy, a section of the journal Frontiers in Oncology

Received: 30 June 2021
Accepted: 27 October 2021
Published: 02 December 2021

Citation:
Leng Y, Dang S, Yin F, Gao T, Xiao X, Zhang Y, Chen L, Qin C, Lai N, Zhan X-Y, Huang K, Luo C, Kang Y, Wang N, Li Y, Liang Y and Huang B (2021) GDPLichi: a DNA Damage Repair-Related Gene Classifier for Predicting Lung Adenocarcinoma Immune Checkpoint Inhibitors Response. Front. Oncol. 11:733533. doi: 10.3389/fonc.2021.733533

GDPLichi: a DNA Damage Repair-Related Gene Classifier for Predicting Lung Adenocarcinoma Immune Checkpoint Inhibitors Response

Yang Leng[1‡], Shiying Dang[1‡], Fei Yin[2], Tianshun Gao[1], Xing Xiao[1], Yi Zhang[1], Lin Chen[1], Changfei Qin[1], Nannan Lai[1], Xiao-Yong Zhan[1], Ke Huang[1], Chuanming Luo[3], Yang Kang[1], Nan Wang[1], Yun Li[2†‡], Yuhong Liang[4*†§] and Bihui Huang[1*†§]*

[1] Scientific Research Center, The Seventh Affiliated Hospital, Sun Yat-sen University, Shenzhen, China, [2] Department of Thoracic Surgery, The Seventh Affiliated Hospital, Sun Yat-sen University, Shenzhen, China, [3] Center for Clinical Neuroscience, The Seventh Affiliated Hospital, Sun Yat-sen University, Shenzhen, China, [4] School of Medicine, Southern University Of Science And Technology, Shenzhen, China

Lung cancer is one of the most common and mortal malignancies, usually with a poor prognosis in its advanced or recurrent stages. Recently, immune checkpoint inhibitors (ICIs) immunotherapy has revolutionized the treatment of human cancers including lung adenocarcinoma (LUAD), and significantly improved patients' prognoses. However, the prognostic and predictive outcomes differ because of tumor heterogeneity. Here, we present an effective method, GDPLichi (Genes of DNA damage repair to predict LUAD immune checkpoint inhibitors response), as the signature to predict the LUAD patient's response to the ICIs. GDPLichi utilized only 7 maker genes from 8 DDR pathways to construct the predictive model and classified LUAD patients into two subgroups: low- and high-risk groups. The high-risk group was featured by worse prognosis and decreased B cells, $CD8^+$ T cells, $CD8^+$ central memory T cells, hematopoietic stem cells (HSC), myeloid dendritic cells (MDC), and immune scores as compared to the low-risk group. However, our research also suggests that the high-risk group was more sensitive to ICIs, which might be explained by increased TMB, neoantigen, immune checkpoint molecules, and immune suppression genes' expression, but lower TIDE score as compared to the low-risk group. This conclusion was verified in three other LUAD cohort datasets (GSE30219, GSE31210, GSE50081).

Keywords: DNA damage repair (DDR), immune check inhibitor (ICI), GDPLichi, lung adenocarcinoma, gene classifier

INTRODUCTION

Lung cancer ranks the second in incidence and top in mortality among malignancies worldwide (1), of which lung adenocarcinoma is the most common subtype (2). The prognosis of advanced and recurrent lung cancer is usually poor because most standard treatments by cytotoxic anticancer drugs only have limited therapeutic effects. In recent years, with a better understanding of immune response regulation,

the immune checkpoint inhibitor (ICI) therapy showed improved survival rates in multiple cancers including non-small-cell lung cancer (NSCLC). The principle of ICIs is to reactivate immune cells by using specific antibodies against inhibitory signaling molecules such as CTLA-4 and PD-1 expressed on tumor and immune cells. Currently, the approved drugs of anti-CTLA-4 (ipilimumab), anti-PD-1 (nivolumab and pembrolizumab), anti-PD-L1 (atezolizumab, avelumab, and durvalumab), and their combinations have performed significant improvements in treating advanced NSCLC patients (3–6). Lung adenocarcinoma accounts for 80% of NSCLC and benefits most from ICIs therapy. However, it was also reported that there were still only partial LUAD patients responsive to ICIs (7).

PD-L1 expression has been widely used as an ICI response predictive marker, but the sensitivity and specificity are not very consistent due to different antibodies and cutoff values used for PD-L1 test (3, 8, 9). Meanwhile, PD-L1 expression cannot accurately reflect the complicated tumor immune microenvironment (10). Recent studies have also reported that tumor mutation burden (TMB) is closely related to the efficacy of ICIs response (11, 12) and can also be used as a predictive marker for the efficacy of ICI treatment. Like PD-L1, the cut-off value of TMB is controversial (13–15). Additionally, TMB alone does not directly produce neoantigen processing by major histocompatibility complex (MHC) class molecules, thus the accuracy of TMB as a predictor for ICI treatment is modest. Neoantigen expressed on tumor cells is one of the main targets for an effective antitumor T-cell response (16), but difficult to be identified. Therefore, identifying novel markers that can efficiently and accurately predict ICI responses is urgent. One promising area for this research is DNA damage repair (DDR). To ensure the integrity of the genome, cells activate DNA damage repair pathways to repair genetic lesions (SNP, Indel, etc.) during the process of DNA replication. DDR consists of eight pathways including miss match repair (MMR), base excision repair (BER), nucleotide excision repair (NER), direct damage repair (DR), homologous dependent recombination (HDR), nonhomologous end joining (NHEJ), fanconi anemia pathway (FA), and translesion DNA synthesis (TLS). Defects in DDR pathways lead to the accumulation of genomic aberrations and an elevated TMB (17–19), thus promoting tumor development (20). Many studies have shown that mutations in DDR pathway genes are associated with ICIs responses (20, 21). Patients who have DDR genomic alterations usually have a better clinical benefit after ICIs therapy (19, 21).

The Tumor Immune Dysfunction and Exclusion (TIDE) algorithm is a computational method that uses gene expression profiles to predict the ICIs response, particularly successful in NSCLC and melanoma (22). TIDE uses a specific set of marker genes to estimate dysfunction of tumor-infiltrating cytotoxic T lymphocyte and exclusion of CTL by an immunosuppressive factor to predict patients' response to ICIs. Patients with lower TIDE scores have a lower chance of antitumor immune escape, thus having a higher response rate of ICIs treatment (22). The TIDE score exhibited a higher accuracy than PD-L1 expression level and TMB in predicting the overall survival of patients treated with ICIs (20, 23, 24). Some studies also have reported its utility in predicting or evaluating the ICIs efficacy (24–28).

We identified seven significant genes (e.g., DUT, MGMT, POLH, RAD1, RAD17, TYMS, and YWHAG) strongly associated with prognosis from DDR pathways using Cox regression analysis.

Patients with lower expression of DUT, TYMS, and YWHAG but higher expression of MGMT, POLH, RAD1, and RAD17 had a better prognosis. Based on the expressions and weights calculated by Cox regression on these genes, we developed a classifier, GDPLichi (Genes of DDR to Predict LUAD immune checkpoint inhibitors), as the signature to predict the ICIs response. LUAD patients were classified into low- and high-risk groups based on the cutoff of the GDPLichi score. Many features, including PDCD1, CTLA4, PD-L1 expression, TMB, and neoantigen, displayed strong discerning abilities in the survival analysis of these two subgroups. Especially, the high-risk subgroup had a worse prognosis but is presumably more efficacious towards ICIs treatment.

MATERIALS AND METHOD

Data Source

To predict the LUAD ICIs response, we built a multi-step approach called GDPLichi described below (**Figure 1** and **Supplementary Figure S1**). The transcriptome gene expression, genomic data, and clinical phenotype data of 526 TCGA-LUAD samples were downloaded from the website xenabrowser (https://xenabrowser.net/datapages/). TCGA raw RNA-Seq transcriptome count data including 526 LUAD samples were further transferred into a transcript per kilobase mullion (TPM). Three validation groups of raw data, including 438 LUAD samples from 3 cohorts [GSE31210 (29), GSE30219 (30), and GSE50081 (31)], were downloaded from Gene Expression Omnibus (GEO) repository. Then raw data were transferred to expression data using the "Oligo" package in R software. For genes with multiple probes, their expression levels were calculated as the maximum expression level of these probes. Finally, all expression data were normalized and converted to Z-scores.

GDPLichi Score

First, a univariate Cox regression model was used to assess the association of 276 DNA damage repair-related genes (**Supplementary File 1**) with the overall survival in the TCGA LUAD cohort. P-value was used to identify key genes and genes with P-value < 0.05 were considered as predictive genes (**Supplementary File 2**). Then, 63 predictive genes were selected for multivariate Cox regression and genes with P-value < 0.05 were considered as risk genes (**Supplementary File 3**). Finally, seven risk genes were obtained by multivariate Cox regression and combined to construct the GDPLichi classifier. By combining the expression values of risk genes and weighting by multivariate Cox regression coefficients, the GDPLichi score for each patient was calculated as follows:

$$\text{GDPLichi score} = \Sigma_{i=1}^{n} expre_i \beta_i$$

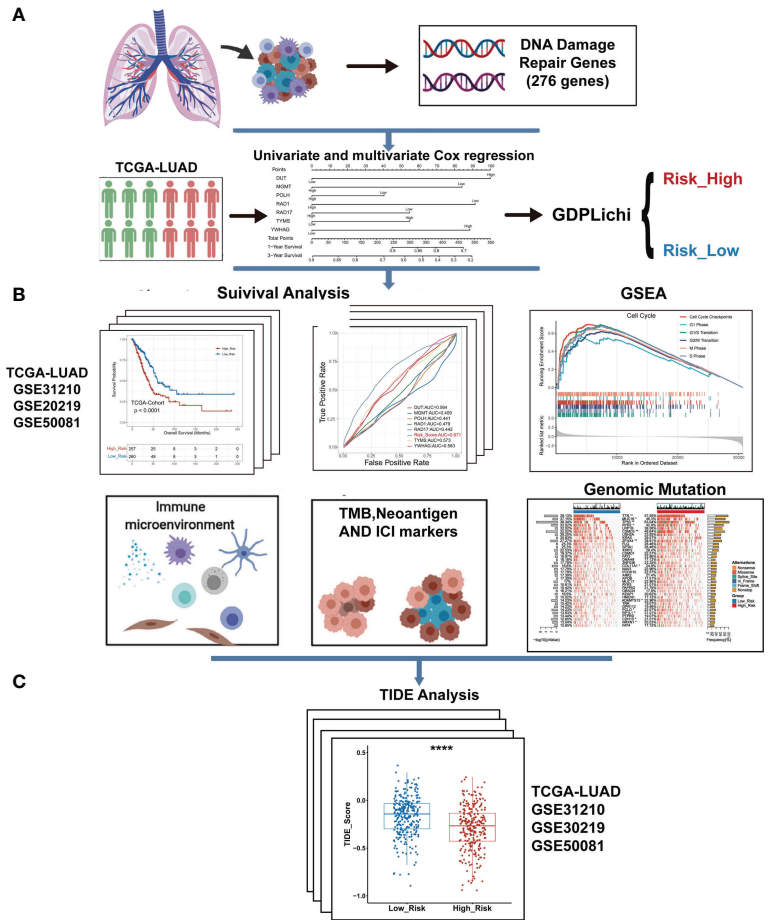

FIGURE 1 | The overall workflow of GDPLichi. **(A)** GDPLichi was constructed by DNA damage-related genes and divided LUAD patients into two subgroups (low- and high-risk). **(B)** GDPLichi can be used for the analyses of survival, GSEA, immune microenvironment, TMB, Neoantigen, immune checkpoint genes (PD-L1, PD-1, CTLA4), and genomic mutation between low- and high-risk subgroups. **(C)** The TIDE algorithm was used to predict the sensitivity to immune checkpoint inhibitors (ICIs) between low- and high-risk groups in four cohorts.

Here n is the number of prognostic genes, $expre_i$ meant the expression value of gene i, and β_i represented the regression coefficient of gene i in the multivariate Cox regression analysis. Using the median GDPLichi score as a cutoff value, TCGA and GEO LUAD patients could be classified into low and high-risk groups.

Gene Set Enrich Analysis, Survival Analysis, Principal Components Analysis, Tumor Microenvironment Analysis, and TIDE

R language 4.0 was applied in this study for the statistical analyses. GSEA was used to explore the pathway enrichment between low- and high-risk groups using the R package "clusterProfiler" (32) on the Reactome pathway database (33) with default parameters. The fold change of gene expressions between two groups was used to rank the genes. The absolute values of the normalized enrichment score (NES) >1 and P-value ≤0.05 were used to screen out significantly enriched pathways. The "survivalROC" package was used to plot the survival ROC curve. The cutoff of survival time was set to 36 months. "Forest plot" was used in the "forestmodel" package and the "factor_separate_line" parameters were set as TRUE. Survival analysis of two groups was carried out by the R package "survminer". PCA was used by the R packages "FactoMineR" and "factoextra" with the values of all genes' expression as the input. We used the "xCell" package (34) to estimate relative subsets of immune cells. TIDE Score was calculated with the TIDE algorithm (22) from the website (http://tide.dfci.harvard.edu). All R package parameters can be found in the source analysis code in main_code.R (**Supplementary File 6**).

Patient Sample Collection

From the TCGA LUAD cohort downloaded from the xenabrowser website, samples with survival, and genomic data were collected. In datasets GSE31210, GSE50081, and GSE30219, lung squamous cell carcinoma samples could be excluded and lung adenocarcinoma with survival data were collected.

RESULT

Construction of GDPLichi

A univariate Cox regression model was used to assess the association of 276 DNA damage repair genes with the overall survival in the TCGA LUAD cohort. There were 63 predictive genes screened out with an initial significance (P <0.05). By using these 63 predictive genes as input for multivariate Cox regression, seven risk genes (DUT, MGMT, POLH, RAD1, RAD17, TYMS, and YWHAG) were screened out (**Figure 2A**) and Kaplan–Meier analysis further confirmed the prognostic value of the individual genes (**Suppelementary Figure S2**). The multivariate Cox regression analysis of the above seven risk genes showed high accuracy in predicting the survival of LUAD patients (**Figure 2B**). By combining the expression values of seven risk genes and weighted by COX regression coefficients, the GDPLichi score for each patient was calculated (Described in 2.2). To further facilitate the application of the GDPLichi, the patients were divided into low- and high-risk groups according to the median value of the GDPLichi score. PCA showed that patients could be distinctively clustered according to the selected signatures (the seven risk genes) in the TCGA LUAD cohort (**Figure 2C**) and three GEO validation cohorts (**Suppelementary Figure S3A**). In addition, Spearman's correlation test indicated that GDPLichi was significantly correlated with the selected genes in the TCGA LUAD cohort (**Figure 2D**) and three GEO validation cohorts (**Figure S3B**).

Identification of LUAD Subgroups With Prognostic Significance According to GDPLichi

LUAD patients were classified into low- or high-risk groups based on the median GDPLichi score described above. The overall survival analysis for these two subgroups showed a significant difference in the TCGA cohort (**Figure 3A**, P<0.0001) and three GEO validation cohorts (**Suppelementary Figure S4A**).

The hazard ratio of the two subgroups in the TCGA cohort is 1.912 (GSE30219: 2.99, GSE31210: 3.79, GSE50081: 2.43). The 95% confidence interval of two subgroups of TCGA cohort is 1.421-2.573 (GSE30219: 1.585-5.641, GSE31210: 1.72-8.351, GSE50081: 1.356-4.356). The difference remained statistically significant after adjusting for age, gender, stage, and smoking

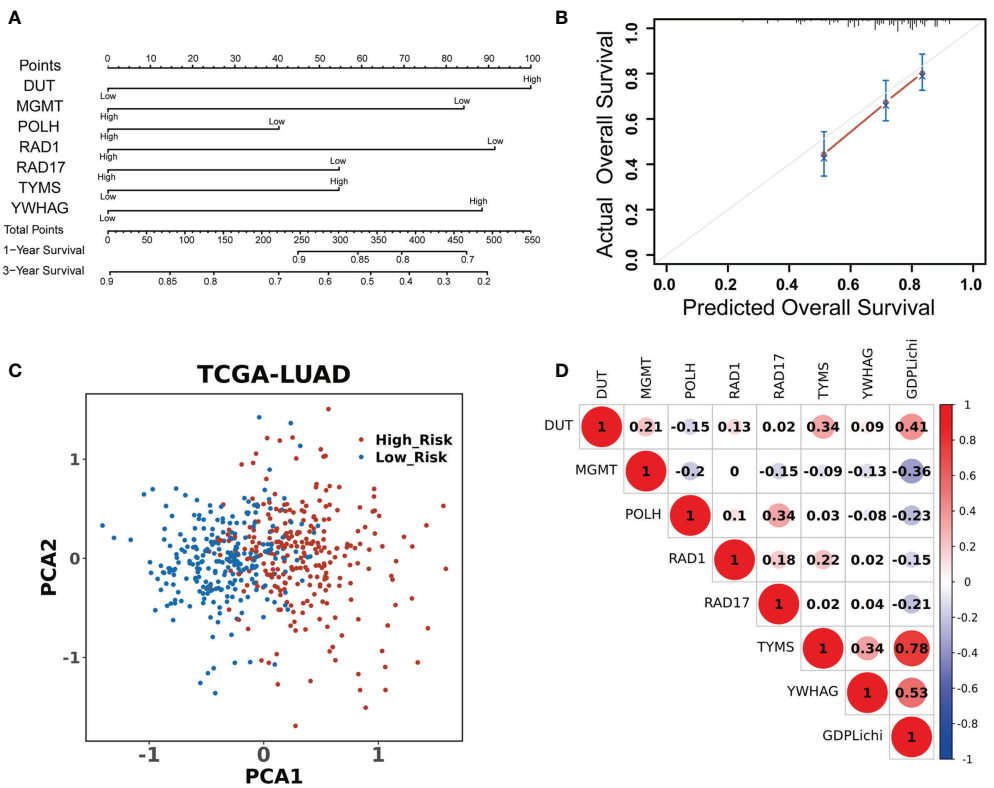

FIGURE 2 | DDR signature accurately predicts the prognosis of LUAD patients. **(A)** Univariate and multivariate Cox regression analyses screened out seven risk genes. The point number represents a score for the relation between the expression of each selected gene and the predicted survival calculated by Cox regression. High and low represent the highest and lowest expression levels of the gene, respectively. Total points were the sum of the individual points from the seven selected genes. Based on the total points, 1-year and 3-year predicted overall survival rates of each LUAD patient were calculated. The higher the number, the lower the predicted survival. **(B)** Multivariate Cox regression analysis of the seven risk genes in predicting the survival of LUAD patients. **(C)** PCA based on the expression profile of the seven risk genes from different risk groups. **(D)** Correlation between the GDPLichi and the seven risk genes in the TCGA LUAD cohort.

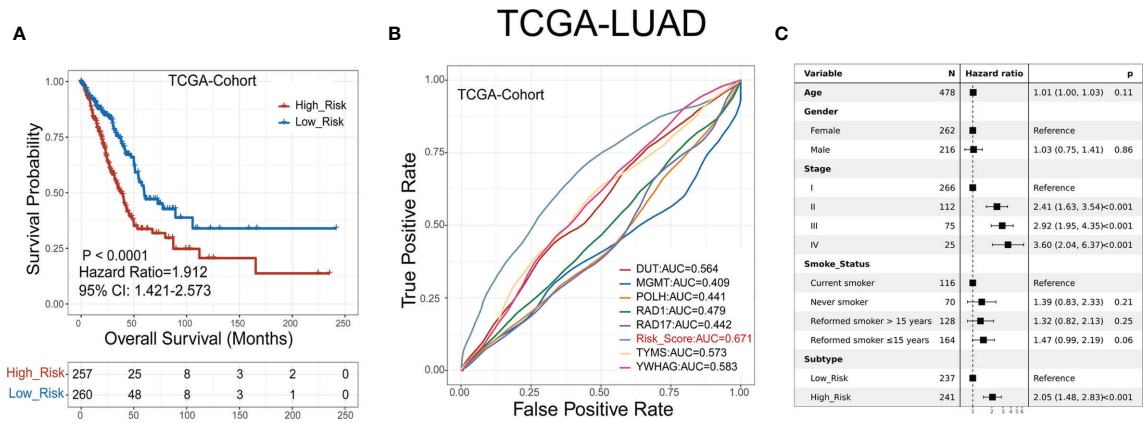

FIGURE 3 | GDPLichi score can function as a prognostic index for LUAD patients. **(A)** Kaplan-Meier plots of the survival probability for low- and high-risk subgroups of TCGA cohort, respectively. **(B)** ROC curves for the performance of the GDPLichi score as well as the seven risk genes of the classifier in TCGA in predicting prognosis. **(C)** Forest plot representation of multivariate Cox model depicting the association between overall survival and LUAD subgroups with other clinical factors considered in the TCGA cohort.

status in the TCGA cohort (**Figure 3C**) and three GEO validation cohorts (**Suppelementary Figure S4C**). To test the practicality of the GDPLichi classifier, we applied ROC (Receiver Operating Characteristic) analyses to the TCGA cohort and found that the GDPLichi score could function as a better prognostic index than any risk gene alone (**Figure 3B**). This result was also validated in the three GEO cohorts (**Suppelementary Figure S4B**). Therefore, the GDPLichi could be a good model to predict the prognosis of LUAD patients.

GSEA Explored the Pathway Enrichment Between Low- and High-Risk Groups

To further investigate the difference of biological mechanisms between low- and high-risk groups divided by GDPLichi, we performed GSEA on the TCGA LUAD cohort. It revealed that cell proliferation-related pathways such as cellular response to hypoxia, MAPK signaling, and noncanonical NF-κB signaling were significantly enriched in the high-risk group (**Figures 4, B**). Meanwhile, cell cycle pathways were also significantly enriched in the high-risk group (**Figures 4B, D**). The results also showed that immune-related pathways such as antigen procession, cross-presentation, interleukin-10 signaling, and MHC class II antigen presentation were significantly enriched (**Figure 4C**). By examining the expression of HLA genes, it was revealed that the expression of MHC II genes in the low-risk group was significantly higher than in the high-risk group (**Figure 4E**). MHC II genes are only expressed in antigen-presenting cells. This may indicate a higher tumor-infiltrating lymphocyte (TIL) in the low-risk group, and ultimately a poorer prognosis.

The Difference in Tumor Immune Microenvironment Between Low- and High-Risk Groups

The "xCell" algorithm was employed to estimate the immune cells in malignant tumor tissues between two subgroups using RNA sequencing data. Our results showed that the immune scores, B cells, hematopoietic stem cells (HSC), myeloid dendritic cells (MDC), $CD8^+$ T cells, and $CD8^+$ central memory T cells were significantly higher in low-risk groups compared to high-risk groups, suggesting a higher TIL in the low-risk group (**Figures 5A–F**). $CD8^+$ T cells, also named cytotoxic T cells, are one of the major tumor killer cells and $CD8^+$ cell exclusion is strongly associated with tumor immune escape. Therefore, we examined the expression of several immune-suppression genes such as TIM-3 (HAVCR2), IDO1, LAG3, PD-L2 (PDCD1LG2), TIGIT, CD276, CD160, VEGFA, VEGFB, SLAMF7, KIR2DL3, and IL1B between low- and high-risk groups. As shown in **Figure 5G**, the high-risk group had a higher expression of immunosuppression genes than the low-risk group, which might account for higher sensitivity to ICIs in the high-risk subgroup of LUAD patients.

The Difference in TMB, Neoantigen, and ICIs-Target Expression Between Low- and High-Risk Subgroups

To predict the sensitivity to ICIs between low- and high-risk groups as classified by the GDPLichi model, we further examined immunotherapy-related markers such as tumor mutation burden (TMB), neoantigen, and expression of PDCD1 (PD-1), CD274 (PD-L1), and CTLA4. The degree of TMB and neoantigen in the high-risk group was significantly higher as compared to the low-risk group in the TCGA-Cohort (**Figures 6A, B**). A significantly higher expression of PD-L1, PDCD1, and CTLA4 was also observed in the high-risk group as compared to the low-risk group in the TCGA-Cohort (**Figure 6C**) as well as the three GEO validation cohorts (**Supplementary Figures S5A–C**). These results indicated that the high-risk group might be more sensitive to immunotherapy.

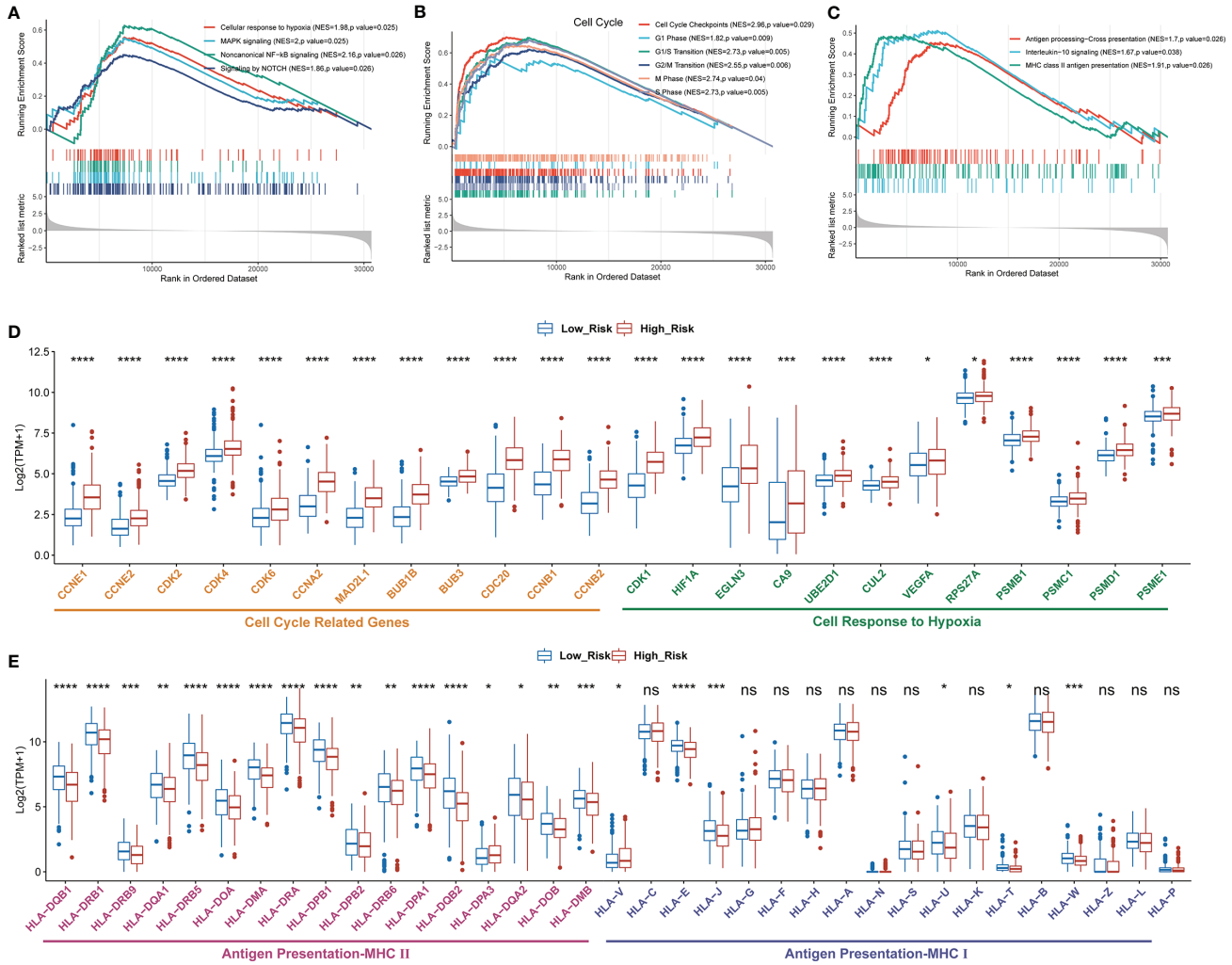

FIGURE 4 | Enriched proliferation-related and cell cycle pathways, but reduced immune-related pathways in the high- as compared to the low-risk group classified by GDPLichi. GSEA plots of proliferation-related pathways **(A)**, cell cycle, **(B)**, and immune-related pathways **(C)**. All transcripts are ranked by the fold change between low- and high-risk subgroups in the TCGA-LUAD cohort. **(D, E)** The difference in the expression of cell cycle-related, cell response to hypoxia, and antigen presentation genes between low and high-risk subgroups. *P < 0.05; **P < 0.01; ***P < 0.001; ****P < 0.0001; ns, no significant difference.

It also suggested that the GDPLichi model may help to predict the response to ICIs of LUAD patients.

Gene Mutation Pattern Between Low- and High-Risk Groups Classified by GDPLichi Model

We identified 12 candidates from the top 25 frequently mutated genes in the TCGA cohort of LUAD patients, which exhibited a significant difference between the low- and the high-risk group classified by GDPLichi (**Figure 7**). Recent studies reported that mutations in the TTN and MUC16 genes indicated high TMB (35, 36) and could be used to predict immunotherapy efficacy (37). TTN mutation status can independently predict immunotherapy prognosis in lung adenocarcinoma patients after ICIs (38). MUC16 mutation was associated with greater response rates associated with ICIs response and overall survival (39). TP53 is a well-known tumor suppressor gene with mutation occurring in more than 50 percent of all malignancies. TP53 mutation is usually associated with a poor prognosis. Some studies also reported that loss of CSMD3 results in increased proliferation of airway epithelial cells in the LUAD (40). Ovarian carcinoma patients with CSMD3 mutation had sustained responses to anti-PD1 without prior chemotherapy (41). Somatic mutations in the ZFHX4 gene are associated with poor overall survival in Chinese lung cancer patients (42). The mutation of RYR2 is a significant biomarker associated with high TMB in LUAD (43). Patients with lung adenocarcinoma with the ADAMTS12 mutation would have a worse prognosis (44). Taken together, these results suggested that the high-risk group might be more sensitive to ICIs and GDPLichi model may predict the response to ICIs.

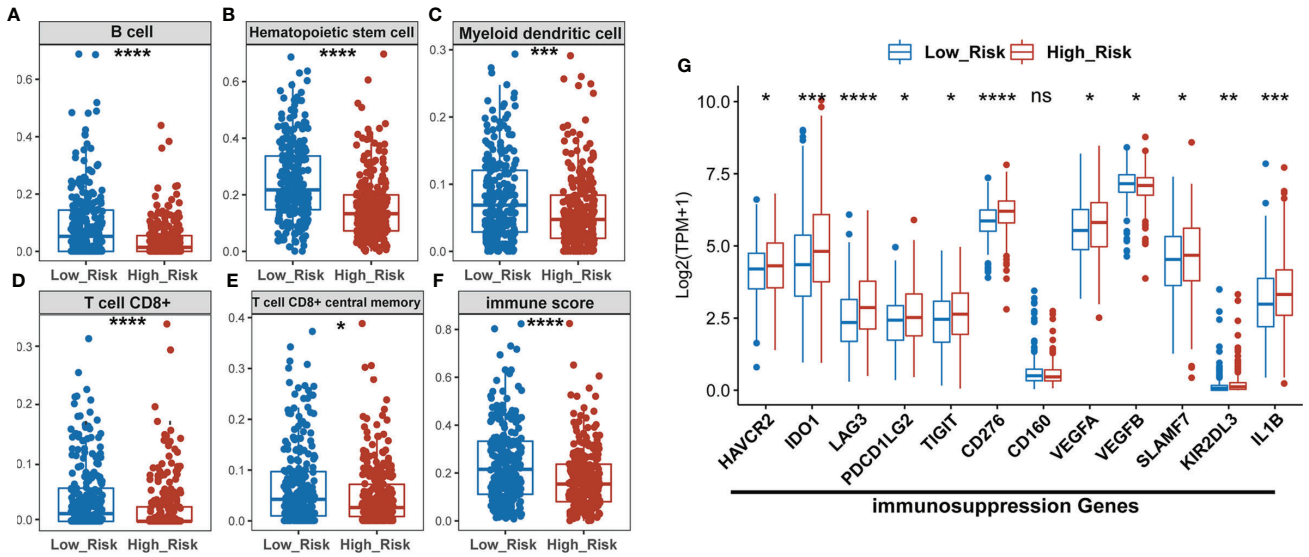

FIGURE 5 | The high-risk LUAD group exhibits relatively lower infiltration of B, HSC, MDC, CD8$^+$ T, and memory T cells, and lower immune scores than the low-risk group, but has higher expression of immuno-suppression genes. **(A–F)** Comparison of infiltrating immune cells (xCell) between low- and high-risk groups using xCell algorism. **(G)** Statistical analysis of the expression of immunosuppression genes between low- and high-risk groups. *P < 0.05; **P < 0.01; ***P < 0.001; ****P < 0.0001; ns, no significant difference.

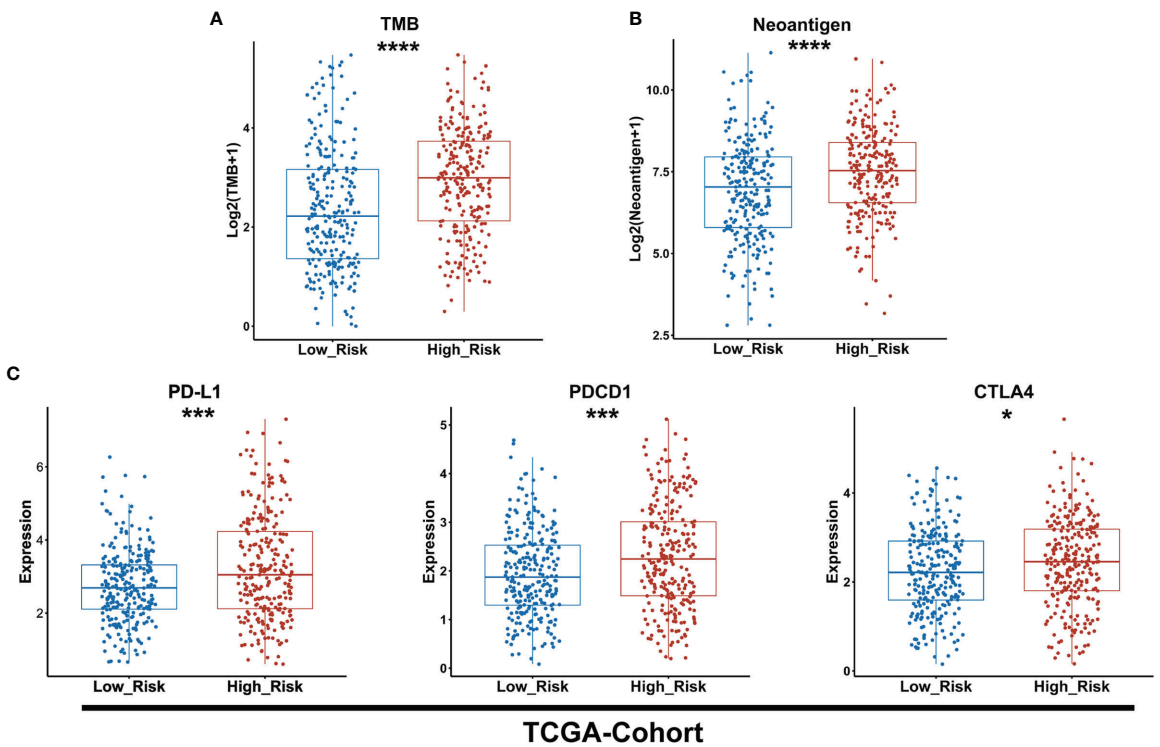

FIGURE 6 | The high-risk group exhibits a higher level of TMB and neoantigen as well as PD-L1, PDCD1, and CTLA4 expression than the lower-risk group. **(A, B)** Boxplot of TMB and neoantigen between low and high-risk groups of the TCGA cohort. **(C)** Statistical analysis of the expression of PD-L1, PDCD1, CTLA4 between low- and high-risk groups in TCGA cohort. *P < 0.05; ***P < 0.001; ****P < 0.0001.

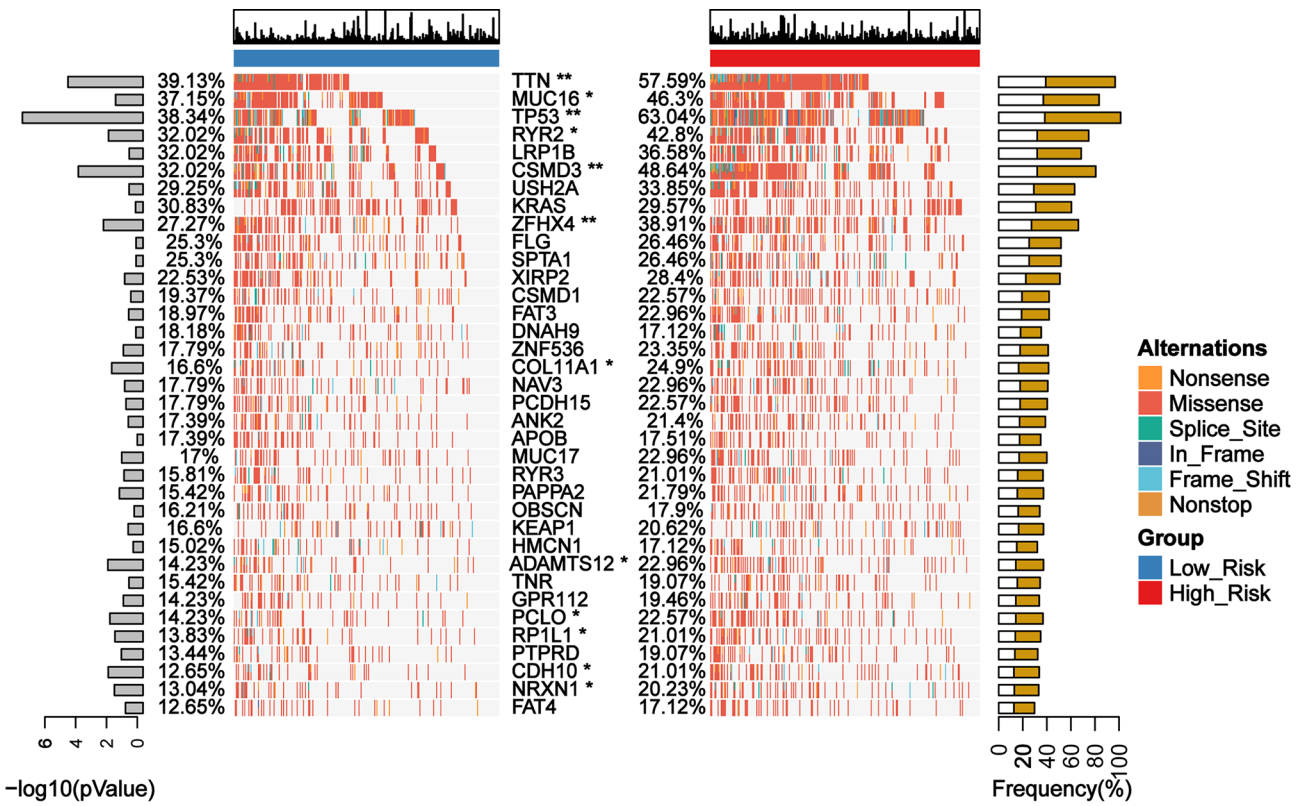

FIGURE 7 | Mutation landscape of genes with significant difference between low- and high-risk subgroups in TCGA LUAD cohort. *P < 0.05; **P < 0.01.

ICIs Response Prediction Between Low- and High-Risk Groups of LUAD Patients Classified by GDPLichi Model

The TIDE algorithm has been proved to help predict ICIs response of LUAD patients with high accuracy (22). Therefore, we calculated the TIDE scores of both low- and high-risk groups of the TCGA LUAD cohort as classified by the GDPLichi model. The results revealed that the TIDE score in the high-risk group was significantly lower than the low-risk group (**Figure 8A**). Similar results were observed in the other three external GEO datasets (**Figures 8B–D**). These results suggested that the high-risk group has a lower chance of antitumor immune escape and exhibiting a higher response rate of ICIs treatment.

DISCUSSION

Lung cancer ranks second in incidence and top in mortality among malignancies worldwide (1). Recently, immunotherapy has become an important new therapeutic approach in treating multiple types of cancer with promising results. It has greatly changed the landscape of cancer care. Many studies have shown that mutations in DDR pathway genes are associated with the prognosis of LUAD patients (20, 21), however, using the DDR gene expression profile as a molecular signature to predict the response to ICIs of LUAD patients has not been reported yet. In this study, we constructed a GDPLichi model based on seven DDR genes (DUT, MGMT, POLH, RAD1, RAD17, TYMS, and YWHAG), to classify LUAD into two distinct subgroups: low- and high-risk groups. Thymidylate synthase (TYMS) is a critical target for cancer chemotherapy (45). Tyrosine 3-Monooxygenase/Tryptophan 5-Monooxygenase Activation Protein Gamma (YWHAG) is also known as 14-3-3γ. A recent study reported that knockdown of YWHAG suppresses epithelial-mesenchymal transition (EMT) and reduces the metastatic potential of human NSCLC (46). O-6-Methylguanine-DNA Methyltransferase (MGMT) catalyzes the transfer of methyl groups from O(6)-alkylguanine and other methylated moieties of the DNA to its molecule. A low protein expression of MGMT was found in the bronchial epithelium of patients with lung cancer as compared to healthy controls, suggesting that there is a negative correlation between MGMT expression and lung cancer risk (47). DNA polymerase eta (POLH) is a DNA polymerase belonging to a subset of tumor suppressor proteins required for maintaining genome integrity (48). RAD1 encodes a component of a heterotrimeric cell cycle checkpoint complex, known as the 9-1-1 complex, that is activated to stop cell cycle progression in response to DNA damage or incomplete DNA replication. RAD17 is a cell cycle checkpoint gene required for cell cycle arrest and DNA damage repair in response to DNA damage. This protein recruits

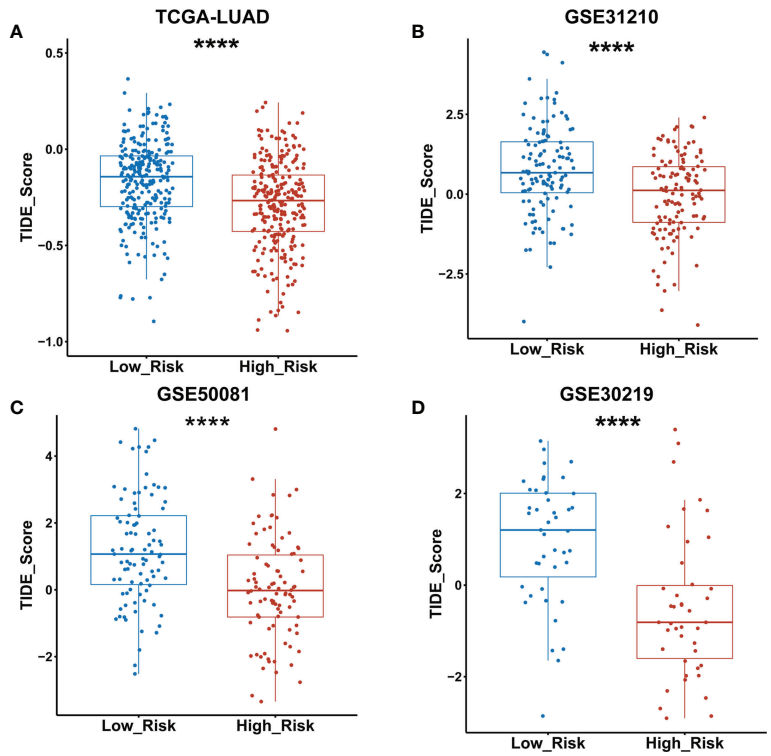

FIGURE 8 | TIDE score was significantly lower in the high- as compared to the low-risk group classified by the GDPLichi model. **(A–D)** Statistical analysis of TIDE scores between low and high-risk groups divided by GDPLichi model in the TCGA LUAD cohort and the three other external validation GEO datasets. ****P < 0.0001.

the RAD1-RAD9-HUS1 checkpoint protein complex onto chromatin after DNA damage and initiates DNA repair.

Gene Set Enrichment Analysis (GSEA) is a computational method that determines whether a priori defined set of genes shows statistically significant, concordant differences between two biological states. GSEA showed that cellular response to hypoxia, MAPK signaling, noncanonical NF-κB signaling, and cell cycle pathways relating to cell proliferation was significantly enriched in the high-risk group, which might account for a higher malignancy and poorer prognosis of LUAD patients in the high-risk group. Oxygen deprivation (hypoxia) is a feature of solid tumors that promotes genomic instability, enhanced aggressiveness, and metastases and is an important factor in treatment resistance and poor survival (49). The MAPK pathways converge in the amplification of key molecules that sustain cell proliferation, growth, and survival processes (50, 51). Noncanonical NF-κB signaling contains NIK phosphorylates IKK/and helps IKK/to phosphorylate p100. Mutations in various upstream regulators (TRAF2, TRAF3, cIAP1&2, CD40) lead to increased stability of NIK and subsequent activation of the noncanonical NF-kB pathway, and this mechanism of activation appears to be important for different cancer types including DLBC and lung cancer (52). The human cell cycle is a tightly regulated process with checkpoints in place to ensure genomic integrity. Recent studies have shown that CDK4 and CDK6 inhibitors can promote T cell activation (53) and reverse T cell exclusion, thus leading to a better response to ICIs (54). Taken together, this suggests that tumor cells in the high-risk group proliferated faster, leading to increased malignancy.

In addition, there were decreased B cells, $CD8^+$ T cells, $CD8^+$ central memory T cells, HSC, MDC, and immune scores found in the high-risk group. The CD8 T cell-dependent killing of cancer cells could produce interferon-gamma (IFN-γ) and then activate antitumor immunity (55). Myeloid dendritic cells (MDC) are crucial for the activation of antigen-specific CD8 T Cells. A recent study reported that anti-tumor effects of DCs can be reduced by a low DC count, low antigen presentation efficiency of tumor-infiltrating DCs, and a weak ability of DC to migrate into tumor (56). Many studies reported that B cell infiltration was associated with a favorable prognosis in NSCLC (57–60). Hematopoietic stem cells (HSC) are a very small group of source cells that can self-renew and generate various blood cells and immune cells. Tumor immune infiltrating cells migrate from blood to tumor tissues and play an important role in immune regulation. Lots of studies have shown that tumor immune infiltrating cells are closely related to the efficacy of ICIs and prognosis (61, 62).

Interestingly, we noticed that there were increased TMB, neoantigen, immune checkpoint molecules, and immunosuppression genes' expression in the high-risk group. Meanwhile, the expression of MHC II genes that express on antigen-presenting cells only in the low-risk group was

significantly lower than in the high-risk group. It has been widely studied that higher TMB, neoantigen, and immune checkpoint molecules are indicators implicated in a better response to ICI treatment (8, 11, 12). Therefore, it is suggested that the high-risk group might be more sensitive to immunotherapies as compared to the low-risk group classified by the GDPLichi model.

We further examined genomic mutations in both the low- and high-risk groups and identified 12 candidates from the first top 25 mutated genes, whose mutation frequency has a significant difference between low- and high-risk groups classified by the GDPLichi model. Most of these genes are associated with TMB (35, 36), which could be used to predict the efficacy of immunotherapy.

The TIDE algorithm is a computational method that uses the expression profile of immune-related genes to predict the ICIs response. It is particularly successful in NSCLC and melanoma (22) and has exhibited a higher accuracy than PD-L1 expression level or TMB alone in predicting overall survival of patients treated with ICIs (13, 19, 20). Further analysis revealed that the TIDE scores in the high-risk group were significantly lower than the low-risk group, suggesting that patient of the high-risk group is more sensitive to response for ICIs. This conclusion was verified in the other external datasets (GSE31210, GSE50081, GSE30219).

In conclusion, we firstly identified two prognostically and clinically relevant subgroups of LUAD using the GDPLichi model which was constructed from seven DDR-risk genes. Patients from the high-risk group showed lower TIDE scores, and are thus more responsive to ICIs. The limit of this research was that it was retrospective, and results should thus be further confirmed by prospective studies.

DATA AVAILABILITY STATEMENT

The datasets presented in this study can be found in online repositories. The names of the repository/repositories and accession number(s) can be found in the article/**Supplementary Material**.

ETHICS STATEMENT

Written informed consent was obtained from the individual(s) for the publication of any potentially identifiable images or data included in this article.

AUTHOR CONTRIBUTIONS

BH, YHL, and YLi designed the study. YLe and SD collected the data and performed the analysis. FY, TG, XX, YZ, LC, CFQ, NL, XZ, CL, YK, KH, and NW helped to analyze the data. YLe and SD wrote the paper. BH, TG, and XZ revised the paper. All the authors read and approved the final manuscript.

FUNDING

This research was supported by the National Natural Science Foundation of China (grant number 81971470 and 32170913) and Shenzhen Science and Technology Commission Fund (program number JCYJ20190809143803732 and JCYJ20210324120602008) to BH and Chinese Postdoctoral Science Foundation (grant number 2020M683062) to NL.

ACKNOWLEDGMENTS

We are grateful for Dr. ShiQiang Zhang's advice on organizing the results.

SUPPLEMENTARY MATERIAL

The Supplementary Material for this article can be found online at: https://www.frontiersin.org/articles/10.3389/fonc.2021.733533/full#supplementary-material

Supplementary Figure S1 | Detailed flowchart of this study.

Supplementary Figure S2 | (A–G) Kaplan-Meier analysis of the genes included for GDPLichi construction (DUT, MGMT, POLH, RAD1, RAD17, TYMS, and YWHAG). **(H)** Example of calculating predicted survival rate related to .

Supplementary Figure S3 | (A) PCA based on the expression profile of the seven risk genes according to different risk groups and **(B)** correlation between the GDPLichi and the seven risk genes in the three GEO validation cohorts.

Supplementary Figure S4 | (A) Kaplan-Meier plots of the survival probability for low- and high-risk subgroups, **(B)** ROC curves of the GDPLichi score and seven risk genes of the classifier, **(C)** Forest plot representation of multivariate Cox model depicted association between overall survival and LUAD subgroups with other clinical factors considered in the three GEO validation cohorts.

Supplementary Figure S5 | (A–C) Statistical analysis of the expression of PD-L1, PDCD1, CTLA4 between low- and high-risk groups in the three GEO validation cohorts

Supplementary Figure S6 | (A) ROC curves for the performance of the GDPLichi score, TMB, PD-L1 expression, and neoantigen in predicting prognosis. **(B–E)** Correlation between the TIDE score and GDPLichi score, TMB, PD-L1 expression, and neoantigen, respectively. **(F)** ROC curves for the performance of the original seven-gene score and three-gene combination (DUT, TYMS, and YWHAG) in predicting prognosis.

Supplementary File 1 | Gene list of DDR-related genes.

Supplementary File 2 | Univariate Cox regression result of DDR-related genes.

Supplementary File 3 | Multivariate Cox regression result of DDR-related genes.

Supplementary File 4 | Jianguoyun source data download link.

Supplementary File 5 | All GSEA significant pathways.

Supplementary File 6 | main_code.R (source analysis R code).

REFERENCES

1. Sung H, Ferlay J, Siegel RL, Laversanne M, Soerjomataram I, Jemal A, et al. Global Cancer Statistics 2020: GLOBOCAN Estimates of Incidence and Mortality Worldwide for 36 Cancers in 185 Countries. *CA Cancer J Clin* (2021) 71:209–49. doi: 10.3322/caac.21660
2. Siegel RL, Miller KD, Jemal A. Cancer Statistics, 2020. *CA Cancer J Clin* (2020) 70:7–30. doi: 10.3322/caac.21590
3. Reck M, Rodriguez-Abreu D, Robinson AG, Hui R, Csoszi T, Fulop A, et al. Pembrolizumab Versus Chemotherapy for PD-L1–Positive Non–Small-Cell Lung Cancer. *N Engl J Med* (2016) 375:1823–33. doi: 10.1056/NEJMoa1606774
4. Herbst RS, Baas P, Kim DW, Felip E, Perez-Gracia JL, Han JY, et al. Pembrolizumab Versus Docetaxel for Previously Treated, PD-L1-Positive, Advanced non-Small-Cell Lung Cancer (KEYNOTE-010): A Randomised Controlled Trial. *Lancet Lond Engl* (2016) 387:1540–50. doi: 10.1016/S0140-6736(15)01281-7
5. Wei SC, Duffy CR, Allison JP. Fundamental Mechanisms of Immune Checkpoint Blockade Therapy. *Cancer Discov* (2018) 8:1069–86. doi: 10.1158/2159-8290.CD-18-0367
6. Akinleye A, Rasool Z. Immune Checkpoint Inhibitors of PD-L1 as Cancer Therapeutics. *J Hematol Oncol J Hematol Oncol* (2019) 12:92. doi: 10.1186/s13045-019-0779-5
7. Niu Y, Lin A, Luo P, Zhu W, Wei T, Tang R, et al. Prognosis of Lung Adenocarcinoma Patients With NTRK3 Mutations to Immune Checkpoint Inhibitors. *Front Pharmacol* (2020) 11:1213. doi: 10.3389/fphar.2020.01213
8. Taube JM, Klein A, Brahmer JR, Xu H, Pan X, Kim JH, et al. Association of PD-1, PD-1 Ligands, and Other Features of the Tumor Immune Microenvironment With Response to Anti–PD-1 Therapy. *Clin Cancer Res* (2014) 20:5064–74. doi: 10.1158/1078-0432.CCR-13-3271
9. Doroshow DB, Bhalla S, Beasley MB, Sholl LM, Kerr KM, Gnjatic S, et al. PD-L1 as a Biomarker of Response to Immune-Checkpoint Inhibitors. *Nat Rev Clin Oncol* (2021) 18:345–62. doi: 10.1038/s41571-021-00473-5
10. Mehnert JM, Monjazeb AM, Beerthuijzen JMT, Collyar D, Rubinstein L, Harris LN. The Challenge for Development of Valuable Immuno-Oncology Biomarkers. *Clin Cancer Res* (2017) 23:4970–9. doi: 10.1158/1078-0432.CCR-16-3063
11. Hollern DP, Xu N, Thennavan A, Glodowski C, Garcia-Recio S, Mott KR, et al. B Cells and T Follicular Helper Cells Mediate Response to Checkpoint Inhibitors in High Mutation Burden Mouse Models of Breast Cancer. *Cell* (2019) 179:1191–206.e21. doi: 10.1016/j.cell.2019.10.028
12. Rizvi NA, Hellmann MD, Snyder A, Kvistborg P, Makarov V, Havel JJ, et al. Mutational Landscape Determines Sensitivity to PD-1 Blockade in non–Small Cell Lung Cancer. *Science* (2015) 348:124–8. doi: 10.1126/science.aaa1348
13. Hellmann MD, Ciuleanu TE, Pluzanski A, Lee JS, Otterson GA, Audigier-Valette C, et al. Nivolumab Plus Ipilimumab in Lung Cancer With a High Tumor Mutational Burden. *N Engl J Med* (2018) 378:2093–104. doi: 10.1056/NEJMoa1801946
14. Hellmann MD, Nathanson T, Rizvi H, Creelan BC, Sanchez-Vega F, Ahuja A, et al. Genomic Features of Response to Combination Immunotherapy in Patients With Advanced Non-Small-Cell Lung Cancer. *Cancer Cell* (2018) 33:843–52.e4. doi: 10.1016/j.ccell.2018.03.018
15. Strickler JH, Hanks BA, Khasraw M. Tumor Mutational Burden as a Predictor of Immunotherapy Response: Is More Always Better? *Clin Cancer Res* (2021) 27:1236–41. doi: 10.1158/1078-0432.CCR-20-3054
16. Bulik-Sullivan B, Busby J, Palmer CD, Davis MJ, Murphy T, Clark A, et al. Deep Learning Using Tumor HLA Peptide Mass Spectrometry Datasets Improves Neoantigen Identification. *Nat Biotechnol* (2018) 37, 55–63. doi: 10.1038/nbt.4313
17. Teo MY, Bambury RM, Zabor EC, Jordan E, Al-Ahmadie H, Boyd ME, et al. DNA Damage Response and Repair Gene Alterations Are Associated With Improved Survival in Patients With Platinum-Treated Advanced Urothelial Carcinoma. *Clin Cancer Res* (2017) 23:3610–8. doi: 10.1158/1078-0432.CCR-16-2520
18. Parikh AR, He Y, Hong TS, Corcoran RB, Clark JW, Ryan DP, et al. Analysis of DNA Damage Response Gene Alterations and Tumor Mutational Burden Across 17,486 Tubular Gastrointestinal Carcinomas: Implications for Therapy. *Oncologist* (2019) 24:1340–7. doi: 10.1634/theoncologist.2019-0034
19. Wang Z, Zhao J, Wang G, Zhang F, Zhang Z, Zhang F, et al. Comutations in DNA Damage Response Pathways Serve as Potential Biomarkers for Immune Checkpoint Blockade. *Cancer Res* (2018) 78:6486–96. doi: 10.1158/0008-5472.CAN-18-1814
20. Knijnenburg TA, Wang L, Zimmermann MT, Chambwe N, Gao GF, Cherniack AD, et al. Genomic and Molecular Landscape of DNA Damage Repair Deficiency Across The Cancer Genome Atlas. *Cell Rep* (2018) 23:239–54.e6. doi: 10.1016/j.celrep.2018.03.076
21. Teo MY, Seier K, Ostrovnaya I, Regazzi AM, Kania BE, Moran MM, et al. Alterations in DNA Damage Response and Repair Genes as Potential Marker of Clinical Benefit From PD-1/PD-L1 Blockade in Advanced Urothelial Cancers. *J Clin Oncol* (2018) 36:1685–94. doi: 10.1200/JCO.2017.75.7740
22. Jiang P, Gu S, Pan D, Fu J, Sahu A, Hu X, et al. Signatures of T Cell Dysfunction and Exclusion Predict Cancer Immunotherapy Response. *Nat Med* (2018) 24:1550–8. doi: 10.1038/s41591-018-0136-1
23. Kaderbhaï C, Tharin Z, Ghiringhelli F. The Role of Molecular Profiling to Predict the Response to Immune Checkpoint Inhibitors in Lung Cancer. *Cancers* (2019) 11(2):201. doi: 10.3390/cancers11020201
24. Wang S, He Z, Wang X, Li H, Liu X-S. Antigen Presentation and Tumor Immunogenicity in Cancer Immunotherapy Response Prediction. *eLife* (2019) 8:e49020. doi: 10.7554/eLife.49020
25. Butler A, Hoffman P, Smibert P, Papalexi E, Satija R. Integrating Single-Cell Transcriptomic Data Across Different Conditions, Technologies, and Species. *Nat Biotechnol* (2018) 36:411–20. doi: 10.1038/nbt.4096
26. Bretz AC, Parnitzke U, Kronthaler K, Dreker T, Bartz R, Hermann F, et al. Domatinostat Favors the Immunotherapy Response by Modulating the Tumor Immune Microenvironment (TIME). *J Immunother Cancer* (2019) 7:294. doi: 10.1186/s40425-019-0745-3
27. Pallocca M, Angeli D, Palombo F, Sperati F, Milella M, Goeman F, et al. Combinations of Immuno-Checkpoint Inhibitors Predictive Biomarkers Only Marginally Improve Their Individual Accuracy. *J Transl Med* (2019) 17:131. doi: 10.1186/s12967-019-1865-8
28. George AP, Kuzel TM, Zhang Y, Zhang B. The Discovery of Biomarkers in Cancer Immunotherapy. *Comput Struct Biotechnol J* (2019) 17:484–97. doi: 10.1016/j.csbj.2019.03.015
29. Okayama H, Kohno T, Ishii Y, Shimada Y, Shiraishi K, Iwakawa R, et al. Identification of Genes Upregulated in ALK-Positive and EGFR/KRAS/ALK-Negative Lung Adenocarcinomas. *Cancer Res* (2012) 72:100–11. doi: 10.1158/0008-5472.CAN-11-1403
30. Rousseaux S, Debernardi A, Jacquiau B, Vitte AL, Vesin A, Nagy-Mignotte H, et al. Ectopic Activation of Germline and Placental Genes Identifies Aggressive Metastasis-Prone Lung Cancers. *Sci Transl Med* (2013) 5:186ra66. doi: 10.1126/scitranslmed.3005723
31. Der SD, Sykes J, Pintilie M, Zhu CQ, Strumpf D, Liu N, et al. Validation of a Histology-Independent Prognostic Gene Signature for Early-Stage, non-Small-Cell Lung Cancer Including Stage IA Patients. *J Thorac Oncol* (2014) 9:59–64. doi: 10.1097/JTO.0000000000000042
32. Yu G, Wang L-G, Han Y, He Q-Y. Clusterprofiler: An R Package for Comparing Biological Themes Among Gene Clusters. *Omics J Integr Biol* (2012) 16:284–7. doi: 10.1089/omi.2011.0118
33. Jassal B, Matthews L, Viteri G, Gong C, Lorente P, Fabregat A, et al. The Reactome Pathway Knowledgebase. *Nucleic Acids Res* (2020) 48:D498–503. doi: 10.1093/nar/gkz1031
34. Aran D, Hu Z, Butte AJ. Xcell: Digitally Portraying the Tissue Cellular Heterogeneity Landscape. *Genome Biol* (2017) 18:220. doi: 10.1186/s13059-017-1349-1
35. Oh J-H, Jang SJ, Kim J, Sohn I, Lee JY, Cho EJ, et al. Spontaneous Mutations in the Single TTN Gene Represent High Tumor Mutation Burden. *NPJ Genomic Med* (2020) 5:33. doi: 10.1038/s41525-019-0107-6
36. Li X, Pasche B, Zhang W, Chen K. Association of MUC16 Mutation With Tumor Mutation Load and Outcomes in Patients With Gastric Cancer. *JAMA Oncol* (2018) 4:1691–8. doi: 10.1001/jamaoncol.2018.2805
37. Yang Y, Zhang J, Chen Y, Xu R, Zhao Q, Guo W, et al. MUC4, MUC16, and TTN Genes Mutation Correlated With Prognosis, and Predicted Tumor Mutation Burden and Immunotherapy Efficacy in Gastric Cancer and Pan-Cancer. *Clin Transl Med* (2020) 10:e155. doi: 10.1002/ctm2.155
38. Wang Z, Wang C, Lin S, Yu X. Effect of TTN Mutations on Immune Microenvironment and Efficacy of Immunotherapy in Lung

Adenocarcinoma Patients. *Front Oncol* (2021) 11:725292. doi: 10.3389/fonc.2021.725292
39. Zhang L, Han X, Shi Y. Association of MUC16 Mutation With Response to Immune Checkpoint Inhibitors in Solid Tumors. *JAMA Netw Open* (2020) 3: e2013201. doi: 10.1001/jamanetworkopen.2020.13201
40. Liu P, Morrison C, Wang L, Xiong D, Vedell P, Cui P, et al. Identification of Somatic Mutations in non-Small Cell Lung Carcinomas Using Whole-Exome Sequencing. *Carcinogenesis* (2012) 33:1270–6. doi: 10.1093/carcin/bgs148
41. Terzic J, Seipel A, Dubuisson J, Tille JC, Tsantoulis P, Addeo A, et al. Sustained Response to Pembrolizumab Without Prior Chemotherapy in High-Grade Serous Ovarian Carcinoma With CSMD3 Mutation. *Gynecol Oncol Rep* (2020) 33:100600. doi: 10.1016/j.gore.2020.100600
42. Qing T, Zhu S, Suo C, Zhang L, Zheng Y, Shi L, et al. Somatic Mutations in ZFHX4 Gene are Associated With Poor Overall Survival of Chinese Esophageal Squamous Cell Carcinoma Patients. *Sci Rep* (2017) 7:4951. doi: 10.1038/s41598-017-04221-7
43. Wang C, Liang H, Lin C, Li F, Xie G, Qiao S, et al. Molecular Subtyping and Prognostic Assessment Based on Tumor Mutation Burden in Patients With Lung Adenocarcinomas. *Int J Mol Sci* (2019) 20. doi: 10.3390/ijms20174251
44. Mohamedi Y, Fontanil T, Cal S, Cobo T, Obaya ÁJ. ADAMTS-12: Functions and Challenges for a Complex Metalloprotease. *Front Mol Biosci* (2021) 8:686763. doi: 10.3389/fmolb.2021.686763
45. Rose MG, Farrell MP, Schmitz JC. Thymidylate Synthase: A Critical Target for Cancer Chemotherapy. *Clin Colorectal Cancer* (2002) 1:220–9. doi: 10.3816/CCC.2002.n.003
46. Raungrut P, Wongkotsila A, Champoochana N, Lirdprapamongkol K, Svasti J, Thongsuksai P. Knockdown of 14-3-3γ Suppresses Epithelial–Mesenchymal Transition and Reduces Metastatic Potential of Human Non-Small Cell Lung Cancer Cells. *Anticancer Res* (2018) 38:3507–14. doi: 10.21873/anticanres.12622
47. Povey AC, Margison GP, Santibáñez-Koref MF. Lung Cancer Risk and Variation in MGMT Activity and Sequence. *DNA Repair* (2007) 6:1134–44. doi: 10.1016/j.dnarep.2007.03.022
48. Barnes RP, Tsao W-C, Moldovan G-L, Eckert KA. DNA Polymerase Eta Prevents Tumor Cell-Cycle Arrest and Cell Death During Recovery From Replication Stress. *Cancer Res* (2018) 78:6549–60. doi: 10.1158/0008-5472.CAN-17-3931
49. Ren W, Mi D, Yang K, Cao N, Tian J, Li Z, et al. The Expression of Hypoxia-Inducible Factor-1α and its Clinical Significance in Lung Cancer: A Systematic Review and Meta-Analysis. *Swiss Med Wkly* (2013) 143:w13855. doi: 10.4414/smw.2013.13855
50. Plotnikov A, Flores K, Maik-Rachline G, Zehorai E, Kapri-Pardes E, Berti DA, et al. The Nuclear Translocation of ERK1/2 as an Anticancer Target. *Nat Commun* (2015) 6:6685. doi: 10.1038/ncomms7685
51. Chapnick DA, Warner L, Bernet J, Rao T. & Liu, X. Partners in Crime: The Tgfβ and MAPK Pathways in Cancer Progression. *Cell Biosci* (2011) 1:42. doi: 10.1186/2045-3701-1-42
52. Cildir G, Low KC, Tergaonkar V. Noncanonical NF-κb Signaling in Health and Disease. *Trends Mol Med* (2016) 22:414–29. doi: 10.1016/j.molmed.2016.03.002
53. Rooney MS, Shukla SA, Wu CJ, Getz G, Hacohen N. Molecular and Genetic Properties of Tumors Associated With Local Immune Cytolytic Activity. *Cell* (2015) 160:48–61. doi: 10.1016/j.cell.2014.12.033
54. Jerby-Arnon L, Shah P, Cuoco MS, Rodman C, Su MJ, Melms JC, et al. A Cancer Cell Program Promotes T Cell Exclusion and Resistance to Checkpoint Blockade. *Cell* (2018) 175:984–97.e24. doi: 10.1016/j.cell.2018.09.006
55. Ribas A, Hu-Lieskovan S. What Does PD-L1 Positive or Negative Mean? *J Exp Med* (2016) 213:2835–40. doi: 10.1084/jem.20161462
56. Shang N, Figini M, Shangguan J, Wang B, Sun C, Pan L, et al. Dendritic Cells Based Immunotherapy. *Am J Cancer Res* (2017) 7:2091–102.
57. Wang S, Liu SS, Ly W, Xu D, Qu H, Zhang L, et al. Tumor-Infiltrating B Cells: Their Role and Application in Anti-Tumor Immunity in Lung Cancer. *Cell Mol Immunol* (2019) 16:6–18. doi: 10.1038/s41423-018-0027-x
58. Liu X, Xu J, Zhang B, Liu J, Liang C, Meng Q, et al. The Reciprocal Regulation Between Host Tissue and Immune Cells in Pancreatic Ductal Adenocarcinoma: New Insights and Therapeutic Implications. *Mol Cancer* (2019) 18:184. doi: 10.1186/s12943-019-1117-9
59. Gottlin EB, Bentley RC, Campa MJ, Pisetsky DS, Herndon JE 2nd, Patz EF Jr, et al. The Association of Intratumoral Germinal Centers With Early-Stage non-Small Cell Lung Cancer. *J Thorac Oncol* (2011) 6:1687–90. doi: 10.1097/JTO.0b013e3182217bec
60. Germain C, Gnjatic S, Tamzalit F, Knockaert S, Remark R, Goc J, et al. Presence of B Cells in Tertiary Lymphoid Structures is Associated With a Protective Immunity in Patients With Lung Cancer. *Am J Respir Crit Care Med* (2014) 189:832–44. doi: 10.1164/rccm.201309-1611OC
61. Al-Shibli KI, Donnem T, Al-Saad S, Persson M, Bremnes RM, Busund LT. Prognostic Effect of Epithelial and Stromal Lymphocyte Infiltration in non-Small Cell Lung Cancer. *Clin Cancer Res* (2008) 14:5220–7. doi: 10.1158/1078-0432.CCR-08-0133
62. Kinoshita T, Muramatsu R, Fujita T, Nagumo H, Sakurai T, Noji S, et al. Prognostic Value of Tumor-Infiltrating Lymphocytes Differs Depending on Histological Type and Smoking Habit in Completely Resected non-Small-Cell Lung Cancer. *Ann Oncol* (2016) 27:2117–23. doi: 10.1093/annonc/mdw319

Conflict of Interest: The authors declare that the research was conducted in the absence of any commercial or financial relationships that could be construed as a potential conflict of interest.

Publisher's Note: All claims expressed in this article are solely those of the authors and do not necessarily represent those of their affiliated organizations, or those of the publisher, the editors and the reviewers. Any product that may be evaluated in this article, or claim that may be made by its manufacturer, is not guaranteed or endorsed by the publisher.

frontiers in Immunology

REVIEW
published: 11 January 2022
doi: 10.3389/fimmu.2021.810388

Factors Determining Long-Term Antitumor Responses to Immune Checkpoint Blockade Therapy in Melanoma

Kimberly Loo[1,2], *James W. Smithy*[1], *Michael A. Postow*[1,3] *and Allison Betof Warner*[1,3]*

[1] Department of Medicine, Memorial Sloan Kettering Cancer Center, New York, NY, United States, [2] Department of Internal Medicine, New York-Presbyterian Hospital and Weill Cornell Medicine, New York, NY, United States, [3] Department of Medicine, Weill Cornell Medical College, New York, NY, United States

With the increasing promise of long-term survival with immune checkpoint blockade (ICB) therapies, particularly for patients with advanced melanoma, clinicians and investigators are driven to identify prognostic and predictive factors that may help to identify individuals who are likely to experience durable benefit. Several ICB combinations are being actively developed to expand the armamentarium of treatments for patients who may not achieve long-term responses to ICB single therapies alone. Thus, negative predictive markers are also of great interest. This review seeks to deepen our understanding of the mechanisms underlying the durability of ICB treatments. We will discuss the currently available long-term data from the ICB clinical trials and real-world studies describing the survivorship of ICB-treated melanoma patients. Additionally, we explore the current treatment outcomes in patients rechallenged with ICB and the patterns of ICB resistance based on sites of disease, namely, liver or CNS metastases. Lastly, we discuss the landscape in melanoma in the context of prognostic or predictive factors as markers of long-term response to ICB.

Keywords: melanoma, immunotherapy, long-term response, biomarkers, survival

OPEN ACCESS

Edited by:
Graham Cook,
University of Leeds, United Kingdom

Reviewed by:
Alexander C. Huang,
University of Pennsylvania, United States
Xianda Zhao,
University of Minnesota, United States

***Correspondence:**
Allison Betof Warner
betofa@mskcc.org

Specialty section:
This article was submitted to Cancer Immunity and Immunotherapy, a section of the journal Frontiers in Immunology

Received: *06 November 2021*
Accepted: *07 December 2021*
Published: *11 January 2022*

Citation:
Loo K, Smithy JW, Postow MA and Betof Warner A (2022) Factors Determining Long-Term Antitumor Responses to Immune Checkpoint Blockade Therapy in Melanoma. Front. Immunol. 12:810388. doi: 10.3389/fimmu.2021.810388

INTRODUCTION

The success of immune checkpoint blockade (ICB) in the treatment of advanced melanoma reinvigorated clinicians and investigators seeking long-term treatment benefit for patients with cancer. ICB was rapidly adopted as frontline therapy for melanoma due to its potential for sustained clinical and survival benefits. The median overall survival (OS) for melanoma shifted from a dismal 9 months with dacarbazine in the pre-ICB era to a median OS of 6.5 years for patients treated with the combination nivolumab + ipilimumab on the CheckMate 067 trial (1). There is even the potential for long-term disease control after treatment discontinuation, a concept previously unrealized in the treatment of metastatic disease.

Despite the considerable promise of ICB, only about half of treated patients experience response, with many others experiencing primary or acquired resistance to ICB (2, 3). Additionally, toxicity from immune checkpoint blockade can be severe and even life-threatening, so identification of patients who are likely to benefit is of the utmost importance (4). Extensive studies are underway to uncover both prognostic and predictive biomarkers of long-term response, with the push to identify

tumor-specific, tumor microenvironment, or T cell markers of long-term responders actively ongoing. Here, we describe the landscape of current clinical trials and real-world studies with long-term survival data following ICB treatment of advanced melanoma including rechallenge studies and highlight the prognostic and predictive biomarkers involved in the molecular determinants of tumor response and unique immune cell populations involved in extending the durability of ICB treatment response.

IMMUNE CHECKPOINT BLOCKADE

Immune checkpoint blockade therapies aimed at harnessing adaptive immunity have driven a therapeutic revolution. Monoclonal antibodies against cytotoxic T lymphocyte antigen-4 (CTLA-4) and programmed death 1 (PD-1) capitalize on the inhibition of immune checkpoint pathways, creating several promising new avenues for new drugs in cancer therapy. CTLA-4 and PD-1 act as negative regulators of T cell immune function at different stages of the immune response (5).

CTLA-4 competitively binds CD80/CD86 with a higher affinity than CD28, which upon binding, dampens T cell activation and delivers inhibitory signals to the T cells (6) and has been shown to largely act in the lymph nodes at the initial priming stage of naive T cell activation by halting autoreactive T cells (7, 8). On the other hand, PD-1 is expressed on tumor cells, cells within the tumor microenvironment (TME), B cells, and natural killer (NK) cells (9, 10). PD-1 expression is induced upon T cell activation and inhibits the T cell receptor (TCR) "stop signal." The activity of PD-1 inhibits kinases involved in T cell activation and affects the duration of T cell to antigen-presenting cell (APC) and T cell to target cell contact (11, 12). PD-1 has been described as another co-inhibitory receptor induced by T cell activation (13). PD-1 acts later in the immune response by regulating previously activated T cells predominantly in peripheral tissues during the T cell effector phase (14). Immune checkpoint blockade consequently utilizes the concept that tumor cells, typically recognized by T cells, have found ways to evade the immune system by utilizing peripheral tolerance (15, 16).

Ipilimumab, a monoclonal antibody against CTLA-4, was approved by the US Food and Drug Administration (FDA) in 2011. Pembrolizumab and nivolumab, both monoclonal antibodies against PD-1, gained FDA approval in 2014. Melanoma has especially benefited from the use of such immune checkpoint blockade agents. From several early clinical trials of these agents, ongoing studies demonstrating long-term survival are maturing. Prolonged overall survival and sustained clinical benefit even in patients who experienced stable disease to these ICB therapies have led to the current widespread use and favor of these agents in the first-line therapy setting in advanced melanoma.

Early promising results of anti-CTLA-4, ipilimumab, and anti-PD-1, pembrolizumab and nivolumab, demonstrated that ipilimumab compared favorably to the current standard melanoma therapies of the time including gp100 peptide vaccine and improved overall survival (OS) (17). Anti-PD-1 antibodies quickly followed suit to add to the repertoire of ICB agents. Initial clinical trials demonstrated response rates of 20%–40% in melanomas treated with anti-PD-1 agents with prolonged stabilization of disease and lower severity and frequencies of grade 3–4 adverse events compared with chemotherapy and ipilimumab (18–21).

Notably, the KEYNOTE-001 study of pembrolizumab demonstrated a robust objective response rate (ORR) in ipilimumab refractory patients (22). The KEYNOTE-002 study demonstrated improved progression-free survival (PFS) in patients who received pembrolizumab compared with those who received investigator choice chemotherapy (23). The KEYNOTE-006 study demonstrated superior OS and PFS in patients treated with pembrolizumab compared with ipilimumab in ICB treatment-naive patients with improved grade 3–4 adverse events (2, 24). The CheckMate 037 trial demonstrated improved ORR in patients treated with nivolumab compared with investigator choice chemotherapy in patients who had previously progressed on ipilimumab or BRAF inhibitors of the BRAF mutant (25). The CheckMate 066 study demonstrated improved median PFS, ORR, and 1-year OS rate in previously untreated BRAF wild-type patients treated with nivolumab compared with dacarbazine (26).

The combination of immunotherapies then followed given the clinical success experienced by ICB monotherapies. Nivolumab in combination with ipilimumab (nivo + ipi) has been associated with response rates of up to 58% and 22% of complete response to treatment (27–29). The CheckMate 067 trial compared the nivo + ipi combination to ipilimumab monotherapy. These results demonstrated significantly improved ORR, PFS, and OS in the nivo + ipi combination group compared with ipilimumab (27). CheckMate 064, a randomized phase II study, compared the sequential treatment of ipilimumab and anti-PD-1 rather than in combination as what the CheckMate 067 trial had conducted. Two arms included a nivolumab induction followed by ipilimumab then nivolumab maintenance arm vs. an ipilimumab induction then nivolumab with nivolumab maintenance. Efficacy outcomes were superior in patients treated with nivolumab frontline therapy compared with initiation with ipilimumab, with statistically similar toxicity rates. Median OS was not reached (30). Substantially improved objective response, PFS, and OS irrespective of BRAF status have propelled the nivo + ipi combination as a standard of care in melanoma, despite increases in grade 3–4 adverse events in patients treated with the combination (3, 31, 32).

LONG-TERM OUTCOMES TO ICB

Across clinical trials and now with years of clinical experience, the early promise of durable melanoma control with ICB is coming to fruition. We are now seeing survival data for 7 years and beyond post-ICB treatment with the tail of survival curves maturing to provide the promise of durable disease control

and long-term treatment outcomes in melanoma ICB-treated patients.

KEYNOTE-001 evaluated 655 patients with advanced melanoma treated with pembrolizumab. With a median follow-up of 55 months, the estimated 5-year OS was 34% in all patients in the study and 41% in treatment-naive patients. The median duration of response was not yet reached at the 5-year timepoint. Seventy-three percent of responses in the entire cohort were ongoing, and 82% of treatment-naive responses were ongoing. The longest response was ongoing at 66 months at the time of data cutoff. Four patients who initially had a complete response (CR) and discontinued therapy ultimately experienced disease progression and were retreated with a second course of pembrolizumab. Two of the four patients had disease response (33).

Similarly, the 5-year *post-hoc* analysis results of the KEYNOTE-006 trial of ipilimumab-naive patients treated with pembrolizumab or ipilimumab were reported (34). Participants with stable disease (SD) or better after receiving at least 24 months of treatment or CR after at least 6 months of pembrolizumab stopped the therapy per protocol. With a median follow-up in survivors of 57.7 months, the median OS was 32.7 months (95% CI: 24.5–41.6) in the pembrolizumab-treated group versus 15.9 months (13.3–22.0) in the ipilimumab-treated group (p = 0.00049). This trial not only confirmed the superiority of PD-1 blockade over ipilimumab, but it also showed that the long-term follow-up data further support the durability of ICB responses.

The exploratory 7-year follow-up data of KEYNOTE-006 (KEYNOTE-587) have recently been presented by Robert et al. at the Society of Melanoma Research 2021 Congress (35). Following the conclusion of KEYNOTE-006, 210 eligible patients transitioned to KEYNOTE-587 for extended follow-up (158 received pembrolizumab, 52 received ipilimumab). The median OS was 32.7 months for pembrolizumab-treated patients versus 15.9 months for ipilimumab-treated patients (HR = 0.70; 95% CI: 0.58–0.83). The 7-year OS rates were 37.8% in pembrolizumab- versus 25.3% in ipilimumab-treated patients. Pembrolizumab was associated with improved clinical outcomes regardless of prior BRAF inhibitor therapy, large tumor burden, elevated LDH, or prior brain metastases.

The CheckMate 067 trial compared nivolumab + ipilimumab with ipilimumab alone. The 6.5-year follow-up data from this study were recently presented, confirming previously reported sustained efficacy. With a minimum follow-up of 6.5 years, the median OS was 72.1 months (38.2–NR), 36.9 months (28.2–NR), and 19.9 months (16.8–24.6) in the nivo + ipi combo, nivolumab monotherapy, and ipilimumab monotherapy arms, respectively. Importantly, the median treatment-free interval (excluding patients who discontinued follow-up prior to subsequent systemic therapy) was 27.6 months in the combination immunotherapy arm, reinforcing the durability of benefit even after treatment discontinuation (1).

Long-term recurrence-free survival results are also beginning to mature for adjuvant ICB for patients with high-risk resected stage III/IV melanoma. The efficacy of adjuvant therapy addresses a slightly different clinical scenario—that of micrometastatic disease. Thus, durable benefit after adjuvant therapy is suggestive of long-term efficacy against microscopic disease as well as detectable metastases. The CheckMate 238 trial demonstrated 4-year results from adjuvant nivolumab versus ipilimumab in resected stage IIIB–C and stage IV melanoma. This multicenter, double blind, randomized controlled phase III trial demonstrated sustained recurrence-free survival benefit in patients treated with nivolumab compared with ipilimumab. Median follow-up was 51.1 months with adjuvant nivolumab and 50.9 months with adjuvant ipilimumab. The 4-year recurrence-free survival was 51.7% (95% CI: 46.8–56.3) in the nivolumab group and 41.2% (36.4–45.9) in the ipilimumab group (p = 0.0003). The 4-year OS was 77.9% with nivolumab and 76.6% with ipilimumab (p = 0.31) (36). This study demonstrates the sustained long-term benefit of adjuvant nivolumab compared with ipilimumab in patients with high-risk resected melanoma, especially also considering a more favorable toxicity profile in anti-PD-1-treated patients. Similarly, KEYNOTE-054 demonstrated improved 3.5-year distant metastasis-free survival with pembrolizumab versus placebo at a median of 42.3 months of follow-up (37). The efficacy of nivolumab and pembrolizumab is therefore expected to be similar (**Table 1**).

It is important to note that most of the long-term data discussed to date have been from clinical trials. Given the differences in clinical trial populations and real-world outcomes, data are needed from patients who received standard of care. In a large single-institution retrospective study of patients treated with anti-PD-1, those who discontinued therapy and had at least 3 months of follow-up (n = 396) were evaluated for durability of long-term response as well as retreatment outcomes following anti-PD-1 disease progression. Median OS was 39 months (31.7–47.2 months) and 5-year OS was 40.8% (33.7–47.8%). One hundred and two (25.8%) patients experienced CR to anti-PD-1. Median follow-up was 21.1 months from the time of CR in patients who did not relapse. This study demonstrated that most CRs to anti-PD-1 were durable, yet the probability of treatment failure at 3 years was 27%. Additionally, of the patients who achieved CR to a single-agent anti-PD-1, 23 of these CR patients later experienced progressive disease (38).

In terms of the immune-related adverse event (irAE) profile experienced during ICB treatment that correlated with long-term response, the development of irAE hypothyroidism and vitiligo within 6 months of treatment was associated with long-term OS (median 43.6 vs. 13.1 months in those without irAEs, p = 0.008) (39). Vitiligo has been observed as an irAE linked with durable response and lower risk of progression or death in melanoma, likely due to the shared antigen between benign melanocytes and melanoma cells (40). Similarly, those who have experienced the irAE of thyroid dysfunction had significantly longer PFS and OS in another study, with prolonged survival long after disease progression (39, 41).

As the ICB arsenal continues to improve long-term survival outcomes across melanoma, the discussion of characteristics of

TABLE 1 | Melanoma clinical trials with long-term survival results.

Trial	Treatment arms	Median follow-up	Median PFS/recurrence-free survival/ intracranial PFS (95% CI)	Median OS/distant metastasis-free survival (95% CI)
KEYNOTE-001 (33) (NCT01295827)	Pembrolizumab monotherapy Total melanoma patients (n = 655); treatment naive (n = 151) or previously untreated (n = 496)	55 months	Median PFS was 8.3 months (95% CI: 5.8–11.1) in all patients and 16.9 months (95% CI: 9.3–35.5) in treatment-naive patients 5-year PFS rates were 21% in all patients, 29% in treatment-naive patients	Median OS was 23.8 months (95% CI: 20.2–30.4) in all patients and 38.6 months (95% CI: 27.2–not reached) in treatment-naive patients 5-year OS rates: 34% in all patients, 41% in treatment-naive patients
KEYNOTE-006 (34) (NCT01866319)	Pembrolizumab monotherapy or ipilimumab monotherapy Total (n = 834); pembrolizumab 10 mg/kg every 2 weeks (n = 279), 10 mg/kg every 3 weeks (n = 277), or ipilimumab 3 mg/kg every 3 weeks (n = 278)	57.7 months	Median PFS was 8.4 months (95% CI: 6.6–11.3) in the combined pembrolizumab groups versus 3.4 months (95% CI: 2.9–4.2) in the ipilimumab group (HR 0.57, 95% CI: 0.48–0.67, $p < 0.0001$)	Median OS was 32.7 months (95% CI: 24.5–41.6) in the combined pembrolizumab groups and 15.9 months (95% CI: 13.3–22.0) in the ipilimumab group (HR 0.73, 95% CI: 0.61–0.88, $p = 0.00049$)
KEYNOTE-587 (35) (NCT03486873)	Pembrolizumab monotherapy or ipilimumab monotherapy Extended follow-up after conclusion of KEYNOTE-006 (n = 210); pembrolizumab (n = 158) or ipilimumab (n = 52)	7-year follow-up data	Not reported	Median OS was 32.7 months for pembrolizumab-treated patients versus 15.9 months for ipilimumab-treated patients (HR 0.70, 95% CI: 0.58–0.83) 7-year OS rates: 37.8% for pembrolizumab and 25.3% for ipilimumab
CheckMate 067 (1) (NCT01844505)	Nivo + ipi or nivolumab monotherapy or ipilimumab monotherapy Nivo + ipi (n = 314), nivolumab only (n = 316), or ipilimumab only (n = 315)	Minimum follow-up of 6.5 years	Median PFS: 11.5 months (95% CI: 8.7–19.3) nivo + ipi, 6.9 months (5.1–10.2) nivolumab, 2.9 months (2.8–3.2) ipilimumab 6.5-year PFS rates: 34% (95% CI: 29%–40%) nivo + ipi, 29% (95% CI: 23%–34%) nivolumab, 7% (95% CI: 4%–11%) ipilimumab	Median OS: 72.1 months (38.2–NR) nivo + ipi, 36.9 months (28.2–NR) nivo, and 19.9 months (16.8–24.6) ipi 6.5-year OS rates: 49% (95% CI: 44%–55%) nivo + ipi, 42% (95% CI: 37%–42%) nivolumab, 23% (95% CI: 19%–28%) ipilimumab
CheckMate 238 (36) (NCT02388906)	Adjuvant nivolumab monotherapy or ipilimumab monotherapy Total (n = 453); adjuvant nivolumab only (n = 453) or adjuvant ipilimumab only (n = 453)	51.1 months in adjuvant nivolumab 50.9 months in adjuvant ipilimumab	4-year recurrence-free survival was 51.7% (95% CI: 46.8–56.3) in the nivolumab group and 41.2% (36.4–45.9) in the ipilimumab group ($p = 0.0003$)	4-year OS was 77.9% in the nivolumab-only group and 76.6% in the ipilimumab-only group ($p = 0.31$)
KEYNOTE-054 (37) (NCT02362594)	Adjuvant pembrolizumab monotherapy or placebo Total (n = 1,019); adjuvant pembrolizumab (n = 514) or adjuvant placebo (n = 505)	42.3 months	3.5-year recurrence-free survival was 59.8% (95% CI: 55.3%–64.1%) in the pembrolizumab group and 41.4% (95% CI: 37.0%–45.8%) in the placebo group (HR 0.59, 95% CI: 0.49–0.70)	3.5-year distant metastasis-free survival was 65.3% (95% CI: 60.9%–69.5%) in the pembrolizumab group and 49.4% (95% CI: 44.8%–53.8%) in the placebo group (HR 0.60, 95% CI: 0.49–0.73, $p < 0.0001$)
CheckMate 204 (93) (NCT02320058)	Nivo + ipi with active melanoma brain metastases Total (n = 119); cohort A: asymptomatic (n = 101) or cohort B: symptomatic and/or steroid requiring (n = 18)	34 months	36-month intracranial PFS rate (icPFS): 54% (95% CI: 43%–64%) cohort A, icPFS 19% (95% CI: 5%–40%) cohort B	OS rate 72% (95% CI: 43%–64%) cohort A, 37% (95% CI: 14%–60%) cohort B
ABC trial (91) (NCT02374242)	Nivo + ipi or nivolumab monotherapy with active melanoma brain metastases (mets) Total (n = 76); asymptomatic brain mets with no prior local brain therapy Cohort A: nivo + ipi (n = 35), cohort B: nivolumab only (n = 25), or cohort C: brain mets, previous local therapy with neuro symptoms and/or with leptomeningeal disease, nivolumab only (n = 16)	54 months	5-year icPFS: 46% cohort A, 15% cohort B, 6% cohort C	5-year OS rates: 51% cohort A, 34% cohort B, 13% cohort C

survivorship, namely, chronic immune toxicities, functional status, and health outcomes, is actively being addressed in survivorship clinics. In patients treated with ipilimumab for metastatic disease or with adjuvant therapy with overall survival of >2 years, Johnson et al. describe the overall excellent functional outcome and toxicities experienced among long-term survivors. While chronic endocrine dysfunction and occasional neurologic toxicities (associated with whole brain

radiation) were seen in a small number of surviving patients, gastrointestinal and dermatologic adverse events were the most frequent, though transient compared with those patients with hypophysitis who required ongoing corticosteroid treatment. Furthermore, surviving patients generally had excellent Eastern Cooperative Oncology Group (ECOG) performance statuses (ECOG 0–1), which is reassuring of life years following ipilimumab treatment (42).

Survivorship and health-related quality of life outcomes in patients experiencing durable responses to anti-PD-1/PD-L1 are also described by Patrinely et al. Among survivors greater than 2 years out from anti-PD-1/PD-L1 treatment for melanoma, renal cell carcinoma, or non-small cell carcinoma, ECOG performance status was 0 or 1 at last follow-up. Chronic irAEs which persisted beyond 12 weeks after anti-PD-1 discontinuation seen at follow-up included hypothyroidism, arthritis, adrenal insufficiently, and neuropathy, though no clear chronic adverse cardiometabolic events were observed (43). Characterization of chronic irAEs of patients treated with anti-PD-1 in the adjuvant setting is described by Patrinely et al. Chronic irAEs were common and persisted with prolonged follow-up, though most were mild low grade 1 or 2. Among patients who received adjuvant anti-PD-1 treatment, endocrinopathies, arthritis, xerostomia, and neurotoxicities were the most common. Additionally, irAEs affecting visceral organs such as the liver, colon, kidneys, and lungs were much less common to become chronic irAEs (44). Collectively, the favorable health-related outcomes among long-term survivors to ICB treatments are overwhelmingly reassuring as patients begin to transition to survivorship clinics for monitoring long after their ICB treatments.

In real-world studies examining patients who electively discontinued anti-PD-1 in the absence of disease progression or treatment limiting toxicity, the duration of anti-PD-1 treatment was shorter compared with the reported treatment course of patients treated on clinical trials (45). In a study of 185 patients treated across multiple centers across Europe and Australia, of the patients who electively discontinued anti-PD-1, those who experienced a CR (63%) and were treated for more than 6 months exhibited a lower risk of relapse after treatment discontinuation. Patients who achieved a PR (24%) or SD (9%) had a higher risk of disease progression after therapy discontinuation (NCT02673970) (46). Further studies to determine the optimal duration of treatment in patients who achieve PR or SD are needed.

In a separate real-world observational cohort study, patients who made a joint decision with their provider to electively discontinue anti-PD-1 therapy at 1 year (>6 and <18 months) were reviewed. Here, the majority of patients with metastatic melanoma following 1 year of anti-PD-1 treatment remained without progression in the long-term follow-up evaluation, with a low risk of disease progression even in patients with residual disease on imaging. Median follow-up in this cohort study was 20.5 months from anti-PD-1 treatment discontinuation with 75% of patients remaining without disease progression, while 25% had disease progression, with a median PFS of 3.9 months (range 0.7–30.9 months) (47). Given this, elective discontinuation of anti-PD-1 therapy may still achieve favorable long-term outcomes while also reducing the immunotherapy-related toxicities and financial burdens associated with prolonged anti-PD-1 treatment.

In a single cohort study examining patients with advanced melanoma treated with anti-PD-1 monotherapy of nivo + ipi, multivariate analysis revealed that patients with a non-CR to treatment as best overall response (BOR) and in cases where immunotherapy was given in the advanced line (where previous lines of treatment included ipilimumab monotherapy, targeted therapy, prior pembrolizumab, or nivo + ipi) should be treated for longer periods of time, with elective discontinuation discouraged prior to the 18-month timepoint (48). Finally, in another study examining CR in patients following anti-PD-1 treatments, 102 patients stopped treatment after a CR after a median duration of 9.4 months. Here, with a median follow-up of 21.1 months from the time of CR, the probability of being alive and not requiring additional treatment was 72.1% with an estimated 3-year OS from the time of CR of 82.7% (95% CI: 67.9%–91.1%) (38).

A prospective, multicenter single-arm interventional study in the Netherlands, the Safe Stop trial, examined patients with melanoma and a confirmed CR or PR to be included in this study examining early discontinuation of first-line monotherapy with the anti-PD-1 therapies pembrolizumab or nivolumab. The primary objective was to examine the rate of response 24 months following anti-PD-1 treatment discontinuation, with secondary objectives examining BOR and duration of response with need and outcomes of anti-PD-1 rechallenge and associated serious adverse events and health-related quality of life measures (49).

Beyond the impressive nature of the 5-plus year landmarked OS rates, the feasibility of determining functional cure rates in melanoma patients treated with ICB is actively emerging. A pooled analysis from several phase II and III studies of ipilimumab-treated patients demonstrated a plateau of survival curves at around year 3. The median OS in this cohort of 254 patients was 11.4 months (95% CI: 10.7–12.1). Follow-up in this cohort was reported for up to 10 years following ipilimumab initiation (50). With a plateau and flattening of the tail of the ipilimumab overall survival curves, thoughts surrounding functional cure rates with patients treated with melanoma are being discussed with much excitement. With the newly maturing ipilimumab data, ongoing analysis of patients treated with PD-1 and examination of the potential plateau curve are ongoing. For the first time, statistical evaluation with cure models may be possible.

We recently examined a subset of melanoma patients treated with ICB regimens who survived at least 5 years (n = 151). The median duration of response among survivors (n = 138) was 93 months. From the 5-year post-initial ICB timepoint, 85% of patients survived an additional 5 years (95% CI: 73%–92%). Among patients who made it to the 5-year post-ICB timepoint without treatment failure (n = 72), the probability of remaining treatment failure free at 7 years was 92% (86%–99%). Of the 151 patients, none ultimately died of melanoma (51). Given this, patients who survived at least 5 years following initial ICB

demonstrated excellent sustained survival and treatment failure free years, a finding which is greatly reassuring to clinicians and patients.

ICB TREATMENT RECHALLENGE

Despite the ability of ICB therapies to provide sustainable antitumor responses in a subset of patients, up to 25%–30% of patients experience recurrence of their melanoma within 1 year of treatment, and more than 50% eventually progress following ICB therapy (20, 52, 53). Approaches to rechallenge or subsequent therapies are being explored for those patients who eventually progress following ICB. Rechallenge regimens utilize repeated treatments with the same therapeutic class of drug following disease progression in patients who experienced previous clinical benefit with prior treatment for unresectable or metastatic disease (54, 54). This is typically considered because there are few effective treatment options for melanoma after progression on ICB. Rechallenge may be considered if initial treatment was discontinued for toxicity or if disease progression necessitates another line of therapy.

Retreatment with monotherapy ipilimumab has resulted in tumor response rates of 12% to 23% (55–57). In patients treated with single-agent anti-PD-1, retreatment with anti-PD-1 or nivo + ipi has led to objective responses in only 15% to 25% of retreated patients. The study by Betof Warner et al. demonstrates that responses to retreatment were infrequent among patients who experienced disease progression on anti-PD-1 and were subsequently treated with either anti-PD-1 or nivo + ipi. Seventy-eight (19.7%) patients who discontinued anti-PD-1 for any reason were subsequently treated with ICB; 45.6% of patients received PD-1 monotherapy and 56.4% received nivo + ipi. A total of 14.7% exhibited a response to PD-1 monotherapy and two patients achieved a CR. Twenty-five percent of patients exhibited a response to nivo + ipi and three patients achieved a CR (38).

Chapman et al. recently reported that in the retreatment of patients using the combination of nivo + ipi, the BOR and time-to-treatment failure (TTF) rates were markedly less favorable following nivo + ipi reinduction compared with the initial treatment course. Rechallenge of 26 patients who received the nivo + ipi combination demonstrated a BOR rate (complete response and partial response) of 74% following the first course of combination treatment versus 23% after reinduction. TTF was also shorter for reinduction compared with the first course in 85% of patients (58). Hepner et al. described the reinduction of 47 patients with ipilimumab (alone or in combination with anti-PD-1) after progressing on nivo + ipi therapy. Modest clinical activity was seen in this cohort despite the recurrence of immune-related adverse events occurring during the reinduction of 40% of this cohort. The response rate to reinduction was 26% at 5 months and the disease control rate was 45%. The median follow-up time of this study was reported as 16 months (95% CI: 10–25 months). The median PFS among responders to reinduction was 14 months (95% CI: 13–NR months). The median OS from reinduction for the entire cohort was 17 months (95% CI: 12–NR months) (59). Finally, Olson et al. have shown that in patients who progressed on anti-PD-1/PD-L1 therapy, retreatment with ipilimumab plus pembrolizumab had a 29% response rate with a median PFS of 5 months, median OS of 24.7 months, and median duration of response 16.6 months (60).

In a review of current studies of ICB treatment rechallenge, the mean disease control rate (DCR) and mean ORR were examined in several rechallenge groups. In rechallenge with anti-PD-1 following disease progression on PD-1, the mean DCR was 45.8% with a mean ORR of 15.5%. The mean DCR of 40.6% and the mean ORR of 20% were noted in patients rechallenged with nivo + ipi following disease progression on anti-PD-1. Rechallenge with anti-CTLA-4 following progression on anti-CTLA-4 demonstrated a mean DCR of 50.9% and a mean ORR of 20.4% (61).

Given the lower objective response rates, shorter time to treatment failure, and increased toxicities associated with ICB retreatment, the risks and benefits of ICB retreatment currently mirror the risk/benefit profile of several chemotherapies used for other malignancies. To obtain more robust prolonged survival on initial ICB regimens, the need to understand the mechanisms of resistance to ICB is heightened as these underlying patterns of resistance may be contributing to the decreased efficacy of retreatment courses. Identifying the cell populations associated with response or resistance to ICB is imperative to guide the development of agents that may provide long-term survival benefit similar to that of ICBs. Additionally, identifying new agents that may utilize different mechanisms of action, either independently or in synergy with ICBs, is imperative to treat those patients who may not respond to ICB and would not benefit from retreatment.

BASELINE PERIPHERAL BLOOD LABORATORY FACTORS ASSOCIATED WITH ICB OUTCOME

Improved survival outcomes to ICB have been observed in patients with favorable prognostic factors. Prognostic factors include measures that are associated with clinical outcomes irrespective of therapy. Conversely, predictive markers include those factors associated with response or lack or response to therapeutic intervention (62, 63). The differentiation between prognostic versus predictive markers of long-term response is an important distinction given the varying relationships between prognostic or predictive biomarkers and clinical outcomes. Here, prognostic markers are thought to be a measure of the natural history of the disease where factors are measured prior to therapy such as lactate dehydrogenase (LDH), baseline neutrophil to lymphocyte ratios (NLR), or tumor burden. While low baseline tumor burden has been associated with favorable prognosis in melanoma, tumor burden can be measured and reported in several ways [i.e., tumor volume, tumor diameter (largest or

combined), or number of metastases] and has not been incorporated into the American Joint Committee on Cancer (AJCC) staging guidelines (64, 65). Here, we describe baseline peripheral blood laboratory prognostic markers associated with long-term ICB response.

Baseline LDH has been a prognostic factor that has been widely utilized in melanoma. LDH has been previously shown to be an independent predictor of overall survival in melanoma and has been incorporated into the AJCC staging classification (66). Increased glycolysis uptake in cancer cells with accelerated metabolism generates elevated levels of LDH as a by-product, which has served as a proxy to assess melanoma tumor burden (67). However, LDH does not always correlate with tumor burden, and tumor size remains an independent prognostic marker (68). The AJCC staging classification has incorporated LDH as a prognostic marker, and studies have described elevated pretreatment LDH with poor OS outcomes in patients treated with ipilimumab and pembrolizumab (66, 69, 70). More recently, several studies have shown that LDH greater than twice the upper limit of normal when measured at baseline prior to ICB therapy correlates with poor response to ipilimumab and anti-PD-1 therapy (71, 72).

In a retrospective study of patients with advanced melanoma who received ICB monotherapy, elevated LDH, the extent of disease, and lymphopenia (<1,000 cells/μl) within 3 months of ICB start were associated with poorer OS and PFS outcomes. CheckMate 067 reported a difference in clinical benefit which was especially robust in patients with BRAF mutation-positive tumors, higher LDH levels (>2× the upper limit of normal, ULN), and those with M1c stage, although the frequency and severity of irAEs were much higher in the nivo + ipi combination regimen compared with nivolumab or ipilimumab monotherapy. Here, there was also a trend for improved survival in patients who received the combination and those with normal LDH or normal LDH with fewer sites of disease (27).

Additional prognostic markers of long-term response have been noted in baseline lymphocyte, neutrophil, and eosinophil levels in the peripheral blood. The absence of lymphocytes given lymphopenia has also been noted as a poor indicator of ICB response. Lymphocytes are crucial mediators in the mechanism of immune checkpoint inhibitors, with circulating lymphocytes often infiltrating tumors. The depletion of such immune cells may be a contributing factor to suboptimal ICB treatment response. Studies have shown that with ipilimumab, increases in absolute lymphocyte count 2–8 weeks after treatment as well as $CD4^+$ and $CD8^+$ T cells at 8–14 weeks were associated with improved OS and clinical response (partial or complete response to therapy) (73).

Eosinophils have been shown to contribute to tumor surveillance and to play an important role in tumor rejection in animal models (74, 75). In studies of ipilimumab-treated patients, high relative eosinophil count (REC) at baseline correlated with improved OS, and increases in REC levels early in treatment were associated with improved clinical response (76). REC ≥1.5% and relative lymphocyte count ≥17.5% were associated with favorable OS in patients treated with pembrolizumab. This was confirmed in a validation cohort and strongly associated with prognosis (77, 78). Additionally, eosinophils also correlate with irAEs. Studies have demonstrated that patients who develop eosinophilia on ICB treatment had significantly longer survival (79).

Elevated baseline NLR and increased NLR early in anti-PD-1 monotherapy treatment in patients with melanoma may serve as additional predictive markers for TTF and OS. A baseline NLR >5 was associated with shorter OS and TTF. An increase in NLR by more than 30% after two treatment cycles was associated with worse OS (median 47 vs. 13.5 months, $p < 0.001$) and trended toward a shorter TTF (12.8 vs. 5.9 months, $p = 0.05$) (80). Several other studies have similarly reported that in stage IV melanoma patients treated with nivolumab or ipilimumab, elevated baseline NLR >5 had significantly worse OS and performance status compared to patients with baseline NLR <5 (81, 82). High platelet to lymphocyte ratios (PLR) have also been shown to correlate with shorter OS but not PFS in melanoma patients. At a PLR cutoff of <120, subgroup analysis of nine studies indicated that PLR served as a significant prognostic indicator in both OS and PFS in patients with melanoma (83).

ICB RESISTANCE BY DISEASE SITES AND LIVER AND BRAIN MICROENVIRONMENTS

Sites of distant metastases have been studied both preclinically and in the clinical setting regarding the increase in mortality, resistance to ICB treatment, and immune tolerance mechanisms that may contribute to overall treatment outcomes. In particular, liver metastases and brain metastases have proven to be challenging in immune-oncology-based therapies. In patients with melanoma, the presence of liver metastases prior to ICB start negatively correlates with immunotherapy efficacy (84, 85). Independent of tumor burden, age, gender, and prior therapies, the presence of melanoma liver metastases is associated with worse outcomes in terms of inferior OS and PFS rates compared to those without liver metastases or those with only lung metastases. Patients with liver metastases were also more likely to have increases in systemic tumor burden compared with those without liver metastases. In the CheckMate 067 trial, participants with liver metastases treated with nivo + ipi had a median OS of 28.2 months compared with 72.1 months in the cohort overall (1).

In addition to the idea that the liver is a tolerogenic organ, many hypothesize that the presence of liver metastases may alter systemic antitumor activity. Studies have reported phenotypic changes to effector tumor-infiltrating lymphocytes in distant biopsy sites in patients with liver metastases (86). Of the patients with liver metastases, the fraction of partially exhausted cytotoxic T cells (peCTLs) was reduced. Moreover, in these patients with low levels of partially exhausted cytotoxic T lymphocytes, the combination nivo + ipi was associated with significantly higher objective response rates when compared with anti-PD-1 monotherapy. Furthermore, specific T cell

populations have been detected in relative abundance in patients who have achieved clinical response to anti-PD-1 therapy. These partially exhausted tumor-infiltrating $CD8^+$ T cells strongly correlated with response and PFS to anti-PD-1 therapy (87). Various populations of $CD8^+$ T cells and their relative location and activation status in patients with liver metastases have been an active area of interest to decipher the underlying mechanism of liver metastases and response to ICB therapy.

In preclinical mouse models, liver metastases were shown to create a systemic immune desert and modulate the immune function in patients with solid tumor cancers. Hepatic peripheral tolerance mechanisms and hepatic monocyte-derived macrophages within the hepatic microenvironment have been proposed as agents of T cell-specific apoptosis and subsequent elimination of crucial antigen-specific T cells leading to systemic immunosuppression (84). Liver metastases were shown to induce systemic tumor-specific $CD8^+$ T cell loss by siphoning activated antigen-specific $CD8^+$ T cells from the circulation. Furthermore, the presence of liver metastases creates a hepatic microenvironment for apoptosis of activated antigen-specific Fas^+CD8^+ T cells following the interaction of these cells with tumor-educated and exposed $FasL^+CD11b^+F4/80^+$ macrophage-derived hepatic myeloid cells. Single-cell RNA sequencing of cells within the hepatic microenvironment in mice models with liver tumors demonstrated a decreased proportion of cells within T cell clusters. Moreover, within the activated T cell population in the hepatic microenvironment, a more enriched population of apoptosis gene signatures was found in those mouse models with liver metastases compared to those without.

Patients with symptomatic CNS melanoma metastases or those requiring steroids following treatment of CNS metastases have previously also exhibited poor treatment outcomes. Patients with melanoma CNS disease historically had a median survival of about 4 months and are further limited by poor functional status, extracranial disease, and age (88, 89). Moreover, very little is known about predictive biomarkers and markers of response in the CNS. Dedicated studies are sorely needed to address this patient population. Ongoing studies, along with clinical experience, suggest that patients with melanoma brain metastases or those with symptomatic CNS lesions and requiring steroids may benefit from immunotherapy.

The phase II CheckMate 204 trial studied nivo + ipi in patients with untreated melanoma brain metastases (90). Patients were divided into two study cohorts: one asymptomatic with no neurologic symptoms or steroid use and the second cohort with neurologic symptoms or in need of steroid use. In the asymptomatic cohort, the intracranial clinical benefit rate (CBR), the proportion of patients with CR + PR + SD for ≥6 months, was 58.4%. In the symptomatic cohort, the intracranial objective response rate was only 16.7% and the CBR was 22.2%. While some intracranial antitumor activity was noted in the symptomatic melanoma brain metastatic group, studies to examine the biologic mechanisms to immunotherapy resistance in these hard-to-treat populations are needed. Similarly, the phase II ABC trial study showed similar results in patients treated with nivo + ipi combination compared with nivolumab monotherapy in patients with asymptomatic brain metastases with no previous local brain therapy (91, 92). A recent systematic review demonstrated a median OS of only 9.0 months in patients with melanoma brain metastases treated with immunotherapy (93).

Recent data presented at the European Society of Melanoma Congress 2021 have reported encouraging results in the management of melanoma brain metastases with the nivo + ipi combination. The 3-year study results of the CheckMate 204 study demonstrated that with a minimum follow-up of 34 months in patients with asymptomatic brain metastases, the investigator-assessed intracranial progression-free survival rate (icPFS) was 54% and the OS rate was 72%. In those patients with symptomatic brain metastases, 36-month icPFS was 19% and OS was 37% (94). Reassuringly, these results suggest that the combination of nivo + ipi serves as a viable standard of care for patients with brain metastases, both asymptomatic and symptomatic, providing hope of a treatment for this vulnerable population.

NEOADJUVANT ICB STUDIES AND BIOMARKERS

Checkpoint blockade therapies have shown additional promise in the neoadjuvant setting. For an additional population of melanoma patients who may derive long-term benefits from ICB therapy, those patients with resectable clinical stage III melanoma may benefit from ICB treatment prior to surgical resection. Melanoma is particularly well suited for neoadjuvant approaches given the potential of improved surgical outcomes from surgery with control of micrometastatic disease prior to surgery and with the high propensity for regional disease that is safely assessable for longitudinal sample and analysis (95). Several studies have demonstrated that high rates of pathologic complete responses and impressive recurrence-free survival rates are attainable following neoadjuvant ICB treatment for stage III melanoma (96–100).

Neoadjuvant ICB studies also identified potential biomarkers of response in terms of early pathologic responses and IFNγ signatures. In a pooled analysis from the International Neoadjuvant Melanoma Consortium of six clinical trials of anti-PD-1-based ICB or BRAF/MEK-targeted therapy, here pathologic complete response (pCR) correlated with improved recurrence-free survival (2-year RFS with pCR 89% vs. no pCR 50%, $p < 0.001$) and OS (2-year pCR OS 95% vs. no pCR 83%, $p = 0.027$). Moreover, in patients with pCR, near pCR, or partial pathologic response, few relapses were seen (2-year RFS 96%), with no patient deaths from melanoma compared with 2-year RFS of patients with pCR from targeted therapy of 79%. Using pathologic response as an early surrogate endpoint for clinical trials may serve as an additional new benchmark for ICB treatment in melanoma (95).

In a separate study, the OpACIN trial compared neoadjuvant with adjuvant ICB nivo + ipi combination therapy. Adjuvant ICB with both ipilimumab and nivolumab had been shown to be

associated with improved relapse-free survival, overall survival, and distant metastasis-free survival compared with placebo of stage III melanoma patients (101, 102). Here, patients with palpable stage III melanoma were randomized 1:1 to receive nivo + ipi whether as four courses in the adjuvant setting or as two courses prior to surgery and two post-surgical courses in the neoadjuvant arm. Pathologic responses were seen in 78% of patients treated in the neoadjuvant arm, where none of the patients in the arm relapsed with a median follow-up of 25.6 months. Additionally, this study reported that IFNγ signature may be used as a biomarker of response in patients treated with neoadjuvant nivo + ipi. Here, a high or intermediate IFNγ RNA signature was a predictor of clinical outcome of patients treated with neoadjuvant nivo + ipi, where none of the patients with a high IFNγ signature had relapsed. Low IFNγ signature was associated with relapse after nivo + ipi, independent of neoadjuvant or adjuvant treatments (97).

The use of favorable IFNγ signatures may therefore serve as a biomarker in additional neoadjuvant ICB trials. In another study of neoadjuvant/adjuvant anti-PD-1 therapy in stage III/IV melanoma, all patients who experienced a rapid antitumor response with a complete or major pathologic response after a single dose of anti-PD-1 remained disease free 3 weeks following treatment. Here, rapid clinical and pathologic responses were associated with the accumulation of exhausted $CD8^+$ T cells 3 weeks following single-dose neoadjuvant/adjuvant anti-PD-1 treatment. A strong neoadjuvant response signature (NRS) was associated with genes involved in adaptive immune response, T cell activation, and migration that also correlated with post-treatment tumor-infiltrating lymphocyte (TIL) responses and RFS. An 18-gene IFNγ T cell-inflamed signature, GEP18, was associated with clinical response in this stage III anti-PD-1-treated melanoma setting. The NRS here strongly enriched for T effector or T memory $CD8^+$ T cell transcriptional factors compared with naive $CD8^+$ T cells. The importance of pre-existing exhausted T cell populations here was again evident with a stronger enrichment of the exhausted $CD8^+$ T cell population compared with the effector T cell population within the neoadjuvant response signature (99). Moreover, a separate study of melanoma patients treated in the neoadjuvant setting demonstrated that treatment stratification based on exhausted T cell (T_{ex}) frequency is possible and may limit adverse events associated with neoadjuvant nivo + ipi. The frequency of Tex cells was defined as the percentage of $CD8^+$ T lymphocytes in pretreatment samples that expressed both inhibitory receptors PD-1 and CTLA-4 within the intratumoral $CD8^+$ T cell population. Here, of the neoadjuvant-treated patients, 10 received anti-PD-1 and 7 nivo + ipi. Of the total patients, 12 achieved a CR, 4 a PR, and 1 with SD. Surgery was performed on 11 of the 17 patients with 8 attaining a pathologic CR. Median RFS and OS were not reached. In this study, patients who received neoadjuvant ICB were enriched for a high Tex population with a mean frequency of 25.7%, demonstrating that immune profile directed neoadjuvant therapy for locally advanced melanoma has the potential of high objective response rates (103).

Finally, early imaging at 3 weeks with ^{18}F-fluorodeoxyglucose (FDG) positron emission tomography–computed tomography (PET-CT) scans at baseline and before surgical resection demonstrated that consistent with pathologic response, radiographic responses were observed after one dose of anti-PD-1, where decreases in tumor size with a ≥20% decrease in tumor size were seen in patients who remained tumor free. Conversely, here, FDG avidity was not associated with response (99). Separately, another phase II study of neoadjuvant nivo + ipi versus nivolumab monotherapy also demonstrated that the role of imaging could serve as an indicator of response in the neoadjuvant setting. Treatment with nivo + ipi yielded high ORR (73%) when measured by RECIST 1.1 as well as pathologic complete response rates (45%) but with substantial grade 3 treatment-related adverse events (73%) compared with modest responses with neoadjuvant nivolumab monotherapy (25% ORR, pCR 25%) though with lower toxicity (8% grade 3 treatment-related AEs) (98). Taken together, pathologic complete responses, IFNγ and exhausted T cell populations, and decreases in tumor size *via* imaging studies are strong forerunners to serve as robust biomarkers of neoadjuvant ICB response.

MOLECULAR DETERMINANTS OF TUMOR RESPONSE TO ICB

With the diverse options for melanoma treatment with ICB alone or in combination, the push for predictive biomarkers to determine the ideal patient populations for each treatment type and to identify early, likely responders to treatment has been a topic of active study. Profiling of tumors of patients and tumor microenvironments for mutations and T cell-inflamed gene expressions is ongoing to help determine the optimal treatments for patients in the frontline or retreatment setting. For patients who have suboptimal responses to ICB, additional studies are ongoing to determine how to best boost the immune response. Additionally, given the poor reproducibility among currently available biomarkers, there remains a paucity of melanoma-specific predictive factors of ICB response that can functionally and reliably be used in the clinical setting.

TUMOR BIOMARKERS, PD-L1

Correlation with response was noted in tumor mutations, neoantigen load, and immune-related gene expression in tumor tissue with $CD8^+$ T cell infiltrates. Activated tumor-infiltrating T cells have been shown to be markers of ICB response, yet the predictive value of these tests has yet to be fully studied (104). PD-L1 expression was an early front-runner as a predictive biomarker. Several early clinical trials explored PD-L1 as a surrogate of ICB response; though given a multitude of reagents and antibodies used across several assays, the reliability of PD-L1 as a biomarker of response remains variable, and PD-L1 expression status has varied in its prediction of melanoma response to ICB (105).

KEYNOTE-001 reported that PD-L1 expression in pretreatment tumor biopsies of melanoma correlated with

response rate, PFS, and OS, though it was also observed that patients with PD-L1-negative tumors also exhibited treatment response (106). KEYNOTE-066 reported OS benefit with pembrolizumab in melanoma compared with ipi across all subgroups except for a small subgroup of patients with PD-L1-negative tumors (2). The phase II CheckMate 064 trial examined patients who received ipi for 12 weeks then nivo for 12 weeks with subsequent nivo maintenance compared with patients who received nivolumab prior to ipilimumab. A higher proportion of patients with baseline PD-L1 expression of 5% or more achieved a response in both sequential treatment groups compared with those with <5% PD-L1 expression. Yet, a higher proportion of patients in the nivo then ipi group were evaluable for baseline PD-L1 expression and had PD-L1 of 5% or more compared with patients in the ipi then nivo group (30).

CheckMate 066 included patients treated with nivolumab versus dacarbazine and showed that nivolumab improves OS in previously untreated melanoma patients and showed that given the magnitude of clinical benefit observed in patients who got nivolumab, PD-L1 status alone is not helpful in the selection of patients for nivo treatment (26). ECHO-301/KEYNOTE-252 stratified patients by PD-L1 expression and BRAF V600 mutation status and randomly assigned 1:1 to the IDO-1 inhibitor plus pembrolizumab or placebo plus pembrolizumab (107).

KEYNOTE-028 examined the T cell-inflamed gene expression profile, PD-L1 expression, and tumor mutational burden efficacy in patients treated with pembrolizumab across 20 solid tumor cancers. Patients with PD-L1-positive tumors were treated with pembrolizumab for 2 years or until confirmed disease progression or toxicity prompted treatment discontinuation. Higher response rates and longer PFS were seen in tumors with higher T cell-inflamed gene expression profiles, PD-L1 expression, and/or tumor mutation burden (TMB). Correlations of TMB with T cell gene expression profile and PD-L1 were low. Patients with high TMB and inflammatory markers (T cell gene expression profile or PD-L1) were the patients with the highest likelihood of response (108).

Despite the studies utilizing PD-1 as surrogates and potential markers of response, the following question remains: why do patients with PD-L1-negative tumors respond and why do the subset of patients with PD-L1-positive tumors not respond to PD-1 pathway blockade? Besides PD-L1 tumor cell expression, PD-L1 expression on immune cell-infiltrating tumors has become another avenue of exploration as a potential predictor of clinical response (109). Additionally, PD-L1 testing based on mRNA level has been feasible, though correlation between PD-L1 expression *via* IHC and RT-PCR is variable between the types of antibody being used. No difference was found between PD-L1 expression between responders and non-responders to therapy with ipilimumab (110).

TUMOR MICROENVIRONMENT, TILs

The TME and the composition of cells within the TME have been identified as potential predictive markers of response in melanoma (111, 112). The current hypothesis proposes that anti-CTLA-4 ipilimumab leads to a more favorable tumor environment for improved efficacy with concurrent or sequential anti-PD-1 therapy. Ipilimumab is thought to increase TILs and IFNγ inducible genes in the TME (113, 114). In turn, this increase in cell populations in the TME increases PD-L1 expression (115). With the increase in PD-L1 expression, the primary ligand for PD-1, the hypothesis proposes an increase in the proportion of patients who experience an improved objective response as well as overall survival in those treated with PD-1.

Classification of the TME into different subtypes has emerged as a way to classify response to ICB based on the presence or absence of TILs and PD-L1 status. The most immunogenic tumors are those with pre-existing $TIL^+/PD\text{-}L1^+$ in the TME and are thought to be the most likely to respond to ICB. Those with $TIL^-/PD\text{-}L1^-$ tumors are the least likely to respond to ICB and seen as an immunologic desert. The $TIL^-/PD\text{-}L1^+$ tumors are thought to be "immune excluded" with a functional PD-L1 pathway and may most benefit from combination ICB to optimize lymphocyte recruitment to the tumor bed. Finally, $TIL^+/PD\text{-}L1^-$ tumors are thought to need alternative strategies beyond the conventional ICB CTLA-4/PD-1 therapies to target additional immunosuppressive pathways (116, 117).

Adaptive immune resistance *via* $CD8^+$ T cells upregulating PD-L1 on melanoma tumor cells has been observed at the invasive tumor margin. *Via* histopathology, of the tumor tissue samples obtained before and after anti-PD-1 treatment, increased expression of $CD8^+$ PD-1 or PD-L1 at the invasive tumor margin correlated with response to anti-PD-1 treatment. Together with a more clonal TCR repertoire, this model suggested a predictive model based on pre-existing $CD8^+$ T cell expression at the tumor-invasive margin following anti-PD-1 treatment may be indicative of response (109).

The gene expression profile of the TME has also been examined as potential predictive biomarkers of ICB response (118). The concept of a T cell-inflamed TME has emerged predictive factors of response to ICB, vaccines, and IL-2 (20, 113, 119). This inflamed TME has been observed in the setting of tumor-infiltrating $CD8^+$ T cells secreting IFNγ, triggering an intratumoral antitumor inflammatory state (120). Thus, across several cancer subtypes with immunotherapy treatment, the inflamed TME *via* the increase in IFNγ-associated gene expression scores is predictive of response to anti-PD-1 therapies (namely, pembrolizumab). Furthermore, the lack of IFNγ-associated gene expression has strongly correlated to a lack of ICB treatment benefit (121–124).

Other markers of response explored have been TMB and T cell-inflamed gene expression profiles (GEP). Both have shown joint predicative utility in stratifying responders and non-responders to pembrolizumab and may be capturing distinct features of neoantigenicity and T cell activation. A study evaluated samples from four KEYNOTE trials and examined the joint predictive utility of the TMB and T cell-inflamed GEP to identify responders versus non-responders to pembrolizumab. In melanoma, both TMB and GEP scores were positively

associated with BOR, with an area under the receiver operating characteristic curve (AOROC) value of 0.602. The correlation between TMB and GEP with predicting response was low (Spearman correlation coefficient $r = 0.252$, $p < 0.05$). TMB showed no association with PD-L1 in melanoma (MEL score $r = 0.049$, $p = 0.65$), whereas GEP was more significantly correlated with PD-L1 ($r = 0.53$, $p < 0.0001$). The most pronounced PFS-associated hazard ratios were observed for TMB high GEP high tumors. In melanoma, the percentage of UV-light-induced mutations correlated with TMB ($r = 0.77$; $p < 1 \times 10^{-10}$) and was significantly associated with response ($p = 0.02$). This suggests that non-synonymous mutations arising from a variety of mutagenic processes are capable of enhancing the antigenicity of tumors with comparable effects on the response to anti-PD-1 treatment (125).

DURABILITY OF ICB RESPONSE: UNDERSTANDING THE UNIQUE IMMUNE CELL POPULATIONS

Immunologic memory is thought to be a characteristic of durable responses to ICB therapy. CTLA-4 inhibition increases T cell priming and promotes T cell diversity, acting on both functionally impaired cytotoxic T cells and helper T cells, while PD-1 inhibition promotes the clonal expansion of previously activated, functionally impaired $CD8^+$ cytotoxic T cells (33, 126–128). ICB therapies have been shown to act on different populations of immune cells at different stages of immune activation, with the potential of a select immunologic memory T cell subset contributing to durable responses to ICB therapy.

The proportion of pre-existing $CD8^+$ T cells at the invasive tumor margin has been shown to correlate with increased clinical response to anti-PD-1 treatments (109, 129). Intratumoral PD-L1 expression is induced by the IFNγ signaling pathway, chromosomal alterations, or a constitutive oncogenic signaling pathway (130). The IFNγ signaling pathway is thought to be the mechanism behind adaptive resistance, a defense mechanism of tumor cells against the immune system attack by IFNγ secreting CTLs and T_h1 cells. Consequently, a link between clinical efficiency and PD-L1 expression, $CD8^+$ T cell tumor infiltration and somatic burden, or the number of neo-antigens originating from increased mutated genes and abnormal proteins has been proposed (131).

$CD4^+$ T cells have been shown to promote tumor regression *via* IL-2 secretion, by directly eliminating cancer cells or by augmenting tumor-specific $CD8^+$ T cell function (132–135). The role of $CD4^+$ T cells in ICB continues to be an active area of exploration as markers of long-term survival in melanoma, though not all studies have made distinctions between regulatory and effector $CD4^+$ cells. A study examined pre- and post-treatment peripheral blood samples from patients with malignant melanoma treated with anti-PD-1 monoclonal antibodies. Using mass cytometry assays and screening by high dimensional clustering, three microclusters of $CD4^+$ T cells and a subset of central memory $CD4^+$ T cells with a $CD27^+FAS^-CD45RA^-CCR7^+$ phenotype were identified in long-term survivors to anti-PD-1 and not identified in non-responders to anti-PD-1 therapy (136). CD27 is a lymphocyte-specific member of the TNF receptor superfamily, expressed by $CD45RA^+CCR7^+$ naive $CD4^+$ T cells, and is further upregulated following T cell receptor signaling, yet decreased expression with effector $CD4^+$ T cell differentiation (137, 138). FAS is a member of the TNF receptor superfamily and has been shown to have pro- and anti-apoptotic T cell effects (139). Activated T cells have been known to express FAS, while naive $CD4^+$ T cells do not. With the expression of $CD27^+$ and FAS^- T central memory $CD4^+$ T cells, this intermediate population may be indicative of a fraction of cells differentiating from naive to central memory cells. This intermediate population may be indicative of cells just egressed from draining lymph nodes to peripheral blood following TCR stimulation *via* cognate antigens. However, $CD27^+FAS^-$ central memory $CD4^+$ T cells have not been shown to express PD-1, suggesting that therapeutic anti-PD-1 monoclonal antibodies do not directly interact with this T cell subset.

Transcriptome and immune profiling of melanoma tumor biopsies of patients treated with anti-PD-1 monotherapy or nivo + ipi have identified activated T cell signatures and populations of T cells unique to the responders to ICB. Transcription factors TBET and eomesodermin (EOMES) are drivers of immune cell development and have been shown to link the long-term renewal of memory $CD8^+$ T cells to their effector potency. TBET and EOMES are master regulators of effector T cell and memory formation and induce helper T cell effector function in $CD8^+$ cytotoxic T cells *via* the upregulation of IFNγ and granzyme B (GZMB), a cytotoxic granule and T cell activation marker (140, 141). Taken together, transcriptome and immune profiling have identified a population of $CD8^+/CD4^+EOMES^+CD69^+CD45RO^+$ (and $TBET^{high}$) effector memory T cells in responders to nivo + ipi. This population of cells though has not been seen in non-responders to the combination therapy. Additionally, this effector memory T cell population was associated with longer PFS and tumor shrinkage in anti-PD-1 monotherapy-treated patients (142). This specific memory T cell population associated with the response to anti-PD-1 monotherapy and nivo + ipi combination therapy demonstrates the potential of utilizing immune infiltrates as markers of durable response to ICB.

Additionally, a subset of immune effector cells has been identified as a way to identify patients who are likely to respond to ICB treatment. This population of peripheral T cells with the $CD3^+/CD4^-/CD8^+/CD45RA^-/CD45RO^{high}/CD27^-/CCR7^-$ signature following one cycle of ICB has been associated with T cell evolution in response to treatment. This dynamic awakening of the immune system was identified using T cell receptor sequencing in plasma cell-free DNA and peripheral blood mononuclear cells. Along with a phenotypic analysis of peripheral T cell subsets of melanoma patients treated with ICB, early peripheral T cell turnover and TCR repertoire dynamics are associated with ICB response. Additionally, the timeline of this immune awakening within 3 weeks of ICB initiation provides promise to monitor patient responses using minimally invasive liquid biopsies (143).

Checkpoint blockade has also been shown to mediate the response of tumor-infiltrating $CD8^+$ T lymphocytes. The chronic activation of this TIL population has been thought to create a state of terminal differentiation or exhaustion of these tumor-specific T cells. Given this, the identification of a subset of exhausted T cells and central memory cells associated with the expression of PD-1 and transcription factor Tcf1 has been studied. A population of $Tcf1^+PD\text{-}1^+$ TILs has been shown to mediate the response to ICB and, in turn, generate additional populations of $Tcf1^+PD\text{-}1^+$ and differentiated $Tcf1^-PD\text{-}1^+$ cells. The Tcf1 transcription factor was not required for the generation of the $Tcf1^+PD\text{-}1^+$ TIL population, though essential for the stem-like function of these cells. Additionally, the ablation of this $Tcf1^+PD\text{-}1^+$ TIL population has been associated with restricted responses to ICB. Taken together, this study proposes that checkpoint inhibition relies less on the reversal of T cell exhaustion and more on the proliferation of this stem-like TIL subset, which is likely implicated in ICB response (144).

Differences between biomarkers associated with efficacy to CTLA-4 versus PD-1 monoclonal antibody treatments have also emerged. A study utilizing mass cytometry profiling of peripheral blood mononuclear cell (PBMC) samples from melanoma patients suggested a difference in anti-PD-1-treated but not anti-CTLA-4-treated patients. In those treated with anti-PD-1, differences between responders and non-responders with a CD69 and MIP-1ß NK cell population were seen. Here, natural killer cell subsets, but not memory $CD4^+$ or $CD8^+$ T cell subsets, correlated with clinical response to anti-PD-1 therapy, whereas these $CD4^+$ or $CD8^+$ memory T cells differed between responders and non-responders to anti-CTLA-4 therapy (145).

Melanoma bulk-tumor transcriptomic and single-cell (sc) RNAseq data have identified other potential biomarkers of response and survival in patients treated with sequential ICB therapy (anti-CTLA-4 then anti-PD-1). In patients treated with sequential anti-CTLA-4 then anti-PD-1, the $CD8^+/CD4^+$ T cell signature associated with IFNγ signaling or cytolytic activity failed to predict an antitumor response. Conversely, early memory $CD8^+/$

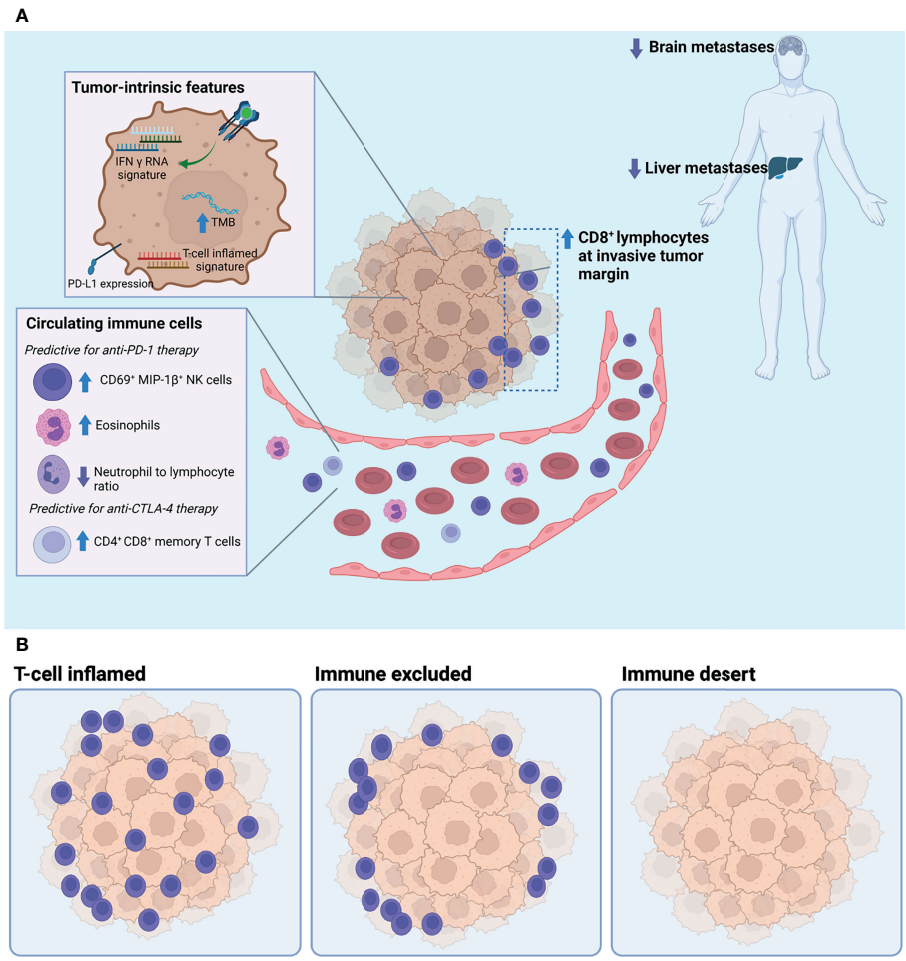

FIGURE 1 | **(A)** Tumor-intrinsic and circulating biomarkers associated with response to immune checkpoint blockade. **(B)** Three archetypical tumor microenvironments defined by the degree of T cell infiltration: T cell inflamed, immune excluded, and immune desert. Of these, the T cell-inflamed phenotype has been positively associated with response to immune checkpoint blockade. TMB, tumor mutational burden.

$CD4^+$ T cell signatures [associated with the transcription factor, T cell factor 1 (TCF-1)-driven stem-like transcriptional program, characteristic of resisting cell death or apoptosis] have been shown to be predictors of ORR to ICB and survival following anti-CTLA-4 and anti-PD-1 sequential therapy. This suggests that sequencing of ICB therapy may impact the T cell repertoire and influence the value of predictive immune biomarkers (146).

Separately, chemotherapy and immunotherapy treatment scheduling may also affect the ICB response. Preclinical mouse models have demonstrated that tumor draining lymph nodes affect the tumor antigen-specific T cell response. Removal of tumor draining lymph nodes concurrently with established primary tumors did not affect the ICB response on localized secondary tumors given the distribution of antigen-specific T cells in peripheral lymphatic organs and the immunotolerance in tumor draining lymph nodes. Yet, in this study, tumor responses were proven with the sequential administration of 5-fluorouracil (5-FU) and ICB compared with the concurrent administration of 5-FU and ICB where immune profiling revealed that the utilization of 5-FU as an induction treatment decreased immunosuppressive cells in the tumor microenvironment, increased tumor visibility to immune cells, and limited chemotherapy-induced T cell depletion. Here, in preclinical models, traditional cytotoxic treatment in sequence with ICB influenced immunotherapy response in localized secondary tumors and may be a strategy utilized in the clinical setting to induce long-term tumor responses (147).

Given these promising hints of potential biomarkers, the importance of understanding the biology surrounding the tumor microenvironment, the modulation of NK cells, and the role that both effector or exhausted $CD8^+$ T cells and TILs play in responders versus non-responders to ICB therapy is imperative to develop clinically informative predictive biomarkers of response (**Figure 1**).

CONCLUSION

Across several clinical trials, the long-term survivorship of patients treated with immune checkpoint blockade therapies continues to shed light on the durability and promising nature of the treatment of those with advanced melanoma. Several trials with follow-up and landmark OS rates of at least 5 years demonstrate just how widely immunotherapies have revolutionized the landscape of melanoma treatment in the last decade. The potential for long-term survival, durable responses, and even possible cure models in melanoma provides an abundance of hope. For patients who do not experience the benefit of long-term response, escalation of care with either rechallenge of ICB or additional therapies is under study and development.

With long-term survival now more attainable than ever, clinicians are looking toward markers that may stratify melanoma patients for ICB therapies with durable clinical responses. Research currently focused on identifying both robust prognostic and predictive biomarkers of response to ICB is underway. To maximize therapeutic potential and minimize undesirable toxicities, the translational potential of neoadjuvant pathologic complete responses, baseline blood chemistry serologies, tumor and microenvironment TIL composition, and additional immune cell populations contributing to lasting T cell memories have been identified as potential biomarkers of long-term response. The future development of therapies alone or in combination with current ICBs and improvements in the diagnostic accuracy of biomarkers are promising to achieve long-term survival and possible cure for advanced melanoma.

AUTHOR CONTRIBUTIONS

KL wrote, reviewed, and edited the article. AW and MP reviewed and edited the article. JS designed the figure. All authors contributed to the article and approved the submitted version.

FUNDING

The authors were supported by the Cancer Center Support Grant P30 CA08748 from the National Institutes of Health/National Cancer Institute.

ACKNOWLEDGMENTS

The figure was created using BioRender.com (2021).

REFERENCES

1. Wolchok JD, Chiarion-Sileni V, Gonzalez R, Grob J-J, Rutkowski P, Lao CD, et al. CheckMate 067: 6.5-Year Outcomes in Patients (Pts) With Advanced Melanoma. *J Clin Oncol* (2021) 39:9506–6. doi: 10.1200/JCO.2021.39.15_suppl.9506
2. Robert C, Schachter J, Long GV, Arance A, Grob JJ, Mortier L, et al. Pembrolizumab Versus Ipilimumab in Advanced Melanoma. *N Engl J Med* (2015) 372:2521–32. doi: 10.1056/NEJMoa1503093
3. Larkin J, Chiarion-Sileni V, Gonzalez R, Grob JJ, Cowey L, Lao CD, et al. Combined Nivolumab and Ipilimumab or Monotherapy in Untreated Melanoma. *N Engl J Med* (2015) 373:23–34. doi: 10.1056/NEJMoa1504030
4. Postow MA, Sidlow R, Hellmann MD. Immune-Related Adverse Events Associated With Immune Checkpoint Blockade. *N Engl J Med* (2018) 378:158–68. doi: 10.1056/NEJMra1703481
5. Buchbinder EI, Desai A. CTLA-4 and PD-1 Pathways. *Am J Clin Oncol* (2016) 39:98–106. doi: 10.1097/COC.0000000000000239
6. Hurst JH. Cancer Immunotherapy Innovator James Allison Receives the 2015 Lasker~DeBakey Clinical Medical Research Award. *J Clin Invest* (2015) 125:3732–6. doi: 10.1172/JCI84236
7. Fife BT, Bluestone JA. Control of Peripheral T Cell Tolerance and Autoimmunity via the CTLA-4 and PD-1 Pathways. *Immunol Rev* (2008) 224:166–82. doi: 10.1111/j.1600-065X.2008.00662.x
8. Krummel MF, Allison JP. CD28 and CTLA-4 Have Opposing Effects on the Response of T Cells to Stimulation. *J Exp Med* (1995) 182:459–65. doi: 10.1084/jem.182.2.459
9. Terme M, Ullrich E, Aymeric L, Meinhardt K, Desbois M, Delahaye N, et al. IL-18 Induces PD-1-Dependent Immunosuppression in Cancer. *Cancer Res* (2011) 71:5393–9. doi: 10.1158/0008-5472.CAN-11-0993

10. Fanoni D, Tavecchio S, Recalcati S, Venegoni L, Fiorani R. New Monoclonal Antibodies Against B-Cell Antigens: Possible New Strategies for Diagnosis of Primary Cutaneous B-Cell Lymphomas. *Immunol Lett* (2011) 134:157–60. doi: 10.1016/j.imlet.2010.09.022
11. Fife BT, Pauken KE, Eagar TN, Obu T, Wu J, Tang Q, et al. Interactions Between PD-1 and PD-L1 Promote Tolerance by Blocking the TCR-Induced Stop Signal. *Nat Immunol* (2009) 10:1185–92. doi: 10.1038/ni.1790
12. Freeman GJ, Long AJ, Iwai Y, Bourque K, Chernova T, Nishimura H, et al. Engagement of the Pd-1 Immunoinhibitory Receptor by a Novel B7 Family Member Leads to Negative Regulation of Lymphocyte Activation. *J Exp Med* (2000) 192:1027–34. doi: 10.1084/jem.192.7.1027
13. Chae YK, Arya A, Iams W, Cruz MR, Chandra S, Choi J, et al. Current Landscape and Future of Dual Anti-CTLA4 and PD-1/PD-L1 Blockade Immunotherapy in Cancer; Lessons Learned From Clinical Trials With Melanoma and Non-Small Cell Lung Cancer (NSCLC). *J Immunother Cancer* (2018) 6:39. doi: 10.1186/s40425-018-0349-3
14. Keir ME, Butte MJ, Freeman GJ, Sharpe AH. PD-1 and Its Ligands in Tolerance and Immunity. *Annu Rev Immunol* (2008) 26:677–704. doi: 10.1146/annurev.immunol.26.021607.090331
15. Dunn GP, Old LJ, Schreiber RD. The Immunobiology of Cancer Immunosurveillance and Immunoediting. *Immunity* (2004) 21:137–48. doi: 10.1016/j.immuni.2004.07.017
16. Poschke I, Mougiakakos D, Kiessling R. Camouflage and Sabotage: Tumor Escape From the Immune System. *Cancer Immunol Immunother CII* (2011) 60:1161–71. doi: 10.1007/s00262-011-1012-8
17. Hodi FS, O'Day SJ, McDermott DF, Weber RW, Sosman JA, Haanen JB, et al. Improved Survival With Ipilimumab in Patients With Metastatic Melanoma. *N Engl J Med* (2010) 363:711–23. doi: 10.1056/NEJMx100063
18. Hamid O, Robert C, Daud A, Hodi S, Hwu W-J, Kefford R, et al. Safety and Tumor Responses With Lambrolizumab (Anti-PD-1) in Melanoma. *N Engl J Med* (2013) 369:134–44. doi: 10.1056/NEJMoa1305133
19. Brahmer JR, Drake CG, Wollner I, Powderly JD, Picus J, Sharfman WH, et al. Phase I Study of Single-Agent Anti-Programmed Death-1 (MDX-1106) in Refractory Solid Tumors: Safety, Clinical Activity, Pharmacodynamics, and Immunologic Correlates. *J Clin Oncol Off J Am Soc Clin Oncol* (2010) 28:3167–75. doi: 10.1200/JCO.2009.26.7609
20. Topalian SL, Hodi FS, Brahmer JR, Gettinger SN, Smith DC, McDermott DF, et al. Safety, Activity, and Immune Correlates of Anti–PD-1 Antibody in Cancer. *N Engl J Med* (2012) 366:2443–54. doi: 10.1056/NEJMoa1200690
21. Brahmer JR, Tykodi SS, Chow LQM, Hwu W-j, Topalian SL, Hwu P, et al. Safety and Activity of Anti-PD-L1 Antibody in Patients With Advanced Cancer. *N Engl J Med* (2012) 366:2455–65. doi: 10.1056/NEJMoa1200694
22. Robert C, Ribas A, Wolchok JD, Hodi S, Hamid O, Kefford R, et al. Anti-Programmed-Death-Receptor-1 Treatment With Pembrolizumab in Ipilimumab-Refractory Advanced Melanoma: A Randomised Dose-Comparison Cohort of a Phase 1 Trial. *Lancet Lond Engl* (2014) 384:1109–17. doi: 10.1016/S0140-6736(14)60958-2
23. Ribas A, Puzanov I, Dummer R, Schadendorf D, Hamid O, Robert C, et al. Pembrolizumab Versus Investigator-Choice Chemotherapy for Ipilimumab-Refractory Melanoma (KEYNOTE-002): A Randomised, Controlled, Phase 2 Trial. *Lancet Oncol* (2015) 16:908–18. doi: 10.1016/S1470-2045(15)00083-2
24. Schachter J, Ribas A, Long GV, Arance A, Grob J-J, Mortier L, et al. Pembrolizumab Versus Ipilimumab for Advanced Melanoma: Final Overall Survival Results of a Multicentre, Randomised, Open-Label Phase 3 Study (KEYNOTE-006). *Lancet Lond Engl* (2017) 390:1853–62. doi: 10.1016/S0140-6736(17)31601-X
25. Weber JS, D'Angelo SP, Minor D, Hodi FS, Gutzmer R, Neyns B, et al. Nivolumab Versus Chemotherapy in Patients With Advanced Melanoma Who Progressed After Anti-CTLA-4 Treatment (CheckMate 037): A Randomised, Controlled, Open-Label, Phase 3 Trial. *Lancet Oncol* (2015) 16:375–84. doi: 10.1016/S1470-2045(15)70076-8
26. Robert C, Long GV, Brady B, Dutriaux C, Maio M, Mortier L, et al. Nivolumab in Previously Untreated Melanoma Without BRAF Mutation. *N Engl J Med* (2015) 372:320–30. doi: 10.1056/NEJMoa1412082
27. Larkin J, Chiarion-Sileni V, Gonzalez R, Grob J-J, Rutkowski P, Lao CD, et al. Five-Year Survival With Combined Nivolumab and Ipilimumab in Advanced Melanoma. *N Engl J Med* (2019) 381:1535–46. doi: 10.1056/NEJMoa1910836
28. Wolchok JD, Kluger H, Callahan MK, Postow MA, Rizvi NA, Lesokhin AM, et al. Safety and Clinical Activity of Combined PD-1 (Nivolumab) and CTLA-4 (Ipilimumab) Blockade in Advanced Melanoma Patients. *N Engl J Med* (2013) 369:122–33. doi: 10.1056/NEJMoa1302369
29. Postow MA, Chesney J, Pavlick AC, Robert C, Grossmann K, McDermott D, et al. Nivolumab and Ipilimumab Versus Ipilimumab in Untreated Melanoma. *N Engl J Med* (2015) 372:2006–17. doi: 10.1056/NEJMoa1414428
30. Weber JS, Gibney G, Sullivan RJ, Sosman JA, Slingluff CL Jr, Lawrence DP, et al. Sequential Administration of Nivolumab and Ipilimumab With a Planned Switch in Patients With Advanced Melanoma (CheckMate 064): An Open-Label, Randomised, Phase 2 Trial. *Lancet Oncol* (2016) 17:943–55. doi: 10.1016/S1470-2045(16)30126-7
31. Wolchok JD, Kluger H, Callahan MK, Postow MA, Rizvi NA, Lesokhin AM, et al. Nivolumab Plus Ipilimumab in Advanced Melanoma. *N Engl J Med* (2013) 369:122–33. doi: 10.1056/NEJMoa1302369
32. Hodi FS, Chapman PB, Sznol M, Lao C, Gonzalez R, Smylie M, et al. Safety and Efficacy of Combination Nivolumab Plus Ipilimumab in Patients With Advanced Melanoma: Results From a North American Expanded Access Program (CheckMate 218). *Melanoma Res* (2021) 31:67–75. doi: 10.1097/CMR.0000000000000708
33. Hamid O, Robert C, Daud A, Ahsan S, Ibrahim N, Ribas A, et al. Five-Year Survival Outcomes for Patients With Advanced Melanoma Treated With Pembrolizumab in KEYNOTE-001. *Ann Oncol Off J Eur Soc Med Oncol* (2019) 30:582–8. doi: 10.1093/annonc/mdz011
34. Robert C, Ribas A, Schachter J, Arance A, Grob J-J, Mortier L, et al. Pembrolizumab Versus Ipilimumab in Advanced Melanoma (KEYNOTE-006): Post-Hoc 5-Year Results From an Open-Label, Multicentre, Randomised, Controlled, Phase 3 Study. *Lancet Oncol* (2019) 20:1239–51. doi: 10.1016/S1470-2045(19)30388-2
35. *New Research for KEYTRUDA® (Pembrolizumab) at Society for Melanoma Research (SMR) 2021 Congress Reinforces Merck's Commitment to Patients With Melanoma Across Stages of Disease [Internet]*. Kenilworth, NJ: Merck.com (2021). Available at: https://www.merck.com/news/new-research-for-keytruda-pembrolizumab-at-society-for-melanoma-research-smr-2021-congress-reinforces-mercks-commitment-to-patients-with-melanoma-across-stages-of-disease/.
36. Ascierto PA, Del Vecchio M, Mandalá M, Gogas H, Arance AM, Dalle S, et al. Adjuvant Nivolumab Versus Ipilimumab in Resected Stage IIIB-C and Stage IV Melanoma (CheckMate 238): 4-Year Results From a Multicentre, Double-Blind, Randomised, Controlled, Phase 3 Trial. *Lancet Oncol* (2020) 21:1465–77. doi: 10.1016/S1470-2045(20)30494-0
37. Eggermont AMM, Blank CU, Mandalà M, Long GV, Atkinson VG, Dalle S, et al. Adjuvant Pembrolizumab Versus Placebo in Resected Stage III Melanoma (EORTC 1325-MG/KEYNOTE-054): Distant Metastasis-Free Survival Results From a Double-Blind, Randomised, Controlled, Phase 3 Trial. *Lancet Oncol* (2021) 22:643–54. doi: 10.1016/S1470-2045(21)00065-6
38. Warner AB, Palmer JS, Shoushtari AN, Goldman DA, Panageas KS, Hayes SA, et al. Long-Term Outcomes and Responses to Retreatment in Patients With Melanoma Treated With PD-1 Blockade. *J Clin Oncol* (2020) 38:1655–63. doi: 10.1200/JCO.19.01464
39. Byun HK, Chang JS, Jung M, Koom WS, Chung KY, Oh H, et al. Prediction of Immune-Checkpoint Blockade Monotherapy Response in Patients With Melanoma Based on Easily Accessible Clinical Indicators. *Front Oncol* (2021) 11:659754. doi: 10.3389/fonc.2021.659754
40. Teulings H-E, Limpens J, Jansen SN, Zwinderman AH, Reitsma JB, Spuls PI, et al. Vitiligo-Like Depigmentation in Patients With Stage III-IV Melanoma Receiving Immunotherapy and Its Association With Survival: A Systematic Review and Meta-Analysis. *J Clin Oncol Off J Am Soc Clin Oncol* (2015) 33:773–81. doi: 10.1200/JCO.2014.57.4756
41. Sakakida T, Ishikawa T, Uchino J, Chihara Y, Komori S, Asai J, et al. Clinical Features of Immune-Related Thyroid Dysfunction and Its Association With Outcomes in Patients With Advanced Malignancies Treated by PD-1 Blockade. *Oncol Lett* (2019) 18:2140–7. doi: 10.3892/ol.2019.10466
42. Johnson DB, Friedman DL, Berry E, Decker I, Ye F, Zhao S, et al. Survivorship in Immune Therapy: Assessing Chronic Immune Toxicities, Health Outcomes, and Functional Status Among Long-Term Ipilimumab

Survivors at a Single Referral Center. *Cancer Immunol Res* (2015) 3:464–9. doi: 10.1158/2326-6066.CIR-14-0217
43. Patrinely JR, Young AC, Quach H, Friedman DL, Moslehi JJ, Johnson DB, et al. Survivorship in Immune Therapy: Assessing Toxicities, Body Composition and Health-Related Quality of Life Among Long-Term Survivors Treated With Antibodies to Programmed Death-1 Receptor and Its Ligand. *Eur J Cancer Oxf Engl 1990* (2020) 135:211–20. doi: 10.1016/j.ejca.2020.05.005
44. Patrinely JR Jr, Johnson R, Lawless AR, Bhave P, Sawyers A, Dimitrova M, et al. Chronic Immune-Related Adverse Events Following Adjuvant Anti–PD-1 Therapy for High-Risk Resected Melanoma. *JAMA Oncol* (2021) 7:744–8. doi: 10.1001/jamaoncol.2021.0051
45. Robert C, Marabelle A, Herrscher H, Caramella C, Rouby P, Fizazi K, et al. Immunotherapy Discontinuation — How, and When? Data From Melanoma as a Paradigm. *Nat Rev Clin Oncol* (2020) 17:707–15. doi: 10.1038/s41571-020-0399-6
46. Jansen YJL, Rozeman EA, Mason R, Atkinson V, Blank CU, Neyns B, et al. Discontinuation of Anti-PD-1 Antibody Therapy in the Absence of Disease Progression or Treatment Limiting Toxicity: Clinical Outcomes in Advanced Melanoma. *Ann Oncol Off J Eur Soc Med Oncol* (2019) 30:1154–61. doi: 10.1093/annonc/mdz110
47. Pokorny R, McPherson JP, Haaland B, Grossmann KF, Luckett C, Voorhies BN, et al. Real-World Experience With Elective Discontinuation of PD-1 Inhibitors at 1 Year in Patients With Metastatic Melanoma. *J Immunother Cancer* (2021) 9:e001781. doi: 10.1136/jitc-2020-001781
48. Asher N, Israeli-Weller N, Shapira-Frommer R, Ben-Betzalel G, Schachter J, Meirson T, et al. Immunotherapy Discontinuation in Metastatic Melanoma: Lessons From Real-Life Clinical Experience. *Cancers* (2021) 13:3074. doi: 10.3390/cancers13123074
49. Mulder EEAP, de Joode K, Litière S, ten Tije AJ, Suijkerbuijk KPM, Boers-Sonderen MJ, et al. Early Discontinuation of PD-1 Blockade Upon Achieving a Complete or Partial Response in Patients With Advanced Melanoma: The Multicentre Prospective Safe Stop Trial. *BMC Cancer* (2021) 21:323. doi: 10.1186/s12885-021-08018-w
50. Schadendorf D, Hodi FS, Robert C, Weber JS, Margolin K, Hamid O, et al. Pooled Analysis of Long-Term Survival Data From Phase II and Phase III Trials of Ipilimumab in Unresectable or Metastatic Melanoma. *J Clin Oncol* (2015) 33:1889–94. doi: 10.1200/JCO.2014.56.2736
51. Loo K, Goldman DA, Panageas K, Callahan MK, Chapman PB, Momtaz P, et al. Characteristics and Probability of Survival for Patients With Advanced Melanoma Who Live Five or More Years After Initial Treatment With Immune Checkpoint Blockade (ICB). *J Clin Oncol* (2021) 39:9534–4. doi: 10.1200/JCO.2021.39.15_suppl.9534
52. Michielin O, Atkins MB, Koon HB, Dummer5 R, Ascierto PA. Evolving Impact of Long-Term Survival Results on Metastatic Melanoma Treatment. *J Immunother Cancer* (2020) 8:e000948. doi: 10.1136/jitc-2020-000948
53. Kim T, Amaria RN, Spencer C, Reuben A, Cooper ZA, Wargo JA, et al. Combining Targeted Therapy and Immune Checkpoint Inhibitors in the Treatment of Metastatic Melanoma. *Cancer Biol Med* (2014) 11:237–46. doi: 10.7497/j.issn.2095-3941.2014.04.002
54. Zaremba A, Eggermont AMM, Robert C, Long GV, Schadendorf D, Zimmer L, et al. The Concepts of Rechallenge and Retreatment With Immune Checkpoint Blockade in Melanoma Patients. *Eur J Cancer Oxf Engl 1990* (2021) 155:268–80. doi: 10.1016/j.ejca.2021.07.002
55. Lebbé C, Weber JS, Maio M, Cykowski L, McHenry MB, Wolchok JD, et al. Survival Follow-Up and Ipilimumab Retreatment of Patients With Advanced Melanoma Who Received Ipilimumab in Prior Phase II Studies. *Ann Oncol Off J Eur Soc Med Oncol* (2014) 25:2277–84. doi: 10.1093/annonc/mdu441
56. Robert C, Schadendorf D, Messina M, Hodi FS, O'Day S. Efficacy and Safety of Retreatment With Ipilimumab in Patients With Pretreated Advanced Melanoma Who Progressed After Initially Achieving Disease Control. *Clin Cancer Res Off J Am Assoc Cancer Res* (2013) 19:2232–9. doi: 10.1158/1078-0432.CCR-12-3080
57. Chiarion-Sileni V, Pigozzo J, Ascierto PA, Simeone E, Maio M, Calabrò L, et al. Ipilimumab Retreatment in Patients With Pretreated Advanced Melanoma: The Expanded Access Programme in Italy. *Br J Cancer* (2014) 110:1721–6. doi: 10.1038/bjc.2014.126
58. Chapman PB, Jayaprakasam VS, Panageas KS, Callahan M, Postow MA, Shoushtari AN, et al. Risks and Benefits of Reinduction Ipilimumab/Nivolumab in Melanoma Patients Previously Treated With Ipilimumab/Nivolumab. *J Immunother Cancer* (2021) 9:e003395. doi: 10.1136/jitc-2021-003395
59. Hepner A, Atkinson VG, Larkin J, Burrell RA, Carlino MS, Johnson DB, et al. Re-Induction Ipilimumab Following Acquired Resistance to Combination Ipilimumab and Anti-PD-1 Therapy. *Eur J Cancer Oxf Engl 1990* (2021) 153:213–22. doi: 10.1016/j.ejca.2021.04.021
60. Olson DJ, Eroglu Z, Brockstein B, Poklepovic AS, Bajaj M, Babu S, et al. Pembrolizumab Plus Ipilimumab Following Anti-PD-1/L1 Failure in Melanoma. *J Clin Oncol Off J Am Soc Clin Oncol* (2021) 39:2647–55. doi: 10.1200/JCO.21.00079
61. Reschke R, Ziemer M. Rechallenge With Checkpoint Inhibitors in Metastatic Melanoma. *JDDG J Dtsch Dermatol Ges* (2020) 18:429–36. doi: 10.1111/ddg.14091
62. Clark GM. Prognostic Factors Versus Predictive Factors: Examples From a Clinical Trial of Erlotinib. *Mol Oncol* (2008) 1:406–12. doi: 10.1016/j.molonc.2007.12.001
63. Clark GM, Zborowski DM, Culbertson JL, Whitehead M, Savoie M, Seymour L, et al. Clinical Utility of Epidermal Growth Factor Receptor Expression for Selecting Patients With Advanced Non-Small Cell Lung Cancer for Treatment With Erlotinib. *J Thorac Oncol Off Publ Int Assoc Study Lung Cancer* (2006) 1:837–46. doi: 10.1097/01243894-200610000-00013
64. Poklepovic AS, Carvajal RD. Prognostic Value of Low Tumor Burden in Patients With Melanoma [Internet]. *Cancer Netw* (2018).
65. Warner AB, Postow MA. Bigger Is Not Always Better: Tumor Size and Prognosis in Advanced Melanoma. *Clin Cancer Res Off J Am Assoc Cancer Res* (2018) 24:4915–7. doi: 10.1158/1078-0432.CCR-18-1311
66. Balch CM, Gershenwald JE, Soong S-J, Thompson JF, Atkins MB, Byrd DR, et al. Final Version of 2009 AJCC Melanoma Staging and Classification. *J Clin Oncol Off J Am Soc Clin Oncol* (2009) 27:6199–206. doi: 10.1200/JCO.2009.23.4799
67. Fantin VR, St-Pierre J, Leder P. Attenuation of LDH-A Expression Uncovers a Link Between Glycolysis, Mitochondrial Physiology, and Tumor Maintenance. *Cancer Cell* (2006) 9:425–34. doi: 10.1016/j.ccr.2006.04.023
68. Joseph RW, Elassaiss-Schaap J, Kefford R, Hwu W-J, Wolchok JD, Joshua AM, et al. Correction: Baseline Tumor Size Is an Independent Prognostic Factor for Overall Survival in Patients With Melanoma Treated With Pembrolizumab. *Clin Cancer Res Off J Am Assoc Cancer Res* (2018) 24:6098. doi: 10.1158/1078-0432.CCR-18-3340
69. Martens A, Wistuba-Hamprecht K, Foppen MG, Yuan J, Postow MA, Wong P, et al. Baseline Peripheral Blood Biomarkers Associated With Clinical Outcome of Advanced Melanoma Patients Treated With Ipilimumab. *Clin Cancer Res Off J Am Assoc Cancer Res* (2016) 22:2908–18. doi: 10.1158/1078-0432.CCR-15-2412
70. Diem S, Kasenda B, Spain L, Martin-Liberal J, Marconcini R, Gore M, et al. Serum Lactate Dehydrogenase as an Early Marker for Outcome in Patients Treated With Anti-PD-1 Therapy in Metastatic Melanoma. *Br J Cancer* (2016) 114:256–61. doi: 10.1038/bjc.2015.467
71. Kelderman S, Heemskerk B, van Tinteren H, van den Brom RRH, Hospers GAP, van den Eertwegh AJM, et al. Lactate Dehydrogenase as a Selection Criterion for Ipilimumab Treatment in Metastatic Melanoma. *Cancer Immunol Immunother CII* (2014) 63:449–58. doi: 10.1007/s00262-014-1528-9
72. Nosrati A, Tsai KK, Goldinger SM, Tumeh P, Grimes B, Loo K, et al. Evaluation of Clinicopathological Factors in PD-1 Response: Derivation and Validation of a Prediction Scale for Response to PD-1 Monotherapy. *Br J Cancer* (2017) 116:1141–7. doi: 10.1038/bjc.2017.70
73. Martens A, Wistuba-Hamprecht K, Yuan J, Postow MA, Wong P, Capone M, et al. Increases in Absolute Lymphocytes and Circulating CD4+ and CD8+ T Cells Are Associated With Positive Clinical Outcome of Melanoma Patients Treated With Ipilimumab. *Clin Cancer Res Off J Am Assoc Cancer Res* (2016) 22:4848–58. doi: 10.1158/1078-0432.CCR-16-0249
74. Ikutani M, Yanagibashi T, Ogasawara M, Tsuneyama K, Yamamoto S, Hattori Y, et al. Identification of Innate IL-5–Producing Cells and Their Role

in Lung Eosinophil Regulation and Antitumor Immunity. *J Immunol* (2012) 188:703–13. doi: 10.4049/jimmunol.1101270
75. Carretero R, Sektioglu IM, Garbi N, Salgado OC, Beckhove P, Hämmerling GJ. Eosinophils Orchestrate Cancer Rejection by Normalizing Tumor Vessels and Enhancing Infiltration of CD8(+) T Cells. *Nat Immunol* (2015) 16:609–17. doi: 10.1038/ni.3159
76. Schindler K, Harmankaya K, Kuk D, Mangana J, Michielin O, Hoeller C, et al. Correlation of Absolute and Relative Eosinophil Counts With Immune-Related Adverse Events in Melanoma Patients Treated With Ipilimumab. *J Clin Oncol* (2014) 32:9096–6. doi: 10.1200/jco.2014.32.15_suppl.9096
77. Weide B, Martens A, Hassel JC, Berking C, Postow MA, Bisschop K, et al. Baseline Biomarkers for Outcome of Melanoma Patients Treated With Pembrolizumab. *Clin Cancer Res* (2016) 22:5487–96. doi: 10.1158/1078-0432.CCR-16-0127
78. Moreira A, Leisgang W, Schuler G, Heinzerling L. Eosinophilic Count as a Biomarker for Prognosis of Melanoma Patients and Its Importance in the Response to Immunotherapy. *Immunotherapy* (2017) 9:115–21. doi: 10.2217/imt-2016-0138
79. Krishnan T, Tomita Y, Roberts-Thomson R. A Retrospective Analysis of Eosinophilia as a Predictive Marker of Response and Toxicity to Cancer Immunotherapy. *Future Sci OA* (2020) 6:FSO608. doi: 10.2144/fsoa-2020-0070
80. Bartlett EK, Flynn JR, Panageas KS, Ferraro RA, Sta. Cruz JM. High Neutrophil-to-Lymphocyte Ratio (NLR) Is Associated With Treatment Failure and Death in Patients Who Have Melanoma Treated With PD-1 Inhibitor Monotherapy. *Cancer* (2020) 126:76–85. doi: 10.1002/cncr.32506
81. Capone M, Giannarelli D, Mallardo D, Madonna G, Festino L, Grimaldi AM, et al. Baseline Neutrophil-to-Lymphocyte Ratio (NLR) and Derived NLR Could Predict Overall Survival in Patients With Advanced Melanoma Treated With Nivolumab. *J Immunother Cancer* (2018) 6:74. doi: 10.1186/s40425-018-0383-1
82. Cassidy MR, Wolchok RE, Zheng J, Panageas KS, Wolchok JD, Coit D, et al. Neutrophil to Lymphocyte Ratio Is Associated With Outcome During Ipilimumab Treatment. *EBioMedicine* (2017) 18:56–61. doi: 10.1016/j.ebiom.2017.03.029
83. Zhang F, Gong W. Prognostic Value of the Platelet-To-Lymphocyte Ratio in Patients With Melanoma: A Meta-Analysis. *Front Oncol* (2020) 10:1116. doi: 10.3389/fonc.2020.01116
84. Yu J, Green MD, Li S, Sun Y, Journey SN, Choi JE, et al. Liver Metastasis Restrains Immunotherapy Efficacy *via* Macrophage-Mediated T Cell Elimination. *Nat Med* (2021) 27:152–64. doi: 10.1038/s41591-020-1131-x
85. Lee JC, Mehdizadeh S, Smith J, Young A, Mufazalov IA, Mowery CT, et al. Regulatory T Cell Control of Systemic Immunity and Immunotherapy Response in Liver Metastasis. *Sci Immunol* (2020) 5:eaba0759. doi: 10.1126/sciimmunol.aba0759
86. Loo K, Tsai KK, Mahuron K, Liu J, Pauli ML, Sandoval PM, et al. Partially Exhausted Tumor-Infiltrating Lymphocytes Predict Response to Combination Immunotherapy. *JCI Insight* (2017) 2:93433. doi: 10.1172/jci.insight.93433
87. Daud AI, Loo K, Pauli ML, Sanchez-Rodriguez R, Sandoval PM. Tumor Immune Profiling Predicts Response to Anti-PD-1 Therapy in Human Melanoma. *J Clin Invest* (2016) 126:3447–52. doi: 10.1172/JCI87324
88. Cagney DN, Martin AM, Catalano PJ, Redig AJ, Lin NU, Lee EQ, et al. Incidence and Prognosis of Patients With Brain Metastases at Diagnosis of Systemic Malignancy: A Population-Based Study. *Neuro-Oncol* (2017) 19:1511–21. doi: 10.1093/neuonc/nox077
89. Sperduto PW, Jiang W, Brown PD, Yu J, Chiang V, Mehta M, et al. Estimating Survival in Melanoma Patients With Brain Metastases: An Update of the Graded Prognostic Assessment for Melanoma Using Molecular Markers (Melanoma-molGPA). *Int J Radiat Oncol* (2017) 99:812–6. doi: 10.1016/j.ijrobp.2017.06.2454
90. Tawbi HA-H, Forsyth PAJ, Hodi FS, Lao CD, Moschos SJ, Hamid O, et al. Efficacy and Safety of the Combination of Nivolumab (NIVO) Plus Ipilimumab (IPI) in Patients With Symptomatic Melanoma Brain Metastases (CheckMate 204). *J Clin Oncol* (2019) 37:9501–1. doi: 10.1200/JCO.2019.37.15_suppl.9501
91. Long GV, Atkinson V, Lo S, Sandhu S, Guminski AD, Brown MP, et al. Combination Nivolumab and Ipilimumab or Nivolumab Alone in Melanoma Brain Metastases: A Multicentre Randomised Phase 2 Study. *Lancet Oncol* (2018) 19:672–81. doi: 10.1016/S1470-2045(18)30139-6
92. Long GV, Atkinson V, Lo S, Guminski AD, Sandhu SK, Brown MP, et al. Five-Year Overall Survival From the Anti-PD1 Brain Collaboration (ABC Study): Randomized Phase 2 Study of Nivolumab (Nivo) or Nivo+ Ipilimumab (Ipi) in Patients (Pts) With Melanoma Brain Metastases (Mets). *J Clin Oncol* (2021) 39:9508–8. doi: 10.1200/JCO.2021.39.15_suppl.9508
93. van Opijnen MP, Dirven L, Coremans IEM, Taphoorn MJB, Kapiteijn EHW. The Impact of Current Treatment Modalities on the Outcomes of Patients With Melanoma Brain Metastases: A Systematic Review. *Int J Cancer* (2020) 146:1479–89. doi: 10.1002/ijc.32696
94. Margolin K, Tawbi H, Forsyth P, Hodi FS, Alagazi A, Hamid O, et al. *CheckMate 204: 3-Year Outcomes of Treatment With Combination Nivolumab (NIVO) Plus Ipilimumab (IPI) for Patients (Pts) With Active Melanoma Brain Metastases (MBM) [Internet]* (2021). Available at: https://oncologypro.esmo.org/meeting-resources/esmo-congress-2021/checkmate-204-3-year-outcomes-of-treatment-with-combination-nivolumab-nivo-plus-ipilimumab-ipi-for-patients-pts-with-active-melanoma-brain-m.
95. Menzies AM, Amaria RN, Rozeman EA, Huang AC, Tetzlaff MT, van de Wiel BA, et al. Pathological Response and Survival With Neoadjuvant Therapy in Melanoma: A Pooled Analysis From the International Neoadjuvant Melanoma Consortium (INMC). *Nat Med* (2021) 27:301–9. doi: 10.1038/s41591-020-01188-3
96. Amaria RN, Menzies AM, Burton EM, Scolyer RA, Tetzlaff MT, Antdbacka R, et al. Neoadjuvant Systemic Therapy in Melanoma: Recommendations of the International Neoadjuvant Melanoma Consortium. *Lancet Oncol* (2019) 20:e378–89. doi: 10.1016/S1470-2045(19)30332-8
97. Blank CU, Rozeman EA, Fanchi LF, Fanchi LF, Sikorska K, van de Wiel B, et al. Neoadjuvant Versus Adjuvant Ipilimumab Plus Nivolumab in Macroscopic Stage III Melanoma. *Nat Med* (2018) 24:1655–61. doi: 10.1038/s41591-018-0198-0
98. Amaria RN, Reddy SM, Tawbi HA, Davies MA, Ross MI, Glitza IC, et al. Neoadjuvant Immune Checkpoint Blockade in High-Risk Resectable Melanoma. *Nat Med* (2018) 24:1649–54. doi: 10.1038/s41591-018-0197-1
99. Huang AC, Orlowski RJ, Xu X, Mick R, George SM, Yan PK, et al. A Single Dose of Neoadjuvant PD-1 Blockade Predicts Clinical Outcomes in Resectable Melanoma. *Nat Med* (2019) 25:454–61. doi: 10.1038/s41591-019-0357-y
100. Rozeman EA, Menzies AM, van Akkooi ACJ, Adhikari C, Bierman C, van de Wiel BA, et al. Identification of the Optimal Combination Dosing Schedule of Neoadjuvant Ipilimumab Plus Nivolumab in Macroscopic Stage III Melanoma (OpACIN-Neo): A Multicentre, Phase 2, Randomised, Controlled Trial. *Lancet Oncol* (2019) 20:948–60. doi: 10.1016/S1470-2045(19)30151-2
101. Eggermont AMM, Chiarion-Sileni V, Grob J-J, Dummer R, Wolchok JD, Schmidt H, et al. Prolonged Survival in Stage III Melanoma With Ipilimumab Adjuvant Therapy. *N Engl J Med* (2016) 375:1845–55. doi: 10.1056/NEJMoa1611299
102. Weber J, Mandala M, Del Vecchio M, Gogas HJ, Arance AM, Cowey CL, et al. Adjuvant Nivolumab Versus Ipilimumab in Resected Stage III or IV Melanoma. *N Engl J Med* (2017) 377:1824–35. doi: 10.1056/NEJMoa1709030
103. Levine LS, Mahuron KM, Tsai KK, Wu C, Mattis DM, Pauli ML, et al. Tumor Immune Profiling-Based Neoadjuvant Immunotherapy for Locally Advanced Melanoma. *Ann Surg Oncol* (2020) 27:4122–30. doi: 10.1245/s10434-020-08648-7
104. Jessurun CAC, Vos JAM, Limpens J, Luiten RM. Biomarkers for Response of Melanoma Patients to Immune Checkpoint Inhibitors: A Systematic Review. *Front Oncol* (2017) 7:233. doi: 10.3389/fonc.2017.00233
105. Hogan SA, Levesque MP, Cheng PF. Melanoma Immunotherapy: Next-Generation Biomarkers. *Front Oncol* (2018) 8:178. doi: 10.3389/fonc.2018.00178
106. Daud AI, Wolchok JD, Robert C, Hwu W-J, Weber JS, Ribas A, et al. Programmed Death-Ligand 1 Expression and Response to the Anti–Programmed Death 1 Antibody Pembrolizumab in Melanoma. *J Clin Oncol* (2016) 34:4102–9. doi: 10.1200/JCO.2016.67.2477
107. Long GV, Dummer R, Hamid O, Gajewski TF, Caglevic C, Dalle S, et al. Epacadostat Plus Pembrolizumab Versus Placebo Plus Pembrolizumab

in Patients With Unresectable or Metastatic Melanoma (ECHO-301/KEYNOTE-252): A Phase 3, Randomised, Double-Blind Study. *Lancet Oncol* (2019) 20:1083–97. doi: 10.1016/S1470-2045(19)30274-8
108. Ott PA, Bang Y-J, Piha-Paul SA, Abdul Razak AR, Bennouna J, Soria J-C, et al. T Cell–Inflamed Gene-Expression Profile, Programmed Death Ligand 1 Expression, and Tumor Mutational Burden Predict Efficacy in Patients Treated With Pembrolizumab Across 20 Cancers: KEYNOTE-028. *J Clin Oncol* (2019) 37:318–27. doi: 10.1200/JCO.2018.78.2276
109. Tumeh PC, Harview CL, Yearley JH, Shintaku P, Taylor EJM, Robert L, et al. PD-1 Blockade Induces Responses by Inhibiting Adaptive Immune Resistance. *Nature* (2014) 515:568–71. doi: 10.1038/nature13954
110. Brüggemann C, Kirchberger MC, Goldinger SM, Weide B, Konrad A, Erdmann M, et al. Predictive Value of PD-L1 Based on mRNA Level in the Treatment of Stage IV Melanoma With Ipilimumab. *J Cancer Res Clin Oncol* (2017) 143:1977–84. doi: 10.1007/s00432-017-2450-2
111. Weide B, Martens A, Zelba H, Stutz C, Derhovanessian E, Di Giacomo AM, et al. Myeloid-Derived Suppressor Cells Predict Survival of Patients With Advanced Melanoma: Comparison With Regulatory T Cells and NY-ESO-1- or Melan-A-Specific T Cells. *Clin Cancer Res Off J Am Assoc Cancer Res* (2014) 20:1601–9. doi: 10.1158/1078-0432.CCR-13-2508
112. Gebhardt C, Sevko A, Jiang H, Lichtenberger R, Reith M, Tarnanidis K, et al. Myeloid Cells and Related Chronic Inflammatory Factors as Novel Predictive Markers in Melanoma Treatment With Ipilimumab. *Clin Cancer Res Off J Am Assoc Cancer Res* (2015) 21:5453–9. doi: 10.1158/1078-0432.CCR-15-0676
113. Ji R-R, Chasalow SD, Wang L, Hamid O, Schmidt H, Cogswell J, et al. An Immune-Active Tumor Microenvironment Favors Clinical Response to Ipilimumab. *Cancer Immunol Immunother* (2012) 61:1019–31. doi: 10.1007/s00262-011-1172-6
114. Tarhini AA, Edington H, Butterfield LH, Lin Y, Shuai Y, Tawbi H, et al. Immune Monitoring of the Circulation and the Tumor Microenvironment in Patients With Regionally Advanced Melanoma Receiving Neoadjuvant Ipilimumab. *PloS One* (2014) 9:e87705. doi: 10.1371/journal.pone.0087705
115. Taube JM, Young GD, McMiller TL, Chen S, Salas JT, Pritchard TS, et al. Differential Expression of Immune-Regulatory Genes Associated With PD-L1 Display in Melanoma: Implications for PD-1 Pathway Blockade. *Clin Cancer Res Off J Am Assoc Cancer Res* (2015) 21:3969–76. doi: 10.1158/1078-0432.CCR-15-0244
116. Teng MWL, Ngiow SF, Ribas A, Smyth MJ. Classifying Cancers Based on T Cell Infiltration and PD-L1. *Cancer Res* (2015) 75:2139–45. doi: 10.1158/0008-5472.CAN-15-0255
117. Tray N, Weber JS, Adams S. Predictive Biomarkers for Checkpoint Immunotherapy: Current Status and Challenges for Clinical Application. *Cancer Immunol Res* (2018) 6:1122–8. doi: 10.1158/2326-6066.CIR-18-0214
118. Gajewski TF, Louahed J, Brichard VG. Gene Signature in Melanoma Associated With Clinical Activity: A Potential Clue to Unlock Cancer Immunotherapy. *Cancer J Sudbury Mass* (2010) 16:399–403. doi: 10.1097/PPO.0b013e3181eacbd8
119. Gajewski TF, Schreiber H, Fu Y-X. Innate and Adaptive Immune Cells in the Tumor Microenvironment. *Nat Immunol* (2013) 14:1014–22. doi: 10.1038/ni.2703
120. Spranger S, Spaapen RM, Zha Y, Williams J, Meng Y, Ha T, et al. Up-Regulation of PD-L1, IDO, and Tregs in the Melanoma Tumor Microenvironment Is Driven by CD8+ T Cells. *Sci Transl Med* (2013) 5:200ra116. doi: 10.1126/scitranslmed.3006504
121. Ribas A, Robert C, Hodi FS, Wolchok JD, Joshua AM, Hwu W-J, et al. Association of Response to Programmed Death Receptor 1 (PD-1) Blockade With Pembrolizumab (MK-3475) With an Interferon-Inflammatory Immune Gene Signature. *J Clin Oncol* (2015) 33:3001–1. doi: 10.1200/jco.2015.33.15_suppl.3001
122. Piha-Paul SA, Bennouna J, Albright A, Nebozhyn M, McClanahan T, Ayers M, et al. T Cell Inflamed Phenotype Gene Expression Signatures to Predict Clinical Benefit From Pembrolizumab Across Multiple Tumor Types. *J Clin Oncol* (2016) 34:1536–6. doi: 10.1200/JCO.2016.34.15_suppl.1536
123. Plimack ER, Bellmunt J, Gupta S, Berger R, Montgomery RB, Heat K, et al. Pembrolizumab (MK-3475) for Advanced Urothelial Cancer: Updated Results and Biomarker Analysis From KEYNOTE-012. *J Clin Oncol* (2015) 33:4502–2. doi: 10.1200/jco.2015.33.15_suppl.4502
124. Shankaran V, Muro K, Bang Y-J, Geva R, Virgil D, Catenacci T, et al. Correlation of Gene Expression Signatures and Clinical Outcomes in Patients With Advanced Gastric Cancer Treated With Pembrolizumab (MK-3475). *J Clin Oncol* (2015) 33:3026–6. doi: 10.1200/jco.2015.33.15_suppl.3026
125. Cristescu R, Mogg R, Ayers M, Albright A, Murphy E, Yearley J, et al. Pan-Tumor Genomic Biomarkers for PD-1 Checkpoint Blockade–Based Immunotherapy [Internet]. *Science* (2018) 362(6411):eaar3593. doi: 10.1126/science.aar3593
126. Takahashi T, Tagami T, Yamazaki S, Uede T, Shimizu J, Sakaguchi N, et al. Immunologic Self-Tolerance Maintained by CD25(+)CD4(+) Regulatory T Cells Constitutively Expressing Cytotoxic T Lymphocyte-Associated Antigen 4. *J Exp Med* (2000) 192:303–10. doi: 10.1084/jem.192.2.303
127. Inozume T, Hanada K-I, Wang QJ, Ahmadzadeh M, Wunderlich JR, Rosenberg SA. Selection of CD8+PD-1+ Lymphocytes in Fresh Human Melanomas Enriches for Tumor-Reactive T Cells. *J Immunother Hagerstown Md 1997* (2010) 33:956–64. doi: 10.1097/CJI.0b013e3181fad2b0
128. Wei SC, Levine JH, Cogdill AP, Zhao Y, AnangN-AAS, Andrews MC, et al. Distinct Cellular Mechanisms Underlie Anti-CTLA-4 and Anti-PD-1 Checkpoint Blockade. *Cell* (2017) 170:1120–33.e17. doi: 10.1016/j.cell.2017.07.024
129. Herbst RS, Soria J-C, Kowanetz M, Fine GD, Hamid O, Gordon MS, et al. Predictive Correlates of Response to the Anti-PD-L1 Antibody MPDL3280A in Cancer Patients. *Nature* (2014) 515:563–7. doi: 10.1038/nature14011
130. Topalian SL, Taube JM, Anders RA, Pardoll DM. Mechanism-Driven Biomarkers to Guide Immune Checkpoint Blockade in Cancer Therapy. *Nat Rev Cancer* (2016) 16:275–87. doi: 10.1038/nrc.2016.36
131. Rizvi NA, Mazières J, Planchard D, Stinchcombe TE, Dy GK, Antonia SJ, et al. Activity and Safety of Nivolumab, an Anti-PD-1 Immune Checkpoint Inhibitor, for Patients With Advanced, Refractory Squamous Non-Small-Cell Lung Cancer (CheckMate 063): A Phase 2, Single-Arm Trial. *Lancet Oncol* (2015) 16:257–65. doi: 10.1016/S1470-2045(15)70054-9
132. Antony PA, Piccirillo CA, Akpinarli A, et al. CD8+ T Cell Immunity Against a Tumor/Self-Antigen Is Augmented by CD4+ T Helper Cells and Hindered by Naturally Occurring T Regulatory Cells. *J Immunol Baltim Md 1950* (2005) 174:2591–601. doi: 10.4049/jimmunol.174.5.2591
133. Pardoll DM, Topalian SL. The Role of CD4+ T Cell Responses in Antitumor Immunity. *Curr Opin Immunol* (1998) 10:588–94. doi: 10.1016/S0952-7915(98)80228-8
134. Xie Y, Akpinarli A, Maris C, Hipkiss EL, Lane M, Kwon E-KM, et al. Naive Tumor-Specific CD4(+) T Cells Differentiated In Vivo Eradicate Established Melanoma. *J Exp Med* (2010) 207:651–67. doi: 10.1084/jem.20091921
135. Quezada SA, Simpson TR, Peggs KS, Merghoub T, Vider J, Fan X, et al. Tumor-Reactive CD4(+) T Cells Develop Cytotoxic Activity and Eradicate Large Established Melanoma After Transfer Into Lymphopenic Hosts. *J Exp Med* (2010) 207:637–50. doi: 10.1084/jem.20091918
136. Takeuchi Y, Tanemura A, Tada Y, Katayama I, Kumanogoh A, Nishikawa H, et al. Clinical Response to PD-1 Blockade Correlates With a Sub-Fraction of Peripheral Central Memory CD4+ T Cells in Patients With Malignant Melanoma. *Int Immunol* (2018) 30:13–22. doi: 10.1093/intimm/dxx073
137. Hintzen RQ, de Jong R, Lens SM, Brouwer M, Baars P, van Lier RA, et al. Regulation of CD27 Expression on Subsets of Mature T-Lymphocytes. *J Immunol Baltim Md 1950* (1993) 151:2426–35.
138. Schiött A, Lindstedt M, Johansson-Lindbom B, Roggen E, Borrebaeck CAK. CD27- CD4+ Memory T Cells Define a Differentiated Memory Population at Both the Functional and Transcriptional Levels. *Immunology* (2004) 113:363–70. doi: 10.1111/j.1365-2567.2004.01974.x
139. Paulsen M, Janssen O. Pro- and Anti-Apoptotic CD95 Signaling in T Cells. *Cell Commun Signal CCS* (2011) 9:7. doi: 10.1186/1478-811X-9-7
140. Intlekofer AM, Takemoto N, Wherry EJ, Longworth SA, Northrup JT, Palanivel VR, et al. Effector and Memory CD8+ T Cell Fate Coupled by T-Bet and Eomesodermin. *Nat Immunol* (2005) 6:1236–44. doi: 10.1038/ni1268
141. Knox JJ, Cosma GL, Betts MR, McLane LM. Characterization of T-Bet and Eomes in Peripheral Human Immune Cells. *Front Immunol* (2014) 5:217. doi: 10.3389/fimmu.2014.00217

142. Gide TN, Quek C, Menzies AM, Longworth SA, Northrup JT, Palanivel VR, et al. Distinct Immune Cell Populations Define Response to Anti-PD-1 Monotherapy and Anti-PD-1/Anti-CTLA-4 Combined Therapy. *Cancer Cell* (2019) 35:238–55.e6. doi: 10.1016/j.ccell.2019.01.003
143. Valpione S, Galvani E, Tweedy J, Mundra PA, Banyard A, Middlehurst P, et al. Immune-Awakening Revealed by Peripheral T Cell Dynamics After One Cycle of Immunotherapy. *Nat Cancer* (2020) 1:210–21. doi: 10.1038/s43018-019-0022-x
144. Siddiqui I, Schaeuble K, Chennupati V, Luther SA, Speiser DE, Held W, et al. Intratumoral Tcf1+PD-1+CD8+ T Cells With Stem-Like Properties Promote Tumor Control in Response to Vaccination and Checkpoint Blockade Immunotherapy. *Immunity* (2019) 50:195–211.e10. doi: 10.1016/j.immuni.2018.12.021
145. Subrahmanyam PB, Dong Z, Gusenleitner D, Giobbie-Hurder A, Severgnini M, Zho J, et al. Distinct Predictive Biomarker Candidates for Response to Anti-CTLA-4 and Anti-PD-1 Immunotherapy in Melanoma Patients. *J Immunother Cancer* (2018) 6:18. doi: 10.1186/s40425-018-0328-8
146. Vanmeerbeek I, Borras DM, Sprooten J, Bechter O, Tejpar S, Garg AD, et al. Early Memory Differentiation and Cell Death Resistance in T Cells Predicts Melanoma Response to Sequential Anti-CTLA4 and Anti-PD1 Immunotherapy. *Genes Immun* (2021) 22:108–19. doi: 10.1038/s41435-021-00138-4
147. Zhao X, Kassaye B, Wangmo D, Lou E, Subramanian S. Chemotherapy But Not the Tumor Draining Lymph Nodes Determine the Immunotherapy Response in Secondary Tumors. *iScience* (2020) 23:101056. doi: 10.1016/j.isci.2020.101056

Conflict of Interest: The authors declare that the research was conducted in the absence of any commercial or financial relationships that could be construed as a potential conflict of interest.

Publisher's Note: All claims expressed in this article are solely those of the authors and do not necessarily represent those of their affiliated organizations, or those of the publisher, the editors and the reviewers. Any product that may be evaluated in this article, or claim that may be made by its manufacturer, is not guaranteed or endorsed by the publisher.

frontiers in Immunology

ORIGINAL RESEARCH
published: 03 February 2022
doi: 10.3389/fimmu.2022.809971

Association of Peripheral Blood Biomarkers With Response to Anti-PD-1 Immunotherapy for Patients With Deficient Mismatch Repair Metastatic Colorectal Cancer: A Multicenter Cohort Study

Yi-Kan Cheng[1,2,3†], Dong-Wen Chen[2,3,4†], Ping Chen[5,6,7†], Xiaosheng He[2,3,4], Pei-Si Li[2,3,4], Zhen-Sen Lin[2,3,4], Shao-Xia Chen[5,6,8], Shu-Biao Ye[2,3,4] and Ping Lan[2,3,4*]*

[1] Department of Radiation Oncology, The Sixth Affiliated Hospital, Sun Yat-sen University, Guangzhou, China, [2] Guangdong Institute of Gastroenterology, Guangzhou, China, [3] Guangdong Provincial Key laboratory of Colorectal and Pelvic Floor Diseases, The Sixth Affiliated Hospital of Sun Yat-sen University, Guangzhou, China, [4] Department of Colorectal Surgery, The Sixth Affiliated Hospital, Sun Yat-sen University, Guangzhou, China, [5] State Key Laboratory of Oncology in South China, Guangzhou, China, [6] Collaborative Innovation Center for Cancer Medicine, Sun Yat-sen University Cancer Center, Guangzhou, China, [7] Department of VIP Region, Sun Yat-sen University Cancer Center, Guangzhou, China, [8] Department of Anesthesiology, Cancer Center, Sun Yat-Sen University, Guangzhou, China

Purpose: Deficient mismatch repair (dMMR) is an established biomarker for the response to the programmed cell death (PD)-1 inhibitors in metastatic colorectal cancer (mCRC). Although patients with dMMR mCRC could achieve a high incidence of disease control and favorable progression-free survival (PFS), reported response rates to PD-1 inhibitors are variable from 28% to 52%. We aimed to explore the additional predictive biomarkers associated with response to anti-PD-1 immunotherapy in patients with dMMR mCRC.

Methods: This multicenter cohort study enrolled patients with dMMR mCRC receiving anti-PD-1 immunotherapy at the Sixth Affiliated Hospital of Sun Yat-sen University and Sun Yat-sen University Cancer Center between December 2016 and December 2019. The total information of 20 peripheral blood biomarkers, including T cells (frequency of CD4+ T cell, frequency of CD8+ T cell, and ratio of CD4+/CD8+), carcinoembryonic antigen (CEA), inflammatory markers, and lipid metabolism markers, was collected. The association between response or survival and peripheral blood parameters was analyzed.

Results: Among the tested parameters, the ratio of CD4+/CD8+ and frequency of CD4+ T cell were significantly associated with PFS (p = 0.023, p = 0.012) and overall survival (OS; p = 0.027, p = 0.019) in a univariate analysis. A lower level of CD4+/CD8+ ratio or frequency of CD4+ T cell showed a significant association with better overall response rates (ORRs; p = 0.03, p = 0.01). The ratio of CD4+/CD8+ and frequency of CD4+ T cell maintained significance in multivariate Cox model for PFS (HR = 9.23, p = 0.004; HR = 4.83, p = 0.02) and OS (HR = 15.22, p = 0.009; HR = 16.21, p = 0.025).

OPEN ACCESS

Edited by:
Roberta Zappasodi,
Cornell University, United States

Reviewed by:
Kirsten A. Ward-Hartstonge,
University of Otago, New Zealand
Serena Meraviglia,
University of Palermo, Italy

***Correspondence:**
Shu-Biao Ye
yeshb6@mail.sysu.edu.cn
Ping Lan
lanping@mail.sysu.edu.cn

†These authors have contributed equally to this work

Specialty section:
This article was submitted to Cancer Immunity and Immunotherapy, a section of the journal Frontiers in Immunology

Received: 05 November 2021
Accepted: 10 January 2022
Published: 03 February 2022

Citation:
Cheng Y-K, Chen D-W, Chen P, He X, Li P-S, Lin Z-S, Chen S-X, Ye S-B and Lan P (2022) Association of Peripheral Blood Biomarkers With Response to Anti-PD-1 Immunotherapy for Patients With Deficient Mismatch Repair Metastatic Colorectal Cancer: A Multicenter Cohort Study. Front. Immunol. 13:809971. doi: 10.3389/fimmu.2022.809971

Conclusion: This study indicated that the ratio of CD4+/CD8+ and the frequency of CD4+ T cell might be crucial independent biomarkers within dMMR mCRC to better identify patients for anti-PD-1 immunotherapy. If validated in prospective clinical trials, the ratio of CD4+/CD8+ and the frequency of CD4+ T cell might aid in guiding the treatment of PD-1 inhibitors among patients with dMMR mCRC.

Keywords: ratio of CD4+/CD8+, frequency of CD4+ T cell, deficient mismatch repair (dMMR), colorectal cancer (CRC), anti-PD-1 immunotherapy

INTRODUCTION

Colorectal cancer (CRC) is the fourth most common cause of cancer-related death globally, and there is an increasing incidence of CRC (1, 2). DNA deficient mismatch repair (dMMR)/microsatellite instability-high (MSI-H) is a well-established biomarker for the response to programmed cell death (PD)-1 inhibitors in metastatic CRC (mCRC), for which the US Food and Drug Administration (FDA) has approved PD-1 inhibitors for treating the patients with dMMR mCRC (3). Although promising efficacy of anti-PD-1 immunotherapy has been reported in locally advanced colon cancer with dMMR tumors (4), the overall response (OR) rates (ORRs) in MSI-H mCRC patients are variable from 28% to 52% (3, 5, 6), which were likely attributed to tumor heterogeneity. Moreover, the analysis of tumor mutational burden (TMB) in tumor sampling helps to further identify MSI-H mCRC patients who respond to PD-1 inhibitors (7), but this invasive way to obtain tissues might cause treatment delay. Hence, identification of new biomarkers from the easily accessible peripheral blood is critical for selecting patients who respond better to PD-1 inhibitors.

Tumor-infiltrating lymphocytes (frequency of CD8+ T cells) mainly contribute to the antitumor immune response and are a reliable prognostic indicator for CRC (8, 9). However, it is not an optimal predictor for anti-PD-1 immunotherapy. Several peripheral blood indexes, including T cells ($CD4^+$ and $CD8^+$ T lymphocytes) and systemic inflammation (neutrophil-to-lymphocyte ratio (NLR), absolute neutrophil count (ANC), C-reactive protein (CRP), and lactate dehydrogenase (LDH)), have been associated with response or survival outcomes in patients with melanoma and non-small cell lung cancer (NSCLC) receiving immune checkpoint inhibitors (ICIs) (10–15). In addition, lipid metabolism has been demonstrated to play an important role in the promotion of migration (16) and invasion (17) and be related to tumor immune milieu (18). However, it remains unclear whether the peripheral blood profiling could detect the responses to anti-PD-1 immunotherapy in MSI-H mCRC patients. Thus, this multicenter study analyzed 41 mCRC patients with dMMR tumors to investigate the potential association between peripheral biomarkers with response to anti-PD-1 immunotherapy.

Abbreviations: dMMR, deficient mismatch repair; PD-1, programmed cell death protein 1; mCRC, metastatic colorectal cancer; PFS, progression-free survival; CEA, carcinoembryonic antigen; OS, overall survival; ORR, overall response rate; MSI-H, microsatellite instability-high; FDA, Food and Drug Administration; TMB, tumor mutational burden; NLR, neutrophil-to-lymphocyte ratio; ANC, absolute neutrophil count; CRP, C-reactive protein; LDH, lactate dehydrogenase; NSCLC, non-small cell lung cancer; ICIs, immune checkpoint inhibitors; PLR, platelet-to-lymphocyte ratio; LMR, lymphocyte-to-monocyte ratio; ALB, albumin; CHO, cholesterol; TG, triglyceride; LDL, low-density lipoprotein; HDL, high-density lipoprotein; ApoA1, apolipoprotein A1; ApoB, apolipoprotein B; HRs, hazard ratios; CR, complete response; PR, partial response; SD, stable disease; PD, progressive disease; TAMs, tumor-associated macrophages.

MATERIALS AND METHODS

Patients

A total of 41 mCRC patients with dMMR tumors who have been treated with anti-PD-1 inhibitor (nivolumab, pembrolizumab, triprizumab, toripalimab, and camrelizumab) were identified at the Sixth Affiliated Hospital of Sun Yat-sen University and Sun Yat-sen University Cancer Center between December 2016 and December 2019 (**Figure 1**). The end of the follow-up was June 30, 2020. The study was approved by the institutional review

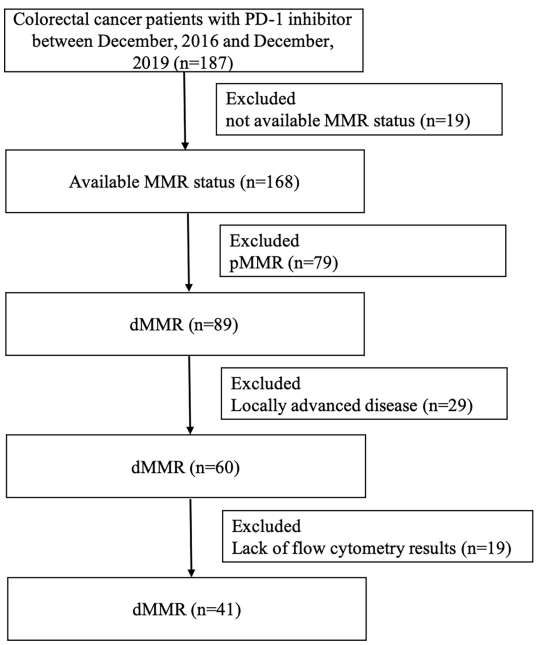

FIGURE 1 | Flowchart depicting patient selection. PD-1, programmed cell death 1; MMR, mismatch repair; dMMR, deficient mismatch repair; pMMR, proficient mismatch repair.

board of the Sixth Affiliated Hospital of Sun Yat-sen University. Written informed consent from patients was waived due to the retrospective nature of our study (**Table 1**).

Pretreatment clinicopathologic features and treatment history were collected from the individual database at these two institutions, which included age, sex, stage, tumor location, histologic subtype, carcinoembryonic antigen (CEA), mutational status (KRAS and BRAF), T cells [CD4+ T cell (CD3+ CD4+ T cell), CD8+ T cell (CD3+CD8 T cell), and ratio of CD4+/CD8+], inflammatory biomarkers [neutrophils, lymphocytes, monocytes, platelets, NLR, platelet-to-lymphocyte ratio (PLR) and lymphocyte-to-monocyte ratio (LMR), LDH, CRP, and albumin (ALB)], and lipid metabolism markers [cholesterol (CHO), triglyceride (TG), low-density lipoprotein (LDL), high-density lipoprotein (HDL), apolipoprotein A1 (ApoA1), and apolipoprotein B (ApoB)]. Pretreatment values were defined as those obtained before the initiation of anti-PD-1 immunotherapy.

TABLE 1 | Patients' characteristics.

Characteristics	No. (%) of Patients (n = 41)	CR/PR (n = 23)	SD/PD (n = 18)	p-Value[a]
Age, years, median (range)	41 (20–77)	35 (20–68)	47 (21–77)	0.16
Gender				0.13
Male	22 (54)	10 (43)	12 (67)	
Female	19 (46)	13 (57)	6 (33)	
Grade				0.40
High	5 (12)	4 (17)	1 (6)	
Moderate	14 (34)	8 (35)	6 (33)	
Low	15 (37)	6 (26)	9 (50)	
NA	7 (17)	5 (22)	2 (11)	
Tumor location				0.73
Colon	30 (73)	16 (70)	14 (78)	
Rectum	11 (27)	7 (30)	4 (22)	
Known KRAS status[b]				1.0
Mutant	16 (73)	8 (73)	8 (73)	
Wild-type	6 (27)	3 (27)	3 (27)	
Known BRAF status[c]				1.0
Mutant	2 (9)	1 (9)	1 (9)	
Wild-type	20 (91)	10 (91)	10 (91)	
Frequency of CD4+ T cells, %, median (range)	37 (23–61)	32 (23–51)	41 (25–61)	0.013
Frequency of CD4+ T cells, %				0.01
>39.5	16 (39)	5 (22)	11 (61)	
≤39.5	25 (61)	18 (78)	7 (39)	
Frequency of CD8+ T cells, %, median (range)	27 (12–53)	28 (15–53)	24 (12–46)	0.24
Ratio of CD4/CD8, %, median (range)	1.3 (0.5–4.6)	1.1 (0.5–2.3)	1.9 (0.6–4.6)	0.12
Ratio of CD4/CD8, %				0.03
>1.64	15 (37)	5 (22)	10 (56)	
≤1.64	26 (63)	18 (78)	8 (44)	
CEA, ng/ml, median (range)	9.3 (1.1–754.6)	5.0 (1.4–754.6)	44.0 (1.1–596.1)	0.03
CRP, mg/L, median (range)	14.4 (0.2–201.7)	12.5 (0.2–201.7)	16.3 (0.5–181.8)	0.47
LDH, U/L, median (range)	197.2 (130.9–931.2)	171.9 (135.5–931.2)	228.0 (130.9–567.3)	0.19
Neutrophils, 10E9/L, median (range)	4.1 (0.6–20.7)	3.3 (0.6–10.9)	4.7 (1.2–20.7)	0.17
Lymphocytes, 10E9/L, median (range)	1.3 (0.3–2.8)	1.3 (0.3–2.2)	1.3 (0.5–2.8)	0.88
NLR, median (range)	3.3 (0.6–26.0)	2.9 (0.6–26.0)	3.6 (1.0–17.6)	0.34
Monocytes, 10E9/L, median (range)	0.6 (0.2–1.8)	0.5 (0.2–1.8)	0.6 (0.3–1.0)	0.72
Platelets, 10E9/L, median (range)	272.0 (111.6–479.7)	265.0 (111.6–444.0)	276.9 (126.0–479.7)	0.82
PLR, median (range)	180.5 (61.5–900.0)	180.5 (61.5–900.0)	182.7 (66.8–622.4)	0.94
LMR, median (range)	2.1 (0.5–9.3)	2.1 (0.5–9.3)	2.2 (1.1–7.7)	0.81
ALB, g/L, median (range)	40.8 (23.0–49.5)	40.9 (26.4–49.5)	40.5 (23.0–48.1)	0.62
CHO, mmol/L, median (range)	4.4 (3.4–6.8)	4.8 (3.5–6.8)	4.0 (3.4–5.2)	0.45
TG, mmol/L, median (range)	1.2 (0.5–3.9)	1.1 (0.7–3.9)	1.4 (0.5–3.4)	0.79
HDL, mmol/L, median (range)	1.2 (0.5–5.1)	1.3 (0.6–5.1)	1.1 (0.5–1.7)	0.11
LDL, mmol/L, median (range)	2.8 (0.8–7.7)	2.8 (1.2–3.8)	2.4 (2.0–7.7)	0.63
ApoA1, g/L, median (range)	1.2 (0.3–1.7)	1.2 (0.7–1.7)	1.1 (0.3–1.5)	0.29
ApoB, g/L, median (range)	0.8 (0.4–1.5)	0.9 (0.4–1.5)	0.8 (0.4–1.2)	0.45

CR, complete response; PR, partial response; SD, stable disease; PD, progressive disease; CEA, carcinoembryonic antigen; CRP, C-reactive protein; LDH, lactate dehydrogenase; ALB, albumin; NLR, neutrophil-to-lymphocyte ratio; PLR, platelet-to-lymphocyte ratio; LMR, lymphocyte-to-monocyte ratio; CHO, cholesterol; TG, triglyceride; HDL, high-density lipoprotein; LDL, low-density lipoprotein; ApoA1, apolipoprotein A1; ApoB, apolipoprotein B.

[a]*p-Values were estimated by Fisher's exact test and Mann–Whitney U test for categorical variables and continuous variables, respectively.*

[b]*A total of 22 patients were tested with KRAS.*

[c]*A total of 22 patients were tested with BRAF.*

Flow Cytometry

We obtained the peripheral blood samples before patients received anti-PD-1 immunotherapy. The antibodies for staining were Ab anti-CD4 (APC-labeled CD4, clone SK3), anti-CD8 (PE-labeled CD8, clone SK1), anti-CD3 (FITC-labeled CD3, clone SK7), and anti-CD45 (PerCP-labeled CD45, clone 2D1 [HLe-1]). All the above Abs (BD Biosciences, San Jose, CA, USA) included isotype-matched negative controls. Well-mixed, anticoagulated whole blood measuring 100 µl was vortexed gently with 20 µl of abs and was incubated for 15 min in the dark at room temperature according to the procedure of BD Multitest™ CD3/CD8/CD45/CD4 kit (No. 340499, BD, USA). A total of 450 µl of 1× BD FACS lysing solution was then added and incubated for 15 min in the dark at room temperature. The stained cells were analyzed on a BD FACS Canto II flow cytometry system with FACS Diva software (BD Biosciences) (**Figure 2**).

Statistical Analysis

Tumor response was evaluated according to the Response Evaluation Criteria in Solid Tumors (RESICT), version 1.1. The disappearance of all target lesions was defined as complete response (CR). Baseline sum diameters were taken as reference according to the RESICT criteria. Partial response (PR) was defined as at least a 30% decrease in the sum of diameters of target lesions. Progressive disease (PD) was defined as at least a 20% increase in the sum of diameters of target lesions. In addition to the relative increase of 20%, the sum must also demonstrate an absolute increase of at least 5 mm. Neither sufficient shrinkage to qualify for PR nor sufficient increase to qualify for PD was defined as stable disease (SD). Progression-free survival (PFS) was defined as the duration from the date of immunotherapy initiation to clinical or radiographic progression or death. Overall survival (OS) was defined as the duration from the date of immunotherapy initiation to death. Fisher's exact test and Mann–Whitney U test were performed to compare distribution between groups based on response for categorical variables and continuous variables, respectively. Univariate Cox regression model was performed to estimate the hazard ratios (HRs) and 95% CIs of survival based on clinicopathologic parameters and peripheral blood indexes. The receiver operating characteristic (ROC) curve analysis was used to determine the cutoff point for the continuous variables including peripheral blood parameters. The Kaplan–Meier method was used to perform survival analysis, with p-values compared by the log-rank test. Only parameters with statistical significance in a univariate analysis were included in multivariable analysis. HRs and 95% CIs of survival were estimated by multivariate Cox regression models. A two-tailed p-value <0.05 was considered statistically significant. All statistical analyses were performed in R software (version 3.5.1; http://www.Rproject.org).

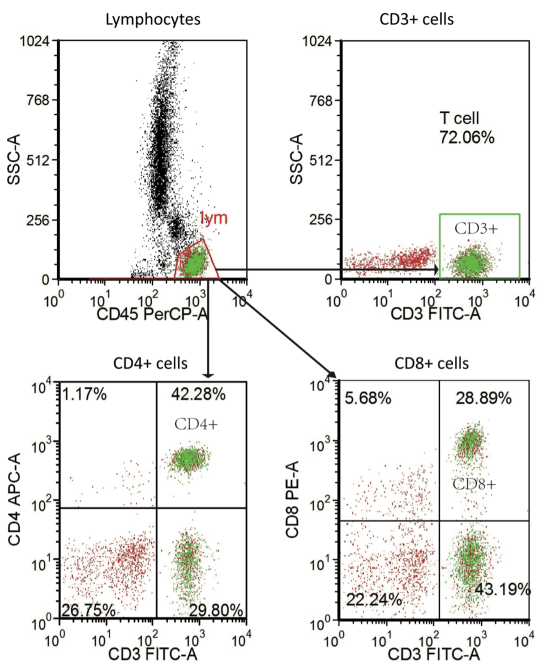

FIGURE 2 | Representative flow-cytometry gating strategy for quantifying the numbers of various immune cell subsets in PBMC. PBMC, peripheral blood mononuclear cell.

RESULTS

Patients Characteristics

A total of 41 mCRC patients with dMMR tumors were identified to be treated with PD-1 inhibitors. Clinical outcomes are depicted in **Table S1**. Overall, 4 patients achieved a CR, 19 patients achieved a PR, 10 patients achieved SD, and 8 patients achieved a PD, which led to an ORR of 56% (23/41). The details of the patients' clinicopathologic characteristics are shown in **Table 1**. The median age for the entire cohort was 41 years (range 20–77), and 54% of patients were male. KRAS mutations were observed in 73% (16/22) of patients, while BRAF mutations in 9% (2/22). A total of 30 patients (73%) had colon tumors. The median values of the frequency of CD4+ T cells, frequency of CD8+ T cell, and ratio of CD4+/CD8+ for the entire cohort were 37 (23–61), 27 (12–53), and 1.3 (0.5–4.6), respectively.

Association Between Biomarkers and Objective Response

Characteristics and OR were compared between responders (CR/PR) and non-responders (SD/PD). The frequency of CD4+ T cell and CEA as continuous variables were significantly associated with ORR (all the p-values <0.05, **Table 1**), while other investigated parameters were similar despite the significant association of a lower level for the ratio of CD4/CD8 T cells with ORR (p = 0.03). For mutation data, KRAS or BRAF mutations did not show any significant difference (**Table 1**).

Association Between Biomarkers and Survival

Among all tested parameters correlated with PFS, gender, age, tumor location, tumor grade, stage, and KRAS as well as BRAF status did not affect PFS or OS by using a Cox regression model

(**Tables 2**, **S2**). The frequency of CD4+ T cell, ratio of CD4+/CD8+, HDL, and ApoA1 were associated with PFS in a univariate Cox regression model (**Table 2**). The frequency of CD4+ T cell, ratio of CD4+/CD8+, NLR, HDL, and ApoA1 were associated with OS in a univariate Cox regression model (**Table S2**). With the use of ROC curves, the cutoff values of the above variables for PFS were identified (**Table 2** and **Figure 3**). The potential survival-related factors (HDL, ApoA1, and NLR) were not significantly associated with the frequency of CD4+ T cell or ratio of CD4+/CD8+ (**Table S3**). The frequency of CD4+ T cell and ratio of CD4+/CD8+ remained significant in a multivariate analysis for both PFS and OS (**Tables 3**, **S4**). The optimal predictive cut-points of CD4+/CD8+ ratio and frequency of CD4+ T cell were 1.64 and 39.5, respectively. For the group with a low level of CD4+/CD8+ ratio, 18 of 26 (69%) cases had an OR (CR+PR), while only 5 of 15 (33%) had an OR ($p = 0.03$) for the group with a higher value of CD4+/CD8+ ratio (**Table 1** and **Figure 4**). Log-rank analysis revealed that a lower level of CD4+/CD8+ ratio was associated with a better PFS ($p = 0.002$) and OS ($p = 0.007$) (**Figure 4**). In a multivariate analysis, the ratio of CD4+/CD8+ remained significant in predicting PFS ($p = 0.004$, HR = 9.23, 95% CI = 2.04–41.7) and OS ($p = 0.009$, HR = 15.22, 95% CI = 2.00–115.8) (**Tables 3**, **S3**). For the group with a lower level of the frequency of CD4+ T cell, 18 of 25 (72%) cases had an OR (CR+PR), while only 5 of 16 (31%) had an OR ($p = 0.01$) for the group with a higher value of the frequency of CD4+ T cell (**Table 1** and **Figure 5**). Log-rank analysis revealed that a lower level of the frequency of CD4+ T cell was associated with a better PFS ($p = 0.017$) and OS ($p = 0.0495$) (**Figure 5**). In a multivariate analysis, the frequency of CD4+ T cell remained significant in predicting PFS ($p = 0.02$, HR = 4.83, 95% CI = 1.28–18.27) and OS ($p = 0.025$, HR = 16.21, 95% CI = 1.43–184.2) (**Tables 3**, **S4**). Furthermore, NLR was significantly associated with OS in both univariate and multivariate analyses.

DISCUSSION

Anti-PD-1 immunotherapy is approved by the FDA for refractory dMMR CRC. In the present multicenter cohort study, the response rate for 41 patients with dMMR mCRC treated with anti-PD-1 inhibitors was analyzed, and the potential blood parameters were identified as predictive biomarkers for response. Although TMB has a potentially predictive value for anti-PD-1 therapy in MSI-H mCRC patients, the identification of peripheral blood biomarkers is crucial because the access of biomarkers from the blood is easier than that from tumor tissues. Considering the limited experience with anti-PD-1 therapy in patients with dMMR mCRC, the evidence of potential blood biomarkers for these patients was scarce. To the best of our knowledge, the present study with 41 patients with dMMR mCRC is the first multicenter study to show that the baseline level of the frequency of CD4+ T cell and the ratio of CD4+/CD8+ are independent potential biomarkers for ORR and survival in dMMR mCRC patients. Moreover, the present study indicated the potential prognostic value for NLR regarding OS.

TABLE 2 | Progression-free survival and associations with clinicopathologic features using Cox regression.

Clinicopathologic Parameters	HR	95% CI	p-Value
Age (years)			
Continuous	1.03	0.99–1.07	0.11
Gender			
Female versus male	1.74	0.51–6.0	0.38
Location			
Rectum versus colon	0.53	0.16–1.83	0.32
Grade			
High versus moderate/low	0.038	0.0–16.09	0.29
KRAS mutation			
Yes versus no	0.30	0.06–1.50	0.14
BRAF mutation			
Yes versus no	0.04	0.00–2,165.88	0.56
Frequency of CD4+ T cell[a] (%)			
Continuous	1.09	1.02–1.16	0.012
>39.5 versus ≤39.5	4.05	1.17–13.97	0.027
Frequency of CD8+ T cell[a] (%)			
Continuous	0.94	0.87–1.01	0.09
Ratio of CD4+/CD8+[a] (%)			
Continuous	1.81	1.08–3.01	0.023
>1.64 versus ≤1.64	5.99	1.58–22.70	0.008
CEA (ng/ml)			
Continuous	1.002	1.00–1.004	0.09
CRP (mg/L)			
Continuous	1.007	0.997–1.02	0.15
LDH (U/L)			
Continuous	1.002	0.999–1.004	0.26
Neutrophils[a] (10E9/L)			
Continuous	1.27	1.09–1.49	0.002
>4.35 versus ≤ 4.35	1.14	0.35–3.76	0.82
Lymphocytes (10E9/L)			
Continuous	0.77	0.25–2.35	0.65
NLR			
Continuous	1.09	0.99–1.19	0.07
Monocytes (10E9/L)			
Continuous	1.39	0.22–8.72	0.73
Platelets (10E9/L)			
Continuous	0.997	0.99–1.003	0.32
LMR			
Continuous	0.83	0.57–1.22	0.34
PLR			
Continuous	0.999	0.996–1.003	0.68
Alb (g/L)			
Continuous	0.92	0.84–1.01	0.09
CHO (mmol/L)			
Continuous	0.21	0.04–1.21	0.08
TG (mmol/L)			
Continuous	1.57	0.74–3.31	0.24
HDL[a] (mmol/L)			
Continuous	0.11	0.02–0.82	0.03
>0.875 versus ≤ 0.875	0.15	0.04–0.54	0.004
LDL (mmol/L)			
Continuous	1.84	1.11–3.05	0.07
ApoA1[a] (g/L)			
Continuous	0.03	0.002–0.40	0.008
>0.865 versus ≤ 0.865	0.14	0.04–0.50	0.003
ApoB (g/L)			
Continuous	0.39	0.02–7.31	0.53

HR, hazard ratio; CEA, carcinoembryonic antigen; CRP, C-reactive protein; LDH, lactate dehydrogenase; ALB, albumin; NLR, neutrophil-to-lymphocyte ratio; PLR, platelet-to-lymphocyte ratio; LMR, lymphocyte-to-monocyte ratio; CHO, cholesterol; TG, triglyceride; HDL, high-density lipoprotein; LDL, low-density lipoprotein; ApoA1, apolipoprotein A1; ApoB, apolipoprotein B.

[a]*Optimal cutoff points were estimated by receiver operating characteristic (ROC) curve analysis.*

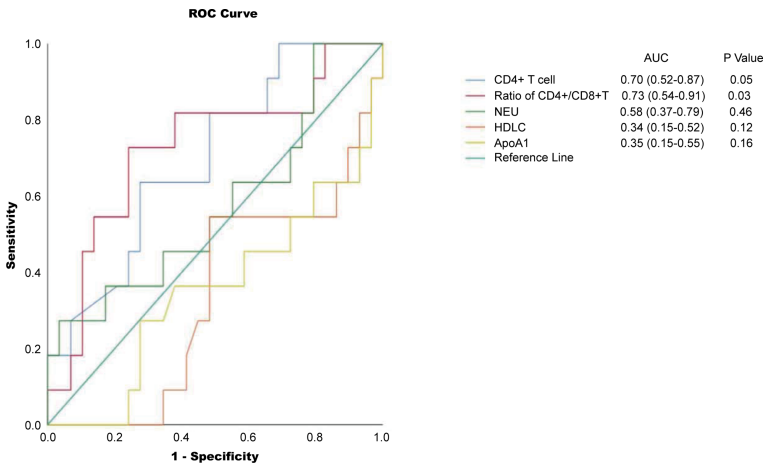

FIGURE 3 | ROC curves for the cutoff points for frequency of CD4+ T cell, ratio of CD4+/CD8+, NEU, HDL, and ApoA1. NEU, neutrophils; HDL, high-density lipoprotein; ApoA1, apolipoprotein A1; ROC, receiver operating characteristic.

TABLE 3 | Multivariate survival analysis after variable selection for progression-free survival.

Clinicopathologic Parameters[#]	HR	95% CI	p-Value	HR	95% CI	p-Value
HDL[a] (mmol/L)						
>0.875 versus ≤0.875	0.36	0.04–3.31	0.37	0.13	0.01–1.44	0.10
ApoA1 (g/L)						
>0.865 versus ≤0.865	0.28	0.03–2.67	0.27	0.56	0.06–5.26	0.61
Frequency of CD4+ T cell[a] (%)						
>39.5 versus ≤39.5	4.83	1.28–18.27	0.02			
Ratio of CD4+/CD8+[a] (%)						
>1.64 versus ≤1.64				9.23	2.04–41.69	0.004

HR, hazard ratio; HDL, high-density lipoprotein; ApoA1, apolipoprotein A1.
[#]Since frequency of CD4+ T cell was strongly correlated with ratio of CD4+/CD8+ with rho value of 0.73 ($p < 0.001$), these two parameters were separately included in the Cox model.
[a]Optimal cutoff points were estimated by receiver operating characteristic (ROC) curve analysis.

Previously, pretreatment counts of peripheral blood cells or LDH have been investigated as potential biomarkers for clinical outcomes in patients with melanoma (10, 11, 19) and NSCLC (13, 14, 20) treated with ICIs. Even though the present study showed that NLR could potentially predict OS, it failed to indicate the predictive value of NLR for ORR and PFS in anti-PD-1 therapy, which indicated that dMMR mCRC might be distinct with melanoma or NSCLC. As far as we know, this study enrolled 41 dMMR mCRC patients firstly to show that pretreatment frequency of CD4+ T cell and the ratio of CD4+/CD8+ are independent potential biomarkers for both ORR and survival. Our analysis thus showed that a low ratio of CD4 T cell (≤39.5) was significantly associated with a better ORR and PFS/OS in dMMR patients with mCRC. The potential mechanism may be that CD4+ lymphocytes are anergised rather than being stimulated, which therefore correlate with a poor prognosis (21). Moreover, the domain type of the frequency of CD4+ T cell in the peripheral blood may be regulatory T cells, which have been recently reported to inhibit the antitumor activity of cytotoxic frequency of CD4+ T cell and then negatively affect the response and survival of patients undergoing anti-PD-1 immunotherapy (22). Moreover, the ratio of CD4+/CD8+ is a predictor for ORR and survival. This may be explained not only by the potential pro-tumor activity of the regulatory frequency of CD4+ T cell but also by the antitumor of the frequency of CD8+ T cell. More frequency of CD8+ T cells in the blood represents systematic antitumor immune features, and they could migrate to the tumor site, lymph nodes, and distal sites to enhance antitumor ability (17, 23, 24), which was consistent with the findings from a recent study (12) to investigate the peripheral blood cells to predict response to anti-PD-1 immunotherapy in melanoma. They found that the frequency of CD8+ T cells in the peripheral blood responders was reduced as compared with that in the blood of non-responders, which also indicated the crucial role in response to anti-PD-1 therapy. Moreover, the NICHE trial indicated that increased the frequency of CD8+ T cell counts in CRC might reflect an underlying immune activation (4).

Although our data revealed that HDL and ApoA1 were significantly associated with PFS and OS in a univariate analysis, the significance of HDL and ApoA1 was not maintained in a multivariate analysis. ApoA1, a prominent protein component in HDL, not only has antiapoptotic, anti-inflammatory, and antioxidant functions (25) but also alters

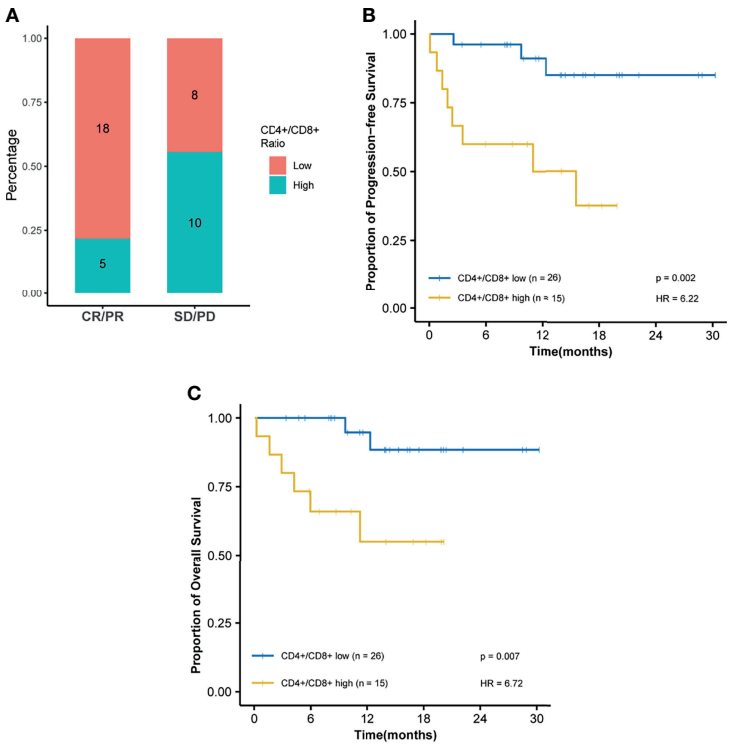

FIGURE 4 | The ratio of CD4+/CD8+ is predictive of response and survival outcome. Optimal cutoff point was calculated by receiver operating characteristic (ROC) curve analysis to dichotomize patients into high and low groups. **(A)** Ratio of CD4+/CD8+ distribution is visualized by a histogram between treatment response groups (CR, complete response; PR, partial response; SD, stable disease; PD, progressive disease). **(B)** Kaplan–Meier survival curves for progression-free survival. **(C)** Kaplan–Meier survival curves for overall survival.

tumor-associated macrophages (TAMs) from a pro-tumor M2 to an antitumor M1 phenotype (26) and modulates regulatory T cells (27). A recent study (18) also inferred that high ApoA1 correlated with higher TIL, which might be the reason for its potential positive impact on PFS.

The limitations of the present study include a relatively small sample size of patients and its retrospective nature. Another limitation lies in the absence of external validation of the associations detected in the present study, which need a further large-scale study to validate our findings. Since the present study has not performed the associations for other variables, especially TMB, which has been indicated to have a predictive value in dMMR cancers, future integrative analyses of circulating immune-based biomarkers with genomic and epigenetic biomarkers for clinical response or survival and prospective trials of MSI-H cancers are warranted to validate their predictive potential. In addition, the specific subtypes of peripheral leukocytes excluding CD4+ and CD8+ immune cells have not been analyzed, although these immune cells had different roles and prognoses in response to anti-PD-1 therapy. Thus, these findings require high content data-generating technologies to explore the potential mechanism for the circulating immune system and its correlation with the tumor immune microenvironment.

This is the first multicenter study to reveal that the frequency of CD4+ T cell and ratio of CD4+/CD8+ are biomarkers to predict the response to anti-PD-1 therapy and survival within a dMMR mCRC population. The finding indicates that patients with very low frequency of CD4+ T cell or low ratio of CD4+/CD8+ might respond well to PD-1 inhibitors, and this subset of patients might be further selected to receive first-line treatment with anti-PD-1 immunotherapy, which was consistent with the recent concept that anti-PD-1 immunotherapy is moved to first-line treatment for mCRC (28). These findings might provide a potential explanation for the variability in response to ant-PD-1 immunotherapy in numerous prospective clinical trials among dMMR mCRC patients and support the potential predictive role of the frequency of CD4+ T cell and ratio of CD4+/CD8+ in anti-PD-1 immunotherapy.

CONCLUSION

In summary, this multicenter cohort indicated that the ratio of CD4+/CD8+ and the frequency of CD4+ T cell might be crucial independent biomarkers within dMMR mCRC to better identify patients for anti-PD-1 immunotherapy. If validated in

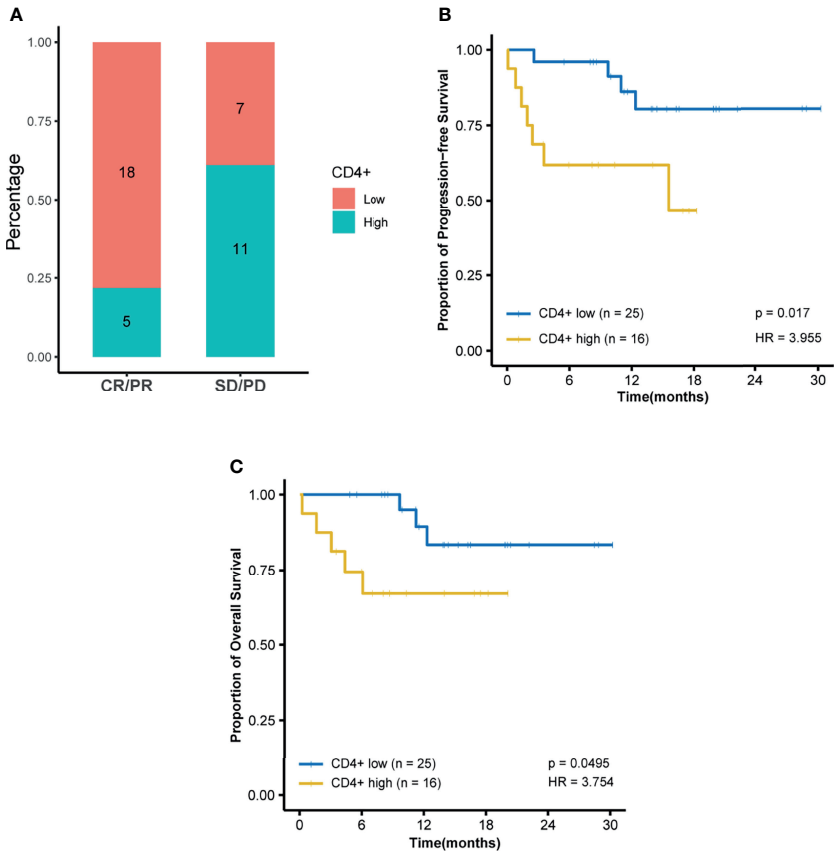

FIGURE 5 | Frequency of CD4+ T cell is predictive of response and survival outcome. Optimal cutoff point was calculated by receiver operating characteristic (ROC) curve analysis to dichotomize patients into high and low groups. **(A)** Frequency of CD4+ T-cell distribution is visualized by a histogram between treatment response groups (CR, complete response; PR, partial response; SD, stable disease; PD, progressive disease). **(B)** Kaplan–Meier survival curves for progression-free survival and **(C)** Kaplan–Meier survival curves for overall survival.

prospective clinical trials, the ratio of CD4+/CD8+ and the frequency of CD4+ T cell might aid in guiding the treatment of PD-1 inhibitors among patients with dMMR mCRC.

DATA AVAILABILITY STATEMENT

The raw data supporting the conclusions of this article will be made available by the authors, without undue reservation.

ETHICS STATEMENT

The studies involving human participants were reviewed and approved by the Medical Ethics Committee of the Sixth Affiliated Hospital of Sun Yat-sen University, Guangzhou, China (no. 2020ZSLYEC-216). The patients/participants provided their written informed consent to participate in this study. Written informed consent was obtained from the individual(s) for the publication of any potentially identifiable images or data included in this article.

AUTHOR CONTRIBUTIONS

Conception and design: PL, S-BY, and Y-KC. Financial support: PL, Y-KC, and S-BY. Provision of study materials or patients: PL and Y-KC. Collection and assembly of data: D-WC and PC. Data analysis and interpretation: S-BY, Y-KC, and D-WC. Manuscript writing: All authors. Final approval of manuscript: All authors.

FUNDING

This study was supported by Key-Area Research and Development Program of Guangdong Province (2019B020229002), Science and Technology Planning Project of Guangzhou (No. 201902020009), the National Natural Science Foundation of China (Grant No. 81801111), and National Key Clinical Discipline, The National Key Research and Development Program of China (2017YFC1308800).

ACKNOWLEDGMENTS

We thank all staff members of the Department of Colorectal Surgery at the Sixth Affiliated Hospital of Sun Yat-sen University and the Sun Yat-sen University Cancer Center.

SUPPLEMENTARY MATERIAL

The Supplementary Material for this article can be found online at: https://www.frontiersin.org/articles/10.3389/fimmu.2022.809971/full#supplementary-material

REFERENCES

1. Siegel RL, Miller KD, Fedewa SA, Ahnen DJ, Meester RGS, Barzi A, et al. Colorectal Cancer Statistics, 2017. *CA Cancer J Clin* (2017) 67:177–93. doi: 10.3322/caac.21395
2. Siegel RL, Miller KD, Jemal A. Cancer Statistics, 2017. *CA Cancer J Clin* (2017) 67:7–30. doi: 10.3322/caac.21387
3. Le DT, Uram JN, Wang H, Bartlett BR, Kemberling H, Eyring AD, et al. PD-1 Blockade in Tumors With Mismatch-Repair Deficiency. *N Engl J Med* (2015) 372:2509–20. doi: 10.1056/NEJMoa1500596
4. Chalabi M, Fanchi LF, Dijkstra KK, Van den Berg JG, Aalbers AG, Sikorska K, et al. Neoadjuvant Immunotherapy Leads to Pathological Responses in MMR-Proficient and MMR-Deficient Early-Stage Colon Cancers. *Nat Med* (2020) 26:566–76. doi: 10.1038/s41591-020-0805-8
5. Le DT, Durham JN, Smith KN, Wang H, Bartlett BR, Aulakh LK, et al. Mismatch Repair Deficiency Predicts Response of Solid Tumors to PD-1 Blockade. *Science* (2017) 357:409–13. doi: 10.1126/science.aan6733
6. Overman MJ, McDermott R, Leach JL, Lonardi S, Lenz HJ, Morse MA, et al. Nivolumab in Patients With Metastatic DNA Mismatch Repair-Deficient or Microsatellite Instability-High Colorectal Cancer (CheckMate 142): An Open-Label, Multicentre, Phase 2 Study. *Lancet Oncol* (2017) 18:1182–91. doi: 10.1016/S1470-2045(17)30422-9
7. Schrock AB, Ouyang C, Sandhu J, Sokol E, Jin D, Ross JS, et al. Tumor Mutational Burden is Predictive of Response to Immune Checkpoint Inhibitors in MSI-High Metastatic Colorectal Cancer. *Ann Oncol* (2019) 30:1096–103. doi: 10.1093/annonc/mdz134
8. Mlecnik B, Bindea G, Angell HK, Maby P, Angelova M, Tougeron D, et al. Integrative Analyses of Colorectal Cancer Show Immunoscore Is a Stronger Predictor of Patient Survival Than Microsatellite Instability. *Immunity* (2016) 44:698–711. doi: 10.1016/j.immuni.2016.02.025
9. Pages F, Mlecnik B, Marliot F, Bindea G, Ou FS, Bifulco C, et al. International Validation of the Consensus Immunoscore for the Classification of Colon Cancer: A Prognostic and Accuracy Study. *Lancet* (2018) 391:2128–39. doi: 10.1016/S0140-6736(18)30789-X
10. Ferrucci PF, Gandini S, Battaglia A, Alfieri S, Di Giacomo AM, Giannarelli D, et al. Baseline Neutrophil-to-Lymphocyte Ratio Is Associated With Outcome of Ipilimumab-Treated Metastatic Melanoma Patients. *Br J Cancer* (2015) 112:1904–10. doi: 10.1038/bjc.2015.180
11. Ferrucci PF, Ascierto PA, Pigozzo J, Del Vecchio M, Maio M, Antonini Cappellini GC, et al. Baseline Neutrophils and Derived Neutrophil-to-Lymphocyte Ratio: Prognostic Relevance in Metastatic Melanoma Patients Receiving Ipilimumab. *Ann Oncol* (2016) 27:732–8. doi: 10.1093/annonc/mdw016
12. Krieg C, Nowicka M, Guglietta S, Schindler S, Hartmann FJ, Weber LM, et al. High-Dimensional Single-Cell Analysis Predicts Response to Anti-PD-1 Immunotherapy. *Nat Med* (2018) 24:144–53. doi: 10.1038/nm.4466
13. Soyano AE, Dholaria B, Marin-Acevedo JA, Diehl N, Hodge D, Luo Y, et al. Peripheral Blood Biomarkers Correlate With Outcomes in Advanced Non-Small Cell Lung Cancer Patients Treated With Anti-PD-1 Antibodies. *J Immunother Cancer* (2018) 6:129. doi: 10.1186/s40425-018-0447-2
14. Tanizaki J, Haratani K, Hayashi H, Chiba Y, Nakamura Y, Yonesaka K, et al. Peripheral Blood Biomarkers Associated With Clinical Outcome in Non-Small Cell Lung Cancer Patients Treated With Nivolumab. *J Thorac Oncol* (2018) 13:97–105. doi: 10.1016/j.jtho.2017.10.030
15. Nixon AB, Schalper KA, Jacobs I, Potluri S, Wang IM, Fleener C. Peripheral Immune-Based Biomarkers in Cancer Immunotherapy: Can We Realize Their Predictive Potential? *J Immunother Cancer* (2019) 7(1):325. doi: 10.1186/s40425-019-0799-2
16. Jiang L, Xiao L, Sugiura H, Huang X, Ali A, Kuro-o M, et al. Metabolic Reprogramming During TGFbeta1-Induced Epithelial-to-Mesenchymal Transition. *Oncogene* (2015) 34:3908–16. doi: 10.1038/onc.2014.321
17. Fisher KE, Pop A, Koh W, Anthis NJ, Saunders WB, Davis GE. Tumor Cell Invasion of Collagen Matrices Requires Coordinate Lipid Agonist-Induced G-Protein and Membrane-Type Matrix Metalloproteinase-1-Dependent Signaling. *Mol Cancer* (2006) 5:69. doi: 10.1186/1476-4598-5-69
18. Guo G, Wang Y, Zhou Y, Quan Q, Zhang Y, Wang H, et al. Immune Cell Concentrations Among the Primary Tumor Microenvironment in Colorectal Cancer Patients Predicted by Clinicopathologic Characteristics and Blood Indexes. *J Immunother Cancer* (2019) 7:179. doi: 10.1186/s40425-019-0656-3
19. Weide B, Martens A, Hassel JC, Berking C, Postow MA, Bisschop K, et al. Baseline Biomarkers for Outcome of Melanoma Patients Treated With Pembrolizumab. *Clin Cancer Res* (2016) 22:5487–96. doi: 10.1158/1078-0432.CCR-16-0127
20. Bagley SJ, Kothari S, Aggarwal C, Bauml JM, Alley EW, Evans TL, et al. Pretreatment Neutrophil-to-Lymphocyte Ratio as a Marker of Outcomes in Nivolumab-Treated Patients With Advanced Non-Small-Cell Lung Cancer. *Lung Cancer* (2017) 106:1–7. doi: 10.1016/j.lungcan.2017.01.013
21. Diederichsen AC, Hjelmborg J, Christensen PB, Zeuthen J, Fenger C. Prognostic Value of the CD4+/CD8+ Ratio of Tumour Infiltrating Lymphocytes in Colorectal Cancer and HLA-DR Expression on Tumour Cells. *Cancer Immunol Immunother* (2003) 52:423–8. doi: 10.1007/s00262-003-0388-5
22. Oh DY, Kwek SS, Raju SS, Li T, McCarthy E, Chow E, et al. Intratumoral CD4 (+) T Cells Mediate Anti-Tumor Cytotoxicity in Human Bladder Cancer. *Cell* (2020) 181:1612–1625 e1613. doi: 10.1016/j.cell.2020.05.017
23. Herbst RS, Soria JC, Kowanetz M, Fine GD, Hamid O, Gordon MS, et al. Predictive Correlates of Response to the Anti-PD-L1 Antibody MPDL3280A in Cancer Patients. *Nature* (2014) 515:563–7. doi: 10.1038/nature14011
24. Kluger HM, Zito CR, Barr ML, Baine MK, Chiang VL, Sznol M, et al. Characterization of PD-L1 Expression and Associated T-Cell Infiltrates in Metastatic Melanoma Samples From Variable Anatomic Sites. *Clin Cancer Res* (2015) 21:3052–60. doi: 10.1158/1078-0432.CCR-14-3073
25. Besler C, Luscher TF, Landmesser U. Molecular Mechanisms of Vascular Effects of High-Density Lipoprotein: Alterations in Cardiovascular Disease. *EMBO Mol Med* (2012) 4:251–68. doi: 10.1002/emmm.201200224
26. Zamanian-Daryoush M, Lindner D, Tallant TC, Wang Z, Buffa J, Klipfell E, et al. The Cardioprotective Protein Apolipoprotein A1 Promotes Potent Anti-Tumorigenic Effects. *J Biol Chem* (2013) 288:21237–52. doi: 10.1074/jbc.M113.468967
27. Wilhelm AJ, Zabalawi M, Owen JS, Shah D, Grayson JM, Major AS, et al. Apolipoprotein A-I Modulates Regulatory T Cells in Autoimmune LDLr-/-, ApoA-I-/- Mice. *J Biol Chem* (2010) 285:36158–69. doi: 10.1074/jbc.M110.134130
28. Andre T, Amonkar M, Norquist JM, Shiu KK, Kim TW, Jensen BV, et al. Health-Related Quality of Life in Patients With Microsatellite Instability-High or Mismatch Repair Deficient Metastatic Colorectal Cancer Treated With First-Line Pembrolizumab Versus Chemotherapy (KEYNOTE-177): An Open-Label, Randomised, Phase 3 Trial. *Lancet Oncol* (2021) 22(5):665–77. doi: 10.1016/S1470-2045(21)00064-4

Conflict of Interest: The authors declare that the research was conducted in the absence of any commercial or financial relationships that could be construed as a potential conflict of interest.

Publisher's Note: All claims expressed in this article are solely those of the authors and do not necessarily represent those of their affiliated organizations, or those of the publisher, the editors and the reviewers. Any product that may be evaluated in

this article, or claim that may be made by its manufacturer, is not guaranteed or endorsed by the publisher.

frontiers in Immunology

ORIGINAL RESEARCH
published: 24 February 2022
doi: 10.3389/fimmu.2022.839901

An Immune-Related Gene Pair Index Predicts Clinical Response and Survival Outcome of Immune Checkpoint Inhibitors in Melanoma

Junya Yan[1†], Xiaowen Wu[2†], Jiayi Yu[3], Yan Kong[2] and Shundong Cang[1*]*

[1] Department of Oncology, Henan Provincial People's Hospital, Zhengzhou University People's Hospital, Henan University People's Hospital, Zhengzhou, China, [2] Key Laboratory of Carcinogenesis and Translational Research (Ministry of Education/Beijing), Department of Melanoma and Sarcoma, Peking University Cancer Hospital & Institute, Beijing, China, [3] Key Laboratory of Carcinogenesis and Translational Research (Ministry of Education/Beijing), Department of Radiation Oncology, Peking University Cancer Hospital & Institute, Beijing, China

OPEN ACCESS

Edited by:
Alison Taylor,
University of Leeds, United Kingdom

Reviewed by:
Fiona Simpson,
The University of Queensland, Australia
Dmitrii Shek,
Western Sydney Local Health District, Australia
Deepanwita Sengupta,
Stanford University, United States

***Correspondence:**
Yan Kong
k-yan08@163.com
Shundong Cang
cangshundong@163.com

[†]These authors have contributed equally to this work

Specialty section:
This article was submitted to Cancer Immunity and Immunotherapy, a section of the journal Frontiers in Immunology

Received: 20 December 2021
Accepted: 04 February 2022
Published: 24 February 2022

Citation:
Yan J, Wu X, Yu J, Kong Y and Cang S (2022) An Immune-Related Gene Pair Index Predicts Clinical Response and Survival Outcome of Immune Checkpoint Inhibitors in Melanoma. Front. Immunol. 13:839901. doi: 10.3389/fimmu.2022.839901

The durable responses and favorable long-term outcomes are limited to a proportion of advanced melanoma patients treated with immune checkpoint inhibitors (ICI). Considering the critical role of antitumor immunity status in the regulation of ICI therapy responsiveness, we focused on the immune-related gene profiles and aimed to develop an individualized immune signature for predicting the benefit of ICI therapy. During the discovery phase, we integrated three published datasets of metastatic melanoma treated with anti-PD-1 (n = 120) and established an immune-related gene pair index (IRGPI) for patient classification. The IRGPI was constructed based on 31 immune-related gene pairs (IRGPs) consisting of 51 immune-related genes (IRGs). The ROC curve analysis was performed to evaluate the predictive accuracy of IRGPI with AUC = 0.854. Then, we retrospectively collected one anti-PD-1 therapy dataset of metastatic melanoma (n = 55) from Peking University Cancer Hospital (PUCH) and performed the whole-transcriptome RNA sequencing. Combined with another published dataset of metastatic melanoma received anti-CTLA-4 (VanAllen15; n = 42), we further validated the prediction accuracy of IRGPI for ICI therapy in two datasets (PUCH and VanAllen15) with AUCs of 0.737 and 0.767, respectively. Notably, the survival analyses revealed that higher IRGPI conferred poor survival outcomes in both the discovery and validation datasets. Moreover, correlation analyses of IRGPI with the immune cell infiltration and biological functions indicated that IRGPI may be an indicator of the immune status of the tumor microenvironment (TME). These findings demonstrated that IRGPI might serve as a novel marker for treating of melanoma with ICI, which needs to be validated in prospective clinical trials.

Keywords: immune-related gene pair index (IRGPI), immune checkpoint inhibitor (ICI), melanoma, prediction, immune infiltration

INTRODUCTION

Malignant melanoma is an aggressive malignant tumor with a poor clinical prognosis, the incidence of which is increasing globally (1–3). With the development of immunotherapy, immune checkpoint inhibitors (ICI) therapy has been approved as the standard treatment for melanoma (4–8). According to the reports from multiple clinical trials (9–12), the overall response rate (ORR) of PD-1 blockade with nivolumab or pembrolizumab ranged from 26% to 44%, thus indicating almost 50% of patients with severely progressed melanoma do not obtain complete or partial response, with roughly 24% reach a stable disease only. Notably, as the main subtypes of Asian patients with melanoma, only 10~20% of acral and mucosal cases can benefit from ICI therapy (13–15). Therefore, development of novel biomarkers in the hope of better prediction of the response to ICI therapy are urgently required.

Several biomarkers have been developed for predicting the benefit of ICI therapy for melanoma patients, including PD-L1 expression (16), tumor mutation burden (TMB) (17), interferon-γ signal (18, 19), and tumor infiltrating lymphocytes (TILs) (20). However, the immunohistochemistry analysis of PD-L1 varies significantly among different antibodies (21), thereby making it difficult to define the positive threshold of PD-L1 expression. In addition, the whole-genome sequences from 183 melanoma samples revealed that the burden of mutations is more frequent in cutaneous compared with acral and mucosal melanoma (22). Thus, the widespread detection value of TMB in acral and mucosal subtypes are limited.

The past decade has witnessed rapid progress in tumor genomics. Some studies utilized RNA sequencing data to establish immune-related gene signatures for the evaluation of immune response and prognosis in melanoma (23, 24). Unfortunately, none has been confirmed to be translated into clinical application owing to the small size of discovery data and lack of sufficient validation (25). Nowadays, a series of immunotherapy data regarding PD-1/PD-L1 or CTLA-4 blockade in melanoma patients have been reported all over the world. Integrated analyses may provide a complete picture of ICI therapy in different populations and summarize more superior predictive biomarkers. However, the information of gene expression profiling (GEP) was measured using different sequence platforms, which is not applied to normalizing gene expression levels through traditional approaches (26). Furthermore, the potential biological heterogeneity across datasets was also a challenge. Recently one method based on the construction of immune-related gene pairs (IRGPs) from GEP can be an excellent choice, which calculates the relative ranking of gene expression levels without the requirement for data preprocessing and has been demonstrated to establish robust models for the application of cancer classification (27–29). Hence, it is imperative to identify novel biomarkers based on IRGPs for guiding ICI therapy.

In this study, we integrated three published datasets of metastatic melanoma treated with anti-PD-1 (n = 120) and constructed an immune-related gene pair index (IRGPI). The IRGPI was constructed based on 31 immune-related gene pairs (IRGPs) consisting of 51 immune-related genes (IRGs), which may be a promising biomarker for predicting the response of ICI therapy and survival outcomes in melanoma patients. The predictive performance of IRGPI was also validated in Peking University Cancer Hospital (PUCH, n = 55) and VanAllen15 (n = 42) datasets treated with PD-1 or CTLA-4 blockade. Furthermore, the analyses of the TME, the immune cell infiltration, and biological functions of different IRGPI groups were also performed, which demonstrated that IRGPI may be an indicator of the immune status of the TME.

Abbreviations: AUC, Area Under Curve; CR, complete response; ESTIMATE, Estimation of STromal and Immune cells in MAlignant Tumor tissues using Expression data; FDR, false discovery rate; GEP, gene expression profiling; CI, confidence interval; GSEA, gene set enrichment analysis; HLA, human leukocyte antigen; HR, hazard ratio; ICI, immune checkpoint inhibitors; IRGs, immune-related genes; IRGPs, immune-related gene pairs; IRGPI, immune-related gene pair index; ORR, overall response rate; OS, overall survival; PD, progressive disease; PFS, progression-free survival; PUCH, Peking University Cancer Hospital; PR, partial response; RECIST, Response Evaluation Criteria in Solid Tumors; ROC, receiver operating characteristic SD, stable disease; TCGA, The Cancer Genome Atlas; TILs, tumor infiltrating lymphocytes; TME, tumor microenvironment; TMB, tumor mutation burden; Tregs, regulatory T cells.

MATERIALS AND METHODS

Patients and GEP

From March 2016 to March 2019, 55 melanoma patients treated with anti-PD-1 therapy were recruited for this study from PUCH. Formalin-fixed, paraffin-embedded pretreatment tumor samples were obtained from all patients. We separated all the clinical and pathological data by medical record review, including sex, age, primary site, metastasis status, and clinical efficacy. Tumor responses were evaluated using the Response Evaluation Criteria in Solid Tumors (RECIST) version 1.1, including complete response (CR), partial response (PR), stable disease (SD), and progressive disease (PD). CR and PR were regarded as responders, while PD and SD were regarded as non-responders. In this study, overall survival (OS) and progression-free survival (PFS) were used as the primary and secondary survival endpoints, respectively. Gene expression data for the PUCH cohort was based on the Illumina NovaSeq 6000 platform. The details of processing the GEP of the PUCH cohort have been described in our previous study (30). This study was conducted according to the Declaration of Helsinki Principles and approved by the Medical Ethics Committee of PUCH. Informed consent for the use of material in medical research was obtained from all participants.

External Data Acquisition

We obtained RNA-seq and clinical data from four publicly available cohorts of melanoma patients treated with anti-PD-1 or anti-CTLA-4 therapy, including Gide19 (n = 41) (31), Hugo16 (n = 28) (32), Riaz17 (n = 51) (33), and VanAllen15 (n = 42) (34). Data of Gide19 cohort (PRJEB23709) were downloaded from the

European Nucleotide Archive database (ENA; https://www.ebi.ac.uk/ena). Data of Hugo16 cohort (GSE91061) and Riaz17 cohort (GSE78220) were downloaded from the Gene Expression Omnibus database (GEO; https://www.ncbi.nlm.nih.gov/geo/). Data of VanAllen15 cohort (phs000452.v2.p1) were downloaded from the database of Genotypes and Phenotypes (dbGap; http://www.ncbi.nlm.nih.gov/gap). The treatment response to immunotherapy consisted of CR/PR/SD/PD according to RECIST 1.1 guidelines, which were used in our analysis.

Moreover, we downloaded the RNA-sequencing data of all available cutaneous melanoma samples from The Cancer Genome Atlas (TCGA) database through the GDC tool (http://portal.gdc.cancer.gov/). The survival data of these patients were extracted from cbioPortal (http://www.cbioportal.org). Patients with OS less than one month were excluded from our analysis. In addition, we separated the TMB data of melanoma patients in the TCGA-SKCM cohort from The Cancer Immunome Atlas (http://tcia.at/home) (35).

Construction of the IRGPI

We constructed a predictive signature based on IRGs gathered from the ImmPort Web portal (https://www.immport.org/home) (36). Two IRGs constituted one IRGP and formed as "IRG-A|IRG-B". The score of IRGPI was generated through pairwise comparison of gene expression levels in specific samples. When the expression level of IRG-A was higher than IRG-B, the IRGP was assigned a score of 1; otherwise, the IRGP score was 0. IRGPs with score of 0 or 1 in over 80% of the specimens were regarded as IRGPs with constant values, which does not contribute to the difference of patient survival (37). Therefore, we excluded these IRGPs with constant values from our analysis.

The Gide19, Hugo16, and Riaz17 cohorts merged into the meta cohort, which was used for the construction of IRGPI. Firstly, we used the log-rank test to investigate the correlation of each IRGP to patients' OS in the meta cohort. According to the analysis results, IRGPs with a false discovery rate (FDR) < 0.001 were candidates to build the IRGPI. Then, the multivariate Cox regression analyses were performed to obtain the hub IRGPs and the respective coefficients. Finally, the IRGPI formula was defined as follows:

$$\mathbf{IRGPI}=\sum_{i=1}^{n}\mathbf{score\ of\ IRGP}_i * \mathbf{coeffecient}_i$$

Validation of the IRGPI

The predictive and prognostic values of IRGPI for immunotherapy were validated in PUCH and VanAllen15 cohorts. Based on the treatment response to immunotherapy, we conducted the receiver operating characteristic (ROC) curve analysis to estimate the prediction accuracy of IRGPI. Using the cut-off value that generated the maximum Youden index (38), the patients were divided into IRGPI-high and IRGPI-low groups. Then, the log-rank tests were conducted for comparison of the survival outcomes between two IRGPI groups.

Tumor Immune Microenvironment Analysis

The transcriptomic data of TCGA-SKCM (skin cutaneous melanoma) cohort were used for analyzing the association of IRGPI with immune-related features. Using the IRGPI formula, we calculated the IRGPI score of each patient in the TCGA-SKCM cohort. The cut-off value for the IRGPI was determined on the basis of the association with patients' OS by using X-tile software (version 3.6.1) (39). Based on two bioinformatic analyses of GEP data in the TCGA-SKCM cohort, we calculated the enrichment of immune cells between two IRGPI groups. Briefly, we used Estimation of STromal and Immune cells in MAlignant Tumor tissues using Expression data (ESTIMATE) method to calculate the immune score and ESTIMATE score of patients (40). CIBERSORT was further used to distinguish 22 immune cells, such as T cell types, B cell types, NK cells, and myeloid cell types (41). In the signaling analysis, we conducted gene set enrichment analysis (GSEA) to distinguish which immune-related pathways were markedly different between IRGPI-high and IRGPI-low groups.

To further characterize the tumor immune microenvironment between two IRGPI groups, we performed single simple GSEA on some previously published immune-related signatures (19, 42–45) and compared the score between IRGPI-high and IRGPI-low groups.

Statistical Analysis

All statistical analyses were performed using the R software (version 3.6.3) and Prism 8. Survival analyses were performed using the R packages "survival" and "survminer". The signature of IRGPs was obtained using the R package "glmnet". Univariate and multivariate Cox regression analyses were conducted using the R package "survival". ROC curve analyses were performed using the R package "survivalROC". ESTIMATE analysis was conducted using the R package "estimate". CIBERSORT analysis was processed using the R packages "e1701", "preprocessCore", and "limma". All statistical analyses were two-sided, and $P < 0.05$ was considered as statistically significant.

RESULTS

Patients Characteristics

The flowchart of this study design is presented in **Figure 1**. A total of 217 patients treated with ICI from five cohorts were included in this study. We constructed the IRGPI based on the meta cohort (n = 120), which consisted Gide19 (n = 41), Hugo16 (n = 28), and Riaz17 (n = 51) cohorts. The PUCH (n = 55) and VanAllen15 (n = 42) cohorts were used for validation the prediction model. The clinicopathological characteristics are summarized in **Table 1**. The median follow-up is 13.1~32.7 months in five cohorts. Notably, 43.6% of patients in PUCH cohort were acral melanomas, which have been reported to be the main subtype of melanoma in Asians. However, the vast majority of patients in other cohorts were cutaneous melanoma.

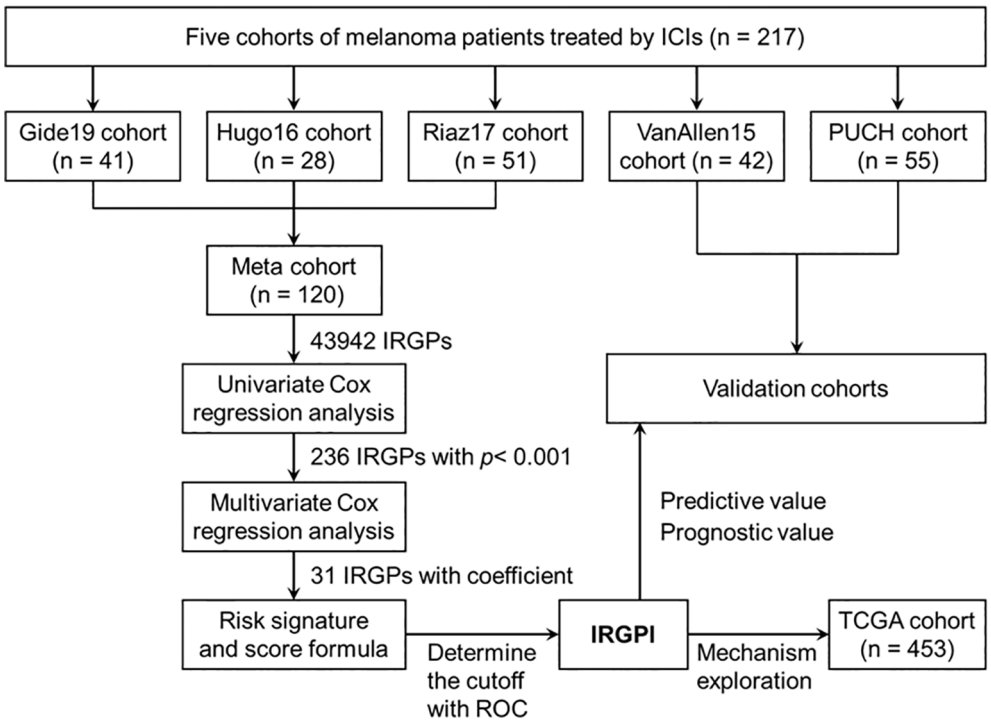

FIGURE 1 | The flowchart showing the scheme of this study.

Construction and Definition of the IRGPI

Among the 2487 IRGs from the ImmPort database, 1138 IRGs commonly occurred in the GEP of five cohorts and 1295044 IRGPs were calculated. We excluded 1251102 IRGPs (96.6%) with constant values in any cohort and 43942 IRGPs remained for subsequent construction of the IRGPI (**Table S1**). According to the univariate Cox regression analyses of the correlation between each IRGP and patients' OS in the meta cohort, 236 IRGPs with adjusted $P < 0.001$ were selected as prognostic IRGPs (**Table S2**). Then, we performed the multivariate Cox regression analyses to filtrate IRGPs to construct the IRGPI. Finally, 31 IRGPs were filtrated to define the IRGPI (**Table 2** and **Figure S1A**). The IRGPI consisted of 51 unique IRGs, most of which encoded molecules involved in antimicrobials, cytokines, and cytokine receptors.

Evaluation of the Prediction Accuracy of IRGPI for the Efficacy of ICI Therapy

Based on the IRGPI formula, we calculated each patient's IRGPI score in the meta cohort and exhibited the result in a heatmap (**Figure 2A**). We conducted ROC curve analysis to evaluate the prediction accuracy of IRGPI for the efficacy of ICI therapy in the meta cohort. With a cut-off value based on the Youden index of -1.221, we found that IRGPI-low group patients were correctly classified as CR/PR with a sensitivity of 71.7% (38/53). Further, IRGPI-high group patients were successfully classified as SD/PD with a specificity of 91.0% (61/67). The overall accuracy of IRGPI was 82.5% (99/120) with AUC of 0.854 (**Figure 2B**). IRGPI-low group showed a higher ORR than IRGPI-high group (71.7% vs. 9.0%; **Figures 2C, E**). Moreover, we evaluated the relationship between the IRGPI score and OS/PFS in the meta cohort. Kaplan-Meier survival analysis revealed that IRGPI-low group patients had significantly longer OS ($P < 0.001$; **Figure 2D**). The median PFS for IRGPI-high group patients was markedly shorter than IRGPI-low group patients in the Gide19 cohort ($P < 0.001$; **Figure S2A**). The pooled hazard ratio (HR) along with 95% confidence interval (CI) for the association between high IRGPI score and OS in 119 cases of patients was 8.02 (3.91~15.19), and no significant heterogeneity among the three datasets was observed ($I^2 = 0\%$, $P = 0.98$, **Figure S1B**). Overall, the IRGPI showed a superior prediction for the benefit of ICI therapy in the meta cohort.

Validation of the Robustness of IRGPI in Predicting the Efficacy of ICI Therapy

To verify the robustness of IRGPI in predicting the efficacy of ICI therapy, we assessed the correlation of IRGPI score with overall response rate and survival outcomes in VanAllen15 and PUCH cohorts. In the VanAllen15 cohort, the IRGPI successfully identified 31 of 42 patients with an overall accuracy of 73.8% and an AUC of 0.767 (**Figure 3A**). Similarly, in the PUCH cohort, the IRGPI demonstrated an overall accuracy of 72.7% (40/55) and AUC of 0.737 (**Figure 3B**). The ORR of IRGPI-high group was lower than IRGPI-low group in VanAllen15 cohort (64.3% vs. 7.1%;

TABLE 1 | Clinicopathological characteristics of five immunotherapy cohorts included in this study.

Patient characteristics	Training cohorts			Validation cohorts	
	Gide19	Hugo16	Riaz17	VanAllen15	PUCH
No. of patients	41	28	51	42	55
Median age in yrs (range)	66 (37-90)	61 (19-84)	–	61 (22-83)	51 (27-72)
Sex, n (%)					
Male	26 (63.4)	20 (71.4)	–	28 (66.7)	17 (30.9)
Female	15 (36.6)	8 (28.6)	–	14 (33.3)	38 (69.1)
Primary site, n (%)					
Acral	–	–	1 (2.0)	–	24 (43.6)
Mucosal	–	3 (10.7)	7 (13.7)	2 (4.8)	8 (14.5)
Cutaneous	–	21 (75.0)	32 (62.7)	37 (88.1)	18 (32.7)
Ocular		–	4 (7.9)	3 (7.1)	–
Unknown	–	4 (14.3)	7 (13.7)	–	5 (9.1)
Metastasis status, n (%)					
M0	–	1 (3.6)	1 (1.9)	1 (2.4)	10 (18.2)
M1a	–	2 (7.1)	11 (21.6)	3 (7.1)	16 (29.1)
M1b	–	3 (10.7)	8 (15.7)	7 (16.7)	18 (32.7)
M1c	–	22 (78.6)	23 (45.1)	31 (73.8)	11 (20.0)
Unknown	–	–	8 (15.7)	–	–
BRAF V600, n (%)	–	12 (42.9)	14 (27.4)	–	–
Prior MAPKi, n (%)	–	12 (42.9)	–	4 (9.5)	–
Treatment, n (%)					
Anti-PD-1	41 (100)	28 (100)	51 (100)	–	55 (100)
Anti-CTLA-4	–	–	–	42 (100)	
Best overall response, n (%)					
CR	4 (9.8)	5 (17.9)	3 (5.9)	–	1 (1.8)
PR	15 (36.6)	10 (35.7)	7 (13.7)	–	13 (23.6)
CR/PR	–	–		19 (45.2)	
SD	6 (14.6)	–	16 (31.4)	–	6 (10.9)
PD	16 (39.0)	13 (46.4)	25 (49.0)	23 (54.8)	35 (63.6)
Median PFS (months)	9.0	–	–	2.8	3.9
Median OS (months)	29.3	32.7	21.1	13.1	28.1

MAPKi, MAPK pathway inhibitors; Anti-PD-1, anti-programmed death-1; Anti-CTLA-4, anti-cytotoxic T lymphocyte antigen-4; CR, complete response; PR, partial response; SD, stable disease; PD, progressive disease; PFS, progression-free survival; OS, overall survival.

Figures 3C and **S3A**) and PUCH cohort (47.4% vs. 13.9%; **Figures 3D** and **S3B**), respectively. As expected, higher IRGPI conferred poor survival outcomes in VanAllen15 cohort (OS: $P < 0.001$, PFS: $P < 0.001$; **Figures 3E** and **S2B**) and PUCH cohort (OS: $P = 0.004$, PFS: $P = 0.015$; **Figures 3F** and **S2C**), respectively. These results confirmed that the IRGPI is reliable for the prediction of ICI therapy responsiveness in VanAllen15 and PUCH cohorts.

Association of IRGPI With Tumor Immune Microenvironment in Melanoma

Reportedly, the infiltration of immune cells, especially $CD8^+$ T cells, is associated with immunotherapy response in many types of cancer (46). Based on the above results, we further investigated the relationship between IRGPI and tumor immune microenvironment features in melanoma patients. The TCGA-SKCM cohort was stratified into IRGPI-high and IRGPI-low groups using X-tile software (**Table S3** and **Figure S4**). Firstly, we calculated the immune score and ESTIMATE score of patients in TCGA-SKCM cohort by ESTIMATE algorithm. The data showed that both the immune score and ESTIMATE score were considerably increased in IRGPI-low group compared with IRGPI-high group (**Figures 4A, B**). Secondly, the CIBERSORT analytical tool was used to estimate the proportions of 22 types of immune cells in each SKCM sample. The results revealed that the infiltration levels of $CD8^+$ T cells, activated memory $CD4^+$ T cells, naive B cells, and NK cells in IRGPI-high group were lower than that in IRGPI-low group, while resting memory $CD4^+$ T cells, M0 and M2 macrophages showed the opposite trend (**Figure 4C**). Finally, we performed GSEA to identify which pathways were enriched at specific IRGPI levels. As shown in **Figure 4D**, the pathways of inflammatory response, interferon response, antigen processing and presentation, and T cell receptor signaling were markedly upregulated in IRGPI-low group.

Correlation of IRGPI to Other Potential Immunotherapy Biomarkers in Melanoma

A series of potential biomarkers have been developed to predict the response of ICI therapy in malignant tumors, such as TMB, immune inhibitory receptor expression levels. We analyzed the relationship between IRGPI and TMB in TCGA-SKCM cohort and the results showed that higher IRGPI conferred lower TMB (**Figure 5A**). As expected, the expression levels of immune inhibitory receptors (including PD-1, CTLA-4, LAG3, TIM-3, and TIGIT) showed the same trend as TMB between IRGPI-high and IRGPI-low groups (**Figure 5B**). Moreover, the

TABLE 2 | Model information of IRGPI.

IRG-A	Full name	Immune pathway	IRG-B	Full name	Immune pathway	Coefficient
CD1B	CD1b molecule	Antigen Processing and Presentation	AMHR2	anti-Mullerian hormone receptor type 2	Cytokine Receptors, TGFb Family Member Receptor	-0.133719837
CD1C	CD1c molecule	Antigen Processing and Presentation	GDNF	glial cell derived neurotrophic factor	Cytokines, TGFb Family Member	-0.006407801
CD1E	CD1e molecule	Antigen Processing and Presentation	NGF	nerve growth factor	Cytokines	-0.118650926
HLA-C	major histocompatibility complex, class I, C	Antigen Processing and Presentation, NaturalKiller Cell Cytotoxicity	SPP1	secreted phosphoprotein 1	Cytokines	-0.000146032
HSPA6	heat shock protein family A (Hsp70) member 6	Antigen Processing and Presentation	PI15	peptidase inhibitor 15	Antimicrobials	-0.006568346
IFNG	interferon gamma	Antigen Processing and Presentation, Antimicrobials, Cytokines, Interferons, NaturalKiller Cell Cytotoxicity, TCR Signaling Pathway	NTS	neurotensin	Cytokines	-0.208747404
RELB	RELB proto-oncogene, NF-kB subunit	Antigen Processing and Presentation	NFATC4	nuclear factor of activated T cells 4	BCR Signaling Pathway, NaturalKiller Cell Cytotoxicity, TCR Signaling Pathway	-0.001379582
CXCL13	C-X-C motif chemokine ligand 13	Antimicrobials, Chemokines, Cytokines	PLAU	plasminogen activator, urokinase	Antimicrobials, Chemokines, Cytokines	-0.042607265
XCL1	X-C motif chemokine ligand 1	Antimicrobials, Chemokines, Cytokines	FABP6	fatty acid binding protein 6	Antimicrobials	-0.179318494
SFTPD	surfactant protein D	Antimicrobials	CR2	complement C3d receptor 2	BCR Signaling Pathway	0.248588976
MMP9	matrix metallopeptidase 9	Antimicrobials	NOX4	NADPH oxidase 4	Antimicrobials	-0.126050935
RBP7	retinol binding protein 7	Antimicrobials	PRF1	perforin 1	NaturalKiller Cell Cytotoxicity	0.040708869
IFIH1	interferon induced with helicase C domain 1	Antimicrobials	VAV3	vav guanine nucleotide exchange factor 3	BCR Signaling Pathway, NaturalKiller Cell Cytotoxicity, TCR Signaling Pathway	-0.601441422
IDO1	indoleamine 2,3-dioxygenase 1	Antimicrobials	CD72	CD72 molecule	BCR Signaling Pathway	-0.238320598
IDO1	indoleamine 2,3-dioxygenase 1	Antimicrobials	SECTM1	secreted and transmembrane 1	Cytokines	-0.16744787
IRF1	interferon regulatory factor 1	Antimicrobials	HMOX1	heme oxygenase 1	Antimicrobials	-0.00086748
IRF1	interferon regulatory factor 1	Antimicrobials	IL1R1	interleukin 1 receptor type 1	Cytokine Receptors, Interleukins Receptor	-0.115025852
ZYX	zyxin	Antimicrobials	IRF9	interferon regulatory factor 9	Antimicrobials	0.117305566
TNFAIP3	TNF alpha induced protein 3	Antimicrobials	IL1R1	interleukin 1 receptor type 1	Cytokine Receptors, Interleukins Receptor	-0.209151382
HMOX1	heme oxygenase 1	Antimicrobials	IL32	interleukin 32	Cytokines	0.199502086
CCR7	C-C motif chemokine receptor 7	Antimicrobials, Chemokine Receptors, Cytokine Receptors	IL11	interleukin 11	Cytokines, Interleukins	-0.036970847
PTGDR	prostaglandin D2 receptor	Antimicrobials, Cytokine Receptors	EGF	epidermal growth factor	Cytokines	-0.088054831
RAC3	Rac family small GTPase 3	BCR Signaling Pathway, NaturalKiller Cell Cytotoxicity	NR1D1	nuclear receptor subfamily 1 group D member 1	Cytokine Receptors	0.174898131
CD19	CD19 molecule	BCR Signaling Pathway	EGF	epidermal growth factor	Cytokines	-0.012058023
INPP5D	inositol polyphosphate-5-phosphatase D	BCR Signaling Pathway	IL1R1	interleukin 1 receptor type 1	Cytokine Receptors, Interleukins Receptor	-0.014592558
CXCR3	C-X-C motif chemokine receptor 3	Chemokine Receptors, Cytokine Receptors	IL11	interleukin 11	Cytokines/Interleukins	-0.12999067
EGF	epidermal growth factor	Cytokines	TNFRSF11A	TNF receptor superfamily member 11a	Cytokine Receptors, TNF Family Members Receptors	0.254354052

(Continued)

TABLE 2 | Continued

IRG-A	Full name	Immune pathway	IRG-B	Full name	Immune pathway	Coefficient
IL33	interleukin 33	Cytokines, Interleukins	RARG	retinoic acid receptor gamma	Cytokine Receptors	-0.27380975
IL7	interleukin 7	Cytokines, Interleukins	PRF1	perforin 1	NaturalKiller Cell Cytotoxicity	0.062199575
IL20RB	interleukin 20 receptor subunit beta	Cytokine Receptors, Interleukins Receptor	TNFRSF10C	TNF receptor superfamily member 10c	Cytokine Receptors, NaturalKiller Cell Cytotoxicity, TNF Family Members Receptors	0.049115859
TEK	TEK receptor tyrosine kinase	Cytokine Receptors	CD28	CD28 molecule	TCR Signaling Pathway	0.046180545

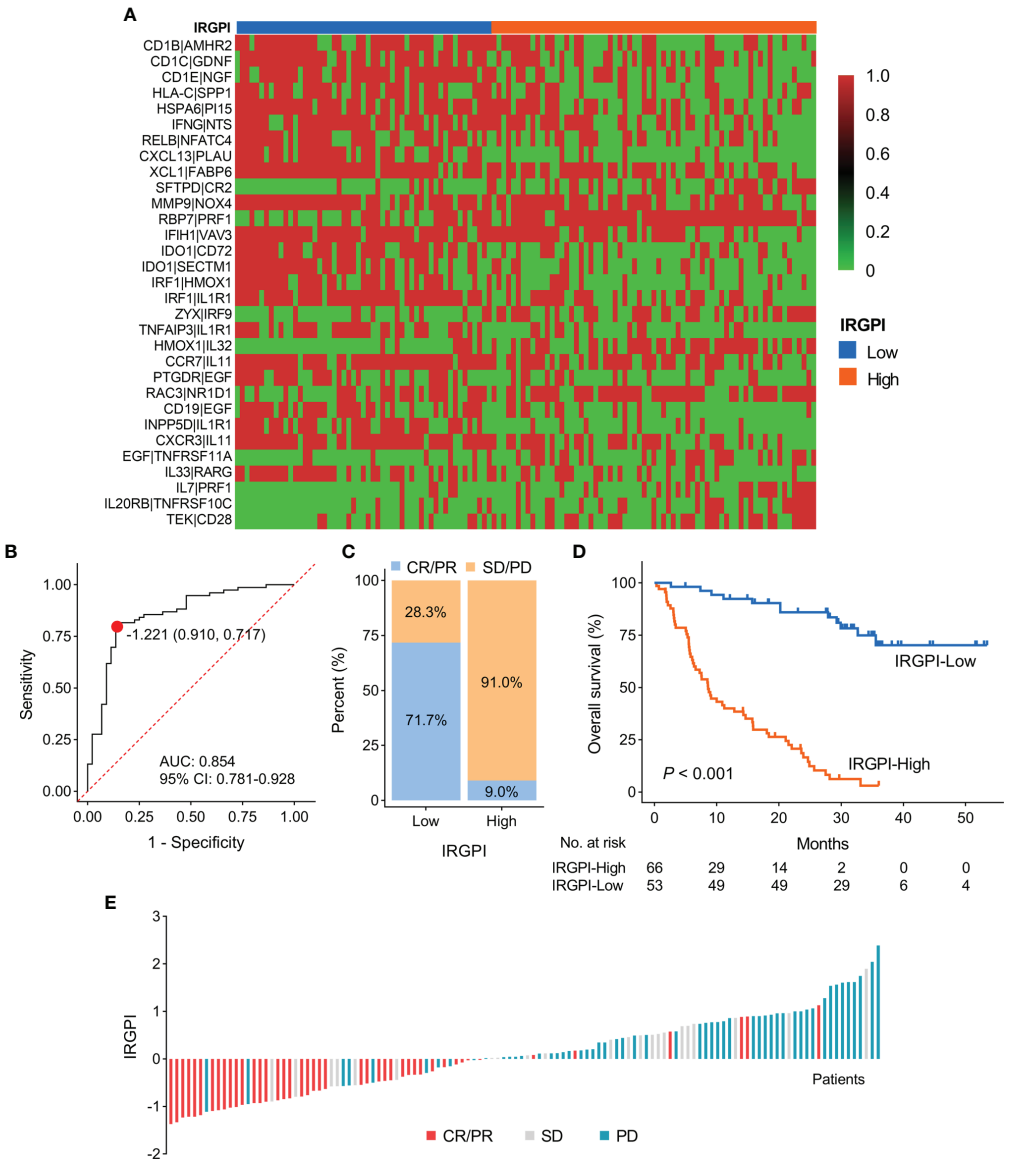

FIGURE 2 | Construction and evaluation of IRGPI in the discovery cohort. **(A)** A heatmap of the identified 31 IRGPs with corresponding IRGPI groups. **(B)** ROC curve for the predictive performance of IRGPI. **(C)** The rate of durable clinical response for patients with high and low IRGPI scores. **(D)** Kaplan-Meier plots of overall survival segregated by IRGPI score with cut-off points selected according to the Youden index. **(E)** Waterfall plot of IRGPI for distinct clinical response groups. IRGPI, immune-related gene pair index; IRGPs, immune-related gene pairs; ROC, receiver operating characteristic; AUC, area under curve; CI, confidence interval.

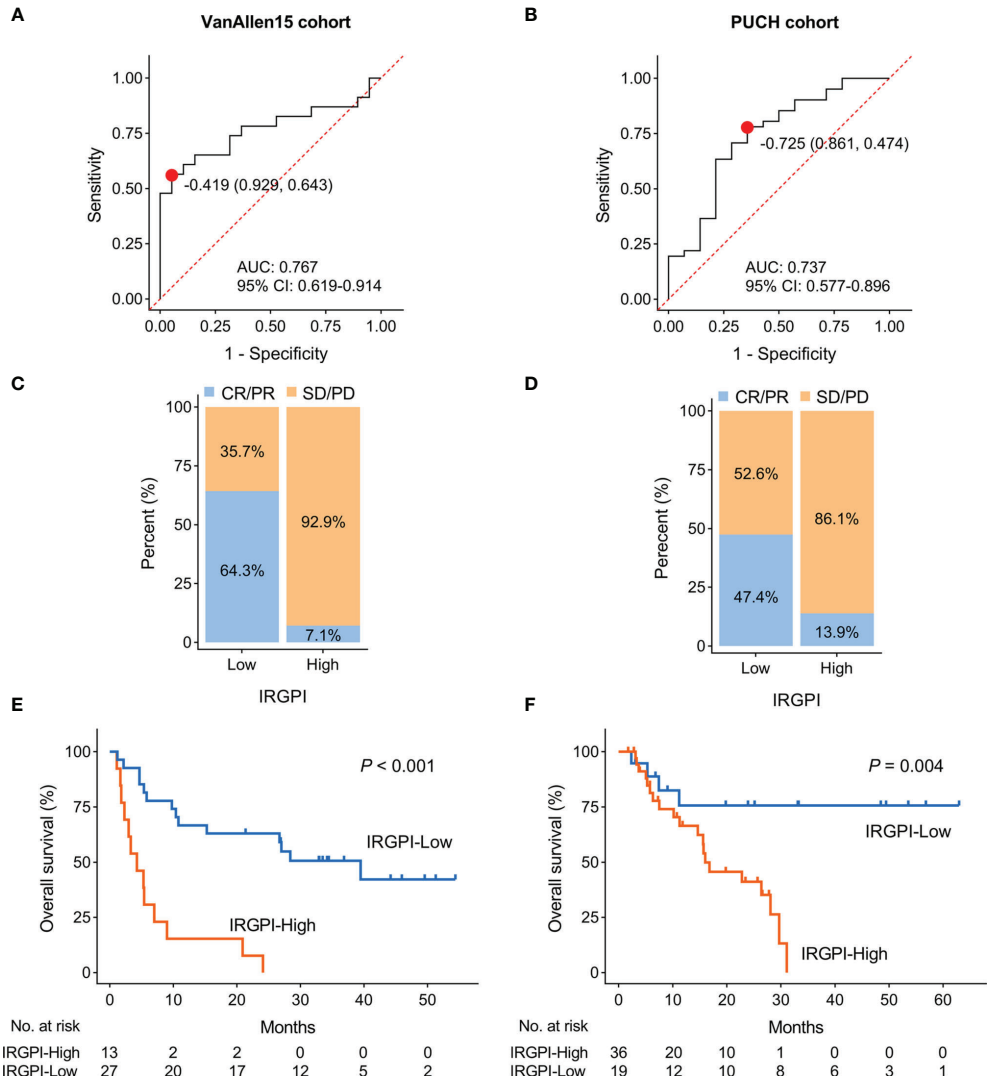

FIGURE 3 | Validation the performance of IRGPI in two cohorts. **(A, B)** ROC curves for the predictive performance of IRGPI in VanAllen15 and PUCH cohorts, respectively. **(C, D)** The rate of durable clinical response for patients with high and low IRGPI scores in VanAllen15 and PUCH cohorts, respectively. **(E, F)** Kaplan-Meier plots of overall survival segregated by IRGPI score with cut-off points selected according to the Youden index in VanAllen15 and PUCH cohorts, respectively. IRGPI, immune-related gene pair index; ROC, receiver operating characteristic; AUC, area under curve; CI, confidence interval.

deficiency of human leukocyte antigen (HLA) could impair antigen presentation and initiate antitumor immunity, which consequently resulting in primary resistance to immunotherapy (47). We then investigated the correlation of IRGPI to the expression levels of HLA members and the data indicated most HLA members were substantially upregulated in IRGPI-low group compared with IRGPI-high group (**Figure 5C**).

Some immune-related GEP signatures have been described to predict the benefit of ICI therapy in melanoma (**Table S4**). We therefore compared these GEP signature scores between IRGPI-high and IRGPI-low groups. Consistent with other biomarkers, these GEP signature scores were significantly downregulated in IRGPI-high group compared with IRGPI-low group (**Figure 5D**).

DISCUSSION

Over the past decades, the incidence of malignant melanoma has continued to increase, but the mortality has decreased, largely due to the rapid development of ICI and targeted therapies (48). Compared with the excellent clinical efficacy of ICI therapy in melanoma, the investigations of its biomarkers are relatively insufficient. The data from the real world revealed that durable responses and favorable long-term outcomes are limited a proportion of melanoma (12). Thus, more attention should be paid to the discovery and establishment of novel biomarkers for selecting patients who may benefit from ICI therapy.

In this study, we integrated the data of ICI therapy of melanoma patients from our center and other four Western

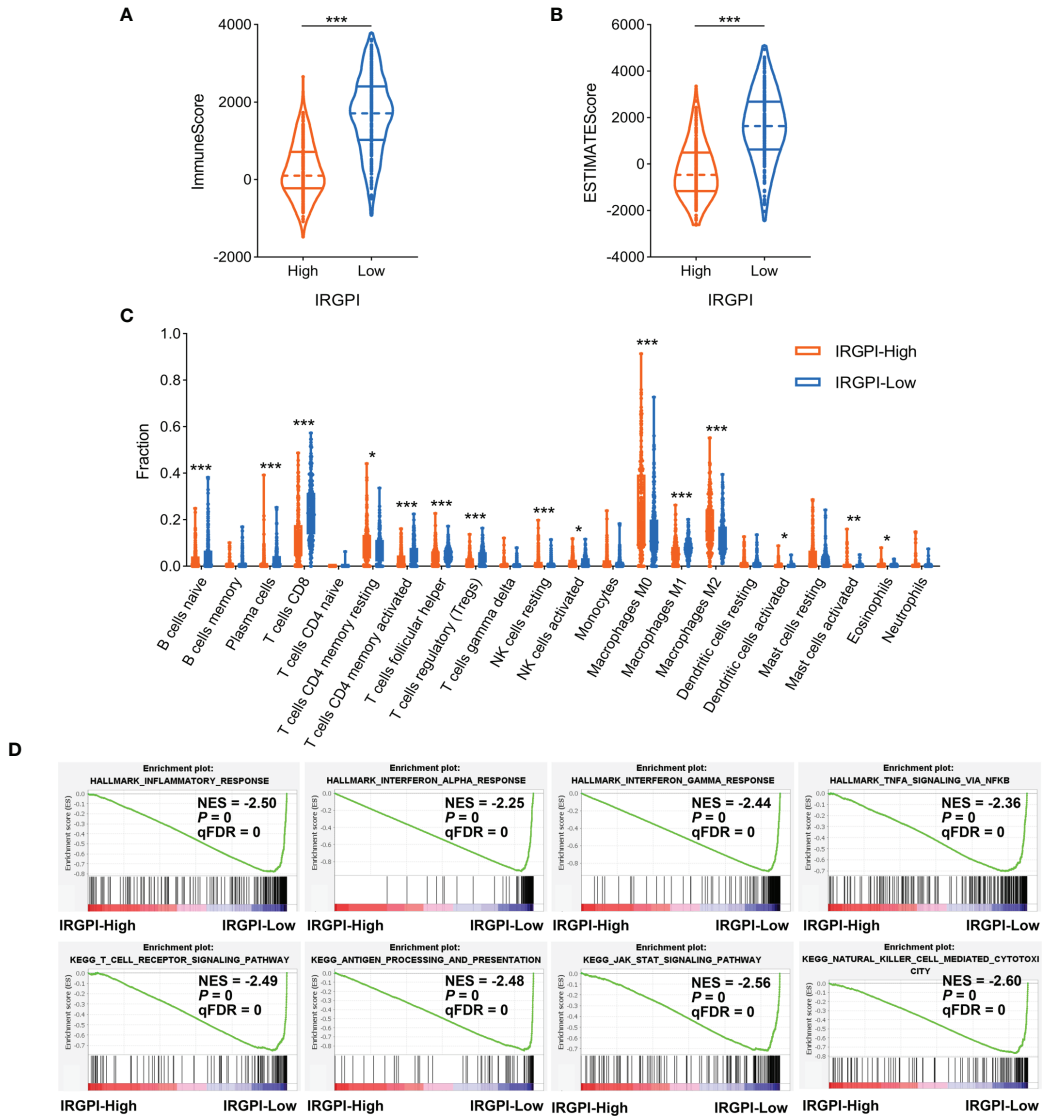

FIGURE 4 | Comparison of immune microenvironment characteristics according to IRGPI status. **(A, B)** ESTIMATE algorithm revealed the ImmuneScore and ESTIMATEScore between IRGPI-high and IRGPI-low groups. **(C)** Evaluation of 22 immune cell infiltrating using the CIBERSORT method. **(D)** GSEA plots of immune-related pathways in comparison between IRGPI-high and IRGPI-low groups. IRGPI, immune-related gene pair index; GSEA, gene set enrichment analysis. *$P < 0.05$, **$P < 0.01$, ***$P < 0.001$.

cohorts (31–34), and constructed an individualized immune predictive signature (IRGPI). The rate of durable clinical response for IRGPI-low patients in the discovery cohort, VanAllen15 and PUCH cohorts were 71.7%, 64.3% and 47.4%, respectively. Further, the percentage of non-responder in IRGPI-high group in discovery cohort, VanAllen15 and PUCH cohorts were 91%, 92.9% and 86.1%, respectively. The AUCs of ROC curve were all more than 0.7 in the discovery and validation cohorts. This reflected the good prediction accuracy and sensitivity of IRGPI for ICI therapy. The patient classification based on IRGPI also showed significantly different survival outcomes. Meanwhile, it is noted that the patients from our center are mainly acral and mucosal subtypes, while the patients from four Western cohorts are mainly cutaneous melanomas, which is consistent with the previous studies (49, 50). Considering the differential subtypes of melanoma and robust prediction accuracy across five cohorts, we reasonably assume that IRGPI is a reliable biomarker for guiding ICI therapy in both Western and Eastern patients with melanoma.

The IRGPI consisted of 51 unique IRGs, of which 36 encoded molecules involved in antimicrobials, cytokines, and cytokine receptors, which play vital roles in the regulation of the response to tumor immune microenvironment. Meanwhile, many of these IRGs have been demonstrated to be correlated with PD-L1 signaling and anti-PD-1 therapy, such as *MMP9* (matrix metallopeptidase 9) and *EGF* (epidermal growth factor).

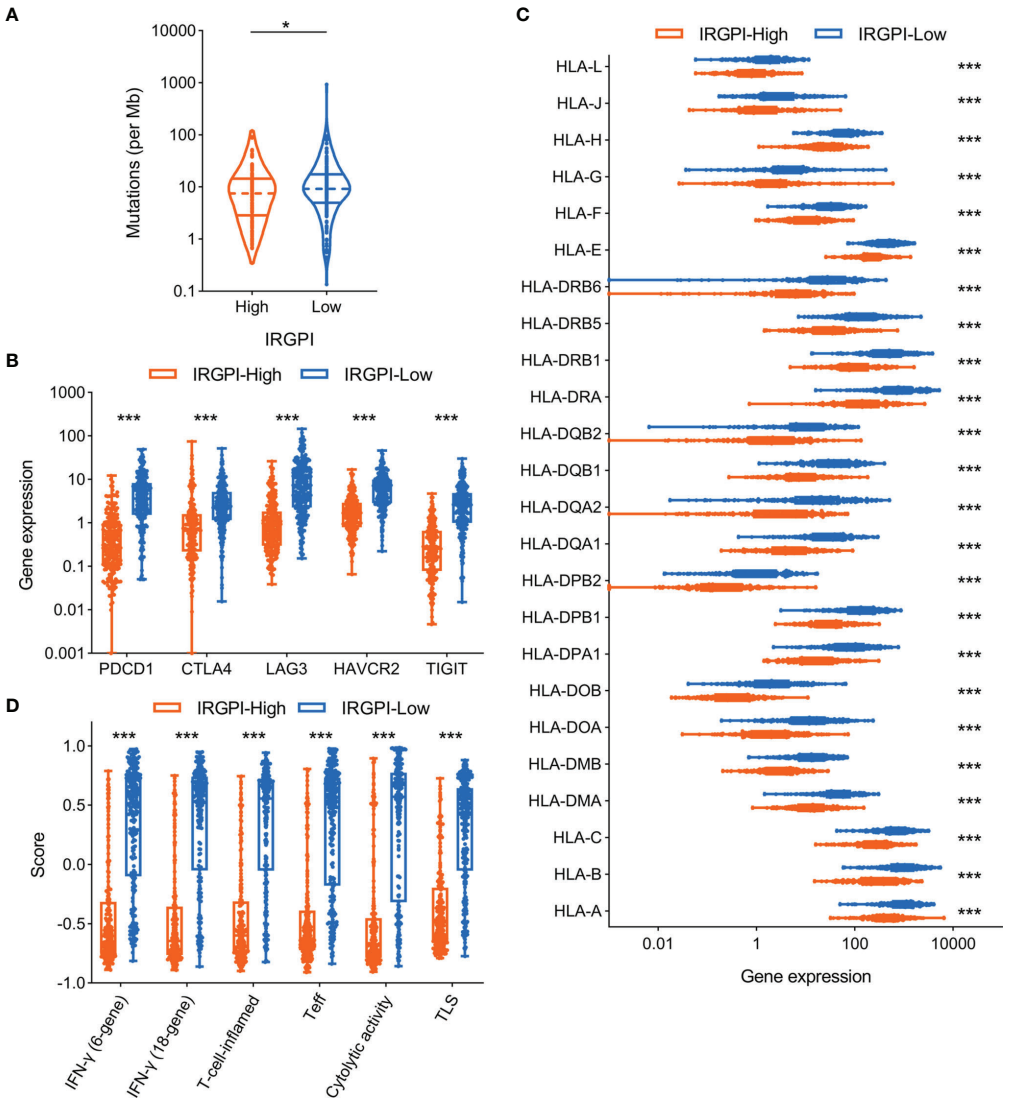

FIGURE 5 | Association of IRGPI to other potential biomarkers in melanoma. **(A)** Comparison of tumor mutation burden level according to IRGPI status. **(B)** Correlation of IRGPI to immune inhibitory receptors, including PDCD1, CTLA4, LAG3, HAVCR2, TIGIT. **(C)** The profile of HLA member expression levels between IRGPI-high and IRGPI-low groups. **(D)** Box plot of the immune-related signatures in comparison of the IRGPI-high and IRGPI-low groups. IRGPI, immune-related gene pair index; HLA, human leukocyte antigen; IFN, interferon; Teff, effective T cells; TLS, tertiary lymphoid structure. $^{*}P < 0.05$, $^{***}P < 0.001$.

Zhao et al. found that TGFβ pathway inhibition promoted the proliferation expansion of stromal fibroblasts, thereby facilitating MMP9-dependent cleavage of PD-L1 surface expression, leading to PD-1 blockade resistance in melanoma models (51). Furthermore, inhibition of MMP9 promoted the therapeutic efficacy of PD-1 blockade, with a marked reduction of tumor burden and extension of survival time (52). Li et al. discovered that the immunosuppressive activity of PD-L1 was tightly regulated by ubiquitination and N-glycosylation, in which glycogen synthase kinase 3β (GSK3β) could induce phosphorylation-dependent proteasome degradation of PD-L1 (53). In addition, EGF could stabilize PD-L1 *via* GSK3β inactivation in basal-like breast cancer (53). Therefore, blocking of EGF signaling using gefitinib resulted in the destabilization of PD-L1, enhancing antitumor T cell immunity and the treatment response of PD-1 blockade in syngeneic mouse models. What's more, some IRGs (including *IFNG*, *PRF1*, *IDO1*, *CXCL13*) were included in an IFN-γ-related T cell-inflamed GEP, which have been developed into a clinical-grade assay for evaluating the treatment efficacy of pembrolizumab in pan-tumors (19). As expected, the GSEA results of our study showed that lower IRGPI conferred upregulated interferon response and inflammatory signaling. The above data and analyses indicated that IRGPI could predict T cell inflammation in melanoma and explain the relationship between IRGPI and ICI therapy responsiveness to some extent.

TILs, especially $CD8^+$ T cells, can be used for predicting ICI therapy responsiveness and survival outcomes (46). In our study, we calculated the relative proportion of 22 types of immune cells based on the CIBERSORT algorithm and the results revealed that melanoma samples with high IRGPI harbored more infiltration of CD8+ T cells, activated memory $CD4^+$ T cells, naive B cells, and NK cells, which further elucidated the reason why IRGPI-high patients with melanoma can benefit from ICI therapy. However, the infiltration levels of regulatory T cells (Tregs) in IRGPI-high patients were also significantly higher compared with that in IRGPI-low patients, which was contradictory with the previous report of Tregs with an immunosuppressive role in TME (54). Further investigations are required to evaluate the infiltration levels of Tregs using immunohistochemistry or flow cytometry.

There are some limitations, unresolved concerns, and potential perspectives in our study. First, the current study combined the data from different datasets, which can sometimes present a selection bias, due to various therapy settings, different pre-existing mutations, and baseline patient characteristics. Although this gene-pair based approach we used in this study does not require normalization of GEP, this bias across cohorts is inevitable. Second, for the IRGPI, there are still some genes whose function are not fully elucidated. Further studies, such as knockdown or overexpression of IRGs in melanoma cell lines, are required to verify the role of these genes. Moreover, the basic experiments were also lacking to examine the immune cell infiltrating and PD-L1 expression of patients treated with ICI therapy. Finally, the patients in PUCH cohort were treated with different anti-PD-1 antibodies from various pharmaceutical companies, which may lead to drug bias. Compared with two previous studies (NCT02821000 and NCT02836795) of PD-1 blockade for treating melanoma patients, the data showed the ORR of two types of anti-PD-1 antibodies in mucosal subtype were 13.3% and 0, respectively (14, 55). Thus, further studies, preferably in a prospective setting, are required to stringently evaluate the correlation of IRGPI to the immunotherapy response and survival outcomes.

CONCLUSIONS

In summary, we constructed an individualized immune predictive signature (IRGPI), which could robustly predict the ICI therapy responsiveness and long-term survival outcomes. In addition, IRGPI may be an indicator of the immune characteristics of the TME in melanoma patients. These findings indicated that IRGPI might serve as a novel marker for treating of melanoma with ICI, which needs to be validated in prospective clinical trials.

DATA AVAILABILITY STATEMENT

The datasets presented in this study can be found in online repositories. The names of the repository/repositories and accession number(s) can be found below: https://ngdc.cncb.ac.cn/search/?dbId=&q=HRA000524.

ETHICS STATEMENT

The studies involving human participants were reviewed and approved by Peking University Cancer Hospital & Institute. The patients/participants provided their written informed consent to participate in this study.

AUTHOR CONTRIBUTIONS

SC and YK were involved in conception and design of the study. JuY performed and evaluated the experiment. XW and JiY helped to analyze the results. YK and XW provided materials or patients. JuY wrote the manuscript. All authors contributed to the article and approved the submitted version.

FUNDING

This work was supported by grants from National Natural Science Foundation of China (82002906, 81902789, 82002897) and CSCO-Roche Cancer Research Fund 2019 (Y-Roche2019/2-0028).

SUPPLEMENTARY MATERIAL

The Supplementary Material for this article can be found online at: https://www.frontiersin.org/articles/10.3389/fimmu.2022.839901/full#supplementary-material

Supplementary Figure 1 | Forest plot of different IRGPI groups. **(A)** Multivariate Cox analysis of 31 hub immune-related gene pairs. **(B)** Forest plot of high IRGPI score with poor OS in patients from three datasets.

Supplementary Figure 2 | The performance of the IRGPI in predicting progression-free survival in three cohorts.

Supplementary Figure 3 | Waterfall plot of IRGPI for distinct clinical response groups in VanAllen15 and PUCH cohorts.

Supplementary Figure 4 | X-tile plots of the IRGPI scores in TCGA-SKCM cohort.

REFERENCES

1. Fecher LA, Cummings SD, Keefe MJ, Alani RM. Toward a Molecular Classification of Melanoma. *J Clin Oncol* (2007) 25(12):1606–20. doi: 10.1200/JCO.2006.06.0442
2. Siegel RL, Miller KD, Fuchs HE, Jemal A. Cancer Statistics, 2021. *CA Cancer J Clin* (2021) 71(1):7–33. doi: 10.3322/caac.21654
3. Chen W, Zheng R, Baade PD, Zhang S, Zeng H, Bray F, et al. Cancer Statistics in China, 2015. *CA Cancer J Clin* (2016) 66(2):115–32. doi: 10.3322/caac.21338

4. Robert C, Ribas A, Schachter J, Arance A, Grob JJ, Mortier L, et al. Pembrolizumab Versus Ipilimumab in Advanced Melanoma (KEYNOTE-006): *Post-Hoc* 5-Year Results From an Open-Label, Multicentre, Randomised, Controlled, Phase 3 Study. *Lancet Oncol* (2019) 20(9):1239–51. doi: 10.1016/S1470-2045(19)30388-2
5. Postow MA, Chesney J, Pavlick AC, Robert C, Grossmann K, McDermott D, et al. Nivolumab and Ipilimumab Versus Ipilimumab in Untreated Melanoma. *N Engl J Med* (2015) 372(21):2006–17. doi: 10.1056/NEJMoa1414428
6. Zou W, Wolchok JD, Chen L. PD-L1 (B7-H1) and PD-1 Pathway Blockade for Cancer Therapy: Mechanisms, Response Biomarkers, and Combinations. *Sci Transl Med* (2016) 8(328):328rv4. doi: 10.1126/scitranslmed.aad7118
7. Eggermont A, Blank CU, Mandala M, Long GV, Atkinson V, Dalle S, et al. Adjuvant Pembrolizumab Versus Placebo in Resected Stage III Melanoma. *N Engl J Med* (2018) 378(19):1789–801. doi: 10.1056/NEJMoa1802357
8. Rozeman EA, Hoefsmit EP, Reijers I, Saw R, Versluis JM, Krijgsman O, et al. Survival and Biomarker Analyses From the OpACIN-Neo and OpACIN Neoadjuvant Immunotherapy Trials in Stage III Melanoma. *Nat Med* (2021) 27(2):256–63. doi: 10.1038/s41591-020-01211-7
9. Ribas A, Puzanov I, Dummer R, Schadendorf D, Hamid O, Robert C, et al. Pembrolizumab Versus Investigator-Choice Chemotherapy for Ipilimumab-Refractory Melanoma (KEYNOTE-002): A Randomised, Controlled, Phase 2 Trial. *Lancet Oncol* (2015) 16(8):908–18. doi: 10.1016/S1470-2045(15)00083-2
10. Hamid O, Robert C, Daud A, Hodi FS, Hwu WJ, Kefford R, et al. Safety and Tumor Responses With Lambrolizumab (Anti-PD-1) in Melanoma. *N Engl J Med* (2013) 369(2):134–44. doi: 10.1056/NEJMoa1305133
11. Topalian SL, Sznol M, McDermott DF, Kluger HM, Carvajal RD, Sharfman WH, et al. Survival, Durable Tumor Remission, and Long-Term Safety in Patients With Advanced Melanoma Receiving Nivolumab. *J Clin Oncol* (2014) 32(10):1020–30. doi: 10.1200/JCO.2013.53.0105
12. Mao L, Qi Z, Zhang L, Guo J, Si L. Immunotherapy in Acral and Mucosal Melanoma: Current Status and Future Directions. *Front Immunol* (2021) 12:680407. doi: 10.3389/fimmu.2021.680407
13. Nakamura Y, Namikawa K, Yoshino K, Yoshikawa S, Uchi H, Goto K, et al. Anti-PD1 Checkpoint Inhibitor Therapy in Acral Melanoma: A Multicenter Study of 193 Japanese Patients. *Ann Oncol* (2020) 31(9):1198–206. doi: 10.1016/j.annonc.2020.05.031
14. Si L, Zhang X, Shu Y, Pan H, Wu D, Liu J, et al. A Phase Ib Study of Pembrolizumab as Second-Line Therapy for Chinese Patients With Advanced or Metastatic Melanoma (KEYNOTE-151). *Transl Oncol* (2019) 12(6):828–35. doi: 10.1016/j.tranon.2019.02.007
15. Tang B, Chi Z, Chen Y, Liu X, Wu D, Chen J, et al. Safety, Efficacy, and Biomarker Analysis of Toripalimab in Previously Treated Advanced Melanoma: Results of the POLARIS-01 Multicenter Phase II Trial. *Clin Cancer Res* (2020) 26(16):4250–9. doi: 10.1158/1078-0432.CCR-19-3922
16. Lin H, Wei S, Hurt EM, Green MD, Zhao L, Vatan L, et al. Host Expression of PD-L1 Determines Efficacy of PD-L1 Pathway Blockade-Mediated Tumor Regression. *J Clin Invest* (2018) 128(2):805–15. doi: 10.1172/JCI96113
17. Kandoth C, McLellan MD, Vandin F, Ye K, Niu B, Lu C, et al. Mutational Landscape and Significance Across 12 Major Cancer Types. *Nature* (2013) 502(7471):333–9. doi: 10.1038/nature12634
18. Grasso CS, Tsoi J, Onyshchenko M, Abril-Rodriguez G, Ross-Macdonald P, Wind-Rotolo M, et al. Conserved Interferon-γ Signaling Drives Clinical Response to Immune Checkpoint Blockade Therapy in Melanoma. *Cancer Cell* (2021) 39(1):122. doi: 10.1016/j.ccell.2020.11.015
19. Ayers M, Lunceford J, Nebozhyn M, Murphy E, Loboda A, Kaufman DR, et al. IFN-γ-Related mRNA Profile Predicts Clinical Response to PD-1 Blockade. *J Clin Invest* (2017) 127(8):2930–40. doi: 10.1172/JCI91190
20. Zito Marino F, Ascierto PA, Rossi G, Staibano S, Montella M, Russo D, et al. Are Tumor-Infiltrating Lymphocytes Protagonists or Background Actors in Patient Selection for Cancer Immunotherapy. *Expert Opin Biol Ther* (2017) 17(6):735–46. doi: 10.1080/14712598.2017.1309387
21. Sunshine JC, Nguyen PL, Kaunitz GJ, Cottrell TR, Berry S, Esandrio J, et al. PD-L1 Expression in Melanoma: A Quantitative Immunohistochemical Antibody Comparison. *Clin Cancer Res* (2017) 23(16):4938–44. doi: 10.1158/1078-0432.CCR-16-1821
22. Hayward NK, Wilmott JS, Waddell N, Johansson PA, Field MA, Nones K, et al. Whole-Genome Landscapes of Major Melanoma Subtypes. *Nature* (2017) 545(7653):175–80. doi: 10.1038/nature22071
23. Zhang JA, Zhou XY, Huang D, Luan C, Gu H, Ju M, et al. Development of an Immune-Related Gene Signature for Prognosis in Melanoma. *Front Oncol* (2020) 10:602555. doi: 10.3389/fonc.2020.602555
24. Yan J, Wu X, Yu J, Zhu Y, Cang S. Prognostic Role of Tumor Mutation Burden Combined With Immune Infiltrates in Skin Cutaneous Melanoma Based on Multi-Omics Analysis. *Front Oncol* (2020) 10:570654. doi: 10.3389/fonc.2020.570654
25. Subramanian J, Simon R. Gene Expression-Based Prognostic Signatures in Lung Cancer: Ready for Clinical Use. *J Natl Cancer Inst* (2010) 102(7):464–74. doi: 10.1093/jnci/djq025
26. Leek JT, Scharpf RB, Bravo HC, Simcha D, Langmead B, Johnson WE, et al. Tackling the Widespread and Critical Impact of Batch Effects in High-Throughput Data. *Nat Rev Genet* (2010) 11(10):733–9. doi: 10.1038/nrg2825
27. Heinäniemi M, Nykter M, Kramer R, Wienecke-Baldacchino A, Sinkkonen L, Zhou JX, et al. Gene-Pair Expression Signatures Reveal Lineage Control. *Nat Methods* (2013) 10(6):577–83. doi: 10.1038/nmeth.2445
28. Li B, Cui Y, Diehn M, Li R. Development and Validation of an Individualized Immune Prognostic Signature in Early-Stage Nonsquamous Non-Small Cell Lung Cancer. *JAMA Oncol* (2017) 3(11):1529–37. doi: 10.1001/jamaoncol.2017.1609
29. Xue YN, Xue YN, Wang ZC, Mo YZ, Wang PY, Tan WQ. A Novel Signature of 23 Immunity-Related Gene Pairs Is Prognostic of Cutaneous Melanoma. *Front Immunol* (2020) 11:576914. doi: 10.3389/fimmu.2020.576914
30. Cui C, Xu C, Yang W, Chi Z, Sheng X, Si L, et al. Ratio of the Interferon-γ Signature to the Immunosuppression Signature Predicts Anti-PD-1 Therapy Response in Melanoma. *NPJ Genom Med* (2021) 6(1):7. doi: 10.1038/s41525-021-00169-w
31. Gide TN, Quek C, Menzies AM, Tasker AT, Shang P, Holst J, et al. Distinct Immune Cell Populations Define Response to Anti-PD-1 Monotherapy and Anti-PD-1/Anti-CTLA-4 Combined Therapy. *Cancer Cell* (2019) 35(2):238–55.e6. doi: 10.1016/j.ccell.2019.01.003
32. Hugo W, Zaretsky JM, Sun L, Song C, Moreno BH, Hu-Lieskovan S, et al. Genomic and Transcriptomic Features of Response to Anti-PD-1 Therapy in Metastatic Melanoma. *Cell* (2016) 165(1):35–44. doi: 10.1016/j.cell.2016.02.065
33. Riaz N, Havel JJ, Makarov V, Desrichard A, Urba WJ, Sims JS, et al. Tumor and Microenvironment Evolution During Immunotherapy With Nivolumab. *Cell* (2017) 171(4):934–949.e16. doi: 10.1016/j.cell.2017.09.028
34. Van Allen EM, Miao D, Schilling B, Shukla SA, Blank C, Zimmer L, et al. Genomic Correlates of Response to CTLA-4 Blockade in Metastatic Melanoma. *Science* (2015) 350(6257):207–11. doi: 10.1126/science.aad0095
35. Charoentong P, Finotello F, Angelova M, Mayer C, Efremova M, Rieder D, et al. Pan-Cancer Immunogenomic Analyses Reveal Genotype-Immunophenotype Relationships and Predictors of Response to Checkpoint Blockade. *Cell Rep* (2017) 18(1):248–62. doi: 10.1016/j.celrep.2016.12.019
36. Bhattacharya S, Andorf S, Gomes L, Dunn P, Schaefer H, Pontius J, et al. ImmPort: Disseminating Data to the Public for the Future of Immunology. *Immunol Res* (2014) 58(2-3):234–9. doi: 10.1007/s12026-014-8516-1
37. Kim S, Lin CW, Tseng GC. MetaKTSP: A Meta-Analytic Top Scoring Pair Method for Robust Cross-Study Validation of Omics Prediction Analysis. *Bioinformatics* (2016) 32(13):1966–73. doi: 10.1093/bioinformatics/btw115
38. Youden WJ. Index for Rating Diagnostic Tests. *Cancer* (1950) 3(1):32–5. doi: 10.1002/1097-0142(1950)3:1<32::aid-cncr2820030106<3.0.co;2-3
39. Camp RL, Dolled-Filhart M, Rimm DL. X-Tile: A New Bio-Informatics Tool for Biomarker Assessment and Outcome-Based Cut-Point Optimization. *Clin Cancer Res* (2004) 10(21):7252–9. doi: 10.1158/1078-0432.CCR-04-0713
40. Becht E, Giraldo NA, Lacroix L, Buttard B, Elarouci N, Petitprez F, et al. Estimating the Population Abundance of Tissue-Infiltrating Immune and Stromal Cell Populations Using Gene Expression. *Genome Biol* (2016) 17(1):218. doi: 10.1186/s13059-016-1070-5
41. Chen B, Khodadoust MS, Liu CL, Newman AM, Alizadeh AA. Profiling Tumor Infiltrating Immune Cells With CIBERSORT. *Methods Mol Biol* (2018) 1711:243–59. doi: 10.1007/978-1-4939-7493-1_12
42. Spranger S, Bao R, Gajewski TF. Melanoma-Intrinsic β-Catenin Signalling Prevents Anti-Tumour Immunity. *Nature* (2015) 523(7559):231–5. doi: 10.1038/nature14404

43. McDermott DF, Huseni MA, Atkins MB, Motzer RJ, Rini BI, Escudier B, et al. Clinical Activity and Molecular Correlates of Response to Atezolizumab Alone or in Combination With Bevacizumab Versus Sunitinib in Renal Cell Carcinoma. *Nat Med* (2018) 24(6):749–57. doi: 10.1038/s41591-018-0053-3
44. Sanchez A, Furberg H, Kuo F, Vuong L, Ged Y, Patil S, et al. Transcriptomic Signatures Related to the Obesity Paradox in Patients With Clear Cell Renal Cell Carcinoma: A Cohort Study. *Lancet Oncol* (2020) 21(2):283–93. doi: 10.1016/S1470-2045(19)30797-1
45. Messina JL, Fenstermacher DA, Eschrich S, Qu X, Berglund AE, Lloyd MC, et al. 12-Chemokine Gene Signature Identifies Lymph Node-Like Structures in Melanoma: Potential for Patient Selection for Immunotherapy. *Sci Rep* (2012) 2:765. doi: 10.1038/srep00765
46. Fu C, Jiang A. Dendritic Cells and CD8 T Cell Immunity in Tumor Microenvironment. *Front Immunol* (2018) 9:3059. doi: 10.3389/fimmu.2018.03059
47. McGranahan N, Rosenthal R, Hiley CT, Rowan AJ, Watkins T, Wilson GA, et al. Allele-Specific HLA Loss and Immune Escape in Lung Cancer Evolution. *Cell* (2017) 171(6):1259–71.e11. doi: 10.1016/j.cell.2017.10.001
48. Curti BD, Faries MB. Recent Advances in the Treatment of Melanoma. *N Engl J Med* (2021) 384(23):2229–40. doi: 10.1056/NEJMra2034861
49. Chi Z, Li S, Sheng X, Si L, Cui C, Han M, et al. Clinical Presentation, Histology, and Prognoses of Malignant Melanoma in Ethnic Chinese: A Study of 522 Consecutive Cases. *BMC Cancer* (2011) 11:85. doi: 10.1186/1471-2407-11-85
50. McLaughlin CC, Wu XC, Jemal A, Martin HJ, Roche LM, Chen VW. Incidence of Noncutaneous Melanomas in the U. *S Cancer* (2005) 103 (5):1000–7. doi: 10.1002/cncr.20866
51. Zhao F, Evans K, Xiao C, DeVito N, Theivanthiran B, Holtzhausen A, et al. Stromal Fibroblasts Mediate Anti-PD-1 Resistance *via* MMP-9 and Dictate Tgfβ Inhibitor Sequencing in Melanoma. *Cancer Immunol Res* (2018) 6 (12):1459–71. doi: 10.1158/2326-6066.CIR-18-0086
52. Ye Y, Kuang X, Xie Z, Liang L, Zhang Z, Zhang Y, et al. Small-Molecule MMP2/MMP9 Inhibitor SB-3CT Modulates Tumor Immune Surveillance by Regulating PD-L1. *Genome Med* (2020) 12(1):83. doi: 10.1186/s13073-020-00780-z
53. Li CW, Lim SO, Xia W, Lee HH, Chan LC, Kuo CW, et al. Glycosylation and Stabilization of Programmed Death Ligand-1 Suppresses T-Cell Activity. *Nat Commun* (2016) 7:12632. doi: 10.1038/ncomms12632
54. Jacobs JF, Nierkens S, Figdor CG, de Vries IJ, Adema GJ. Regulatory T Cells in Melanoma: The Final Hurdle Towards Effective Immunotherapy. *Lancet Oncol* (2012) 13(1):e32–42. doi: 10.1016/S1470-2045(11)70155-3
55. Tang B, Yan X, Sheng X, Si L, Cui C, Kong Y, et al. Safety and Clinical Activity With an Anti-PD-1 Antibody JS001 in Advanced Melanoma or Urologic Cancer Patients. *J Hematol Oncol* (2019) 12(1):7. doi: 10.1186/s13045-018-0693-2

Conflict of Interest: The authors declare that the research was conducted in the absence of any commercial or financial relationships that could be construed as a potential conflict of interest.

Publisher's Note: All claims expressed in this article are solely those of the authors and do not necessarily represent those of their affiliated organizations, or those of the publisher, the editors and the reviewers. Any product that may be evaluated in this article, or claim that may be made by its manufacturer, is not guaranteed or endorsed by the publisher.

frontiers in Immunology

CASE REPORT
published: 17 March 2022
doi: 10.3389/fimmu.2022.815598

Case Report: A PD-L1-Positive Patient With Pleomorphic Rhabdomyosarcoma Achieving an Impressive Response to Immunotherapy

Jiayong Liu[1], Peijie Liu[2], Fuyu Gong[3], Youhui Tian[3] and Xiaochen Zhao[3]*

[1] Key Laboratory of Carcinogenesis and Translational Research (Ministry of Education/Beijing), Department of Bone and Soft Tissue Tumor, Peking University Cancer Hospital & Institute, Beijing, China, [2] Department of Oncology, The First Affiliated Hospital of Henan University, Kaifeng, China, [3] The Medical Department, 3D Medicines Inc., Shanghai, China

There is currently a lack of effective systemic treatment for patients with advanced pleomorphic rhabdomyosarcoma (PRMS). Although programmed death protein 1 (PD-1) inhibitors have shown efficacy in various solid tumors, their effects on PRMS have not been well established. Here, we present a case of a 12-year-old Chinese male adolescent with metastatic PRMS who benefited from the PD-1 inhibitor nivolumab. The patient initially underwent primary tumor resection but failed to respond to subsequent first-line chemotherapy and second-line pazopanib treatment. Pathological examination showed positive PD-L1 expression and tumor-infiltrating lymphocytes in the tumor tissue, and the patient was administered nivolumab as a posterior-line treatment. After attaining a clinically partial response (PR), surgical resection was performed, which was followed by adjuvant nivolumab. At the time of the submission of this manuscript, the patient achieved recurrence-free survival (RFS) lasting 45 months and counting. This is the first clinical evidence that a patient with refractory PRMS was controlled by anti-PD-1 antibody, with an RFS lasting more than 3 years. This case suggests that PD-L1 expression and T-cell infiltration could be used as potential biomarkers for PRMS immunotherapy.

Keywords: pleomorphic rhabdomyosarcoma, immunotherapy, pazopanib, PD-L1, CD8 T cell

OPEN ACCESS

Edited by:
Alison Taylor,
University of Leeds, United Kingdom

Reviewed by:
Jiyang Yu,
St. Jude Children's Research Hospital, United States
Santiago Cabezas-Camarero,
San Carlos University Clinical Hospital, Spain

****Correspondence:***
Jiayong Liu
liujiayong_doc@163.com

Specialty section:
This article was submitted to Cancer Immunity and Immunotherapy, a section of the journal Frontiers in Immunology

Received: *15 November 2021*
Accepted: *18 February 2022*
Published: *17 March 2022*

Citation:
Liu J, Liu P, Gong F, Tian Y and Zhao X (2022) Case Report: A PD-L1-Positive Patient With Pleomorphic Rhabdomyosarcoma Achieving an Impressive Response to Immunotherapy. Front. Immunol. 13:815598. doi: 10.3389/fimmu.2022.815598

INTRODUCTION

Rhabdomyosarcoma (RMS), which originates from the mesenchymal tissue, is the most common type of soft tissue sarcoma (STS) that occurs in childhood and adolescence (1). According to the World Health Organization classification of soft tissue tumors, RMS can be classified into four histological subtypes: alveolar RMS (ARMS), embryonal RMS (ERMS), spindle cell/sclerosing RMS (SRMS), and pleomorphic

Abbreviations: CT, computed tomography; dMMR, mismatch repair deficiency; ICI, immune checkpoint inhibitor; IHC, immunohistochemistry; MSI-H, microsatellite instability-high; MSS, microsatellite-stable status; MTI, medication time interval; PD, progressive disease; PD-1, programmed death protein 1; PR, partial response; PRMS, pleomorphic rhabdomyosarcoma; RMS, rhabdomyosarcoma; SD, stable disease; STS, soft tissue sarcoma; TIL, tumor-infiltrating lymphocytes; TMB, tumor mutation burden; WES, whole exon sequencing.

RMS (PRMS) (2). In comparison to the other RMS subtypes, PRMS is associated with a poor response to standard chemotherapy and a poor prognosis for both local and metastatic disease (3). Nonetheless, anthracycline-based chemotherapy remains the first-line standard treatment for advanced PRMS (4, 5). Pazopanib and regorafenib are multitarget tyrosine kinase inhibitors (TKIs) that are recommended as second-line treatment options for nonspecific STS, including PRMS (6).

Monoclonal antibodies against programmed death-1 (PD-1) and programmed death-ligand 1 (PD-L1) could help activate cytolytic T lymphocytes by blocking the PD-L1/PD-1 signaling pathway to prevent tumors from achieving immune evasion. Immune checkpoint inhibitor (ICI)-based immunotherapy has shown promising efficacy in various malignancies (7–9). Evidence regarding ICI efficacy in RMS remains scarce (10). A multicenter phase 2 clinical trial showed that ICIs exhibited promising efficacy and an acceptable safety profile in advanced STS (11). However, a retrospective study revealed that RMS showed no response to the anti-PD-1 antibody pembrolizumab (12). A phase I/II study (NCT02304458) is underway to explore the use of nivolumab as a single agent or in combination with ipilimumab in refractory solid tumors, including RMS. Predictive biomarkers should be investigated to identify the subset of patients who respond to immunotherapy.

Here, we present a case of a patient with advanced PRMS who failed to respond to chemotherapy and antiangiogenic therapy but achieved a partial response (PR) with nivolumab treatment. Subsequently, the patient underwent R0 resection on the recurrent lesions, followed by nivolumab treatment as adjuvant and maintenance immunotherapy. At the time of submission of this manuscript, the patients achieved recurrence-free survival (RFS) lasting 45 months and counting (**Figure 1A**).

CASE PRESENTATION

A 12-year-old Chinese male adolescent was referred due to a mass in his left elbow. In January 2017, surgical treatment was performed due to the rapid growth of the mass. Immunohistochemistry (IHC) results of the tumor specimens showed highly positive expression of DESMIN, MYOD1, and MYOGLB (**Figures 1B–E**) . *PAX3-FOXO* gene fusion was not detected by using fluorescence *in situ* hybridization (FISH). In February 2017, computed tomography (CT) of the chest and an enhanced CT scan of the left elbow revealed recurrence, showing two locoregionally relapsed lesions and multiple lung metastases (**Figures 2A1–A3**). Accordingly, the patient was diagnosed with poorly differentiated PRMS, stage IV (pT2N0M1).

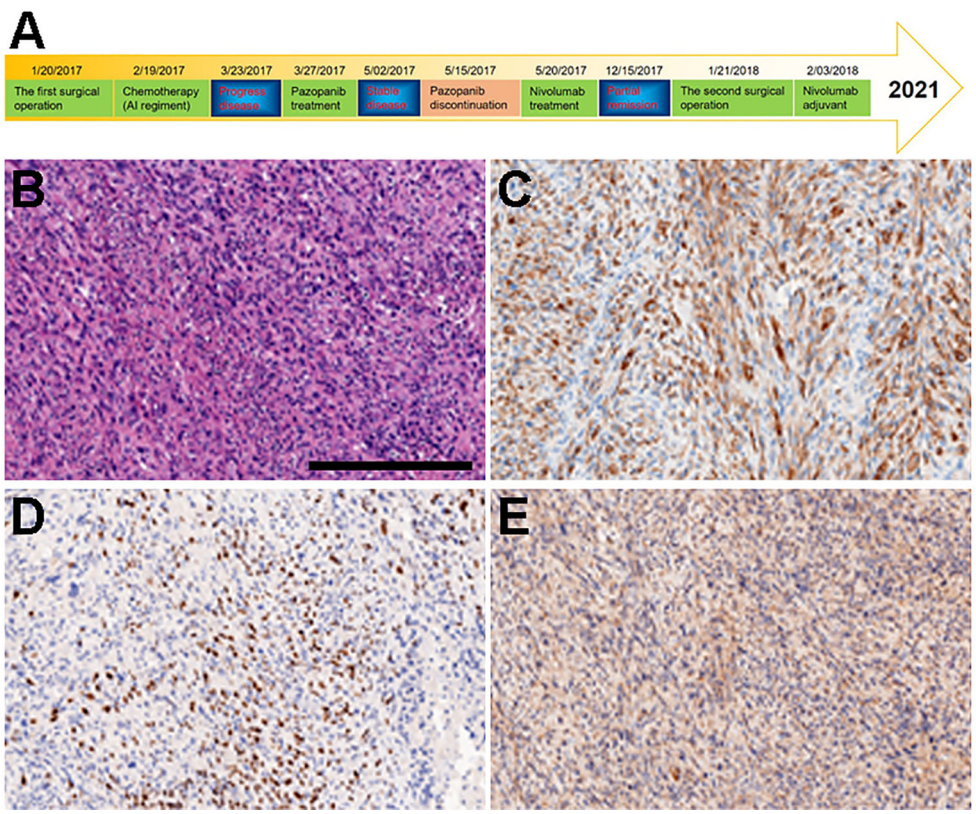

FIGURE 1 | Diagnosis and treatment schematic plot and IHC of primary tumor tissue obtained from surgery. **(A)** Diagnosis and treatment schematic plot. **(B)** H&E. **(C)** DESMIN. **(D)** MYOD1. **(E)** MYGLB.

Given his good physical condition, the patient was treated with endosarc (a recombinant human endostatin) in combination with chemotherapy (doxorubicin and ifosfamide). Progressive disease (PD) and serious treatment-related adverse events, such as nausea and myelosuppression, occurred after one cycle of chemotherapy (**Figures 2B1–B3**). This indicated a failure of the first-line chemotherapy. Starting on March 27, 2017, pazopanib monotherapy was administered following a multidisciplinary discussion. Although stable disease (SD) was achieved 1 month later (**Figures 2C1–C3**), the patient experienced severe adverse effects, including asthenia, myelosuppression, and nausea. The use of pazopanib was discontinued.

Under the consent of the patient's guardian, the surgical tissue sample was tested for the feasibility of immunotherapy. More than 30% of the tumor cells expressed PD-L1 (as tested by the SP263 assay on the Ventana platform), and tumor-infiltrating T cells appeared in the tumor region (**Figure 3**). Whole exon sequencing (WES) revealed a microsatellite-stable (MSS) status and HLA-I locus heterozygosity. The tumor mutation burden (TMB) was 2.05 mut/Mb (**Table 1**). Based on these findings, nivolumab monotherapy (100 mg Q2W) was initiated on May 20, 2017. CT scans exhibited a significant remission of the lung lesions after four courses of nivolumab treatment. One of the primary lesions had PR, but the other had little change (**Figures 2D1–D3**). Taken together, the total tumor volume was reduced by 87%, demonstrating that PR was achieved.

On January 21, 2018, the patient underwent R0 resection after 19 cycles of nivolumab immunotherapy. Another WES was performed on the surgical tumor tissue obtained during the second surgery and showed a TMB of 4.79 mut/Mb (**Table 1**). Upon submission of this manuscript, the patient continued to receive maintenance monotherapy with nivolumab. The most recent CT scan indicated no recurrence or metastasis. The patient has achieved an RFS of 45 months and counting (**Figures 2E1–E3**). Moreover, the toxicity associated with nivolumab treatment was tolerable through the whole course of immunotherapy.

DISCUSSION

Unlike other RMS subtypes, PRMS is a rare subtype that is noted more commonly in adults rather than in children and teenagers (1). There are no effective treatments and accurate prognostic biomarkers for PRMS, especially for refractory disease. Here, we reviewed the clinical courses and prognosis of 15 patients with metastatic or recurrent PRMS (**Table 2**) and found that surgical resection was still the best option. Adjuvant therapy, such as chemotherapy and immunotherapy, would benefit the patients further. The majority of patients died within a year of diagnosis. Nonetheless, long-term event-free survival has been achieved in two patients with adjuvant immunotherapy following surgical resection or immunotherapy alone (15). These two patients, in particular, were younger than the others. This indicates that ICI-based immunotherapy could be a promising treatment option for refractory PRMS, especially in teenagers. According to WHO classification, PRMS was not classified as a separate disease diagnosis in pediatric patients but was categorized as incorporated in ERMS diffuse anaplasia (23, 24). This highlights that age is a vital risk stratification factor for RMS.

The expression of PD-L1 in tumor cells correlates with inferior prognosis in STS patients, suggesting that the PD-1/PD-L1 axis could be a promising therapeutic biomarker (25). In many advanced malignant tumors, including STS (11, 26), monoclonal antibodies targeting the PD-1/PD-L1 axis have demonstrated considerable antitumor effects with a controllable toxicity profile. One of the essential approaches to improve the therapeutic benefit is to stratify patients using reliable biomarkers (27, 28).

In many solid tumors, such as non-small-cell lung cancer (NSCLC), PD-L1 expression in tumor cells and tumor-infiltrating lymphocytes (TILs) have strong predictive effects for anti-PD-1/L1 therapy (8). Little is known about the predictive significance of PD-L1 expression in STS. In a phase 2 study of pembrolizumab in advanced STS and bone sarcoma, three patients (4%) were identified as PD-L1 positive (TPS >1%) (9). Two of the three PD-L1-positive patients achieved an evaluable response: one complete response (CR) and one PR. Moreover, in another phase 2 clinical trial evaluating the efficacy and safety of cyclophosphamide plus pembrolizumab in 57 STS patients (29), only one patient presented a high level of PD-L1 expression (immune proportion score >10%) and achieved PR. A favorable response was also observed in a 17-year-old PD-L1-positive patient (TPS = 75%) with metastatic histiocytic sarcoma treated with nivolumab (30). Moreover, Tlemsani et al. reported the first case of a patient with PRMS (TPS = 60%), high levels of PD-L1 expression, and mismatch repair deficiency (dMMR). This patient was administered nivolumab monotherapy and achieved a long-term CR (15). Given the above data, PD-L1 expression may serve as a predictive biomarker for anti-PD-1/L1 treatment in STS patients.

The PD-L1 expression in STS patients varied among the studies. According to Perisano et al., 68.3% of high-grade sarcomas displayed positive PD-L1 expression (31). Chowdhury's study revealed that RMS had the highest (86%) PD-L1-positive expression (TPS > 5%) when compared to other common pediatric tumors (32). Similar to the clinical result in NSCLC (33), our study also found that the proportion of $CD8^+$ TIL seemed to be positively correlated with PD-L1 expression, implying that $CD8^+$ TIL infiltration could become another effective indicator of immune response (32). The patient in our case presented with positive PD-L1 expression (TPS = 30%) and increased infiltration of $CD8^+$ T cell (**Figure 3**). Given the impressive clinical response, we hypothesized that PD-L1-positive expression and/or TILs could be useful biomarkers for predicting the response to PD-1 blockade in PRMS.

Deficient mismatch repair/microsatellite instability-high (dMMR/MSI-H) has been identified as a powerful predictor of ICIs in multiple solid tumors, particularly colorectal and gastric cancer (8–11). The prevalence of dMMR/MSI-H in STS is 2.3% (34). In Doyle's study, no response was observed in three dMMR PRMS patients treated with pembrolizumab. Lewin et al.

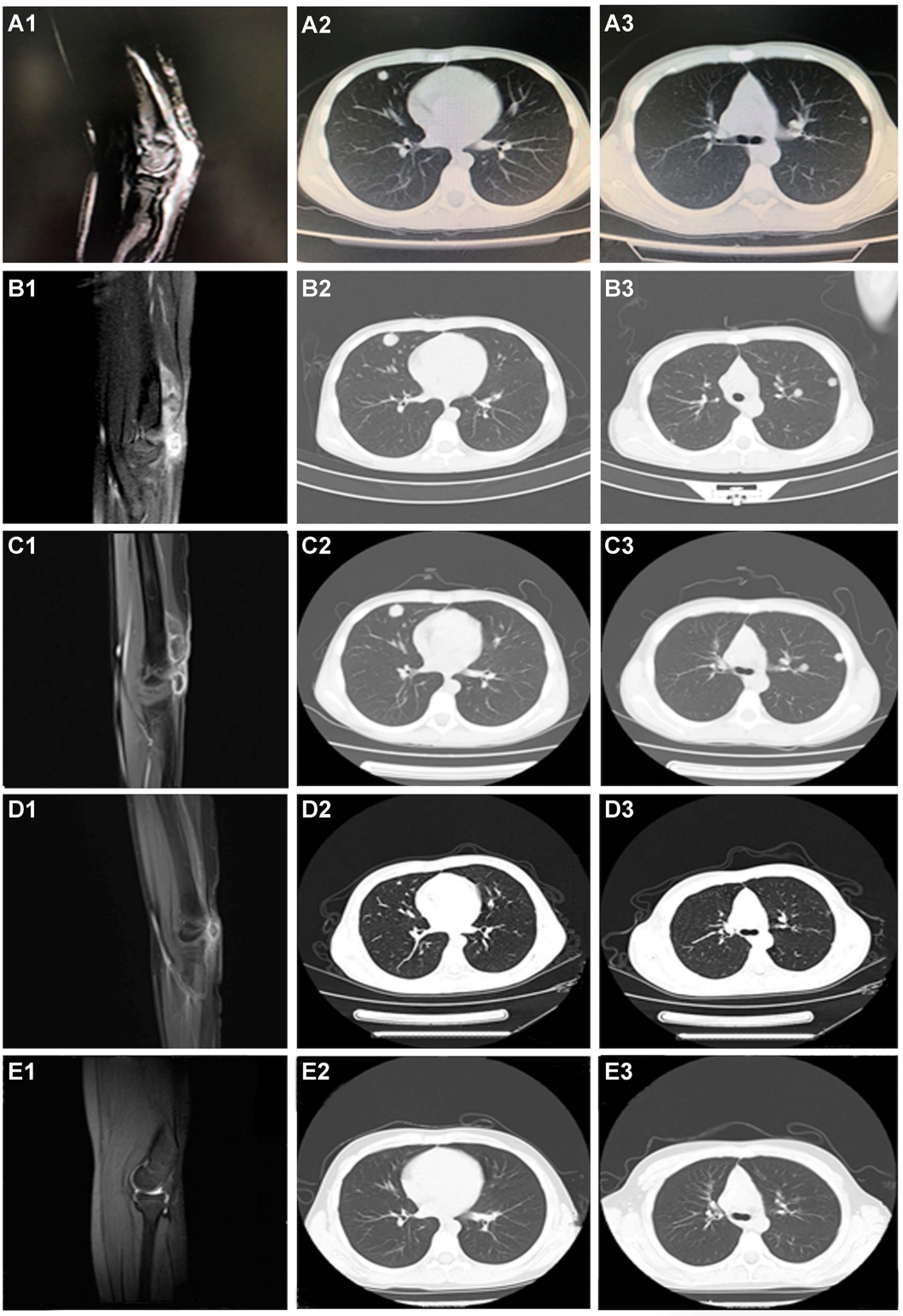

FIGURE 2 | CT scanning during the whole treatment. **(A1–A3)** Before any systemic treatment. **(B1–B3)** After one cycle of chemotherapy and endostar. **(C1–C3)** After 1 month of pazopanib. **(D1–D3)** After four cycles of nivolumab. **(E1–E3)** The last followed up scanning. The first column was the limb viewport; the middle and last column was the lung viewport.

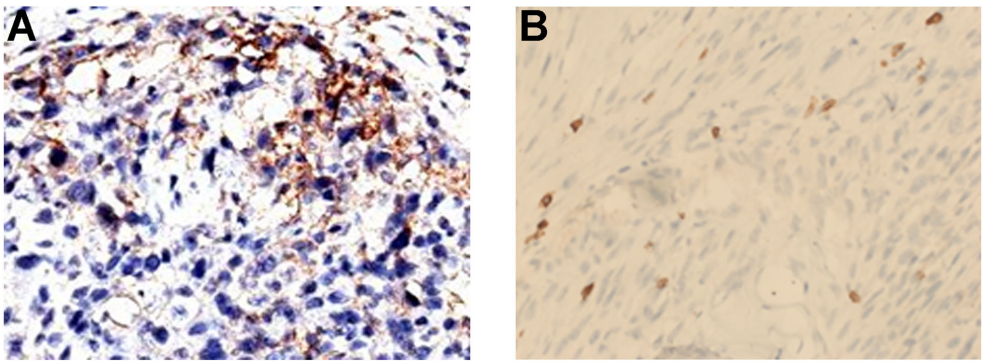

FIGURE 3 | IHC assay of tumor tissue obtained from the first surgery. **(A)** PD-L1. **(B)** CD8.

reported that two dMMR cases with alveolar soft part sarcoma responded to durvalumab (anti-PD-L1) alone or in combination with tremelimumab (anti-CTLA-4) (35). The patient in our study was microsatellite stable (MSS) but benefited from nivolumab. Thus, the predictive value of dMMR/MSI-H for STS with anti-PD-1/L1 treatment remains debatable. In Doyle's study, dMMR patients exhibited significantly higher TMB than proficient mismatch repair (pMMR) patients, consistent with previous clinical studies (36). High TMB has been reported as a potential biomarker to screen patients who may benefit from ICI therapy (37). However, TMB has no predictive ability for STS with anti-PD-1/L1 treatment due to the small patient population (35). Studies with larger sample sizes are needed to assess the predictive effects of dMMR/MSI-H and TMB in STS and PRMS.

Moreover, prior pazopanib treatment may have reinforced the brilliant response to nivolumab. The combination of atezolizumab (PD-L1 antibody) and bevacizumab [vascular endothelial growth factor (VEGF) antibody] has been recommended as the preferred first-line systemic therapy regimen in hepatocellular carcinoma (HCC) based on the favorable objective response rate (ORR) and survival benefit reported (38). Similarly, the clinical study of

TABLE 1 | The results of WES.

	Primary surgical tissue	Second surgical tissue
Somatic variations	*TP53 p.R213**	*TP53 p.R213**
	SMAD2 p.P305A	*SMAD2 p.P305A*
		JUN p.A111-F114del
Tumor mutation burden	2.05 Muts/Mb	4.79 Muts/Mb
Microsatellite instability	MSS	MSS
Neogenic antigen	32	54

**Nonsense mutation.*

TABLE 2 | Fifteen cases of refractory PRMS including this one.

No.	Age	Location	Treatment	Metastasis and recurrent	Prognosis	Reference
1	80	Neck	Surg, chemo	Skin	Died of disease	(13)
2	70	Left thigh	Chemo	Lung	Alive without disease 12 months	(14)
3	19	Right thigh	Immu	Lung	Durable CR after 12 months	(15)
4	78	Sacrum	Surg	Liver, lung	Died of disease after 12 months	(16)
5	43	Leg	NA	Lung	Died of disease after 6 months	(17)
6	77	Arm	Surg, chemo	Regional LN	Alive without disease 13 months	(18)
7	72	Scalp	Surg, chemo	Skin, regional LN	Alive uncertain disease status 23 months	(18)
8	78	Leg	Surg	Lung	Died of disease after 12 months	(18)
9	41	Orbit	Surg, chemo	Lung, bone, local recurrence	Died of disease after 6 months	(19)
10	65	Submandibular	Surg, chemo	Local recurrence	Alive without disease 12 months	(20)
11	89	cheek	Surg	Local recurrence	Died of disease after 2 months	(21)
12	90	Uterine	Surg	NA	Dies of disease after 6 months	(14)
13	80	Uterine	Surg, chemo	NA	Died of disease after 6 months	(14)
14	50	Back	Surg, chemo	Regional LN	Alive with disease 2 months	(22)
15	12	Left elbow	Surg, immu	Lung metastasis	Durable CR after 45 months	Present case

Chemo, chemotherapy; Immu, immunotherapy; LN, lymph nodes; NA, not available; Surg, surgery.

lenvatinib plus pembrolizumab demonstrated an impressive ORR. By blocking the FGFR4-GSK3β axis, lenvatinib reshaped Treg differentiation and reduced tumor PD-L1 levels, resulting in improved anti-PD-1 efficacy (39). In this case, the patient achieved SD after receiving pazopanib treatment (**Figures 2C1–C3**). Although the TKI was terminated due to severe adverse effects 1 month later, it is rational to speculate that pazopanib may have contributed to refining the tumor immune microenvironment and paved the way for the effects of nivolumab. Our findings suggest that TKI plus immunotherapy might be an effective option for PRMS.

CONCLUSION

Here, we described a Chinese male adolescent PRMS patient with positive PD-L1 expression and TILs who achieved a remarkable response to nivolumab following TKI therapy. The PD-L1 and CD8 statuses were informative in guiding therapy decisions for this patient. Our findings could pave the way for a better understanding of the predictive biomarkers of anti-PD-1 therapies in PRMS.

DATA AVAILABILITY STATEMENT

The original contributions presented in the study are included in the article/supplementary material. Further inquiries can be directed to the corresponding author.

ETHICS STATEMENT

The studies involving human participants were reviewed and approved by Peking University Cancer Hospital. Written informed consent to participate in this study was provided by the participants' legal guardian/next of kin.

AUTHOR CONTRIBUTIONS

JL conceived the study. PL Liu took care of the patient. YL supervised patient care. FG, YT, and XZ from 3DMed Clinical Laboratory Inc. performed WES and immunohistochemistry on tumor tissue. JL evaluated and prepared images for the manuscript. All authors contributed to the article and approved the submitted version.

FUNDING

This work was supported by grants from the National Natural Science Foundation of China (Grant No. 81802689).

ACKNOWLEDGMENTS

We gratefully acknowledge the patient and his family for allowing us to publish this clinical case, and appreciate Ting Bei's (3D Medicines Inc.) amendment opinions and revising work.

REFERENCES

1. Miwa S, Yamamoto N. Recent Advances and Challenges in the Treatment of Rhabdomyosarcoma. *Cancers (Basel)* (2020) 12(7):1758. doi: 10.3390/cancers12071758
2. Jo VY, Fletcher CD. WHO Classification of Soft Tissue Tumours: An Update Based on the 2013 (4th) Edition. *Pathology* (2014) 46(2):95–104. doi: 10.1097/pat.0000000000000050
3. Noujaim J, Thway K, Jones RL, Miah A, Khabra K, Langer R, et al. Adult Pleomorphic Rhabdomyosarcoma: A Multicentre Retrospective Study. *Anticancer Res* (2015) 35(11):6213–7.
4. Ruiz-Mesa C, Goldberg JM, Coronado Munoz AJ, Dumont SN, Trent JC. Rhabdomyosarcoma in Adults: New Perspectives on Therapy. *Curr Treat Options Oncol* (2015) 16(6):27. doi: 10.1007/s11864-015-0342-8
5. Chen C, Dorado Garcia H, Scheer M, Henssen AG. Current and Future Treatment Strategies for Rhabdomyosarcoma. *Front Oncol* (2019) 9:1458. doi: 10.3389/fonc.2019.01458
6. van der Graaf WT, Blay JY, Chawla SP, Kim DW, Bui-Nguyen B, Casali PG, et al. Pazopanib for Metastatic Soft-Tissue Sarcoma (PALETTE): A Randomised, Double-Blind, Placebo-Controlled Phase 3 Trial. *Lancet* (2012) 379(9829):1879–86. doi: 10.1016/s0140-6736(12)60651-5
7. Levi J, Lam T, Goth SR, Yaghoubi S, Bates J, Ren G. Imaging of Activated T Cells as an Early Predictor of Immune Response to Anti-PD-1 Therapy. *Cancer Res* (2019) 79(13):3455–65. doi: 10.1158/0008-5472.can-19-0267
8. Dyson KA, Stover BD, Grippin A, Mendez-Gomez HR, Lagmay J, Mitchell DA, et al. Emerging Trends in Immunotherapy for Pediatric Sarcomas. *J Hematol Oncol* (2019) 12(1):78. doi: 10.1186/s13045-019-0756-z
9. Silva MA, Triltsch N, Leis S, Kanchev I, Tan TH, Van Peel B, et al. Biomarker Recommendation for PD-1/PD-L1 Immunotherapy Development in Pediatric Cancer Based on Digital Image Analysis of PD-L1 and Immune Cells. *J Pathol Clin Res* (2020) 6(2):124–37. doi: 10.1002/cjp2.152
10. Salvador-Coloma C, Saigí M. Identification Of Actionable Genetic Targets In Primary Cardiac Sarcomas. *Onco Targets Ther* (2019) 12:9265–75. doi: 10.2147/ott.s214319
11. Tawbi HA, Burgess M, Bolejack V, Van Tine BA, Schuetze SM, Hu J, et al. Pembrolizumab in Advanced Soft-Tissue Sarcoma and Bone Sarcoma (SARC028): A Multicentre, Two-Cohort, Single-Arm, Open-Label, Phase 2 Trial. *Lancet Oncol* (2017) 18(11):1493–501. doi: 10.1016/s1470-2045(17)30624-1
12. Paoluzzi L, Cacavio A, Ghesani M, Karambelkar A, Rapkiewicz A, Weber J, et al. Response to Anti-PD1 Therapy With Nivolumab in Metastatic Sarcomas. *Clin Sarcoma Res* (2016) 6:24. doi: 10.1186/s13569-016-0064-0
13. Ansai S, Takeda H, Koseki S, Hozumi Y, Kondo S. A Patient With Rhabdomyosarcoma and Clear Cell Sarcoma of the Skin. *J Am Acad Dermatol* (1994) 31(5 Pt 2):871–6. doi: 10.1016/s0190-9622(94)70249-7
14. Ashley CW, Da Cruz Paula A, Ferrando L, Gularte-Mérida R. Genetic Characterisation of Adult Primary Pleomorphic Uterine Rhabdomyosarcoma and Comparison With Uterine Carcinosarcoma. *Histopathology* (2021) 79(2):176–86. doi: 10.1111/his.14346
15. Tlemsani C, Leroy K, Gimenez-Roqueplo AP, Mansuet-Lupo A, Pasmant E, Larousserie F, et al. Chemoresistant Pleomorphic Rhabdomyosarcoma: Whole Exome Sequencing Reveals Underlying Cancer Predisposition and Therapeutic Options. *J Med Genet* (2020) 57(2):104–8. doi: 10.1136/jmedgenet-2018-105594
16. Miracco C, Materno M, De Santi MM, Pirtoli L, Ninfo V. Unusual Second Malignancies Following Radiation Therapy: Subcutaneous Pleomorphic Rhabdomyosarcoma and Cutaneous Melanoma. Two Case Reports. *J Cutan Pathol* (2000) 27(8):419–22. doi: 10.1034/j.1600-0560.2000.027008419.x

17. Stock N, Chibon F, Binh MB, Terrier P, Michels JJ, Valo I, et al. Adult-Type Rhabdomyosarcoma: Analysis of 57 Cases With Clinicopathologic Description, Identification of 3 Morphologic Patterns and Prognosis. *Am J Surg Pathol* (2009) 33(12):1850–9. doi: 10.1097/PAS.0b013e3181be6209
18. Marburger TB, Gardner JM, Prieto VG, Billings SD. Primary Cutaneous Rhabdomyosarcoma: A Clinicopathologic Review of 11 Cases. *J Cutan Pathol* (2012) 39(11):987–95. doi: 10.1111/cup.12007
19. Scatena C, Massi D, Franchi A, De Paoli A, Canzonieri V. Rhabdomyosarcoma of the Skin Resembling Carcinosarcoma: Report of a Case and Literature Review. *Am J Dermatopathol* (2012) 34(1):e1–6. doi: 10.1097/DAD.0b013e31822381fas
20. Sabater-Marco V, Zapater Latorre E, Martorell Cebollada M. Postradiation Cutaneous Pleomorphic Rhabdomyosarcoma With Extracellular Collagen Deposits Reminiscent of So-Called Amianthoid Fibers. *J Cutan Pathol* (2014) 41(3):316–21. doi: 10.1111/cup.12282
21. Li JJ, Forstner D, Henderson C. Cutaneous Pleomorphic Rhabdomyosarcoma Occurring on Sun-Damaged Skin: A Case Report. *Am J Dermatopathol* (2015) 37(8):653–7. doi: 10.1097/dad.0000000000000191
22. Watanabe M, Ansai SI, Iwakiri I, Fukumoto T, Murakami M. Case of Pleomorphic Rhabdomyosarcoma Arising on Subcutaneous Tissue in an Adult Patient: Review of the Published Works of 13 Cases Arising on Cutaneous or Subcutaneous Tissue. *J Dermatol* (2017) 44(1):59–63. doi: 10.1111/1346-8138.13549
23. Rudzinski ER, Anderson JR, Hawkins DS, Skapek SX, Parham DM, Teot LA. The World Health Organization Classification of Skeletal Muscle Tumors in Pediatric Rhabdomyosarcoma: A Report From the Children's Oncology Group. *Arch Pathol Lab Med* (2015) 139(10):1281–7. doi: 10.5858/arpa.2014-0475-OA
24. Skapek SX, Ferrari A, Gupta AA, Lupo PJ, Butler E, Shipley J, et al. Rhabdomyosarcoma. *Nat Rev Dis Primers* (2019) 5(1):1. doi: 10.1038/s41572-018-0051-2
25. Kim C, Kim EK, Jung H, Chon HJ, Han JW, Shin KH, et al. Prognostic Implications of PD-L1 Expression in Patients With Soft Tissue Sarcoma. *BMC Cancer* (2016) 16:434. doi: 10.1186/s12885-016-2451-6
26. Reck M, Rodríguez-Abreu D, Robinson AG, Hui R, Csőszi T, Fülöp A, et al. Pembrolizumab Versus Chemotherapy for PD-L1-Positive Non-Small-Cell Lung Cancer. *N Engl J Med* (2016) 375(19):1823–33. doi: 10.1056/NEJMoa1606774
27. Le DT, Uram JN, Wang H, Bartlett BR, Kemberling H, Eyring AD, et al. PD-1 Blockade in Tumors With Mismatch-Repair Deficiency. *N Engl J Med* (2015) 372(26):2509–20. doi: 10.1056/NEJMoa1500596
28. Topalian SL, Taube JM, Anders RA, Pardoll DM. Mechanism-Driven Biomarkers to Guide Immune Checkpoint Blockade in Cancer Therapy. *Nat Rev Cancer* (2016) 16(5):275–87. doi: 10.1038/nrc.2016.36
29. Toulmonde M, Penel N, Adam J, Chevreau C, Blay JY, Le Cesne A, et al. Use of PD-1 Targeting, Macrophage Infiltration, and IDO Pathway Activation in Sarcomas: A Phase 2 Clinical Trial. *JAMA Oncol* (2018) 4(1):93–7. doi: 10.1001/jamaoncol.2017.1617
30. Bose S, Robles J. Favorable Response to Nivolumab in a Young Adult Patient With Metastatic Histiocytic Sarcoma. *Pediatr Blood Cancer* (2019) 66(1):. doi: 10.1002/pbc.27491
31. Perisano C, Vitiello R, Sgambato A, Greco T, Cianni L, Ragonesi G, et al. Evaluation of PD1 and PD-L1 Expression in High-Grade Sarcomas of the Limbs in the Adults: Possible Implications of Immunotherapy. *J Biol Regul Homeost Agents* (2020) 34(4 Suppl. 3):289–94. Congress of the Italian Orthopaedic Research Society.
32. Chowdhury F, Dunn S, Mitchell S, Mellows T, Ashton-Key M, Gray JC. PD-L1 and CD8+PD1+ Lymphocytes Exist as Targets in the Pediatric Tumor Microenvironment for Immunomodulatory Therapy. *OncoImmunology* (2015) 4(10):e1029701. doi: 10.1080/2162402X.2015.1029701
33. Kim H, Kwon HJ, Han YB, Park SY, Kim ES, Kim SH, et al. Increased CD3+ T Cells With a Low FOXP3+/CD8+ T Cell Ratio can Predict Anti-PD-1 Therapeutic Response in Non-Small Cell Lung Cancer Patients. *Mod Pathol* (2019) 32(3):367–75. doi: 10.1038/s41379-018-0142-3
34. Doyle LA, Nowak JA, Nathenson MJ, Thornton K, Wagner AJ. Characteristics of Mismatch Repair Deficiency in Sarcomas. *Mod Pathol* (2019) 32(7):977–87. doi: 10.1038/s41379-019-0202-3
35. Lewin J, Davidson S, Anderson ND, Lau BY, Kelly J, Tabori U, et al. Response to Immune Checkpoint Inhibition in Two Patients With Alveolar Soft-Part Sarcoma. *Cancer Immunol Res* (2018) 6(9):1001–7. doi: 10.1158/2326-6066.cir-18-0037
36. Chalmers ZR, Connelly CF, Fabrizio D, Gay L, Ali SM, Ennis R, et al. Analysis of 100,000 Human Cancer Genomes Reveals the Landscape of Tumor Mutational Burden. *Genome Med* (2017) 9(1):34. doi: 10.1186/s13073-017-0424-2
37. Hellmann MD, Ciuleanu TE, Pluzanski A, Lee JS, Otterson GA, Audigier-Valette C, et al. Nivolumab Plus Ipilimumab in Lung Cancer With a High Tumor Mutational Burden. *N Engl J Med* (2018) 378(22):2093–104. doi: 10.1056/NEJMoa1801946
38. Finn RS, Qin S, Ikeda M, Galle PR, Ducreux M, Kim TY, et al. Atezolizumab Plus Bevacizumab in Unresectable Hepatocellular Carcinoma. *N Engl J Med* (2020) 382(20):1894–905. doi: 10.1056/NEJMoa1915745
39. Yi C, Chen L. Lenvatinib Targets FGF Receptor 4 to Enhance Antitumor Immune Response of Anti-Programmed Cell Death-1 in HCC. *Hepatology* (2021) 74(5):2544–60. doi: 10.1002/hep.31921

Conflict of Interest: Authors FG, YT and XZ are employed by 3DMed Clinical Laboratory Inc.

The remaining authors declare that the research was conducted in the absence of any commercial or financial relationships that could be construed as a potential conflict of interest.

Publisher's Note: All claims expressed in this article are solely those of the authors and do not necessarily represent those of their affiliated organizations, or those of the publisher, the editors and the reviewers. Any product that may be evaluated in this article, or claim that may be made by its manufacturer, is not guaranteed or endorsed by the publisher.

frontiers | Frontiers in Immunology

CASE REPORT
published: 28 April 2022
doi: 10.3389/fimmu.2022.870406

Case Report: Maintenance Nivolumab in Complete Responder After Multimodality Therapy in Metastatic Pancreatic Adenocarcinoma

Shih-Hung Yang[1,2], *Jen-Chieh Lee*[3], *Bang-Bin Chen*[4], *Sung-Hsin Kuo*[1,2], *Chiun Hsu*[1,2,5] *and Li-Yuan Bai*[6*]

[1] Department of Oncology, National Taiwan University Hospital, Taipei, Taiwan, [2] Graduate Institute of Oncology, National Taiwan University College of Medicine, Taipei, Taiwan, [3] Department of Pathology, National Taiwan University Hospital, Taipei, Taiwan, [4] Department of Medical Imaging and Radiology, National Taiwan University Hospital, Taipei, Taiwan, [5] National Taiwan University Cancer Center, National Taiwan University College of Medicine, Taipei, Taiwan, [6] Division of Hematology and Oncology, Department of Internal Medicine, China Medical University Hospital, Taichung, Taiwan

OPEN ACCESS

Edited by:
Alison Taylor,
University of Leeds, United Kingdom

Reviewed by:
Antonio Barbieri,
G. Pascale National Cancer Institute Foundation (IRCCS), Italy
Naziye Ak,
Istanbul University, Turkey

***Correspondence:**
Li-Yuan Bai
lybai6@gmail.com

Specialty section:
This article was submitted to Cancer Immunity and Immunotherapy, a section of the journal Frontiers in Immunology

Received: *06 February 2022*
Accepted: *01 April 2022*
Published: *28 April 2022*

Citation:
Yang S-H, Lee J-C, Chen B-B, Kuo S-H, Hsu C and Bai L-Y (2022) Case Report: Maintenance Nivolumab in Complete Responder After Multimodality Therapy in Metastatic Pancreatic Adenocarcinoma. Front. Immunol. 13:870406. doi: 10.3389/fimmu.2022.870406

Maintenance therapy is rarely considered in pancreatic ductal adenocarcinoma (PDAC). We describe the case of a 57-year-old man with metastatic PDAC treated with an initially full but subsequently de-escalated dose of combination chemotherapy due to intolerance to neurotoxicity. After a complete response to combined radiofrequency ablation for the liver metastasis and radiotherapy for the pancreatic tumor was achieved, chemotherapy was terminated and maintenance therapy was applied: nivolumab plus cytokine-induced killer cell therapy initially and then a de-escalated dosing interval of nivolumab monotherapy subsequently. No adverse events occurred during nivolumab therapy for more than 2 years, and the patient remains disease-free. To date, this is the first report of maintenance nivolumab after successful multimodality therapy in metastatic PDAC.

Keywords: pancreatic ductal adenocarcinoma, maintenance therapy, chemotherapy, nivolumab, case report

INTRODUCTION

Pancreatic ductal adenocarcinoma (PDAC) remains the most challenging neoplasm. Multiagent chemotherapy regimens—such as gemcitabine plus nab-paclitaxel or the combination of 5-fluorouracil, folinic acid, irinotecan, and oxaliplatin (FOLFIRINOX)—remain the mainstay of treatment for patients with metastatic PDAC who have good performance status (PS) (1, 2). Although multiagent chemotherapy has notable toxicities (1, 2), mitigating these toxicities in the face of a deteriorating condition during the disease course may eventually jeopardize patients by precluding adequate chemotherapy doses in any effective regimen. Furthermore, how patients with metastatic PDAC who develop an extremely rare durable complete response (CR) to multiagent chemotherapy can be chronically managed remains unknown.

In the absence of defective mismatch repair (dMMR) or a high tumor mutation burden (TMB), immune checkpoint inhibitors (ICIs) have demonstrated modest efficacy in chemotherapy-treated

PDAC (3). In first-line settings, the addition of nivolumab or pembrolizumab to gemcitabine plus nab-paclitaxel has resulted in manageable toxicities with a greater disease control rate and duration of response than those achieved with chemotherapy alone (1, 4, 5).

Here, we report a case of metastatic PDAC on long-term maintenance nivolumab after achieving CR with multimodal therapy without toxicities.

CASE PRESENTATION

A 57-year-old man without any relevant medical history presented to our hospital in October 2018 with a 2-week history of epigastralgia. Mild epigastric tenderness was noted. The initial Eastern Cooperative Oncology Group PS was 0. Notably, his mother and sister had developed breast cancer at 80 and 42 years old, respectively. An abdominal computed tomography (CT) scan (**Figure 1A**) revealed a 5-cm mass at the pancreatic body with liver metastases and the staging of cT4N1M1. A liver biopsy revealed an adenocarcinoma with positive cytokeratin 7 staining through immunohistochemistry. The initial level of CA 19-9 was 62.7 U/ml.

Initially, the patient was enrolled in a clinical trial (NCT03162510) and treated with the SOLAR regimen consisting of oxaliplatin (75 mg/m^2, day 1), nab-paclitaxel (150 mg/m^2, day 1), S-1 (120 mg per day, days 1–7), and leucovorin in October 2018. Partial response was revealed by a CT scan after three cycles of chemotherapy. Dose de-escalation of chemotherapy was performed starting in the sixth cycle for grade 4 neutropenia. Eventually, he was withdrawn from the protocol-based chemotherapy after the 11th cycle due to intolerance to numbness. A CT scan in February 2019 demonstrated continuing shrinkage of the liver tumors and a nearly resolved pancreatic mass. He received radiofrequency ablation (RFA) for the residual liver tumor in April 2019, and reduced doses of the same chemotherapy agents were restarted concomitantly. After RFA, no [18F]-fluorodeoxyglucose uptake of liver tumors was identified through positron emission tomography (**Figure 1B**). During September and October 2019, radiotherapy to the pancreatic tumor (55 Gy) and regional lymphatic area (50 Gy) in 25 fractions was administered with reduced doses of the same chemotherapy agents.

Biweekly nivolumab (200 mg, 2.4 mg/kg) was added to the chemotherapy and radiotherapy starting in October 2019. After radiotherapy, S-1 was continued with add-on cytokine-induced killer (CIK) cell therapy, but de-escalated oxaliplatin and nab-paclitaxel were terminated in December 2019 due to severe numbness. Maintenance nivolumab therapy was performed with CIK cell therapy but without S-1 starting in February 2020. Finally, CIK cell therapy was also terminated in

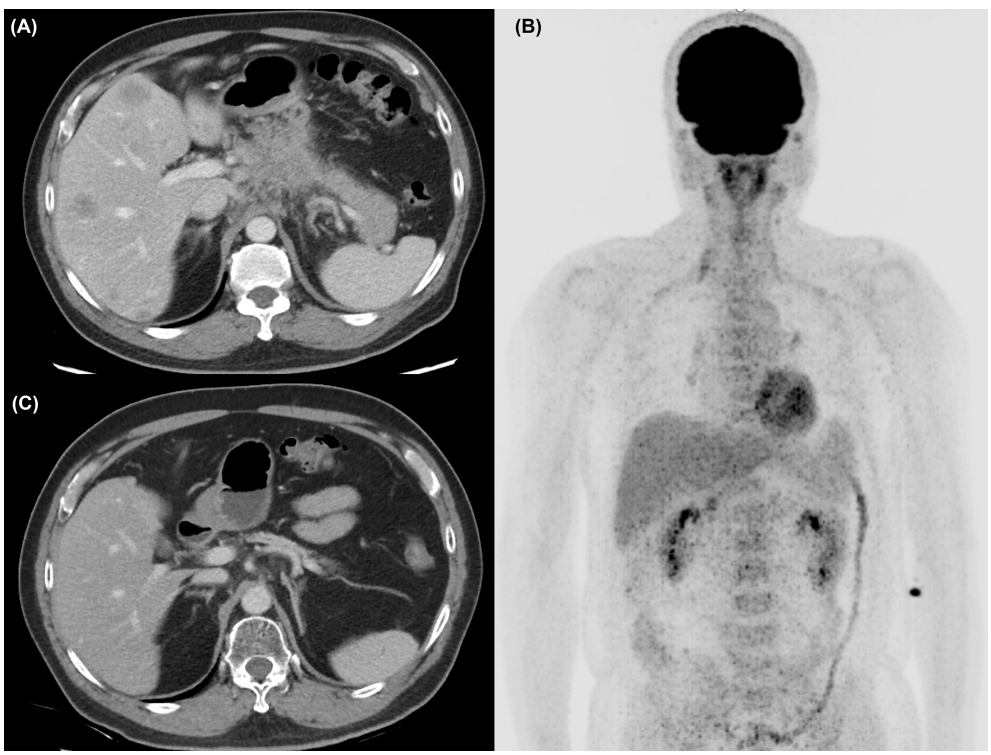

FIGURE 1 | **(A)** The abdominal computed tomography (CT) scan revealed a 5-cm mass at the pancreatic body with liver metastases at diagnosis. **(B)** After chemotherapy and RFA of liver metastasis, no [18F]-FDG uptake was identified at PET scan. **(C)** At 32 months after initial diagnosis, the patient remains disease-free under maintenance nivolumab alone.

December 2020 due to continuing CR. No adverse events were observed with nivolumab therapy and gradual prolongation of the dosing interval (2 → 4 → 6 weeks) due to financial concerns. At present, the patient is still receiving maintenance nivolumab alone every 6 weeks and remains disease-free (**Figure 1C**). The treatment course is summarized in **Figure 2**. Genetic analysis of the biopsy from liver metastasis failed due to an inadequate amount of tissue (immunohistochemistry in the **Supplemental Figures**). However, genetic analysis from peripheral blood mononuclear cells revealed heterozygous mutations of *ATM* (exon4: C283A to Q95K) and *FANCI* (exon29: C3081G to S1027R).

DISCUSSION

Maintenance therapy in metastatic PDAC has been reported from randomized trials. In the PACT-12 phase II trial, enrolled patients were treated with 6 months of first-line chemotherapy without progression (6). Even without responders, patients receiving maintenance sunitinib had a significantly higher rate of being progression-free at 6 months (PF-6m) than those only under observation (22.2% vs. 3.6%, $P < 0.01$) and better median progression-free survival (PFS; 3.2 vs. 2.0 months, $P < 0.01$) (6). The improvement of median overall survival (OS) was not significant [10.6 vs. 9.2 months; hazard ratio (HR) = 0.71; $P = 0.11$] and was probably related to more than 80% of the patients in both arms receiving second-line therapy at progression (6). By contrast, the phase III POLO trial enrolled patients with metastatic PDAC and a germline *BRCA1* or *BRCA2* mutation under disease control with ≥16 weeks of first-line platinum-based chemotherapy (7). Patients receiving maintenance olaparib had significantly longer median PFS than those on placebo (7.4 vs. 3.8 months; HR = 0.53; $P = 0.004$) as well as a superior response rate (20% vs. 10%) and PF-6m rate (53% vs. 23%) (7). Therefore, the efficacy of maintenance targeted therapy may still rely on a biological match between the drug and the tumor target. Olaparib-based maintenance therapy was not considered in our patient after the withdrawal from the platinum-containing SOLAR regimen because the genetic alterations of the tumor were not initially confirmed. The analyses of germline mutations in the blood sample were requested by the patient and performed during the nivolumab maintenance therapy. Although no germline mutation of *BRCA1* or *BRCA2* was identified, the tumor was highly suspected to have a BRCAness phenotype due to the dramatic response to the platinum-based chemotherapy and alterations in *ATM* and *FANCI*. Considering the supportive data in pancreatic cancer cell lines, targeting pathways involving homologous recombination may be useful as maintenance therapy in patients with *ATM* mutation (8).

For chemosensitive cancers, the concept of maintenance chemotherapy as a de-escalated extension of standard therapy to reduce toxicities is mainly considered in patients with tumors that are adequately stably controlled. By contrast, in advanced PDAC, maintenance chemotherapy is usually overlooked both in real-world practice and clinical trials, probably due to the poor efficacy of the chemotherapy, which results in short OS in the majority of patients. Notably, the prognosis of de-escalated maintenance chemotherapy is still dismal, with limited median PFS after reintroduction of the original regimen at progression (9). The neurotoxicity of oxaliplatin was found to be even higher after FOLFIRINOX was resumed because of a larger cumulative dose comparing to the arm of continuing FOLFIRINOX (9). Cumulative toxicity, such as neurotoxicity, may require

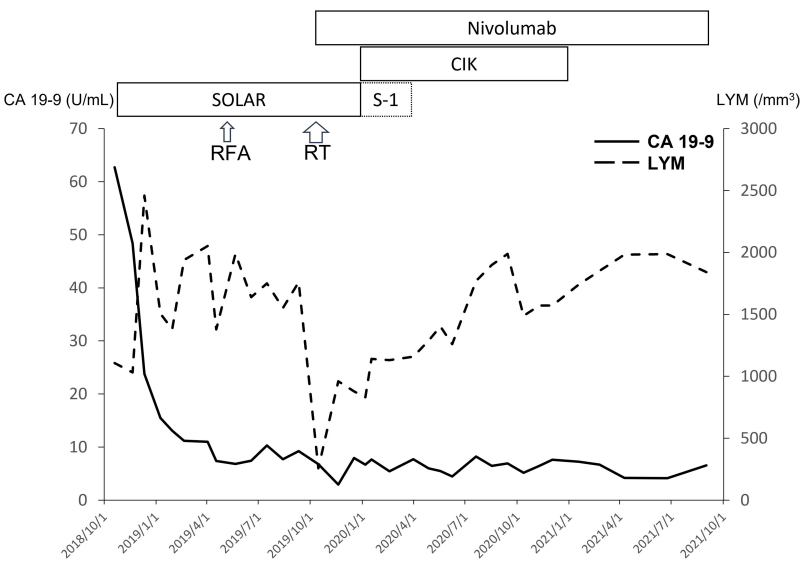

FIGURE 2 | With extreme response to the SOLAR regimen, the level of CA 19-9 decreased rapidly. The lymphocyte count (LYM) decreased after chemotherapy and RT initially but recovered with maintenance nivolumab ± CIK cell therapy.

management because in more than 40% of patients with metastatic PDAC, progression had not occurred after 6 months of first-line chemotherapy (1, 2). The results of the randomized phase II PANOPTIMOX-PRODIGE 35 trial indicated that use of a maintenance LV5FU2 regimen after disease control with eight cycles of FOLFIRINOX resulted in a comparable median PFS and OS to the complete 12 cycles of FOLFIRINOX (9). However, the highest neurotoxicity occurred later, and the median time to deterioration of quality of life in the maintenance arm was longer (9).

In the present case, after achieving an extreme response to the chemotherapy, gradual dose de-escalation of the chemotherapy combined with local treatment targeting the liver metastasis and pancreatic tumor was adopted to achieve minimal residual disease. Subsequently, gradually de-escalated maintenance immunotherapy was implemented with initially concomitant CIK cell therapy plus nivolumab followed by nivolumab alone. Indeed, a meaningful benefit has rarely been observed when ICIs have been used for blockade of the programmed cell death protein 1 (PD-1)/programmed death ligand 1 pathway in metastatic PDAC without high TMB or dMMR, even in the setting of clinical trials enrolling patients with good PS (3–5). Although information about TMB was not available, the key reason for the durable benefits of maintenance nivolumab with or without CIK cell therapy in our case may have been the balance between the extremely small tumor load and the potentially weak antitumor activity of immunotherapy for PDAC. One phase II study randomized patients with metastatic PDAC who responded or had stable disease (SD) when administered FOLFIRINOX into two groups: those with maintenance granulocyte–macrophage colony-stimulating factor-allogeneic pancreatic tumor cells (GVAX) plus ipilimumab and those for whom FOLFIRINOX was continued (10). No tumor response was observed in patients with GVAX plus ipilimumab, even the beneficial immune reactions in a patient with SD were elicited (10). Median PFS and OS were significantly worse in the immunotherapy arm (10). The failure of this trial may partially reflect the inability of weak maintenance immunotherapy to overcome insufficient prior debulking of tumors with chemotherapy. RFA in our case may have been beneficial for maintenance nivolumab due to direct reduction of the tumor burden. Remodeling of the immune microenvironment at distant non-RFA tumor sites was demonstrated in an animal model (11). As for CIK cell therapy, it is permitted and under the regulation and supervision of the Ministry of Health and Welfare in Taiwan. Infused CIK cells may provide additional source of antitumor cytotoxicity and cytokines to overcome the immunosuppressive tumor microenvironment (12).

CONCLUSION

Studies are increasingly investigating ICIs in advanced PDAC, but meaningful benefits have rarely been observed. In conclusion, our case supports further exploration of maintenance nivolumab in patients achieving optimal tumor reduction through multimodality therapy, given the relative safety of anti–PD-1 therapy compared with long-term chemotherapy.

DATA AVAILABILITY STATEMENT

The original contributions presented in the study are included in the article/**Supplementary Material**. Further inquiries can be directed to the corresponding author.

ETHICS STATEMENT

Ethical review and approval was not required for the study on human participants in accordance with the local legislation and institutional requirements. Written informed consent for participation was not required for this study in accordance with the national legislation and the institutional requirements.

AUTHOR CONTRIBUTIONS

Study design: S-HY, S-HK, and CH; Data collection and analysis: S-HY, J-CL, B-BC, and L-YB; Manuscript preparation: S-HY, J-CL, B-BC, and L-YB. All authors contributed to the article and approved the submitted version.

ACKNOWLEDGMENTS

Celgene for nab-paclitaxel and TTY Biopharm for oxaliplatin and S-1 in the clinical trial of the SOLAR regimen.

SUPPLEMENTARY MATERIAL

The Supplementary Material for this article can be found online at: https://www.frontiersin.org/articles/10.3389/fimmu.2022.870406/full#supplementary-material

Supplementary Figure | The immunohistochemical staining of the residual tissues from liver biopsy demonstrated negative staining of CD3, CD4, CD8, CD20, and PD-L1 in the tumor nest.

REFERENCES

1. Von Hoff DD, Ervin T, Arena FP, Chiorean EG, Infante J, Moore M, et al. Increased Survival in Pancreatic Cancer With Nab-Paclitaxel Plus Gemcitabine. *N Engl J Med* (2013) 369:1691–703. doi: 10.1056/NEJMoa1304369
2. Conroy T, Desseigne F, Ychou M, Bouché O, Guimbaud R, Bécouarn Y, et al. FOLFIRINOX Versus Gemcitabine for Metastatic Pancreatic Cancer. *N Engl J Med* (2011) 364:1817–25. doi: 10.1056/NEJMoa1011923
3. O'Reilly EM, Oh DY, Dhani N, Renouf DJ, Lee MA, Sun W, et al. Durvalumab With or Without Tremelimumab for Patients With Metastatic Pancreatic Ductal Adenocarcinoma: A Phase 2 Randomized Clinical Trial. *JAMA Oncol* (2019) 5:1431–8. doi: 10.1001/jamaoncol.2019.1588
4. Weiss GJ, Blaydorn L, Beck J, Bornemann-Kolatzki K, Urnovitz H, Schütz E, et al. Phase Ib/II Study of Gemcitabine, Nab-Paclitaxel, and Pembrolizumab in Metastatic Pancreatic Adenocarcinoma. *Invest New Drugs* (2018) 36:96–102. doi: 10.1007/s10637-017-0525-1

5. Wainberg ZA, Hochster HS, Kim EJ, George B, Kaylan A, Chiorean EG, et al. Open-Label, Phase I Study of Nivolumab Combined With Nab-Paclitaxel Plus Gemcitabine in Advanced Pancreatic Cancer. *Clin Cancer Res* (2020) 26:4814–22. doi: 10.1158/1078-0432.CCR-20-0099
6. Reni M, Cereda S, Milella M, Novarino A, Passardi A, Mambrini A, et al. Maintenance Sunitinib or Observation in Metastatic Pancreatic Adenocarcinoma: A Phase II Randomised Trial. *Eur J Cancer* (2013) 49:3609–15. doi: 10.1016/j.ejca.2013.06.041
7. Golan T, Hammel P, Reni M, Van Cutsem E, Macarulla T, Hall MJ, et al. Maintenance Olaparib for Germline BRCA-Mutated Metastatic Pancreatic Cancer. *N Engl J Med* (2019) 381:317–27. doi: 10.1056/NEJMoa1903387
8. Gout J, Perkhofer L, Morawe M, Arnold F, Ihle M, Biber S, et al. Synergistic Targeting and Resistance to PARP Inhibition in DNA Damage Repair-Deficient Pancreatic Cancer. *Gut* (2021) 70:743–60. doi: 10.1136/gutjnl-2019-319970
9. Dahan L, Williet N, Le Malicot K, Phelip JM, Desrame J, Bouché O, et al. Randomized Phase II Trial Evaluating Two Sequential Treatments in First Line of Metastatic Pancreatic Cancer: Results of the PANOPTIMOX-PRODIGE 35 Trial. *J Clin Oncol* (2021) 39:3242–50. doi: 10.1200/JCO.20.03329
10. Wu AA, Bever KM, Ho WJ, Fertig EJ, Niu N, Zheng L, et al. A Phase II Study of Allogeneic GM-CSF-Transfected Pancreatic Tumor Vaccine (GVAX) With Ipilimumab as Maintenance Treatment for Metastatic Pancreatic Cancer. *Clin Cancer Res* (2020) 26:5129–39. doi: 10.1158/1078-0432.CCR-20-1025
11. Fei Q, Pan Y, Lin W, Zhou Y, Yu X, Hou Z, et al. High-Dimensional Single-Cell Analysis Delineates Radiofrequency Ablation Induced Immune Microenvironmental Remodeling in Pancreatic Cancer. *Cell Death Dis* (2020) 11:589. doi: 10.1038/s41419-020-02787-1
12. Han Y, Mu D, Liu T, Zhang H, Zhang J, Li S, et al. Autologous Cytokine-Induced Killer (CIK) Cells Enhance the Clinical Response to PD-1 Blocking Antibodies in Patients With Advanced Non-Small Cell Lung Cancer: A Preliminary Study. *Thorac Cancer* (2021) 12:145–52. doi: 10.1111/1759-7714.13731

Conflict of Interest: Ono Pharmaceutical Co., Ltd. supported nivolumab for an ongoing investigator-initiated clinical trial in pancreatic cancer at National Taiwan University Hospital (principal investigator: S-HY).

The remaining authors declare that the research was conducted in the absence of any commercial or financial relationships that could be construed as a potential conflict of interest.

Publisher's Note: All claims expressed in this article are solely those of the authors and do not necessarily represent those of their affiliated organizations, or those of the publisher, the editors and the reviewers. Any product that may be evaluated in this article, or claim that may be made by its manufacturer, is not guaranteed or endorsed by the publisher.

frontiers | Frontiers in Immunology

SYSTEMATIC REVIEW
published: 06 May 2022
doi: 10.3389/fimmu.2022.861723

Effect of Concomitant Use of Analgesics on Prognosis in Patients Treated With Immune Checkpoint Inhibitors: A Systematic Review and Meta-Analysis

Ziyang Mao[1†], Xiaohui Jia[1†], Panpan Jiang[1], Qinyang Wang[1], Yajuan Zhang[1], Yanlin Li[1], Xiaolan Fu[1], Min Jiao[1], Lili Jiang[1], Zhiyan Liu[2] and Hui Guo[1,3,4*]*

[1] Department of Medical Oncology, The First Affiliated Hospital of Xi'an Jiaotong University, Xi'an, China, [2] Department of Respiratory and Critical Care Medicine, Respiratory and Critical Care Medicine, The Affiliated Hospital of Northwest University, Xi'an No. 3 Hospital, Xi'an, China, [3] Centre for Translational Medicine, The First Affiliated Hospital of Xi'an Jiaotong University, Xi'an, China, [4] Key Laboratory of Environment and Genes Related to Diseases, Xi'an Jiaotong University, Ministry of Education of China, Xi'an, China

OPEN ACCESS

Edited by:
Alison Taylor,
University of Leeds, United Kingdom

Reviewed by:
Fei Zhou,
Shanghai Pulmonary Hospital, China
Ran Wang,
Anhui Medical University, China
Irena Ilic,
University of Belgrade, Serbia

***Correspondence:**
Hui Guo
guohui@xjtufh.edu.cn
Zhiyan Liu
1441999403@qq.com

†These authors share first authorship

Specialty section:
This article was submitted to Cancer Immunity and Immunotherapy, a section of the journal Frontiers in Immunology

Received: 25 January 2022
Accepted: 06 April 2022
Published: 06 May 2022

Citation:
Mao Z, Jia X, Jiang P, Wang Q, Zhang Y, Li Y, Fu X, Jiao M, Jiang L, Liu Z and Guo H (2022) Effect of Concomitant Use of Analgesics on Prognosis in Patients Treated With Immune Checkpoint Inhibitors: A Systematic Review and Meta-Analysis. Front. Immunol. 13:861723. doi: 10.3389/fimmu.2022.861723

Background: Drug–drug interactions (DDIs) pose new challenges beyond traditional pharmacodynamics in the context of optimizing the treatment options with immune checkpoint inhibitors (ICIs). To alleviate cancer-related pain, analgesics are of absolute vital importance as chronic medications used by cancer patients. However, the possible outcome of ICI treatment concomitant with analgesics remains unclear.

Methods: Original articles describing the possible influence of analgesics use on ICI treatment published before December 1, 2021 were retrieved from PubMed, Embase, and the Cochrane Library. Odds ratio (OR) with 95% confidence interval (CI) for objective response rate (ORR), hazard ratio (HR) with 95% CI for progression-free survival (PFS), and overall survival (OS) were calculated using the random-effects or fixed-effects model, and heterogeneity was assessed using the χ^2-based *Q*-test. Publication bias was examined by funnel plot analysis.

Results: A total of 11 studies involving 4,404 patients were included. The pooled OR showed that opioid use decreased the response of opioid users to ICIs compared to non-opioid users (OR = 0.49, 95% CI = 0.37–0.65, $p < 0.001$). Compared to patients who did not receive opioids, opioid users had an increased risk of progression and mortality (HR = 1.61, 95% CI = 1.37–1.89, $p < 0.001$; HR = 1.67, 95% CI =1.30–2.14, $p < 0.001$, respectively). Furthermore, the concomitant use of non-steroidal anti-inflammatory drugs (NSAIDs) was not significantly associated with differences in ORR, PFS, and OS in patients treated with ICIs (OR = 1.40, 95% CI = 0.84–2.32, $p = 0.190$; HR = 0.90, 95% CI = 0.77–1.06, $p = 0.186$; HR = 0.90, 95% CI = 0.71–1.14, $p = 0.384$, respectively).

Conclusion: The concomitant use of opioids during ICI treatment has an adverse effect on patient prognosis, while the use of NSAIDs is not significantly associated with the prognosis in patients treated with ICIs.

Keywords: immune checkpoint inhibitors, analgesics, drug–drug interactions, prognosis, meta-analysis

INTRODUCTION

Drug–drug interactions (DDIs) are an important concern in the context of anticancer therapy due to the narrow therapeutic index and inherent toxicity of anticancer agents (1). Concomitant medications can affect the efficacy of systemic therapy through their effects on pharmacodynamics, including changes in drug absorption, distribution, metabolism, or elimination (1). Recently, DDIs have posed new challenges beyond traditional pharmacodynamics in the era of the rapid development of immune checkpoint inhibitors (ICIs). By blocking cytotoxic T-lymphocyte-associated 4 (CTLA-4) and programmed cell death protein/ligand 1 (PD-1/PD-L1), ICIs can activate the anticancer function of exhausted T cells and can elicit remarkable survival benefits to patients with multiple malignancies (2). However, ICIs are not consistently effective across different individuals (2). Although tumoral PD-L1 expression has been evaluated to predict the response to ICI therapy to a certain extent in clinical practice, it is not an entirely reliable biomarker (3). For instance, among the melanoma patients who failed to respond to ICI therapy, 48%–56% of patients were positive for PD-L1 expression (4, 5). Another conspicuous biomarker, the tumor mutation burden (TMB) is considered to be positively correlated with the efficacy of ICI therapy (6). Nevertheless, the results of the KEYNOTE-158 trial showed that there was no significant difference in prognosis between the TMB-high and TMB-low cohort among patients with advanced solid tumors receiving pembrolizumab (7). Considering these cases, exploring additional factors influencing efficacy of ICIs is urgent, among which DDI has received considerable attention from researchers.

Several studies have highlighted the link between DDI and the response to ICI therapy. Steroids, antibiotics, and proton pump inhibitors (PPIs) have been demonstrated to influence prognosis in patients treated with ICIs compared to those receiving ICI treatment (8–10). Furthermore, Cortellini et al. demonstrated worse outcomes in patients receiving steroids or PPIs might be attributed to adverse disease features, while the impact of antibiotics on clinical outcomes is presumably a consequence of immune modulation (11). Conversely, Ni et al. revealed that statins can promote anticancer immunity by downregulating PD-L1 expression (12). Accordingly, a retrospective cohort study confirmed that administration of statins during ICI treatment was associated with improved prognosis in patients with malignant pleural mesothelioma or advanced non-small cell lung cancer (NSCLC) (13). Thus, DDIs play an important role in the influence of concomitant medications on the efficacy of ICIs.

In addition to the above medications, analgesics use is also critical to cancer patients. Approximately 30%–50% of cancer patients will experience moderate to severe pain, usually at multiple sites, with different etiologies and potential mechanisms (14). As for the therapeutic approach, the World Health Organization (WHO) recommends an analgesic ladder based on pain intensity [i.e., non-steroidal anti-inflammatory drugs (NSAIDs) for mild pain leading up to strong opioids for severe chronic pain] (15). However, the possible influence of DDIs between ICIs and analgesics on the efficacy of ICIs, including opioids and NSAIDs, remains unclear and lacks clinical evidence. Many preclinical studies have highlighted that opioids can promote tumor progression and metastasis directly as opioid receptors are overexpressed in several tumors (16, 17), which, in turn, may impair the response to treatment with ICIs. Furthermore, opioids can suppress the immune system in various ways, such as by affecting T-cell function, upregulating regulatory T cells (Tregs), and interfering with the composition of the intestinal microbiota that damages the entire immune system (18–21). Conversely, *via* their inhibition of cyclooxygenase-2 (COX-2), NSAIDs may be beneficial for the treatment of ICIs, since overexpression of COX-2 has been found in a wide range of tumors, and is associated with malignant tumor phenotypes and negative regulation of anticancer immunity (22–25).

Several retrospective cohort studies have explored the association of analgesics use with the efficacy of ICIs in advanced cancer patients (26–36). Most evidence suggests that opioids could cause a poor prognosis in patients treated with ICIs, while NSAIDs do not weaken the efficacy of ICIs. However, these are all retrospective cohort studies with a small sample size and conclusions are not sufficiently convincing. The exact effect of analgesics on ICI treatment deserves to be further explored, with due consideration on both pain alleviation and efficacy of ICI treatment, which are crucial for optimizing benefits to patients. Therefore, additional higher-level evidence-based research is needed to dispel doubts and better guide clinical practice. Given the above evidence, we conducted this meta-analysis to determine the effect of concomitant use of analgesics on outcomes in patients receiving treatment with ICIs.

MATERIALS AND METHODS

This meta-analysis was performed in accordance with the preferred reporting items for systematic reviews and meta-analyses (PRISMA) guidelines (37). We designed a formal protocol for this meta-analysis, which was registered in the Prospective Register of Systematic Reviews (PROSPERO CRD42021288940).

Search Strategy

We systematically conducted an electronic search using PubMed, Embase, and the Cochrane Library to identify potentially

relevant studies. Results from International conferences, such as the American Society of Clinical Oncology (ASCO), the European Society of Medical Oncology (ESMO), and the American Association for Cancer Research (AACR) were also selected to avoid any loss of information. Studies were identified using free text including the following terms: neoplasm, malignancy, ICIs, anti-PD1, anti-PD-L1, opioids, and NSAIDs, as well as specific drug names. The search was limited to studies published in English and published before December 1, 2021. Two authors (ZM and XJ) established the comprehensive search strategy, which is presented in **Table S1**.

Inclusion and Exclusion Criteria

A study was included when all the following criteria were met: (a) involved patients with solid tumors or hematological malignancy treated with ICIs; (b) explored the DDI between ICIs and analgesics (opioids and NSAIDs); (c) involved primary endpoints, such as objective response rate (ORR), progression-free survival (PFS), and overall survival (OS); and (d) provided sufficient data to calculate the odds ratio (OR) or hazard ratio (HR) with 95% confidence interval (CI). Accordingly, the exclusion criteria were as follows: (a) lack of related or sufficient data; (b) designed as single-arm or dosage-finding studies; and (c) published as a meta-analysis, editorial, review, or case report. Two authors (ZM and XJ) checked the studies, and disagreements were decided by two senior investigators (HG and ZL).

Data Extraction and Quality Assessment

The studies that met the inclusion criteria were selected and analyzed by two authors (PJ and QW). The following elements were extracted for each included study: first author's surname, publication year, country of origin, sample size, type of concomitant analgesics received, type of study design, analysis, cancer type, ICIs type, line of treatment, median PFS and OS, OR for ORR with 95% CI, HR for PFS, and OS with 95% CI. Discrepancies were solved by the other two authors (YZ and YL).

Three independent authors (XF, MJ, and LJ) assessed the quality of the included studies by using the Quality Assessment of Newcastle–Ottawa Scale (NOS) for cohort studies (38). Discrepancies were resolved through discussion among all researchers. The total scores ranged from 0 (worst) to 9 (best), and NOS scores >6 indicated high-quality studies (38).

Statistical Analysis

ORs with 95% CI for ORR from included studies were utilized to calculate the pooled OR. HRs with 95% CI for PFS or OS were synthesized in this meta-analysis. ORR was defined as proportion of complete response (CR) and partial response (PR) according to the Response Evaluation Criteria in Solid Tumors (RECIST) criteria (version 1.1) (39). PFS was defined as the time from initiation of ICIs to the date of disease progression or death from any cause, while OS was defined as the time from initiation of ICI treatment to the date of death from any cause. The heterogeneity of the pooled results was evaluated using the χ^2-based Q-test and quantified using the I^2 test. If p was < 0.10 for the Q-test or I^2 was >50%, we recognized significant heterogeneity, and the random-effects model was utilized to synthesize the data. Otherwise, the fixed-effects model was adopted (40). Subgroup analysis was performed mainly according to the cancer type and ICI type. Funnel plots were constructed to evaluate publication bias. Sensitivity analysis was used to examine the stability of the outcome. All statistical tests were two-sided and a p-value < 0.05 was considered statistically significant. Review Manager, version 5.3 (The Nordic Cochrane Centre, The Cochrane Collaboration, Copenhagen, Denmark) was used for all pooled analysis and GraphPad Prism, version 9.0.0 (GraphPad Software Inc., La Jolla, CA, USA) was used to construct graphical charts.

RESULTS

Selection of Eligible Studies

Figure 1 shows the flowchart used for the identification of eligible studies and the inclusion and exclusion criteria. A total of 417 studies were identified from the electronic databases. After removing duplicates and screening titles and abstracts, 57 potentially relevant studies remained for further eligibility evaluation. After a complete evaluation, 46 ineligible studies were excluded and 11 studies that explored the effect of concomitant analgesics on the survival of patients receiving ICIs were ultimately included in this meta-analysis.

Characteristics of the Included Studies

All included studies (26–36) were retrospective, and a total of 4,404 participants were enrolled. Among them, two studies (31, 35) evaluated both NSAIDs and opioids, five studies (30, 32–34, 36) that only evaluated NSAIDs, and four studies (26–29) only evaluated opioids. Four studies (27, 30, 31, 33) only included patients with NSCLC and two studies (34, 36) only included melanoma patients. The remaining studies (26, 28, 29, 32, 35) included both NSCLC and melanoma or other types of cancer. Additional characteristics of these studies are listed in **Table 1**. The quality of these studies quantified by the NOS criteria ranged from 6 to 9, showing that all studies were of high quality and qualified for analysis. Details of the quality assessment are shown in **Table S2**.

Concomitant Use of Opioids on ICIs Efficacy

Five studies reported the influence of opioid use on ORR in patients treated with ICIs. The pooled OR showed that the use of opioids decreased the response of opioid users to ICI treatment compared to non-opioid users (OR = 0.49, 95% CI = 0.37–0.65, p < 0.001) (**Figure 2A**). Furthermore, low heterogeneity was detected in the heterogeneity test (I^2 = 32%, Q-test p = 0.210).

Four studies used PFS as an indicator of outcome. The analysis of this study showed that compared to non-opioid users, the use of opioids increased the risk of progression by 61% among opioid users (HR = 1.61, 95% CI = 1.37–1.89, p < 0.001) (**Figure 2B**). Furthermore, no significant heterogeneity was observed in these studies (I^2 = 0%, Q-test p = 0.470).

OS data were available in six studies. Because the heterogeneity test showed a high level of heterogeneity (I^2 =

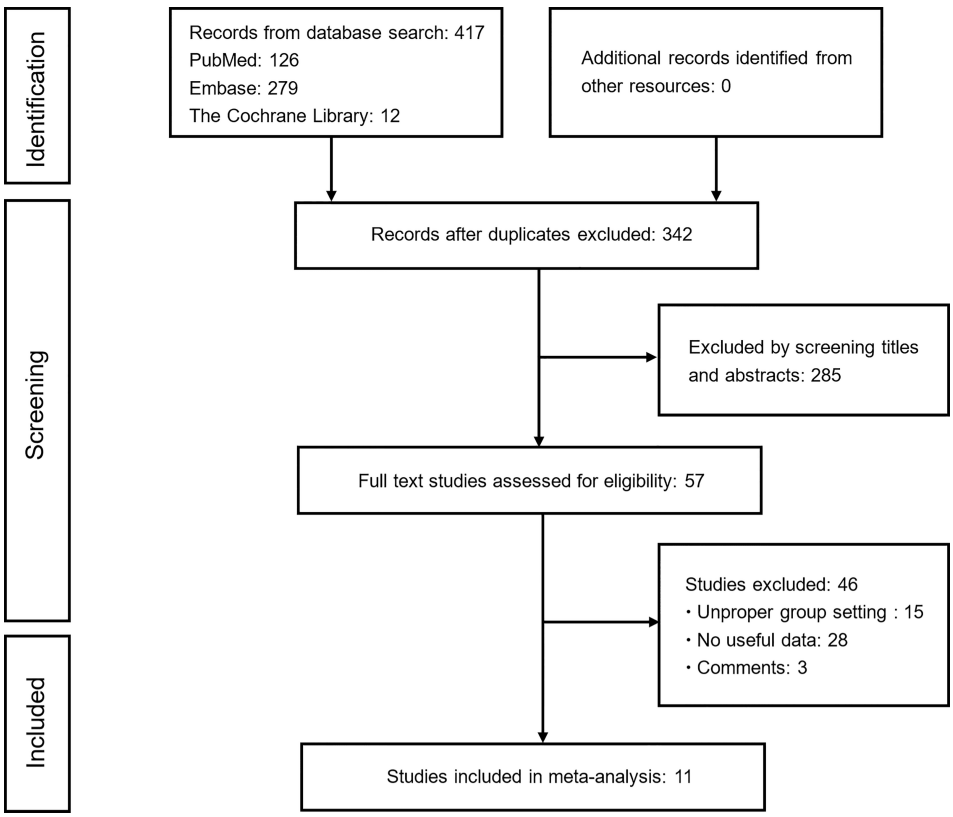

FIGURE 1 | Flowchart of study selection. Based on the inclusion and exclusion criteria, 11 studies were included in this study.

69%, *Q*-test $p = 0.007$) in these studies, we used a random-effects model for analysis. The pooled data for HR showed that the concomitant use of opioids was significantly associated with a poorer OS in patients receiving ICIs (HR = 1.67, 95% CI =1.30–2.14, $p < 0.001$) (**Figure 2C**).

Concomitant Use of NSAIDs on the Efficacy of ICIs

Seven studies evaluated the effect of concomitant use of NSAIDs on ORR in patients receiving ICI treatment. A highly significant heterogeneity was observed in these studies ($I^2 = 75\%$, *Q*-test $p < 0.001$); thus, the random-effects model was adopted for analysis. The pooled OR showed that the use of NSAIDs did not significantly influence ORR in patients during ICI treatment (OR = 1.40, 95% CI = 0.84–2.32, $p = 0.190$) (**Figure 3A**).

Five studies reported PFS data. Our analysis showed that compared to non-NSAID users, NSAID use did not significantly influence PFS among NSAID users (HR = 0.90, 95% CI = 0.77–1.06, $p = 0.186$) (**Figure 3B**). Furthermore, no significant heterogeneity was detected in all five studies ($I^2 = 21\%$, *Q*-test $p = 0.210$).

OS data were available in seven studies. Due to the high heterogeneity ($I^2 = 54\%$, $p = 0.030$), a random-effects model was used for the analysis. The pooled HR data showed that the concomitant use of NSAIDs was not significantly associated with OS in patients treated with ICIs (HR = 0.90, 95% CI = 0.71–1.14, $p = 0.384$) (**Figure 3C**).

Subgroup Analysis

A further subgroup analysis was performed according to the following variables: cancer type (NSCLC and melanoma) and ICI type (anti-CTLA-4, anti-PD-1, and anti-PD-L1). The results are presented in **Table 2**. These were basically consistent with the results of the entire population: opioid use during ICI treatment was significantly associated with a poor prognosis, while NSAID use did not influence prognosis in ICI-treated patients. In particular, NSAIDs were significantly associated with better PFS in patients in the anti-PD-1 subgroup (HR = 0.74, 95% CI = 0.58-0.96, $p = 0.020$).

Sensitivity Analysis

Regarding the comparison between opioid users and nonopioid users, the pooled ORs for ORR were stable in the sensitivity analysis, ranging from 0.42 [95% CI = 0.30–0.50, after excluding the study by Cortellini et al., 2020 (35)] to 0.55 [95% CI = 0.39–0.78, after excluding the study by Gaucher et al., 2021 (29)] (**Figure S1A**). The pooled HRs for PFS were also stable in the sensitivity analysis, ranging from 1.56 [95% CI = 1.32–1.85, after excluding Iglesias–Santamaría et al., 2020 (28)] to 1.82 (95% CI = 1.44–2.30, after excluding Botticelli et al., 2021) (**Figure S1B**). In

TABLE 1 | Baseline characteristics of studies included in the meta-analysis.

Concomitant medications	Study (years)	Country	Study design	Cancer type	ICIs treatment	Line of ICIs treatment	Patients (n) (Users/non-users)	Outcome	ORR(%) (Users vs non-users)	mPFS (months) (Users vs non-users)	mOS (months) (Users vs non-users)	Type of analysis
Opioids	Iglesias–Santamaría et al., 2020 (28)	Spain	Retrospective	Melanoma, NSCLC, Others	Atezo, Nivo, Pembro, Nivo + Ipi	≥1	55/47	PFS/OS	NA	4.5 vs 8.1	8.6 vs 26.3	Multivariate
	Cortellini et al., 2020 (35)	Italy	Retrospective	Melanoma, NSCLC, Others	Atezo, Nivo, Pembro, Others	≥1	68/944	ORR/ PFS/OS	32.2 vs 38.6	NA	NA	Multivariate
	Taniguchi et al., 2020 (27)	Japan	Retrospective	NSCLC	Nivo	≥1	38/38	ORR/ PFS/OS	2.6 vs 21.1	1.2 vs 2.1	4.2 vs 9.6	Univariate
	Botticelli et al., 2021 (26)	Italy	Retrospective	Melanoma, NSCLC, Others	Atezo, Nivo, Pembro, Avelu	≥1	42/151	ORR/ PFS/OS	31.0 vs 52.3	3.0 vs 19.0	4.0 vs 35.0	Multivariate
	Miura et al., 2021 (31)	Japan	Retrospective	NSCLC	Nivo, Pembro	≥1	114/186	ORR/OS	13.9 vs 26.9	NA	5.7 vs 15.9	Multivariate
	Gaucher et al., 2021 (29)	France	Retrospective	Melanoma NSCLC Others	Ipi, Nivo, Pembro, Nivo + Ipi	1/2/3	173/199	ORR/ PFS/OS	16.2 vs 33.7	NA	8.5 vs 29.4	Multivariate
NSAIDs	Failing et al., 2016 (36)	US	Retrospective	Melanoma	Ipi	1	31/128	ORR/ PFS/OS	71.0 vs 64.1	NA	NA	Multivariate
	Cortellini et al., 2020 (35)	Italy	Retrospective	Melanoma, NSCLC, Others	Atezo, Nivo, Pembro, Others	≥1	59/953	ORR/ PFS/OS	27.3 vs 38.2	NA	NA	Multivariate
	Wang et al., 2020 (34)	Multicountry	Retrospective	Melanoma,	Nivo, Pembro	1	122/208	ORR/ PFS/OS	43.4 vs 41.3	8.5 vs 5.2	25.7 vs 27.3	Univariate
	Svaton et al., 2020 (33)	Czech	Retrospective	NSCLC	Nivo	1/2/3/4/5/6	45/178	PFS/OS	33.3 vs 28.1	6.9 vs 5.3	16.8 vs 12.8	Multivariate
	Wang et al., 2020 (32)	US	Retrospective	Melanoma, NSCLC	PD-1/L1 inhibitors, CTLA-4 inhibitors	NA	Melanoma: 32/58 NSCLC: 20/17	ORR/OS	Melanoma: 59.3 vs 19.0 NSCLC: 75.0 vs 35.3	NA	Melanoma: 25.4 vs 22.1 NSCLC: 37.7 vs 14.3	Multivariate
	Miura et al., 2021 (31)	Japan	Retrospective	NSCLC	Nivo, Pembro	≥1	140/160	ORR/OS	18.6 vs 27.5	NA	8.8 vs 15.9	Multivariate
	Kanai et al., 2021 (30)	Japan	Retrospective	NSCLC	Atezo, Nivo, Pembro	2/3	65/133	ORR/ PFS/OS	20.0 vs 12.0	3.45 vs 3.94	7.85 vs 15.11	Univariate

ORR, objective response rate; mPFS, median progression-free survival; mOS, median overall survival; NSCLC, non-small cell lung cancer; NSAIDs, non-steroidal anti-inflammatory drugs; Ipi, Ipilimumab; Atezo, Atezolizumab; Nivo, Nivolumab; Pembro, Pembro- lizumab; Avelu, Avelumab; PD-1/L1, programmed cell death protein/ligand 1; CTLA-4, T-lymphocyte-associated 4; NA, not available.

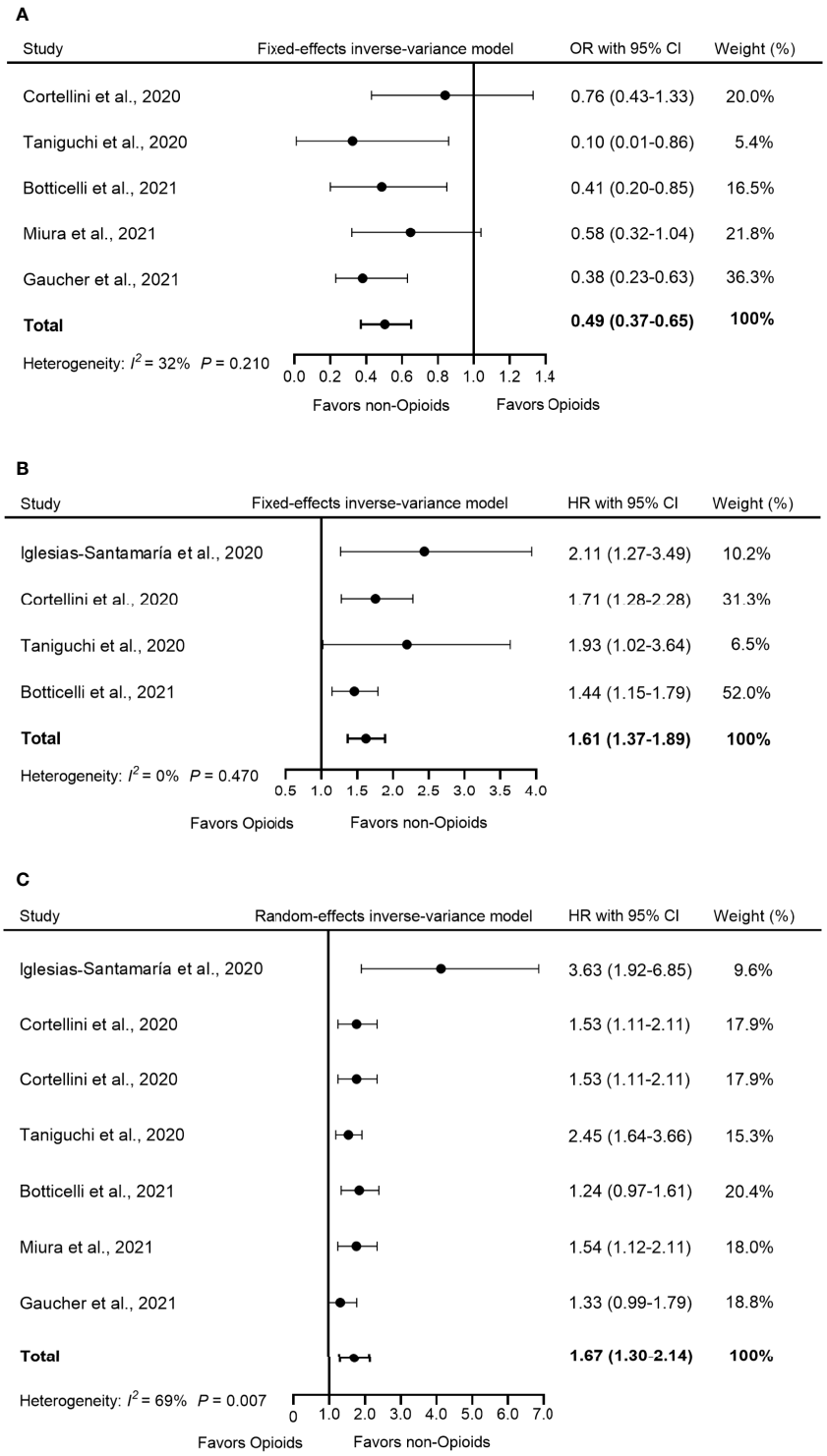

FIGURE 2 | Forest plot of the correlation between concomitant use of opioids and **(A)** ORR, **(B)** PFS, and **(C)** OS in patients receiving ICIs. The pooled OR of ORR was 0.49 (95% CI = 0.37–0.65, $p < 0.001$) and the fixed-effects model was adopted. The pooled HR of PFS was 1.61 (95% CI = 1.37–1.89, $p < 0.001$) and the fixed-effects model was adopted. The combined HR of OS was 1.67 (95% CI = 1.30–2.14, $p < 0.001$) and the random-effects model was adopted. By definition, OR > 1 or HR < 1 implied a better prognosis for opioid users. ORR, objective response rate; PFS, progression-free survival; OS, overall survival; OR, odds ratio; HR, hazard ratio; CI, confidence interval; ICIs, immune checkpoints inhibitors.

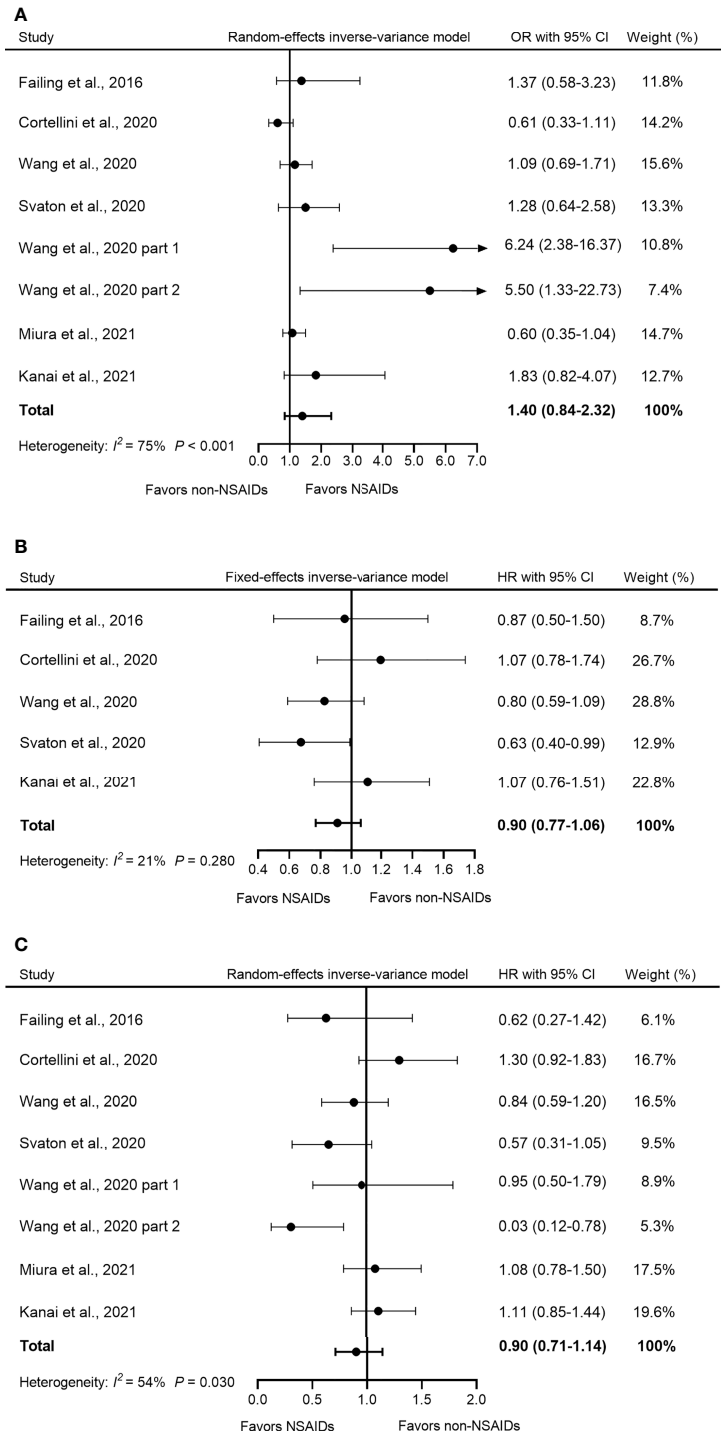

FIGURE 3 | Forest plot of the correlation between concomitant use of NSAIDs and **(A)** ORR, **(B)** PFS, and **(C)** OS in patients receiving ICIs. The study of Wang et al. (2020) included two parts: melanoma and NSCLC with reported OR and OS respectively, so we named them "Wang et al., 2020 part 1" and "Wang et al., 2020 part 2". The pooled OR of ORR was 1.40 (95% CI = 0.84–2.32, p = 0.190) and the random-effects model was adopted. The pooled HR of PFS was 0.90 (95% CI = 0.77–1.06, p = 0.186) and the fixed-effects model was adopted. The combined HR of OS was 0.90 (95% CI = 0.71–1.14, p = 0.384) and the random-effects model was adopted. By definition, OR > 1 or HR < 1 implied a better prognosis for NSAID users. NSAIDs, non-steroidal anti-inflammatory drugs; ORR, objective response rate; PFS, progression-free survival; OS, overall survival; OR, odds ratio; HR, hazard ratio; CI, confidence interval; ICIs, immune checkpoints inhibitors.

addition, the pooled HRs for OS did not change significantly in the sensitivity analysis and ranged from 1.52 [95% CI = 1.24–1.86, after excluding Iglesias–Santamaría et al., 2020 (28)] to 1.81 [95% CI = 1.36–2.41, after excluding Botticelli et al., 2021 (26)] (**Figure S1C**).

Comparison of NSAID users and non-NSAID users showed that the pooled ORs for ORR were stable in the sensitivity analysis, ranging from 1.11 (95% CI = 0.74–1.68, after excluding Wang et al., 2020 part 1) to 1.61 [95% CI = 0.93–2.87, after excluding Cortellini et al., 2020 (35) or 95% CI = 0.94–2.77, after excluding Miura et al., 2021 (31)] (**Figure S2A**). The pooled HR for PFS was also stable, ranging from 0.85 [95% CI = 0.70–1.03, after excluding Cortellini et al., 2020 (35)] to 0.95 (95% CI = 0.78–1.15, after excluding Wang et al., 2020 or 95% CI = 0.80–1.13, after excluding Svaton et al., 2020) (**Figure S2B**). Similarly, the pooled HRs for OS did not significantly influence the sensitivity analysis, ranging from 0.68 (95% CI = 0.90–1.19, after excluding Wang et al., 2020) to 0.99 (95% CI = 0.82–1.19, after excluding Wang et al., 2020 part 2) (**Figure S2C**).

Publication Bias Analysis

Funnel plots were used to determine whether there was evidence of publication bias for pooled HRs for ORR, PFS, or OS analysis. In general, the funnel plots were distributed symmetrically, and the publication bias was modest (**Figures S3A–F**).

DISCUSSION

DDIs represent a key area of interest in the context of the urgent need to accelerate the selection process for distinguishing patients who will benefit from ICI therapy. Of all the medications that cancer patients require on a daily basis, analgesics represent a considerable proportion (14). However, the potential effect of ICI interactions with analgesics on alleviating cancer pain remains undetermined. In this study, we found that the use of opioids during ICI treatment showed an adverse effect on the prognosis of patients, while the concomitant use of NSAIDs could not significantly influence the prognosis in patients receiving ICIs.

Opioids are feasible analgesics for severe pain; they act by activating the μ opioid receptor (MOR), which results in a decrease in afferent nociceptive neuronal depolarization, thus producing the analgesic effect (41). However, many preclinical studies have reported that the interaction between opioids and MOR can affect the development of multiple cancers through different mechanisms. Morphine (an opioid)-induced phosphorylation of the epidermal growth factor receptor (EGFR) occurs *via* MOR in NSCLC cell lines, facilitating tumor proliferation and invasion (16). Morphine can also activate the MAPK/ERK signaling pathway in microvascular endothelial cells, which stimulates angiogenesis of breast tumors (17). Furthermore, in colon cancer, morphine can induce the secretion of urokinase plasminogen activator (uPA) that plays a crucial role in the degradation of the extracellular matrix, facilitating tumor invasion and metastasis. Opioid antagonists such as naloxone can reverse morphine-induced upregulation of uPA (42). In summary, opioids can directly promote tumor growth, which could impair the efficacy of ICIs.

In addition to the intrinsic traits of tumors, the efficacy of ICIs also depends on anticancer immunity. Opioids are potentially an incentive to the immunosuppressive tumor microenvironment (TME), which can be an impediment to treatment with ICIs. An *in vitro* study has shown that morphine can block IL-2 transcription, an iconic cytokine involved in the activation of $CD8^+$ T cells (18). Furthermore, opioids such as morphine and β-endorphin can induce a significant increase in cAMP, which ultimately blocks the initiation of T-cell receptor signaling and results in impairment of $CD8^+$ T cell function in the activation stage (18). In terms of antigen-presenting cell (APC) function in T cells, morphine can downregulate major histocompatibility complex class II expression, which inhibits the activation and proliferation of the $CD4^+$ T cells. Inactivation of $CD4^+$ T cells will further cause a decrease in the secretion of IL-2 and IFN-γ, impairing cytotoxic T lymphocyte-mediated tumor killing activity (43). Not all immune cells are conducive to the anticancer response, such as Tregs (44). Cornwell et al. demonstrated that long-term exposure to morphine can upregulate circulating Tregs ($CD25^+Foxp3^+$) levels in peripheral blood mononuclear cell samples by approximately five times in the rhesus monkey (19). In addition, another study also showed that the number of Tregs in breast cancer patients who have undergone surgery and were treated with sufentanil or fentanyl (belonging to opioids) increased significantly after 7 days (45).

There is convincing evidence supporting a link between gut dysbiosis and the efficacy of ICIs. Both quantitative and qualitative imbalances in the microbiota can potentially decrease the patient's response to ICIs (46, 47). Long-term use of opioids has been definitely associated with gastrointestinal side effects, including constipation, bloating, nausea, and vomiting (41). Specifically, opioids can suppress protective mucus and bicarbonate secretion from the intestinal epithelium and weaken coordinated myenteric activity, thus delaying transit time and potentially increasing the risk of bacterial translocation in the human body (20). *In vivo* and *in vitro*, morphine has been shown to destroy the intestinal epithelial integrity by damaging the distribution of tight junction protein (ZO-1) in intestinal epithelial cells. As a result, the risk of *Escherichia coli* bacteria translocation to the mesenteric lymph nodes of mice increases after morphine treatment, inducing damage to the immune system (21). Furthermore, chronic morphine treatment can significantly alter the intestinal microbiota composition and induce a prominent proliferation of pathogenic Gram-positive bacteria and a decrease in bile-deconjugating bacterial strains. Intriguingly, morphine-induced microbial dysbiosis and intestinal barrier destruction can be rescued by transplanting the placebo-treated microbiota into morphine-treated animals (48).

Contrary to opioids, NSAIDs probably play a role in the inhibition of malignancies. The analgesic action of NSAIDs,

TABLE 2 | Results of subgroup analysis.

Concomitant medications	Analysis	ORR				PFS				OS			
		Association			Heterogeneity	Association			Heterogeneity	Association			Heterogeneity
		N	OR (95% CI)	*P*	I^2	N	HR (95% CI)	*P*	I^2	N	HR (95% CI)	*P*	I^2
Opioids	**Total**	6	0.49 (0.37-0.65)	**<0.001**	32%	4	1.61 (1.37-1.89)	**<0.001**	0%	6	1.67 (1.30-2.14)	**<0.001**	69%
	Cancer type												
	NSCLC	2	0.48 (0.28-0.84)	**0.010**	59%	2	2.04 (1.37-3.03)	**<0.001**	0%	2	2.75 (1.94-3.91)	**<0.001**	0%
	Melanoma	–	–	–	–	–	–	–	–	–	–	–	–
	ICIs type												
	Anti-CTLA-4	–	–	–	–	–	–	–	–	–	–	–	–
	Anti-PD-1	2	0.48 (0.28-0.84)	**0.010**	59%	1	1.93 (1.02-3.65)	**0.040**	0%	2	1.91 (1.21-3.01)	**0.005**	68%
	Anti-PD-L1	–	–	–	–	–	–	–	–	–	–	–	–
NSAIDs	**Total**	8*	1.40 (0.84-2.32)	0.190	75%	5	0.90 (0.77-1.06)	0.186	21%	8*	0.90 (0.71-1.14)	0.384	54%
	Cancer type												
	NSCLC	4	1.41 (0.65-3.06)	0.380	73%	2	0.84 (0.50-1.41)	0.510	70%	4	0.80 (0.52-1.22)	0.310	72%
	Melanoma	3	1.97 (0.74-5.25)	0.170	81%	2	0.82 (0.62-1.07)	0.164	0%	3	0.83 (0.62-1.11)	0.211	0%
	ICIs type												
	Anti-CTLA-4	1	1.37 (0.58-3.23)	0.470	0%	1	0.87 (0.50-1.51)	0.620	0%	1	0.62 (0.27-1.42)	0.260	0%
	Anti-PD-1	3	0.93 (0.60-1.44)	0.740	46%	2	0.74 (0.58-0.96)	**0.020**	0%	3	0.87 (0.63-1.18)	0.360	43%
	Anti-PD-L1	–	–	–	–	–	–	–	–	–	–	–	–

*ORR, objective response rate; PFS, progression-free survival; OS, overall survival; HR, hazard ratio; NSCLC, non-small cell lung cancer; NSAIDs, non-steroidal anti-inflammatory drugs; NOS, Newcastle–Ottawa Scale.Annotation: *The study by Wang SJ et al. included two parts and showed the HR and 95% CI respectively, and the total number refers to cohorts rather than studies.*

particularly selective COX-2 inhibitors, has been explained on the basis of their inhibition of enzymes that synthesize prostaglandin E2 (PGE2) (49). Substantial evidence from preclinical studies has shown that overexpression of COX-2/PGE2 in multiple cancers is associated with many malignant phenotypes. In NSCLC, PGE2 can bind to the EP3 receptor, which promotes EGFR translocation. EGFR entering the nucleus can promote the expression of c-myc, cyclin D1, and PTGS2, and can contribute to tumor cell proliferation (22). Furthermore, COX-2/PGE2 can upregulate the expression of vascular endothelial growth factor receptor-1 in colon cancer by binding to EP3. This process can increase tumor angiogenesis and metastasis (23). In addition, COX-2/PGE2 can upregulate β1-integrin expression, to facilitate the invasion and migration of tumor cells (50). Consequently, NSAIDs are potentially able to favor cancer prophylaxis and regression by inhibiting COX-2/PGE2, which may partly explain why NSAIDs may improve survival in patients receiving ICIs to a certain extent compared to opioids.

In addition to directly regulating tumor progression, COX-2/PGE2 can also mediate reprogramming of the TME, leaving the TME in an immunosuppressive state. The malate–aspartate shuttle (MAS) system is critical to maintaining the redox equilibrium between mitochondria and cytoplasm in various cells (51). COX-2/PGE2 can seriously damage the MAS system in $CD8^+$ T cells. As a result, there is a marked decrease in the content of aspartic acid and of various enzymes in the MAS system, resulting in the growth arrest of $CD8^+$ T cells (24, 25). This might represent the key mechanism by which COX-2/PGE2 downregulates $CD8^+$ T cells in the TME. COX-2/PGE2 can also inhibit the secretion of CCL5 and XCL1 by natural killer (NK) cells and the expression of CCR5 and XCR1 in conventional type 1 dendritic cells (cDC1), which can impair the function of NK cells and the accumulation of cDC1 in the TME, which are responsible for tumor immunity (24). Furthermore, downregulation of RIPK3 in myeloid-derived suppressor cells (MDSCs) can promote the activation of the COX-2/PGE2 axis and can generate a large amount of PGE2, which promotes the polarization of MDSCs to M2-type macrophages. At the same time, PGE2 can further reduce RIPK3 levels, forming a positive feedback loop to further promote the immunosuppressive activity of MDSCs (52). Taken together, NSAIDs, as inhibitors of COX-2/PGE2, are potentially able to reverse the immunosuppressive TME by increasing the infiltration of

$CD8^+$ T cells or other killer cells and by suppressing the function of MDSCs. Therefore, compared to opioids, NSAIDs and ICIs have synergistic effects, which may increase the therapeutic response of patients to ICIs.

Studies evaluating NSAIDs have also reported a lack of beneficial effect of concomitant use with ICIs [such as Miura et al., 2021 (31), Kanai et al., 2021 (30)], whereas Svaton et al. (2020) (33) reported higher ORR and longer OS and PFS in NSAID users, although the differences in most results were not statistically significant. A possible explanation is that the time of administration of NSAIDs may have affected the results. In Svaton et al. (33), patients started taking NSAIDs 1 month before treatment with ICIs. However, NSAIDs were used in Miura et al. (31) only at the start of ICI treatment. This suggests that only the prolonged administration of NSAIDs may improve the efficacy of treatment with ICIs. Clinicians should reasonably control the duration of NSAID treatment when combined with ICIs. Furthermore, NSAID users in Kanai et al. (30) had a higher prevalence of bone metastasis. It has been reported that bone metastasis can hinder the development of T cells and, thus, undermine the efficacy of ICI treatment (53). Therefore, future research on NSAIDs should give greater consideration to the effects of cancer pain associated with bone metastasis on outcome.

To our knowledge, this is the first meta-analysis to assess the influence of analgesics on the treatment of ICIs. Our study provides some useful information to oncologists in their clinical practice. Chronic use of opioids should be limited or replaced with NSAIDs as much as possible, to prevent the negative impact on concomitant treatment with ICIs and improve survival rates. For patients experiencing severe pain that is inadequately treated with NSAIDs, proper management of opioids is crucial to balance a pain-free period without influencing the outcome of ICI treatment. Opioids with weak or no immune modulation, such as buprenorphine, oxycodone, hydromorphone, and tramadol should be given before morphine, fentanyl, or codeine, which possess powerful immunosuppressive effects (54). In addition, it is necessary to apply some biological agents to regulate the gut microbiota and increase the efficacy of ICI treatment during the period when opioids are applied.

Certainly, our study has some intrinsic limitations. First, all included studies were retrospective designs, possibly lacking scientific control over variables, which could have led to deviations between results and actual clinical practice. Second, all studies included in this meta-analysis were published in English, which may have introduced a certain degree of bias. Third, some important characteristics, including age, sex, PD-L1 expression, line of ICI treatment, and pain grade, were not included in the subgroup analysis due to unavailability, and may have affected the universality of our findings.

CONCLUSION

In summary, this study revealed that concomitant use of opioids is associated with a poor prognosis in patients treated with ICIs, while use of NSAIDs did not alter the efficacy of ICI treatment. Our findings provide important information for balancing management of cancer pain relief and efficacy of ICI treatment.

DATA AVAILABILITY STATEMENT

The original contributions presented in the study are included in the article/**Supplementary Material**. Further inquiries can be directed to the corresponding authors.

AUTHOR CONTRIBUTIONS

HG and ZL designed the study. ZM and XJ performed literature search and wrote the original manuscript. PJ and QW conceived the project and prepared the figures and tables. YZ and YL participated in the drafting and editing of the manuscript. XF and MJ provided statistical analysis. LJ committed to interpreting the results. HG revised the manuscript. ZM and XJ revised the draft and approved the final version to be submitted. All authors had full access to all data, critically revised the paper, approved the final analysis, and took responsibility for all aspects of the work.

ACKNOWLEDGMENTS

The authors are grateful to Dr. Kejun Nan of the Oncology Hospital of the Xi'an International Medical Center Hospital for his valuable guidance on writing assistance.

SUPPLEMENTARY MATERIAL

The Supplementary Material for this article can be found online at: https://www.frontiersin.org/articles/10.3389/fimmu.2022.861723/full#supplementary-material

Supplementary Figure 1 | Sensitivity analysis for the correlation between concomitant use of opioids and **(A)** ORR, **(B)** PFS, **(C)** OS in patients receiving ICIs. Pooled ORs or HRs with 95% CI of the remaining studies were presented with accordingly removed studies. By definition, OR>1 or HR<1 implied a better prognosis for opioids users. ORR, objective response rate; PFS, progression-free survival; OS, overall survival; OR, odds ratio; HR, hazard ratio; CI, confidence interval; ICIs, immune checkpoints inhibitors.

Supplementary Figure 2 | Sensitivity analysis for the correlation between concomitant use of NSAIDs and **(A)** ORR, **(B)** PFS, **(C)** OS in patients receiving ICIs. Pooled ORs or HRs with 95% CI of the remaining studies were presented with accordingly removed studies. By definition, OR>1 or HR<1 implied a better prognosis for NSAIDs users. NSAIDs, non-steroidal anti-inflammatory drugs; ORR, objective response rate; PFS, progression-free survival; OS, overall survival; OR, odds ratio; HR, hazard ratio; CI, confidence interval; ICIs, immune checkpoints inhibitors.

Supplementary Figure 3 | Publication bias. Analysis for studies evaluating opioids: **(A)** Begg's funnel plot of OR of ORR; Begg's funnel plot of HR of **(B)** PFS

and **(C)** OS. Analysis for studies evaluating NSAIDs: **(D)** Begg's funnel plot of OR of ORR; Begg's funnel plot of HR of **(E)** PFS and **(F)** OS. NSAIDs, non-steroidal anti-inflammatory drugs; ORR, objective response rate; PFS, progression-free survival; OS, overall survival; OR, odds ratio; HR, hazard ratio.

REFERENCES

1. Scripture CD, Figg WD. Drug Interactions in Cancer Therapy. *Nat Rev Cancer* (2006) 6(7):546–58. doi: 10.1038/nrc1887
2. Bagchi S, Yuan R, Engleman EG. Immune Checkpoint Inhibitors for the Treatment of Cancer: Clinical Impact and Mechanisms of Response and Resistance. *Annu Rev Pathol* (2021) 16:223–49. doi: 10.1146/annurev-pathol-042020-042741
3. Fundytus A, Booth CM, Tannock IF. How Low Can You Go? PD-L1 Expression as a Biomarker in Trials of Cancer Immunotherapy. *Ann Oncol Off J Eur Soc Med Oncol* (2021) 32(7):833–6. doi: 10.1016/j.annonc.2021.03.208
4. Weber JS, D'Angelo SP, Minor D, Hodi FS, Gutzmer R, Neyns B, et al. Nivolumab Versus Chemotherapy in Patients With Advanced Melanoma Who Progressed After Anti-CTLA-4 Treatment (CheckMate 037): A Randomised, Controlled, Open-Label, Phase 3 Trial. *Lancet Oncol* (2015) 16(4):375–84. doi: 10.1016/S1470-2045(15)70076-8
5. Robert C, Long GV, Brady B, Dutriaux C, Maio M, Mortier L, et al. Nivolumab in Previously Untreated Melanoma Without BRAF Mutation. *N Engl J Med* (2015) 372(4):320–30. doi: 10.1056/NEJMoa1412082
6. Chan TA, Yarchoan M, Jaffee E, Swanton C, Quezada SA, Stenzinger A, et al. Development of Tumor Mutation Burden as an Immunotherapy Biomarker: Utility for the Oncology Clinic. *Ann Oncol* (2019) 30(1):44–56. doi: 10.1093/annonc/mdy495
7. Marabelle A, Fakih M, Lopez J, Shah M, Shapira-Frommer R, Nakagawa K, et al. Association of Tumour Mutational Burden With Outcomes in Patients With Advanced Solid Tumours Treated With Pembrolizumab: Prospective Biomarker Analysis of the Multicohort, Open-Label, Phase 2 KEYNOTE-158 Study. *Lancet Oncol* (2020) 21(10):1353–65. doi: 10.1016/S1470-2045(20)30445-9
8. Meriggi F, Zaniboni A. Antibiotics and Steroids, the Double Enemies of Anticancer Immunotherapy: A Review of the Literature. *Cancer Immunol Immunother* (2021) 70(6):1511–7. doi: 10.1007/s00262-020-02786-3
9. Petrelli F, Iaculli A, Signorelli D, Ghidini A, Dottorini L, Perego G, et al. Survival of Patients Treated With Antibiotics and Immunotherapy for Cancer: A Systematic Review and Meta-Analysis. *J Clin Med* (2020) 9(5). doi: 10.3390/jcm9051458
10. Li M, Zeng C, Yao J, Ge Y, An G. The Association Between Proton Pump Inhibitors Use and Clinical Outcome of Patients Receiving Immune Checkpoint Inhibitors Therapy. *Int Immunopharmacol* (2020) 88:106972. doi: 10.1016/j.intimp.2020.106972
11. Cortellini A, Di Maio M, Nigro O, Leonetti A, Cortinovis DL, Aerts JG, et al. Differential Influence of Antibiotic Therapy and Other Medications on Oncological Outcomes of Patients With Non-Small Cell Lung Cancer Treated With First-Line Pembrolizumab Versus Cytotoxic Chemotherapy. *J Immunother Cancer* (2021) 9(4). doi: 10.1136/jitc-2021-002421
12. Ni W, Mo H, Liu Y, Xu Y, Qin C, Zhou Y, et al. Targeting Cholesterol Biosynthesis Promotes Anti-Tumor Immunity by Inhibiting Long Noncoding RNA SNHG29-Mediated YAP Activation. *Mol Ther* (2021) 29(10):2995–3010. doi: 10.1016/j.ymthe.2021.05.012
13. Cantini L, Pecci F, Hurkmans DP, Belderbos RA, Lanese A, Copparoni C, et al. High-Intensity Statins Are Associated With Improved Clinical Activity of PD-1 Inhibitors in Malignant Pleural Mesothelioma and Advanced Non-Small Cell Lung Cancer Patients. *Eur J Cancer* (2021) 144:41–8. doi: 10.1016/j.ejca.2020.10.031
14. Wiffen PJ, Wee B, Derry S, Bell RF, Moore RA. Opioids for Cancer Pain - An Overview of Cochrane Reviews. *Cochrane Database Syst Rev* (2017) 7(7):Cd012592. doi: 10.1002/14651858
15. Anekar AA, Cascella M. WHO Analgesic Ladder. In: *StatPearls*. Treasure Island (FL: StatPearls Publishing (1990).
16. Fujioka N, Nguyen J, Chen C, Li Y, Pasrija T, Niehans G, et al. Morphine-Induced Epidermal Growth Factor Pathway Activation in Non-Small Cell Lung Cancer. *Anesth Analg* (2011) 113(6):1353–64. doi: 10.1213/ANE.0b013e318232b35a
17. Gupta K, Kshirsagar S, Chang L, Schwartz R, Law PY, Yee D, et al. Morphine Stimulates Angiogenesis by Activating Proangiogenic and Survival-Promoting Signaling and Promotes Breast Tumor Growth. *Cancer Res* (2002) 62(15):4491–8.
18. Börner C, Warnick B, Smida M, Hartig R, Lindquist JA, Schraven B, et al. Mechanisms of Opioid-Mediated Inhibition of Human T Cell Receptor Signaling. *J Immunol* (2009) 183(2):882–9. doi: 10.4049/jimmunol.0802763
19. Cornwell WD, Lewis MG, Fan X, Rappaport J, Rogers TJ. Effect of Chronic Morphine Administration on Circulating T Cell Population Dynamics in Rhesus Macaques. *J Neuroimmunol* (2013) 265(1-2):43–50. doi: 10.1016/j.jneuroim.2013.09.013
20. Wang F, Roy S. Gut Homeostasis, Microbial Dysbiosis, and Opioids. *Toxicol Pathol* (2017) 45(1):150–6. doi: 10.1177/0192623316679898
21. Meng J, Yu H, Ma J, Wang J, Banerjee S, Charboneau R, et al. Morphine Induces Bacterial Translocation in Mice by Compromising Intestinal Barrier Function in a TLR-Dependent Manner. *PloS One* (2013) 8(1):e54040. doi: 10.1371/journal.pone.0054040
22. Bazzani L, Donnini S, Finetti F, Christofori G, Ziche M. PGE2/EP3/SRC Signaling Induces EGFR Nuclear Translocation and Growth Through EGFR Ligands Release in Lung Adenocarcinoma Cells. *Oncotarget* (2017) 8(19):31270–87. doi: 10.18632/oncotarget.16116
23. Fujino H, Toyomura K, Chen XB, Regan JW, Murayama T. Prostaglandin E_2 Regulates Cellular Migration *via* Induction of Vascular Endothelial Growth Factor Receptor-1 in HCA-7 Human Colon Cancer Cells. *Biochem Pharmacol* (2011) 81(3):379–87. doi: 10.1016/j.bcp.2010.11.001
24. Böttcher JP, Bonavita E, Chakravarty P, Blees H, Cabeza-Cabrerizo M, Sammicheli S, et al. NK Cells Stimulate Recruitment of Cdc1 Into the Tumor Microenvironment Promoting Cancer Immune Control. *Cell* (2018) 172(5):1022–1037.e14. doi: 10.1016/j.cell.2018.01.004
25. Franco F, Wenes M, Ho PC. Sparks Fly in PGE2-Modulated Macrophage Polarization. *Immunity* (2018) 49(6):987–9. doi: 10.1016/j.immuni.2018.12.002
26. Botticelli A, Cirillo A, Pomati G, Cerbelli B, Scagnoli S, Roberto M, et al. The Role of Opioids in Cancer Response to Immunotherapy. *J Transl Med* (2021) 19(1):119. doi: 10.1186/s12967-021-02784-80
27. Taniguchi Y, Tamiya A, Matsuda Y, Adachi Y, Enomoto T, Azuma K, et al. Opioids Impair Nivolumab Outcomes: A Retrospective Propensity Score Analysis in Non-Small-Cell Lung Cancer. *BMJ Support Palliat Care* (2020). doi: 10.1136/bmjspcare-2020-002480
28. Iglesias-Santamaría A. Impact of Antibiotic Use and Other Concomitant Medications on the Efficacy of Immune Checkpoint Inhibitors in Patients With Advanced Cancer. *Clin Transl Oncol* (2020) 22(9):1481–90. doi: 10.1007/s12094-019-02282-w
29. Gaucher L, Adda L, Séjourné A, Joachim C, Guillaume C, Poulet C, et al. Associations Between Dysbiosis-Inducing Drugs, Overall Survival and Tumor Response in Patients Treated With Immune Checkpoint Inhibitors. *Ther Adv Med Oncol* (2021) 13:17588359211000591. doi: 10.1177/17588359211000591
30. Kanai O, Ito T, Saito Z, Yamamoto Y, Fujita K, Okamura M, et al. Effect of Cyclooxygenase Inhibitor Use on Immunotherapy Efficacy in Non-Small Cell Lung Cancer. *Thorac Cancer* (2021) 12(6):949–57. doi: 10.1111/1759-7714.13845
31. Miura K, Sano Y, Niho S, Kawasumi K, Mochizuki N, Yoh K, et al. Impact of Concomitant Medication on Clinical Outcomes in Patients With Advanced Non-Small Cell Lung Cancer Treated With Immune Checkpoint Inhibitors: A Retrospective Study. *Thorac Cancer* (2021) 12(13):1983–94. doi: 10.1111/1759-7714.14001
32. Wang SJ, Khullar K, Kim S, Yegya-Raman N, Malhotra J, Groisberg R, et al. Effect of Cyclo-Oxygenase Inhibitor Use During Checkpoint Blockade Immunotherapy in Patients With Metastatic Melanoma and Non-Small Cell Lung Cancer. *J Immunother Cancer* (2020) 8(2). doi: 10.1136/jitc-2020-000889
33. Svaton M, Zemanova M, Zemanova P, Kultan J, Fischer O, Skrickova J, et al. Impact of Concomitant Medication Administered at the Time of Initiation of Nivolumab Therapy on Outcome in Non-Small Cell Lung Cancer. *Anticancer Res* (2020) 40(4):2209–17. doi: 10.21873/anticanres.14182

34. Wang DY, McQuade JL, Rai RR, Park JJ, Zhao S, Ye F, et al. The Impact of Nonsteroidal Anti-Inflammatory Drugs, Beta Blockers, and Metformin on the Efficacy of Anti-PD-1 Therapy in Advanced Melanoma. *Oncologist* (2020) 25 (3):e602–5. doi: 10.1634/theoncologist.2019-0518
35. Cortellini A, Tucci M, Adamo V, Stucci LS, Russo A, Tanda ET, et al. Integrated Analysis of Concomitant Medications and Oncological Outcomes From PD-1/PD-L1 Checkpoint Inhibitors in Clinical Practice. *J Immunother Cancer* (2020) 8(2). doi: 10.1136/jitc-2020-001361
36. Failing JJ, Finnes HD, Kottschade LA, Allred JB, Markovic SN. Effects of Commonly Used Chronic Medications on the Outcomes of Ipilimumab Therapy in Patients With Metastatic Melanoma. *Melanoma Res* (2016) 26 (6):609–15. doi: 10.1097/CMR.0000000000000299
37. Hutton B, Salanti G, Caldwell DM, Chaimani A, Schmid CH, Cameron C, et al. The PRISMA Extension Statement for Reporting of Systematic Reviews Incorporating Network Meta-Analyses of Health Care Interventions: Checklist and Explanations. *Ann Intern Med* (2015) 162(11):777–84. doi: 10.7326/M14-2385
38. Wells G, Shea B, O'Connell D, Peterson J, Welch V, Losos M, et al. *The Newcastle-Ottawa Scale (NOS) for Assessing the Quality of Nonrandomized Studies in Meta-Analyses*. Ottawa Hospital Research Institute (2000). Available at: http://www.ohri.ca/programs/clinical_epidemiology/oxford.asp.
39. Eisenhauer EA, Therasse P, Bogaerts J, Schwartz LH, Sargent D, Ford R, et al. New Response Evaluation Criteria in Solid Tumours: Revised RECIST Guideline (Version 1.1). *Eur J Cancer* (2009) 45(2):228–47. doi: 10.1016/j.ejca.2008.10.026
40. Higgins JP, Thompson SG. Quantifying Heterogeneity in a Meta-Analysis. *Stat Med* (2002) 21(11):1539–58. doi: 10.1002/sim.1186
41. Al-Hasani R, Bruchas MR. Molecular Mechanisms of Opioid Receptor-Dependent Signaling and Behavior. *Anesthesiology* (2011) 115(6):1363–81. doi: 10.1097/ALN.0b013e318238bba6
42. Gach K, Szemraj J, Fichna J, Piestrzeniewicz M, Delbro DS, Janecka A. The Influence of Opioids on Urokinase Plasminogen Activator on Protein and mRNA Level in MCF-7 Breast Cancer Cell Line. *Chem Biol Drug Des* (2009) 74(4):390–6. doi: 10.1111/j.1747-0285.2009.00875.x
43. Beagles K, Wellstein A, Bayer B. Systemic Morphine Administration Suppresses Genes Involved in Antigen Presentation. *Mol Pharmacol* (2004) 65(2):437–42. doi: 10.1124/mol.65.2.437
44. Barbi J, Pardoll D, Pan F. Treg Functional Stability and Its Responsiveness to the Microenvironment. *Immunol Rev* (2014) 259(1):115–39. doi: 10.1111/imr.12172
45. Gong L, Qin Q, Zhou L, Ouyang W, Li Y, Wu Y, et al. Effects of Fentanyl Anesthesia and Sufentanil Anesthesia on Regulatory T Cells Frequencies. *Int J Clin Exp Pathol* (2014) 7(11):7708–16.
46. Humphries A, Daud A. The Gut Microbiota and Immune Checkpoint Inhibitors. *Hum Vaccin Immunother* (2018) 14(9):2178–82. doi: 10.1080/21645515.2018.1442970
47. Tian M, Zhang S, Tseng Y, Shen X, Dong L, Xue R, et al. Gut Microbiota and Immune Checkpoint Inhibitors-Based Immunotherapy. *Anticancer Agents Med Chem* (2021). doi: 10.1080/21645515.2018.1442970
48. Banerjee S, Sindberg G, Wang F, Meng J, Sharma U, Zhang L, et al. Opioid-Induced Gut Microbial Disruption and Bile Dysregulation Leads to Gut Barrier Compromise and Sustained Systemic Inflammation. *Mucosal Immunol* (2016) 9(6):1418–28. doi: 10.1038/mi.2016.9
49. Ferrer MD, Busquets-Cortés C, Capó X, Tejada S, Tur JA, Pons A, et al. Cyclooxygenase-2 Inhibitors as a Therapeutic Target in Inflammatory Diseases. *Curr Med Chem* (2019) 26(18):3225–41. doi: 10.2174/0929867325666180514112124
50. Pan J, Yang Q, Shao J, Zhang L, Ma J, Wang Y, et al. Cyclooxygenase-2 Induced β1-Integrin Expression in NSCLC and Promoted Cell Invasion *via* the EP1/MAPK/E2F-1/FoxC2 Signal Pathway. *Sci Rep* (2016) 6:33823. doi: 10.1038/srep33823
51. Borst P. The Malate-Aspartate Shuttle (Borst Cycle): How It Started and Developed Into a Major Metabolic Pathway. *IUBMB Life* (2020) 72(11):2241–59. doi: 10.1002/iub.2367
52. Yan G, Zhao H, Zhang Q, Zhou Y, Wu L, Lei J, et al. RIPK3-PGE(2) Circuit Mediates Myeloid-Derived Suppressor Cell-Potentiated Colorectal Carcinogenesis. *Cancer Res* (2018) 78(19):5586–99. doi: 10.1158/0008-5472.CAN-17-3962
53. Jiao S, Subudhi SK, Aparicio A, Ge Z, Guan B, Miura Y, et al. Differences in Tumor Microenvironment Dictate T Helper Lineage Polarization and Response to Immune Checkpoint Therapy. *Cell* (2019) 179(5):1177–1190.e13. doi: 10.1016/j.cell.2019.10.029
54. Zajączkowska R, Leppert W, Mika J, Kocot-Kępska M, Woroń J, Wrzosek A, et al. Perioperative Immunosuppression and Risk of Cancer Progression: The Impact of Opioids on Pain Management. *Pain Res Manag* (2018) 2018:9293704. doi: 10.1155/2018/9293704

Conflict of Interest: The authors declare that the research was conducted in the absence of any commercial or financial relationships that could be construed as a potential conflict of interest.

Publisher's Note: All claims expressed in this article are solely those of the authors and do not necessarily represent those of their affiliated organizations, or those of the publisher, the editors and the reviewers. Any product that may be evaluated in this article, or claim that may be made by its manufacturer, is not guaranteed or endorsed by the publisher.

frontiers | Frontiers in Immunology

ORIGINAL RESEARCH
published: 01 July 2022
doi: 10.3389/fimmu.2022.893198

Artificial Intelligence-Assisted Score Analysis for Predicting the Expression of the Immunotherapy Biomarker PD-L1 in Lung Cancer

Guoping Cheng[1,2†], Fuchuang Zhang[3†], Yishi Xing[3†], Xingyi Hu[1,2,4], He Zhang[5], Shiting Chen[3], Mengdao Li[3], Chaolong Peng[3], Guangtai Ding[6], Dadong Zhang[3], Peilin Chen[3*], Qingxin Xia[5*] and Meijuan Wu[1,2*]*

[1] Department of Pathology, The Cancer Hospital of the University of Chinese Academy of Sciences (Zhejiang Cancer Hospital), Hangzhou, China, [2] Institute of Basic Medicine and Cancer, Chinese Academy of Sciences, Hangzhou, China, [3] 3D Medicines Inc., Shanghai, China, [4] The Second Clinical Medical College, Zhejiang Chinese Medical University, Hangzhou, China, [5] Department of Pathology, Affiliated Cancer Hospital of Zhengzhou University, Zhengzhou, China, [6] School of Computer Engineering and Science, Shanghai University, Shanghai, China

Programmed cell death ligand 1 (PD-L1) is a critical biomarker for predicting the response to immunotherapy. However, traditional quantitative evaluation of PD-L1 expression using immunohistochemistry staining remains challenging for pathologists. Here we developed a deep learning (DL)-based artificial intelligence (AI) model to automatically analyze the immunohistochemical expression of PD-L1 in lung cancer patients. A total of 1,288 patients with lung cancer were included in the study. The diagnostic ability of three different AI models (M1, M2, and M3) was assessed in both PD-L1 (22C3) and PD-L1 (SP263) assays. M2 and M3 showed improved performance in the evaluation of PD-L1 expression in the PD-L1 (22C3) assay, especially at 1% cutoff. Highly accurate performance in the PD-L1 (SP263) was also achieved, with accuracy and specificity of 96.4 and 96.8% in both M2 and M3, respectively. Moreover, the diagnostic results of these three AI-assisted models were highly consistent with those from the pathologist. Similar performances of M1, M2, and M3 in the 22C3 dataset were also obtained in lung adenocarcinoma and lung squamous cell carcinoma in both sampling methods. In conclusion, these results suggest that AI-assisted diagnostic models in PD-L1 expression are a promising tool for improving the efficiency of clinical pathologists.

Keywords: PD-L1, NSCLC, automated scoring, AI, pathological diagnosis

Abbreviations: PD-L1, programmed cell death ligand 1; IHC, immunohistochemistry; DL, deep learning; AI, artificial intelligence; TME, tumor microenvironment; EGFR, epidermal growth factor receptor; HER2, human epidermal growth factor receptor 2; TPS, tumor proportion score; CNNs, convolutional neural networks; WSI, whole-slide image; LCC, linear correlation coefficient; CPS, combined positive score; IP, PD-L1-positive immune cells patch; NSCLC, non-small cell lung cancer; CK, cytokeratin.

OPEN ACCESS

Edited by:
Alison Taylor,
University of Leeds, United Kingdom

Reviewed by:
Sharia Hernandez,
University of Texas MD Anderson Cancer Center, United States
Arutha Kulasinghe,
The University of Queensland, Australia

***Correspondence:**
Dadong Zhang
dadong.zhang@3dmedcare.com
Peilin Chen
peilin.chen@3dmedcare.com
Qingxin Xia
15838552920@163.com
Meijuan Wu
wumj@zjcc.org.cn

†These authors have contributed equally to this work and share first authorship

Specialty section:
This article was submitted to Cancer Immunity and Immunotherapy, a section of the journal Frontiers in Immunology

Received: *10 March 2022*
Accepted: *27 May 2022*
Published: *01 July 2022*

Citation:
Cheng G, Zhang F, Xing Y, Hu X, Zhang H, Chen S, Li M, Peng C, Ding G, Zhang D, Chen P, Xia Q and Wu M (2022) Artificial Intelligence-Assisted Score Analysis for Predicting the Expression of the Immunotherapy Biomarker PD-L1 in Lung Cancer. Front. Immunol. 13:893198. doi: 10.3389/fimmu.2022.893198

INTRODUCTION

Immunotherapy is one of the important pharmacological options for lung cancer treatment (1, 2). As a major immune checkpoint biomarker, programmed cell death ligand 1 (PD-L1) expression is widely considered a gold standard for predicting the response to immunotherapy (3). In the clinical context, the choice of immunotherapeutic strategies mainly depends on the levels of PD-L1 expression in tumor cells. Normally, a higher expression level of PD-L1 in tumor cells is associated with the patient's better response to immunotherapy (4). Thus, efficient and accurate assessment of PD-L1 expression plays a critical role in cancer immunotherapy. However, there are still some challenges for the traditional methods of interpretation of PD-L1-positive tumor cells.

Moreover, the tumor microenvironment (TME) is a dynamic structure that is considered to play a role in tumor initiation and progression (5, 6). The extensive interaction among the TME, tumor cells, and immune cells provides novel opportunities for therapeutic strategies of cancer (7). Previous studies have shown multiple biomarkers in the TME and their predictive role in disease outcomes (6). Moreover, biomarkers within the TME may help us identify the beneficiaries of immunotherapy (6). Thus, the characteristics of the TME and its components make them ideal candidates for cancer-specific pathological diagnosis and precision treatments.

The application space of digital pathology and scanners has expanded greatly with the development of artificial intelligence (AI). AI-based automatic learning and diagnosis models could easily solve complex problems during medical image analysis (8). Deep learning (DL) and machine learning could promote further optimization of the AI-based image-processing models (9). DL methods have shown great advantages in image identification and classification (10), especially in cell classification (11), cancer detection (12), pathological diagnosis (13), and characterization of the spatial organization of immune cells in the TME (14). Previous studies have shown the application of DL in the analysis of multiple biomarkers in immunohistochemistry (IHC) staining, including epidermal growth factor receptor, human epidermal growth factor receptor 2, and Ki67 (15–17). AI-based quantitative diagnosis could also reduce the disadvantages of traditional methods, such as time consumption, lack of reproducibility, and interobserver variability (18, 19). Thus, AI-based automatic diagnosis models for tumor-specific biomarkers have promising application prospects in precise stratified medicine.

Specifically, several studies have shown the evaluation of AI models for PD-L1 expression in non-small cell lung carcinoma (20, 21). Whole-slide images of PD-L1-stained slides were automatically annotated with an AI model (22). PD-L1 expression on tumor cells and immune cells was further labeled, detected, and calculated. Interestingly, the algorithms of image-based scoring are highly consistent with those of pathologists when assessing PD-L1 expression (23). However, existing models have poor specificity and accuracy for pathological sections with low PD-L1 expression, especially at tumor proportion score (TPS) cutoff values of 1% (24, 25).

In this study, we explored and optimized three different AI model-based workflows for automatically detecting the positive PD-L1 expression in both 22C3 and SP263 assays. A highly accurate performance of the AI-assisted DL diagnostic models was shown in lung adenocarcinoma and lung squamous cell carcinoma of both sampling methods, especially for PD-L1 expression at 1% cutoff. Moreover, the M2 workflow was able to further improve the accuracy of the results. Our results indicate that AI-based diagnostic models are a promising approach to assist pathologists in the accurate diagnosis of PD-L1 expression.

MATERIALS AND METHODS

Materials

A total of 1,288 formalin-fixed, paraffin-embedded lung cancer samples from Zhejiang Cancer Hospital were obtained. All samples were processed in the 3DMed Clinical Laboratory (accredited by CAP and CLIA). Among these, 1,204 samples were prepared and stained using the PD-L1 IHC 22C3 pharmDx assay (Dako, Carpenteria, CA, USA) developed on the Dako Autostainer Link 48 platform according to the kit's manufacturer recommendations. In total, 84 samples were prepared and stained using PD-L1 IHC SP263 assays (Ventana Medical Systems, Tucson, AZ, USA) developed on the Ventana BenchMark platform.

Clinicopathological characteristics (*e.g.*, age, gender, and tumor type) of lung cancer were included in this study. The detailed patient demographics and PD-L1 results are summarized in **Table 1**. This study was approved by the Zhejiang Cancer Hospital Ethics Committee (IRB-2020-310 and IRB-2021-439). All slides were digitized by a KFBIO FK-Pro-120 slide scanner at ×20 magnification (0.475 μm/pixel). Furthermore, 627 PD-L1 (22C3)-staining whole-slide images (WSIs) were used to develop prediction models, and the remaining WSIs were used as test sets (**Table 1**). The training WSIs were manually annotated by two graduate students majoring in pathology, and all annotations were confirmed by pathologists. The TPSs of all slides were estimated by one trained pathologist and confirmed by another.

TPS Algorithm

TPS was calculated as the percentage of viable tumor cells exhibiting weak to strong partial or complete membranous staining. In order to accurately calculate TPS, we proposed a two-stage workflow based on DL: first, classification models were used to detect patches containing tumor cells, and then an object detection model was used to locate and count the tumor cells.

The Development of Classification Models

Among the samples, more than 600 slides were selected for patch classification. To distinguish tumor cells containing patches from the others, we proposed two different classification models using convolutional neural networks with different input image sizes, namely, 256 × 256 pixels and 128 × 128 pixels, respectively (**Figure 1**). To train the networks with an input image size of 256 × 256 pixels, patches were randomly obtained and checked

TABLE 1 | Clinicopathological characteristics of lung cancer.

Characteristic	Training set(*N* = 627)	Validation set (22C3)(*N* = 577)	Validation set (SP263)(*N* = 84)
Age, years			
Average	61	62	59
Range	25–91	21–91	30–83
Gender			
Male	385	308	43
Female	242	269	41
Tissue source			
Lung	538	532	79
Lymph nodes	53	22	4
Other	36	23	1
Sampling methods			
Surgical operation	305	282	30
Needle biopsy	220	198	48
Other biopsies	74	63	4
Pleural effusion	12	18	1
Other	16	16	1
Tumor tissue type			
Lung adenocarcinoma	425	497	67
Lung squamous cell carcinoma	102	67	16
Other	100	13	1
TPS			
<1%	316	442	63
1–50%	167	88	10
≥50%	144	47	11
CPS			
<1%	145	278	38
≥1%	471	280	45
NA	11	19	1

TPS, tumor proportion score; CPS, combined positive score; NA, not available.

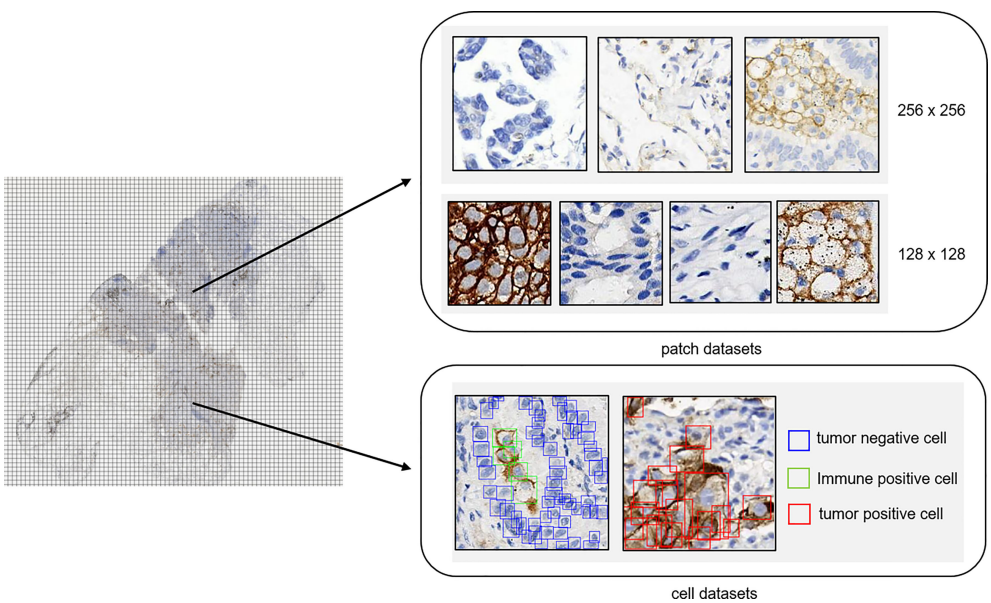

FIGURE 1 | Annotation dataset for tumor detection. Patch datasets and cell datasets annotated in the whole-slide images of PD-L1 staining. Both 256 × 256 patch size and 128 × 128 patch size were included in the patch datasets. In the cell datasets, PD-L1-positive tumor cells, PD-L1-positive immune cells, and PD-L1-negative tumor cells were labeled with different colors.

from the WSI annotation areas and then grouped into three categories: patches containing tumor cells but no PD-L1 positive immune cells (category 1: 124,459), patches containing both PD-L1 negative tumor cells and PD-L1 positive immune cells (category 2: 14,069; immune cells include macrophages and lymphocytes), and patches excluding tumor cells [category 3: 131,672; this category was comprised of various no-tumor tissues, including negative immune cells (macrophages and lymphocytes), hemorrhage, necrosis tissue, and stromal cells] (**Supplementary Figure S1**). Two classification models were constructed for different tasks: model (12_3), trained with patches among all three categories, was designed to classify the patches into tumor cell-containing patches (category 1 + category 2) and no-tumor cell-containing patches (category 3) and model (1_2), using category 1 and category 2 as training data sets, was constructed to classify the tumor cell-containing patches into PD-L1-positive immune cell-containing patches or no-PD-L1-positive immune cell-containing patches.

As for the development of networks with an input image size of 128 × 128, patches with a size of 128 × 128 were randomly obtained and checked from the WSI annotation areas and then grouped into four categories: patches containing PD-L1-positive tumor cells (category 4: 37,583), patches containing PD-L1-negative tumor cells (category 5: 45,107), patches containing PD-L1-positive immune cells (category 6: 38,192; immune cells including macrophages and lymphocytes), and other patches [category 7: 65,786; this category was comprised of various no-tumor tissues including negative immune cells (macrophages and lymphocytes), hemorrhage, necrosis tissue, and stromal cells]. The patches were fed into the network for model training.

All datasets for model training were randomly split into training and validation sets in a ratio of 8:2. Data augmentation was performed during the training by random flip, rotation, and blur. We employed MobileNetV2 architecture pretrained on ImageNet as the basic classification model. The MobileNetV2 architecture was the same as in a previous paper (26), with the depth multiplier and width multiplier both being 1 and using global max pooling for feature extraction. We removed the top layer (classify layer) in the original model and added a dropout layer and a dense layer for our task.

Cell Detection

We built our own object detection model based on the YOLO head to quantitatively classify, locate, and count the PD-L1 tumor cells. We used CSPDarknet53 as our backbone (27); our feature network resembled BiFPN (28). Cell tags were labeled into patches of 128 × 128 pixel size and were grouped into PD-L1-negative tumor cells (105,508), PD-L1-positive tumor cells (24,523), and PD-L1-positive immune cells (10,429) (**Supplementary Figure S1**). In the data augmentation step, the same strategies were applied. In the training step, we used fivefold cross-validation and label smoothing (0.1) to avoid overfitting. From the predicted output of the cell detection model, only PD-L1-positive tumor cells and PD-L1-negative cells remained to calculate the TPS.

Flow Chart of the Study

The flow chart of the DL model is shown in **Figure 2**. In brief, 627 pathological sections of lung cancer tissue staining samples with PD-L1 (22C3) were used for the DL model building. During the training, a subset of the WSIs was first selected, annotated, and fed into the network for training. Then, the remaining WSIs were used for the evaluation and refinement of the DL model performance. Both the established classification model and the cell detection model were then combined for the next test. Then, 577 slides stained by PD-L1 (22C3) and 84 slides stained by PD-L1 (SP263) were used for the independent testing of the DL model. Based on the cell detection of the combined DL models, the TPS of WSIs was obtained.

WSI Inference Workflow

The WSI inference workflow is shown in **Figure 3**. Three different workflows (top, M1; middle, M2; and bottom, M3) were used for the calculation of the TPS. For M1, the patches were divided into tumor and other regions by model (12_3); the YOLO model was further used for the detection of PD-L1-

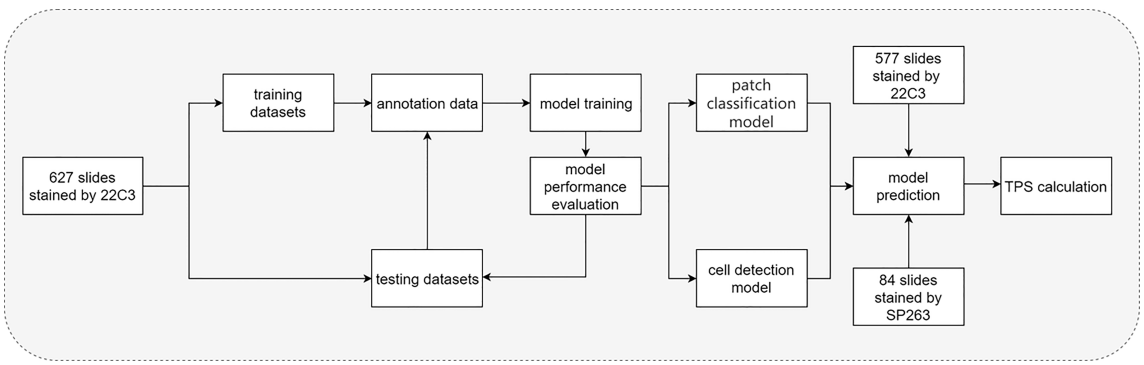

FIGURE 2 | Flow chart of the study. Flow chart of tumor proportion score assessed with artificial intelligence-based diagnostic models in the pathological sections of lung cancer tissue samples stained with PD-L1 (22C3).

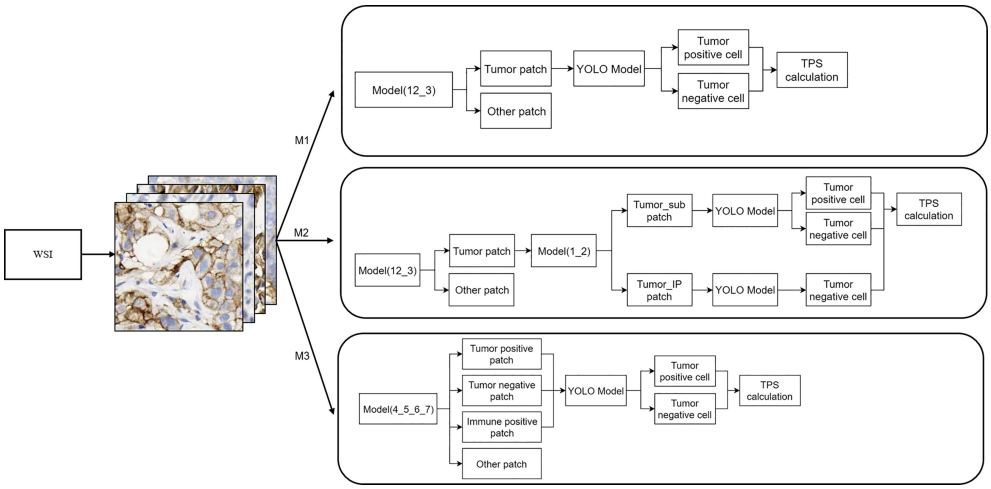

FIGURE 3 | Whole-slide image inference workflow. A whole-slide image was analyzed with different artificial intelligence model-based workflows (M1, M2, and M3). The detailed information of these three workflows is shown here.

positive and PD-L1-negative tumor cells. M2 included further algorithm optimization based on M1. The tumor patches in M2 workflow were further divided into patches with or without PD-L1-positive immune cells by model (1_2), and then the YOLO model was used for the detection of PD-L1-positive or PD-L1-negative tumor cells inside the patches. Compared with M1, M2 could filter out PD-L1-positive immune cells, which would otherwise be misdiagnosed as PD-L1-positive tumor cells. After optimization, the performance of the M2 model was greatly improved. As for the M3 workflow, the patches were first classified into four groups—tumor-positive patch, tumor-negative patch, immune positive patch, and other patch—followed by the detection of PD-L1-positive and PD-L1-negative cells using the YOLO model and then TPS calculation, as shown in **Figure 3**.

Evaluation Metrics and Statistical Analyses

The linear correlation coefficient (LCC) was used for comparison with the TPS of AI models and the TPS given by the pathologists. Cohen's kappa was also calculated for the agreement between pathologists and AI models. The Kappa values were interpreted as poor (<0.40), moderate (0.40–0.75), or excellent (≥0.75). Statistical significance was set at p <0.05. The accuracy evaluation was represented by several metrics, including specificity, sensitivity, precision, accuracy, and F1 score. All statistical analyses were performed using Python (version 3.6).

RESULTS

Clinicopathological Characteristics of Patients With Lung Cancer

More than half of the sections (57.1%) were from male patients, and 42.9% were from female patients (**Table 1**). The sampling methods mainly included surgical operation, needle biopsy, other biopsy, and pleural effusion, and the total number of the corresponding samples was 617, 466, 141, and 31, respectively (**Table 1**). As for the tumor tissue types, there were 989 with lung adenocarcinoma and 185 with lung squamous cell carcinoma. The PD-L1 TPS (<1, 1–49, and ≥50%) and combined positive score (CPS) (<1 and ≥1%) assessments are also recorded in **Table 1**.

DL Model Performance Evaluation in the PD-L1 (22C3) and PD-L1 (SP263) Assays

To evaluate the performance of the experimental DL models, the test dataset was used for further analysis. TPS cutoff values of 1% (**Figures 4A, D**) and 50% (**Figures 4B, E**) were selected for the PD-L1 (22C3) (**Figures 4A–C**) and PD-L1 (SP263) (**Figures 4D–F**) assays in M1, M2, and M3. In the PD-L1 (22C3) assay, M2 and M3 showed improved performance in TPS calculation (**Figures 4A–C**), especially at 1% cutoff (M2: specificity, 0.9502; sensitivity, 0.9407; precision, 0.8523; accuracy, 0.9480; F1-score, 0.8944; kappa score, 0.8600; M3: specificity, 0.9457; sensitivity, 0.9407; precision, 0.8411; accuracy, 0.9445; F1-score, 0.8881; kappa score, 0.8510). Highly accurate performance in the PD-L1 (SP263) assay was also achieved for both M2 and M3 (M2: specificity, 0.9677; sensitivity, 0.9524; precision, 0.9091; accuracy, 0.9639; F1-score, 0.9302; kappa score, 0.9060 at 1% TPS cutoff values; M3: specificity, 0.9677; sensitivity, 0.9523; precision, 0.9091; accuracy, 0.9639; F1-score, 0.9302; kappa score, 0.9060 at 1% TPS cutoff values) (**Figures 4D–F**). Above all, the experimental DL models shown here obtained a high-precision score of PD-L1 expression.

LCC in the 22C3 and SP263 Assays

To evaluate the consistency between the results of the DL model and the judgment of the pathologist, LCC was used for the analysis of M1, M2, and M3 in the PD-L1 (22C3) and PD-L1

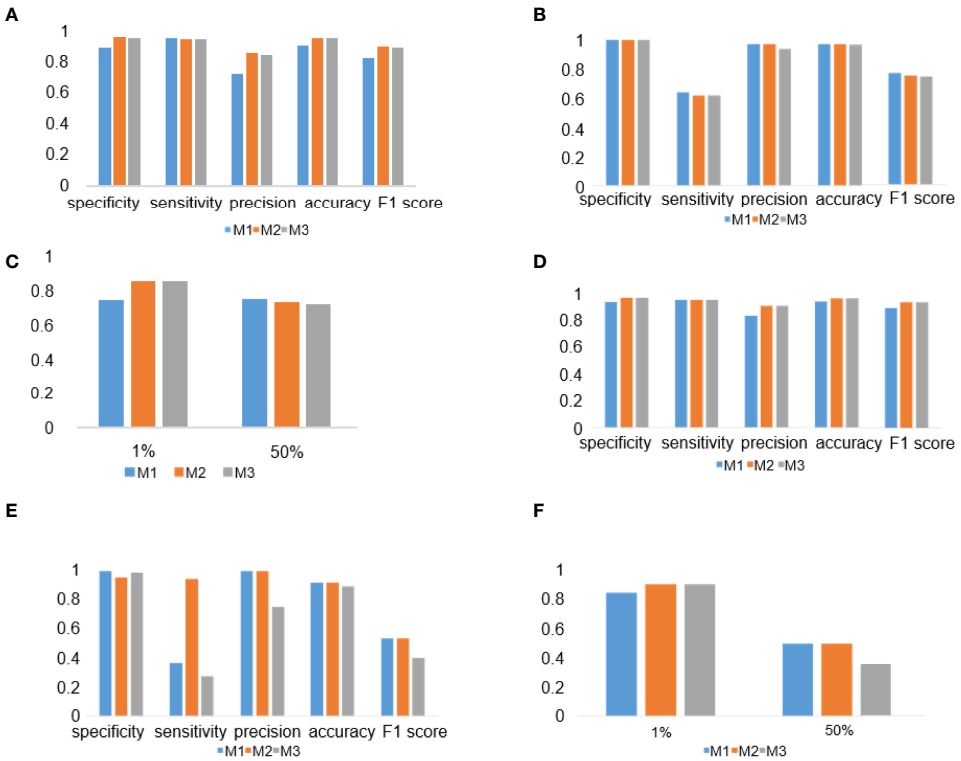

FIGURE 4 | Deep learning (DL) model performance evaluation in the PD-L1 (22C3) and PD-L1 (SP263) assays. **(A–C)** Histograms of DL model performance with PD-L1 (22C3) assay test. **(D–F)** Histograms of DL model performance with PD-L1 (SP263) assay test. Tumor proportion score cutoff values of 1% **(A**, **D)** and 50% **(B**, **E)**. Kappa score analysis **(C**, **F)**.

(SP263) assays (**Table 2**). In the PD-L1 (22C3) dataset, M2 and M3 obtained a higher LCC score compared with M1 (M1: 95% CI, 0.791–0.844; M2: 95% CI, 0.858–0.892; M3: 95% CI, 0.854–0.892). A similar trend of the LCC score was also shown in the PD-L1 (SP263) set. The LCC values in M1, M2, and M3 of the PD-L1 (SP263) dataset were 0.825 (95% CI, 0.749–0.879), 0.867 (95% CI, 0.812–0.907) and 0.832 (95% CI, 0.766–0.882) respectively.

Examples of Tumor Detection and PD-L1 Calculation

An illustrative example of the process of tumor recognition with the 256 patch size is shown in **Figure 5A**. After obtaining PD-L1 IHC WSIs, tumor sections were detected and calculated by the DL model (**Figure 5A**). Moreover, based on pathological characteristics and PD-L1 staining, cells in the patches were further detected by object detection model and labeled with different colors for visualization (**Figure 5B**). Blue, green, and red represented PD-L1-negative tumor cells, PD-L1-positive immune cells, and PD-L1-positive tumor cells, respectively.

PD-L1-Positive Immune Cell Patch Filter Module

The effectiveness of the PD-L1-positive immune cell patch filter module in the M2 workflow is shown in **Figure 6**. The predicted tumor patch and immune patch are indicated with blue and green squares, respectively, and the predicted PD-L1-negative tumor cells and PD-L1-positive tumor cells are indicated with blue and red dots, respectively (**Figure 6A**). In the M1 workflow, most of the false positive samples of TPS have CPS ≥1% (**Figure 6B**). Compared with the M2 workflow, the M1 workflow does not have an immune filter module, so it usually leads to an increase in TPS because the M1 model easily misjudges PD-L1-positive immune cells as PD-L1-positive tumor cells (**Figure 6A**), which leads to a higher positive tumor ratio than normal (**Figure 6B**). The M2 workflow can greatly reduce the misjudging of PD-L1-positive immune cells as PD-L1-positive tumor cells through the filter module. Among the false positive samples in the M2 workflow, 42% of the samples have CPS ≥1 compared to that in the M1 workflow at 67%.

DL Model Performance in Different Tumor Types and Surgical Methods

To check the performance of the model more comprehensively, we stratified the testing results of the three workflows by different tumor types (**Figures 7A–D**) and surgical methods (**Figures 7E–H**). Compared with the M1 workflow, M2 and M3 showed better performance with TPS cutoff values of 1% in both lung adenocarcinoma (**Figure 7A**) (M2: specificity, 0.9569; sensitivity,

TABLE 2 | Linear correlation coefficient in 22C3 and SP263 assay.

	Model	LCC	95% CI
22C3	M1	0.819	0.791–0.844
	M2	0.878	0.858–0.892
	M3	0.874	0.854–0.892
SP263	M1	0.825	0.749–0.879
	M2	0.867	0.812–0.907
	M3	0.832	0.766–0.882

Linear correlation coefficient among different artificial intelligence diagnostic models (M1, M2, and M3) in both PD-L1 (22C3) and PD-L1 (SP263) assays.

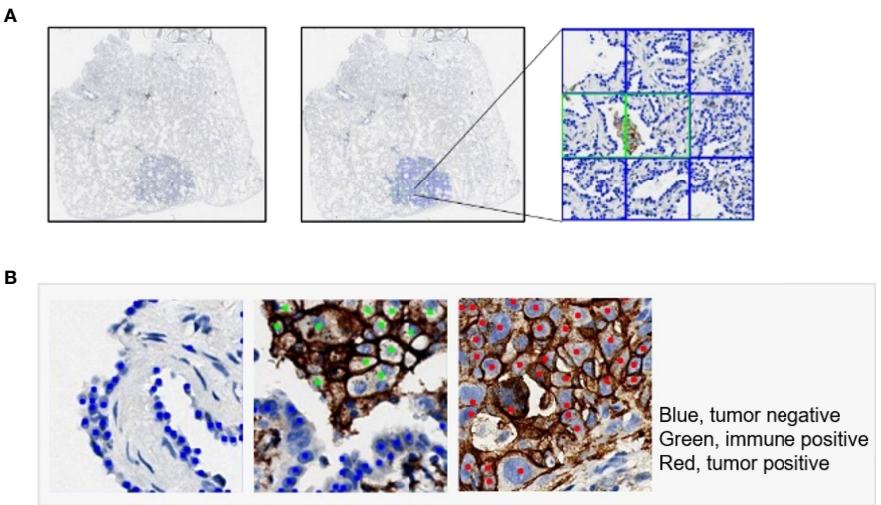

FIGURE 5 | Examples of tumor detection and PD-L1 calculation. **(A)** Example of whole-slide image analysis for tumor recognition with the 256 patch. **(B)** Examples of cells detected by the YOLO model: PD-L1-negative tumor cell (blue), PD-L1-positive immune cell (green), and PD-L1-positive tumor cell (red).

0.9320; precision, 0.8496; accuracy, 0.9517; F1-score, 0.8889; M3: specificity, 0.9543; sensitivity, 0.9320; precision, 0.8421; accuracy, 0.9497; F1-score, 0.8848) and lung squamous cell carcinoma (**Figure 7B**) (M2: specificity, 0.9024; sensitivity, 0.9615; precision, 0.8621; accuracy, 0.9254; F1-score, 0.9091; M3: specificity, 0.9024; sensitivity, 0.9615; precision, 0.8621; accuracy, 0.9254; F1-score, 0.9091). In terms of TPS cutoff values of 50%, M2 showed higher sensitivity but lower specificity when compared with M1 and M3 in both lung adenocarcinoma (**Figure 7C**) and lung squamous cell carcinoma (**Figure 7D**). A similar performance of M1, M2, and M3 in the 22C3 dataset was also shown in the samples from surgery (**Figures 7E, G**) and needle biopsy (**Figures 7F, H**). Thus, our DL models achieved a high-precision score of PD-L1 (22C3) in lung adenocarcinoma and lung squamous cell carcinoma in both sampling methods (surgery and needle biopsy).

DISCUSSION

An increasing number of studies have confirmed that PD-L1 is a critical predictive biomarker of non-small cell lung cancer (NSCLC) response to immunotherapy (29, 30). A higher percentage of positive PD-L1 expression is associated with a higher probability of responding to immunotherapy (31, 32). Thus, efficient and accurate assessment of PD-L1 expression is a critical step for clinical intervention. However, there are some problems with the traditional methods of evaluating PD-L1 expression levels. In this study, we developed three AI-based workflows that can be used for the quantitative scoring of PD-L1 expression in digital whole slides of lung cancer. These three fully automated AI-based workflows showed high specificity and accuracy in the PD-L1 expression of tumor cells, especially at 1% cutoff. Moreover, the high performance of our AI diagnostic models was further confirmed in lung adenocarcinoma and lung squamous cell carcinoma of both sampling methods (surgical sampling and needle biopsy).

In clinical practice, the experience of clinical pathologists has a certain impact on the identification of PD-L1 expression results (22). The assessment results of trained pathologists' evaluation of PD-L1 expression are usually more accurate than those of untrained pathologists (33). It takes extensive professional learning and training for an untrained pathologist to become experienced (34). Previous studies have indicated that the assessment of PD-L1 expression by untrained pathologists has lower intraclass consistency compared with that by highly trained pathologists (35). Moreover, manually counting tumor

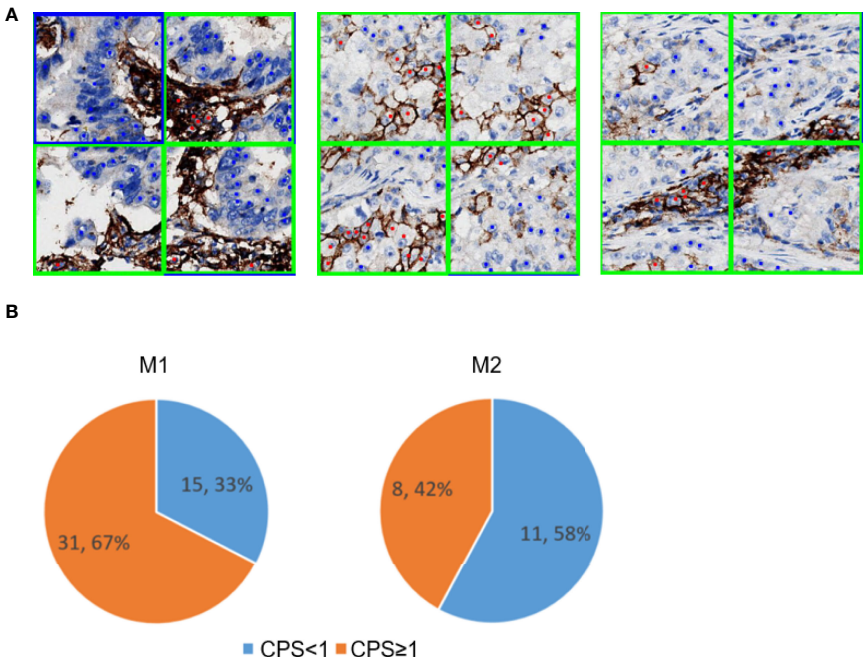

FIGURE 6 | PD-L1-positive immune cells patch filter module. **(A)** Predicted tumor and immune patch annotated with blue and green squares, respectively. The predicted PD-L1-negative tumor cells and PD-L1-positive tumor cells are indicated with blue and red dots, respectively. **(B)** Performance of the immune filter module in M1 (left) and M2 (right). These pie charts show the percentage of false positive slides with CPS <1 and ≥1.

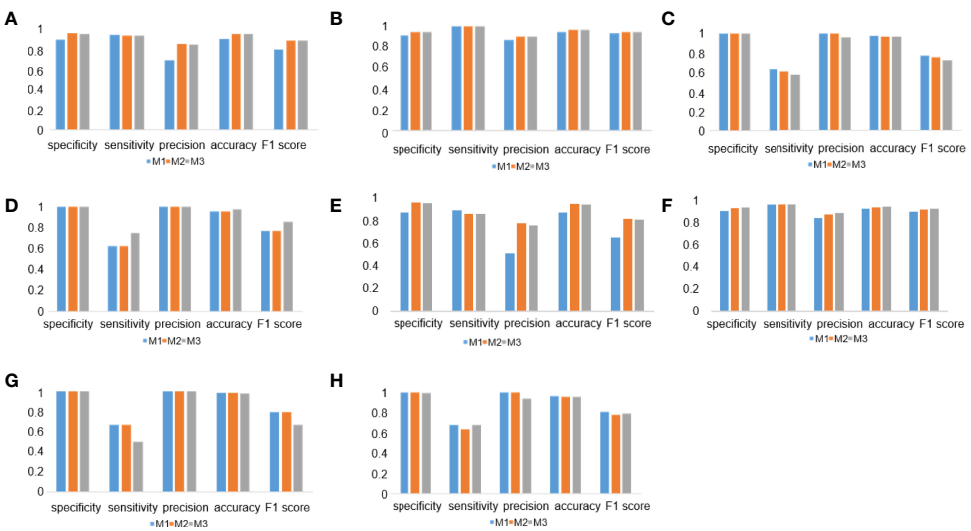

FIGURE 7 | Deep learning (DL) model performance in different tumor types and surgical methods. **(A–D)** Histograms of DL model performance of lung adenocarcinoma **(A, C)** and lung squamous cell carcinoma **(B, D)** at the cutoff of 1% **(A, B)** and 50% **(C, D)**. **(D–F)** Histograms of DL model performance of samples from surgery **(E, G)** and needle biopsy **(F, H)** at the cutoff 1% **(E, F)** and 50% **(G, H)**.

cells for the interpretation of PD-L1 expression levels is of low efficiency and poor repeatability (24). Because of the intratumoral heterogeneity and variability of the whole slides of tumor tissues, it is a difficult task for a pathologist to get a precise assessment of all PD-L1-expressing tumor cells (36). Thus, the exploration of accurate and efficient automated diagnosis technology is urgently needed for the precise evaluation of PD-L1 expression in clinical practice.

The abovementioned challenges have been solved to a certain extent with the development of DL models (37). Previous studies

have indicated that the diagnosis result of an AI model is highly consistent with that of highly trained pathologists and even better than that of untrained pathologists (22, 37). With fully automated labeling and calculation ability, a DL-based AI diagnostic model could assess the expression of PD-L1 (20) similar to a pathologist's cognition of different cells. The exploration of the random forest assessment-based PD-L1 scoring algorithm indicated that the results of AI-based diagnostic models showed a high concordance with those of pathologists (38). Moreover, a previous study showed that different PD-L1-positive cells and other regions could be detected at a pixel level with a DL model (25). These results have indicated the promising application of the DL-based AI diagnostic model in PD-L1 scoring assessment for tumor immunotherapy in NSCLC.

However, the interpretation of slides with low PD-L1 expression is still a challenge for AI models (24, 25, 39). In this study, we focused on distinguishing PD-L1-positive tumor cells from PD-L1-positive immune cells. Our DL-based AI diagnostic workflows showed a high performance in PD-L1 scoring, especially at 1% cutoff. The M2 and M3 workflows showed high precision detection, and all five indicators performed well, especially for PD-L1 expression below 1%. We noticed that, in some cases, stromal cells in the tumor cell-containing patches were predicted as PD-L1-negative tumor cells in the YOLO model, leading to a lower TPS value and false negatives, especially at 50% cutoff value. In our proposed workflows, we compared two different patch sizes used in the classification models, namely, the 256 patch and the 128 patch. We speculated that the 128 patch would be superior to the 256 patch because cells in the 128 patch were more likely to be of the same type compared to the cells in the 256 patch, and this would reduce the counts of misdiagnosed stromal cells in the tumor cell-containing patches. However, the results shown in the classification models with these two different patch sizes almost have the same performance.

The tumor segmentation model reported in the literature requires a large amount of labeling work because it needs to be done at the pixel level (40). The patch classification model used in our study was easier to obtain. Moreover, it seems that the patch classification model has a strong ability to classify tissues with different structural patterns (41). In our study, compared to the M1 workflow, the M2 workflow ensured a higher accuracy of the results owing to its ability to distinguish PD-L1-positive tumor cells from PD-L1-positive immune cells. It is important to test the performance of AI models in samples with different histological subtypes or from different sampling methods encountered by pathologists in clinical practice. The AI diagnostic models shown here were tested in lung squamous cell carcinoma and lung adenocarcinoma, and the results show that there were no differences between histological subtypes. We also found that the proposed AI diagnostic models performed well both in samples from surgery and needle biopsy. Of the 18 pleural effusions samples, four negative samples were predicted as false positive, and one positive sample was predicted as false negative. Compared to the histological samples, the cytological samples have less structure information. It would pose a challenge for the AI model to distinguish tumor cells from other tissue cells in pleural effusions. In the future, more pleural effusion samples are needed to train our model and test its interpretation power of PD-L1 expression.

In current clinical practice, several assays for detecting PD-L1 expression using IHC analysis have been developed for different platforms, and some studies have evaluated various IHC assays for their reproducibility and sensitivity based on the respective scoring criteria (33). The results showed highly comparable staining by the 22C3, 28–8, and SP263 assays and lower sensitivity of the SP142 assay for determining TPS on TCs (33, 42). In this study, although the AI models were only trained with 22C3 immunostaining samples, our AI diagnostic models could effectively identify PD-L1-positive cells in both 22C3 and SP263 staining samples. In the future, it is valuable for us to evaluate the ability of the proposed AI diagnostic models in samples stained by other PD-L1 IHC assays.

There were some limitations in the current study. First, the sample size of this study was small, especially for pleural effusions. More slides need to be considered in a future study. Second, this study lacked multicenter external verification. Multicenter research could make our research results more convincing and could test the generalization ability of our AI models on slides from different sources. Third, the detection results of PD-L1 high-expression samples need to be further optimized. Fourth, factors such as the morphology and structural similarity between some PD-L1-positive immune cells and PD-L1-positive tumor cells as well as the presence of other confounding factors (*e.g.*, poor quality of staining or the destruction of the structure of a tissue during sample preparation) may have affected the identification. It is still a challenge for the AI model to classify them. Immunostaining with more specific biomarkers (like CK for tumor cell or CD68 for macrophages) is a potential solution.

What is more, many studies have shown that PD-L1 expression alone is insufficient for patient selection in most malignancies, and a lot of new potential biomarkers are being studied for precision cancer immunotherapy (43). Increasing studies have indicated that the TME plays an important role in immunopathology and predicting clinical outcomes (44). Some predictive biomarkers in the components of TME have been widely used in immune checkpoint inhibitor therapies (45). The interactions between tumor and immune cells in the TME and their impact on the efficacy of tumor immunotherapy need more exploration. With the development of spatial TME profiling technologies (44), more comprehensive immunotherapy biomarker expression information will be further enhanced. DL is another emerging potential method that could assist in exploring the complexity of the TME, especially the spatial organization of tumor-infiltrating immune cells in the TME (14).

In summary, we explored and optimized three different AI model-based workflows for automatically detecting the positive PD-L1 expression in both 22C3 and SP263 assays. A highly

accurate performance of the AI-assisted DL diagnostic models was shown in lung adenocarcinoma and lung squamous cell carcinoma of both sampling methods, especially for PD-L1 expression at 1% cutoff. Moreover, M2 could further improve the accuracy of the results. Our results indicate that AI-based diagnostic models are a promising approach to assist pathologists in making an accurate assessment of PD-L1 expression.

DATA AVAILABILITY STATEMENT

The original contributions presented in the study are included in the article/**Supplementary Material**, further inquiries can be directed to the corresponding authors.

ETHICS STATEMENT

The studies involving human participants were reviewed and approved by The Ethics Committee of Zhejiang Cancer Hospital (IRB-2020-310 and IRB-2021-439). The patients/participants provided their written informed consent to participate in this study. The animal study was reviewed and approved by The Ethics Committee of Zhejiang Cancer Hospital. Written informed consent was obtained from the owners for the participation of their animals in this study. Written informed consent was obtained from the individual(s) for the publication of any potentially identifiable images or data included in this article.

AUTHOR CONTRIBUTIONS

Conceptualization: MW, QX, GC, PC, and DZ. Methodology and investigation: GC, FZ, YX, XH, HZ, SC, ML, PC, GD, and PC. Visualization: GC, PC, FZ, and YX. Funding acquisition: GC and MW. Project administration and supervision: MW, QX, GC, PC, DZ, and FZ. Writing—original draft: FZ, GC, and YX. Writing—review and editing: MW, QX, PC, and DZ. All authors contributed to the article and approved the submitted version.

FUNDING

This work was supported by the Medical Health Science and Technology Project of Zhejiang Provincial Health Commission (2021KY579) and Zhejiang Provincial Natural Science Foundation of China under Grant (LGF20H160008).

ACKNOWLEDGMENTS

We appreciate the support and participation of the physicians and patients in this study.

SUPPLEMENTARY MATERIAL

The Supplementary Material for this article can be found online at: https://www.frontiersin.org/articles/10.3389/fimmu.2022.893198/full#supplementary-material

REFERENCES

1. Guo H, Li W, Qian L, Cui J. Clinical Challenges in Neoadjuvant Immunotherapy for non-Small Cell Lung Cancer. *Chin J Cancer Res* (2021) 33(2):203–15. doi: 10.21147/j.issn.1000-9604.2021.02.08
2. Yang L, Wang L, Zhang Y. Immunotherapy for Lung Cancer: Advances and Prospects. *Am J Clin Exp Immunol* (2016) 5(1):1–20.
3. Incorvaia L, Fanale D, Badalamenti G, Barraco N, Bono M, Corsini LR, et al. Programmed Death Ligand 1 (PD-L1) as a Predictive Biomarker for Pembrolizumab Therapy in Patients With Advanced Non-Small-Cell Lung Cancer (NSCLC). *Adv Ther* (2019) 36(10):2600–17. doi: 10.1007/s12325-019-01057-7
4. Han Y, Liu D, Li L. PD-1/PD-L1 Pathway: Current Researches in Cancer. *Am J Cancer Res* (2020) 10(3):727–42.
5. Anderson NM, Simon MC. The Tumor Microenvironment. *Curr Biol* (2020) 30(16):R921–5. doi: 10.1016/j.cub.2020.06.081
6. Sadeghi Rad H, Monkman J, Warkiani ME, Ladwa R, O'Byrne K, Rezaei N, et al. Understanding the Tumor Microenvironment for Effective Immunotherapy. *Med Res Rev* (2021) 41(3):1474–98. doi: 10.1002/med.21765
7. Baghban R, Roshangar L, Jahanban-Esfahlan R, Seidi K, Ebrahimi-Kalan A, Jaymand M, et al. Tumor Microenvironment Complexity and Therapeutic Implications at a Glance. *Cell Commun Signal* (2020) 18(1):59. doi: 10.1186/s12964-020-0530-4
8. Lundervold AS, Lundervold A. An Overview of Deep Learning in Medical Imaging Focusing on MRI. *Z Med Phys* (2019) 29(2):102–27. doi: 10.1016/j.zemedi.2018.11.002
9. Suganyadevi S, Seethalakshmi V, Balasamy K. A Review on Deep Learning in Medical Image Analysis. *Int J Multimed Inf Retr* (2021) 11(1):19–38. doi: 10.1007/s13735-021-00218-1
10. Chan HP, Samala RK, Hadjiiski LM, Zhou C. Deep Learning in Medical Image Analysis. *Adv Exp Med Biol* (2020) 1213:3–21. doi: 10.1007/978-3-030-33128-3_1
11. Chen CL, Mahjoubfar A, Tai LC, Blaby IK, Huang A, Niazi KR, et al. Deep Learning in Label-Free Cell Classification. *Sci Rep* (2016) 6:21471. doi: 10.1038/srep21471
12. Yan X, Ding J, Cheng HD. A Novel Adaptive Fuzzy Deep Learning Approach for Histopathologic Cancer Detection. *Annu Int Conf IEEE Eng Med Biol Soc* (2021) 2021:3518–21. doi: 10.1109/EMBC46164.2021.9630824
13. Serag A, Ion-Margineanu A, Qureshi H, McMillan R, Saint Martin MJ, Diamond J, et al. Translational AI and Deep Learning in Diagnostic Pathology. *Front Med (Lausanne)* (2019) 6:185. doi: 10.3389/fmed.2019.00185
14. Saltz J, Gupta R, Hou L, Kurc T, Singh P, Nguyen V, et al. Spatial Organization and Molecular Correlation of Tumor-Infiltrating Lymphocytes Using Deep Learning on Pathology Images. *Cell Rep* (2018) 23(1):181–193 e7. doi: 10.1016/j.celrep.2018.03.086
15. Khameneh FD, Razavi S, Kamasak M. Automated Segmentation of Cell Membranes to Evaluate HER2 Status in Whole Slide Images Using a Modified Deep Learning Network. *Comput Biol Med* (2019) 110:164–74. doi: 10.1016/j.compbiomed.2019.05.020
16. Saha M, Chakraborty C, Arun I, Ahmed R, Chatterjee S. An Advanced Deep Learning Approach for Ki-67 Stained Hotspot Detection and Proliferation Rate Scoring for Prognostic Evaluation of Breast Cancer. *Sci Rep* (2017) 7(1):3213. doi: 10.1038/s41598-017-03405-5
17. Dong Y, Hou L, Yang W, Han J, Wang J, Qiang Y, et al. Multi-Channel Multi-Task Deep Learning for Predicting EGFR and KRAS Mutations of non-Small Cell Lung Cancer on CT Images. *Quant Imaging Med Surg* (2021) 11(6):2354–75. doi: 10.21037/qims-20-600
18. Ahuja AS. The Impact of Artificial Intelligence in Medicine on the Future Role of the Physician. *PeerJ* (2019) 7:e7702. doi: 10.7717/peerj.7702
19. Ahmad Z, Rahim S, Zubair M, Abdul-Ghafar J. Artificial Intelligence (AI) in Medicine, Current Applications and Future Role With Special Emphasis on its Potential and Promise in Pathology: Present and Future Impact, Obstacles

Including Costs and Acceptance Among Pathologists, Practical and Philosophical Considerations. A Comprehensive Review. *Diagn Pathol* (2021) 16(1):24. doi: 10.1186/s13000-021-01085-4
20. Tian P, He B, Mu W, Liu K, Liu L, Zeng H, et al. Assessing PD-L1 Expression in non-Small Cell Lung Cancer and Predicting Responses to Immune Checkpoint Inhibitors Using Deep Learning on Computed Tomography Images. *Theranostics* (2021) 11(5):2098–107. doi: 10.7150/thno.48027
21. Wiesweg M, Mairinger F, Reis H, Goetz M, Kollmeier J, Misch D, et al. Machine Learning Reveals a PD-L1-Independent Prediction of Response to Immunotherapy of non-Small Cell Lung Cancer by Gene Expression Context. *Eur J Cancer* (2020) 140:76–85. doi: 10.1016/j.ejca.2020.09.015
22. Wu J, Liu C, Liu X, Sun W, Li L, Gao N, et al. Artificial Intelligence-Assisted System for Precision Diagnosis of PD-L1 Expression in non-Small Cell Lung Cancer. *Mod Pathol* (2021) 35(3):403–11. doi: 10.1038/s41379-021-00904-9
23. Baxi V, Edwards R, Montalto M, Saha S. Digital Pathology and Artificial Intelligence in Translational Medicine and Clinical Practice. *Mod Pathol* (2021) 35(1):23–32. doi: 10.1038/s41379-021-00919-2
24. Pan B, Kang Y, Jin Y, Yang L, Zheng Y, Cui L, et al. Automated Tumor Proportion Scoring for PD-L1 Expression Based on Multistage Ensemble Strategy in non-Small Cell Lung Cancer. *J Transl Med* (2021) 19(1):249. doi: 10.1186/s12967-021-02898-z
25. Liu J, Zheng Q, Mu X, Zuo Y, Xu B, Jin Y, et al. Automated Tumor Proportion Score Analysis for PD-L1 (22C3) Expression in Lung Squamous Cell Carcinoma. *Sci Rep* (2021) 11(1):15907. doi: 10.1038/s41598-021-95372-1
26. Sandler M HA, Zhu M, Zhmoginov A, Chen L. MobileNetV2: Inverted Residuals and Linear Bottlenecks IEEE *Conference on Computer Vision and Pattern Recognition (CVPR)*. (2018).
27. Bochkovskiy A WC, Liao H. *Yolov4: Optimal Speed and Accuracy of Object Detection*, Vol. 17. (2020).
28. Tan M PR, Le Q. Efficientdet: Scalable and Efficient Object Detection. *arXiv e-prints* (2019) 10:10781–90.
29. Grigg C, Rizvi NA. PD-L1 Biomarker Testing for non-Small Cell Lung Cancer: Truth or Fiction? *J Immunother Cancer* (2016) 4:48. doi: 10.1186/s40425-016-0153-x
30. Teixido C, Vilarino N, Reyes R, Reguart N. PD-L1 Expression Testing in non-Small Cell Lung Cancer. *Ther Adv Med Oncol* (2018) 10:1758835918763493. doi: 10.1177/1758835918763493
31. Yu H, Boyle TA, Zhou C, Rimm DL, Hirsch FR. PD-L1 Expression in Lung Cancer. *J Thorac Oncol* (2016) 11(7):964–75. doi: 10.1016/j.jtho.2016.04.014
32. Garon EB, Rizvi NA, Hui R, Leighl N, Balmanoukian AS, Eder JP, et al. Pembrolizumab for the Treatment of non-Small-Cell Lung Cancer. *N Engl J Med* (2015) 372(21):2018–28. doi: 10.1056/NEJMoa1501824
33. Hirsch FR, McElhinny A, Stanforth D, Ranger-Moore J, Jansson M, Kulangara K, et al. PD-L1 Immunohistochemistry Assays for Lung Cancer: Results From Phase 1 of the Blueprint PD-L1 IHC Assay Comparison Project. *J Thorac Oncol* (2017) 12(2):208–22. doi: 10.1016/j.jtho.2016.11.2228
34. Wang X, Chen P, Ding G, Xing Y, Tang R, Peng C, et al. Dual-Scale Categorization Based Deep Learning to Evaluate Programmed Cell Death Ligand 1 Expression in non-Small Cell Lung Cancer. *Med (Baltimore)* (2021) 100(20):e25994. doi: 10.1097/MD.0000000000025994
35. Chang S, Park HK, Choi YL, Jang SJ. Interobserver Reproducibility of PD-L1 Biomarker in Non-Small Cell Lung Cancer: A Multi-Institutional Study by 27 Pathologists. *J Pathol Transl Med* (2019) 53(6):347–53. doi: 10.4132/jptm.2019.09.29
36. Rehman JA, Han G, Carvajal-Hausdorf DE, Wasserman BE, Pelekanou V, Mani NL, et al. Quantitative and Pathologist-Read Comparison of the Heterogeneity of Programmed Death-Ligand 1 (PD-L1) Expression in non-Small Cell Lung Cancer. *Mod Pathol* (2017) 30(3):340–9. doi: 10.1038/modpathol.2016.186
37. Nielsen KB, Lautrup ML, Andersen JKH, Savarimuthu TR, Grauslund J. Deep Learning-Based Algorithms in Screening of Diabetic Retinopathy: A Systematic Review of Diagnostic Performance. *Ophthalmol Retina* (2019) 3(4):294–304. doi: 10.1016/j.oret.2018.10.014
38. Wu J, Lin D. A Review of Artificial Intelligence in Precise Assessment of Programmed Cell Death-Ligand 1 and Tumor-Infiltrating Lymphocytes in Non-Small Cell Lung Cancer. *Adv Anat Pathol* (2021) 28(6):439–45. doi: 10.1097/PAP.0000000000000322
39. Wu J, Liu C, Liu X, Sun W, Li L, Gao N, et al. Artificial Intelligence-Assisted System for Precision Diagnosis of PD-L1 Expression in non-Small Cell Lung Cancer. *Mod Pathol* (2022) 35(3):403–11. doi: 10.1038/s41379-021-00904-9
40. Lee K, Lockhart JH, Xie M, Chaudhary R, Slebos RJC, Flores ER, et al. Deep Learning of Histopathology Images at the Single Cell Level. *Front Artif Intell* (2021) 4:754641. doi: 10.3389/frai.2021.754641
41. Carter JH. The Immune System as a Model for Pattern Recognition and Classification. *J Am Med Inform Assoc* (2000) 7(1):28–41. doi: 10.1136/jamia.2000.0070028
42. Tsao MS, Kerr KM, Kockx M, Beasley MB, Borczuk AC, Botling J, et al. PD-L1 Immunohistochemistry Comparability Study in Real-Life Clinical Samples: Results of Blueprint Phase 2 Project. *J Thorac Oncol* (2018) 13(9):1302–11. doi: 10.1016/j.jtho.2018.05.013
43. Cristescu R, Mogg R, Ayers M, Albright A, Murphy E, Yearley J, et al. Pan-Tumor Genomic Biomarkers for PD-1 Checkpoint Blockade-Based Immunotherapy. *Science* (2018) 362(6411):eaar3593. doi: 10.1126/science.aar3593
44. Sadeghi Rad H, Bazaz SR, Monkman J, Ebrahimi Warkiani M, Rezaei N, O'Byrne K, et al. The Evolving Landscape of Predictive Biomarkers in Immuno-Oncology With a Focus on Spatial Technologies. *Clin Transl Immunol* (2020) 9(11):e1215. doi: 10.1002/cti2.1215
45. Bai R, Lv Z, Xu D, Cui J. Predictive Biomarkers for Cancer Immunotherapy With Immune Checkpoint Inhibitors. *biomark Res* (2020) 8:34. doi: 10.1186/s40364-020-00209-0

Conflict of Interest: FZ, YX, SC, ML, PC, DZ and CP are current or former employees of the company 3D Medicines Inc.

The remaining authors declare that the research was conducted in the absence of any commercial or financial relationships that could be construed as a potential conflict of interest.

Publisher's Note: All claims expressed in this article are solely those of the authors and do not necessarily represent those of their affiliated organizations, or those of the publisher, the editors and the reviewers. Any product that may be evaluated in this article, or claim that may be made by its manufacturer, is not guaranteed or endorsed by the publisher.

frontiers | Frontiers in Oncology

TYPE Original Research
PUBLISHED 25 October 2022
DOI 10.3389/fonc.2022.887383

OPEN ACCESS

EDITED BY
Roberta Zappasodi,
Cornell University, United States

REVIEWED BY
Gang Sun,
The First Affiliated Hospital of People's Liberation Army General Hospital, China
Tiziana Schioppa,
University of Brescia, Italy

*CORRESPONDENCE
Yi Hu
huyi301zlxb@sina.com

SPECIALTY SECTION
This article was submitted to Cancer Immunity and Immunotherapy, a section of the journal Frontiers in Oncology

RECEIVED 01 March 2022
ACCEPTED 29 July 2022
PUBLISHED 25 October 2022

CITATION
Wu Z, Zhang S, Li L, Huang Z, Huang D and Hu Y (2022) The gut microbiota modulates responses to anti–PD-1 and chemotherapy combination therapy and related adverse events in patients with advanced solid tumors. *Front. Oncol.* 12:887383. doi: 10.3389/fonc.2022.887383

The gut microbiota modulates responses to anti–PD-1 and chemotherapy combination therapy and related adverse events in patients with advanced solid tumors

Zhaozhen Wu[1,2,3], Sujie Zhang[1], Lingling Li[1,3], Ziwei Huang[1], Di Huang[1] and Yi Hu[1,3]*

[1]Department of Medical Oncology, the Fifth Medicine Center of Chinese People's Liberation Army (PLA) General Hospital, Beijing, China, [2]Beijing Chest Hospital, Beijing, China, [3]School of Medicine, Nankai University, Tianjin, China

Background: Immune checkpoint inhibitors (ICIs) targeting programmed cell death protein 1 (PD-1) have been widely used in treating different malignancies. Several studies have reported that the gut microbiota modulates the response and adverse events (AEs) to ICIs in melanoma, non–small cell lung cancer (NSCLC), renal cell cancer and hepatocellular carcinoma, but data on other cancer types and ICI combination therapy are limited.

Methods: Stool samples were collected from patients with cancer who received anti–PD-1 and chemotherapy combination treatment and were analyzed by fecal metagenomic sequencing. The microbiota diversity and composition were compared between the responder (R) and non-responder (NR) groups and the AE vs. the non-AE (NAE) groups. In addition, associated functional genes and metabolic pathways were identified.

Results: At baseline, the microbiota diversity of the groups was similar, but the genera *Parabacteroides*, *Clostridia bacterium UC5.1_2F7*, and *Bifidobacterium dentium* were enriched in the R group, whereas *Bacteroides dorei* and 11 species of *Nocardia* were enriched in the NR group. At 6 weeks, the beta diversity was significantly different between the R and NR groups. Further analysis found that 35 genera, such as *Alipes*, *Parabacteroides*, *Phascolarctobacterium*, *Collinsella*, *Ruminiclostridium*, *Porphyromonas*, and *Butyricimonas* and several genera of the *Fibrobacteraceae* family, were frequently distributed in the R group, whereas 17 genera, including *Enterococcus*, *Lachnoclostridium*, *Hungatella*, and *Bilophila* and several genera of the *Pseudonocardiaceae* and *Beijerinckiaceae* families, were more abundant in the NR group. A total of 66 and 52 Kyoto Encyclopedia of Genes and Genomes (KEGG) orthologs (KOs) were significantly enriched in the R and NR groups, respectively. In addition, pathway analysis revealed functional

differences in the gut microbacteria in the R group, including the enrichment of anabolic pathways and DNA damage repair (DDR) pathways. Dynamic comparisons of the bacterial composition at baseline, 6 weeks, and 12 weeks showed that the abundance of *Weissella* significantly increased in the R group at 6 weeks and the abundance of *Fusobacterium* and *Anaerotruncus* significantly increased in the NR group at 12 weeks. Linear discriminant analysis effect size analysis indicated that bacteria of *Bacteroidetes*, especially *Bacteroides*, were enriched in the NAE group, whereas flora of *Firmcutes*, such as *Faecalibacterium prausnitzii*, *Bacteroides fragilis*, and *Ruminococcus lactaris*, were enriched in the AE group.

Conclusion: Beta diversity and differences in the gut microbiota modulated AEs and the response to anti–PD-1 blockade combined with chemotherapy, by regulating related anabolic and DDR pathways. Dynamic changes in the intestinal microbiome may predict the efficacy of PD-1 inhibitor–based therapy.

KEYWORDS

gut microbiota, response, adverse events, anti–PD-1 therapy, solid tumors

Introduction

In recent years, immune checkpoint inhibitors (ICIs), which target the cytotoxic T lymphocyte antigen-4 (CTLA-4) or programmed cell death protein 1 (PD-1)/PD-1 ligand (PD-L1) pathway, have been shown to be effective in the treatment of different malignancies (1) with a lower incidence of side effects. However, only a subset of patients with cancer derives benefits from these agents. Several biomarkers, such as PD-L1, tumor mutation burden and other molecular characteristics, microsatellite instability, and Epstein–Barr virus (2–7), were suggested to help select potential beneficiaries, but none of them was accurate. It is thus critical to further understand the determinants driving response and explore potential biomarkers.

Increasing evidence suggests that the gut microbiome plays a significant role in the response to both immunotherapy and chemotherapy. Significantly, it has been reported that the diversity and composition of the intestinal microbiota influence ICI responses in both mouse models and patients. In murine models, it was demonstrated that *B. thetaiotaomicron* and *B. fragilis* were associated with the response to CTLA-4 blockade (8), and *Bifidobacterium* was associated with the response to PD-L1 blockade (9, 10). *Clostridiales* and *Bacteroidales* were recently reported to be associated with favorable and unfavorable responses, respectively, to anti–PD-1 immunotherapy in a cohort of 112 patients with melanoma (11). It was reported that an elevation of *Prevotella/Bacteroides* ratio was related with a favorable response to anti–PD-1 therapy in advanced-stage gastrointestinal cancer (12). In addition, *Ruminococcaceae* was found to be associated with a favorable response to ICI in NSCLC (13). Moreover, *Akkermansia muciniphila* was found to enhance the efficacy of PD-1 blockade in epithelial tumors in an interleukin-12 (IL-12)–dependent manner (14, 15). In addition to the influence of the gut microbiome on the response to immunotherapy, several studies have reported the efficacy of chemotherapeutic drugs, such as cyclophosphamide and platinum, to be modulated by gut microbiota (16, 17). This is important because combination therapies with anti–PD-1/PD-L1 and other drugs, such as chemotherapy and anti-angiogenesis drugs, are more commonly used than single- agent ICIs in real-word clinical settings. Therefore, we aimed to explore the effect of the gut microbiota on PD-1 inhibitor–based combined therapy.

Method

Study design and fecal sample collection

In total, 27 patients with cancer treated with anti–PD-1 combined with chemotherapy every 3 weeks in the Oncology Department of Chinese PLA General Hospital were enrolled in this study. No antibiotics were used during this treatment regimen, and all patients had signed informed consent forms and donated their stool samples for this study. Stool samples from 24 patients at baseline (day 0), 6 weeks, and 12 weeks were

collected and immediately stored at −80°C until DNA extraction was performed, whereas the stool samples from three patients with AEs were collected only at baseline. The gut microbiota was analyzed by metagenomic sequencing. Clinicopathological data and treatment information were independently collected and recorded by two physicians, and all patients were classified as responders (R, complete response, partial response, or stable disease ≥ 6 months; n = 16) and non-responders (NR; disease progression or stable disease < 6 months; n = 8) based on radiological evaluation by two radiologists according to the Response Evaluation Criteria in Solid Tumors, version 1.1 (RECIST 1.1). Patients were classified as the AE group and the non-AE (NAE) group according to the National Cancer Institute Common Terminology Criteria for Adverse Events, version 4.0 (CTCAE 4.0). This study was approved by the Institutional Ethics Committee of Chinese PLA General Hospital, Beijing, China (approval number: S2019-184-01).

DNA extraction and metagenomic sequencing

The gut bacterial composition was evaluated by fecal metagenomic sequencing. Briefly, bacterial genomic DNA was extracted using the QIAamp DNA Stool Mini Kit (Qiagen, Hilden, Germany). After the integrity and concentration of DNA was determined, individual libraries were constructed with the NEBNext Ultra DNA Library Prep Kit for Illumina (BGI, Shenzhen, China), loaded onto the BGISEQ-500 RS platform (BGI, Shenzhen, China), and then were sequenced according to a 2 × 100-bp paired-end read protocol. Quality filtering, trimming, and demultiplexing were performed as described previously (18). A total of 70 datasets were generated. Overall, 85.84% of the raw reads were considered as high quality, with an average length of 150 bp and an average Q30 score of 88.54% (eTable 1). The species accumulation curves are shown in eFigure 1.

Taxonomic and gene profiling

All high-quality reads were aligned to the Homo sapiens (human) genome assembly hg38 using SOAPalign 2.21 (https://anaconda.org/bioconda/soapaligner) with default parameters to remove human reads. The retained clean reads were aligned to ~1 M clade-specific marker genes from approximately 17,000 reference genomes to estimate relative phylotype abundance using MetaPhlAn (version 2.5.0). For gene annotation, the clean reads were aligned to the integrated gene catalog (IGC) by using SOAPalign 2.21 with the default parameters; only the reads with both ends mapped to the same gene were used in the subsequent analysis. An average IGC mapping rate of 53% was achieved. Functional annotations

TABLE 1 Clinical data of patients in the R and NR groups.

Characteristic	R group (n = 16)	NR group (n = 8)	P value
Gender			1.000
Male	10	5	
Female	6	3	
age			0.362
<65	13	5	
≥65	3	3	
ECOG			0.249
0–1	15	6	
≥2	1	2	
Smoking history			0.388
Current or former	8	2	
Never	8	6	
Antibiotic use			1.000
In ≤1month	3	2	
No	13	6	
Metastasis number			1.000
number<2	12	6	
number≥2	4	2	
CNS metastasis			0.536
yes	2	0	
no	14	8	
Liver metastasis			0.065
yes	2	0	
no	14	8	
Lung metastasis			0.621
yes	5	1	
no	11	7	
Bone metastasis			0.363
yes	4	4	
no	12	4	
PD-L1 expression			0.191
<1%	3	4	
≥1%	12	3	
unknown	1	1	
TMB			0.095
<10m/Mb	5	6	
≥10m/Mb	6	0	
unknown	5	2	
Lymphocyte number			0.167
$<0.8*10^9$/L	3	4	
$\geq 0.8*10^9$/L	13	4	
LDH			1.000
<250U/L	11	5	
≥250U/L	5	3	
Treatment lines			0.741
1	7	5	
1~2	5	2	
≥3	4	1	

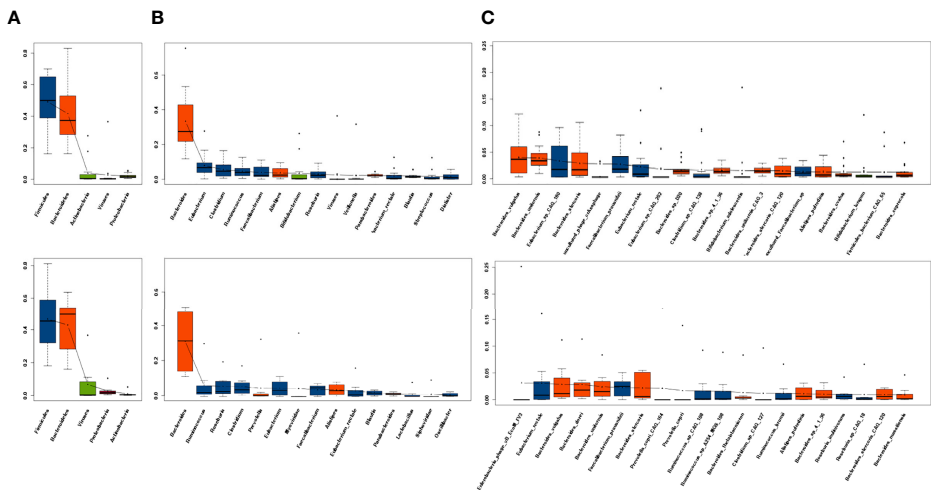

FIGURE 1
Dominant microbiota composition at baseline. **(A)** The top 5 phyla, **(B)** top 10 genera, and **(C)** top 20 species in the R group (n = 16, upper) and NR group (n = 8, lower) are listed separately. Red indicates *Bacteroidetes* and blue indicates *Firmicutes*.

were carried out *via* BLASTP searches against the Kyoto Encyclopedia of Genes and Genomes (KEGG) database (e-value ≤$1e^{-5}$ and high-scoring segment pair scoring >60). The KEGG ortholog (KO) abundance was estimated by accumulating the relative abundance of all genes belonging to this feature. All of the above procedures were carried out as previously described (19).

Statistical analysis

Clinical characteristics and demographic data were summarized *via* descriptive statistical analysis, and the Fisher's exact test was used to compare differences between two groups using SPSS 20.0 software (IBM, SPSS, Chicago, IL, USA). Two-sided P-values were evaluated, and $P < 0.05$ was considered statistically significant. The Shannon and Simpson indices were used to calculate alpha diversity, and principal coordinates analysis (PCoA) and the analysis of similarities (ANOSIM) test with the Bray–Curtis distance were used to evaluate beta diversity. A non-parametric Wilcoxon rank sum test was applied to analyze the statistical significance of diversity indices, taxa, and KOs between the R and NR groups. The linear discriminant analysis (LDA) effect size (LEfSe) algorithm was further used to identify the phylotypes that had a significantly different abundance in different groups; phylotypes with an LDA score cutoff of 2.0 and $P < 0.05$ in built-in rank sum test were regarded as statistically significant. A ternary plot in the R language (ggtern package) was used to compare differences among three groups. Spearman sequential correlation analysis was used to estimate the correlation between two variables (microbiota family and metabolic pathways in KEGG database, by R language), and only significant correlations with $P < 0.01$ and rho > 0.5 are shown. The network was visualized with Cytoscape 3.0.2.

Results

Patient characteristics

In total, 27 patients with cancer (including three patients without serial stool samples) were enrolled in our study, including 12 patients with non–small cell lung cancer (NSCLC), nine patients with digestive system cancers, and one patient each with ovarian, bladder, and prostate cancer, separately. We collected patients' demographics and clinicopathological data, including baseline antibiotic use (within 1 month), metastasis, number of treatment regimens received, PD-L1 expression, tumor mutation burden, lymphocyte number, and Lactate dehydrogenase (LDH). We placed these patients in the R or NR group, and the clinical characteristics were balanced between these groups (Table 1).

Dominant microbiota composition and diversity

The top five phyla, top 10 genera, and top 20 species in the R group and the NR group at baseline are listed separately. At baseline, Gram-positive *Firmicutes* and Gram-negative *Bacteroidetes* dominated the fecal microbiota of both the R

and NR groups at the phylum level, which was in accordance with the previous findings in healthy human (20), followed by *Actinobacteria*, *Viruses*, and *Proteobacteria* in the R group and *Viruses*, *Proteobacteria*, and *Actinobacteria* in the NR group (Figure 1A). At the genus level, the dominant microbiome at baseline was similar between the two groups, except for *Alistipes* and *Bifidobacterium*, which seemed to be more abundant in the R group, and *Myoviridae* and *Siphoviridae*, which seemed to be more dominant in the NR group (Figure 1B). At the species level, the top 20 species of two groups almost all belonged to *Firmicutes* and *Bacteroidetes* (Figure 1C). The microbiome composition of 24 patients at baseline is shown in eFigure 3A.

The dynamic analysis of the dominant microbiota at the phylum, genus, and species levels showed a significant decrease in *uncultured phage crAssphage* at 12 weeks compared with baseline in the NR group ($P = 0.047$; eFigure 2F); however, no other significant differences at baseline, 6 weeks, and 12 weeks were observed in either the R group (eFigures 2A, C, E) or the NR group (eFigures 2D, F, 3B).

Alpha diversity was higher in the R group than in the NR group at baseline and 6 weeks, but the differences were not significant ($P > 0.05$; Figures 2A, B). Alpha diversity was higher at 12 weeks than at baseline in the R group, but a significant difference was not observed ($P > 0.05$; Figure 2C), whereas alpha diversity significantly decreased at 12 weeks compared with baseline in the NR group ($0.01 < P < 0.05$; Figure 2D). Although beta diversity determined by PCoA and ANOSIM indicated no significant difference at baseline between the R group and the NR group ($P > 0.05$; Figures 3A, B), beta diversity was significantly different by both PCoA ($P_1 = 0.045$; Figure 3C) and ANOSIM ($P = 0.005$, $R = 0.34$; Figure 3D) at 6 weeks. These results suggest that the intragroup diversity (measured by alpha diversity) was similar at baseline and 6 weeks in the two groups but significantly decreased at 12 weeks in the NR group. In addition, the intergroup diversity (indicated by beta diversity) was significantly different between the R and NR groups at 6 weeks.

Comparison of the gut microbiota composition and genes between the two groups

To further investigate whether the composition of the gut microbiota influenced the response to anti–PD-1–based combination therapy, we compared the relative abundance of gut microbiome components at the genus and species levels in further detail between the R group and the NR group. At baseline, LEfSe analysis of the two groups indicated that the genera *Parabacteroides*, *Bacterium OL_1* and *Clostridia bacterium UC5.1_2F7* genus, and 15 species, including *Bifidobacterium dentium*, were enriched in the R group, whereas the genus *Bacteroidia bacterium UC5.1_2G11* and 19 species including *Bacteroides dorei* and 11 species of *Nocardia* genus were enriched in the NR group (Figures 4A, B). At 6 weeks, differences in the microbiome were more noticeable. A total of 35 genera, such as *Alipes*, *Parabacteroides*, *Phascolarctobacterium*, *Collinsella*, *Ruminiclostridium*, *Porphyromonas*, *Butyricimonas*, and several genera of *Fibrobacteraceae* family, were frequently founed in the R group; whereas 17 genera, including *Enterococcus*, *Lachnoclostridium*, *Hungatella*, *Bilophila*, several genera of *Pseudonocardiaceae*, and *Beijerinckiaceae* families, were more abundant in the NR group (Figure 4C). At the species level, 66 species in the R group and 17 species in the NR group were identified as being differentially abundant by LEfSe analysis. Eubacterium siraeum, Bacteroides uniformis, *Bacteroides xylanisolvens*, *Bacteroides salyersiae*, *Bacteroides caccae CAG_21*, *Bacteroides fragilis*, *Alistipes putredinis*, *Parabacteroides merdae*, *Ruminococcus bromii*, *Lactobacillus kitasatonis*, *Collinsella aerofacien*, and many short-chain fatty acid (SCFA)–producing species were included in the R group, and *Hungatella hathewayi*, several species of the genus *Enterococcus* genus, *Erysipelotrichaceae bacterium I46*, *Bilophila wadsworthia*, and *Lactobacillus phage A2* were included in the NR group (eFigure 3B). The difference in the composition of the gut microbiome at 12 weeks could not be quantified because five samples in the NR group were not obtained, which resulted in an imbalance in case numbers.

We further compared longitudinal differences in the gut microbiota at baseline, 6 weeks, and 12 weeks. LEfSe analysis identified three species in the R group: *Bacteroides uniformis CAG_3* (D0), *Weissella cibaria* (W6), and Enterobacteria phage SfV(W12) (Figure 5A). At the genus level, *Weissella* was significantly enriched at 6 weeks in the R group (Figure 5B), whereas *Fusobacterium* and *Anaerotruncus* were significantly enriched at 12 weeks in the NR group (Figure 5C). Ternary plots generated at the species level yielded similar results to LEfSe analysis (data not shown), and ternary plots generated at the genus level showed the differential enrichment of species of the genera *Weissella, Fusobacterium*, and *Anaerotruncus genus* (Figures 5D, E).

At 6 weeks, ANOSIM showed a significant difference in genes related to the microbiome between the two groups ($P = 0.004$, $R = 0.347$). Coabundance genes (CAG) analysis found 65 differential genes at different taxonomic levels (eTable 2). Some distinct microbiota components between the two groups also showed significant differences at the genetic level; these included *Alipes*, *Parabacteroides merdae*, *Eubacterium siraeum*, *Bacteroides caccae*, *Lactobacillus salivarius*, *Bacteroides fragilis*, and *Barnesiella intestinihominis YIT 11860* in the R group and *Bilophila* and *Bilophila wadsworthia* in the NR group (eTable 2).

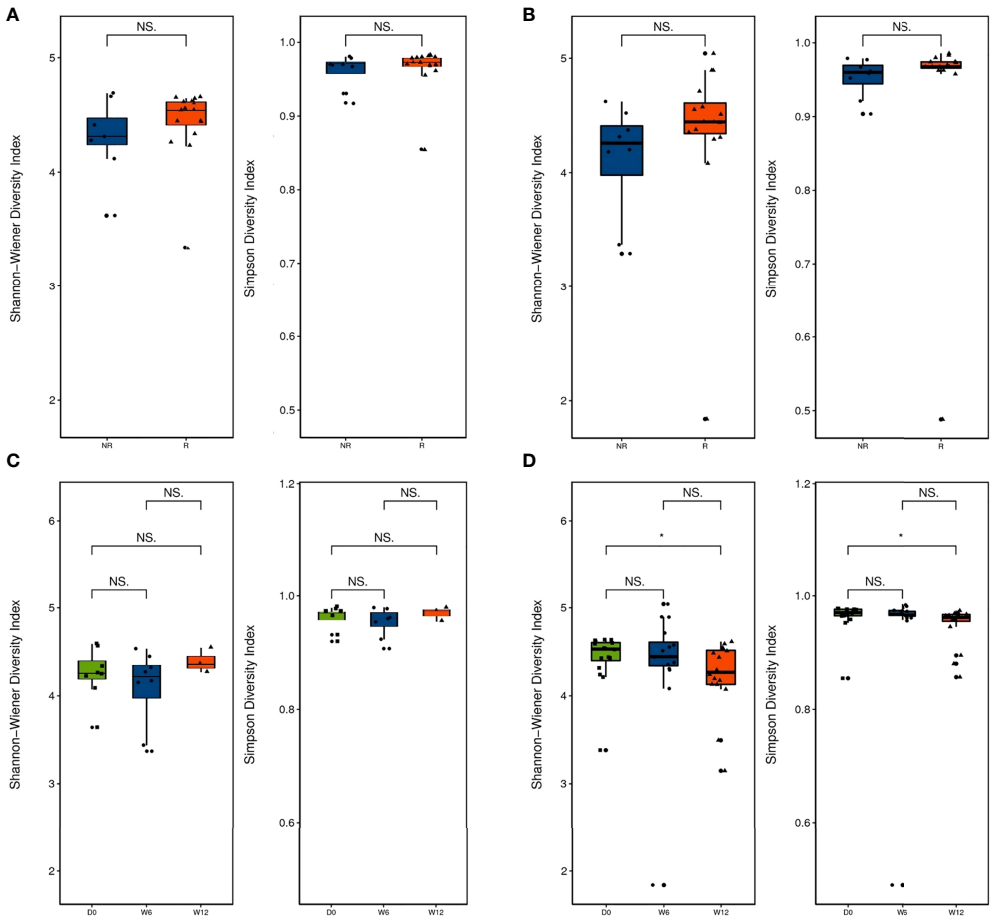

FIGURE 2
Diversity of the gut microbiota between the R group (n = 16) and NR group (n = 8, except at 12 weeks). **(A)** Alpha diversity was evaluated by the Shannon and Simpson indices at baseline and **(B)** 6 weeks. **(C)** Comparison of alpha diversity by the Shannon and Simpson indices at baseline, 6 weeks, and 12 weeks in the R group and **(D)** the NR group (n = 3 at 12 weeks). NS and *indicate values of P > 0.05, P < 0.05, respectively.

Analysis of functional genes and enriched pathway

Functional gene families associated with bacteria in the two groups were further investigated. ANOSIM showed a significant intergroup difference in KEGG orthologs only at 6 weeks (P = 0.004, R = 0.335). A total of 66 and 52 KOs with significant differences were more enriched in the R and NR groups, respectively (eTable 3), and a heatmap of samples and distinct KOs is shown (Figure 6A). Analysis at different functional levels all indicated that the gut microbiota of the R group was more enriched in biochemical functions than that of the NR group (Figure 6B). Further correlation analysis of differentially abundant microbiota and KEGG pathways revealed functional differences in the gut microbiota in the R group, including the enrichment of anabolic pathways and DNA damage repair (DDR) pathways, such as amino acid metabolism, the biosynthesis of other secondary metabolites, and cancer: overview, energy metabolism, glycan biosynthesis and metabolism, part of lipid metabolism, and transcription and translation at both the genus level (eFigure 4) and species level (eFigure 5).

Correlation of the gut microbiota and immune-related adverse events

On the basis of the presence or absence of AEs, seven patients were placed in the AE group and 20 patients were in the NAE group, and data from these 27 patients were analyzed. All immune-related adverse events (irAEs) were ≥ grade 2, including five cases of pneumonitis and two patients of immunotherapy-induced colitis. With the exception of one patient with grade 2 pneumonitis, who restarted

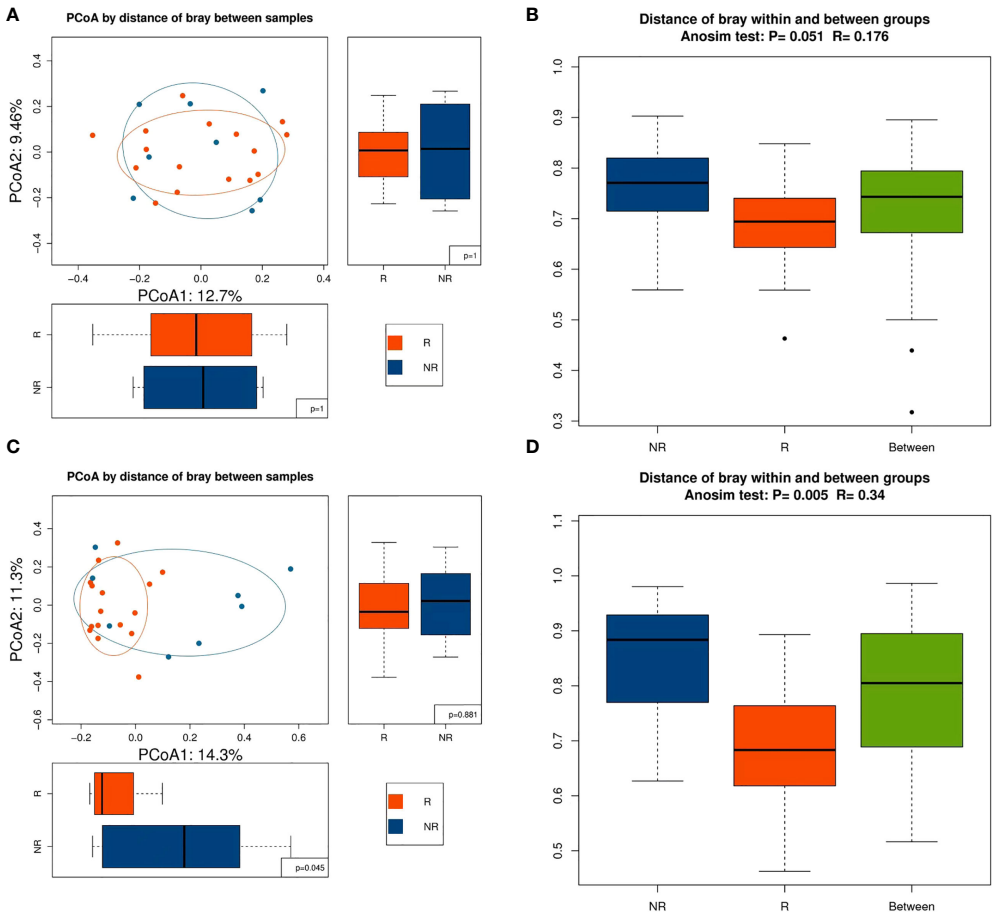

FIGURE 3
Beta diversity between the R (n = 16) and NR (n = 8) groups. **(A)** Beta diversity was evaluated by PCoA and **(B)** ANOSIM at baseline. **(C)** Beta diversity was evaluated by PCoA and **(D)** ANOSIM at 6 weeks.

immunotherapy after pneumonitis was well-controlled, patients with irAEs discontinued immunotherapy.

Although alpha diversity (at the species level) showed no significant difference between the AE group and NAE group ($P > 0.05$; Figure 7A), PCoA of beta diversity indicated that there was a significant intergroup difference between these two groups ($P = 0.036$; Figure 7B). At the phylum level, *Firmicutes* and *Proteobacteria* were more abundant in the AE group, and *Bacteroidetes* was more abundant in the NAE group (Figure 7C). At the genus level, LEfSe analysis identified 38 AE-enriched genera and 16 NAE-enriched genera, including many genera from the *Bacteroides* (Figure 7D). At the species level, LEfSe analysis indicated that 12 species (most of them belonging to *Firmicutes*) were correlated with non-AEs, whereas 13 species of *Firmcutes*, such as *Faecalibacterium prausnitzii*, and *Bacteroides* sp. *2_1_56FAA* (*Bacteroides fragilis*) were enriched in the AE group (Figure 7E).

The results of LEfSe analysis revealed that 12 and 48 KOs were significantly different in the AE and NAE groups, and distinct KOs within the groups are listed in the heatmap (eFigure 6A). FishTaco analysis suggested that NAE-enriched species of *Bacteroides* promoted type I polyketide biosynthesis (eFigure 6B). Further investigation found that irAEs were positively correlated with energy metabolism, membrane transport, transcription, and translation and that irAEs were negatively correlated with streptomycin metabolism, penicillin and cephalosporin biosynthesis, glycan biosynthesis and metabolism, sphingolipid metabolism, and steroid hormone biosynthesis (eFigure 7).

Discussion

Recent work has highlighted the key role of the gut microbiota in mediating tumor responses to chemotherapeutic agents and ICIs as well as irAEs (15, 21, 22). Akkermansia muciniphila (Akk) has been reported to be associated with clinical benefit of ICI in patients with NSCLC or kidney cancer (14, 23), and intestinal Akk was reported to be

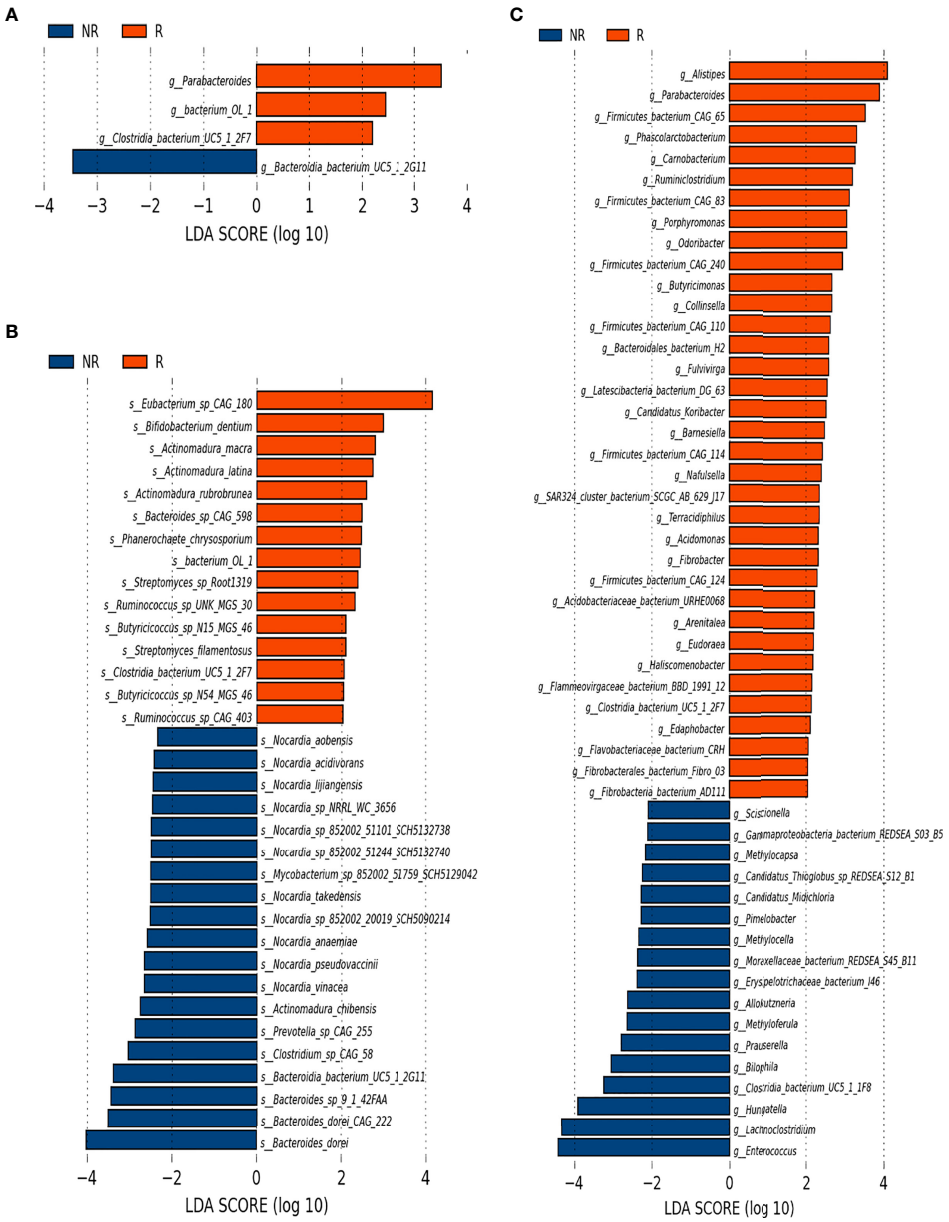

FIGURE 4
Microbiota composition differences between the R group (n = 16) and the NR group (n = 8). **(A)** The relative abundance of R-enriched and NR-enriched genera and **(B)** species at baseline. **(C)** The relative abundance of differentially abundant genera at 6 weeks, as identified by LEfSe analysis (Kruskal–Wallis sum rank test, $P < 0.05$).

accompanied by a richer commensalism, including *Bifidobacterium adolescentis* and *Eubacterium hallii* (15). The diversity of gut microbiota was reported to influence the response to ICIs (19, 24), and in our study, the Shannon and Simpson indices were higher in the R group than in the NR group, but a significant difference was not reached, perhaps due to the small case number. Longitudinal comparisons showed that alpha diversity increased in the R group and decreased in the NR group at 12 weeks. Our study also showed that beta diversity markedly influenced the efficacy of PD-1 blockade–based combination therapy. Baseline beta diversity evaluated by ANOSIM showed a critical P-value of 0.051 (Figure 3B), and beta diversity evaluated by PCoA was not significantly different at baseline between the R group and the NR group ($P_1 = 1$, $P_2 = 1$; Figure 3A); this might have been due to the strict standards of patient selection and sample collection. Beta diversity at 6 weeks by both two methods showed a significant difference between the R group and the NR group, and this result was consistent with a

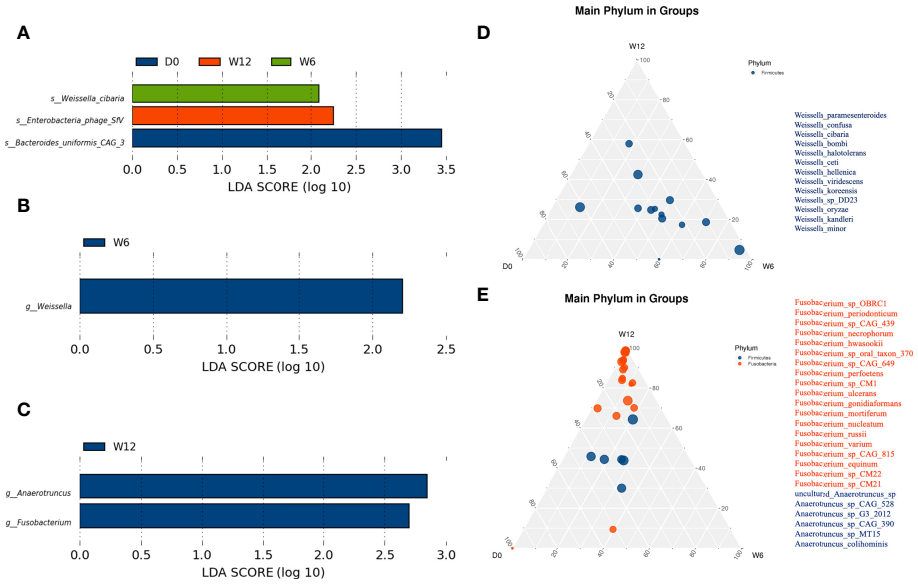

FIGURE 5
Dynamic analysis of the gut microbiota longitudinally. **(A)** Differential species in the R group (n = 16) at baseline, 6 weeks, and 12 weeks. **(B, C)** Differential genera in the R group (n = 16) and the NR group (n = 8 at 6 weeks, n = 3 at 12 weeks). **(D, E)** At the genus level, significantly different species were identified by ternary plots between the R group (n = 16) and NR group (n = 8) at 6 weeks.

previous study that showed that the beta diversity became significantly lower as early as week 6 (19). It is worthy of further study on the relationship of beta diversity and the efficacy of immunotherapy at different timepoints.

We identified differentially enriched gut microbiota at both baseline and 6 weeks in the R and NR groups; *Parabacteroides* and *Bifidobacterium dentium* were more abundant in the R group at baseline, which was in accordance with previous studies

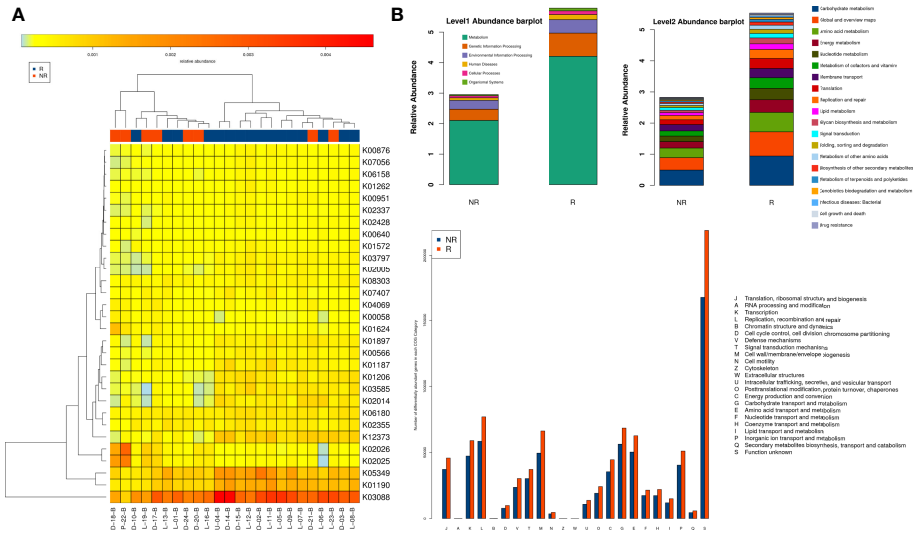

FIGURE 6
Comparison of functional genes and metabolic pathways at 6 weeks in the R group (n = 16) and the NR group (n = 8). **(A)** Heatmap of samples and differential KOs based on LEfSe analysis. **(B)** The gut microbiota of the R group was more enriched in biochemical and metabolic pathways at different functional levels, as evaluated with the KEGG and EggNOG databases.

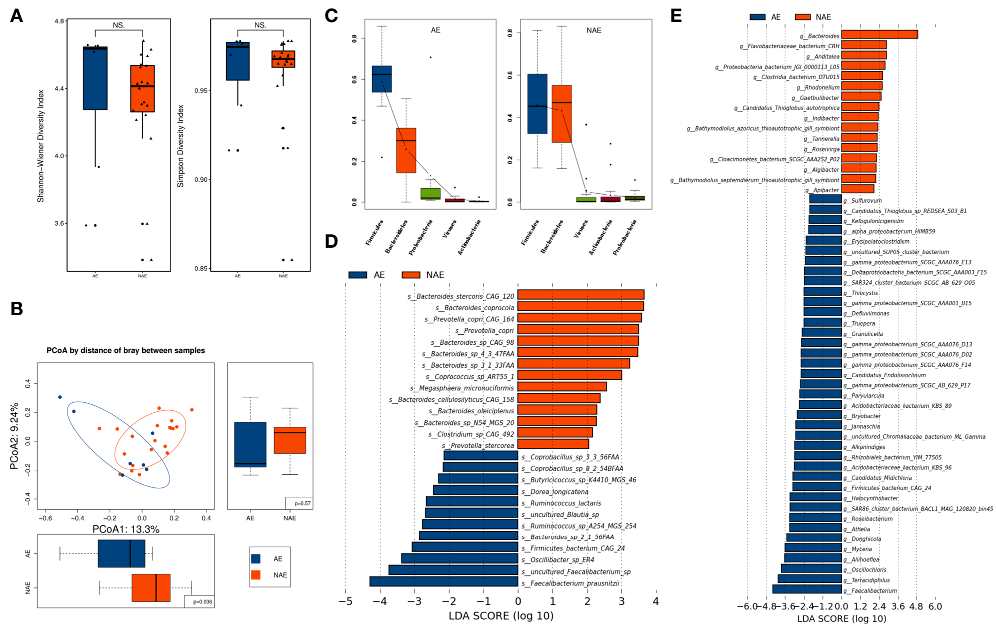

FIGURE 7
The correlation of the baseline gut microbiome and irAEs. **(A)** Alpha diversity was determined by the Shannon and Simpson indices at the species level between the AE group (n = 7) and the NAE group (n = 20). **(B)** Beta diversity was evaluated by PCoA analysis at the species level. **(C)** Dominant gut microbiota at the phylum level. **(D)** Differentially abundant microbiota components were identified by LEfSe analysis at the genus and **(E)** species levels.

(9, 25). The differential enrichment between the two groups was more notable at 6 weeks than at baseline; 35 genera and 66 species were enriched in the R group. Among these enriched microbiota components, *Alipes* (14), *Bacteroides fragilis* (8), Eubacterium siraeum (14), *Ruminococcus bromii* (19), *Collinsella aerofacien* and *Parabacteroides merdae* (25), *Bacteroides caccae CAG_21* (26), and *Bacteroides salyersiae* and *Bacteroides xylanisolvens* (27) were previously reported to be favorable for antitumor responses to ICI. At the same time, we identified 17 genera and 17 species that were significantly enriched in the NR group, of which *Hungatella hathewayi* had been previously reported to induce resistance to ICIs in renal cell carcinoma (27). Analysis at the genetic level further confirmed that *Alistipes*, *Parabacteroides merdae*, and *Eubacterium* sp. *CAG_180* were enriched in the R group, and this consistency at the genus, species, and genetic levels supported the validity of our results.

Although previous investigations reported interesting results and conclusions, we found little congruence among the different studies in the specific bacteria that were found to be favorable for antitumor responses. Therefore, longitudinal detection may play an important role. In our study, the longitudinal analysis of the composition of gut microbiota showed that the abundance of *Weissella*, especially *Weissella cibaria*, increased in the R group, whereas the abundance of *Fusobacteria* increased in the NR group. *Weissella cibaria*, a kind of lactic acid bacteria, has been reported to have the potential to prevent cancer (28), and different studies have indicated that *Fusobacteria* modulates the tumor microenvironment, leading to colon cancer growth and poor outcomes (29, 30).

We also found that patients with a higher abundance of *Bacteroidetes* in the gut microbiota were more likely to be protected from irAEs (pneumonitis and colitis) in our study, especially *Bacteroides* at the genus level and *Faecalibacterium prausnitzii* at the species level. This might be explained by the fact that *Bacteroidetes* promoted the biosynthesis and metabolism of anti-inflammatory components, including streptomycin metabolism, penicillin and cephalosporin biosynthesis, glycan biosynthesis and metabolism, sphingolipid metabolism, and steroid hormone biosynthesis (eFigure 8).

Increasing evidence has shown that the mechanisms through which microbacteria promote ICI responses could involve promoting the biosynthesis of amino acids and SCFAs, which regulate the immune response by inhibiting histone deacetylase (31). Our results indicated that anabolic pathways, including amino acid and fatty acid biosynthesis and metabolism, were correlated with gut microbiota components enriched in the R group. In addition, we found that DDR pathways, including homologous recombination, mismatch repair, DNA replication, and nonhomologous end joining, were markedly related to gut microbiota components that were enriched in the R group. Chemotherapy induces additional DNA damage, and a high

level of the DDR was correlated with better efficacy of ICIs (32), which might be one of the reasons why those microbiota promoted the response to ICI-based combination therapy.

Mechanistically, the microbiome has been reported to affect tumor-specific $CD8^+$ T cells *via* TLR4 or TLR9/MyD88 signaling and the IL-12 pathway (33, 34). One study showed that *B. fragilis* facilitated the efficacy of CTLA-4 blockade *via* IL-12–induced Th1 response and dendritic cell maturation (8), and another study showed that *Akkermansia muciniphila* modulated the efficacy of PD-1 blockade in an IL-12–dependent manner by upregulating the recruitment of $CCR9^+CXCR3^+CD4^+$ T cells to tumor beds (14). We examined PD-L1 expression and lymphocyte numbers, but correlation analysis with the gut microbiota showed no significant differences between the N and R groups. Therefore, the absence of further mechanistic exploration of cytokines such as IL-12 and interferon-γ and lymphocyte classification and function was a limitation of our study.

To our knowledge, this is the first study to report the relationship between gut microbiome and combined anti–PD-1 treatment/chemotherapy in cancer *via* the dynamic detection of the gut microbiome using metagenomic sequencing. Nevertheless, there are some limitations in our study. First, the drugs, cancer types, and treatment lines were not exactly the same between groups; therefore, a correlation analysis of the gut microbiome and survival could not be conducted. Second, immunophenotyping was not performed and used to analyze how the gut microbiota affected the tumor microenvironment. Last, fecal bacteria transplantation and gavage administration of probiotics were not carried out, as this was a preliminary study. In future studies, we will conduct these experiments with the identified "favorable" species, such as *Bifidobacterium*, and the predictive model constructed in our study could be attempted to verify by other cohort in the future.

Despite differences among our study and other similar studies regarding study design, experimental methods and measurements, or subject population dynamics, our results, together with those of other studies, supported that the gut microbiota might be used to noninvasively predict the efficacy and irAEs of ICI-based therapy. In addition, the combination of favorable microbiota with PD-1 blockade–based therapy is promising.

Data availability statement

The datasets presented in this study can be found in online repositories. The names of the repository/repositories and accession number(s) can be found below: https://www.ncbi.nlm.nih.gov/bioproject/PRJNA847263.

Ethics statement

The studies involving human participants were reviewed and approved by Institutional ethics committee of Chinese PLA General Hospital. The patients/participants provided their written informed consent to participate in this study.

Author contributions

ZW and YH conceived and designed the study. ZW and LL collected samples and completed the laboratory experiments. ZW and DH collected the data. ZW, SZ, and ZH analyzed the data. ZW, SZ, and LL drafted the manuscript. The other authors revised the manuscript. All authors have reviewed and approved the manuscript.

Funding

This study was supported by the Major Research plan of the National Health Commission (No.GWJJ2021100304) and by the Military Health Special Research Project (No.20BJZ37).

Conflict of interest

The authors declare that the research was conducted in the absence of any commercial or financial relationships that could be construed as a potential conflict of interest.

The reviewer GS declared a shared parent affiliation with the author(s) to the handling editor at the time of review.

Publisher's note

Supplementary material

The Supplementary Material for this article can be found online at: https://www.frontiersin.org/articles/10.3389/fonc.2022.887383/full#supplementary-material

References

1. Havel JJ, Chowell D, Chan TA. The evolving landscape of biomarkers for checkpoint inhibitor immunotherapy. *Nat Rev Cancer* (2019) 19(3):133–50. doi: 10.1038/s41568-019-0116-x

2. Zhou J, Mahoney KM, Giobbie-Hurder A, Zhao F, Lee S, Liao X, et al. Soluble PD-L1 as a biomarker in malignant melanoma treated with checkpoint blockade. *Cancer Immunol Res* (2017) 5(6):480–92. doi: 10.1158/2326-6066.CIR-16-0329

3. Garon EB, Rizvi NA, Hui R, Leighl N, Balmanoukian AS, Eder JP, et al. Pembrolizumab for the treatment of non-small-cell lung cancer. *N Engl J Med* (2015) 372(21):2018–28. doi: 10.1056/NEJMoa1501824

4. Hellmann MD, Ciuleanu TE, Pluzanski A, Lee JS, Otterson GA, Audigier-Valette C, et al. Nivolumab plus ipilimumab in lung cancer with a high tumor mutational burden. *New Engl J Med* (2018) 378(22):2093–104. doi: 10.1056/NEJMoa1801946

5. Domingo E, Camps C, Kaisaki PJ, Parsons MJ, Mouradov D, Pentony MM, et al. Mutation burden and other molecular markers of prognosis in colorectal cancer treated with curative intent: results from the QUASAR 2 clinical trial and an Australian community-based series. *Lancet Gastroenterol Hepatol* (2018) 3(9):635–43. doi: 10.1016/S2468-1253(18)30117-1

6. Kim ST, Cristescu R, Bass AJ, Kim KM, Odegaard JI, Kim K, et al. Comprehensive molecular characterization of clinical responses to PD-1 inhibition in metastatic gastric cancer. *Nat Med* (2018) 24(9):1449–58. doi: 10.1038/s41591-018-0101-z

7. Le DT, Durham JN, Smith KN, Wang H, Bartlett BR, Aulakh LK, et al. Mismatch repair deficiency predicts response of solid tumors to PD-1 blockade. *Science* (2017) 357(6349):409–13. doi: 10.1126/science.aan6733

8. Vetizou M, Pitt JM, Daillere R, Lepage P, Waldschmitt N, Flament C, et al. Anticancer immunotherapy by CTLA-4 blockade relies on the gut microbiota. *Science* (2015) 350(6264):1079–84. doi: 10.1126/science.aad1329

9. Sivan A, Corrales L, Hubert N, Williams JB, Aquino-Michaels K, Earley ZM, et al. Commensal bifidobacterium promotes antitumor immunity and facilitates anti-PD-L1 efficacy. *Science* (2015) 350(6264):1084–9. doi: 10.1126/science.aac4255

10. Mager LF, Burkhard R, Pett N, Cooke NCA, Brown K, Ramay H, et al. Microbiome-derived inosine modulates response to checkpoint inhibitor immunotherapy. *Science* (2020) 369(6510):1481–9. doi: 10.1126/science.abc3421

11. Gopalakrishnan V, Spencer CN, Nezi L, Reuben A, Andrews MC, Karpinets TV, et al. Gut microbiome modulates response to anti-PD-1 immunotherapy in melanoma patients. *Science* (2018) 359(6371):97–103. doi: 10.1126/science.aan4236

12. Peng Z, Cheng S, Kou Y, Wang Z, Jin R, Hu H, et al. The gut microbiome is associated with clinical response to anti-PD-1/PD-L1 immunotherapy in gastrointestinal cancer. *Cancer Immunol Res* (2020) 8(10):1251–61. doi: 10.1158/2326-6066.CIR-19-1014

13. Hakozaki T, Richard C, Elkrief A, Hosomi Y, Benlaifaoui M, Mimpen I, et al. The gut microbiome associates with immune checkpoint inhibition outcomes in patients with advanced non-small cell lung cancer. *Cancer Immunol Res* (2020) 8(10):1243–50. doi: 10.1158/2326-6066.CIR-20-0196

14. Routy B, Le Chatelier E, Derosa L, Duong CPM, Alou MT, Daillere R, et al. Gut microbiome influences efficacy of PD-1-based immunotherapy against epithelial tumors. *Science* (2018) 359(6371):91–7. doi: 10.1126/science.aan3706

15. Derosa L, Routy B, Thomas AM, Iebba V, Zalcman G, Friard S, et al. Intestinal akkermansia muciniphila predicts clinical response to PD-1 blockade in patients with advanced non-small-cell lung cancer. *Nat Med* (2022) 28(2):315–24. doi: 10.1038/s41591-021-01655-5

16. Iida N, Dzutsev A, Stewart CA, Smith L, Bouladoux N, Weingarten RA, et al. Commensal bacteria control cancer response to therapy by modulating the tumor microenvironment. *Science* (2013) 342(6161):967–70. doi: 10.1126/science.1240527

17. Viaud S, Saccheri F, Mignot G, Yamazaki T, Daillere R, Hannani D, et al. The intestinal microbiota modulates the anticancer immune effects of cyclophosphamide. *Science* (2013) 342(6161):971–6. doi: 10.1126/science.1240537

18. Fang C, Zhong H, Lin Y, Chen B, Han M, Ren H, et al. Assessment of the cPAS-based BGISEQ-500 platform for metagenomic sequencing. *Gigascience* (2018) 7(3):1–8. doi: 10.1093/gigascience/gix133

19. Zheng Y, Wang T, Tu X, Huang Y, Zhang H, Tan D, et al. Gut microbiome affects the response to anti-PD-1 immunotherapy in patients with hepatocellular carcinoma. *J Immunother Cancer* (2019) 7(1):193. doi: 10.1186/s40425-019-0650-9

20. Human Microbiome Project C. Structure, function and diversity of the healthy human microbiome. *Nature* (2012) 486(7402):207–14. doi: 10.1038/nature11234

21. Andrews MC, Duong CPM, Gopalakrishnan V, Iebba V, Chen WS, Derosa L, et al. Gut microbiota signatures are associated with toxicity to combined CTLA-4 and PD-1 blockade. *Nat Med* (2021) 27(8):1432–41. doi: 10.1038/s41591-021-01406-6

22. McCulloch JA, Davar D, Rodrigues RR, Badger JH, Fang JR, Cole AM, et al. Intestinal microbiota signatures of clinical response and immune-related adverse events in melanoma patients treated with anti-PD-1. *Nat Med* (2022) 28(3):545–56. doi: 10.1038/s41591-022-01698-2

23. Akk abundance alters survival in patients with NSCLC on ICIs. *Cancer Discovery* (2022) 12(4):OF8. doi: 10.1158/2159-8290.CD-RW2022-027

24. Zhang C, Wang J, Sun Z, Cao Y, Mu Z, Ji X. Commensal microbiota contributes to predicting the response to immune checkpoint inhibitors in non-small-cell lung cancer patients. *Cancer Sci* (2021) 112(8):3005–17. doi: 10.1111/cas.14979

25. Matson V, Fessler J, Bao R, Chongsuwat T, Zha Y, Alegre ML, et al. The commensal microbiome is associated with anti-PD-1 efficacy in metastatic melanoma patients. *Science* (2018) 359(6371):104–8. doi: 10.1126/science.aao3290

26. Frankel AE, Coughlin LA, Kim J, Froehlich TW, Xie Y, Frenkel EP, et al. Metagenomic shotgun sequencing and unbiased metabolomic profiling identify specific human gut microbiota and metabolites associated with immune checkpoint therapy efficacy in melanoma patients. *Neoplasia* (2017) 19(10):848–55. doi: 10.1016/j.neo.2017.08.004

27. Derosa L, Routy B, Fidelle M, Iebba V, Alla L, Pasolli E, et al. Gut bacteria composition drives primary resistance to cancer immunotherapy in renal cell carcinoma patients. *Eur Urol* (2020) 78: 195–206. doi: 10.1016/j.eururo.2020.04.044

28. Kwak SH, Cho YM, Noh GM, Om AS. Cancer preventive potential of kimchi lactic acid bacteria (Weissella cibaria, lactobacillus plantarum). *J Cancer Prev* (2014) 19(4):253–8. doi: 10.15430/JCP.2014.19.4.253

29. Zhou Z, Chen J, Yao H, Hu H. Fusobacterium and colorectal cancer. *Front Oncol* (2018) 8:371. doi: 10.3389/fonc.2018.00371

30. Mima K, Nishihara R, Qian ZR, Cao Y, Sukawa Y, Nowak JA, et al. Fusobacterium nucleatum in colorectal carcinoma tissue and patient prognosis. *Gut* (2016) 65(12):1973–80. doi: 10.1136/gutjnl-2015-310101

31. Andrews MC, Reuben A, Gopalakrishnan V, Wargo JA. Concepts collide: Genomic, immune, and microbial influences on the tumor microenvironment and response to cancer therapy. *Front Immunol* (2018) 9:946. doi: 10.3389/fimmu.2018.00946

32. Wang Z, Zhao J, Wang G, Zhang F, Zhang Z, Zhang F, et al. Comutations in DNA damage response pathways serve as potential biomarkers for immune checkpoint blockade. *Cancer Res* (2018) 78(22):6486–96. doi: 10.1158/0008-5472.CAN-18-1814

33. Paulos CM, Wrzesinski C, Kaiser A, Hinrichs CS, Chieppa M, Cassard L, et al. Microbial translocation augments the function of adoptively transferred self/tumor-specific CD8+ T cells *via* TLR4 signaling. *J Clin Invest* (2007) 117(8):2197–204. doi: 10.1172/JCI32205

34. Yin P, Liu X, Mansfield AS, Harrington SM, Li Y, Yan Y, et al. CpG-induced antitumor immunity requires IL-12 in expansion of effector cells and down-regulation of PD-1. *Oncotarget* (2016) 7(43):70223–31. doi: 10.18632/oncotarget.11833

frontiers | Frontiers in Immunology

TYPE Original Research
PUBLISHED 24 November 2022
DOI 10.3389/fimmu.2022.880959

OPEN ACCESS

EDITED BY
Alison Taylor,
University of Leeds, United Kingdom

REVIEWED BY
Peter Hart,
Roosevelt University College of Pharmacy, United States
Yu-Chan Chang,
National Yang Ming Chiao Tung University, Taiwan

*CORRESPONDENCE
Ivan J. Cohen
ivan.cohen@pennmedicine.upenn.edu

SPECIALTY SECTION
This article was submitted to Cancer Immunity and Immunotherapy, a section of the journal Frontiers in Immunology

RECEIVED 22 February 2022
ACCEPTED 20 September 2022
PUBLISHED 24 November 2022

CITATION
Cohen IJ, Pareja F, Socci ND, Shen R, Doane AS, Schwartz J, Khanin R, Morris EA, Sutton EJ and Blasberg RG (2022) Increased tumor glycolysis is associated with decreased immune infiltration across human solid tumors. *Front. Immunol.* 13:880959. doi: 10.3389/fimmu.2022.880959

Increased tumor glycolysis is associated with decreased immune infiltration across human solid tumors

Ivan J. Cohen[1*], Fresia Pareja[2], Nicholas D. Socci[3], Ronglai Shen[4], Ashley S. Doane[5], Jazmin Schwartz[6], Raya Khanin[3], Elizabeth A. Morris[7], Elizabeth J. Sutton[7] and Ronald G. Blasberg[1,8,9]

[1]Gerstner Sloan Kettering Graduate School of Biomedical Sciences, Memorial Sloan Kettering Cancer Center, New York, NY, United States, [2]Department of Pathology, Memorial Sloan Kettering Cancer Center, New York, NY, United States, [3]Bioinformatics Core, Memorial Sloan Kettering Cancer Center, New York, NY, United States, [4]Department of Epidemiology and Biostatistics, Memorial Sloan Kettering Cancer Center, New York, NY, United States, [5]Computational Biology and Medicine Tri-Institutional PhD Program, Weill Cornell Medicine, New York, NY, United States, [6]Department of Medical Physics, Memorial Sloan Kettering Cancer Center, New York, NY, United States, [7]Department of Radiology, Memorial Sloan Kettering Cancer Center, New York, NY, United States, [8]Department of Neurology, Memorial Sloan Kettering Cancer Center, New York, NY, United States, [9]Molecular Pharmacology and Chemistry Program, Memorial Sloan Kettering Cancer Center, New York, NY, United States

Response to immunotherapy across multiple cancer types is approximately 25%, with some tumor types showing increased response rates compared to others (i.e. response rates in melanoma and non-small cell lung cancer (NSCLC) are typically 30-60%). Patients whose tumors are resistant to immunotherapy often lack high levels of pre-existing inflammation in the tumor microenvironment. Increased tumor glycolysis, acting through glucose deprivation and lactic acid accumulation, has been shown to have pleiotropic immune suppressive effects using *in-vitro* and *in-vivo* models of disease. To determine whether the immune suppressive effect of tumor glycolysis is observed across human solid tumors, we analyzed glycolytic and immune gene expression patterns in multiple solid malignancies. We found that increased expression of a glycolytic signature was associated with decreased immune infiltration and a more aggressive disease across multiple tumor types. Radiologic and pathologic analysis of untreated estrogen receptor (ER)-negative breast cancers corroborated these observations, and demonstrated that protein expression of glycolytic enzymes correlates positively with glucose uptake and negatively with infiltration of $CD3^+$ and $CD8^+$ lymphocytes. This study reveals an inverse relationship between tumor glycolysis and immune infiltration in a large cohort of multiple solid tumor types.

KEYWORDS

tumor metabolism, immunotherapy, tumor microenvironment, solid tumors, glycolysis, immune infiltration

Introduction

Immune checkpoint blockade (ICB) with PD1/PDL1-, or CTLA4-blocking antibodies has shown encouraging results, either as monotherapy or in combination with other checkpoint inhibitors or with standard chemotherapies (1, 2). As a monotherapy, some of the best responses were observed in melanoma (objective response rate (ORR) of 45%) (3), PDL1-positive non-small cell lung cancer (NSCLC; ORR 45%) (4–6) and multiple Mismatch-Repair deficient (MMRd) tumor types (ORR of 40-53%) (7–9). The combination of anti-PD1 and anti-CTLA-4 therapies has also shown excellent responses with an ORR in the 40-60% range and long duration of these responses (3, 10–12). ICB also generates improved responses in combination with standard chemotherapies, most notably in lung and breast cancer, with a ~40% increase in 2-year overall survival rates in the immunotherapy-containing arm vs. the chemotherapy-only arm in multiple clinical trials (13–20). Further, multiple studies have recently shown the benefits of neoadjuvant or adjuvant ICB in multiple tumor types (21–27). Since the initial FDA approval of immunotherapy for melanoma and lung cancers, immunotherapies have been cleared by the FDA for various additional tumor types, including head and neck, renal, hepatocellular, colorectal, urothelial, gastric, cervical, breast and Merkel cell carcinomas (28). Moreover, the use of pembrolizumab was recently approved by the FDA in Microsatellite Instability-high (MSI-h) patients, irrespective of the tumor type (29). Although highly encouraging, the majority of patients treated with immunotherapy still fail to respond. This lack of response is likely due in part to the hostile tumor microenvironment (TME) found in solid tumors and its effect on immune infiltrating cells (30).

The Warburg effect describes the preferential utilization of glycolysis in tumor cells even in the presence of oxygen (31). Signaling *via* different oncogenic pathways has been shown to result in increased expression of glycolytic genes with an ensuing increase in glycolytic rates and cell proliferation. Signaling *via* MYC results in the upregulation of various glycolytic genes, such as *LDHA* (32); signaling *via* AKT and BRAF leads to increased glucose uptake in tumor cells (33, 34); and *TP53* inactivation results in increased glycolysis (35). This results in a metabolic tumor microenvironment (mTME) characterized by glucose depletion, lactic acid accumulation and an acidic pH, among other metabolic changes (36–38). Lactic acid is a highly immune-suppressive metabolite that can directly affect many steps involved in mounting a successful anti-tumor immune response (39). Independent studies using mouse models of breast cancer and melanoma have shown that depletion of lactate dehydrogenase A (LDHA) from tumor cells led to a dramatic increase in tumor-infiltrating T-cells and NK cells (40, 41). In addition, activated $CD4^+$ and $CD8^+$ T cells are highly dependent on glucose (38, 42), whereas regulatory T cells (Tregs) can function effectively in low glucose, high lactate microenvironments. In fact, Tregs have been shown to metabolize lactic acid to fuel their proliferation and support their immune suppressive capacity (43, 44), and inhibition of tumor glycolysis was shown to lead to Treg functional destabilization and increased efficacy of ICB in mouse models of breast cancer and melanoma (45).

Given that one of the best predictors for response to immunotherapy is pre-existing inflammation within tumors (46), we focused on understanding a potential mechanism of immune exclusion that may be important to improve the response to ICB. We hypothesized that increased tumor glycolysis would be associated with decreased immune infiltration across a variety of non-hematologic solid tumor types. Using gene expression profiles from The Cancer Genome Atlas (TCGA) and other independent datasets, we found that increased tumor glycolysis was associated with decreased immune infiltration across multiple cancer types. Our findings may help define not only a subset of patients where ICB is unlikely to be effective, but may also reveal new strategies for the combination of ICB and treatments targeting tumor cell metabolism.

Materials and methods

Data processing

Gene expression (RNA) data was downloaded from the National Cancer Institute Genomic Data Commons (NCI GDC) Pan Cancer Atlas Publications website (https://gdc.cancer.gov/about-data/publications/pancanatlas) (47). Clinical data was downloaded from the TCGA-Clinical Data Resource (CDR) Outcome site. We focused our analysis on non-hematologic solid tumor types, and excluded Acute Myeloid Leukemia (LAML), Thymoma (THYM) and Diffuse Large B Cell Lymphoma (DLBC) (n = 30 solid tumor types). Primary and Metastatic tumor samples were included in our study (TCGA Barcode Sample Type Codes 01 and 06). The expression values from the NCI GDC were transformed into log base 2 values.

Gene expression data from the METABRIC (48) study was downloaded from the cBioPortal (https://www.cbioportal.org/datasets) (49); data from GSE65904 (melanoma) and GSE119267 (lung adenocarcinoma) was downloaded from the National Center for Biotechnology Information Gene Expression Omnibus (NCBI GEO). Expression values from GSE65904 were transformed into log base 2 values unless otherwise noted.

EGFR, KRAS and BRAF mutation status were obtained from the cBioPortal for each indicated tumor type. For LUAD, we selected cases with either EGFR L858R mutations or KRAS G12C/V/D/A/S. For SKCM, we selected cases with BRAF

V600E mutations. For BRCA, increased androgen receptor (AR) expression cases were counted if they exhibited either (i) high-level amplification of the AR region or (ii) AR mRNA expression >2 standard deviations from the mean relative to all other BRCA cases.

Protein abundance data [as measured by mass spectrometry by the Clinical Proteomics Tumor Analysis Consortium (CPTAC)] for 875 tumor samples across seven cancer types (breast, lung, ovarian, pancreatic, endometrial, brain and colon cancer) was downloaded from the cBioPortal. The Z-score transformed protein abundance values were downloaded and used as is in this study. The GSE140343 lung adenocarcinoma (LUAD) proteomics and clinical data (n=103) was downloaded from Xu, et al. (50) and used as is (only tumor samples were analyzed in our study, not the matching normal tissue samples).

Metabolite abundance data was downloaded from Tang et al. (51) and used as is. ssGSEA T-cell estimates were calculated as above and the relationships between Glucose or Lactate, and different ssGSEA T-cell estimates were plotted.

Glycolysis and immune signatures

To determine the expression of the glycolysis-related fluorodeoxyglucose (FDG) uptake signature (52), we calculated the Weighted Mean of the genes in this signature for each sample according to the weights in Palaskas, et al. (FDGScore = weightedMean(gene.symbols, gene.weights, na.rm = T) (Supp Table S1). This was performed using the log base 2 transformed expression values for each dataset. For genes with more than one probe, the weights of each probe were added as in Supp Table S1. To estimate the abundance of T-cell subsets, the single-sample GSEA (ssGSEA) method described by Şenbabaoğlu, et al. was followed [gsva(expression.data, list.of.immune.pathways, method="ssgsea")] (53). The expression values without log base 2 were used to estimate immune-cell proportions with ssGSEA. To calculate the enrichment of the 50 Hallmark gene sets from the Molecular Signatures Database (MSigDB) (54), ssGSEA values were calculated as described above for the estimation of T-cell subset abundance, but using the Hallmark gene sets.

To determine the relationships between our signatures (FDGScore, Hallmarks_Glycolysis, and multiple ssGSEA-based T-cell estimates) and clinical parameters (Tumor Stage, Patient Age at Diagnosis, Patient Gender) we used multiple statistical tests. To study the association of our signatures and Tumor Stage, we performed linear regression between our signatures and Tumor Stage, where Tumor Stage was defined numerically from 1 to 4 (Stage I to IV) for TCGA and METABRIC, and defined numerically from 1 to 3 (Primary Tumor, Regional Metastasis, Distant Metastasis) for GSE65904, and we reported the resulting Beta Coefficient (B) and p-value. To study the association of our signatures and Patient Age at Diagnosis (Age), we calculated the Spearman correlation coefficient (rho, r) between our signatures and Age, and we reported the rho and p-value. To study the association between our signatures and Patient Gender, we performed a two-sided t-test between our signatures and Gender, and we reported the male/female expression percentage and p-value.

Survival analysis

To perform survival analysis on the publicly available datasets (TCGA, METABRIC, GSE65904), patients were stratified into tertiles based on the expression of the different gene signatures (FDGScore, CD8 T Cells) in the tumors. For FDGScore, the log base 2 expression values were used; for CD8 T cells, the raw ssGSEA output was used without any transformation.

The overall survival between patients in the top tertile ("high") vs. those in the bottom tertile ("low") was compared using Cox Proportional Hazards Regression analysis with a cutoff of 4,000 days for TCGA and 10 years for METABRIC and GSE65904. Both univariate and multivariate analyses were performed for each gene signature (FDGScore, Hallmarks_Glycolysis, CD8 T cells) and for other available covariates, depending on the study (Age, Gender, Stage, Prior therapies).

For TCGA, the TCGA-Clinical Data Resource (CDR) Outcome file (https://gdc.cancer.gov/about-data/publications/pancanatlas) was used, as per TCGA recommendations (55).

To perform survival analysis on the MSKCC cohort of 49 patients with ER-negative breast cancer, patients were stratified into tertiles based on their expression of LDHA and CD8 by IHC staining. Patients were stratified into the highest LDHA expression tertiles (LDHA H-Score > 180, "LDHA.High"), the highest Mean Glycolysis H Score tertile (Mean Glycolysis H Score > 180, "Gly.High"), the highest CD8 expression tertile (Stromal $CD8^+$ % > 20, "CD8.High"), and patients which were not in either of the above top tertiles. The recurrence free survival (RFS) was compared between patients in the Gly.High group vs. non-Gly.High and between CD8.High group vs. non-CD8.High in this cohort using Cox Proportional Hazards Regression and Kaplan-Meier analysis. Data cutoff date for tumor recurrence was November 2 2018.

Cases

Following institutional review board (IRB) approval (Protocol # 17-236A), cases were retrieved from the Pathology archives of Memorial Sloan Kettering Cancer Center (MSKCC). Patient consents were obtained as described in the protocol, and 49 ER-negative primary breast cancers were reviewed by a pathologist (FP) and classified according to the definitions of the World Health Organization (56). Tumors were graded according to the Nottingham grading system (57). ER and HER2 status were retrieved from the electronic medical records at our institution,

and the extent of stromal tumor-infiltrating lymphocytes (sTILs) was evaluated following the recommendation put forward by the International TILs Working Group 2016 (58).

Immunohistochemistry

Representative formalin-fixed paraffin-embedded whole tissue sections from the 49 ER-negative primary breast cancers were subjected to immunohistochemistry as previously described in the MSKCC Department of Pathology Immunohistochemistry Core Laboratory (59, 60). In brief, sections were incubated for 30 min with the anti-CD3 antibody (Leica Biosystems, Clone LN10) at a 1:200 dilution, anti-CD8 antibody (Dako Omnis, Clone C8/144B) at a 1:100 dilution, anti-LDHA antibody (Cell Signaling, Clone C4B5; #3582) at a 1:300 dilution, or anti-GLUT1 (Polyclonal from AbCam) antibody at a 1:400 dilution. All antibody incubations were followed by a 30 min ER2 pre-treatment (Bond) on a Leica Bond RX platform, followed by Bond Poymer Refine Detection (Leica Biosystems; #DS9800).

Immunohistohemical expression of LDHA and GLUT1 was assessed using the H-score, a semi-quantitative approach based on the sum of individual scores for each intensity (0, negative; 1+, weak; 2+, moderate; 3+, strong) and the percentage of tumor cells displaying a particular expression intensity. The final score is computed with the formula: [1x(%cells 1+) +2 x(%cells 2+) +3x (% cells 3+)] and ranges from 0 to 300. We also computed a composite score of both markers by simply averaging the H-score for GLUT1 and LDHA (Mean Glycolysis H-score).

Immunohistochemical assessment of CD3 and CD8 expression in TILs was recorded as the % of stromal TILs displaying immunoreactivity for these markers. All analyses were performed with observers blinded to the clinical and radiologic features of the cases.

Imaging

Eighteen of the 49 patients in the MSKCC cohort underwent FDG-PET imaging. The patients ranged in age from 25 – 71 years, and were injected with an average of 431 ± 49 MBq of FDG and imaged at an average of 68 ± 18 min PI on various GE discovery PET scanners (LS,STE, 690, 710) mid-skull to mid-thigh.

Volumetric Regions of Interest (VOIs) were drawn on FDG-PET images over the breast lesion of interest. For each lesion VOI, the maximum and peak standardized uptake values (SUV_{max} and SUV_{peak}, respectively) were calculated. The standardized uptake value (SUV) is defined as the tracer uptake in a region divided by the injected activity and patient weight.

SUV_{max} hottest voxel within a defined VOI and SUV_{peak} is calculated by averaging the SUV for all the pixels within a 1 cc sphere containing the lesion VOI such that this average is the largest of all possible such spheres. Both SUV metrics are used to assess the most metabolically active region of a tumor.

Results

Inverse correlation between the expression of glycolysis-related genes and immune genes across multiple solid tumor types

Typical response rates to ICB in solid tumor types outside of melanoma, PDL1-positive NSCLC and MMR-deficient tumors is ~5-20% (61–64). Thus, we sought to determine whether increased tumor glycolysis may be associated with decreased immune infiltration. If true, this may (i) allow the identification of patients who may be resistant to ICB; and (ii) reveal tumor glycolysis as a potential target for combination therapies with ICB (44, 45). To initially determine how expression of glycolysis-related genes correlated with tumor immune infiltration, we created a minimal selection of glycolysis genes (one for each of the 10 steps of glycolysis, plus the glucose transporter GLUT1 (*SLC2A1*), lactate dehydrogenase A (*LDHA*) and the lactate transporters *SLC16A1* and *SLC16A3*) and immune genes (consisting of the 'identity' genes *CD3, CD4, CD8* and the cytotoxicity genes Granzyme A (*GZMA*) and Perforin 1 (*PRF1*)). This list included glycolysis rate-limiting genes such as *HK2*, *PFKP* and *PKM2* (65, 66). We then performed a preliminary analysis of the expression patterns of these genes in the 30 non-hematologic solid tumor types in the Pan Cancer TCGA cohort (n=9,875). We observed robust co-expression within the glycolysis and immune gene subsets, but minimal inverse correlations between the glycolysis and immune genes, with the strongest negative correlation observed between *GPI* and *CD4*: $r = -0.08$, $p = 2.16e^{-15}$) (Supp Figures S1A, B).

When divided into individual cancer types and subtypes, however, there were strong inverse correlation patterns between specific glycolysis and immune genes, especially in the Basal and Her2 subtypes of breast cancer (BRCA) (with the strongest negative correlations occurring between *SLC2A1* and *CD8A*: $r = -0.32$, $p = 1.72e^{-7}$), skin cutaneous melanoma (SKCM) (*SLC16A1* vs. *CD3E*: $r = -0.42$, $p = 9.83e^{-22}$), and lung adenocarcinoma (LUAD) (*TPI1* vs. *CD4*: $r = -0.22$, $p = 4.66e^{-7}$) (Figure 1A; Supp Figure S1B). We sought to validate these findings in independent datasets, including the METABRIC breast cancer cohort (23); the GSE65904 dataset [comprised of 214 melanoma samples (67)], and a cohort of 155 LUAD samples (GSE119267) for which gene expression profiles were publicly available (68). We observed similar expression patterns in these datasets, wherein some glycolytic genes showed strong and

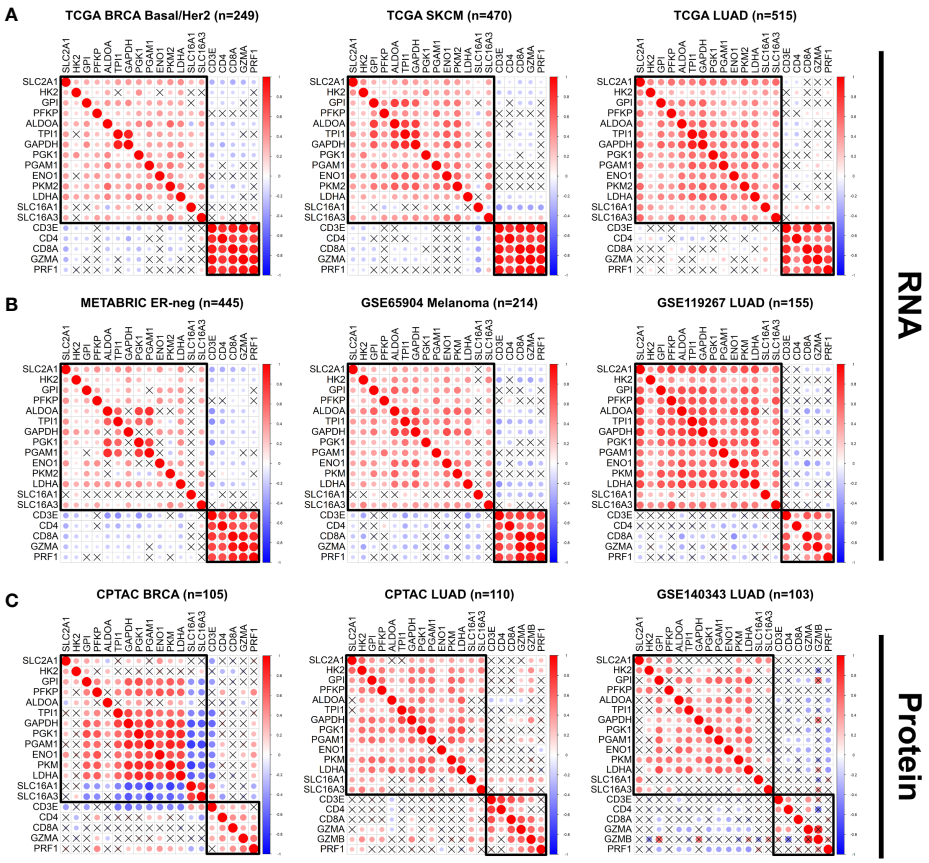

FIGURE 1
The expression of glycolysis- and immune-related genes is negatively correlated across multiple solid tumor types. **(A, B)** The correlation between expression of selected glycolysis and immune genes was plotted for individual tumor types in the TCGA dataset **(A)** Basal/Her2 Breast Cancer (BRCA), Skin Cutaneous Melanoma (SKCM), Lung Adenocarcinoma (LUAD), and in the independent datasets **(B)** ER-negative METABRIC, GSE65904 Melanoma, GSE119267 LUAD). **(C)** The correlation between protein abundance of specific glycolysis and immune proteins was plotted for specific tumor types in the CPTAC cohort (BRCA, LUAD) and the GSE140343 LUAD cohort. Red = positive correlation; blue = negative correlation. The size and intensity of the circles are proportional to the Pearson r coefficient. Pearson correlation coefficients that were not statistically significant (p>0.05) are marked with an X.

significant inverse correlations with specific immune genes in specific tumor types (with the strongest negative correlations occurring in ER-negative breast cancer from METABRIC: *TPI1* vs. *CD3E*: r = -0.44, p = $2.39e^{-22}$; GSE65904 Melanoma: *LDHA* vs. *CD3E*: r = -0.43, p = $6.03e^{-11}$; GSE119267 *LUAD*: *ENO1* vs. *CD8A*: r = -0.43, p = $2.57e^{-8}$) (Figure 1B; Supp Figures S1A, B). Additionally, the expression of the glycolysis rate-limiting genes *HK2, PFKP* and *PKM2* showed expression patterns similar to non-rate-limiting genes in the Pan Cancer TCGA cohort. The correlation between the rate-limiting genes *HK2* vs. *CD4* was r = -0.03, p = 0.01; *PFKP* vs. *CD4*: r = 0.05, p = $3.43e^{-6}$; *PKM2* vs. *CD4*: r = 0.09, p = $6.14e^{-21}$). Similarly, the correlation between specific non-rate limiting glycolysis genes was *GAPDH* vs. *CD4*: r = 0.005, p = 0.61, *ALDOA* vs. *CD4*: r = -0.02, p = 0.02 (Supp Figure S1A).

We then delved deeper into the molecular subtypes of breast cancer, lung adenocarcinoma and melanoma. We found that in contrast to breast cancer samples from the ER-negative and Basal/Her2 subtypes, samples from the ER-positive/LumA-LumB subtypes showed weaker negative correlations (*TCGA BRCA LumA/LumB*: *ALDOA* vs. *CD8A*: r = -0.22, p = $2.0e^{-9}$; *METABRIC ER-positive*: *ALDOA* vs. *CD3E*: r = -0.24, p = $1.24e^{-20}$) (Supp Figures S1A, B). Additionally, a cohort of breast cancer patients with increased expression of the androgen receptor gene (*AR*) showed a paucity of statistically significant negative correlations between glycolysis and immune genes (Supp Figure S2A). Within the SKCM cohort, we found that tumors with a BRAF V600E mutation lost the strong negative correlations observed in the *BRAF* WT cohort between multiple glycolytic genes and immune genes, with the exception of *LDHA* and *SLC16A1* (strongest negative correlation between *SLC16A1* vs. *CD3E*: r = -0.34, p = $9.68e^{-6}$) (Supp Figure S2B). Similar results were observed in LUAD tumors with either *EGFR* L858R or *KRAS* G12 mutations, wherein a significant portion of the negative associations between glycolysis and immune genes lost statistical significance (no significant negative correlations observed in the *EGFR* L858R cohort;

strongest negative correlation in the *KRAS* G12 cohort: *TPI1* vs. *CD4*: r = -0.018, p = 0.038) (Supp Figures S2C, D).

We performed similar analyses on available proteomics datasets from (i) the Clinical Proteomic Tumor Analysis Consortium (CPTAC) (69–76) and (ii) a LUAD cohort of 103 tumor samples (GSE140343) (50). We again found strong negative correlations in the protein abundance of specific glycolysis and immune genes in the CPTAC BRCA (GAPDH vs. CD3E: r = -0.58, p = $8.38e^{-8}$) and CPTAC LUAD (ALDOA vs. CD3D: r = -0.26, p = 0.019) cohorts, and in the GSE140343 LUAD cohort (LDHA vs. PRF1: r = -0.41, p = 0.003) (Figure 1C). We also found significant negative correlations in the PAAD (ENO1 vs. CD3E: r = -0.46, p = $4.030e^{-7}$), UCEC (TPI1 vs. GZMB: r = -0.31, p = 0.015), GBM (PFKP vs. CD3E: r = 0.50, p = $7.42e^{-3}$), OVCA (GPI vs. CD4: r = -0.28, p = $9.69e^{-3}$) and LUSC (SLC2A1 vs. CD3E: r = -0.44, p = $2.52e^{-6}$) cohorts, but minimal negative correlations in the CPTAC COAD (HK2 vs. CD8A: r = -0.35, p = 0.02) cohort (Supp Figure S3A). Moreover, our analyses revealed a robust negative correlation between LDHA protein abundance and the extent of immune-cell and $CD8^+$ T cell infiltration in the GSE140343 LUAD proteomics cohort, where the negative associations between LDHA and immune cell infiltration were stronger in the EGFR wildtype (WT) cases compared to the EGFR mutant cases (Supp Figures S3B, C). Thus, our preliminary analysis on both mRNA and protein datasets (TCGA, METABRIC, GSE65904, GSE119267, CPTAC BRCA, PAAD, UCEC, GBM, OVCA, LUSC and GSE140343) suggest that increased tumor glycolysis may lead to decreased immune infiltration across multiple solid tumor types.

Increased expression of a glycolysis signature is associated with depletion of $CD8^+$ T-cells in most solid tumor types

To quantify the expression patterns of glycolysis and immune related genes, we applied a previously developed signature that predicts fluorodeoxyglucose (FDG) uptake in patients and in cell lines (52). This signature, referred to as FDGScore in our study, has the advantage of having been developed by assessing FDG uptake both in patients (ensuring clinical relevance) and cell lines *in-vitro*, ensuring that the signature takes into account uptake and retention of the radiotracer without confounding factors found in purely clinical data sets, such as tumor size, heterogeneity, vessel quantity, and radiotracer delivery. In addition, to estimate the proportion of different immune cell types within tumors from TCGA as well as other datasets, we implemented the single-sample GSEA (ssGSEA) method (53, 77). This method has the advantage of (i) producing near-Gaussian curves of the immune estimates; and (ii) ease of implementation into independent datasets.

We first characterized the expression patterns of FDGScore in our cohorts, and found that increased FDGScore expression was significantly associated with Tumor Stage across the entire Pan Cancer TCGA cohort (Regression Beta Coefficient (B) = 0.16, p = $6.65e^{-42}$) and the METABRIC cohort (B = 0.29, p = $1.03e^{-95}$), but not in the GSE65904 Melanoma cohort (B = 0.05, p = 0.398) (Supp Figures S4A–C). When analyzed in individual tumor types, we found that 8/30 (27%) of tumor types showed a statistically significant association between FDGScore and Tumor Stage (Supp Table S2). Further, we observed minimal differences in FDGScore expression with increasing Age or Male vs. Female Gender, both at the PanCancer level and within individual tumor types (Supp Figures S4A–C and Supp Table S2).

We then sought to determine the correlation between the estimate of the proportion of all the T-cell subsets (by the ssGSEA method) and our FDG signature (FDGScore) across the entire TCGA cohort (n=9,875). We found that FDGScore was most negatively correlated with the CD8 T cell estimate (Pearson rho = -0.29, p < $1.42e^{-186}$) and the central memory T cell estimate (T_{cm}; r = -0.29 and p < $3.02e^{-192}$) (Figure 2A). When conducting the analyses in individual tumor types we found that FDGScore was significantly negatively correlated with the CD8 T cell estimate in 23/30 tumor types tested (Pearson r range: -0.57 - -0.09). Similarly, FDGScore was negatively correlated with the Tcm estimate across all cancer types in a statistically significant manner with the exception of CHOL (Pearson r range: -0.72 – 0.19) (Supp Table 3).

We then focused on BRCA, SKCM and LUAD and found that they were among the top 10 tumor types with the strongest negative correlations between FDGScore expression and the CD8 T cell estimate (*BRCA Basal/Her2*: r = -0.42, p = $6.15e^{-12}$; *SKCM*: r = -0.39, p = $1.21e^{-18}$; *LUAD*: r = -0.40, p < $2.36e^{-21}$) and the T_{cm} estimate (*BRCA Basal/Her2*: r = -0.52, p = 6.35e-19; *SKCM*: r = -0.59, p = $3.96e^{-45}$; *LUAD*: r = -0.54, p < $1.75e^{-39}$) (Figures 2B–D and Supp Table 3). These observations extended to our independent datasets, with negative associations found between FDGScore and CD8 T cells (*METABRIC ER-negative*: r = -0.42, p < $2.69e^{-20}$; *GSE65904 (Melanoma)*: r = -0.34, p = $3.67e^{-7}$; *GSE119267 (LUAD)*: r = -0.44, p = $7.02e^{-09}$) and T_{cm} cells (*METABRIC ER-negative*: r = -0.26, p < $2.58e^{-8}$; *GSE65904 (Melanoma)*: r = -0.30, p = $7.17e^{-6}$; *GSE119267 (LUAD)*: r = -0.40, p = $2.13e^{-7}$) (Supp Figures S5A–C). Further, within breast cancer subtypes, we found that the LumA/LumB subtype of BRCA in TCGA, and the ER-positive subtype in METABRIC had weaker negative correlations between FDGScore and immune cell infiltration, although statistical significance was maintained (Supp Figures S6A). These results support our hypothesis that increased tumor glycolysis may create a microenvironment that is hostile to infiltrating T-cells, especially $CD8^+$ T-cells and T_{cm} cells.

We then sought to validate the findings obtained with the FDGScore signature using a different glycolysis gene signature. We chose to focus on the Molecular Signatures Database "Hallmark" Gene Set Collection (54). From this collection of 50 "Hallmark" gene sets, we selected the "Glycolysis" gene set and quantified its associations with FDGScore and the various ssGSEA-derived T-cell estimates, as above. We observed a strong positive correlation between HM_Glycolysis and FDGScore across all tumor types we tested (Pearson r range = 0.40-0.78).

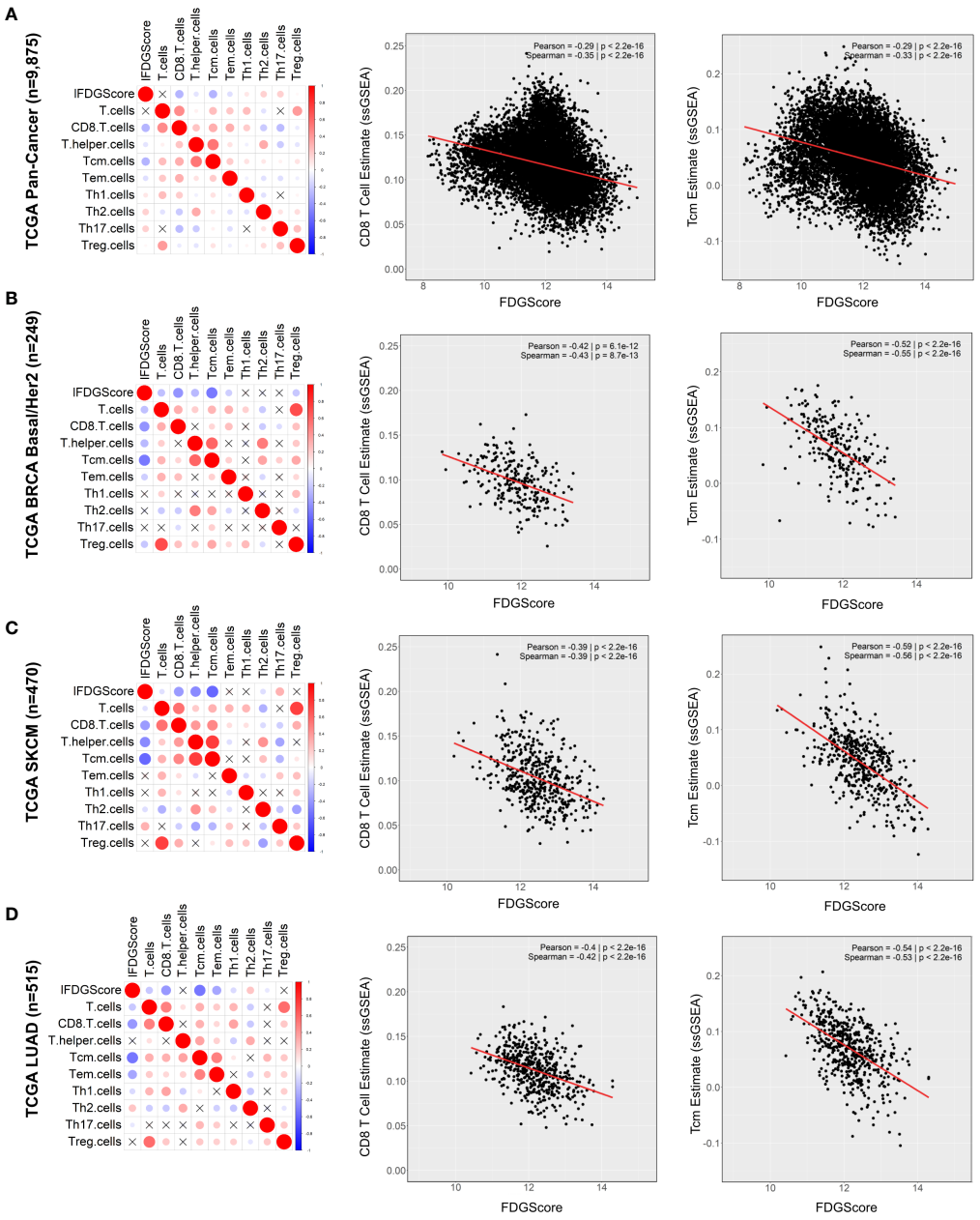

FIGURE 2
Expression of the glycolysis signature FDGScore is inversely correlated with multiple estimates of T cell infiltration across solid tumors. **(A–D)** The correlation profiles of the FDG uptake signature (FDGScore) and the estimates of T cell subset abundance (as measured by ssGSEA) were calculated and plotted for the entire TCGA Pan Cancer cohort **(A)** and for individual tumor types within TCGA **(B–D)** (left). The expression of the FDGScore vs. CD8 (middle) and Tcm (right) T cell estimates is also shown with the calculated Pearson and Spearman coefficients. Red = positive correlation; blue = negative correlation. The size and intensity of the circles are proportional to the Pearson r coefficient. Pearson correlation coefficients that were not statistically significant (p>0.05) are marked with an X.

(Supp Table 3). In accordance with our FDGScore-based findings, we observed a robust negative correlation between the Hallmark Glycolysis gene signature (referred to as HM_Glycolysis in our study) and T cell estimates across multiple solid tumor types. Across the entire TCGA cohort, HM_Glycolysis was strongly negatively correlated with the CD8 T cell estimate (Pearson r = -0.40, p < 2.2e-200) and the T_{cm} estimate (r = -0.65, p = 4.18e-284) (Supp Figure S7A and Supp Table 3). As above, we quantified these relationships within individual tumor types and found that 27/30 solid tumor types in the TCGA dataset showed a statistically significant negative association between HM_Glycolysis and the CD8 T cell estimate

(Supp Table 3). In addition, similar to our observations with FDGScore, we observed robust negative associations between HM_Glycolysis and the CD8 and T_{cm} estimates in the TCGA BRCA Basal/Her2, SKCM and LUAD cohorts (Supp Figures S7B–D). We also observed negative associations in the METABRIC ER-negative, GSE65904 and GSE119273 cohorts (Supp Figures S8A–C), and weaker negative correlations in the TCGA BRCA LumA/LumB and METABRIC ER-positive cohorts (Supp Figures S9A, B). Thus, using a different glycolysis signature from the Broad MSigDB, we validated our initial findings and showed that increased expression of a different glycolysis signature is strongly and significantly associated with decreased expression of multiple T-cell estimates across most solid tumor types we studied.

Additionally, to investigate whether the abundance of lactate itself was associated with the levels of T cell infiltration in human tumors, we leveraged the metabolomics dataset published by Tang et al. (51). The authors collected a cohort of 23 breast tumors that were fully characterized by TCGA (15/23 cases being LumA/LumB subtypes, 8/23 being Basal/Her2 subtypes), and they further analyzed the metabolome of these tumors by gas-chromatography/mass spectroscopy (GC/MS) and liquid-chromatography/mass spectroscopy (LC/MS), which included both glucose and lactate. We found that FDGScore was negatively correlated with glucose levels (r = -0.52, p = 0.012) and positively correlated with lactate levels (r = 0.49, p = 0.017) (Supp Figures S10A, B). We further observed that lactate levels were negatively correlated with multiple ssGSEA-based T cell estimates (lactate vs. Tcm: r = -0.45, p = 0029; lactate vs. T Helper: r = -0.44, p = 0.037; lactate vs. CD8: r = -0.31, p = 0.15) (Supp Figures S10A, C). Taken together, in addition to the transcriptomic and proteomic data presented above, the analysis of a metabolomic dataset lends further support to the notion that increased levels of glycolysis and lactate accumulation are associated with decreased immune infiltration in human breast tumors.

Expression of FDGScore and CD8 T-cell signatures is associated with prognosis

We next sought to determine whether FDGScore and the CD8-T cell ssGSEA estimate correlate with patient survival. Our analyses in all patients of the Pan Cancer TCGA cohort revealed that high FDGScore expression was associated with poor prognosis (HR = 2.47, 95% CI = 2.24-2.72, p = $4.25e^{-73}$) whereas CD8 T cell estimates was associated with improved prognosis (HR = 0.63, 95% CI = 0.58-0.69, p = $2.46e^{-23}$) in univariate analysis (Figure 3A; Supp Table S4). We also found that a high FDGScore expression was associated with poor prognosis in specific individual tumor types (*METABRIC HR*: 1.70, 95% CI = 1.43-2.01, p = $7.^{18e-10}$; *TCGA SKCM HR*: 1.39, 95% CI = 0.98-1.97, p = 0.0598; *TCGA LUAD HR*: 2.31, 95% CI = 1.58-3.39, p = $1.76e^{-5}$), while a high CD8 T-cell signature was consistently associated with improved prognosis (*METABRIC HR*: 0.78, 95% CI = 0.66-0.92, p = $3.66e^{-3}$; *TCGA SKCM HR*: 0.60, 95% CI = 0.43-0.86, p = $4.51e^{-3}$; *TCGA LUAD HR*: 0.62, 95% CI = 0.43-0.90, p = $1.12e^{-2}$) (Figures 3B–D; Supp Table S4). In contrast to the stronger negative correlations found in the Basal/Her2/ER-negative cohorts of the TCGA BRCA and METABRIC cohorts compared to the Luminal/ER-positive cohorts, we found minimal differences in prognosis between Basal/Her2/ER-negative and Luminal/ER-positive breast cancer cohorts (Supp Figures S11A-D). Additionally, we again sought to validate our findings using the HM_Glycolysis signature and similarly found that increased HM_Glycolysis expression was associated with poor prognosis both in the entire Pan Cancer TCGA cohort as well as within the individual tumor types that we studied (Supp Figures S12A-D).

Further, FDGScore was independently associated with poor prognosis in the entire Pan Cancer TCGA cohort in multivariate analysis (HR = 2.47, 95% CI = 2.24-2.72, p = $4.25e^{-73}$), while the CD8 T cell estimate was associated with improved prognosis (HR = 0.69, 95% CI = 0.61-0.77, p = $3.20e^{-10}$) (Supp Table S5). Similarly, HM_Glycolysis was also independently associated with poor prognosis in the Pan Cancer TCGA cohort (HR = 1.62, p = $3.08e^{-25}$) (Supp Table S5). When analyzed within individual tumor types, many of the associations with prognosis remained significant (FDGScore remained significantly associated with prognosis in the TCGA LUAD, METABRIC and GSE65904 cohorts; while the CD8 T cell estimate remained significantly associated with improved prognosis in the TCGA LUAD and SKCM cohorts; Supp Table S5). These data suggest that increased expression of glycolytic genes is significantly associated with poor prognosis, while increased expression of the CD8 T-cell signature is modestly and significantly associated with improved prognosis across multiple tumor types.

Increased protein expression of glycolytic enzymes is associated with decreased immune infiltration in primary ER-negative breast tumors

ER-negative breast cancer was found to display significant negative correlations between glycolysis and immune infiltration by transcriptomic and proteomic profiling (Figures 1, 2). To corroborate these observations, we assessed the protein expression levels of surrogate markers of glycolytic activity and immune infiltration in 49 treatment-naïve, primary breast cancers, including 39 triple-negative breast cancers (TNBC; i.e., ER-negative, PR-negative and HER2-negative) and 10 ER-negative/HER2-positive breast cancers using IHC staining (Supp Table S6). The median age of the patients was 47 years old (range: 25-71) and the median size of the tumors was 2.4 cm

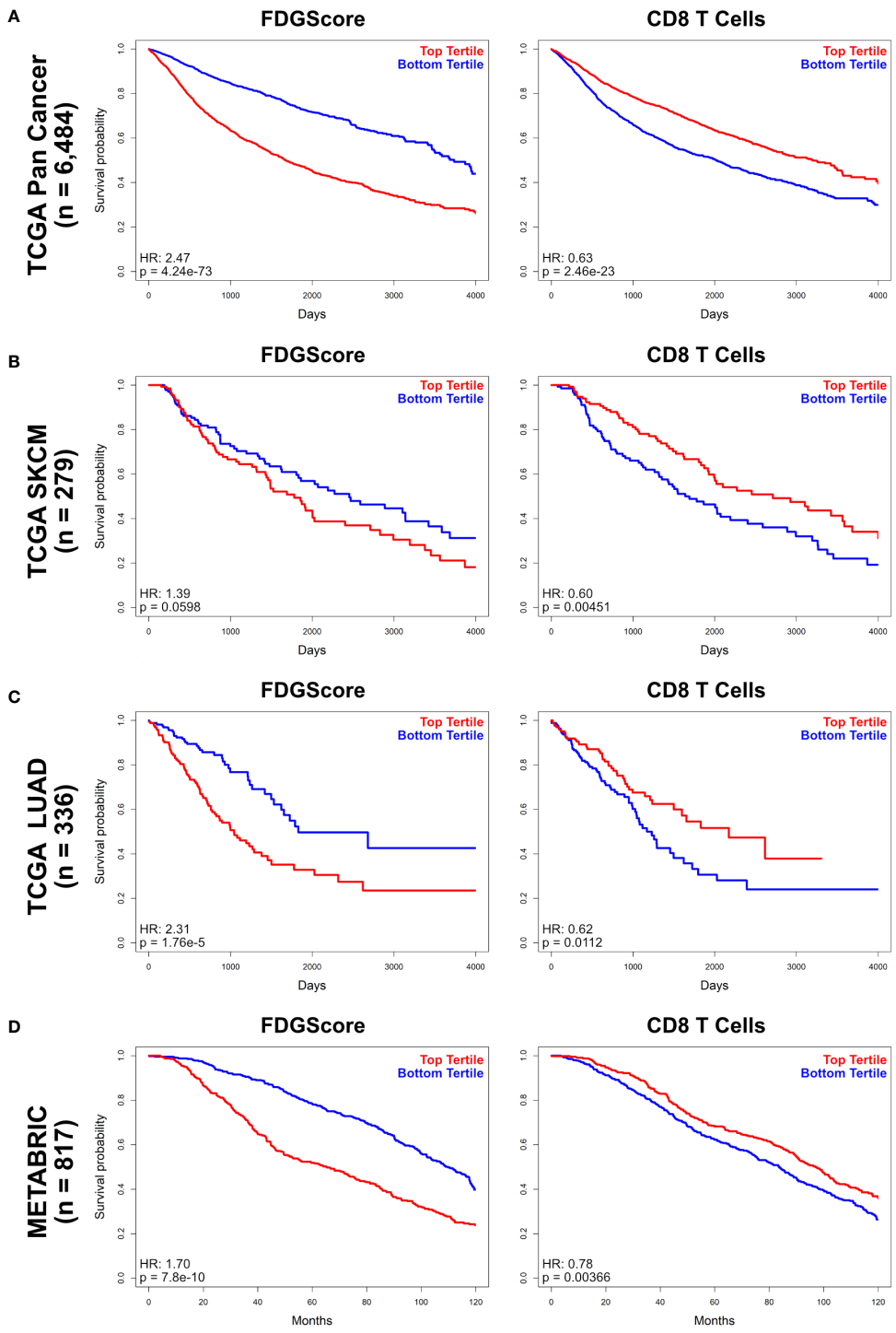

FIGURE 3
Overall survival by FDGScore and the CD8 T cell estimate in solid tumors. **(A–D)** Kaplan-Meier survival analysis was performed for the entire TCGA cohort **(A)**, as well as individually for the TCGA SKCM **(B)**, TCGA LUAD **(C)** and METABRIC **(D)** cohorts. The disease-specific survival probability of patients was measured in the top tertile vs the bottom tertile of expression of either FDGScore (*left*) or CD8 T cell estimate (*right*) for each cancer type, and the Hazard Ratio (HR) was calculated.

(range: 0.9 – 5 cm). Fifty-one percent (25/49) and 45% (22/49) of tumors were of T1 and T2 stage, respectively, whilst one tumor was of T3 and another one T4 (1/49; 2% each). Fifty-six percent (27/48) of patients were node positive, and 18/49 of patients had undergone an FDG PET scan prior to therapy or surgery.

Our analysis revealed a strong positive correlation between FDG uptake and GLUT1 expression (Pearson r = 0.67; p = 0.002) (Figure 4A) that was further enhanced in the Mean Glycolysis H-Score (see Methods) (Pearson r = 0.70; p = 0.001) (Supp Figure S13A). These results suggest that the expression of glycolytic markers can be used as an indicator of glycolytic activity in breast tumors. We then quantified the relationship between FDG uptake and immune-cell infiltration and found no significant associations between FDG uptake and either total stromal TILs, $CD3^+$ or $CD8^+$ TILs (Supp Figure S13B). We also studied how expression of glycolytic enzymes and immune infiltration affects patient recurrence-free survival ('RFS'). Notably, we found that increased expression of glycolytic markers was associated with poor prognosis (HR 3.44, p = 0.0529), whereas a numerical association between stromal immune infiltration and longer RFS (HR = $1.2e^{-8}$, p = 0.99) was observed, although this analysis did not reach statistical significance, likely due to the small sample size and number of events (Supp Figure S13C).

Next, we sought to determine the relationship between the expression of the glycolytic enzyme LDHA and the extent of lymphocytic infiltration. We separated our samples into either the top tertile of LDHA expression vs. the bottom 2 tertiles of LDHA expression. We found that tumors with the highest levels of tumor-cell LDHA expression displayed a significantly reduced infiltration of stromal TILs (*left*), and of $CD3^+$ (*middle*) and $CD8^+$ (*right*) lymphocytes (Figure 4B; p = 0.001, 0.003 and 0.015, respectively). Moreover, the extent of $CD8^+$ stromal tumor-infiltrating lymphocytes (sTILs) inversely correlated with the LDHA expression when used as a continuous variable (Pearson rho = -0.37, p = 0.01) (Figure 4C). Given that the association between CD8 sTIL % and LDHA H Score was not linear, we also calculated the odds of a tumor having both high CD8 sTIL % and high LDHA H Score, and found that the probability for a tumor to be in the top tertile for both was 0, although this test did not reach statistical significance (p = 0.16), likely due to low n. Further, three clusters with different extents of CD8-positive sTILs and LDHA expression levels were identified (LDHA.High, CD8.High, or Neither). We sought to determine whether patients in these three clusters would have differences in their recurrence-free survival. Our analysis revealed that patients in the CD8.High group (with high levels of $CD8^+$ stromal TILs and low LDHA), tended to have a better recurrence-free survival than those in the remaining two clusters (Figure 4D). Although statistical significance was not achieved (due to a low "n"), no patients in cluster 3 had a recurrence event as of data cutoff. In contrast, patients in the LDHA.High or Neither groups had high and moderate LDHA levels and low $CD8^+$ TILs, respectively, and 20-40% of patients in these clusters experienced tumor recurrence. Taken together, these findings show that increased metabolic tumor activity is associated with immune exclusion and poor prognosis.

Discussion

Numerous published studies have demonstrated a direct and strong inhibitory effect of tumor glycolysis and lactic acid on immune cell function, mostly using *in-vitro* and *in-vivo* models of disease (41, 42, 78, 79). Given the robust effect observed in these studies, we hypothesized that this immune suppressive effect of tumor glycolysis may be widespread and would also be observed in patients, across multiple solid tumor types. Indeed, we demonstrate that in most solid tumor types in the TCGA dataset, as well as in select independent datasets, there is a strong negative correlation between expression of two glycolysis signatures and CD8 and memory T-cell infiltration.

The Warburg effect, discovered in the 1920's, is a common finding across multiple cancer types (80). Multiple lines of evidence suggest that the Warburg effect, in addition to being important for providing the metabolic building blocks for rapid cell proliferation (81), is highly immune suppressive. The depletion of glucose and the concomitant accumulation of lactic acid has been shown to directly affect multiple immune cell types, inhibiting anti-tumor immune cells while promoting the formation, survival and function of pro-tumorigenic immune cells. For example, two recent studies have elegantly shown that Tregs become destabilized and lose their immune-suppressive potential with increased glucose uptake and increased glycolytic rates that may be found in tumors with decreased tumor glycolysis (44, 45). In contrast, Tregs with decreased glucose uptake show increased uptake of extracellular lactate and increased immune suppressive potential. Further, recent studies have also shown that glycolytic metabolites can directly regulate the nutrient-sensing PI3K/mTOR pathway (82–84), and that glycolysis and lactic acid can directly affect gene expression by promoting histone acetylation and lactylation (85, 86), expanding the tumor-promoting effects of the Warburg effect. In this study, we propose that glycolysis-induced local immune suppression in solid tumors is yet another critical contribution of the Warburg effect to tumor progression, and this may help explain why the Warburg effect is central to tumorigenesis across multiple tumor types.

We initially showed that expression of specific glycolysis-related genes is negatively correlated with expression of immune-related genes across multiple tumor types, both at the mRNA and protein level. In our study, we did not observe differences in the expression pattern of the glycolysis rate-limiting genes *HK2, PFKP* and *PKM2* when compared to the expression of non-rate limiting steps of glycolysis. We expanded

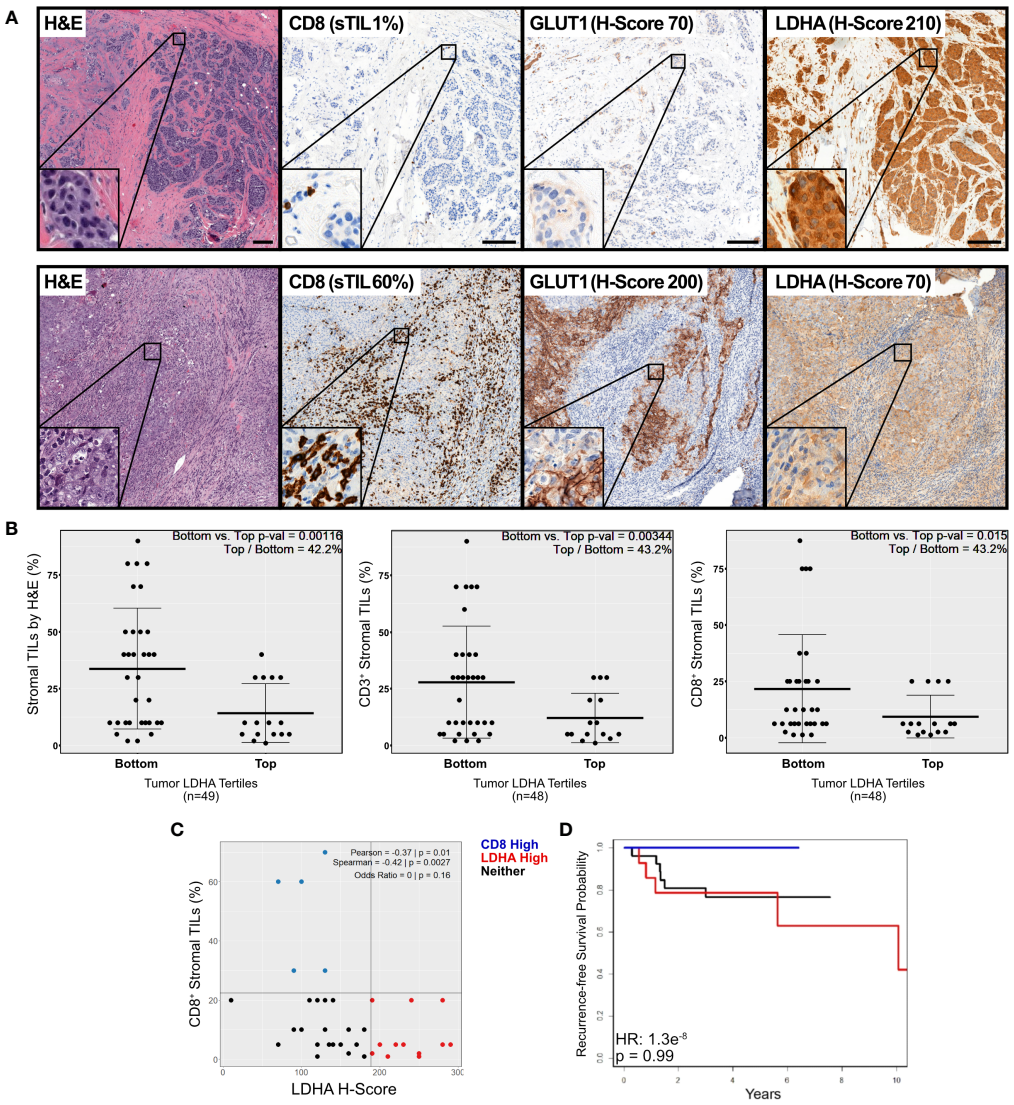

FIGURE 4
IHC staining of primary breast tumor samples reveals an inverse association between expression of glycolytic and immune markers. **(A)** Representative micrographs of immunohistochemical staining for CD8, GLUT1 and LDHA in our cohort of 49 primary, untreated ER-negative breast tumor samples. Shown are selected sections of tumors with high LDHA expression and low stromal $CD8^+$ T-cell infiltrate (*top*), and with low LDHA expression and high stromal $CD8^+$ T-cell infiltration (*bottom*). **(B)** The extent of stromal lymphocytic infiltration (sTILs) was quantified (by H&E staining, *left*; or by IHC staining of $CD3^+$ (*middle*) or $CD8^+$ (*right*) T cells) and plotted in tumors in the top tertile of LDHA expression vs. tumors in the bottom 2 tertiles of LDHA expression, as measured by the H-Score. **(C)** The percentage of stromal $CD8^+$ TILs was plotted against the LDHA H-Score, and data was color coded according to whether the sample was in CD8 High (*blue*), LDHA High (*red*) or Neither (*black*) group. The Odds Ratio for CD8 High and LDHA High was calculated and displayed. **(D)** Recurrence-free survival was calculated and Kaplan-Meier plots were plotted for all tumors according to their phenotype as described in **(C)**.

our observations by studying the relationship between established glycolysis (52) and immune (53) signatures. We found a strong inverse relationship between the glycolysis and the CD8 T-cell signatures in 23/30 solid tumor types in the TCGA cohort (Supp Table 3). We further observed that the Central Memory T-cell signature was significantly negatively correlated with expression of the FDGScore (Supp Table 3). This suggested that increased glycolysis may not only blunt CD8 T-cell infiltration, but it may also negatively affect the phenotype of T_{cm} T-cells, another critical component of the anti-tumor immune response. We validated these findings using the well-established "Hallmarks" gene signatures from the MSigDB, and found similar negative associations between HM_Glycolysis and the CD8 and T_{cm} estimates (Supp Table 3). Additionally, we leveraged the metabolomic dataset from Tang et al. (51) to show that the levels of lactate itself were negatively associated with T

cell infiltration (Supp Figure S9). We corroborated these findings by analyzing 49 primary and treatment-naïve breast tumor samples, where we observed a strong inverse relationship between the expression of glycolysis markers (GLUT1 and LDHA) and stromal infiltration of $CD3^+$ and $CD8^+$ T-cells (Figure 4). We found that expression of GLUT1 and LDHA correlated strongly with ^{18}F-FDG uptake as measured by PET (Supp Figure S13A). Further, in agreement with the transcriptomic analyses performed here, there was a strong negative correlation between expression of LDHA protein and all 3 immune variables ($CD3^+$, $CD8^+$ and total lymphocyte counts, Figure 4B). Thus, we consistently show a strong inverse relationship between expression of glycolytic and immune markers across multiple solid tumor types.

A potential caveat of our approach is that we studied the relationships between just two glycolysis signatures and a single method for estimating immune cell abundance (ssGSEA). However, while numerous other glycolysis-related signatures have been described (87–95), these signatures are (i) mostly composed of genes that are not directly involved in glycolysis (such as *COL5A1, HMMR, STC1*, among others); and (ii) have been developed by their association with prognosis/survival rather than with the metabolic activity of tumors. We initially chose the glycolysis signature described by Palaskas, et al. (52) given that (i) this signature was developed by the direct measurement of FDG uptake in cell lines and in patients; and (ii) this signature is composed solely by genes involved in glucose metabolism. Additionally, to validate our findings, we chose the Hallmarks-Glycolysis gene signature as it was developed by the Molecular Signatures Database (MSigDB). The Hallmark gene lists were created using a combination of bioinformatic approaches and expert curation that led to Hallmark gene sets with reduced variation and redundancy while attaining increased coherent expression within each Hallmark gene list (54). The HM_Glycolysis signature showed highly concordant expression with FDGScore across tumor types, and showed negative associations with various T-cell estimates to a similar degree as we observed when using FDGScore (Supp Table 3).

Currently, there are multiple methods for estimating immune-cell abundance (96). We chose the ssGSEA approach taken by Senbabaoglu, et al. (53) given that (i) it produces normally distributed scores for multiple immune cell types, making downstream statistical analyses more straightforward; and (ii) ease of implementation to independent datasets, as demonstrated in previous studies that used ssGSEA for immune deconvolution of various solid tumors (77, 97). However, although our mRNA analysis may be limited to individual gene signatures, these findings are consistent with the proteomic analysis by the CPTAC described in Figure 1 and Supp Figure S3, and with our IHC analysis of human breast tumor tissues described in Figure 4. Although our mRNA studies are based on a number of different cohorts and encompass >10,000 patient samples, a limitation of our study is that the IHC findings are based on a limited number of patients (49 breast cancer patients). Thus, further studies to confirm our observations using protein-based methods in diverse tumor types are warranted. Another caveat of our study is that while we show strong negative associations between glycolysis and immune-cell infiltration, the prognostic value of the FDGScore and T-cell signatures, and IHC staining of glycolytic and immune markers, although statistically significant in many cases, is not universally strong and statistically significant. Although the associations between our glycolysis and immune gene signatures showed robust associations with overall survival in the Pan Cancer TCGA cohort of 30 solid tumor types (Figure 3A), the association between our gene signatures and prognosis were modest when analyzed within individual tumor types (Figures 3B, C and Supp Tables S4, S5). We speculate that the robust associations in the Pan Cancer cohort may arise from increased variability in gene signature expression and prognosis between the 30 solid tumor types studied, while the modest associations observed within individual tumor types may arise from decreased variability within individual disease types.

We note that a number of studies have quantified the relationship between FDG uptake and TIL abundance in solid tumors, with some studies showing a positive (albeit small) correlation between FDG uptake and TIL counts (98, 99). In our study, we did not observe a significant correlation between FDG uptake and TIL counts in our cohort of 49 breast cancer patients (Supp Figure S13B). In contrast, throughout our study we have shown a significantly negative association between tumor glycolysis and immune infiltration. These contrasting results could be explained by the fact that while the FDGScore signature is indeed *associated* with FDG uptake, it is mainly composed of glycolysis and glucose metabolism genes. As such, FDGScore expression in tumors should be viewed primarily as a measure of tumor glycolysis rather than a direct surrogate of FDG uptake. In fact, in an analysis of a cohort of 20 breast tumor samples (100) we similarly observed that FDGScore, but not SUV_{max}, was significantly negatively associated with the ssGSEA CD8 T cell signature (data not shown), suggesting that while FDGScore is associated with FDG uptake as measured by PET, they are not identical.

Tumor glycolysis is a critical component of tumor growth. In addition to fueling cell proliferation, it can directly regulate the mTOR pathway (82–84), regulate translation of immune-related mRNAs (79), and affect histone modification (85, 86). Additionally, increased tumor glycolysis and lactate production is known to directly inhibit effector T-cell function while promoting regulatory T-cell function (45). Our study has important limitations, such as the observational character of our analyses, the lack of validation of our findings at the protein level in larger cohorts, and the weak association of FDGScore and prognosis across multiple tumor types. However, we aimed to determine whether the association between tumor glycolysis and

immune exclusion described in pre-clinical models of disease was also true across a wide range of solid human malignancies.

Despite the limitations mentioned, taken together our study indeed shows that tumor glycolysis is associated with exclusion of CD8 T-cells across most solid tumor types. In combination with the published literature demonstrating the causal effect of tumor glycolysis on immune exclusion in selected mouse models of disease, our study raises the interesting possibility that inhibiting tumor glycolysis may lead to increased immune cell infiltration across multiple solid tumor types, and thus may serve to increase the efficacy of immune checkpoint blockade. The combination of glycolysis inhibition in tumor cells with immune checkpoint blockade has been recently shown to lead to dramatically improved efficacy of ICB in mouse models of breast cancer and melanoma (45). In addition, an inhibitor of the lactate transporter MCT1 (AZD3965) has been shown to increase immune-cell infiltration into solid tumors in pre-clinical models (101), and has also entered phase I clinical trials, showing safety and on-target effects as measured by changes in urinary lactate (102). Whether inhibiting glycolysis and/or lactate transport in combination with ICB in highly glycolytic tumors will increase the efficacy of ICB in patients remains to be determined.

Data availability statement

The original contributions presented in the study are included in the article/Supplementary Material. Further inquiries can be directed to the corresponding author.

Ethics statement

The studies involving human participants were reviewed and approved by MSKCC IRB Protocol #17-236A. Written informed consent for participation was not required for this study in accordance with the national legislation and the institutional requirements.

Author contributions

IC and RGB conceived the study. IC, FP and ES reviewed the MSK cases. FP and IC performed IHC analysis. IC performed the bioinformatics analyses. NS, RK, RS, and AD provided advice and guidance on the bioinformatic and biostatistical analyses. IC, FP and RGB wrote the manuscript, which was reviewed by all co-authors. RGB, ES and EM supervised the study. All authors contributed to the article and approved the submitted version.

Funding

The authors wish to acknowledge assistance from the NCI R01-CA215136 grant, the Breast Research Fund at MSKCC, and the Cancer Center Support Grant P30 CA008748. FP is partially funded by an NIH/NCI P50 CA247749 grant.

Acknowledgments

IC specifically thanks Dr. Jorge Reis-Filho for his conceptual assistance with the biostatistical analyses and guidance during his graduate studies and thesis writing, which led to the formulation of this manuscript. The authors also wish to thank Drs. Marina Asher and Irina Linkov for their assistance with IHC staining of primary breast tumor tissue.

Conflict of interest

The authors declare that the research was conducted in the absence of any commercial or financial relationships that could be construed as a potential conflict of interest.

Publisher's note

Supplementary material

The Supplementary Material for this article can be found online at: https://www.frontiersin.org/articles/10.3389/fimmu.2022.880959/full#supplementary-material

SUPPLEMENTARY FIGURE S1
Co-expression patterns of glycolysis and immune related genes within individual tumor types. **(A, B)** RNA expression data was downloaded from TCGA and other datasets (see Methods), and the correlation between expression of selected glycolysis and immune genes was plotted (red = positive correlation; blue = negative correlation. X marks correlation coefficients with p>0.05). Correlation profiles of mRNA expression of selected glycolysis- and immune-related genes across multiple solid tumor types from the TCGA and independent cohorts are shown **(A)**. **(B)** The expression of specific glycolysis and immune genes was plotted for specific tumor types and the Pearson and Spearman correlation coefficients were calculated.

SUPPLEMENTARY FIGURE S2

Co-expression patterns of glycolysis and immune related genes within specified subtypes of breast cancer, lung cancer, and melanoma. **(A-D)** Correlation profiles of mRNA expression of selected glycolysis- and immune-related genes across specific tumor subtypes from the TCGA are shown: A) AR-Normal vs. AR-High BRCA; B) BRAF WT vs. V600E MUT SKCM; C) EGFR WT vs. L858R MUT LUAD and D) KRAS WT vs. G12 MUT LUAD.

SUPPLEMENTARY FIGURE S3

Abundance of glycolytic proteins is associated with decreased immune infiltration. **(A)** Correlation profiles of protein abundance of selected glycolysis- and immune-related genes in selected tumor types from CPTAC. **(B)** The LDHA protein abundance was plotted against the percentage of immune cells in H&E-stained tumor biopsies [as reported in Xu, Zhang, et al. (50)]. Data is presented in the entire cohort *(left)*, and in the EGFR WT *(middle)* and MUT *(right)* cohorts. **(C)** LDHA protein abundance was plotted in samples classified as having low, middle or high levels of CD8 T cell infiltration as measured by IHC staining and scoring [as reported in Xu, Zhang, et al. (50)]. Data is presented in the entire cohort *(left)*, and separated into the individual EGFR WT *(middle)* and MUT *(right)* cohorts.

SUPPLEMENTARY FIGURE S4

Expression of FDGScore across clinical characteristics of multiple cohorts. **(A)** FDGScore expression was plotted in relation to the (i) tumor stage; (ii) patient age at diagnosis; and (iii) gender in the Pan Cancer TCGA cohort. **(B)** FDGScore expression was plotted in relation to (i) tumor stage and (ii) patient age at diagnosis in the breast METABRIC cohort. **(C)** FDGScore expression was plotted in relation to (i) tumor stage; (ii) patient age at diagnosis and (iii) gender in the GSE65904 Melanoma cohort. The relationship between FDGScore and Stage was determined by calculating a linear regression to obtain the B coefficient. The relationship between FDGScore and Age was determined by calculating a Spearman rank correlation to obtain the correlation coefficient. The relationship between FDGScore and Gender was determined by performing a t-test between FDGScore expression in Male/Female.

SUPPLEMENTARY FIGURE S5

Expression of FDGScore is negatively correlated with T cell estimates within individual tumor types. **(A-C)** The correlation profiles of the FDG uptake signature (FDGScore) and the estimates of T cell subset abundance (as measured by ssGSEA) were calculated and plotted for the ER-negative METABRIC (A), GSE65904 (B) and GSE119267 (C) cohorts *(left)*. The expression of the FDGScore vs. CD8 *(middle)* and Tcm *(right)* T cell estimates is also shown with the calculated Pearson and Spearman coefficients.

SUPPLEMENTARY FIGURE S6

Expression of FDGScore is negatively correlated with T cell estimates within Luminal and ER-positive breast tumor types. **(A-B)** The correlation profiles of the FDG uptake signature (FDGScore) and the estimates of T cell subset abundance (as measured by ssGSEA) were calculated and plotted for the Luminal A and Luminal B subtypes of the TCGA BRCA cohort (A) and for the ER-positive subtype of the METABRIC cohort (B) *(left)*. The expression of the FDGScore vs. CD8 *(middle)* and Tcm *(right)* T cell estimates is also shown with the calculated Pearson and Spearman coefficients.

SUPPLEMENTARY FIGURE S7

HM_Glycolysis expression is inversely correlated with estimates of $CD8^+$ and $T_{cm}T$ cells across most solid tumor types. **(A-D)** The correlation profiles of the HM_Glycolysis signature and the estimates of T cell subset abundance (as measured by ssGSEA) were calculated and plotted for the entire TCGA Pan Cancer cohort (A) and for individual tumor types within TCGA (B-D) *(left)*. The expression of the HM_Glycolysis vs. CD8 *(middle)* and Tcm *(right)* T cell estimates is also shown with the calculated Pearson and Spearman coefficients.

SUPPLEMENTARY FIGURE S8

Expression of HM_Glycolysis is negatively correlated with T cell estimates within individual tumor types. **(A-C)** The correlation profiles of the HM_Glycolysis signature and the estimates of T cell subset abundance (as measured by ssGSEA) were calculated and plotted for the ER-negative METABRIC (A), GSE65904 (B) and GSE119267 (C) cohorts *(left)*. The expression of the FDGScore vs. CD8 *(middle)* and Tcm *(right)* T cell estimates is also shown with the calculated Pearson and Spearman coefficients.

SUPPLEMENTARY FIGURE S9

Expression of HM_Glycolysis is negatively correlated with T cell estimates within the Luminal and ER-positive breast tumor types.**(A-C)** The correlation profiles of the HM_Glycolysis signature and the estimates of T cell subset abundance (as measured by ssGSEA) were calculated and plotted for the TCGA BRCA LumA/LumB (A) and METABRIC ER-positive (B) cohorts. The expression of the FDGScore vs. CD8 *(middle)* and Tcm *(right)* T cell estimates is also shown with the calculated Pearson and Spearman coefficients.

SUPPLEMENTARY FIGURE S10

Glucose and lactate abundance in a cohort of 23 human breast tumors. **(A)** Glucose and lactate metabolite levels were obtained from the Tang et. al. dataset and the correlation between glucose, lactate, FDGScore and multiple T cell estimates were plotted. ((**B)** FDGScore expression was plotted vs. the levels of glucose and lactate. **(C)** Multiple T cell estimates were plotted vs. lactate abundance levels in the Tang dataset.

SUPPLEMENTARY FIGURE S11

Overall survival by FDGScore and the CD8 T cell estimate in individual subtypes of breast cancer. **(A-D)** Kaplan-Meier survival analysis was performed for the Luminal A/B (A) and Basal/Her2 (B) subtypes of the TCGA BRCA cohort; and for the ER-positive (C) and ER-negative (D) subtypes of the METABRIC cohort. The disease-specific survival probability of patients was measured in the top tertile vs the bottom tertile of expression of either FDGScore *(left)* or the CD8 T cell estimate *(right)* for each cancer type, and the Hazard Ratio (HR) was calculated.

SUPPLEMENTARY FIGURE S12

Overall survival by HM_Glycolysis in solid tumors. **(A-D)** Kaplan-Meier survival analysis was performed for the entire TCGA cohort (A), as well as individually for the TCGA SKCM (B), TCGA LUAD (C) and METABRIC (D) cohorts. The disease-specific survival probability of patients was measured in the top tertile vs the bottom tertile of expression of HM_Glycolysis for each cancer type, and the Hazard Ratio (HR) was calculated.

SUPPLEMENTARY FIGURE S13

Expression of glycolytic and immune markers in relation to FDG uptake in primary breast tumors. **(A)** Volumetric Regions of Interest (ROIs) were drawn on FDG-PET scans for 18 pts with available scans, and the SUV Peak was calculated and plotted against the GLUT1 H Score *(left)*, the LDHA H Score *(middle)* and the Mean Glycolysis H Score *(right)* in the MSK cohort of 49 patients with treatment-naïve ER-negative primary breast cancer; see Methods. **(B)** SUV Peak was plotted against the percentage of stromal TILs *(left)*, stromal CD3+ lymphocytes *(middle)* and stromal CD8+ lymphocytes *(right)*. **(C)** Recurrence-free survival was calculated and Kaplan-Meier plots were plotted for patients in the highest tertile of the Mean Glycolysis H Score *(left)* or stromal CD8+ lymphocytes *(right)* and compared to patients in the bottom 2 tertiles.

References

1. Galluzzi L, Chan TA, Kroemer G, Wolchok JD, López-Soto. A. The hallmarks of successful anticancer immunotherapy. *Sci Trans Med* (2018) 10:eaat7807. doi: 10.1126/scitranslmed.aat7807

2. Kraehenbuehl L, Weng C-H, Eghbali S, Wolchok JD, Merghoub. T. Enhancing immunotherapy in cancer by targeting emerging immunomodulatory pathways. *Nat Rev Clin Oncol* (2022) 19:37–50. doi: 10.1038/s41571-021-00552-7

3. Larkin J, Chiarion-Sileni V, Gonzalez R, Grob J-J, Rutkowski P, Lao CD, et al. Five-year survival with combined nivolumab and ipilimumab in advanced melanoma. *New Engl J Med* (2019) 381:1535–46. doi: 10.1056/NEJMoa1910836

4. Reck M, Rodríguez-Abreu D, Robinson AG, Hui R, Csőszi T, Fülöp A, et al. Pembrolizumab versus chemotherapy for PD-L1–positive non–Small-Cell lung cancer. *New Engl J Med* (2016) 375:1823–33. doi: 10.1056/NEJMoa1606774

5. Garon EB, Rizvi NA, Hui R, Leighl N, Balmanoukian AS, Eder JP, et al. Pembrolizumab for the treatment of non–Small-Cell lung cancer. *New Engl J Med* (2015) 372:2018–28. doi: 10.1056/NEJMoa1501824

6. Sezer A, Kilickap S, Gümüş M, Bondarenko I, Özgüroğlu M, Gogishvili M, et al. Cemiplimab monotherapy for first-line treatment of advanced non-small-cell lung cancer with PD-L1 of at least 50%: A multicentre, open-label, global, phase 3, randomised, controlled trial. *Lancet* (2021) 397:592–604. doi: 10.1016/S0140-6736(21)00228-2

7. Le DT, Durham JN, Smith KN, Wang H, Bartlett BR, Aulakh LK, et al. Mismatch repair deficiency predicts response of solid tumors to PD-1 blockade. *Science* (2017) 357:409–13. doi: 10.1126/science.aan6733

8. Le DT, Uram JN, Wang H, Bjarne R, Kemberling H, et al. PD-1 blockade in tumors with mismatch-repair deficiency. *New Engl J Med* (2015) 372:2509–20. doi: 10.1056/NEJMoa1500596

9. André, Thierry, Shiu K-K, Kim TW, Jensen BV, Jensen LH, et al. Pembrolizumab in Microsatellite-Instability–high advanced colorectal cancer. *New Engl J Med* (2020) 383:2207–18. doi: 10.1056/NEJMoa2017699

10. Hellmann MD, Paz-Ares L, Caro RB, Zurawski B, Kim S-W, Costa EC, et al. Nivolumab plus ipilimumab in advanced non–Small-Cell lung cancer. *New Engl J Med* (2019) 381:2020–31. doi: 10.1056/NEJMoa1910231

11. Motzer RJ, Tannir NM, McDermott DF, Frontera OArén, Melichar B, Choueiri TK, et al. Nivolumab plus ipilimumab versus sunitinib in advanced renal-cell carcinoma. *New Engl J Med* (2018) 378:1277–90. doi: 10.1056/NEJMoa1712126

12. Hellmann MD, Ciuleanu T-E, Pluzanski A, Lee JS, Otterson GA, Audigier-Valette C, et al. Nivolumab plus ipilimumab in lung cancer with a high tumor mutational burden. *New Engl J Med* (2018) 378:2093–104. doi: 10.1056/NEJMoa1801946

13. Paz-Ares L, Ciuleanu T-E, Cobo M, Schenker M, Zurawski B, Menezes J, et al. First-line nivolumab plus ipilimumab combined with two cycles of chemotherapy in patients with non-small-cell lung cancer (CheckMate 9LA): an international, randomised, open-label, phase 3 trial. *Lancet Oncol* (2021) 22:198–211. doi: 10.1016/S1470-2045(20)30641-0

14. Cortes J, Cescon DW, Rugo HS, Nowecki Z, Im S-A, Yusof MMd, et al. Pembrolizumab plus chemotherapy versus placebo plus chemotherapy for previously untreated locally recurrent inoperable or metastatic triple-negative breast cancer (KEYNOTE-355): A randomised, placebo-controlled, double-blind, phase 3 clinical trial. *Lancet* (2020) 396:1817–28. doi: 10.1016/S0140-6736(20)32531-9

15. Cascone T, William WN, Weissferdt A, Leung CH, Lin HY, Pataer A, et al. Neoadjuvant nivolumab or nivolumab plus ipilimumab in operable non-small cell lung cancer: the phase 2 randomized NEOSTAR trial. *Nat Med* (2021) 27:504–14. doi: 10.1038/s41591-020-01224-2

16. Provencio M, Nadal E, Insa A, García-Campelo MaríaR, Casal-Rubio Joaquín, Dómine M, et al. Neoadjuvant chemotherapy and nivolumab in resectable non-small-cell lung cancer (NADIM): An open-label, multicentre, single-arm, phase 2 trial. *Lancet Oncol* (2020) 21:1413–22. doi: 10.1016/S1470-2045(20)30453-8

17. Borghaei H, Langer CJ, Gadgeel S, Papadimitrakopoulou VA, Patnaik A, Powell SF, et al. 24-month overall survival from KEYNOTE-021 cohort G: Pemetrexed and carboplatin with or without pembrolizumab as first-line therapy for advanced nonsquamous non–small cell lung cancer. *J Thorac Oncol* (2019) 14:124–29. doi: 10.1016/j.jtho.2018.08.004

18. Socinski MA, Jotte RM, Cappuzzo F, Orlandi F, Stroyakovskiy D, Nogami N, et al. Atezolizumab for first-line treatment of metastatic nonsquamous NSCLC. *New Engl J Med* (2018) 378:2288–301. doi: 10.1056/NEJMoa1716948

19. Horn L, Mansfield AS, Szczęsna A, Havel L, Krzakowski M, Hochmair MJ, et al. First-line atezolizumab plus chemotherapy in extensive-stage small-cell lung cancer. *New Engl J Med* (2018) 379:2220–29. doi: 10.1056/NEJMoa1809064

20. Schmid P, Adams S, Rugo HS, Schneeweiss A, Barrios CH, Iwata H, et al. Atezolizumab and nab-paclitaxel in advanced triple-negative breast cancer. *N Engl J Med* (2018) 379:2108–21. doi: 10.1056/NEJMoa1809615

21. Eggermont AMM, Blank CU, Mandalà M, Long GV, Atkinson VG, Dalle Stéphane, et al. Adjuvant pembrolizumab versus placebo in resected stage III melanoma (EORTC 1325-MG/KEYNOTE-054): distant metastasis-free survival results from a double-blind, randomised, controlled, phase 3 trial. *Lancet Oncol* (2021) 22:643–54. doi: 10.1016/S1470-2045(21)00065-6

22. Rozeman EA, Menzies AM, Akkooi ACJv, Adhikari C, Bierman C, Wiel BAvde, et al. Identification of the optimal combination dosing schedule of neoadjuvant ipilimumab plus nivolumab in macroscopic stage III melanoma (OpACIN-neo): a multicentre, phase 2, randomised, controlled trial. *Lancet Oncol* (2019) 20:948–60. doi: 10.1016/S1470-2045(19)30151-2

23. Ascierto PA, Vecchio MD, Mandalá M, Gogas H, Arance AM, Dalle S, et al. Adjuvant nivolumab versus ipilimumab in resected stage IIIB–c and stage IV melanoma (CheckMate 238): 4-year results from a multicentre, double-blind, randomised, controlled, phase 3 trial. *Lancet Oncol* (2020) 21:1465–77. doi: 10.1016/S1470-2045(20)30494-0

24. Zimmer L, Livingstone E, Hassel JC, Fluck M, Eigentler T, Loquai C, et al. Adjuvant nivolumab plus ipilimumab or nivolumab monotherapy versus placebo in patients with resected stage IV melanoma with no evidence of disease (IMMUNED): A randomised, double-blind, placebo-controlled, phase 2 trial. *Lancet* (2020) 395:1558–68. doi: 10.1016/S0140-6736(20)30417-7

25. Kelly RJ, Ajani JA, Kuzdzal J, Zander T, Cutsem EV, Piessen G, et al. Adjuvant nivolumab in resected esophageal or gastroesophageal junction cancer. *New Engl J Med* (2021) 384:1191–203. doi: 10.1056/NEJMoa2032125

26. Bajorin DF, Witjes JA, Gschwend JürgenE, Schenker M, Valderrama BegoñaP, Tomita Y, et al. Adjuvant nivolumab versus placebo in muscle-invasive urothelial carcinoma. *New Engl J Med* (2021) 384:2102–14. doi: 10.1056/NEJMoa2034442

27. Forde PM, Chaft JE, Smith KN, Anagnostou V, Cottrell TR, Hellmann MD, et al. Neoadjuvant PD-1 blockade in resectable lung cancer. *New Engl J Med* (2018) 378:1976–86. doi: 10.1056/NEJMoa1716078

28. Ribas A, Wolchok. JD. Cancer immunotherapy using checkpoint blockade. *Science* (2018) 359:1350–55. doi: 10.1126/science.aar4060

29. Marcus L, Lemery SJ, Keegan P, Pazdur R. FDA approval summary: Pembrolizumab for the treatment of microsatellite instability-high solid tumors. *Clin Cancer Res: Clincanres* (2019) 4070:2018. doi: 10.1158/1078-0432.CCR-18-4070

30. Leone RD, Powell JD. Metabolism of immune cells in cancer. *Nat Rev Cancer* (2020) 20:516–31. doi: 10.1038/s41568-020-0273-y

31. Warburg O. The metabolism of carcinoma cells. *J Cancer Res* (1925) 9:148–63. doi: 10.1158/jcr.1925.148

32. Shim H, Dolde C, Lewis BC, Wu C-S, Dang G, Jungmann RA, et al. c-myc transactivation of LDH-a: Implications for tumor metabolism and growth. *Proc Natl Acad Sci* (1997) 94:6658–63. doi: 10.1073/pnas.94.13.6658

33. Elstrom RL, Bauer DE, Buzzai M, Karnauskas R, Harris MH, Plas DR, et al. Akt stimulates aerobic glycolysis in cancer cells. *Cancer Res* (2004) 64:3892–99. doi: 10.1158/0008-5472.CAN-03-2904

34. Hall A, Meyle KD, Lange MK, Klima M, Sanderhoff M, Dahl C, et al. Dysfunctional oxidative phosphorylation makes malignant melanoma cells addicted to glycolysis driven by the (V600E)BRAF oncogene. *Oncotarget* (2013) 4:584–99. doi: 10.18632/oncotarget.965

35. Matoba S, Kang J-G, Patino WD, Wragg A, Boehm M, Gavrilova O, et al. p53 regulates mitochondrial respiration. *Science* (2006) 312:1650–53. doi: 10.1126/science.1126863

36. Walenta S, Wetterling M, Lehrke M, Schwickert G, Sundfor K, Rofstad EK, et al. High lactate levels predict likelihood of metastases, tumor recurrence, and restricted patient survival in human cervical cancers. *Cancer Res* (2000) 60(4):916–21.

37. Wike-Hooley JL, van den Berg AP, Zee Jvd, Reinhold. HS. Human tumour pH and its variation. *Eur J Cancer Clin Oncol* (1985) 21:785–91. doi: 10.1016/0277-5379(85)90216-0

38. Chang CH, Qiu J, O'Sullivan D, Buck MD, Noguchi T, Curtis JD, et al. Metabolic competition in the tumor microenvironment is a driver of cancer progression. *Cell* (2015) 162:1229–41. doi: 10.1016/j.cell.2015.08.016

39. Cohen IJ, Blasberg R. Impact of the tumor microenvironment on tumor-infiltrating lymphocytes: Focus on breast cancer. *Breast Cancer (Auckl)* (2017) 11:1178223417731565. doi: 10.1177/1178223417731565

40. Serganova I, Cohen IJ, Vemuri K, Shindo M, Maeda M, Mane M, et al. LDH-a regulates the tumor microenvironment *via* HIF-signaling and modulates the immune response. *PloS One* (2018) 13:e0203965. doi: 10.1371/journal.pone.0203965

41. Brand A, Singer K, Koehl GE, Kolitzus M, Schoenhammer G, Thiel A, et al. LDHA-associated lactic acid production blunts tumor immunosurveillance by T and NK cells. *Cell Metab* (2016) 24:657–71. doi: 10.1016/j.cmet.2016.08.011

42. Ho PC, Bihuniak JD, Macintyre AN, Staron M, Liu X, Amezquita R, et al. Phosphoenolpyruvate is a metabolic checkpoint of anti-tumor T cell responses. *Cell* (2015) 162:1217–28. doi: 10.1016/j.cell.2015.08.012

43. Angelin A, Gil-de-Gómez L, Dahiya S, Jiao J, Guo L, Levine MH, et al. Foxp3 reprograms T cell metabolism to function in low-glucose, high-lactate environments. *Cell Metab* (2017) 25:1282–93.e7. doi: 10.1016/j.cmet.2016.12.018

44. Watson MJ, Vignali PDA, Mullett SJ, Overacre-Delgoffe AE, Peralta RM, Grebinoski S, et al. Metabolic support of tumour-infiltrating regulatory T cells by lactic acid. *Nature* (2021) 591:645–51. doi: 10.1038/s41586-020-03045-2

45. Zappasodi R, Serganova I, Cohen IJ, Maeda M, Shindo M, Senbabaoglu Y, et al. CTLA-4 blockade drives loss of treg stability in glycolysis-low tumours. *Nature* (2021) 591:652–58. doi: 10.1038/s41586-021-03326-4

46. Zappasodi R, Wolchok JD, Merghoub T. Strategies for predicting response to checkpoint inhibitors. *Curr Hematol Malig Rep* (2018) 13:383–95. doi: 10.1007/s11899-018-0471-9

47. Hoadley KA, Yau C, Hinoue T, Wolf DM, Lazar AJ, Drill E, et al. Cell-of-Origin patterns dominate the molecular classification of 10,000 tumors from 33 types of cancer. *Cell* (2018) 173:291–304.e6. doi: 10.1016/j.cell.2018.03.022

48. Curtis C, Shah SP, Chin S-F, Turashvili G, Rueda OM, Dunning MJ, et al. The genomic and transcriptomic architecture of 2,000 breast tumours reveals novel subgroups. *Nature* (2012) 486:346–52. doi: 10.1038/nature10983

49. Cerami E, Gao J, Dogrusoz U, Gross BE, Sumer SO, Aksoy BülentA, et al. The cBio cancer genomics portal: An open platform for exploring multidimensional cancer genomics data. *Cancer Discovery* (2012) 2:401–04. doi: 10.1158/2159-8290.CD-12-0095

50. Xu J-Y, Zhang C, Wang X, Zhai L, Ma Y, Mao Y, et al. Integrative proteomic characterization of human lung adenocarcinoma. *Cell* (2020) 182:245–61.e17. doi: 10.1016/j.cell.2020.05.043

51. Tang X, Lin C-C, Spasojevic I, Iversen ES, Chi J-T, Marks. JR. A joint analysis of metabolomics and genetics of breast cancer. *Breast Cancer Res* (2014) 16:415. doi: 10.1186/s13058-014-0415-9

52. Palaskas N, Larson SM, Schultz N, Komisopoulou E, Wong J, Rohle D, et al. 18F-fluorodeoxy-glucose positron emission tomography marks MYC-overexpressing human basal-like breast cancers. *Cancer Res* (2011) 71:5164–74. doi: 10.1158/0008-5472.CAN-10-4633

53. Senbabaoglu Y, Gejman RS, Winer AG, Liu M, Van Allen EM, de Velasco G, et al. Tumor immune microenvironment characterization in clear cell renal cell carcinoma identifies prognostic and immunotherapeutically relevant messenger RNA signatures. *Genome Biol* (2016) 17:231. doi: 10.1186/s13059-016-1092-z

54. Liberzon A, Birger C, Thorvaldsdottir H, Ghandi M, Mesirov JP, Tamayo P. The molecular signatures database (MSigDB) hallmark gene set collection. *Cell Syst* (2015) 1:417–25. doi: 10.1016/j.cels.2015.12.004

55. Liu J, Lichtenberg T, Hoadley KA, Poisson LM, Lazar AJ, Cherniack AD, et al. An integrated TCGA pan-cancer clinical data resource to drive high-quality survival outcome analytics. *Cell* (2018) 173:400–16.e11. doi: 10.1016/j.cell.2018.02.052

56. Tumours B. WHO classification of tumours. *Lyon France: Int Agency Res Canc* (2019).

57. Elston CW, Ellis IO. Pathological prognostic factors in breast cancer. i. the value of histological grade in breast cancer: Experience from a large study with long-term follow-up. *Histopathology* (1991) 19:403–10. doi: 10.1111/j.1365-2559.1991.tb00229.x

58. Salgado R, Denkert C, Demaria S, Sirtaine N, Klauschen F, Pruneri G, et al. The evaluation of tumor-infiltrating lymphocytes (TILs) in breast cancer: recommendations by an international TILs working group 2014. *Ann Oncol* (2015) 26:259–71. doi: 10.1093/annonc/mdu450

59. Pareja F, Toss MS, Geyer FC, da Silva EM, Vahdatinia M, Sebastiao APM, et al. Immunohistochemical assessment of HRAS Q61R mutations in breast adenomyoepitheliomas. *Histopathology* (2020) 76:865–74. doi: 10.1111/his.14057

60. Pareja F, da Silva EM, Frosina D, Geyer FC, Lozada JR, Basili T, et al. Immunohistochemical analysis of IDH2 R172 hotspot mutations in breast papillary neoplasms: Applications in the diagnosis of tall cell carcinoma with reverse polarity. *Modern Pathol* (2020) 33:1056–64. doi: 10.1038/s41379-019-0442-2

61. Winer EP, Lipatov O, Im S-A, Goncalves A, Muñoz-Couselo E, Lee KS, et al. Pembrolizumab versus investigator-choice chemotherapy for metastatic triple-negative breast cancer (KEYNOTE-119): A randomised, open-label, phase 3 trial. *Lancet Oncol* (2021) 22:499–511. doi: 10.1016/S1470-2045(20)30754-3

62. Kojima T, Shah MA, Muro K, Francois E, Adenis A, Hsu C-H, et al. Randomized phase III KEYNOTE-181 study of pembrolizumab versus chemotherapy in advanced esophageal cancer. *J Clin Oncol* (2020) 38:4138–48. doi: 10.1200/JCO.20.01888

63. Shitara K, Cutsem EV, Bang Y-J, Fuchs C, Wyrwicz L, Lee K-W, et al. Efficacy and safety of pembrolizumab or pembrolizumab plus chemotherapy vs chemotherapy alone for patients with first-line, advanced gastric cancer: The KEYNOTE-062 phase 3 randomized clinical trial. *JAMA Oncol* (2020) 6:1571–80. doi: 10.1001/jamaoncol.2020.3370

64. Marabelle Aurélien, Fakih M, Lopez J, Shah M, Shapira-Frommer R, Nakagawa K, et al. Association of tumour mutational burden with outcomes in patients with advanced solid tumours treated with pembrolizumab: prospective biomarker analysis of the multicohort, open-label, phase 2 KEYNOTE-158 study. *Lancet Oncol* (2020) 21:1353–65. doi: 10.1016/S1470-2045(20)30445-9

65. Feng J, Li J, Wu L, Yu Q, Ji J, Wu J, et al. Emerging roles and the regulation of aerobic glycolysis in hepatocellular carcinoma. *J Exp Clin Cancer Res* (2020) 39:126. doi: 10.1186/s13046-020-01629-4

66. Wu Z, Wu J, Zhao Q, Fu S, Jin J. Emerging roles of aerobic glycolysis in breast cancer. *Clin Transl Oncol* (2020) 22:631–46. doi: 10.1007/s12094-019-02187-8

67. Cirenajwis H, Ekedahl H, Lauss M, Harbst K, Carneiro A, Enoksson J, et al. Molecular stratification of metastatic melanoma using gene expression profiling: Prediction of survival outcome and benefit from molecular targeted therapy. *Oncotarget* (2015) 6:12297–309. doi: 10.18632/oncotarget.3655

68. Subat S, Inamura K, Ninomiya H, Nagano H, Okumura S, Ishikawa. Y. Unique MicroRNA and mRNA interactions in EGFR-mutated lung adenocarcinoma. *J Clin Med* (2018) 7:419. doi: 10.3390/jcm7110419

69. Vasaikar S, Huang C, Wang X, Petyuk VA, Savage SR, Wen Bo, et al. Proteogenomic analysis of human colon cancer reveals new therapeutic opportunities. *Cell* (2019) 177:1035–49.e19. doi: 10.1016/j.cell.2019.03.030

70. Gillette MA, Satpathy S, Cao S, Dhanasekaran SM, Vasaikar SV, Krug K, et al. Proteogenomic characterization reveals therapeutic vulnerabilities in lung adenocarcinoma. *Cell* (2020) 182:200–25.e35. doi: 10.1016/j.cell.2020.06.013

71. Dou Y, Kawaler EA, Cui Zhou D, Gritsenko MA, Huang C, Blumenberg L, et al. Proteogenomic characterization of endometrial carcinoma. *Cell* (2020) 180:729–48.e26. doi: 10.1016/j.cell.2020.01.026

72. Wang LB, Karpova A, Gritsenko MA, Kyle JE, Cao S, Li Y, et al. Proteogenomic and metabolomic characterization of human glioblastoma. *Cancer Cell* (2021) 39:509–28.e20. doi: 10.1016/j.ccell.2021.01.006

73. Satpathy S, Krug K, Jean Beltran PM, Savage SR, Petralia F, Kumar-Sinha C, et al. A proteogenomic portrait of lung squamous cell carcinoma. *Cell* (2021) 184:4348–71.e40. doi: 10.1016/j.cell.2021.07.016

74. Cao L, Huang C, Cui Zhou D, Hu Y, Lih TM, Savage SR, et al. Proteogenomic characterization of pancreatic ductal adenocarcinoma. *Cell* (2021) 184:5031–52.e26. doi: 10.1016/j.cell.2021.08.023

75. Krug K, Jaehnig EJ, Satpathy S, Blumenberg L, Karpova A, Anurag M, et al. Proteogenomic landscape of breast cancer tumorigenesis and targeted therapy. *Cell* (2020) 183:1436–56.e31. doi: 10.1016/j.cell.2020.10.036

76. Zhang H, Liu T, Zhang Z, Payne SH, Zhang B, McDermott JE, et al. Integrated proteogenomic characterization of human high-grade serous ovarian cancer. *Cell* (2016) 166:755–65. doi: 10.1016/j.cell.2016.05.069

77. Hakimi A, Attalla K, DiNatale RG, Ostrovnaya I, Flynn J, et al. A pan-cancer analysis of PBAF complex mutations and their association with immunotherapy response. *Nat Commun* (2020) 11:4168. doi: 10.1038/s41467-020-17965-0

78. Fischer K, Hoffmann P, Voelkl S, Meidenbauer N, Ammer J, Edinger M, et al. Inhibitory effect of tumor cell–derived lactic acid on human T cells. (2007) 109(9):3812–9. doi: 10.1182/blood-2006-07-035972

79. Chang C-H, Curtis JD, Maggi LB, Faubert B, Villarino AV, O'Sullivan D, et al. Posttranscriptional control of T cell effector function by aerobic glycolysis. *Cell* (2013) 153:1239–51. doi: 10.1016/j.cell.2013.05.016

80. Warburg O, Wind F, Negelein E. THE METABOLISM OF TUMORS IN THE BODY. *J Gen Physiol* (1927) 8:519–30. doi: 10.1085/jgp.8.6.519

81. Ward PS, Thompson CB. Metabolic reprogramming: a cancer hallmark even warburg did not anticipate. *Cancer Cell* (2012) 21:297–308. doi: 10.1016/j.ccr.2012.02.014

82. Orozco JM, Krawczyk PA, Scaria SM, Cangelosi AL, Chan SH, Kunchok T, et al. Dihydroxyacetone phosphate signals glucose availability to mTORC1. *Nat Metab* (2020) 2:893–901. doi: 10.1038/s42255-020-0250-5

83. Xu Ke, Yin Na, Peng M, Stamatiades EG, Shyu A, Li P, et al. Glycolysis fuels phosphoinositide 3-kinase signaling to bolster T cell immunity. *Science* (2021) 371:405–10. doi: 10.1126/science.abb2683

84. Haas R, Cucchi D, Smith J, Pucino V, Macdougall CE, Mauro. C. Intermediates of metabolism: From bystanders to signalling molecules. *Trends Biochem Sci* (2016) 41:460–71. doi: 10.1016/j.tibs.2016.02.003

85. Peng M, Yin Na, Chhangawala S, Xu Ke, Leslie CS, Li. MO. Aerobic glycolysis promotes T helper 1 cell differentiation through an epigenetic mechanism. *Science* (2016) 354:481–84. doi: 10.1126/science.aaf6284

86. Zhang Di, Tang Z, Huang He, Zhou G, Cui C, Weng Y, et al. Metabolic regulation of gene expression by histone lactylation. *Nature* (2019) 574:575–80. doi: 10.1038/s41586-019-1678-1

87. Yao J, Li R, Liu X, Zhou X, Li J, Liu T, et al. Prognostic implication of glycolysis related gene signature in non-small cell lung cancer. *J Cancer* (2021) 12:885–98. doi: 10.7150/jca.50274

88. Zhang L, Zhang Z, Yu Z. Identification of a novel glycolysis-related gene signature for predicting metastasis and survival in patients with lung adenocarcinoma. *J Transl Med* (2019) 17:423. doi: 10.1186/s12967-019-02173-2

89. Tang J, Luo Y, Wu G. A glycolysis-related gene expression signature in predicting recurrence of breast cancer. *Aging (Albany NY)* (2020) 12:24983–94. doi: 10.18632/aging.103806

90. Yu S, Hu C, Cai L, Du X, Lin F, Yu Q, et al. Seven-gene signature based on glycolysis is closely related to the prognosis and tumor immune infiltration of patients with gastric cancer. *Front Oncol* (2020) 10(1778). doi: 10.3389/fonc.2020.01778

91. Liu J, Li S, Feng G, Meng H, Nie S, Sun R, et al. Nine glycolysis-related gene signature predicting the survival of patients with endometrial adenocarcinoma. *Cancer Cell Int* (2020) 20:183. doi: 10.1186/s12935-020-01264-1

92. Jiang F, Wu C, Wang M, Wei K, Wang J. Identification of novel cell glycolysis related gene signature predicting survival in patients with breast cancer. *Sci Rep* (2021) 11(1):3986. doi: 10.1038/s41598-021-83628-9

93. Xu F, Guan Y, Xue L, Huang S, Gao K, Yang Z, et al. The effect of a novel glycolysis-related gene signature on progression, prognosis and immune microenvironment of renal cell carcinoma. *BMC Cancer* (2020) 20(1):1207. doi: 10.1186/s12885-020-07702-7

94. Wei J, Huang K, Chen Z, Hu M, Bai Y, Lin S, et al. Characterization of glycolysis-associated molecules in the tumor microenvironment revealed by pan-cancer tissues and lung cancer single cell data. *Cancers (Basel)* (2020) 12(7):1788. doi: 10.3390/cancers12071788

95. Wu Z, Wen Z, Li Z, Yu M, Ye G. Identification and prognostic value of a glycolysis-related gene signature in patients with bladder cancer. *Med (Baltimore)* (2021) 100(3):e23836. doi: 10.1097/MD.0000000000023836

96. Sturm G, Finotello F, Petitprez F, Zhang JD, Baumbach J, Fridman WH, et al. Comprehensive evaluation of transcriptome-based cell-type quantification methods for immuno-oncology. *Bioinformatics* (2019) 35(14):i436–i445. doi: 10.1093/bioinformatics/btz363

97. Harbison RA, Pandey R, Considine M, Leone RD, Murray-Stewart T, Erbe R, et al. Interrogation of T cell-enriched tumors reveals prognostic and immunotherapeutic implications of polyamine metabolism. *Cancer Res Commun* (2022) 2:639–52. doi: 10.1158/2767-9764.CRC-22-0061

98. Murakami W, Tozaki M, Sasaki M, Hida AI, Ohi Y, Kubota K, et al. Correlation between (18)F-FDG uptake on PET/MRI and the level of tumor-infiltrating lymphocytes (TILs) in triple-negative and HER2-positive breast cancer. *Eur J Radiol* (2020) 123:108773. doi: 10.1016/j.ejrad.2019.108773

99. An YS, Kim SH, Roh TH, Park SH, Kim TG, Kim JH. Correlation between (18)F-FDG uptake and immune cell infiltration in metastatic brain lesions. *Front Oncol* (2021) 11:618705. doi: 10.3389/fonc.2021.618705

100. Osborne JR, Port E, Gonen M, Doane A, Yeung H, Gerald W, et al. 18F-FDG PET of locally invasive breast cancer and association of estrogen receptor status with standardized uptake value: Microarray and immunohistochemical analysis. *J Nucl Med* (2010) 51:543–50. doi: 10.2967/jnumed.108.060459

101. Beloueche-Babari M, Galobart TC, Delgado-Goni T, Wantuch S, Parkes HG, Tandy D, et al. Monocarboxylate transporter 1 blockade with AZD3965 inhibits lipid biosynthesis and increases tumour immune cell infiltration. *Br J Cancer* (2020) 122:895–903. doi: 10.1038/s41416-019-0717-x

102. Halford SER, Jones P, Wedge S, Hirschberg S, Katugampola S, Veal G, et al. A first-in-human first-in-class (FIC) trial of the monocarboxylate transporter 1 (MCT1) inhibitor AZD3965 in patients with advanced solid tumours. *J Clin Oncol* (2017) 35:2516–16. doi: 10.1200/JCO.2017.35.15_suppl.2516

Frontiers in Immunology

Explores novel approaches and diagnoses to treat immune disorders.

The official journal of the International Union of Immunological Societies (IUIS) and the most cited in its field, leading the way for research across basic, translational and clinical immunology.

Discover the latest Research Topics

See more →

Frontiers

Avenue du Tribunal-Fédéral 34
1005 Lausanne, Switzerland
frontiersin.org

Contact us

+41 (0)21 510 17 00
frontiersin.org/about/contact